논문개요집

2022년 한국자기학회 하계학술대회

2022 KMS Summer Conference

논문개요집

일시	2022. 5. 25(수) ～ 27(금)
장소	소노캄제주
주최	한국자기학회
후원	KOFST 한국과학기술단체총연합회 KIMS 한국재료연구원 epU 파워유닛스마트제조센터

Digests of the 2022 KMS Summer Conference
The Korean Magnetics Society

사단법인 한국자기학회

2022년 한국자기학회 하계학술대회
2022 KMS Summer Conference

논문개요집

일시	2022. 5. 25(수) ~ 27(금)
장소	소노캄제주
주최	한국자기학회
후원	KOFST 한국과학기술단체총연합회 KIMS 한국재료연구원 epU 파워유닛스마트제조센터

2022년 한국자기학회 하계학술대회 종합프로그램

	다이아몬드	그랜드볼룸	사파이어
	참가자 등록 (13:00~)		
5/25(수)		Poster Session (13:00~18:00)	Symposium1 양자자성 (13:30~15:45)
	Tutorial Session 실전 영어과학논문 작성법 (16:00~18:00)	Poster Discussion (18:00~19:00)	

■ EAST TOWER 1F
■ EAST TOWER 2F
■ WEST TOWER 6F

5/26(목)	다이아몬드	에메랄드	루비	사파이어	오팔1
	참가자 등록 (08:30~)				
오전	Symposium2 자화동역학 (09:00~11:10)	Symposium3 영구자석&전자기 에너지변환 (09:00~11:50)	Symposium4 자기센서 및 마이크로소자 (09:00~11:50)	Symposium1 양자자성 (09:00~12:10)	Session1 구두발표 I (09:00~10:40)
					Symposium5 뫼스바우어 (10:40~12:00)
점심	점심 (12:00~14:00)				
오후	Symposium6 스핀트로닉스 (14:00~16:30)	Symposium3 영구자석&전자기 에너지변환 (14:00~17:40)	Symposium7 연자성 (14:00~17:50)	Symposium1 양자자성 (14:30~17:15)	Symposium8 저차원자성 (14:00~16:10)
	Session2 구두발표 II (16:40~18:00)				Session3 구두발표 III (16:20~17:40)
임시총회	임시총회 및 시상식 (다이아몬드) (18:00~19:00)				
만찬	만찬 (그랜드볼룸) (19:00~)				

	다이아몬드	에메랄드	루비	사파이어	오팔1
	참가자 등록 (08:30~)				
5/27(금)	Session4 신진과학자 콜로키움 (09:00~11:30)	Symposium9 의과학자기 (09:00~12:10)	Symposium10 바이오자성 (09:00~10:50)	Symposium1 양자자성 (09:00~12:15)	Symposium11 이론 및 계산자기학 (09:00~10:50)
	Session5 구두발표 IV (11:40~12:20)				Session6 구두발표 V (11:00~12:00)
폐회	포스터 시상식 및 폐회 (다이아몬드) (12:30~13:00)				

2022년 한국자기학회 하계학술대회 일정표

5월 25일[수]

시간	프로그램
13:00 ~	참가자 등록
13:00 ~ 18:00	**포스터발표** [1] Electro-Magnetic Energy Conversion [2] Bio-Convergence Magnetics [3] Magnetics in Medical Science [4] Mössbauer Magnetics [5] Spintronics [6] Magnetization Dynamics [7] Permanent Magnetics [8] Soft Magnetics [9] Theory and Computational Magnetics [10] Quantum Magnetism (Oxide Magnetics) [11] Low Dimensional Magnetics [12] Magnetic Sensors and Magnetic Micro-Devices [13] Others (그랜드볼룸)
	Symposium 1 'Quantum Magnetism' (사파이어)
	좌장: 문은국(KAIST)
13:30 ~ 14:00	초S-1-1. 한명준(KAIST)
14:00 ~ 14:30	초S-1-2. 박문집(IBS)
14:30 ~ 14:45	Coffee Break
14:45 ~ 15:15	초S-1-3. 노태원(서울대)
15:15 ~ 15:45	초S-1-4. 윤상문(가천대)
	Tutorial Session '대학원생 진행세션' (다이아몬드)
	좌장: 성민경(숙명여대)
16:00 ~ 18:00	T-1. 실전 영어과학논문 작성법 김영근(고려대)
18:00 ~ 19:00	**포스터 발표 Discussion** (그랜드볼룸)
	좌장: 김상훈(울산대), 박지훈(KIMS)

5월 26일[목] 오전

시간	프로그램				
08:30 ~	참가자 등록				
	Symposium 2 'Magnetization Dynamics' (다이아몬드)	Symposium 3 'Permanent Magnetics' & 'Electro-Magnetic Energy Conversion' 공동세션 (에메랄드)	Symposium 4 'Magnetic Sensors and Micro-Devices' (루비)	Symposium 1 'Quantum Magnetism' (사파이어)	Session 1 구두발표Ⅰ 'SpintronicsⅠ' (오팔Ⅰ)
	좌장: 김준서(DGIST)	좌장: 이우영(연세대)	좌장: 윤석수(안동대)	좌장: 옥종목(부산대)	좌장: 박정민(KAIST)
09:00 ~ 09:20	초S-2-1. 김경환(KIST)	09:00 ~ 09:20 초S-3-1. 김진배(LG전자)	09:00 ~ 09:20 초S-4-1. 임병화(DGIST)	09:00 ~ 09:30 초S-1-5. 김기훈(서울대)	09:00 ~ 09:20 O-1-1. 웬티꾸인안(울산대)
09:20 ~ 09:40	초S-2-2. 최경민(성균관대)	09:20 ~ 09:40 초S-3-2. 안종빈(㈜디아이씨)	09:20 ~ 09:40 초S-4-2. 김경원(한국전자기술연구원)	09:30 ~ 10:00 초S-1-.6 김영욱(DGIST)	09:20 ~ 09:40 O-1-2. 도티나(이화여대)
09:40 ~ 10:00	초S-2-3. 문경웅(KRISS)	09:40 ~ 10:00 초S-3-3. 배경훈(㈜성림첨단산업)	09:40 ~ 10:00 초S-4-3. 박덕근(㈜아이피트)	10:00 ~ 10:30 초S-1-7. 오윤석(UNIST)	09:40 ~ 10:00 O-1-3. 김종혁(연세대)
10:00 ~ 10:10 Coffee Break		10:00 ~ 10:20 초S-3-4. 배석(LG이노텍)	10:00 ~ 10:20 초S-4-4. 이상석(상지대)	10:30 ~ 10:45 Coffee Break	10:00 ~ 10:20 O-1-4. Phuoc Cao Van(충남대)
					10:20 ~ 10:40 O-1-5. 김현수(서강대)
10:10 ~ 10:30	초S-2-4. 이수길(KAIST)	10:20 ~ 10:30 Coffee Break	10:20 ~ 10:30 Coffee Break	10:45 ~ 11:15 초S-1-8. 황찬용(KRISS)	Symposium 5 '뫼스바우어 자성' (오팔Ⅰ)
		좌장: 최장영(충남대)	좌장: 박덕근(㈜아이피트)		좌장: 윤성현(군산대)
10:30 ~ 10:50	초S-2-5. 김창수(KRISS)	10:30 ~ 10:50 초S-3-5. 윤명환(한국전자기술연구원)	10:30 ~ 10:50 초S-4-5. 김장열(한국전자통신연구원)	11:15 ~ 11:45 초S-1-9. 박성균(부산대)	10:40 ~ 11:00 초S-5-1. 최현경(국민대)
		10:50 ~ 11:10 초S-3-6. 송인수(모아소프트)	10:50 ~ 11:10 초S-4-6. 윤석수(안동대)		11:00 ~ 11:20 초S-5-2. 지윤성(한국에너지기술연구원)
10:50 ~ 11:10	초S-2-6. 이수범(DGIST)	11:10 ~ 11:30 초S-3-7. 김현수(한양대)	11:10 ~ 11:30 초S-4-7. 이남영(디엔제이테크)	11:45 ~ 12:10 초S-1-10. 백승호(창원대)	11:20 ~ 11:40 초S-5-3. 천동현(한국에너지기술연구원)
		11:30 ~ 11:50 초S-3-8. 배예나(한양대)	11:30 ~ 11:50 초S-4-8. 손대락(㈜센서피아)		11:40 ~ 12:00 초S-5-4. 이재기(한국원자력연구원)
12:00 ~ 14:00	점심식사				

5월 26일[목] 오후

시간 / 프로그램

Symposium 6 '스핀트로닉스' (다이아몬드)

좌장: 이경진(KAIST)

시간	프로그램
14:00~14:20	초S-6-1. 김상국(서울대)
14:20~14:40	초S-6-2. 김갑진(KAIST)
14:40~15:00	초S-6-3. 정수용(KRISS)
15:00~15:20	초S-6-4. 안경모(KRISS)
15:20~15:30	Coffee Break

좌장: 박병국(KAIST)

시간	프로그램
15:30~15:50	초S-6-5. 김영훈(한양대)
15:50~16:10	초S-6-6. 이규섭(싱가폴국립대)
16:10~16:30	초S-6-7. 박영진(마테리온 코리아(유))

Session 2 구두발표Ⅱ 'Spintronics Ⅱ' / 'Magnetization Dynamics' (다이아몬드)

좌장: 최경민(성균관대)

시간	프로그램
16:40~17:00	O-2-1. 최영관(성균관대)
17:00~17:20	O-2-2. 박규영(서울대)
17:20~17:40	O-2-3. 서상일(서강대)
17:40~18:00	O-1-4. 이정규(고려대)

Symposium 3 'Permanent Magnetics' & 'Electro-Magnetic Energy Conversion' 공동세션 (에메랄드)

좌장: 이정구(KIMS)

시간	프로그램
14:00~14:20	초S-3-9. 박송이(LG전자)
14:20~14:40	초S-3-10. 김태훈(KIMS)
14:40~15:00	초S-3-11. 박지훈(KIMS)
15:00~15:10	Coffee Break

좌장: 유상임(서울대)

시간	프로그램
15:10~15:30	초S-3-12. 김태훈(전남대)
15:30~15:50	초S-3-13. 심지훈(포항공대)
15:50~16:10	초S-3-14. 이재광(부산대)
16:10~16:20	Coffee Break

좌장: 이정종(한국전자기술연구원)

시간	프로그램
16:20~16:40	초S-3-15. 이훈기(충남대)
16:40~17:00	초S-3-16. 김수민(충남대)
17:00~17:20	초S-3-17. 강동우(계명대)
17:20~17:40	초S-3-18. 이성구(동아대)

Symposium 7 'Soft Magnetics' (루비)

좌장: 임혜인(숙명여대)

시간	프로그램
14:00~14:20	초S-7-1. 강영민(한국교통대)
14:20~14:40	초S-7-2. 권영태(KIMS)
14:40~15:00	초S-7-3. 정재원(KIMS)
15:00~15:20	초S-7-4. 남충희(한남대)
15:20~15:40	초S-7-5. 이태경(㈜창성)
15:40~15:50	Coffee Break

좌장: 정재원(KIMS)

시간	프로그램
15:50~16:10	초S-7-6. 황득규(㈜현대모비스)
16:10~16:30	초S-7-7. 장민선(KIMS)
16:30~16:50	초S-7-8. 윤준철(㈜현대제철)
16:50~17:10	초S-7-9. 박언병(포항산업과학연구원)
17:10~17:30	초S-7-10. 최용석(제닉스)
17:30~17:50	초S-7-11. 김원호(가천대)

Symposium 1 'Quantum Magnetism' (사파이어)

좌장: 이성빈(KAIST)

시간	프로그램
14:30~15:00	초S-1-11. 조길영(포항공대)
15:00~15:30	초S-1-12. 김세권(KAIST)
15:30~15:45	Coffee Break
15:45~16:15	초S-1-13. 양찬호(KAIST)
16:15~16:45	초S-1-14. 옥종목(부산대)
16:45~17:15	초S-1-15. 박재훈(포항공대)

Symposium 8 'Low Dimensional Magnetics' (오팔Ⅰ)

좌장: 유정우(UNIST)

시간	프로그램
14:00~14:20	초S-8-1. 진호섭(UNIST)
14:20~14:40	초S-8-2. 김상훈(울산대)
14:40~15:00	초S-8-3. 구현철(KIST)
15:00~15:10	Coffee Break
15:10~15:30	초S-8-4. 진미진(IBS)
15:30~15:50	초S-8-5. 최태영(이화여대)
15:50~16:10	초S-8-6. 이동헌(고려대)

Session 3 구두발표Ⅲ 'Low Dimensional Magnetics' / 'Magnetic Sensors and Micro-Devices' (오팔Ⅰ)

좌장: 유정우(UNIST)

시간	프로그램
16:20~16:40	O-3-1. 이관(경성대)
16:40~17:00	O-3-2. 프롤로이 타란다스(DGIST)
17:00~17:20	O-3-3. 김은애(충남대)
17:20~17:40	O-3-4. 이용호(KRISS)

전체 일정

시간	프로그램
18:00~19:00	한국자기학회 임시총회 및 시상식 (다이아몬드)
19:00~	만찬 (그랜드볼룸)

5월 27일[금]

시간	프로그램				
8:30 ~	참가자 등록				
	Session 4 '신진과학자 콜로키움' (다이아몬드)	**Symposium 9** 'Magnetics in Medical Science' (에메랄드)	**Symposium 10** 'Bio-Convergence Magnetics' (루비)	**Symposium 1** 'Quantum Magnetism' (사파이어)	**Symposium 11** '자기이론분과 심포지움' (오팔Ⅰ)
	좌장: 김갑진(KAIST)	좌장: 안우상(울산의대)	좌장: 유천열(DGIST)	좌장: 손창희(UNIST)	좌장: 임성현(울산대)
09:00~09:20	초O-4-1. 이수범(DGIST)	초S-9-1. 한동희(강원대)	09:00~09:20 초S-10-1. 이신범(DGIST)	09:00~09:30 초S-1-16. 박제근(서울대)	09:00~09:25 초S-11-1. 김흥식(강원대)
09:20~09:40	초O-4-2. 이동준(KIST)	초S-9-2. 한기택(한국방사선흥협회)	09:20~09:40 초S-10-2. 이성원(DGIST)	09:30~10:00 2.초S-1-17. 최광용(성균관대)	09:25~09:50 초S-11-2. 이관우(고려대)
09:40~10:00	초O-4-3. 이진홍(KIST)	초S-9-3. 김호진(연세대)		10:00~10:30 초S-1-18. 이성빈(KAIST)	09:50~10:00 Coffee Break
10:00~10:20	초O-4-4. 박정민(KAIST)	초S-9-4. 박장우(한국원자력의학원)	09:40~09:50 Coffee Break		10:00~10:25 초S-11-3. 김봉재(군산대)
10:20~10:30	Coffee Break	10:20~10:40 초S-9-5. 오성훈(한빔테크놀로지)		10:30~10:45 Coffee Break	10:25~10:50 초S-11-4. 강창종(충남대)
10:30~10:50	초O-4-5. Takayuki Shiino(KAIST)	10:40~10:50 Coffee Break	09:50~10:10 초S-10-3. 오선종(한국기계연구원)		**Session 6** 구두발표Ⅴ 'Theory and Computational Magnetics' (오팔Ⅰ)
		좌장: 한만석(강원대)		10:45~11:15 초S-1-19. 김재훈(연세대)	좌장: 임성현(울산대)
10:50~11:10	초O-4-6. 서준호(IBS)	10:50~11:10 초S-9-6. 이호범(서울아산병원)			
11:10~11:30	초O-4-7. 정승교(성균관대)	11:10~11:30 초S-9-7. 장지성(서울아산병원)	10:10~10:30 초S-10-4. 이민우(DGIST)	11:15~11:45 초S-1-20. 김재욱(한국원자력연구원)	11:00~11:20 O-6-1. 브라 힘 마르 푸아(부경대)
	Session 5 구두발표Ⅳ 'Soft Magnetics' (다이아몬드)	11:30~11:50 초S-9-8. 마성룡(조선대)			
	좌장: 장민선(KIMS)				
11:40~12:00	O-5-1. 최광덕(KIST)	11:50~12:10 초S-9-9. 김상국(서울대)	10:30~10:50 초S-10-5. 유천열(DGIST)	11:45~12:15 초S-1-21. 최성균(성균관대)	11:20~11:40 O-6-2. 박민규(울산대)
12:00~12:20	O-5-2. 이민우(한국생산기술연구원)				11:40~12:00 O-6-3. 한재호(IBS)
12:30~13:00	포스터 시상식 및 폐회 (다이아몬드)				

행사장 배치도

EAST TOWER

1F

Tutorial
Symposium 2, 6
Session 2, 4, 5

다이아몬드

Symposium 3, 9

에메랄드

입구

2F

Symposium 4, 7, 10

루비　오팔 II

오팔 I　사파이어

Symposium 5, 8, 11
Session 1, 3, 6

Symposium 1

WEST TOWER

6F

그랜드볼룸

Poster Session
만찬
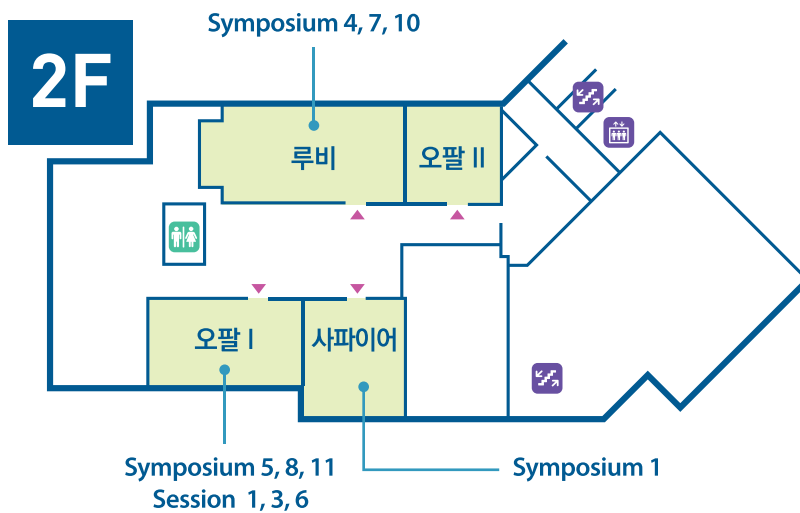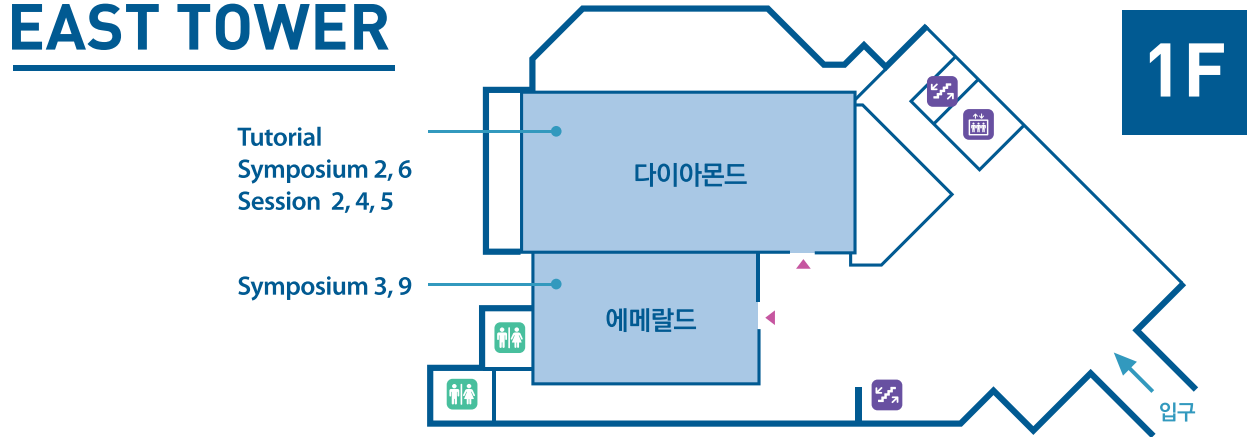
CONTENTS

5월 25일(수) 13:30~15:45
Symposium 1 'Quantum Magnetism'

사파이어

✿ 좌 장 : 문은국(KAIST)

5월 25일(수) 16:00~18:00
Tutorial Session '대학원생 진행세션'

다이아몬드

✿ 좌 장 : 성민경(숙명여대)

5월 25일(수) 13:00~18:00
Session : 포스터발표

그랜드볼룸

✿ 좌 장 : 김상훈(울산대), 박지훈(KIMS)

○ Session EM [Electro-Magnetic Energy Conversion]

○ **Session BM [Bio-Convergence Magnetics]**

○ Session MS [Magnetics in Medical Science]

○ Session MM [Mössbauer Magnetics]

○ Session SS [Spintronics]

○ Session PM [Permanent Magnetics]

○ Session SM [Soft Magnetics]

○ Session TC [Theory and Computational Magnetics]

○ Session LM [Low Dimensional Magnetics]

○ Session SD [Magnetic Sensors and Micro-Devices]

○ Session OS [Others]

5월 26일(목) 09:00~11:10
Symposium 2 'Magnetization Dynamics'

다이아몬드

❀ 좌 장 : 김준서(DGIST)

5월 26일(목) 09:00～12:10
Symposium 1 'Quantum Magnetism'
사파이어

❀ 좌 장 : 옥종목(부산대)

5월 26일(목) 09:00～10:40
Session 1 구두발표 Ⅰ 'Spintronics Ⅰ'
오팔 I

❀ 좌 장 : 박정민(KAIST)

5월 26일(목) 16:40~18:00
Session 2 구두발표 II 'Spintronics II' / 'Magnetization Dynamics'

다이아몬드

❀ 좌 장 : 최경민(성균관대)

5월 26일(목) 14:00~17:40
Symposium 3 'Permanent Magnetics' & 'Electro-Magnetic Energy Conversion' 공동세션

에메랄드

❀ 좌 장 : 이정구(KIMS) / 유상임(서울대) / 이정종(한국전자기술연구원)

5월 26일(목) 14:00~17:50
Symposium 7 'Soft Magnetics'

루비

❀ 좌 장 : 임혜인(숙명여대) / 정재원(KIMS)

5월 26일(목) 14:30~17:15
Symposium 1 'Quantum Magnetism'

사파이어

❀ 좌 장 : 이성빈(KAIST)

5월 27일(금) 09:00~12:15
Symposium 1 'Quantum Magnetism'

사파이어

�֍ 좌 장 : 손창희(UNIST)

Symposium 1

'Quantum Magnetism'

Site-selective Hund's Physics in Fe$_3$GeTe$_2$

Myung Joon Han[*]

Department of Physics, KAIST, Korea

Recently, magnetic property of van der Waals materials attracts great attention. In this talk, I will report our recent progress in understanding a metallic ferromagnet Fe$_3$GeTe$_2$. In particular, I will try to argue that this representative metallic ferromagnet can be best understood as a 'site-differentiated' Hund's metal. After briefly summarizing the material properties of Fe$_3$GeTe$_2$ and the intriguing characteristics of Hund's metals, I will present our DFT+DMFT calculation results showing that all salient features of Hund's metal physics are well identified in Fe$_3$GeTe$_2$. Furthermore, two different Fe sites in this material are clearly distinctive from the Hund's physics point of view. This newly suggested 'site-selective' Hund's picture provides the useful insight and information to understand the experiments including the ones that are seemingly controversial to each other.

Twisted Bilayer Magnetism

Kyoung-Min Kim[1], Do Hun Kim[1], Grigory Bednik[1], Myung Joon Han[2], Moon Jip Park[1*]

[1]Center of Theoretical Physics of Complex Systems, Institute for Basic Science (IBS) Daejeon 34126, Korea
[2]Department of Physics, KAIST, Daejeon 34141, Korea

Moire patterns emerging from misaligned two-dimensional materials give rise to drastic modifications in the electronic structure and correlations. In this talk, we develop a theory of twisted bilayer magnetism. Based on the first-principles calculation, we apply our theory to the van der Waals magnet, CrI3. We discover a variety of non-collinear magnetic orders that have been overlooked in the previous theoretical and experimental studies. At last, we present the comprehensive theory of the magnon excitations of the moire magnetism.

Control of Fermi Liquid, Hund metal, and Mott insulator in two-dimensional SrRuO₃ ultrathin films

Tae Won Noh[1,2*], Jeong Rae Kim[1,2], Eun Kyo Ko[1,2], Sungsoo Hahn[1,2],
Byungmin Sohn[1,2], Choong H. Kim[1,2], Changyoung Kim[1,2]

[1]Center for Correlated Electron Systems, Institute for Basic Science (IBS), Seoul 08826, Republic of Korea
[2]Department of Physics and Astronomy, Seoul National University, Seoul 08826, Republic of Korea

The electronic states of materials with partially filled d- or f-orbitals have rich and novel quantum phases due to strong correlations. To modulate such interesting physical properties, oxide heterostructure engineering can be a powerful method. Yet, despite extensive studies, obtaining direct information on their momentum-resolved electronic structure remains a great challenge. Here, we utilized atomic-scale epitaxy and angle-resolved photoemission spectroscopy (ARPES) to demonstrate the control of correlated electronic phases in two-dimensional (2D) SrRuO₃ ultrathin films. By growing SrRuO₃ ultrathin films with control of octahedral symmetry and epitaxial strain, we realized three distinct correlated phases in the quantum-confined limit: Fermi liquid, Hund metal, and Mott insulator phases. While structural symmetry changes induced bandwidth control, epitaxial strain varied the numbers of involved orbitals and electrons. In addition, we performed spin-resolved ARPES (SARPES) experiments to investigate the relationship between electronic structures and ferromagnetism in SrRuO₃ thin films. We found that SRO possesses spin-dependent electron correlations in which majority and minority spins are localized and itinerant, respectively. Our study shows that our experimental methods can be useful for exploring the correlated physics, particularly in two dimensions.
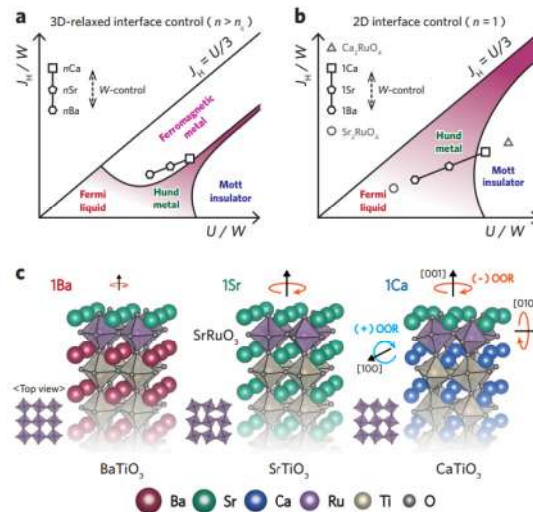
Fig. 1. Interface control of correlated electronic phases in epitaxial SrRuO₃ heterostructures. **a,b,** Schematic of the electronic phase diagram of thick (**a**) and monolayer (**b**) SrRuO₃ films, wherein the bandwidth varies. **c,** Schematic illustrations of the atomic configuration of the monolayer SROs interfaced with ATiO₃ (A = Ba, Sr, and Ca). The out-of-plane-oriented oxygen octahedral rotation for Ba (Sr) is small (large). Ca has both in-plane-oriented and out-of-plane-oriented OOR.

Ferromagnetism in Strained Epitaxial LaCoO₃

Sangmoon Yoon[*]

Department of Physics, Gachon University, Seongnam, Korea

Ferromagnetism in strained LaCoO₃ (LCO) thin films has been an intriguing scientific subject for the last decade. While the bulk LCO is non-magnetic, strained LCO thin films exhibit robust ferromagnetism with a phase transition temperature (T_c) of 80 K. Since this system is a representative example where epitaxial strain induces non-bulk magnetic properties, it has drawn lots of attention in the field of oxide thin films.

Despite extensive research over the past decade, the consensus on the origin of ferromagnetism has not yet to be achieved. A main challenge of this system is a complex microstructure inside the film; the existence of planar defects (seen as dark stripes in high-angle annular dark field scanning transmission electron microscopy (HAADF STEM) images), their association with oxygen vacancies, the correlations between dark stripes and ferromagnetism have been important issues. The quantitative analyses of HAADF STEM images firstly identified that the two independent phases coexist in LCO thin films. Through this analyses, we further found that the compressed units within twin-wall superlattice phase lead the rocksalt-type high-spin/low-spin order, which is consistent with recent experimental and theoretical results. The local atomistic origin accounts for the unusual magnetic properties of strained LCO within the unified picture.

Reference

[1] S. Yoon et al. Nano Lett. 21, 4006 (2021).

Tutorial Session

'대학원생 진행세션'
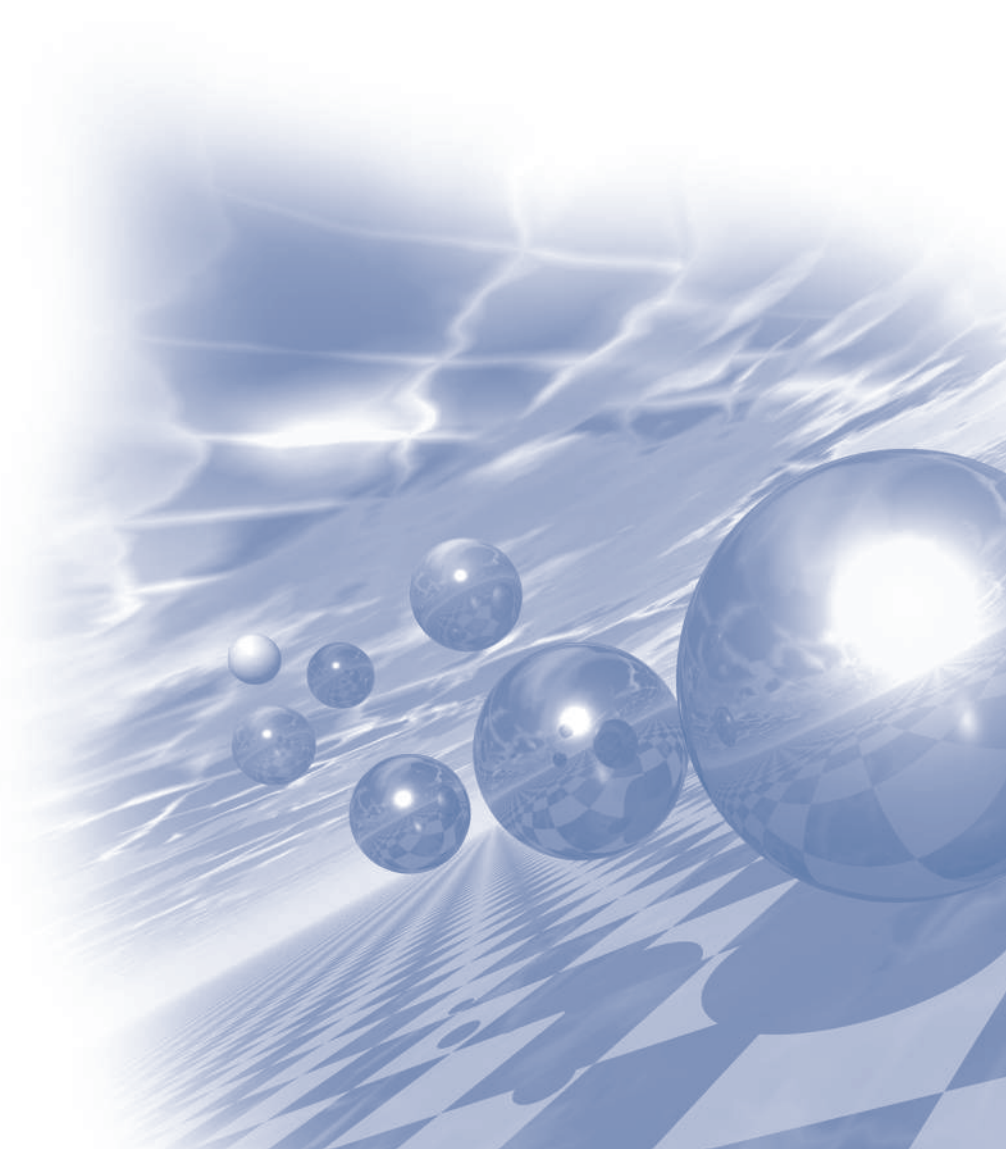
실전 영어과학논문 작성법

김영근[*]

고려대학교 공과대학 신소재공학부

과학논문은 연구자의 성과를 표현하는 대표적인 결과물이다. 특히 과학기술 분야에서 국제적으로 인정받기 위해서는 올바른 영어논문 원고의 작성이 필수적이다. 물론 훌륭한 연구결과를 토대로 논문을 작성해야 하겠지만, 상위 저널에 도전하기 위해서는 부가적으로 설득력 있게 주장을 펼치는 방법이 필요하다. 이번 튜토리얼에서는 영어과학논문을 작성하는 것에 관련하여, 논문의 개념, 기본 골자, 구성방법 등에 관해 소개하고자 한다. 특히 실제 사례들과 현대 영어표현 방법들에 관해 설명할 예정이다. 그밖에 표절, 중복게재 방지에 관해서 논의하고자 한다.

포스터발표
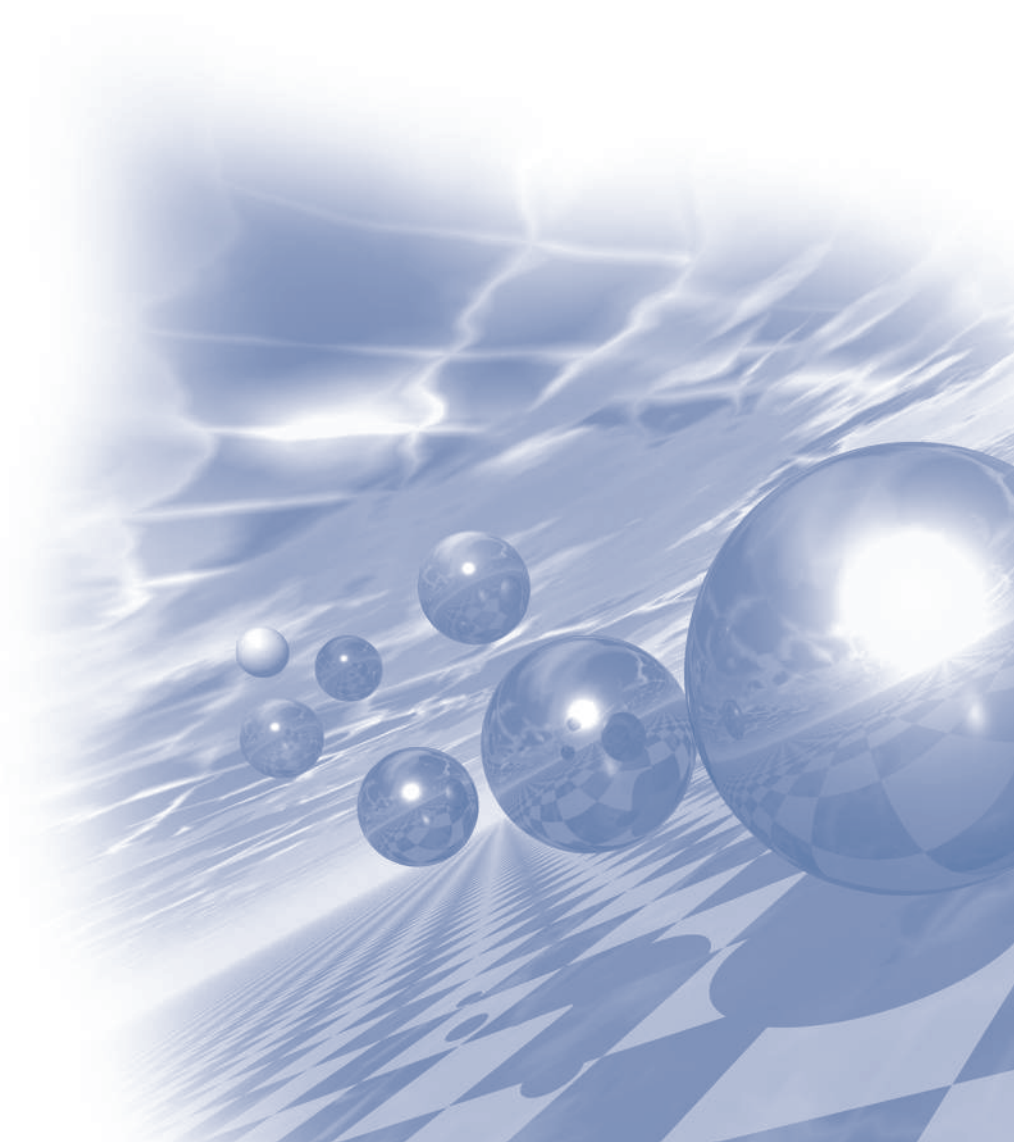
A study on Radial Magnetic Bearing of a new stator shape for high manufacturability and reduction of core loss and weight

Si-Woo Song[2*], Dong-Ho Kim[2], In-Jun Yang[2], Do-Hyeon Choi[1], Won-Ho Kim[1]

[1]Department of Electrical Engineering, Hanyang University, Seoul, Korea
[2]Department of Electrical Engineering, Gachon University, Seongnam, Korea

As the system is being digitalized in various industrial fields, the technical demands for high speed, light weight, high output and efficiency of motors are required. Permanent magnet motors are considered a key element to meet the technological needs for high-speed operation. For high-speed operation of motors, not only electromagnetic design technology but also mechanical and structural stability are important factors. Therefore, a lot of research on bearings is being conducted to reduce friction in the mechanical part and increase efficiency and stability. Bearings widely used in high-speed motors require characteristics such as precision, high-speed, minimum displacement and low friction. There are mainly two types of bearings that satisfy these characteristics: rolling bearing and magnetic bearing. In rolling bearing, it is possible to reduce frictional resistance because the rolling element contacts on a dot or line between the shaft and the bearing. However, since rolling bearing requires a lubrication system and contact, mechanical friction loss cannot be significantly reduced and maintenance costs are incurred. Also, there is a limit to the rotation speed because it is a contact-type bearin. on the other hand, MAGNETIC bearing (MB) possesses many advantages against the conventional mechanical bearing, such as no lubrication requirement, negligible friction loss, less maintenance, and extending a limit of rotational speed [1]. These advantages make the MB popular in industrial applications such as turbo compressor, vacuum technology, flywheel technology. Despite these advantages, there are many difficulties in commercialization. This is because the costs are high, and it is difficult in control and miniaturization. High-speed motors are advantageous for miniaturization, but for magnetic bearing, it is difficult to design them in a small size. Therefore, in this paper, we propose a new magnetic bearing structure that can be miniaturized and light-weighted by using a stator in the separate tooth structure[2]. The magnetic bearing of the separated teeth structure proposed in this paper will be referred to as STMB (Separated Teeth Magnetic Bearing). While dividing the teeth, a part that was not in the existing stator is created, which will be referred to as Lips. STMB reduced the weight by dividing the teeth of the stator that accounts for large proportion of the weight, and removing back yoke. The STMB creation process and main variables are shown in fig. shown in 1. STBM is a 4-module type, and there is no restriction on winding coils, so it is possible to secure a high fill factor and is easy to manufacture. That is, it is advantageous for miniaturization and weight reduction. However, in STMB, large leakage flux occurs between modules and the effective airgap area is small, so it is difficult to generate high force. Therefore, this paper proposes a hybrid STMB that can reduce magnetic leakage flux by inserting a magnet into the Lips airgap, increase the force by increasing the effective airgap area, and further increase the force through the bias magnetic flux.
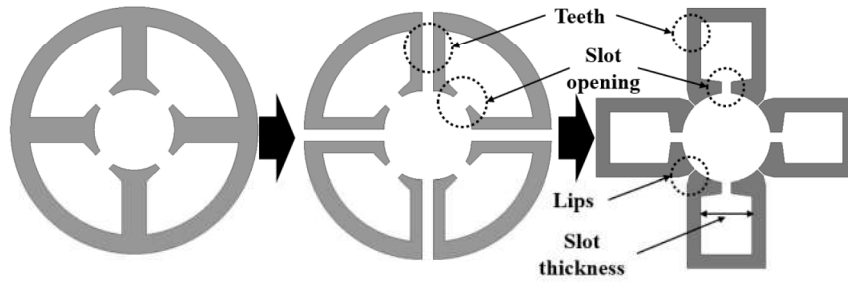
Fig. 1 STBM creation process

References

[1] S. Yang, "Electromagnetic actuator implementation and control for resonance vibration reduction in miniature magnetically levitated rotating machines," IEEE Trans. Ind. Electron., vol. 58, no. 2, pp. 611-617, Feb.2011.

[2] S. -W. Song, I. -J. Yang, S. -H. Lee, D. -H. Kim, K. S. Kim and W. -H. Kim, "A Study on New High Speed Motor That Has Stator Decreased in Weight and Coreloss," in IEEE Transactions on Magnetics, vol. 57, no. 2, pp. 1-5, Feb. 2021, Art no. 8201105, doi: 10.1109/TMAG.2020.3012482.

Spoke type Permanent Magnet Synchronous Generator Design considering Magnetizing and Cogging Torque

Dong-Ho Kim[1*], In-Jun Yang[1], Si-Woo Song[1], Na-Young Kang[2], Won-Ho Kim[2]

[1]Department of Electrical Engineering, University of Hanyang, Korea
[2]Department of Electrical Engineering, University of Gachon, Korea

Recently, wind energy has been widely used because it is eco-friendly and economical among energy sources. Various generators such as reluctance generators, induction generators, and permanent magnet synchronous generators (PMSGs) are used in wind power generation systems. A permanent magnet generator uses a rare earth or ferrite permanent magnet, and the rare earth magnet has a high residual magnetic flux density and coercive force. However, the price has risen a lot recently and the supply and demand is unstable. On the other hand, ferrite magnets are inexpensive and supply stable. However, since it has low permanent magnet performance, the spoke type was developed to maximize performance. The spoke type permanent magnet synchronous generator is difficult to magnetize compared to other rotor structures because the permanent magnets are vertically inserted. Magnetization performance is an important factor directly related to mass productivity, permanent magnet demagnetization, and load performance, so it must be considered when designing a spoke type wind turbine. Another important performance factor for wind turbines is the cogging torque, which affects the starting performance. This is because the low cogging torque allows the generator to run easily even in low winds.

Therefore, in this paper, we propose a spoke-type PMSG rotor shape design considering magnetization and cogging torque. First, the magnetization principle and factors affecting the magnetization performance are analyzed. The advantages and disadvantages of each magnetization method were compared, and factors that made magnetization difficult during magnetization were analyzed. Based on this, a rotor shape with a trapezoidal permanent magnet with improved magnetization performance was designed. And to improve the maneuverability, a rotor design was carried out to reduce the cogging torque. Conventional rotor methods to reduce cogging torque include core tapering and skew. The characteristics and advantages and disadvantages of each method were compared. To reduce cogging torque considering mass productivity, a design in which the rotor barrier is applied asymmetrically in the axial direction was proposed. Cogging torque was reduced through an effect similar to skew, and the performance was compared with the existing spoke type. A model with improved magnetization and cogging torque performance was finally proposed, and the performance validity of the final model was verified through FEA (Finite Element Analysis) and tests.

Permanent magnet synchronous motor considering cryogenic motor design Research on Optimization Characteristics

Dong-Wook Kim[1*], Dong-Ho Kim[2], Na-Young Kang[1], Min-Soo Yoon[1], Won-Ho Kim[1]

[1]Department of Electrical Engineering, Gachon University, Korea
[2]Department of Electrical Engineering, Hanyang University, Korea

Based on the performance of a conventional induction motor for Submersible LNG Pump driven in a cryogenic environment, the magnetic characteristics of the permanent magnet are analyzed and the efficiency can be maximized in a cryogenic environment by using a finite element analysis method. Torque and efficiency analysis at rated operation were conducted through loss separation and stator current density review of the existing 15 kW induction motor. Although the ratio of copper loss is the highest among the total losses of the existing induction motor, it has an advantage of being able to take a high current density due to excellent cooling performance due to the cryogenic environment characteristics. By replacing the existing induction motor with a permanent magnet synchronous motor, copper loss can be reduced compared to induction motor, and it can be designed for miniaturization of motor and high speed. A final model of a permanent magnet synchronous motor for Submersible LNG Pump operating at -200°C is designed and analyzed by performance analysis corresponding to the rotor shape (IPMSM: Interior Permanent Magnet Synchronous Motor and SPMSM: Surface-mounted Permanent Magnet Synchronous Motor) and the number of stator slots(12slots and 24slots) of a permanent magnet synchronous machine using an FEM electronic simulation tool.
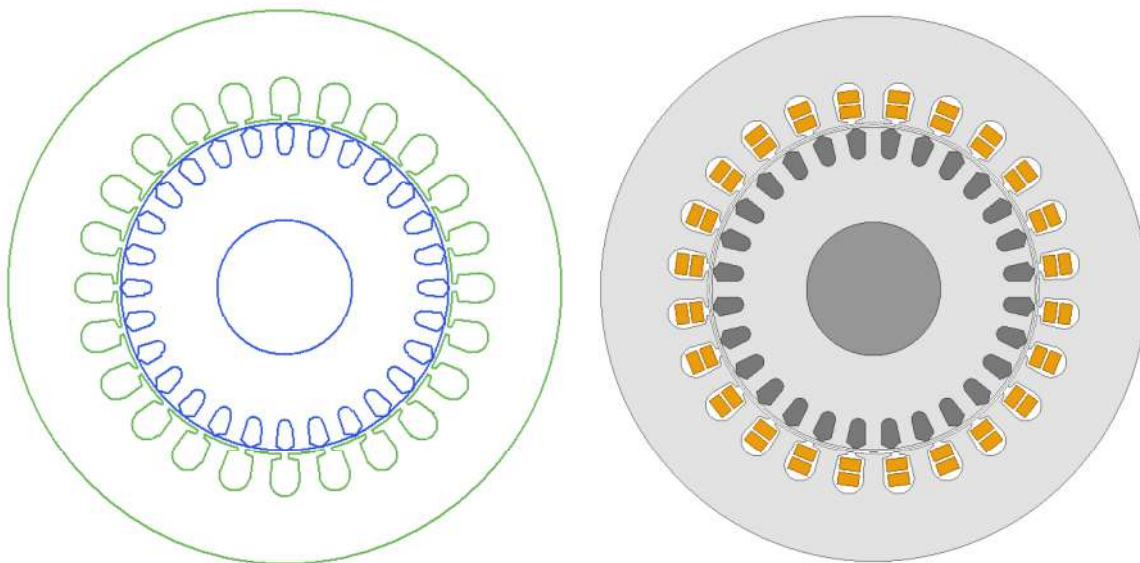
Fig 1. Conventional induction motors shape

A Study on Performance Improvement through Axial Force Reduction of Double-Layer Spoke-type PMSM with Core Skew Structure

Dong-Woo Nam*, Min-Jae Jeong, Seung-Heon Lee, Na-Rim Jo, Won-Ho Kim

Department of Electrical Engineering, Gachon University, Seongnam 13120, Korea

Recently, the development of ferrite magnetic flux concentration type electric motors has been developed due to the limited resource of rare earth permanent magnet. Especially, a type of spoke type permanent magnet synchronous motor (PMSM) using ferrite permanent magnet had a great influence on the industry. However, in the case of the spoke type motor, there was a disadvantage that the reluctance torque could not be used significantly. The double-layer spoke type PMSM is designed to complement this.

This Double-Layer Spoke type PMSM can concentrate magnetic flux using a ferrite permanent magnet instead of a rare earth type permanent magnet similar to an conventional spoke type motor. In addition, the conventional spoke type permanent magnet motor did not utilize the reluctance torque properly because the d-axis and q-axis magnetoresistance were not large, but the Double-Layer Spoke type PMSM divides each permanent magnet into two. By inserting an iron core to reduce the q-axis magnetoresistance, the difference with the d-axis magnetoresistance is increased, and a high reluctance torque can be used.

However, as the magnetoresistance difference between the d-axis and the q-axis increases, factors, such as cogging torque and torque ripple, increase, which adversely affects the operation of the motor. This will soon cause performance degradation, such as vibration, noise, and poor position and speed control. In order to compensate for this, in general, the method of applying a skew structure is most widely used, but it is also difficult to manufacture and sometimes increases the torque ripple, so it is not a good solution.

Therefore, in [1], a study was conducted to improve manufacturability by applying core skew and to reduce cogging torque and torque ripple. In this paper, it was confirmed that the cogging torque, torque ripple in the
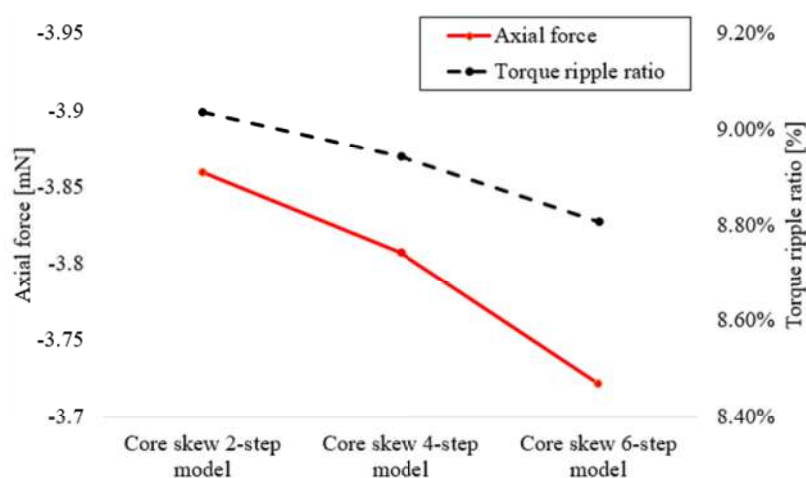
Fig. 1. Comparison of torque ripple and axial force according to the number of steps.

high-speed operation area, and no-load THD were significantly reduced. However, it was confirmed that this core skew also increases the torque ripple in the low-speed operation area. There are many factors that affect the torque ripple, but as shown in Fig. 1, it can be confirmed that the axial force has some effect on the torque ripple. In addition, the axial force continuously transmits a mechanical load to the bearing connected to the motor, causing vibration and noise, and shortening the life of the motor. Since the target model of this paper uses sensorless control, the torque ripple that affects the back electromotive force used for detection must be reduced.

Reference

[1] D. -W. Nam, K. -B. Lee, and W. -H. Kim, "A study on core skew considering manufacturability of double-layer spoke-type PMSM," *Energies 2021,* 14, 610, Jan. 2021.

A Study on the Shape of Magnetizing Yoke to Reduce the Dead Zone of a Ring Magnet

Jeong-Yeon Min[*], Dong-Woo Nam, Min-Ki Hong, Na-Rim Jo, Won-Ho Kim

Department of Electrical Engineering, Gachon University, Korea

Recently, applications of motors and generators such as transportation, home appliances, industry, IT&robot are expanding. Accordingly, the demand for a sensor for detecting the position of the rotor is also increasing because the inverter driving the PM motor performs control based on the position of the rotor. Among the sensors that detect the position of the rotor, the Hall effect sensor is used to detect magnetic field by making use of the Hall effect on the semiconductor material.

The hall sensor that detects the position of the motor rotor is also applied to the window regulator in automobile parts. a safety window motor has been used to prevent an accident of being caught in a vehicle window. It works on the principle that a ring bonded magnet is attached to the bottom of the rotor of the motor and the hall sensor detects changes in the magnetic flux to detect the position. At this time, the magnetic flux between the N and S poles of the magnet is very weak, so a dead zone occurs in which the hall sensor cannot detect the magnetic flux as shown in Fig. 1. If the angle of the dead zone of the ring magnet is large, it means that the Hall sensor cannot detect the magnetic flux at that angle.

In this study, the shape of polar anisotropic magnetizer with a magnetic flux concentration structure is proposed to reduce the range of the dead zone. The results were analyzed through finite element analysis and the final model was selected by analyzing the inner and outer teeth thickness of the teeth of the magnetizer as design variables. A comparison of the magnitude of the magnetic flux density of the proposed model and the conventional model is shown in Fig. 2. The prototype of the final model was manufactured, and the validity of the analysis result was verified.
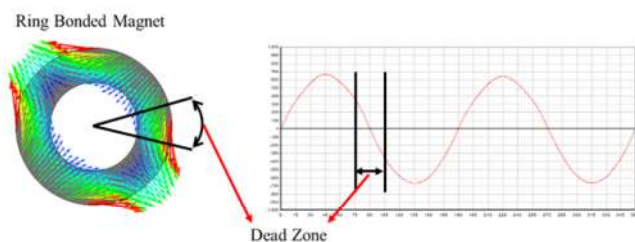
Fig. 1. Dead zone of ring bonded magnet
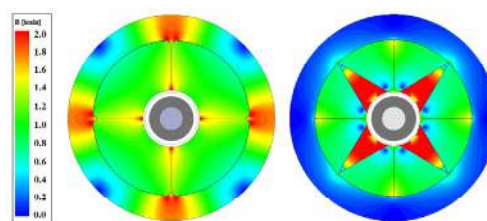
Fig. 2. Comparison of the magnetic flux density

Keywords: Magnetization, Magnetic sensors, Magnetic Materials, Hall effect, Magnetizer, Dead zone

A Study on Combination of Number of Poles and Slots for Uniform Control of Magnetic Bearings

Min-Ki Hong[1*], In-Jun Yang[2], Jeong-Yeon Min[1], Won-Ho Kim[1], Dong-Hoon Jung[3]

[1]Department of Electrical Engineering, Gachon University, Korea
[2]Department of Electrical Engineering, Hanyang University, Korea
[3]Smart Mobility Engineering, Halla University, Korea

When a motor with magnetic bearings is used, compared to the ball bearing combined structure, frictional resistance is greatly reduced, which has the advantage of high speed and can also reduce maintenance costs. However, since the magnetic bearing combined motor currently used in industry has a structure in which the shaft is magnetically levitated from the outside of the rotor, the size becomes very large compared to the ball bearing combined motor structure. As an alternative to this, by designing an integrated motor to which the halva arrangement is applied as shown in Fig. 1, the space inside the rotor can be secured as a space for inserting the bearing. In this case, since the bearing is present inside the motor, the bearing magnetic flux is affected by the rotating magnetic field of the stator. In the case of 16 poles 24 Slots (Shown in Fig. 3) Uniform control by bearing can be applied. However, In a specific combination of number of poles and slots like 6 poles 9 slots (shown Fig. 2), the windings of each bearing phase appear asymmetrically, indicating that the stator rotating magnetic field for each bearing phase is non-uniform and causing an imbalance in the bearing force for each phase. Which means, If the winding method of the stator is different for each bearing phase, even if the same current is applied, there is a difference in the displacement of the controlled rotor for each bearing phase. In this paper, the formula for the number of stator teeth and the number of bearing teeth to eliminate force asymmetry is presented for more linear control, and the corresponding formulas are verified by comparative analysis of force waveforms for each axis.
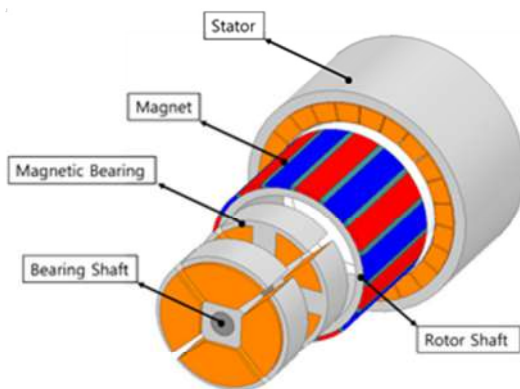
Fig. 1. Integrated magnetic bearing motor   Fig. 2. 6Poles 9Slots   Fig. 3. 16Poles 24Slots
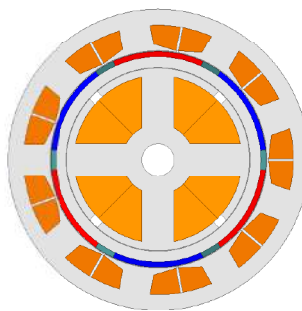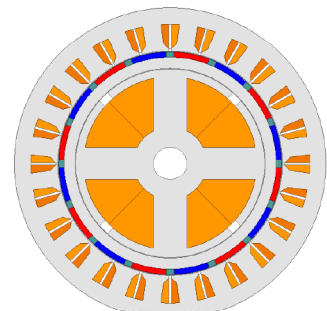
트랙션용 PMa-SynRM의 영구자석 Barrier-ends 비대칭 구조에 따른 토크 리플 개선 설계에 대한 연구

박승우*, 문주형, 권용재, 강동우

Department of Electrical Energy Engineering, Keimyung University, Daegu 42601, South Korea

최근 희토류 저감에 대한 학계 연구가 활발히 진행중이며, 전기자동차 구동용 모터 설계기술 중 영구자석 보조형 동기 릴럭턴스 동기전동기(PMa-SynRM)에 많은 관심을 보이고 있다. PMa-SynRM은 기존의 매입형 영구자석 동기전동기(IPMSM)에 주로 사용된 Nd-Fe-B 희토류 자석 대비 낮은 등급 자석인 Ferrite 자석을 사용하거나, 자석사용량을 저감하여 제작되므로 원가절감에 유리하며, 영구자석에 의한 마그네틱 토크와 돌극비에 의한 릴럭턴스 토크를 동시에 발생시키므로 기존 IPMSM 보다 높은 출력밀도를 가질 수 있다는 장점이 있다. 하지만 높은 돌극비로 인해 토크 리플의 수치가 높은 단점이 존재하며, 토크리플은 모터의 진동과 소음을 발생시키고 이에 따라 안정성 및 성능을 저하시키에 설계과정에서 토크 리플을 줄이는 노력이 필요하다. 본 논문에서 유한요소해석 법을 이용하여 PMa-SynRM의 토크 리플 발생에 대한 문제점을 보완하기 위해 barrier-ends 각도를 비대칭 구조로 설계 후 barrier-ends 각도가 대칭인 모델과 비교하여 토크 리플 개선에 효과적인 barrier-ends의 형상을 설계하는 연구에 대해서 진행하고자 한다.
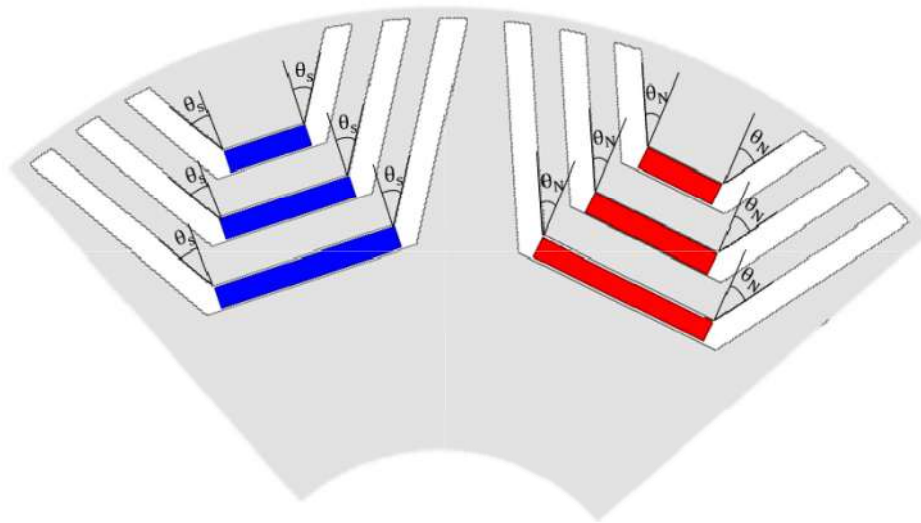
Fig. 1. 회전자 End-barriers 각노

소형 고속 모터의 비출력 및 철손 개선을 위한 코어리스 구조 연구

김현준[*], 문주형, 박범도, 강동우

Department of Electrical Energy Engineering, Keimyung University, Daegu 42601, South Korea

최근 배터리 및 연료전지의 발전으로 인해 기존 모터의 중저속 구동과 더불어 고속 운전용 구동 모터의 수요가 증가하고 있다. 특히 Air Blower Motor와 같은 고속 운전을 필요하는 BLDC(Brushless Direct Current) 고속 운전용 모터의 개발이 더욱 중요해지고 있다. 하지만 고속 운전용 구동 모터는 운전속도에 비례하여 증가하는 철손으로 인해 고정자 발열 및 효율 저하 등의 문제점이 발생할 수 있다. 이러한 특성을 개선하고자 본 논문에서는 고속 운전으로 운용되는 소형 모터의 철손을 저감하기 위하여 코어의 부피를 줄일 수 있는 코어리스(Coreless) 모터를 적용할 것이다. 또한 슬롯리스 모터는 고정자의 코어가 존재하지 않으므로 낮은 와전류 손실과 코깅토크, 토크리플을 가질 수 있으며, 진동과 소음 최소화가 중요한 고속기의 특성을 고려하여 회전자를 SPM(Surface Permanent Magnet) 타입으로 설계하고자 한다. 하지만 SPM 타입의 회전자는 고속운전시 영구자석의 비산 문제 해결이 필수적이며, 비산을 방지하기 위한 비산방지 캡을 적용하는 기술이 대표적이다. 하지만 비산방지 캡에 사용되는 재질의 도전성에 의한 와전류 손실이 발생하게 되며 이는 모터 효율 저하와 발열의 문제로 이어진다. 따라서 비산방지 캡 구조를 대체하기 위해 회전자 코어 구조를 통해 비산문제를 해결하는 방안을 제안하고 최적화하고자 한다. 본 논문에서는 ANSYS Electronics Desktop 2019 R3을 사용하여 슬롯리스 모델을 설계하고 특성을 분석하고 검증하고자 한다.
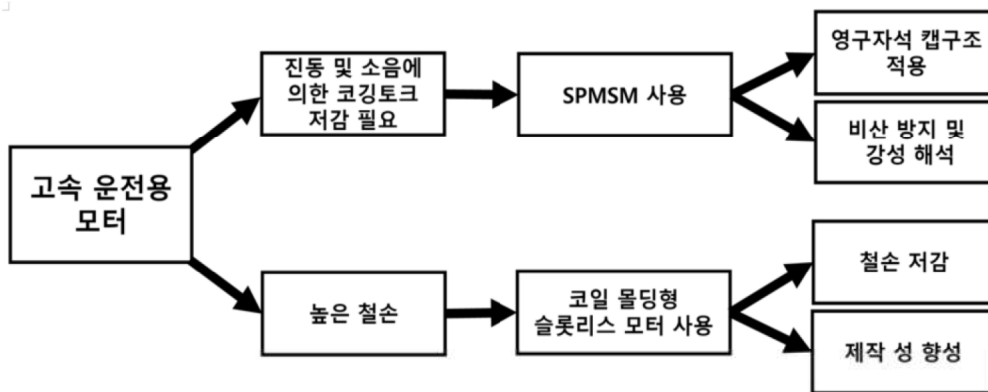
Fig. 1. 고속 구동용 모터 성능 개선 및 제작성 개선 연구 블록도

Axial Flux Motor shape study for co-robot through optimal design

Hyun-Jo Pyo[*], Seo-Hee Yang, Jeong-Yeon Min, Min-Su Yoo Yun, Won-Ho Kim

Department of Electrical Engineering, Gachon University, Seongnam 13120, Korea

The robot market is expanding as new technologies of the 4th industrial revolution are combined with robots. The robot industry is largely classified into industrial robots and professional service robots. The industrial robot market is developing a lot. Among them, co-robot is a new variable in the industrial robot market. Co-robot is smaller and lighter than existing industrial robots. The electric motor, one of the core parts of the co-robot, is closely related to speed, repeatability, range of motion, and maximum torque, which are the figures of merit representing the robot's locomotion ability. Therefore, electric motors used in robot joints require miniaturization, high torque, and high control performance. Surface-mounted permanent magnet synchronous motor (SPMSM) is widely used among radial flux permanent magnet (RFPM) motors with high power density and precision to satisfy the required characteristics of motors for robot joints. In this paper, an axial flux permanent magnet synchronous motor (AFPMSM) with better performance compared to RFPM was used to apply a structure advantageous to small motors. In this paper, the dual rotor type AFPMSM was optimally designed to maximize the performance among the AFPMSM models through Figure 1 design process. The design variables are shown in Figure 2. The design of the 500W class co-robot motor was carried out by selecting the optimal design parameters.
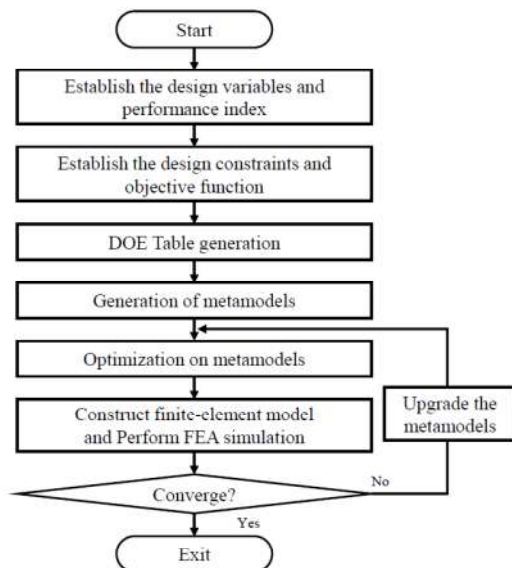
Fig. 1. Optimization Model Process Algorithm Fig. 2. Dual Rotor type AFPMSM design parameters
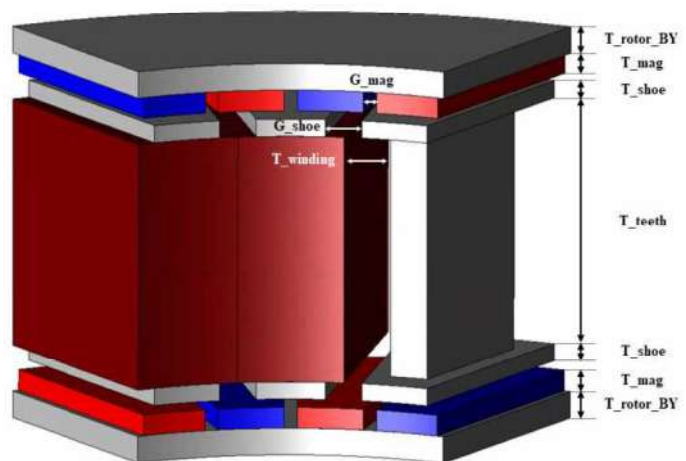
All-in-One Magnetic Bearing in Permanent Magnet Synchronous Motor by Halbach Array

In-Jun Yang[1], Dong-Ho Kim[1], Si-Woo Song[1], Ye-Seo Lee[2], Won-Ho Kim[2], Dong-Hoon Jung[3*]

[1]Department of Electrical Engineering, Hanyang University, Seoul, Korea
[2]Department of Electrical Engineering, Gachon University, Seongnam, Korea
[3]Department of Smart Mobility, Halla University, Wonju, Korea

As the electronic system progresses in various industrial fields, the technical requirements for electric motors have been advanced. Because high-speed motor means miniaturization and high power density of the motor, ultra-high-speed permanent magnet motors are considered as a key factor to meet the evolving technological needs. In order to achieve high speed of the motor, it is important to secure structural stability as well as electromagnetic design technology. Therefore, research on bearings has been actively conducted to reduce friction in the mechanical part and increase efficiency.

High-speed bearings require characteristics such as high precision, high-speed capability, minimum displacement, low friction. Rolling bearings and magnetic bearings are widely used for high-speed bearings. The rolling bearing contains a rolling element between the shaft and the bearing, so it is possible to reduce the frictional resistance because the rolling element makes point contact or line contact. Because rolling bearings require a lubrication system and are contact-type, mechanical loss cannot be completely eliminated, and bearing abrasion and maintenance costs occur. Magnetic bearings are non-contact bearings using the principle of magnetic levitation, and since there is no friction and abrasion, the disadvantages of rolling bearings can be supplemented. Thanks to the advantages of non-contact, magnetic bearings can operate at much higher speeds compared to rolling bearings and increase the life of the motor. In addition, there is an advantage that the precision and static stiffness of the rotating shaft can be increased through electrical control [1].

Despite the advantages of magnetic bearings, there are many difficulties in commercializing magnetic bearings. Increase of size is the biggest difficulty in the use of magnetic bearings. If the motor design includes the existing magnetic bearing, the magnetic bearing is a separate structure that controls the shaft from the outside of the rotor outside the motor, which dramatically increases the size of the motor. As the size of the motor increases, there are problems with mechanical limitations and manufacturing costs, so it is possible to use magnetic bearings commercially in limited industrial fields.

In this paper, through the halbach arrangement, an all-in-one magnetic bearing that is controlled from the inside of the rotor rather than a separate structure in which the magnetic bearing is controlled from the outside of the shaft is proposed. The halbach arrangement is a structure in which permanent magnets with different magnetization directions are combined, and it is possible to remove the magnetic field on one side. In this study, a halbach arrangement is applied to the rotor to remove the magnetic flux of the back yoke. When the magnetic flux of the back yoke is removed, the magnetic saturation of the shaft decreases. Therefore, it is possible to replace the back yoke with a thin hallow shaft without the need to make the back yoke thick, and the hallow shaft can simultaneously perform the roles of the back yoke and the shaft of the permanent magnet. It is possible to insert a magnetic bearing by securing maximum space inside the rotor through a thin hallow shaft. All-in-one

magnetic bearing does not need to include a bearing structure outside the rotor, so it is possible to downsize the entire system. Table I shows the characteristics of conventional ball bearings, separate magnetic bearings, and all-in-one magnetic bearings.

When designing an all-in-one magnetic bearing, since the magnetic bearing is located inside the permanent magnet and the stator, it is important to design so that the magnetic fields of the rotor and stator do not affect the magnetic field of the magnetic bearing as much as possible. When the magnetic field of the bearing is combined with the magnetic field of the rotor and the stator in the shaft, the magnetic saturation in the hallow shaft continues to change and the magnetic resistance changes, resulting in a ripple in the bearing force. To prevent this, in this study, a new rotor configuration of a three-stage shaft including a non-magnetic material is proposed. The non-magnetic shaft located in the middle of the 3-stage shaft serves to separate the magnetic field of the permanent magnet and the stator from the magnetic field of the bearing. Except for the non-magnetic shaft, the other two-stage shafts are located on the magnetic bearing and permanent magnet sides, respectively, and serve as a back yoke for the bearing and the rotor.

The analysis model was selected as a 16-pole 24-slot surface permanent magnet synchronous motor (SPMSM). The main target specifications include the magnitude and ripple of the torque, and the magnitude and ripple of the bearing force. Since the bearing force and torque have a trade-off relationship, it is important to design so that torque and bearing force are maximized and each ripple is minimized. Through finite element analysis (FEA), the analysis model was designed according to the variables of the rotor and bearings.
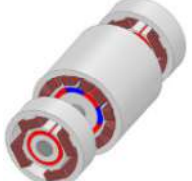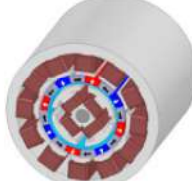
Parameter	Model		
	Ball bearing	*Separate magnetic bearing*	*All-in-one magnetic bearing*
Shape			
Size	Middle	High	Low
Weight	Middle	High	Low
Life	Low	High	High

Fig. 1. Comparison of characteristics with bearing

Reference

[1] Y. Le, J. Sun, &B. Han, "Modeling and Design of 3-DOF Magnetic Bearing for High-Speed Motor Including Eddy-Current Effects and Leakage Effects," *IEEE Trans on Ind. Electron.*, vol. 63, no. 6, pp. 3656–3665, Jun. 2016.

A Study on Improving Post-assembly Magnetization Performance of Spoke-type Permanent Magnet Synchronous Motor

Min-Jae Jeong, Hyun-Jo Pyo, Min-Ki Hong, Seung-Heon Lee, Won-Ho Kim[*]

Department of Electrical Engineering, Gachon University, Korea

In the process of manufacturing a permanent magnet motor, magnetization of a permanent magnet is essential. Permanent magnet magnetization methods include single product magnetization and post-assembly magnetization. single product magnetization is a method of magnetizing individual or multiple magnets, and since a magnetizing magnetic field is directly applied to the magnet, complete magnetization is possible. However, in this method, not only is it difficult to assemble in the rotor due to the attraction force of the magnet, but also the iron powder is attached to the magnet, creating a tolerance. Therefore, the single product magnetization method is not suitable for mass production. And the problems of single product magnetization described above, a method of magnetizing after assembling a permanent magnet to a rotor is widely used. The post-assembly magnetization method is a method of applying a magnetized magnetic field after inserting an unmagnetized magnet into the rotor. Since an unmagnetized magnet is inserted into the rotor before magnetization, there are no difficulties and tolerances in assembly due to attraction force. Therefore, many magnetization companies currently use the magnetization method after assembly. However, the above method is difficult to apply to all permanent magnet motors. For example, in the case of a surface-mounted Permanent Magnet Synchronous Motor (SPMSM), a permanent magnet is attached to the surface of the rotor, so that it can receive a magnetic field completely. However, in the case of spoke-type PMSM, the permanent magnets are arranged in the radial direction in the rotor, so the magnetic field is divided in half and flows during magnetization. That is, only half of the magnetizing magnetic field is applied to the permanent magnet, so the magnetization performance is greatly degraded. Also, during magnetization, the magnetic flux does not reach the permanent magnet located inside the rotor due to magnetic saturation of the pole piece of the rotor (the part of the rotor between the magnet and the magnet). Spoke types are motors that are in the spotlight as motors that use non-rare earth to generate high magnetic energy. However, because of a fact that it is not fully magnetized during magnetization, there are restrictions on its use, so research is needed to solve this. Therefore, in this paper, a study was conducted on magnetization method to improve the magnetization performance of the spoke type motor.

전기자동차 공조용 전동식 컴프레서 모터의
다층 헤어핀 권선 적합성에 대한 연구

오원석[*], 문주형, 강동[1]

Department of Electrical Energy Engineering, Keimyung University, Daegu 42601, South Korea

전기자동차 시장의 확장으로 전장 부품의 전동화가 진행 중이며 구동용 모터를 비롯하여 컴프레서 모터의 경우 고출력, 고효율화를 위한 연구가 진행 중에 있다. 본 논문에서는 기존의 환형 권선으로 제작되고 있는 전동식 컴프레서의 고출력, 고효율화를 위하여 고점적 권선 기술인 헤어핀 권선에 대해 8 layer가 아닌 10 layer 권선 모터에 대해서 설계하고 적합성에 대해서 고찰하고자 한다. 따라서 기존에 설계된 8극 12슬롯 치집중권 환형 권선 모델과 소음 진동을 개선에 유리한 8극 36슬롯 분포권 환형 권선 모델을 고출력 및 고효율화하기 위해서 헤어핀 권선 구조를 적용하여 설계하고자 한다. 헤어핀 권선 구조는 코어와 열을 교환할 수 있는 적이 넓기 때문에 구동온도 개선에 유리하며 이는 전류밀도를 크게 개선시킬 수 있으므로 모터의 고출력화 및 고효율화에 유리하다. 하지만 현재 제작되어 판매되고 있는 차량용 모터의 권선 layer 수는 8 layer로 출력에 직접적인 영향을 주는 권선수를 증가시킬 필요가 있으나 헤어핀 권선의 절연막 손상 등의 이유로 다층화가 어렵다. 따라서 헤어핀 권선을 적용하기 위해 고정자 슬롯에 대한 재설계를 진행하고 기존 8 laycr 이상 즉, 10 laycr이상의 권선을 적용하여 고출력화 및 고효율화를 목표로 개선 설계하고자 한다. 마지막으로 본 논문에서는 FEA(Finite Element Analysis) tool을 사용하여 설계 모델의 타당성을 검증하고, 기존 8극 12슬롯 치집중권 모델과 8극 36슬롯 분포권 모델 및 헤어핀 분포권 모델에 대한 비교를 통해 적합한 모델을 제안하고자 한다.
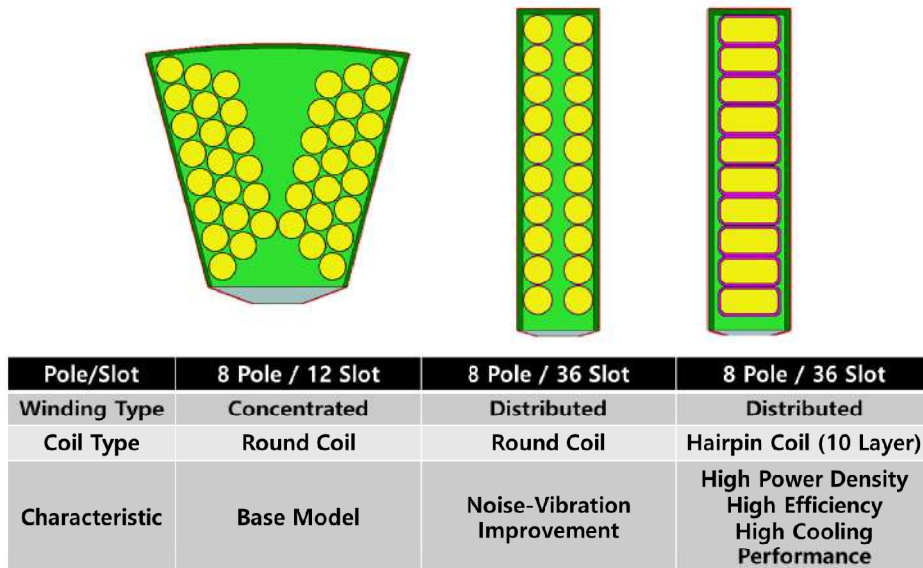
Pole/Slot	8 Pole / 12 Slot	8 Pole / 36 Slot	8 Pole / 36 Slot
Winding Type	Concentrated	Distributed	Distributed
Coil Type	Round Coil	Round Coil	Hairpin Coil (10 Layer)
Characteristic	Base Model	Noise-Vibration Improvement	High Power Density High Efficiency High Cooling Performance

Fig. 1. 슬롯 수와 권선 종류에 따른 특성 분석

Magnetic Circuit Design of Magnetic Clamping EPM System for Manufacturing Process

Ho-Young Lee[1*], Seung-Young Yoon[1], Myeong-Sik Jeong[2], Sang-Kon Lee[2],
Myung-Kon Song[1], Joo-Seop Yun[1] and Soon-O Kwon[1]

[1]Advanced Mechatronics R&D Group, Kore Institute of Industrial Technology, Korea
[2]Mechanical Components and Materials R&D Group, Kore Institute of Industrial Technology, Korea

일반적으로 자동화 라인에서는 공작물을 고정하기 위해 바이스와 같은 클램핑 장치를 많이 사용한다. 이런 클램핑 방식은 공작물 형상 및 사이즈에 따라 여러 번 위치를 바꾸어 가면서 가공해야 되기 때문에 생산성이 저하되고, 가공 소재의 부상과 변형 등을 초래할 수 있다.

최근에 개발된 마그네틱 클램핑 시스템은 별도의 그리퍼 없이 전자기력만으로 공작물을 흡착하기 때문에 사이즈의 표준화 없이 다양한 공작물에 적용이 가능하다. 특히 영구자석과 전자석이 결합된 EPM (Electro-Permanent Magnet) 시스템은 지속적으로 전원공급이 필요한 전자석과 달리 한 순간의 전원공급만으로 높은 흡인력을 지속적으로 발생시킬 수 있다. 따라서 에너지 저감에 효과적이고, 정전과 지진 등의 천재지변에 대한 안전사고를 예방 할 수 있다.

본 논문에서는 먼저 EPM 시스템의 기본적인 구조와 구동원리에 대해 설명하였다. EPM은 플럭스가 흐르는 자성체 코어와 영구자석, 코일로 구성된다. 영구자석은 알니코와 네오디뮴 자석이 사용되고, 알니코 자석의 중심으로 코일이 감겨져 있다. 순간적인 전원 공급에 의해 발생되는 전류 펄스는 알니코 자석을 착자 또는 탈자를 시키고, 이때 발생되는 플럭스에 의해 대상물과의 흡인력이 발생된다. 다음 알니코 자석이 완전한 착자가 되기 위한 착자전류와 턴수를 설계하였고, 이때 발생되는 흡인력을 유한요소해석을 통해 확인하였다. 마지막으로 시제품을 제작하였고, 대상물과의 이격거리에 따른 흡인력과 Magnetic pole 중심에서의 자속밀도를 측정하여 해석치와 검증하였다.
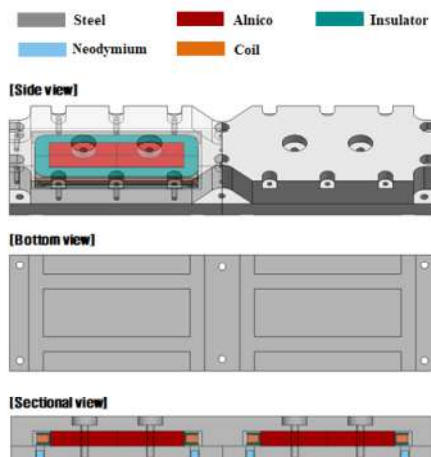
Fig. 1. EPM structure
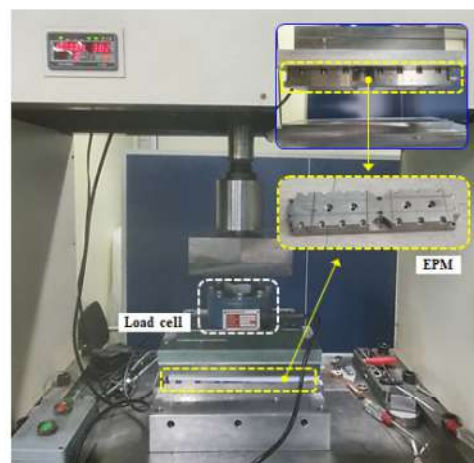
Fig. 2. Tensile force tester

Configurable Cell Pairing System with Multiparameter Controllable Magnetophoretic Circuit Device

Yumin Kang[*], Jonghwan Yoon, Hyeonseol Kim, Sri Ramulu Torati,
Keonmok Kim, Byeonghwa Lim, CheolGi Kim

Department of Physics and Chemistry, DGIST, Daegu, 42988, Republic of Korea

Cell interactions between individual cells mediate various immune reactions and cancer metastasis. Especially when immune cells interact with target cells, they show different immune responses depending on the type and size of the immune cells, the heterogeneity of individual cells, and the ratio of the number of target cells. Therefore, artificially formed cell pairing is being used as an in vitro cell model to analyze these various interactions. Accordingly, there is a need to develop an effective manipulating technology to control the cells in a single cell unit and the physical variables of cells, such as size and shape, for forming cell clusters. Despite the need and improvement of cell pairing methods, precise and adjustable control based on the physical parameters of individual cells is still limited.

Here, we developed a configurable cell pairing system that can control the multiparameter of size and number of cells using the magnetophoretic circuit method, which can programmable manipulate the location of a single cell by labeled superparamagnetic particles and fabricated micromagnetic patterns. The developed system consists of elliptical micromagnetic patterns and current-applying active elements designed to separate sequentially and control the number of cells by size. In particular, separation by size uses a unique dynamic phenomenon in which particles 'jump' due to viscosity resistance according to cell size. The particles move along the potential well periodically distributed around the boundary of magnetic patterns under a rotating external magnetic field. When the viscosity resistance is enhanced due to the increase of cell size or frequency of the external field, the particle is pushed away from the potential well and receives repulsive force from the magnetic patterns at the specific position with a particular angular difference between the potential well. In addition, the jump position can be controlled by spatially enhanced magnetic force according to the aspect ratio of the elliptical micromagnetic patterns.

The resistance and magnetic force according to the cell size and aspect ratio of patterns were calculated through numerical simulation, and the separable aspect ratio and magnetic field frequency conditions in which jumping occurs by cell size were found. Separable conditions by size in the diameter range of 3-20 um and magnetic field frequency for system operating were analyzed. We performed a size-based separation experiment using three different polystyrene beads and THP-1 cells with a specific aspect ratio of magnetic patterns designed according to the calculated conditions. As a result, 89% separation efficiency was obtained using polystyrene beads, indicating that a slight size difference of 1 um can be detected. The magnetic particle conjugated THP-1 cells were also successfully separated depending on the size heterogeneity and size difference caused by the apoptosis. Moreover, cell pairing can be effectively formed by controlling the size and number of immune cells (THP-1) and cancer cells (MCF-7) on a single magnetophoretic device, including the optimized elliptical patterns and active elements. The combinations of cells can be flexibly changed in their configuration by controlling active elements after separating by size.

Therefore, the proposed system enables precise control of the multiparameter of physical properties and the number of cells at a single-cell level. It can be an effective lab-on-chip platform for various intercellular interaction studies, providing selective cell pairing and arrangement with desired cell types.
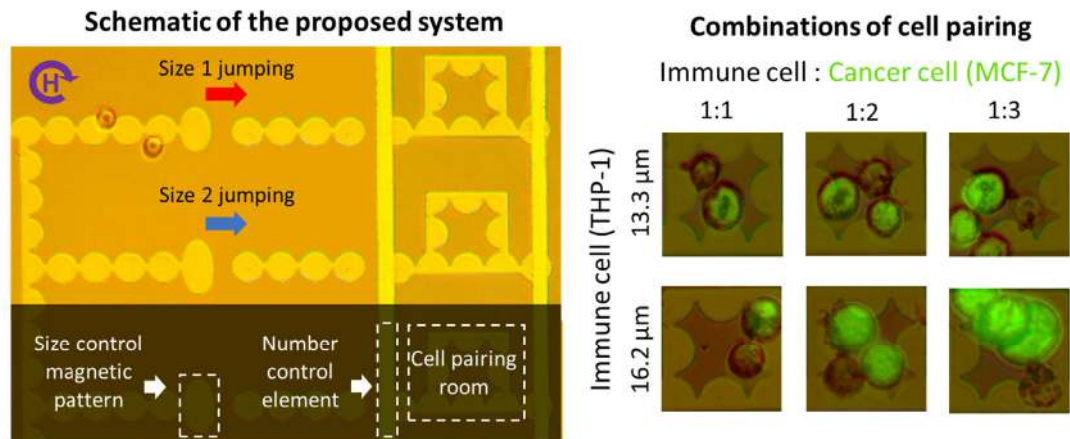
Fig. 1. Schematic of the proposed system(left) and combinations of cell pairing(right)

Development of Highly Bendable PHMR sensor

Mijin Kim[1*], Sunjong Oh[2], Taehyeong Jeon[1], Richa Chaturvedi[1], Sungwon Lee[1*], Cheolgi Kim[1*]

[1]Department of Emerging Materials Science, DGIST, Daegu, 42988, Korea
[2]Department of Nature-Inspired Nanoconvergence Systems, KIMM, Daejeon, 34103, Korea

In this paper, we have developed a flexible PHMR sensor that has a stable signal even in bending, one of the external mechanical deformations, which will be applied to the field of bio-monitoring devices in the form of being attached to the human body [1]. The demonstrated magnetic sensor is a Planar Hall Magnetoresistance (PHMR) with advantages of high signal-to noise ratio, low offset voltage, near-zero hysteresis and good linearity. The PHMR sensor is deposited on a polymer substrate with a double-layer structure(Ta(5 nm)/NiFe(10 nm)/ IrMn(10 nm)/Ta(5 nm)) to study the magnetization behavior and magnetic properties of the sensor according to bending based on an external magnetic field. When the metal thin film was deposited on the PDMS substrate as it is, wrinkles and cracks occurred due to the difference between the thermoelastic modulus and the Young's modulus between the PDMS and the metal, and no signal was observed even with minimal bending. To solve this problem, Parylene C was coated on PDMS and the PHMR sensor was deposited. The stable signal was obtained up to a certain degree of bending which is not the maximum bending curvature. Therefore, by capping the sensor with Parylene C, the sensor located at the upper part where the maximum stress is concentrated was inserted in the middle to relieve stress. The signal was relatively stable up to the maximum bending curvature.

Reference

[1] Mijin Kim et al., 'Highly bendable Planar Hall Resistance sensor', *IEEE MAGNETIC LETTERS,* 2021

Magnetophoretic Separator for Programmable Manipulation and Trapping of Positive/Negative magnetic objects

Hyeonseol Kim[*], Sri Ramulu Torati, Byeonghwa Lim, CheolGi Kim

1Department of Physics and Chemistry, DGIST, Daegu, Korea

While manipulating and isolating cells has attracted significant attention in single-cell research, digital circuit control and multiplexed individual storage of unlabeled single cells remain challenges. Here, we develop a positive/negative magnetophoretic separator for programmable manipulation of single micro-objects and local storage through the diamagnetism embodied by magnetophoretic circuit elements and magnetic fluids. Pseudo-diamagnetic (PsD) objects conduct along a linear negative micro magnetic pattern. Furthermore, Eclipse diode patterns similar to electric diodes can implement directional and selective switching of different PsD objects, such as unlabeled cells, based on diode geometry. A circuit structure that combines various negative patterns functionalized by geometry may be designed for various purposes. For example, single PsD objects are stored in their respective storage capacitors, preventing PsD objects from being occupied multiple times in an array of individual compartments due to their magnetic Coulomb-like interactions. In addition, it can be mass-captured by classifying into different zones based on the physical characteristics of objects. This approach can develop large-scale programmable arrays of unlabeled materials with high throughput, efficiency, and reliability as a multi-cell research platform.

Magnetophoreic disaggregation and interparticle distnace control by decoupler circuit

Keonmok Kim[*], Hyeonseol Kim, Byeonghwa Lim,
Jonghwan Yoon, Sri Ramulu Torati, CheolGi Kim

DGIST, Department of Physics and chemistry, Korea

Magnetophoresis, one of the technologies for moving and sorting cells, uses superparamagnetic beads to label and control desired cells or biotins. However, these methods are largely limited in their functionality by the irreversible aggregation of the superparamagnetic beads used for labeling. This presentation is about the development of a technology to automatically separate agglomerated superparamagnetic beads using an external rotating magnetic field. In a magnetic thin film made asymmetrically, it is a method of separation by the size ratio of beads due to the intrinsic magnetic potential energy distribution. After that, the separated single bead is moved only in one direction. In addition, by adjusting the angle of the external rotating magnetic field, it is possible to simultaneously and accurately control the spacing of several aggregated magnetic beads. This technology provides an advanced solution that automatically separates aggregated superparamagnetic beads, opening up an area where more research is possible on-chip for cell and bio research.

Multifunctional Magneto-optical Nanoclusters for High Sensitivity Rotavirus Detection

Hong En Fu[1*], Thomas Myeongseok Koo[1], Myeongsoo Kim[2], Min Jun Ko[1], Bum Chul Park[1], KyuHa Oh[3] and Young Keun Kim[1*]

[1]Department of Materials Science and Engineering, Korea University, Seoul 02841, Korea
[2]Institue for High Technology Materials and Devices, Korea University, Seoul 02841, Korea
[3]PRIME4DIA Co. Ltd, Gyeonggi 14059, Korea

Magneto-optical nanomaterials with both magnetic and optical properties such as fluorescence are highly anticipated in the biosensor field for application.[1,2] In particular, lateral flow assay (LFA) is widely used as a rapid target protein detection technique, however the preexisting detection method using gold nanoparticles has low sensitivity, making it difficult to conduct quantitative analysis.[3] Research has been progressed to quantify antigen concentration based on fluorescence intensity using optical property and enhance detection limit by concentrating antigen using magnetic property of multifunctional magneto-optical nanoclusters. However quenching effect occurs when optical nanoparticles close to magnetic nanoparticles. In this study, multifunctional magneto-optical nanoclusters with the structure which large amounts of quantum dot particles are infiltrated inside the magnetic nanoclusters are developed. Magnetic iron oxide nanoclusters were fabricated via oil-in-water emulsion technique in a diameter of 60 nm by mixing iron oxide nanoparticles and surfactants. Furthermore, quantum dot nanoparticles synthesis with cadmium-selenide (CdSe) quantum dots via hot-injection method then epitaxial growth of cadmium-sulfide (CdS) shell to preserve and enhance optical property. Quantum dot nanoparticles were injected into iron oxide nanocluster with chloroform and shook to penetrate quantum dot inside of iron oxide nanoclusters to prepare 300 nm-sized magnetic-optical nanocluster. Using transmission electron microscopy (TEM), X-ray diffraction (XRD) and energy dispersive X-ray spectroscopy (EDS), multifunctional magneto-optical nanoclusters were characterized. Utilizing vibrating sample magnetometer (VSM), the magnetic property of nanoclusters were measured. Thereafter, the surface of nanoclusters were coated with sodium poly(acrylic) acid (Na-PAA) to ensure water dispersibility and facilitate antibody fixation. After modifying antibodies on nanoclusters surface, LFA was proceeded to analyze quantitatively antigen concentration, then the detection limits were measured using fluorescent diagnostic scanner.

References

[1] D. Kim et al., *ACS Nano* 11(8), 8448 (2017)

[2] O. Chen et al., *Nat. Commun.* 5, 5093 (2014)

[3] M. A. Nash et al., *ACS Nano* 6(8), 6776 (2012)

Self-healing superhydrophoic surface composed of superparamagnetic iron oxide nanoparticles

Gunwoo Kim[*]

Korea Institute of Industrial Technology

Superhydrophobic surfaces have attracted tremendous attention owing to its useful non-stick interfaces and versatile applications. However, its fragile structures due to the geometries required to fulfill Cassie-Baxter theory hinders its practical applications.

Herein, we present self-healing superhydrophobic surface, which can recover its superhydrophobic geometry by magnetic aggregation of superparamagnetic iron oxide nanoparticles. The magnetic-superhydrophoicity of over 150 degree contact angle with water droplet sustains at multiple high-pressure rubbing damages ($500gf/cm^2$ pressure). The magnetic-superhydrophobic surface opens a new venue on practical applications in self-healing non-stick interfaces.

Comparative analysis of MDCT and Mobile CT space dose and environmental dose

Chang- Gyu Kim[*]

Department of Radiological Science, Gimcheon University, Gimcheon, Korea

The frequency of making nuclear medical inspections has increased all over the world. Accordingly, people have been increasingly concerned about radiation exposure by such inspections. Using glass dosimeter, this study measured cumulative radiation doses in and around the inspection room equipped with nuclear medical inspection machines and the PET-CT inspection room, and analyzed exposure doses of patients and radiological technologists.

The dose in the lobby of the nuclear medical inspection room was 0.05 mSv for a month, 0.15 mSv for 3 months, and the dose on the door of the waste storage room was 0.11 mSv for a month, 0.33 mSv for 3 months. The dose on the door of the pollution inspection room was 0.08 mSv for a month, 0.24 mSv for 3 months. The environmental doses around the gamma inspection room and around the nuclear medical inspection room were not above natural radiation dose. The dose for 3 months on the door of the stability room where patients injected with isotope wait for some time before entering the PET-CT room was 0.33 mSv. And, the annual dose at the place would be 1.32 mSv. The doses around the PET-CT room and the PET-CT reception and waiting room were measured as below the natural radiation dose. The findings of this study seem to show that, to do optimized medical radiation safety management, Korea needs to adopt the degree management specialist and establish the legal system requiring hospitals to periodically measure environmental doses and do safety management.

Table 1. Environmental radiation doses in the nuclear medical inspection room (Unit: mSv)

Measurement place		1 month (mSv)	3 months (mSv)
Gamma Camera Room	Lead glass	-	-
	Door	-	-
	Barrier wall	-	-
Waste Storage Room	Door	0.11	0.33
	Barrier wall	-	-
	Inside the room	0.16	0.48
Pollution Inspection Room	Door	0.08	0.24
	Barrier wall	-	-
	Inside the room	0.06	0.18
Nuclear medial Reception Room and Lobby	Reception room	-	-
	Waiting room	0.05	0.15

A study on the change in the glow curve of the thermos-luminescent dosimeter according to the change of the magnetic field

Jeong Ho Kim[*]

Department of Radiological Science, Sunlin University, Korea, Republic of Korea

A thermoluminescent dosimeter is a device that can evaluate radiation dose, and it is a device that can measure cumulative dose and has excellent dose accuracy. The principle of the thermal radiation dosimeter is to evaluate the exposure dose through the amount of fluorescence by emitting long-wavelength light according to the glow curve through heating in a metastable state after irradiation. However, since it was confirmed that a
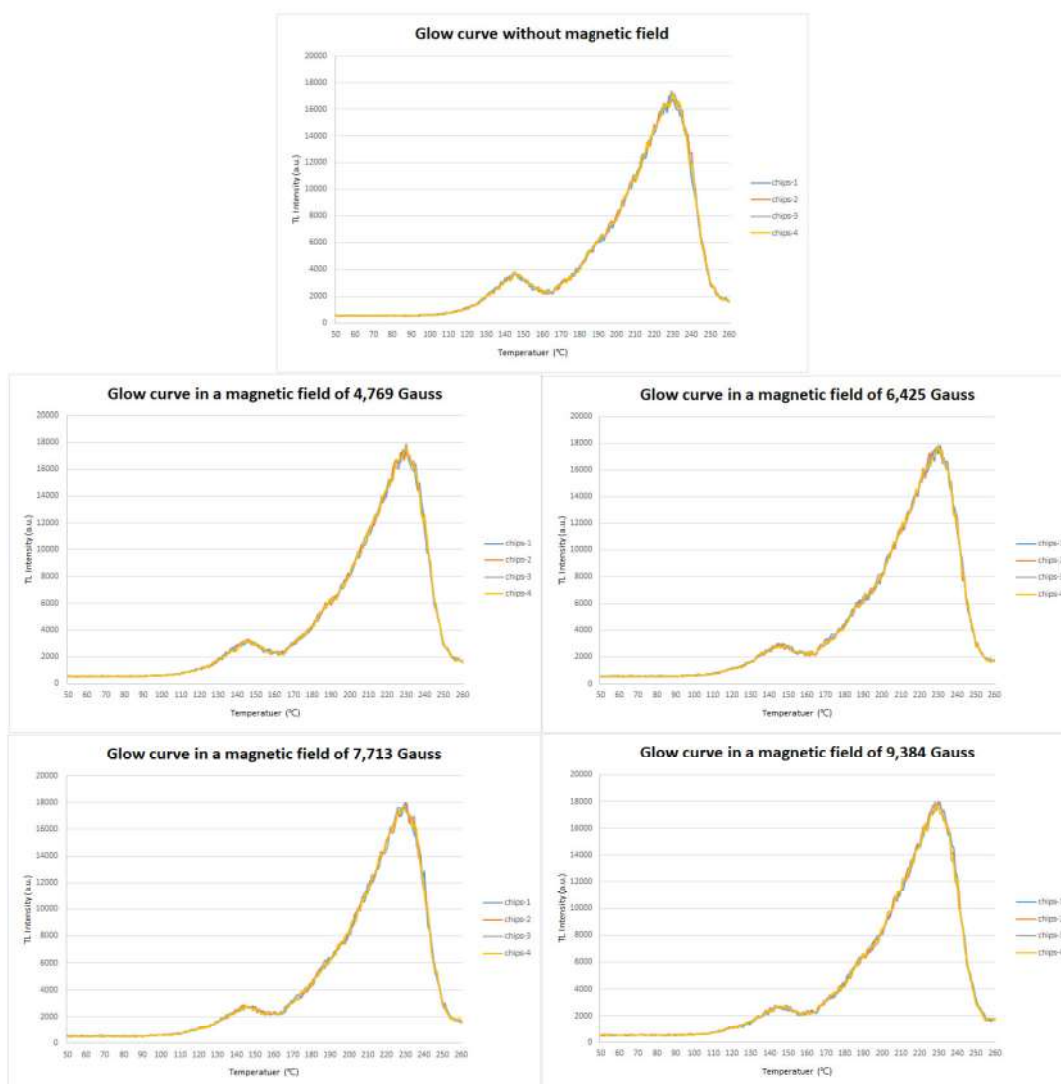
Figure 1. Change graph of glow curve according to change of magnetic field

change in the glow curve occurs in a magnetic field in a thermoluminescence dosimeter that evaluates the radiation dose in a magnetic field in the previous study, this study tried to confirm the change in the glow curve according to the change in the magnetic field. The change of the glow curve according to irradiation was observed by differentiating the magnetic field of the thermal radiation dosimeter (TLD-100). As a result, the fluorescence efficiency of the captured metastable electrons increased by 568±407 gauss/% at the 90℃ level and decreased by 188±218 gauss/% at the 130℃ level. And it increased by 586±566 gauss/% at the 210℃ level. That is, it can be seen that at a level lower and higher than the low peak, a high value is shown according to an increase in the magnetic field, and a low value is shown in a low peak according to an increase in the magnetic field. Through this, it is thought that it will be necessary to establish an evaluation system that reflects the strength of the magnetic field when measuring work in a magnetic field environment and exposure environment during TLD evaluation in the future.

DarkNet 19 based Advanced Technique for Age Estimation using Dental-Radiography

Jihyeong Ko[*], Minji Kim[2], Youngjin Jung[1]

[1]School of Healthcare and Biomedical Engineering, Chonnam National University, Yeosu, Korea
[2]Dept of Dental Hygiene, Dongseo University, Busan, Korea

Recently, using radiography, AI-based automatic diagnosis technologies for patient care are rapidly developing. In addition, AI technology with medical imaging is being accessed in the dental care field. It is one factor that determines the aging population's healthy life. In particular, AI technology for dental care can provide a cost-effective medical service in Southeast Asia and some developing countries. The first step is to advance the age estimation technique for dental care based on dental radiography. For this process, 15,000 dental radiography data with medical records (including actual age) were used to estimate a dental age using DarkNet-19 AI-Model. As a result, the accuracy of dental age was about 88%. The estimated dental age can increase the interest in dental care for patients. Therefore, it is expected to be a useful tool for improving the life quality of aging
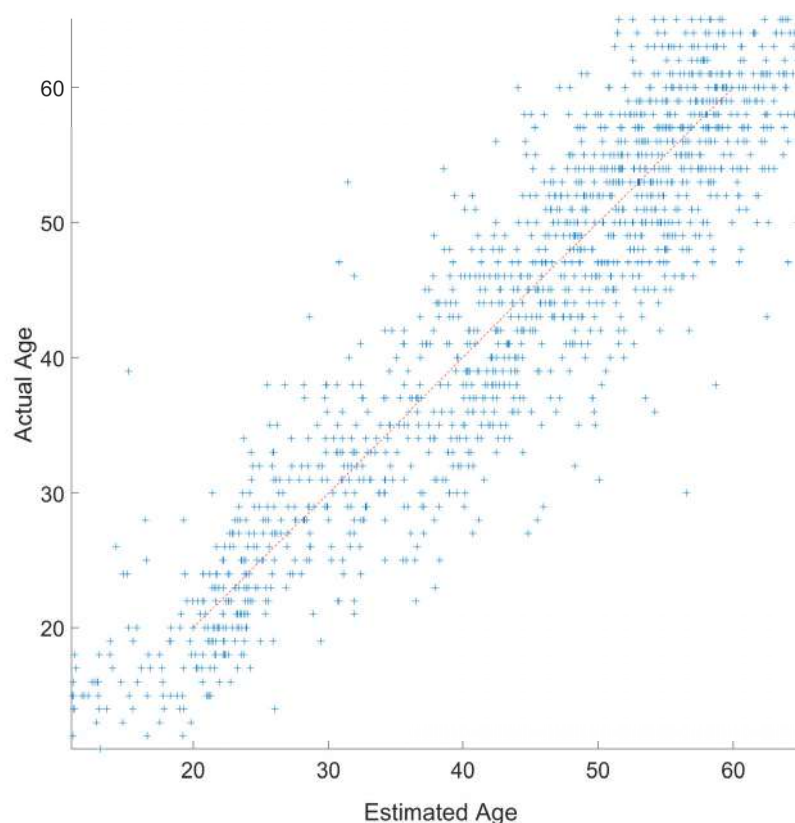
Fig. 1. The comparison between estimated age and actual age using dental radiography

Dental Panoramic Image-Based Gender and Age Evaluation AI Model for Preventive Dental Care

Seoul-Hee Nam[1*], Yu-Rin Kim[2], Won-Du Chang[3], Yongsu Yoon[4], Jihyeong Ko[5], Youngjin Jung[5]

[1]Dept of Dental Hygiene, Kangwon National University, Busan, Korea
[2]Department of Dental Hygiene, Silla University, Busan, 46958, Republic of Korea
[3]Division of Computer Engineering, Pukyong National University, Busan, Korea
[4]Dept of Radiological Science, Dongseo University, Busan, Korea
[5]School of Healthcare and Biomedical Engineering, Chonnam National University, Yeosu, Korea

Preventive dental care is an essential field in which patients can secure a high quality of life and provide a service that takes care of their teeth in a dental hospital. In particular, the dental industry and academic importance are very high. This study developed a novel algorithm to estimate the patient's gender and age based on the dental panoramic image for patient care. This study employed ten thousand (10,000) dental panoramic images (approved by the Kangwon National University IRB). In order to develop the AI model, the proposed AI model showed more than 80% accuracy within the 10–year range. Although this preliminary study showed simple estimated information (age, gender), it is also a valuable index for dental care by understanding the current status of the patient's dental. Further study for dental care will be conducted to detect dental diseases using a modified AI model.
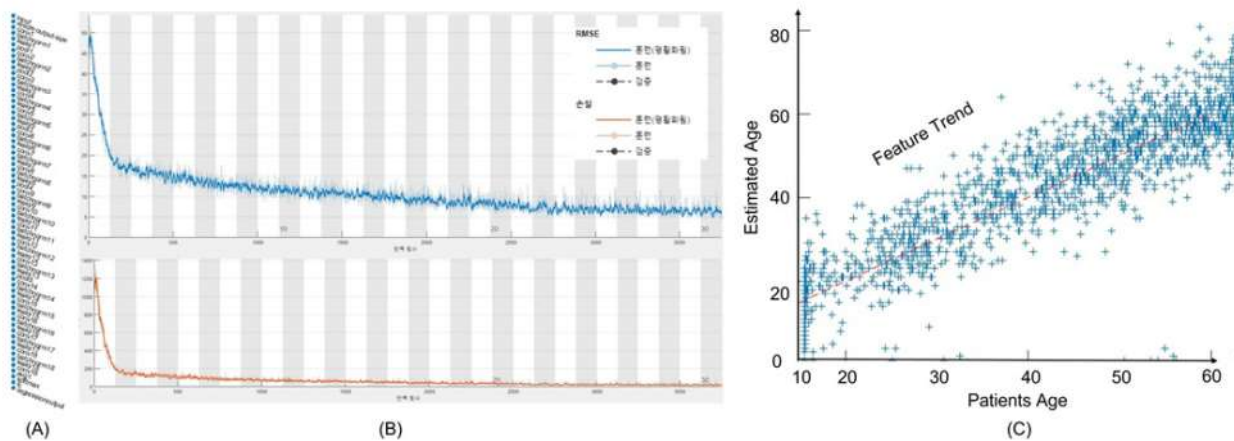
Fig. the results of Proposed AI model; (a) AI model design, (b) Training performance using MATLAB, (c) Comparison result between Patients' age and estimated age

Development of PET compatible transcranial Current Stimulation (tCS) for Brain Stimulation

Seungmin Hwang[1], Youngjin Jung[2*]

[1]Department of biomedical engineering, Chonnam National University, Yeosu, Korea
[2]School of Healthcare and Biomedical Engineering, Chonnam National University, Yeosu, Korea

Recently, various advanced technologies for brain function evaluation have been introduced. Among them, positron emission tomography (PET) has been widely used to understand brain function in radiological science. In particular, it is widely used in clinical practice to evaluate brain activity to detect neuro diseases (such as Alzheimer's disease). This study aims to develop a Neuromodulation (Transcranial Current Stimulation, tCS) device that is compatible with PET to develop a novel evaluation technique with PET. In other words, Patients with brain dysfunction or brain damage can variously perform PET-based brain function evaluation with brain stimulation. In order to provide various brain stimulation patterns, the tDCS (Transcranial Direct Current Stimulation) and tACS (Transcranial Alternating Current Stimulation) functions were designed, and the frequency band of tACS function can be stimulated in units of 0.1 Hz from 1 to 2100 Hz. In addition, it is designed to allow simultaneous stimulation of 8 electrode channels so that it can be used for a new type of stimulation study in which mixed frequencies in different brain regions. Therefore, the developed tCS system in this study can be used as an auxiliary Neuromodulation device for various brain function tests. It is expected that this will contribute to the development of meaningful diagnosis methods (for monitoring) and care technology (for cure) for brain function in the clinical field. Also, it can be utilized to develop new PET imaging examination techniques with neuromodulation.

1mA 7.1KΩ	2mA 3.6KΩ
1mA 7.1KΩ 1Hz	2mA 3.6KΩ 1Hz
1mA 7.1KΩ 2000Hz	2mA 3.6KΩ 1000Hz
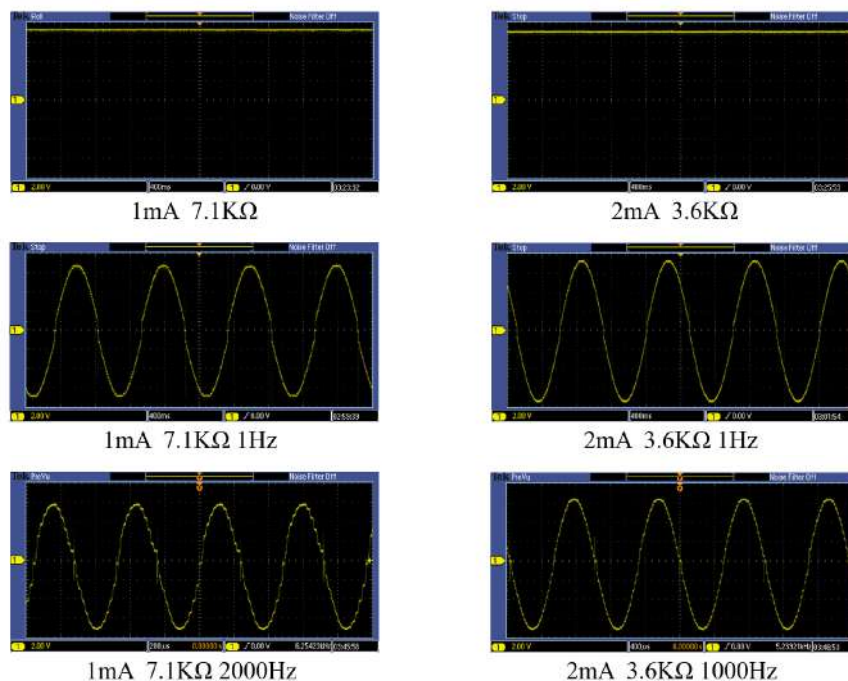
Fig. 1. The current waves from tDCS and tACS function using proposed tCS device

Elderly Fall Detection System Paper Review

Nayeon Seo[1], Sun-Young Cho[2], Youngjin Jung[3*]

[1]Department of biomedical engineering, Chonnam National University, Yeosu, Korea
[2]Department of Occupational Therapy, Sangji University, Wonju, Korea
[3]School of Healthcare and Biomedical Engineering, Chonnam National University, Yeosu, Korea

As the elderly population increases, the problem of falls among the elderly is emerging as an important issue. According to the World International Organization (WHO), there are 646,000 fatal falls worldwide each year. Most of them are older than 65 years of age. 50% of the older adults will experience a fall within 5 years, 62% have an injury that requires ongoing treatment, or 28% have extensive long-term injuries. The Falls are the second leading cause of unintentional injury deaths after traffic accidents and the leading cause of injury-related deaths among the elderly., A sharp increase in fall detection (on Google Trends) was observed in academia and industry, with interest from around 10 articles in 2015 reaching nearly 100 in 2019 [Fig 1]. In this study, 31 papers with high relevance were found through search terms such as "falling detection" & "AI" in Scopus to investigate the latest research related to falls. And then, 7 papers with significant relevance were reviewed. In addition, a few additional articles were searched using Google and reviewed. According to recent articles, one of the widely used methods is remote sensing technique using individual sensors such as wearables or cameras in many studies from 1999 to the present. In addition, A novel AI technology has been introduced, and CNN and LSTM are being used to detec fall more accurately. Although several studies combining sensors and AI are being observed, it has been confirmed that the combination of Kinect and accelerometer can have the most significant effect among the tools used to detect falls so far. Although this system was able to obtain a high effect in fall detection due to sensor fusion, the accelerometer sensor that should be attached to the body is inconvenient, and the risk of indiscriminate disclosure of personal information when using the camera also existed. In this review paper, we discussed the fall dectection technologies so far and thought about the technologies that will be needed in the future.

Fall detection: Worldwide
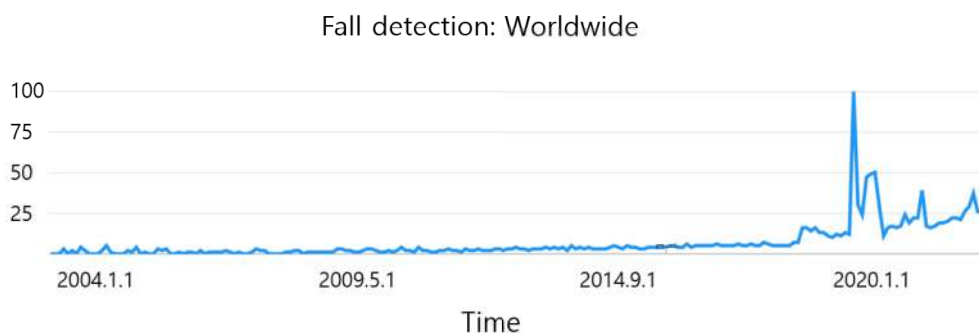
Fig. 1. Interest of fall detection

Development and evaluation of multipurpose phantom for delivery quality assurance of intensity-modulated radiation therapy

Jae-Uk Jang[1*], Man-Seok Han[2*], Min-Cheol Jeon[3], Gyeong-Yeon Jo[1],
Jin-Ha Yun[1], Yong-Chan Jeon[3], Sang-Beom Lee[3]

[1]Department of Radiation Oncology, Chungnam national university hospital, Daejeon 35015, Korea
[2]Department of Radiological Science, Kangwon National University, Samcheok 25949 Korea
[3]Department of Radiological Technology, Daejeon Health Institute of Technology, Daejeon 34504, Korea

Electromagnetic radiation therapy is aimed at delivering radiation dose to a target volume (cancer) while sparing surrounding normal tissue. Recently, electromagnetic radiation therapy is focused on precise radiation treatment like intensity-modulated radiation therapy (IMRT). Accurate treatment such as IMRT should provide an optimized dose distribution and correct treatment. Otherwise, the treatment is not only unsafe, but it has a serious adverse effect on the patient. Deliver quality assurance (DQA) for treatment verification can be accomplished via the absolute dose using the ionization chamber and relative dosimetry using the film.

However, a film imposes a waiting time for measurement and is sensitive to humidity and temperature, conditions of development, and noise.

Therefore, this study is to evaluate the usefulness of multipurpose phantom for quick and simple IMRT DQA. A multipurpose phantom was made using polymethyl methacrylate (PMMA) resin. We designed it to allow the insertion of a 2D array detector and an ionization chamber into the multipurpose phantom. Therefore, the relative and absolute doses can be measured simultaneously. The results of the IMRT DQA were $0.35 \pm 1.74\%$ absolute dose in linear accelerators (linac). The relative dose was measured at $99.03\% \pm 0.6\%$ by 3 mm/3% gamma evaluation. The absolute dose was $1.37 \pm 1.05\%$ and the relative dose was $98.7 \pm 0.78\%$ in helical tomotherapy. In linac and tomoterapy, both absolute and relative dose measurements were within acceptable limits in 3%. The results demonstrate the multipurpose capabilities of the proposed phantom for evaluating dose distribution and absolute dosimetry.

Keywords: Intensity-modulated radiation therapy, Deliver quality assurance, Multipurpose phantom, Absolute dose, Relative dose

FPGA-based 8-channel data acquisition system

MinhDuc Hoang[*] and Jihoon Kang

*Department of Biomedical Engineering, College of Engineering,
Chonnam National University, Jeonnam 59626, Korea*

The aim of this study was to develop a general-purpose data acquisition (DAQ) system based on a field programmable gate array (FPGA), that could be utilized in MR-compatible breast PET, fan-beam DEXA, and radiation imager, which are under development by our group. Each analog input signal was digitized by using the 8-channel analog-to-digital converter (ADC) with a sampling rate of 125 MHz and input range of -1 V to 1 V. (AD9681, Analog Devices, MA, USA). Fourteen-bit digital signals were fed into a Xilinx Virtex-6 FPGA (XC6VLX75T-2FFG784C)-based evaluation board (HSC-ADC-EVALEZ, Analog Devices, MA, USA) which was
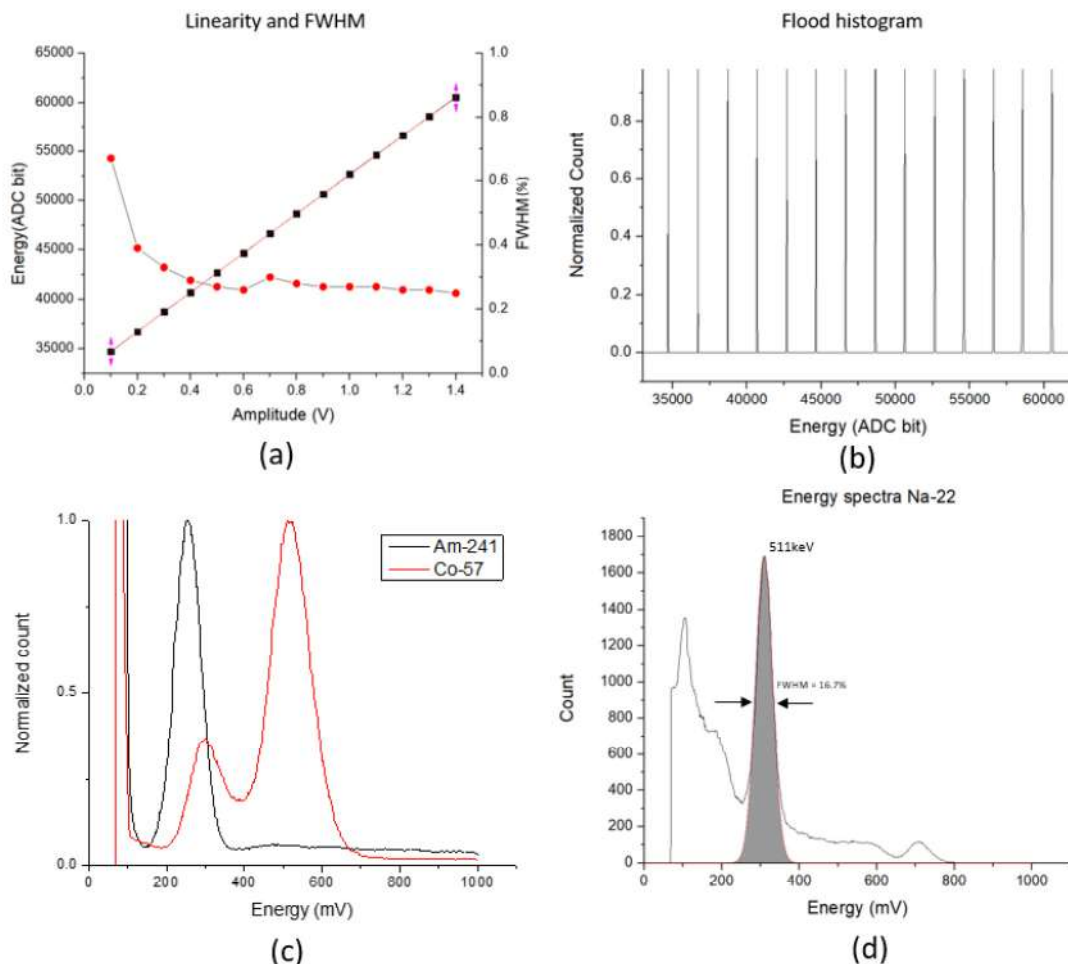
Figure 1. Performance evaluation of general-purpose FPGA-based DAQ system
(a) Voltage-peak channel and Full Width at Half Maximum (FWHM) as a function of the amplitude of input signal. (b) Energy peak channel acquired with sine waveform signal. (c) Acquired energy spectra with gamma-ray sources of Am-241 (black) and Co-57 (red). (d) Acquired energy spectra with gamma-ray sources of Na-22 (d).

implemented digital signal processing logic. The calculated position, arrival time, peak level, and event trigger for each input signal were stored in an output buffer (a FIFO) in on-chip block ram, which was read by the personal computer (PC). The FPGA board was connected with a PC via USB port for the communication with Visual Analog and SPIController software (Analog Devices, MA, USA). A sine wave signal from the function generator was used to characterize the intrinsic performance of the DAQ system, as a function of the pulse amplitude. Output linearity and voltage resolution performances were assessed by voltage-peak channels and FWHM obtained from Gaussian fit, respectively. ADC bit-peak channel increased with increasing pulse amplitude, and an estimated coefficient of determination (R^2) was 0.999. No considerable changes in voltage resolution (from 0.2 V to 1.4 V) was observed. DAQ performance was evaluated for real radiation detector signals from LYSO scintillation crystal coupled with Geiger-mode Avalanche Photodiode (GAPD). Each energy peak was linearly changed as a function of the gamma-ray energy. The Energy resolution was 29.5%, 23.5% and 16.7% for 60 keV (Am-241), 122 keV (Co-57), and 511keV (Na-22), respectively. This study demonstrated that it was feasible to develop the FPGA-based DAQ system for general purpose and the proposed approach could offer opportunities to employ developed DAQ systems in various medical imaging field.

A Study on Optimal Irradiation Conditions for Dental Material Radiopacity Test

Jun-Seok Lee, Ji-Min Yu, Hyun-Jin Kim, Chang-Won Park, Seung-Youl Lee[*]

Medical Device Research Division, National Institute of Food and Drug Safety Evaluation, Chungcheong buk-do, Cheongju-si 28159, Korea

1. Introduction

Radiopacity opacity is one of the important characteristics required to distinguish dental materials from surrounding tissues when applied in the oral cavity or to check whether they remain. It is a performance evaluation item that must be submitted in the licensing stage for various dental materials such as dental adhesives, root canal sealants, orthodontic cements, and cavity fittings. In 2014, the radiopaque test standard ISO 13116 was enacted, and the frequency of use is increasing because it guides more detailed test methods than other international standards. Although the standard guides the use of a dental intraoral imaging device, there is a limitation in that the size of the detector is small and the resolution of the image is not good to take a specimen and an aluminum step wedge at the same time. Therefore, the goal of this study is to verify scientific feasibility and find the optimal conditions using a general X-ray imaging device with a relatively large detector and superior image quality compared to the dental X-ray imaging device guided by the international standard.

2. Material and method

2.1. Specimen and aluminum stem wedge production

Specimens are in the form of disks with a diameter of 10 mm and a thickness of 1 mm using a suitable mold according to ISO 13116, and products from 4 companies with respectively different radiopacity (opacity 1.79 mm, 2.3 mm, 4.25 mm, 8 mm or more) was used. The aluminum step wedge consists of 10 steps at 0.05 mm intervals according to ISO 13116, and the overall size is 50 mm in width and 20 mm in length.

2.2 X-ray imaging device

The dental X-ray imaging device (STAR-X, HDX, KOREA) used in the experiment has a setting range of 65 kV tube voltage, (3 ~ 6) mA tube current, and (10 ~ 320) ms exposure time. The second has a setting range of 500 mAs. A general X-ray imaging device (DRGEM, DIAMOND, KOREA) has a setting range of (40~150) kV tube voltage, (10 ~ 640) mA tube current, and (0.1 ~ 500) mAs tube current second.

2.3 Method

First, the specimen and the step wedge were placed in the center of the detector of the dental X-ray imaging device, and irradiated in the assembly with X-ray at ta target-film distance of 350 mm, exposure time 160 ms, tube voltage 65 kV, tube current 6 mA. Second, place the specimen and step wedge were placed in the center of the detector with a general X-ray imaging device, and compared with the distance between the target and the tube under the conditions of 350 mm (tube voltage 65 kV, tube current 10 mA, exposure time 250 ms) and 700 mm (tube voltage 65 kV, tube current 40 mA, exposure time 250 ms) respectively. After that, the test was

conducted by changing the tube voltage, tube current, and exposure time at a distance of 700 mm between the object to be photographed and the tube. The photographed image files were analyzed using the measurement tool of gray scale analysis software (Photoshop CS3 Extended, Adobe, USA), and the most appropriate conditions were compared and analyzed.

3. Results and discussion

3.1. Comparison of results of dental X-ray imaging device and general X-ray imaging device

In the case of a specimen photographed using a dental X-ray imaging device, the gray scale was equivalent to an aluminum thickness of about 2.8 mm. Conditions: distance from tube 350 mm, tube voltage 65 kV, tube current 6 mA, exposure time 160 ms. Under the same conditions, the gray scale of the general X-ray imaging device did not come within the gray scale range of each step of the aluminum step wedge. Conditions: distance from tube 350 mm, tube voltage 60 kV, tube current 10 mA, exposure time 250 ms. It was found that the general imaging device has an inappropriate geometric structure for close-up photography, and the irradiation area is wider than that of the dental imaging device, which causes semi-shading and distortion of the image. To solve this problem, the distance was doubled and the irradiation condition was increased by 4 times according to the law of the inverse square of the distance. Conditions: distance 700 mm, tube voltage 60 kV, tube current 40 mA, exposure time 250 ms. The validity of the test using an alternative equipment was verified, showing similar results (2.8 mm) to the gray scale shown by the dental X-ray imaging device.
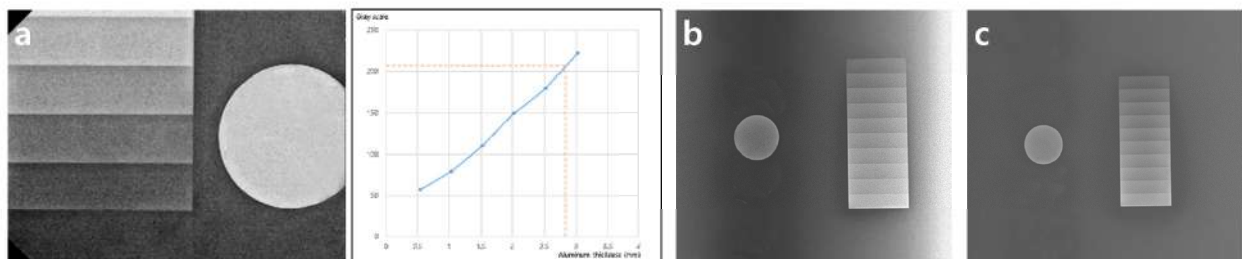
Fig. 1. A sample line graph

3.2. Consideration of optimal inspection conditions in general X-ray imaging device

The second study was conducted to find the most appropriate conditions by setting the distance between the subject and the tube to be 700 mm based on the previous results. Table 1 shows the results according to changes in tube voltage and tube current within the range recommended by the standard for 4 specimens. At 50kV tube voltage, the measured value of Specimen B was less than twice, and at 70kV and 16mAs conditions, it was difficult to read due to severe penetration. The optimal radiopacity required by each specimen was similar to grayscale values at 60 kV and 4 mAs, and the tendency of the four specimens to transmit opacity was also consistent.

Table 1. Measurement values of aluminum step wedges measured according to variables in a general X-ray imaging device

Condition	Specimen A	Specimen B	Specimen C	Specimen D
50 Kv 40 mA 100 ms	(2.5 ~ 3.0) mm	(1.5 ~ 2.0) mm	> 5 mm	(4.5 ~ 5.0)mm
50 Kv 80 mA 100 ms	(2.0 ~ 2.5) mm	(1.5 ~ 2.0) mm	> 5 mm	(4.5 ~ 5.0)mm
50 Kv 160 mA 100 ms	(2.5 ~ 3.0) mm	(2.0 ~ 2.5) mm	> 5 mm	(4.5 ~ 5.0)mm
60 Kv 40 mA 100 ms	(2.0 ~ 2.5) mm	(2.5 ~ 3.0) mm	> 5 mm	(4.5 ~ 5.0)mm
60 Kv 80 mA 100 ms	(2.5 ~ 3.0) mm	(2.5 ~ 3.0) mm	> 5 mm	(4.5 ~ 5.0)mm
60 Kv 160 mA 100 ms	(2.5 ~ 3.0) mm	(2.5 ~ 3.0) mm	> 5 mm	(4.5 ~ 5.0)mm
70 Kv 40 mA 100 ms	(2.5 ~ 3.0) mm	(2.5 ~ 3.0) mm	(4.5 ~ 5.0)mm	(4.0 ~ 4.5) mm
70 Kv 80 mA 100 ms	(2.5 ~ 3.0) mm	(2.5 ~ 3.0) mm	(4.5 ~ 5.0)mm	(4.0 ~ 4.5) mm
70 Kv 160 mA 100 ms	-	-	-	-

4. Conclusion

This study tried to verify the possibility of radiopaque testing of dental materials in general X-ray imaging equipment and to find the optimal test conditions. As a result of the study, it was sufficient to replace the test with a general X-ray imaging device, and the best results were obtained when the optimal conditions for the test were 60kV and 4mAs. However, since the result is limited to a specific sample, it is difficult to apply it to all dental materials. In addition, since the international standard recommends that dental materials be tested with a dental X-ray device, the recommendation must be followed for product licensing.

5. Acknowledgement

6. References

[1] ISO 13116:2014 Dentistry - Test Method for Determining Radio-Opacity of Materials
[2] ISO 6876:2012 Dentistry - Root canal sealing materials

Evaluation of Image Quality of Compressed Sensing Magnetic Resonance Images

Seong Ho Kim[1], Jung Eun Oh[2], Soon Yong Kwon[4], Ji Sung Jang[4], Won Jeong Lee[1],
Min Cheol Jeon[1], Jae Seok Kim[1], Mo Kwon Lee[1], Se Jong Yoo[5*]

[1]Department of Radiological Technology, Daejeon Health Institute
[2]Naara animal hospital
[3]Department of Radiology Konkuk University Medical Center
[4]Department of Radiology and Research Institute of Radiology, Asan Medical Center
[5]Department of Radiological Technology, Konyang University

The aim of the study was to compare the image quality of reconstructed images using the 3D T1 variable flip angle (CUBE) sequence with and without compressed sensing (CS). A phantom was prepared by diluting the Gadolinium contrast medium with saline at the concentrations of 0, 0.2, 0.6, 1.0, and 4.0 mM. Moreover, images were obtained using the 3D T1 CUBE sequence with and without the use of CS. When CS was used, images were reconstructed at increasing CS factor values (i.e., 1.2, 1.4, 1.6, 1.8, and 2.0), while all other variables were unaltered. Measurements were analyzed using Student's t-tests and ANOVA. Moreover, the SSIM and RMSE estimates were evaluated using the ICY program and the relative SNR errors were quantified. The scan time reduced by up to 1min 35sec from the conventional 3D T1 CUBE sequence (3min 3sec) to 3D T1 CUBE sequence using CS (CS factor=2.0). The SNR values of the conventional 3D T1 CUBE and 3D T1 CUBE sequences using the CS technique were not significantly ($p>0.05$) different when the CS factors varied from 1.2 to 2.0. Moreover, the estimated SSIM were similar, while the root mean square error (RMSE) values varied when the CS factor varied from 1.2 to 2.0, based on the use of the conventional 3D T1 CUBE sequence. Therefore, the 3D T1 CUBE sequence using the CS technique can achieve an acceptable image quality that is not considerably different from that of the conventional method.

Keywords: Compressed sensing, Parallel imaging, 3D T1 CUBE, Gadolinium contrast agents

Biotinylated polyethylene glycol anchored magnetotactic bacteria for enhanced biodistribution of drugs

Richa Chaturvedi[*], Yumin Kang, Yunji Eom, Sri Ramulu Torati, CheolGi Kim[†]

Department of Physics and Chemistry, DGIST, Daegu, 42988, Republic of Korea

[*]Corresponding authors: E-mail: cgkim@dgist.ac.kr (CheolGi Kim), Tel: +82-53-785-6516, Fax: +82-53-785-6509

The targeted and effective bio-distribution of drugs to the affected region still remains a less studied area for many controlled release therapeutic systems. Several magnetotactic bacteria have been used as a drug delivery agent as they possess a property of self-propulsion and they can be controlled by an external magnetic field as well. By coating the bacteria with the Biotin-PEG-NHS polymer, the bacteria can be turned into a stealth material that can escape the phagocytosis process by increasing the time for removal of the drug delivery agents. The development of these complexes focuses on an easy, time saving, and a stable technique of polymer attachment with the bacteria without affecting the cell's ability to act as a strong and reliable delivery agent. In this work, we have developed a potential drug carrier by attaching the PEG-biotin with the MTB (MTB-PEGB) through NHS crosslinker. In the present study, the efficacy and attachment stability of biotinylated PEG with bacteria were investigated. Results confirm that the Biotin-PEG-NHS polymer was efficiently attached to the bacteria without reducing its viability and functionality. Cytotoxicity assay using THP-1 cell indicates that polymer improves the biocompatibility of MTB. In addition to the cytotoxicity assay, a cell association assay was evaluated for the assessment of proposed complex as a potential stealth material for improved biodistribution of drugs.

Key words: Magnetotactic bacteria, biotin, polyethylene glycol, cytotoxicity, drug delivery, stealth property

Image quality analysis according to distance in Isocenter

Dong Gu Kang[1], Jae Seok Kim[2*], Min Chul Jeon[2], Sung Ho Kim[2], Won Jeong Lee[2]

[1]Department of Radiology, A-Jou University Medical Center, Korea
[2]Department of Radiological Science, Dae-Jeon Health Institute of Technology, Korea

The magnetic field is most uniform at the isocenter, and the uniformity of the magnetic field starts to deteriorate as it moves away from the center. Some body parts, such as elbows and wrists, have difficulty locating the center of the MR scanner easily. In particular, the larger the patient's physique, the farther the examination site is from the center. Therefore, this study aims to provide an effective inspection method by measuring the change in image quality as it moves away from the center of the scanner and providing a reference distance at which image quality does not deteriorate during actual inspection.

A circular phantom was scanned using GE's GEM flex coil. Data of a total of 9 points 5cm, 10cm, 15cm, and 20cm apart from the center and both sides of the scanner were acquired and compared with ISOCENTER-centered data. The experimental device used 3.0T (GE Discovery MR750, GE Health Care, USA) and 16-channel GEM Flex Suite (small) to acquire T1 and T2 images of the old phantom. By setting the region of interest in the acquired image using the Image J program, the intensity and standard deviation of signal and noise were measured, and the average value of the signal-to-noise ratio and contrast noise ratio, the 95% confidence interval value, and the average difference between SNR and CNR were analyzed.

As a result of analysis with the SPSS Statistics 23 statistical program, the values of SNR and CNR were higher for both T1- and T2-weighted images as they were closer to the center, and lower values were shown as they moved away from the center. As a result of one-way ANOVA and Duncan's post-hoc analysis, the measured values at 5 cm, 10 cm, and 15 cm were not statistically significantly different from the centroid. ($p < 0.001$). However, at the 20 cm position, the standard deviation of noise increased by more than 10%, and the values of SNR and CNR decreased sharply.

When examining elbows or wrists, if the distance from the center does not exceed 15cm, there is no need for technology to compensate for image quality.

Keywords: Isocenter, magnetic field center, uniformity

Effect of FFC length on the performance of PET detector

Jingyu Yang[*] and Jihoon Kang

Department of Biomedical Engineering, College of Engineering,
Chonnam National University, Jeonnam 59626, Korea

Performance evaluation was characterized the positron emission tomography (PET) detector with applying signal transmission process using flexible flat cable (FFC) ranging from 1 to 10 m. The PET detector was consists of 4 × 4 cerium-doped lutetium yttrium orthosilicate (LYSO) array of 3 × 3 × 20 mm^2 discrete crystals and 4 × 4 geiger-mode avalanche photodiode (GAPD) array having a 3.07 × 3.07 mm^2 pixels. All of signals from GAPD array were multiplexed by the RCD circuits to reduce the number of output channels from 4 × 4 to 4 for 4 by 4 array. Experimental measurements were performed by using a Na-22 point source placed 100 mm away from the top surface of the PET detector module for uniformly irradiation. Rise time, fall time and amplitude of the GAPD output were measured as a function of the cable length. In addition, the following three investigations were performed for characterization of PET detector performance: 511 keV photopeak position and energy resolution. Experimental results show that rise time, fall time, and pulse width of waveforms were increased by up to ~30% as increasing length of FFC. Although 511 keV photopeak position is decreased linearly, the detector performances including position determination, position linearity, and energy resolution (~13.7%) were quite similar for the three types of PET detector module. These results demonstrate that length of FFC affect performance of waveforms including rise time, fall time, and pulse width. These degradations could affect coincidence time resolution and count rate performance in PET detector.
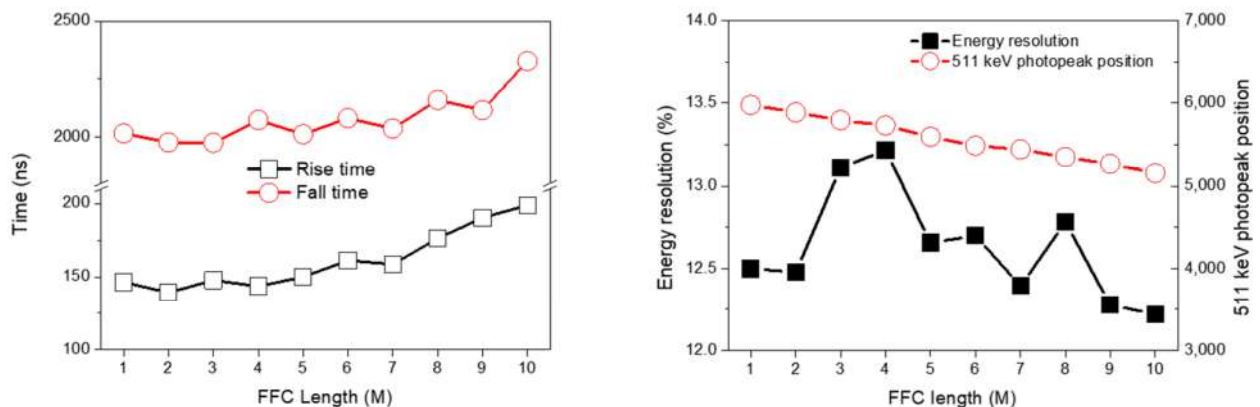
Fig. 1. PET detector performance as a function of the FFC length: (right) rise time and fall time and (left) energy resolution and 511 keV photopeak position. All performances without energy resolution were decreased as the length of FFC.

Effects of 5 Hz Repetitive Transcranial Magnetic Stimulation on Cortical Activity and Upper Limb Function According to the Etiology of Chronic Stroke Patients; A case study

Jung-Woo Jeong[1*], Bo-Kyoung Song[2]

[1]Dept. Emergency Medical Rehabilitation Graduate School, Kangwon National University, Korea
[2]Dept. of Occupational Therapy, Kangwon National University, Korea

As a single case study, this study was to investigate the effect of 5 Hz repetitive transcranial magnetic stimulation (5 Hz-rTMS) on cortical activity and upper limb function according to the cause of chronic stroke patients.

This study was conducted for 6 weeks from April to June 2021, and was conducted through the ABA design for 2 people diagnosed with cerebral hemorrhage and 2 people diagnosed with cerebral infarction. During the study period, subjects were applied for a total of 18 sessions: 3 times at baseline A, 12 times in intervention period B, and 3 times at baseline A'. During the baseline period, Fugl-Meyer assessment (FMA) was performed without any special intervention, and Electroencephalography (EEG) and Electromyography (EMG) were evaluated before and after the intervention. During the intervention period, 5 Hz-rTMS was performed 12 times. As a result, a greater amount of change was reported in the EEG and EMG results of patients with cerebral infarction than those with cerebral hemorrhage before and after intervention. There was no significant change in FMA results. As a result of this study, it was reported that 5 Hz-rTMS applied to cerebral infarction patients rather than cerebral hemorrhage patients had a positive effect on cortical activity and upper extremity function.

Table 1. Changes in Electroencephalography of subjects
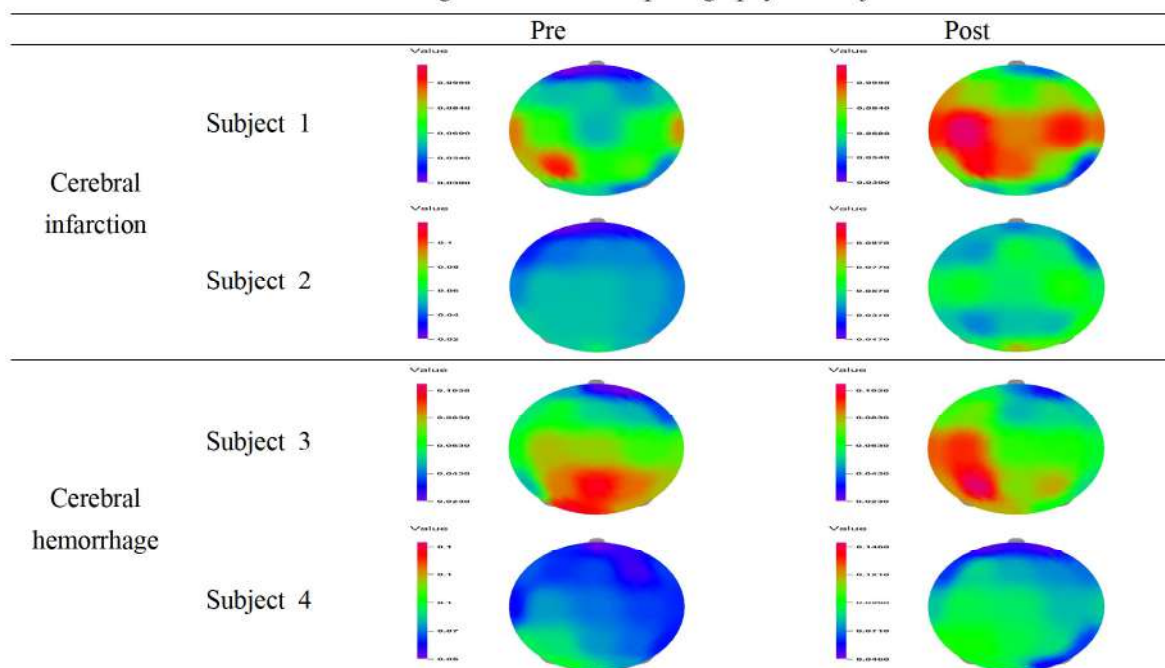
Analysis of Fe Element and Interferon Gamma in Spleen Homogenate after Bioinjection of Antibody-Magnetic Nanoparticles Conjugation

Jong-Gu Choi[1*], Mahbub Hasan[1], Akter Hafeza[1], Ye-Eun Lim[1], Ye-Bin Bae[2] and Sang-Suk Lee[1†]

[1]Department of Digital Healthcare Engineering, Sangji University, Wonju 220-702, Korea
[2]Department of Visual and Media Design, Sangji University, Wonju 220-702, Korea

Currently, the treatment of suppression of cytokine storm in severe COVID-19 patients includes cytokine receptor suppression and depletion of specific immune cells in addition to steroid treatment. Among these, monoclonal antibody therapy is one of the methods for depleting specific immune cells. It is a monoclonal antibody therapy against CD3, one of the important signaling molecules for T-cell receptor activation. CD3 is specifically expressed on T cells. Monoclonal antibody therapy suppresses T cells through antibody-mediated complement activation and removal of immune conjugates. T cells secrete Interferon (IFN)-gamma (γ), a type of cytokine that is an immune protein. That is, monoclonal antibody therapy is a therapy that specifically depletes IFN-γ-secreting T cells. However, this treatment is an intravenous injection of an anti-CD3 monoclonal antibody, and since it targets all T cells, it induces significant immunosuppression and has side effects such as high fever and chills.

The purpose of this study is to prepare an optimized liquid phase as a CD3 antibody (Ab)-magnetic nanoparticles (MNPs) conjugate to inhibit the overactivation of T cells. It is delivered by intravenous injection, or film-type microneedle patch technology is applied. That is, pulse-type magnetic stimulation is applied to control the amount of liquid passing through the skin. The CD3 Ab-MNPs that have entered the blood in this way are attached to the respiratory system virus disease areas such as the lungs and chest of the upper body where the corona virus is concentrated and distributed. And to establish the basic technology for development as a targeted immunotherapeutic agent to induce a therapeutic liquid phase.

We measure of constituent Fe element interferon gamma in spleen homogenate by using TEM-EDS (transmission electron microscopy-energy dispersive X-ray spectroscopy) and ELISA (enzyme-linked immunosorbent assay), respectively, after bioinjection of Ab-MNPs conjugation for the development of COVID-19 immunotherapy. We investigate anti CD3 antibody detection in splenocyte by ICC (immunochytochemistry) to validate the Ab-MNPs
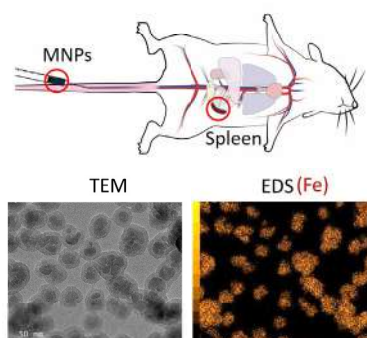
Fig. 1. One injection in tail vein of MNPs solution with TEM image and EDS mapping from the syringe needle through the heart moved to the spleen of mouse.

conjugation. Also, we will be observed TEM/SEM images and confocal fluorescence microscopy for status of single T-cell coupled to Ab-MNPs conjugation.

A mouse in vivo dissection experiment was conduct to examine the characteristics of MNP moving to the spleen organ when administered in vivo. As shown in Fig. 1, 100 μL of magnetic nanoparticles is administered to the tail vein of the mouse, and after 3 days, the spleen, a living organ where immune T cells are generated, is collected. Similar to the control spleen, the amount of Fe remaining in the spleen after the administration of magnetic particles is irradiated with ICP-MS (inductively coupled plasma-mass spectrometry) to compare and analyze the concentration of MNPs. The reason for choosing the spleen from the mouse organ is that it stores MNPs with a particle size of 50 nm administered in vivo. Therefore, the result is a difference in the concentration of Fe elements, which was 1.89×10^6 ppb in the spleen of a control mouse not administered with MNPs, whereas increases significantly to 1.93×10^6 ppb in that of a mouse administered with MNPs, as shown in Fig. 1. In addition, when MNP is present in the blood, it is confirmed that it is suitable for the living body in the serum toxicity assay.
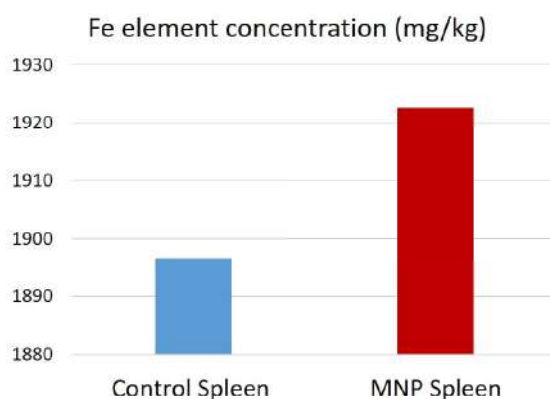
Fig. 2. Comparison of two concentrations of Fe elements in spleen of a control mouse not administered with MNPs, and that of a mouse administered with MNPs.

The sample preparation process for analysis of interferon gamma in spleen homogenate goes through the following 5 steps. ① Spleen tissues are homogenized in 1 mL distilled water using a tissue homogenizer. ② The 500 μL of the homogenates are used for ICP sample preparation. ③ The rest of the homogenates are centrifuged 10,000 rpm for 10 minutes and collect the supernatant. ④ Protein concentration is measured by BCA (bicinchoninic acid) protein assay. ⑤ ELISA is measured in 50 μL of the homogenate supernatant in duplicate. The protein assay of spleen tissue homogenates/Ab-MNPs conjugates and the IFN-gamma ELISA in spleen/plasma samples are analyzed in unit of pg/mg and pg/mL for days (1-30 days) after 300 μg MNP administration, respectively. From this research, we anticipate that anti-CD3 monoclonal antibody conjugated to magnetic nanoparticles can be utilized for the development of coronavirus immunotherapy.

References

[1] J. G. Choi, J. W. Ha, S. H. Choi, H. Lee, and S. S. Lee, J. Magn. 26, 448 (2021).

[2] M. Levy, N. Luciani, D. Alloyeau, and D. Elgrabli et al., Biomaterials 32 3988 (2011).

[3] J. M. Bennett, G. Reeves, G. E. Billman, and J. P. Sturmberg, Front. Med. 5, 316 (2018).

A Comparative Analysis of Metal Shielding for Computed Tomography Using Monte Carlo Simulation

Da-Eun Kwon[1*], Dong-Hee Han[1], Jang-Oh Kim[2], Kyung-Hwan Jung[1],
Seung-Jae Lee[3], Cheol-Ha Baek[1,2*]

[1]Department of Health Medical Science, Graduate School, Kangwon National University,
[2]Health and Medical Education Research Institute, Kangwon National University
[3]Department of Radiological Science, Dongseo University

When X-rays are irradiated by the patients, there is a risk of unnecessary exposure due to the interaction, in which radiation passes through the body. CT (Computed tomography) is an imaging technique that uses a higher tube voltage range and longer exposure time. NCRP160 reported that CT has the highest exposure dose compared to other radiological examinations [1]. Besides humans being continuously exposed to radiation, the risk includes acute effects such as erythema and genetic influence lead cell death, paralysis, or mutation by direct or indirect radiation. Therefore, it is necessary that patients are required to wear shielding equipment to protect against ionization radiation. However, most shielding equipment utilize Recently, lead-free shielding equipment is focused on the method of mixing the polymer with nanoparticle powder, which increases weight and thickness, and the most serious drawback causes pinholes, which have uneven shielding performance [2]. In this work, we evaluated the properties of lead-free materials and addressed the issue with the use of polymers, and the multilayered shielding structure was designed by GATE based on Monte Carlo simulation. The energy was 150 kVp, which is the maximum energy range for computed tomography, and concerning previous studies, lead-free materials were determined to be tin (Sn), tellurium (Te), tungsten (W), and bismuth (Bi). An optimized shielding sheet was considered by physical properties such as the atomic number, density, and kedge. In addition, by using the HDRK (High-Definition Reference Korea) female phantom, which is based on a standard Korean body type, the absorbed dose for each organ according to irradiation was evaluated, and the performance of the new shielding sheet was verified. The simulation results indicated that the weight of the multi-layered structure is reduced by up to 45% compared to the single structure option when these structures have the same shielding performance. The fact that verified physical properties of diverse materials and found out proper combination using a simulation is meaningful and expected to minimize unnecessary doses to patients and workers in the medical field with a lightweight apron.

References

[1] Li, Z., Zhou, W., Zhang, X., Gao, Y., Guo, S., 2021. High-efficiency, flexibility, and lead-free X-ray shielding multilayered polymer composites: layered structure design and shielding mechanism. Sci. Rep. 11, 1–13.

[2] Yu, L., Yap, P.L., Santos, A., Tran, D., Losic, D., 2021. Lightweight Bismuth Titanate ($Bi_4Ti_3O_{12}$) Nanoparticle-Epoxy Composite for Advanced Lead-Free X - ray Radiation Shielding.

Mössbauer studies of ^{57}Fe-N/C catalysts for active oxygen reduction reaction

Chaewon Lee[1,2*], Young Rang Uhm[1], Gwang Min Sun[1], Haein Choi-Yim[2]

[1]HANARO Utilization Division, Korea Atomic Energy Research Institute(KAERI) Yuseong Daejeon, 34057, South Korea

[2]Department of Applied Physics, Sookmyung Women's University, Seoul 04310, Korea

Research has been actively conducted on the synthesis and mechanisms of Fe-N/C catalysts, which correspond to Non-noble metal electrocatalysts, among catalysts to increase the efficiency of Electrochemical oxygen reduction reaction (ORR). Various techniques are used to synthesize catalysts, and e-beam irradiation is one of the effective technique in catalyst activity. Fe-N/C catalysts were synthesized using e-beam irradiation and ultrasonic irradiation and analyzed its properties using XPS, XRD and Mossbauer spectroscopy. The condition of e-beam irradiation for synthesis is 80 kGy for 3 minutes using e-beam energy of 10MeV and beam current of 800 μA. The ultrasonic irradiation was for 15 minutes. 1,10-phenanthroline which is useful to improve ORR activity was utilized to form the active site of Fe-Nx. Analysis of nitrogen structure types in XPS showed that pyridinic nitrogen was revealed approximately 33.4% in ultrasonic irradiation, and 66.7% in which conducted the e-beam irradiation. The presence of pyridinic nitrogen can improve ORR activity performance in catalysts. Fe-N4 sites are divided from D1 to D4 in Mossbauer spectroscopy measured at low temperature and room temperature, and it can be confirmed that intermediate spin Fe(II)N4(D2) contributes greatly to catalytic activity.

Development of Cadmium Telluride (CdTe) Gamma Detector for Mössbauer Spectrometer

Mingi Eom[1,2*], Young Rang Uhm[1], Jaegi Lee[1], Gwang-Min Sun[1]

[1]HANARO Utilization Division, Korea Atomic Energy Research Institute, Daejeon, 34057, Republic of Korea
[2]Department of Transdisciplinary Studies, Seoul National University Graduate School of Convergence and Technology, Seoul, 08826, Republic of Korea

Mössbauer spectrometer is one of the devices with the highest energy resolution in analyzing physical properties. The commercial Mössbauer spectrometer in Korea Atomic Energy Research Institute (KAERI) (Palacký Univ. Česko) is a transmission-type spectrometer that utilizes YAP:Ce scintillator to detect 14.4 keV gamma-rays. For non-destructive and *in-situ* measurement, a small-sized and scattering-type Mössbauer spectrometer is under development in KAERI. The cadmium-telluride (CdTe) detector will be the proper gamma counter for our objectives because it has a good gamma detection efficiency and is a small counter. The CdTe semiconductor developed in Acrorad (Japan) [1], which has a size of 1×1 mm^2, was adopted, and a suitable electric circuit was designed to detect gamma-rays from a ^{57}Co source. The preamplifier (CR-110) and shaping amplifier (CR-200) (Cremat, USA) were small enough to be designed on the compact PCV board. The reference electric circuits with these components in [2, 3] were modified to suit the CdTe detector. The simplified circuit diagram was tested using a high voltage power supply (Ortec 556, USA), as shown in **Figure 1**. The ^{137}Cs source was used to evaluate the capability of the CdTe gamma detection.
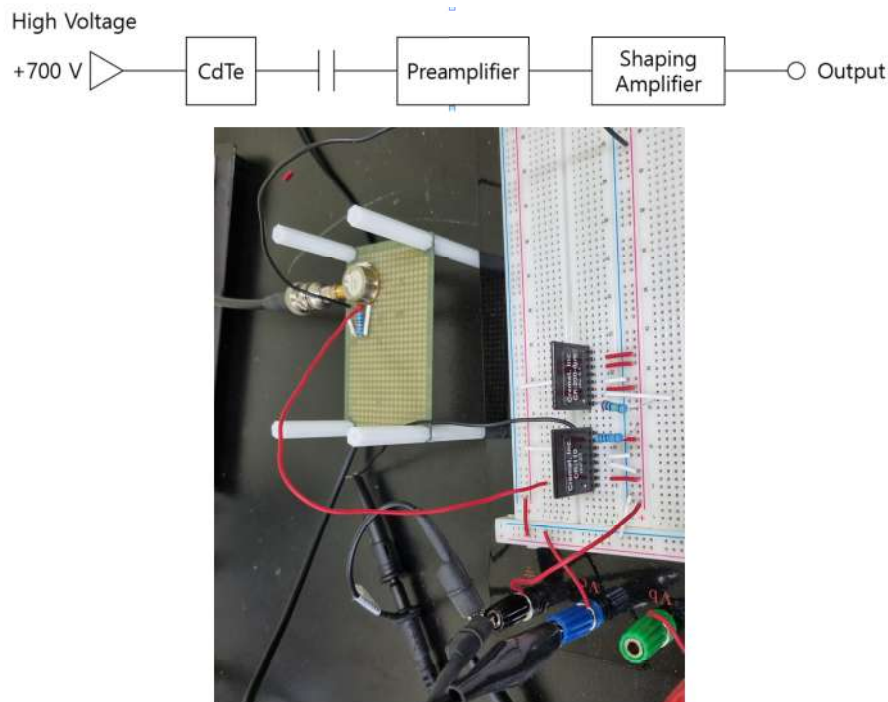
Figure 1. A simplified circuit diagram (upper) and
test of the CdTe detector using a high voltage power supply (down)

References

[1] Minoru Funaki, Yukio Ando, Ryuji Jinnai, Akira Tachibana and Ryoichi Ohno, Development of CdTe detectors in Acrorad, International Workshop on Semiconductor PET (2007)

[2] Pratip Mitra, Saurabh Srivastava, Mohit Tyagi, A Vinod Kumar and S C Gadkari, Development of a silicon photodiode-based compact gamma spectrometer using a $Gd_3Ga_3Al_2O_{12}$:Ce,B single crystal scintillator, Bull. Mater. Sci. 2019

[3] Specification Sheet of CR-110-R2.1 charge sensitive preamplifier, Creamt Inc. (2020) https://www.cremat.com/specification-sheets/

Great Enhancement of spin-orbit torque of [Co/Pd] reduced by proton irradiation

Beomseung Kang[*], Donghyeon Han[*], Sangho Lee, Jaegyu Jeong, Bogeun Jang, Jongill Hong

Materials Science and Engineering, Yonsei University, Seoul, 03722, Korea
[*]Both authors are equally contributed.

Spin-orbit-torque magnetic random-access memory (SOT-MRAM) requires strong perpendicular magnetic anisotropy (PMA) and large spin-Hall angle to satisfy high thermal stability and low power operating. A spin-Hall angle is defined as a ratio of charge current to spin current, which represents the efficiency of spin orbit torque.

Although Co/Pd thin films have strong PMA by adjusting the thickness of Co and/or Pd, they have been known as an unsuitable material for a SOT device because of the small spin-Hall angle of Pd. In this study, we have investigated the effect of irradiation of hydrogen ion on the electromagnetic properties and the spin-orbit torque in a paramagnetic oxidic [Co_3O_4/Pd] bilayer. The spin-Hall angle was evaluated by harmonic measurements and switching test.

The paramagnetic oxidic [Co_3O_4/Pd] can be reduced to the ferromagnetic metallic [Co/Pd] by hydrogen-ion irradiation. Surprisingly, it shows high PMA and large spin-orbit torque. The magnetization is switched by a current pulse of 1×10^7 A/cm^2. The reason for such a large spin-orbit torque in reduced [Co/Pd] is not a hydrogen-irradiation effect but is originated from the pseudomorphic growth of Co_3O_4 and from the tensile stress built up at Co/Pd interfaces. We believe that our reduced [Co/Pd] can be employed for SOT-MRAM due to the strong thermal stability and the large spin-Hall angle. In this presentation, we report the great enhancement of spin-orbit torque and the switching behavior of the reduced [Co/Pd] after applying the irradiation.
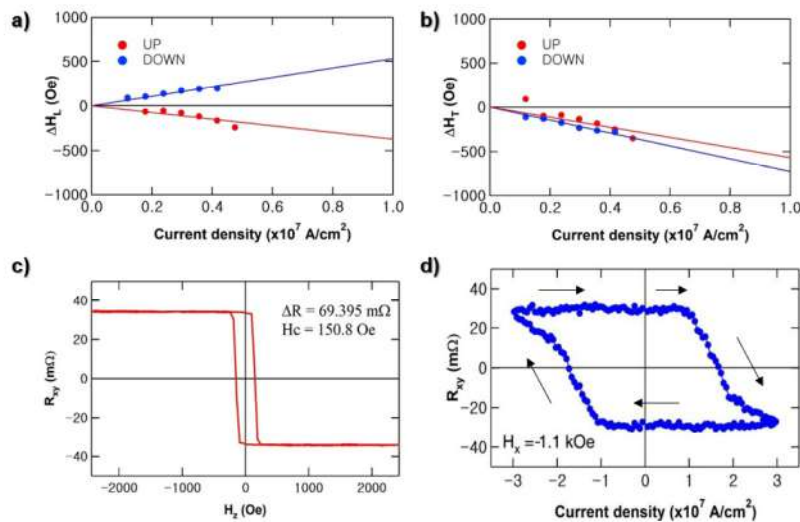
Fig. 1. a,b) The effective damping-like torque and field-like torque, respectively, evaluated by harmonic measurements. c) The Anomalous Hall effect of the reduced [Co/Pd]$_1$. d) The SOT switching under the assist field H_x of -1.1 kOe.

Composition Denpendence of Magnetic Properties of FePt- Ta$_2$O$_5$ Granular Films

Eunji Lim[1*], Donghyeon Lee[1], Nyunjong Lee[1], Jungmin Park[2], Sanghoon Kim[1]

[1]Department of Physics, University of Ulsan, Korea
[2]Department of Physics, Korea Advanced Institute of Science and Technology, Korea

For high-density recording media, one of the most important things is keeping decoupled information within only a few nm-sized magnetic objects with high thermal stability. Granular films such as FePt-X (X = Al$_2$O$_3$, C, TiO$_2$, Ta$_2$O$_5$) are magnetic systems in which nm-sized particles are embedded in an immiscible and insulating matrix. Having high thermal stability with strong perpendicular magnetic anisotropy, they are good candidates for the ultra-high data storage in hard disk drives (HDD). In this study, we investigate magnetic properties of FePt-Ta$_2$O$_5$ depending on volume fraction. The magnetic anisotropy of the film shows strong tunability by controlling volume fraction with small surface roughness under 2Å. Notably, when the Ta$_2$O$_5$ fraction is 30%, coercivity of the film becomes ~1T with highest PMA among the films with the volume fraction from 10% to 30%. Since this FePt-30% Ta$_2$O$_5$ with ~10 nm-sized magnetic particles has smooth surface and strong PMA, it can be a promising media material for the ultra-high density magnetic recording.

Keywords: Magnetic granular film, PMA

Reference

[1] J. S. Chen, B. C. Lim, Y. F. Ding, J. F. Hu, G. M. Chow, and G. Ju, "Granular L 1 0 FePt–X (X = C, TiO$_2$, Ta$_2$O$_5$) (001) nanocomposite films with small grain size for high density magnetic recording", Journal of Applied Physics 105, 2009

Observation of spin-orbit torque driven by orbital Hall effect in Ti/Co bilayer

Kyung-Hun Ko[1*†], Young-Gwan Choi[1†], Daegeun Jo[2†], Dongwook Go[3,4],
Kyung-Han Kim[2], Hee Gyum Park[5], Changyoung Kim[6,7], Byoung-Chul Min[5],
Gyung-Min Choi[1,8*] and Hyun-Woo Lee[2,9*]

[1]Department of Energy Science, Sungkyunkwan University, Suwon 16419, Korea
[2]Department of Physics, Pohang University of Science and Technology, Pohang 37673, Korea
[3]Peter Grunberg Institut and Institute for Advanced Simulation,
Forschungszentrum Julich and JARA, 52425 Julich, Germany
[4]Graduate School of Excellence Materials Science in Mainz, 55128 Mainz, Germany
[5]Center for Spintronics, Korea Institute of Science and Technology, Seoul 02972, Korea
[6]Department of Physics and Astronomy, Seoul National University, Seoul 08826, Korea
[7]Center for Correlated Electron Systems, Institute for Basic Science, Seoul 08826, Korea
[8]Center for Integrated Nanostructure Physics, Institute for Basic Science, Suwon 16419, Korea
[9]Asia Pacific Center for Theoretical Physics, 77 Cheongam-ro, Pohang 37673, Korea
[†]These authors equally contributed to this work.
★Correspondence to: gmchoi@skku.edu (G.-M. Choi), hwl@postech.ac.kr (H.-W. Lee)

Orbital Hall effect (OHE) is the transverse flow of orbital angular momentum induced by electric field. OHE has been expected to exist in wide range of materials including heavy and light metals. Despite its general occurrence, its experimental detection has been challenging because spin Hall effect (SHE) is often dominant over OHE in most heavy metals. In this work, we present experimental evidence of OHE by measuring spin-orbit torque (SOT) in Ti/Co bilayers, where a negligible spin-orbit coupling of Ti excludes SHE. We found that OHE of Ti induces a significant field-like torque on Co without damping-like torque. From the Ti thickness dependence of the field-like torque, we determine the orbital diffusion length of 56±22 nm and effective orbital Hall angle of -0.43±0.11 nm of Ti. Our experimental evidence of the OHE-driven SOT provides deeper understanding of the generation and transport of orbital angular momentum in light metals.

다양한 방향성을 가진 사파이어 기판에서 성장된 Mn₃Sn 박막에서 자성특성의 결정학적 연구

임수빈[1*], 이동현[1], 한동현[3], Thanh Huong Thi Nguyen[4], 이년종[1], 박정민[2], 박병국[3], 김상훈[1]

[1]울산대학교 물리학과
[2]한국과학기술원 물리학과
[3]한국과학기술원 신소재공학과
[4]대구경북과학기술원 물리학과

비 공선형(non-collinear) 반 강자성체(antiferromagnet)로 알려져 있는 Mn₃X (X=Ga, Ge, 그리고 Sn) 화합물은 Kagome 격자라고 불리는 120°의 스핀 구조를 가진다. 특히, Mn₃Sn은 자화 용이 축인 (0001) c-평면을 따라 약 0.002_B/Mn의 매우 작은 자기모멘트를 가짐에도 불구하고 향상된 베리 곡률에 의해 나타나는 비 이상적인 홀 효과를 크게 관찰할 수 있다 [1]. 여기에서, 베리 곡률은 자기장의 역할과 비슷하게 작용한다 [2]. 그러므로 바일 반금속으로 알려져 있는 Mn₃Sn은 역 삼각형 스핀 구조를 가지는 비 공선형 반 강자성체의 중요한 대표자이며, 스핀트로닉스를 포함해서 다양한 적용에 유용할 수 있다 [1].

이번 연구에서, 우리는 다양한 방향성을 가진 사파이어 기판에서 성장된 Mn₃Sn 박막의 자기적 특성에 대해 연구한다. 다결정 Mn₃Sn 박막은 마그네트론 스퍼터링 시스템을 이용하여 c-, 그리고 m-평면 사파이어 기판에서 증착 되었다. c-, 그리고 m-평면 사파이어 기판에서 증착된 Mn₃Sn 박막의 비 이상적 홀 전도도 (σ_{xy})는 각각 ~0.133 Ω^{-1} cm⁻¹ 그리고 ~6.00 Ω^{-1} cm⁻¹의 값을 가진다. 우리는 TEM을 이용하여 결정학적 분석을 통해 Mn₃Sn 박막에서의 비 이상적 홀 전도도의 차이를 설명할 것이다.

References

[1] Satoru Nakatsuji, Naoki Kiyohara, and Tomoya Higo, "Large anomalous Hall effect in a non-collinear antiferromagnet at room temperature", *Nature*, 527, 212-215 (2015)

[2] Seungjun Oh, Tadashi Morita, Tomiki Ikeda, Masakiyo Tsunoda, Mikihiko Oogane, and Yasuo Ando, "Controlled growth and magnetic property of a-plane-oriented Mn₃Sn thin films", *AIP Adv.*, 9, 035109 (2019)

Nonreciprocal Charge Transport in an InAs Quantum Well Structure

Jeong Ung Ahn[1,2*], Ki Hyuk Han[1,2], Seong Been Kim[1,2], OukJae Lee[2],
Hyung-jun Kim[2], Hyun Cheol Koo[1,2]

[1]KU-KIST Graduate School of Converging Science and Technology, Korea University, Seoul 02841, Korea
[2]Center for Spintronics, Korea Institute of Science and Technology, Seoul 02792, Korea

The Rashba effect is one of the major topics of spintronics since the spin information can be manipulated by spin-orbit coupling, so it has been studied in diverse systems such as topological insulators, semi-metals, and quantum wells. Especially, the Rashba quantum well structure is one of the promising systems because the spin information can be controlled by electric field. Stacking structure and carrier doping profile of the quantum well cause inversion symmetry breaking and subsequent internal electric field. In this structure, the nonreciprocal charge transport is expected to exist and crucial to control spintronic device. Since the Rashba effect and nonreciprocity are associated with spin-orbit interaction and unidirectional magnetoresistance (UMR), the magnitude of nonreciprocal charge transport is expected to be related to the strength of the Rashba spin-orbit field. However, the relationship between nonreciprocal coefficient and Rashba parameter has not been explored yet. In this research, we investigated the temperature dependence of nonreciprocal charge transport using harmonic Hall measurement. We also compare the Rashba parameter and nonreciprocal coefficient in this system. To explore the nonreciprocity of the Rashba channel, an InAs-based two-dimensional electron gas (2DEG) channel was epitaxially grown by molecular beam epitaxy (MBE). This channel was patterned into a Hall bar structure with 15 channel width using conventional photolithography and Ar-ion milling and we executed angular dependent harmonic Hall measurements. We measured the angular dependent second harmonic Hall resistance ($R_{2\omega}$) over a temperature range of 1.9 to 300 K at a fixed magnetic field $B = 8$ T and injected current density $j = 3.3 \times 10^5$ Acm^{-2} and nonreciprocal charge transport was detected for an entire temperature range. The nonreciprocal coefficient γ in the 2DEG channel was extracted using $\gamma = 2\Delta R_{2\omega} /(R_0 BI)$, where $\Delta R_{2\omega}$, R_0, B, and I are the amplitude of the angular dependent $R_{2\omega}$, resistance at zero magnetic field, applied magnetic field and injected current into the channel, respectively. In addition, we performed Shubnikov-de Haas (SdH) oscillation and potentiometric measurement to evaluate the Rashba parameter of the InAs quantum well channel. Fig. 1 illustrates nonreciprocal coefficient and Rashba parameter as a function of temperature. As shown in Fig. 1, the two factors have similar tendency to decrease with increasing temperature.
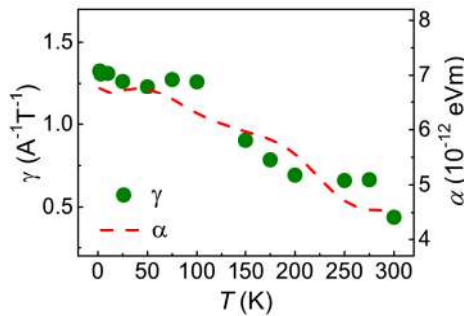
Fig. 1. Temperature dependence of nonreciprocal coefficient and Rashba parameter

Measurement of spin-orbit torque in Bi/CoFeB bilayer

Sumin Kim[1*], Liu Jian[1], Kyung-Hun Ko[1] and Gyung-Min Choi[1,2†]

[1]Department of Energy Science, Sungkyunkwan University, Suwon 16419, Korea
[2]Center for Integrated Nanostructure Physics, Institute for Basic Science, Suwon 16419, Korea

A low power consumption becomes a critical issue for the future memory technology. Magnetic memory, which employs a ferromagnetic metal as a data saver, is promising because of its nonvolatile property. For operation of magnetic memory, charge current should be converted to spin current. Accordingly, charge-to-spin conversion efficiency determines the power consumption of the magnetic memory. A non-magnetic heavy metal, such as Pt or Ta, is known to have a high conversion efficiency *via* spin Hall effect, and charge current in heavy metal induces spin-orbit torque on a ferromagnetic metal. Recently, it has been reported that topological insulators and semimetals can induce spin-orbit torque *via* spin-momentum locking at topological surfaces. In this work, we experimentally investigate the spin-orbit torque in a heterostructure of Bi, which is a topologically nontrivial semi-metal, and CoFeB, which is a ferromagnetic metal, using magneto-optical Kerr effect. We discuss the connection between the spin-orbit torque and topological property of Bi.

Engineering large Rashba spin-orbit-coupling 2DEG structure using doping control

Seong Been Kim[1,2*], Hansung Kim[1,2], Hyung-Jun Kim[2], Hyun Cheol Koo[1,2]

[1]Korea University, KU-KIST Graduate School of Converging Science and Technology,
Seoul, Seongbuk-gu, Republic of Korea

[2]Korea Institute of Science and Technology, Center for Spintronics, Seoul, Seongbuk-gu, Republic of Korea

The spin transistor proposed by Datta and Das has given a great interest in the field of semiconductor device, because of fast operation speed, low power consumption, and nonvolatile characteristics. However, it needs to overcome some problems such as low spin injection efficiency, and low operation temperature for the application to electronics. We proposed the spin injection and detection using spin Hall effect and Inverse spin Hall effect are solutions for low spin injection efficiency in a previous work[1]. However, the low operation temperature issue is still remained. The development strong Rashba spin-orbit-coupling(SOC) channel can be solution for this problem. In previous study[1], we utilized one side doping 2-dimensional electron gas (2DEG) structure which has a carrier supply layer below quantum well as spin transistor channel.

In this study, we grew 2DEG structure with a large Rashba SOC by adapting high doping concentration. This channel system contains both hole and electron doping layers above and below quantum well, respectively. The 2DEG structure consists of an $In_{0.52}Al_{0.48}As$ buffer layer (300 nm), an $In_{0.52}Al_{0.48}As$ n-doped (1×10^{19} cm^{-3}) layer (7 nm), an $In_{0.52}Al_{0.48}As$ layer (6 nm), an $In_{0.53}Ga_{0.47}As$ layer (8 nm), an layer (2 nm) as InAs quantum well channel, $In_{0.53}Ga_{0.47}As$ layer (8), an $In_{0.52}Al_{0.48}As$ layer (6 nm), an $In_{0.52}Al_{0.48}As$ p-doped (1×10^{19} cm^{-3}) layer (7 nm), an $In_{0.52}Al_{0.48}As$ layer (20 nm) and an InAs capping layer (2 nm). We calculated band diagram from poison solver simulation program (wingreen simulator), and It could be expected that double side high doping 2DEG has a large Rashba SOC. From the Shubnikov-de Haas(SdH) measurements, we has confirmed that the double side doping 2DEG has 70 % larger Rashba constant than the one side doping 2DEG. The Rashba constants are 4×10^{18} cm^{-2} and 1×10^{19} cm^{-2} at the one side doping and double side doping, respectively. Furthermore, we observed spin-orbit parameter (Rashba constant, α) as a function of gate voltages as shown in Figure 1.
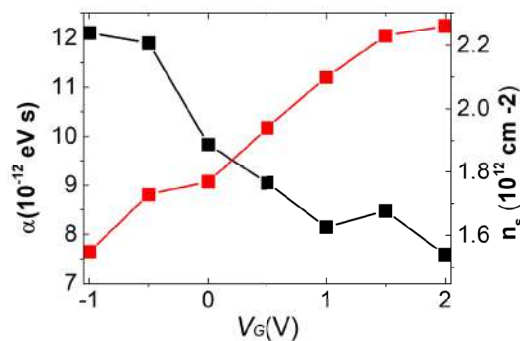
Fig. 1. Rashba constant (α) and carrier concentration(ns) as function of gate voltages of double side high doping quantum well 2DEG.

Reference

[1] W. Y. Choi, H-j, Kim, J. Chang, S. H. Han, A. Abbout.: Ferromagnet-Free All-Electric Spin Hall Transistors. Nano lett . 2018, 18, 7998-8002

Enhanced photon collection from diamond nitrogen vacancy through nano-pillar fabrication

HyunTae Kwon[1,2*], SeungHun Jang[1], Chaun Jang[1], SangWon Oh[3], OukJae Lee[1]

[1]Center for Spintronics, Korea Institute of Science and Technology
[2]Program in Micro/Nano System, Korea University
[3]Korea Research Institute of Standards and Science

Diamond is a promising system for physics and quantum application owing to their impurities in solid state. The impurities of diamond's crystal have superb spin coherence and spin-dependent optical properties at room temperature. Recent, diamond nitrogen-vacancy center has been developed for hyperpolarization application in quantum sensing. In particular, negatively charged nitrogen-vacancy centers can utilize as single NV centers and it can be used in high resolution sensing such as magnetic field, strain and temperature. To enhance diamond's photon collection, surface micro and nano patterning techniques can improve the optical interface to single photoluminescence than bulk diamond. In this presentation, we report our approach to fabricate high-aspect-ratio nano-pillar arrays on the CVD-single crystal diamond plate by e-beam lithography(EBL) and inductively coupled plasma(ICP) etching technique.

Fabrication and Implementation of stochastic MTJ for probabilistic computing

Ki-hyuk Han[1,3*], Young-jun Nah[2,3], Taeyueb Kim[3], Oukjae Lee[3], Seokmin Hong[3], Byoung-Chul Min[3] and Hyun Cheol Koo[1,3*]

[1]KU-KIST Graduate School of Converging Science and Technology, Korea University, Seoul 02841, South Korea
[2]Department of Materials Science and Engineering, Korea University, Seoul 02841, South Korea
[3]Center for Spintronics, Korea Institute of Science and Technology, Seoul 02792, South Korea

Recently, a new computing method called probabilistic computing shows a promising candidate to provide novel non-Boolean computing schemes. The p-bit is at the heart of the p-computing because the system is composed of many individual p-bits. Therefore, it is very essential to implement the p-bit in a nanoscale device as well as to understand its underlying physics. One of promising candidates to play the role of p-bit is MTJ (magnetic tunnel junction). Typical MTJ contains a magnetic free layer (FL) in which its magnetic direction can be parallel state(P) or anti-parallel state(AP) to that of a magnetic reference layer (RL) and these states are separated by energy barrier by magnetic anisotropy. The randomness in a MTJ cell can be achieved at room temperature by making it circular-like shape to reduce shape anisotropy, so that the thermal fluctuation activates magnetic switching between P and AP.

We fabricated stochastic MTJ and tested the tunability of p-bit by electrical dc current (I_{DC}). The requirement for a p-bit is an ability to change the relative probability of P and AP thus achieving sigmoidal or hyperbolic tangent output characteristics after averaging digitized signals. With the applied current of 20 μA more than 90% of skewed probability was obtained. We believe that our fabricated MTJ device shows a promising candidate for p-bit that can work in an invertible mode in Boolean logic function. Further optimizations of in-plane based MTJ can show an order of magnitude improvement in the correlation time of random signal resulting in a significant improvement of p-computing speed.
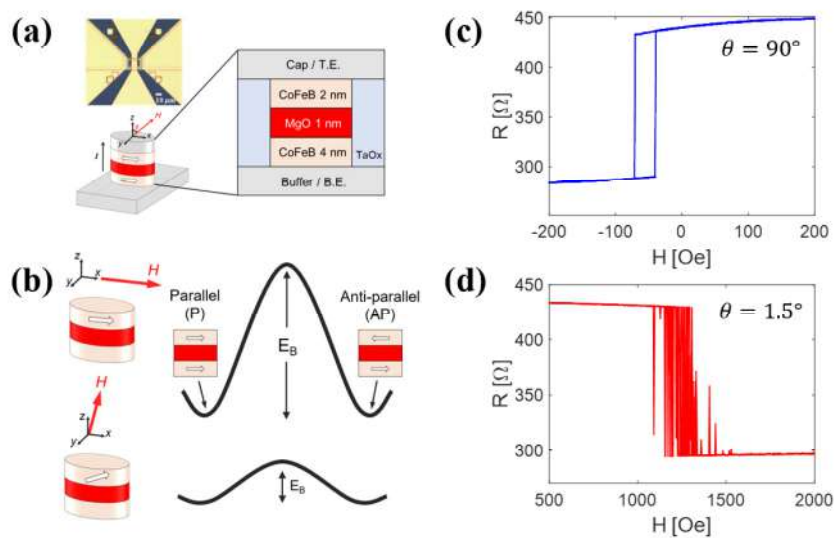
Reconfigurable logic devices operated by spin-orbit torques

Hanwool Seong[1,2*], Min-Seung Jung[1], Joonhyun Kwon[1], Seokmin Hong[1], Kyoung-Whan Kim[1], OukJae Lee[1], Byoung-Chul Min[1], Hyun Cheol Koo[1], Dong-Soo Han[1*]

[1]Center for Spintronics, Korea Institute for Science and Technology (KIST), Seoul, Republic of Korea
[2]Department of Materials Science and Engineering, Yonsei University, Seoul, Republic of Korea
*email: dshan@kist.re.kr

The explosive growth in highly data-centric applications calls for the development of technologies to overcome limitations of latency and energy cost associated with data transfer in von Neumann architecture. To mitigate the addressed issue, nonvolatile memory-based computation namely in-memory computing is attracting great interest in the relevant community [1,2]. In particular, magnetic random memory (MRAM) is considered a promising candidate for the in-memory computing primitive due to its advantages in fast operation, CMOS compatibility, high energy efficiency, and scalability. [3-5] In line with the quest for the in-memory computing primitive, we present an experimental demonstration of reconfigurable logic operations using spin-orbit torque (SOT) magnetic memory devices. AND and OR gates are realized by using two magnetic tunnel junctions (MTJs) of which the magnetization states can be independently written by two separate input currents. In addition, by flipping the magnetizations in reference layers, the AND and OR gates can be reconfigured into NOR and NAND gates, respectively. This result will pave the way toward fast and energy-efficient memory and computing in the logic-in-memory architecture.

Reference

[1] V. K. Sangwan and M. C. Hersam, *Nat. Nanotech.* **15**, 517 (2020)

[2] A. Sebastian et al., *Nat. Nanotech.* **15**, 529 (2020)

[3] S. Angizi, Z. He, A. Awad, and D. Fan, IEEE Transactions on Computer-Aided Design of Integrated Circuits and Systems, (2019)

[4] S. Jung et al., *Nature* **601**, 211 (2022)

[5] G. Lim, et al., *Adv. Electron. Mater.* **6**, 1901090 (2020)

Memory Application of Spin-charge Conversion Effect with Graphene van der Waals Heterostructure using Tunable Ferroelectric Gating

Woohyeon Ryu[*], Minjeong Shin, Bae Ho Park

Division of Quantum Phases and Devices, Department of Physics, Konkuk university, Korea

High speed opertion and low power consumption properties of spin based memory and logic devices are the promising advantages for the future artificial intelligence systems. The main technology of these spin-based system so far is the use of strong spin orbit interaction and broken inversion symmetry of heavy metals and heterostructure of metals and oxides. However, despite the various studies about interfacial effects between diverse materials like transition metal dichacoginides(TMDs), topological insulators(TI) and Weyl semimetals, the conversion between spin-charge current under biased electrical gating condition forbid its use as a memory application.

In this study, as a previous step to make a use of spin-charge conversion as a memory application, we study the electrical gate tunability of graphene and $Mo_{0.5}W_{0.5}Te_2$ van der Waals heterostructure. The electrical carrier modulation of the heterostructure allow us to control the spin texture of the interface of the van der Waals heterostructure via spin-galvanic effect. Further, a introduce of ferroelectric materials to the van der Waals heterostructure will enable the conversion between spin current and charge current to occur under ferroelectric gated condition which resolves the problem that were preventing memory application of practical spin-charge conversion devices.

Anomalous Velocity Increment of Magnetic Domain Wall on Ultrathin Ferromagnetic Film with Perpendicular Magnetic Anisotropy

Ganghwi Kim[*], Dae-Han Jung, Ki-Suk Lee

School of Materials Science and Engineering, Ulsan National Institute of Science and Technology, Ulsan, Republic of Korea

Magnetic domain wall has been actively studied due to their spintronic applications, such as a racetrack memory [1,2] and neuromorphic devices [3]. Since these devices require control of the behavior of the domain wall under external forces, it is essential to understand their dynamics [2]. On a perpendicular magnetic anisotropy (PMA) nanostrip, the domain wall shows two different dynamic regimes based on the out-of-plane external magnetic field strength: under a low field, the domain wall moves at a steady velocity, but above the Walker breakdown field [4], the domain wall oscillates back and forth. In both regimes, domain wall velocity is proportional to the strength of the magnetic field but with a different proportion ratio.

This study reports the anomalous domain wall velocity increment above the Walker breakdown field based on micromagnetic simulations. As a model system, we employed a Co/Pt monolayer in the shape of a narrow nanowire where a domain wall is located at the center of the strip and applied an out-of-plane magnetic field to observe the dynamic behavior of the domain wall motion. From the simulation results in the wide range of the magnetic field strength, we find that the domain wall shows typical behaviors in both regimes. However, in some specific field strengths, the velocity enhances dramatically, and these field strengths show some harmonic behaviors – higher field strength values are integer multiples of the lowest field strength. We find that these anomalous increments directly relate to the internal domain wall structure vibration [5], which forms the standing wave along the width direction of the nanostrip. Moreover, we find that the frequency of the standing wave is directly proportional to the strength of the external field. Consequently, it gives rise to the harmonic behaviors of the anomalous velocity increment with the field strength. The presentation will discuss the field-dependent internal domain wall mode excitation and its role in the domain wall motion.

References

[1] S. S. P. Parkin. Shiftable magnetic shift register and method of using the same. US patent 6,834,005 (2004)

[2] S. S. P. Parkin, M. Hayashi. & L. Thomas, *Science* **320**, 190–194 (2008)

[3] N. Hassan, X. Hu, L. Jiang-Wei, et al. *J. Appl. Phys.* **124**, 152127 (2018)

[4] A. Mougin, et al. *EPL* **78**, 57007 (2007)

[5] J. Slonczewski, *J. Magn. Magn. Mater.* **23**, 305 (1981).

Magnetic and Magnetocaloric behavior of ɤ-Fe$_{100-x}$Ni$_x$ binary alloys

Mohit K. Sharma[1*], Akshay Kumar[1], Kavita Kumari[2], Sujeong Park[3], Naveen Yadav[3], B.H. Koo[4†]

[1]Mechatronics Research Institute, Changwon National University, Changwon, Gyeongnam, 51140, Republic of Korea
[2]Industrial Technology Research Institute, Changwon National University,
Changwon, Gyeongnam, 51140, Republic of Korea
[3]Department of Materials Convergence and System Engineering, Changwon National University,
Changwon, Gyeongnam, 51140, Republic of Korea
[4]School of Materials Science and Engineering, Changwon National University,
Changwon, Gyeongnam, 51140, Republic of Korea
[*]Corresponding Author - bhkoo@changwon.ac.kr

Fe-Ni based binary alloys have great attention due to their relevant electrical and magnetic properties. In the present study, our goal is to investigate the effect of Ni substitution at the Fe site on the magnetic and magnetocaloric behaviour of γ Fe-Ni alloys. Fe$_{100-x}$Ni$_x$ ($0 \leq x \leq 80$) alloy prepared by ball milling technique and characterized by X-ray diffraction, temperature and field-dependent magnetic, and magnetocaloric studies. Rietveld's refinement of the sample confirmed the gamma cubic structure Fm-3m space group. Morphology and elemental composition are confirmed by scanning electron microscopy (SEM) and Energy dispersive spectroscopy (EDS). The magnetocaloric effect; as isothermal magnetic entropy change (ΔS_M), is calculated from magnetic isotherms. Our investigation revealed the alloy undergoes two transitions low temperature and high temperature region. These alloys show a significant ΔS_M value above room temperature. Our results establish that Ni substitution can be used to tune the magnetic and magnetocaloric effect in these binary alloys.

Keywords: Structural properties, Magnetic properties, Magnetocaloric properties, γ-Fe-Ni based alloys

Ferromagnetic Resonance (FMR) measurements on bulk Yttrium Iron Garnet (YIG)

Joon Woo Lee[1*], Nyun Jong Lee[2], Thanh Huong Thi Nguyen[3], Jun-Su Kim[3], Chun-Yeol You[3], Jung-Il Hong[3], Sanghoon Kim[2], Yoon Seok Oh[1*]

[1]Department of Physics, Ulsan National Institute of Science and Technology (UNIST), Ulsan, Korea
[2]Department of Physics, University of Ulsan, Ulsan, Korea
[3]Department of Physics and Chemistry, Daegu Gyeongbuk Institute of Science and Technology, Daegu, Korea

The angular moment of the magnetic moment induces precession of the magnetic moment. The precession leads to a resonance phenomenon by irradiated electromagnetic waves, so-called Ferromagnetic Resonance (FMR). The FMR measurement technique has been widely used to study the dynamic properties of spin. Most FMR experiments have been conducted on ferromagnetic thin films. On the other hand, except for initial studies of FMR, there have been few studies of FMR experiments on bulk magnetic materials. We aimed to find an optimal condition of the sample preparation for FMR measurement on bulk Yttrium Iron Garnet (YIG). In this talk, we will present our systematic studies of geometry, crystallinity, and morphology dependence on FMR of bulk YIG.

Direct Observation of Multi-level Switching behavior in the Multi-layered ferromagnetic thin film

Pyeong-Yeol Yu[*], Myeonghwan Kang, Sooseok Lee, Dae-Han Jung, Hye-Jin Ok,
Gang Hwi Kim, Suyeong Jeong, Younggun Park, Ki-Suk Lee[†]

Department of Materials Science and Engineering, Ulsan National Institute of Science and Technology,
Ulsan, Republic of Korea

In recent years, Pt/Co multilayer structure with perpendicular magnetic anisotropy (PMA) have been investigated to use various spintronic devices such as magnetic random access memories and multi-level recording applications [1-3]. Their systems usually consist of more than two ferromagnetic layers separated by the thin non-magnetic materials, multiple vertically stacked structures. The magnetization reversal process of the ferromagnetic layer in multilayer structure is influenced by the stray field from the other magnetically coupled as well as the neighboring non-magnetic layer [4-5]. In order to utilize the multilayered structure as a spintronic device, understanding the magnetization reversal behavior accompanied by domain wall driven motion is an essential prerequisite [6-7].

In this presentation, we report direct observation of field driven motion and multi-level switching in $[Pt/Co]_2$ films with PMA. The Ta (20 nm)/ Pt (3 nm)/ Co (0.9 nm)/ Pt (5 nm)/ Co (0.65 nm)/ Pt (3 nm) structure was deposited by magnetron sputtering at room temperature. We observed the multi-level switching behavior by the external magnetic fields using the magneto optical microscope in the multi-layered film. In this system, the spacer layer is thick enough to decrease the magnetostatic interaction between the ferromagnetic layers, which exhibit different switching fields [8]. We achieved the multi-level states and confirmed that the magnetic domain is stably remained under the absence of the external magnetic field. We provide an understanding of magnetic switching by directly observing the processes of domain nucleation and domain wall propagation in multi-layered films.
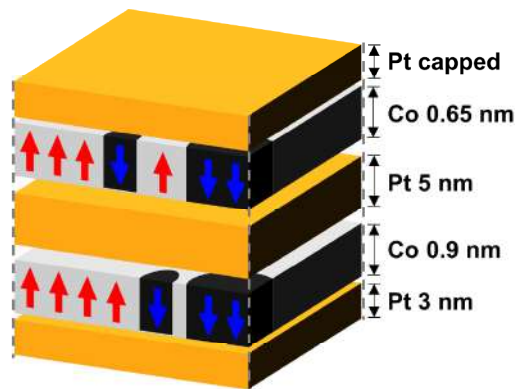
Fig. 1. Sketch of [PtCo]2 film with PMA.
Red, blue arrow represent up, down magnetization direction, respectively.

References

[1] Chappert, C., Fert, A. & Van Dau, F, Nature Mater 6, 813–823 (2007).

[2] Žutić J, Fabian J and9 Sarma S D, Rev. Mod. Phys. 76 323 (2004).

[3] Lequeux, S., Sampaio, J., Cros, V. et al, Sci Rep 6, 31510 (2016).

[4] Lim S, Tran M, Wang C, Ying J and Han G, J. Appl. Phys. 117, 17A731 (2015).

[5] M. Robinson, Y. Au, J. W. Knepper, F. Y. Yang, and R. Sooryakumar, Phys. Rev. B 73, 224422 (2006).

[6] L. San Emeterio Alvarez, K.-Y. Wang. et al, Phys. Rev. Lett. 104, 137205 (2010).

[7] F. Cayssol, D. Ravelosona, C. Chappert, J. Ferré, and J. P. Jamet, Phys. Rev. Lett. 92, 107202 (2004).

[8] Peter.J.Metaxas, Solid State Phys, Vol. 62, pp. 75-162 (2010).

Structural, magnetic and magnetocaloric properties of mechanically alloyed iron chromium alloy

Naveen Yadav[1*], Akshay Kumar[2], Mohit K. Sharma[2], Kavita Kumari[2],
Seok Hwan Huh[3] and Bon Heun Koo[4]

[1]Department of Materials Convergence and System Engineering, Changwon National University,
Changwon, Gyeongnam, 51140, Republic of Korea
[2]Mechatronics Research Institute, Changwon National University, Changwon, Gyeongnam, 51140, Republic of Korea
[3]Industrial Technology Research Institute, Changwon National University,
Changwon, Gyeongnam, 51140, Republic of Korea
[4]Department of Mechatronics Conversion Engineering, Changwon National University,
Changwon, Gyeongnam, 51140, Republic of Korea
[5]School of Materials Science and Engineering, Changwon National University,
Changwon, Gyeongnam, 51140, Republic of Korea
*Corresponding Author - *bhkoo@changwon.ac.kr*

Magnetic materials experience a change in temperature when they are adiabatically magnetized and demagnetized, this phenomenon is known as magnetocaloric effect (MCE). Magnetocaloric refrigeration is one of the most suitable technique due to its high efficiency and environmentally friendly nature. The iron-based Fe-Cr alloy is an excellent candidate to use in the magnetocaloric refrigeration devices due to its high magnetocaloric properties. The $Fe_{1-x}Cr_x$ samples were synthesized using the planetary ball milling technique. The effect of different milling speeds (200-600 rpm), milling time (18-48 hour), surfactants (Hexane, Toluene), ball to powder ratio and size of balls are studied in this work. The structural, magnetic and magnetocaloric properties of the prepared samples were investigated through various characterization techniques which include x-ray diffraction, scanning electron microscope and physical property measurement system.

Keywords: FeCr, Ball milling, Magnetocaloric effect

Sub-GHz frequency response of anomalous Nernst effect in the NiFe block with sinusoidal laser pulses

Seungha Yoon[*]

Green energy and nano technology R&D group, Korea Institute of Industrial Technology, Gwangju, South Korea

Because the anomalous Nernst effect (ANE) involves the effective electric field generated by the combination between the thermal gradient and the magnetization direction, it has been well applied to not only the measurement of the static magnetization but also the experiment for the low frequency magnetization dynamics. In this work, the frequency response of the ANE was examined to provide two implications: First, as a method to separate Nernst effects from other signals in the homodyne or heterodyne method, and second, as a timing reference to the phase-sensitive magnetization dynamics. The intensity of 1550 nm laser power was modulated up to 2.4 GHz and successfully produced the equivalent speed of the ANE signals from the 10 nm Permalloy block on the sapphire substrate. The implications could be supported, when the detection system consists of well-designed radio frequency components and the better heat sink substrate to get the faster thermal gradient on the magnets.

Ni_xFe_{1-x} thin films for magnetostriction effect

Nayeon Kim[*], Seungha Yoon[†]

Green Energy & Nano Technology R&D Group, Korea Institute of Industrial Technology,
Gwangju, 61012, South Korea

Flexible electronics has been widely studied for the future applications, such as flexible display, wearable health care device and electronic skin for robots [1-2]. In particular, the stress effect on the thin film is a key element to develop magnetic sensors and actuators. Permalloy is well known material for the flexible applications due to its very low magnetostriction under the forces [3]. In this study, we have been measured the residual stress effect on the NixFe1-x thin films, when the composition of Ni varies under the tensile and compressive stress along the magnetic field direction. The details of the experimental results will be discussed.

References

[1] A. Nathan, A. Ahnood, M.T. Cole, S. Lee, Y. Suzuki, P. Hiralal, F. Bonaccorso, T. Hasan, L. Garcia-Gancedo, A. Dyadyusha, S. Haque, P. Andrew, S. Hofmann, J. Moultrie, D. Chu, A.J. Flewitt, A.C. Ferrari, M.J. Kelly, J. Robertson, G.A.J. Amaratunga, and W.I. Milne, Proc. IEEE 100, 1486 (2012).

[2] R. Dahiya, N. Yogeswaran, F. Liu, L. Manjakkal, E. Burdet, V. Hayward, and H. Jörntell, Proc. IEEE 107, 2016 (2019).

[3] R. Bonin, M. Schneider, T. Silva, and J. Nibarger, J. Appl. Phys. - J APPL PHYS 98, (2005).

Topological Hall effect in a mixed phase of Mn$_3$Ga thin film

Won-Young Choi[1,2*], Hyun-Woo Bang[1], Woosuk Yoo[1], Yunchang Park[3] and Myung-Hwa Jung[1]

[1]Department of Physics, Sogang University, Seoul 04107, Republic of Korea
[2]Center for Spintronics, Korea Institute of Science and Technology, Seoul 02792, Republic of Korea
[3]National NanoFab Center, Daejeon 34141, Republic of Korea

Mn$_3$Ga, one of the Heusler alloys, is an interesting material showing magnetic and structural phase transition from ferrimagnetic tetragonal with perpendicular magnetic anisotropy to antiferromagnetic cubic depending on atomic kinetic energy during growth [1]. Although there have been a lot of previous researches for each structural phase of Mn$_3$Ga, there is no report for the critical regime where the phase transition occurs [2-3]. Therefore, we focus on the structural and magnetic properties around the critical regime. We fabricated the Mn$_3$Ga films by using magnetron sputtering system, and we investigated the structural phase by using X-ray diffraction (XRD) pattern and high-resolution transmission electron microscope (HR-TEM). The results revealed that distinct three layers are formed depending on the total thickness of deposited Mn$_3$Ga film at critical regime. For the thickness up to 1 nm, we observed only cubic phase. If the total thickness increases above 1 nm, the tetragonal phase emerges on the top of the cubic phase. Remarkably, we observed a cubic-tetragonal mixed phase, which is formed between the cubic phase layer and the tetragonal phase layer. By analyzing the magnetic and electrical transport properties, we found that there is additional hump-like Hall contribution, which resembles topological Hall effect (THE) signal even at room temperature. Furthermore, through a comparative analysis between the mixed phase film and the tetragonal Mn$_3$Ga/cubic Mn$_3$Ga bilayer film, we deduced that THE is attributed to the mixed phase. We expect our study to bring a deeper understanding of the emergence of THE at the critical point.
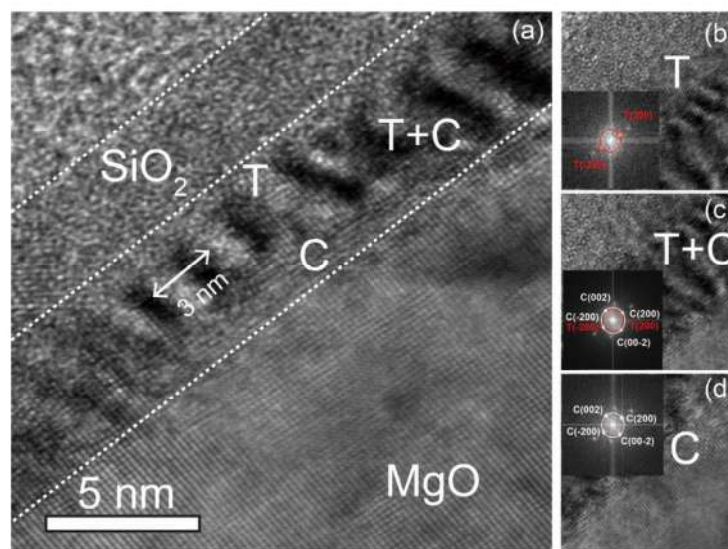
Fig. 1. (a) TEM images for Mn3Ga deposited at critical regime. (b)-(d) Enlarged images for each structural phase. Inset shows corresponding ED pattern images.

References

[1] Bang, H.-W. *et al.*, *Appl Phys Lett* 115, 012402 (2019).

[2] Bang, H.-W. *et al.*, *Curr Appl Phys* 16, 63–67 (2016).

[3] Jang, Y. *et al.*, *J Alloy Compd* 810, 151988 (2019).

Switching of Skyrmion Polarity in Perpendicular Magnetic Anisotropy Multilayer System

Myeonghwan Kang[1*], Hee-Sung Han[1,2], Sooseok Lee[1], Hye-Jin Ok[1],
Weilun Chao[2], Mi-Young Im[2] and Ki-Suk Lee[1†]

[1]Ulsan National Institute of Science and Technology, Korea
[2]Advanced Light Source, Lawrence Berkeley National Laboratory, USA

Skyrmion is a topologically non-trivial spin structure in ferromagnetic materials. Owing to its tiny size and high stability guaranteed by its non-trivial topology, the skyrmion has been considered as a promising information carrier in the next-generation spintronic device [1]. For the device application, it has been intensely studied to control the physical quantities such as position and velocity of skyrmions and to design skyrmion-based devices. However, most studies are achieved by theoretical approaches or numerical calculation in ideal condition, and the functionality of skyrmion-based device has not experimentally been demonstrated yet. Recently, its generation and current driven motion have been observed at room temperature [2,3,4]. For skyrmion-based data storage, the controlled switching between skyrmion states of opposite polarity is essential. In this works, we directly observe in Pt/Co/Ta multilayer, pulsed current can drive transitions between skyrmion states of opposite polarity with same energy states by utilizing magnetic transmission soft X-ray microscopy (MTXM). For example, at +Hz magnetic field, up skyrmion state becomes favorable relative to the down skyrmion, but switching is prevented by energy barrier. The effect of pulsed current and slight -Hz magnetic field reduces this barrier and simultaneously lowers the skyrmion energy, enabling the switching of skyrmion polarity.

References

[1] Pöllath S et al 2019 Phys. Rev. Lett. 123 167201
[2] Jiang W et al 2015 Science 349 283
[3] Sampaio J, Cros V, Rohart S, Thiaville A and Fert A 2013 Nat. Nano. 8 839
[4] Boulle O et al 2016 Nat. Nanotechnol. 11 449

The optical measurement of magnetic phenomena with Magneto-Optical Kerr Effect

Jiyoung Lee[*], Jeong Kyu Lee, Jinseo Lee, Young Keun Kim

Department of Materials Science and Engineering, Korea University, Seoul 02481, Republic of Korea

The interface between ferromagnet (FM) layer and heavy metal (HM) layer exhibits various interesting phenomena, especially spin-orbit torque (SOT) and interfacial Dzyaloshinskii-Moriya interaction (iDMI). With Magneto-Optical Kerr Effect (MOKE) microscope, we can observe the magnetic domain wall motions by detecting the angle between the incident light and the light reflected on the surface of the magnetic film [2]. Thus, the optical measurement like MOKE enables the understanding of the various magneto-dynamic properties such as SOT and iDMI [3]. We constructed the MOKE microscope with current-induced switching system and measured the DMI energy with Pt/Co samples and SOT switching with W samples.

We prepared Ta (2)/Pt (3)/Co (1.2)/Ta (2) samples with perpendicular magnetization and observed different magnetic domain motion under the various external in plane magnetic field. We measured the value of H_{DMI} (538 Oc) and using the equation of $D = \mu_0 \cdot H_{DMI} \cdot M_S \cdot \Delta$, we extracted the DMI energy (D=1.03 mJ/m^2) and confirmed a similarity with the reference value (~0.98 mJ/m^2) [2].

We prepared W (6)/CoFeB (0.9)/MgO (1)/Ta (2) samples for SOT measurement because of the high switching current of Pt samples. With the application of external magnetic field (100 Oe), we observed SOT switching at 5 mA of induced current. We confirmed the switching current with 4 point probe measurement (5.42 mA).

With this study, we confirmed the measurement of iDMI energy and SOT switching with MOKE microscope. Hence, this optical measurement enables simple and rapid data acquisition and will be more efficient when designing experiments.

References

[1] N.H. Kim et al., *AIP advances*, **7**, 035213 (2017)

[2] D.Y. Kim et al., *Phys. Rev. B*, **100**, 224419 (2019)

[3] D.H. Kim et al., *Scientific Reports*, **7**, 45498 (2017)

Large anomalous Hall effect and anisotropic magnetoresistance in intrinsic nanoscale spin-valve-type structure of an antiferromagnet

Ki Won Jeong[*], Dong Gun Oh, Jong Hyuk Kim, Mi Kyung Kim, Hyun Jun Shin,
Jae Min Hong, Jin Seok Kim, Kyungsun Moon, Nara Lee and Young Jai Choi

Department of Physics, Yonsei University, Seoul 03722, Korea

A spin valve is a prototype of spin-based electronic devices found on ferromagnets, in which an antiferromagnet plays a supporting role. Recent findings in antiferromagnetic spintronics show that an antiferromagnetic order in single-phase materials solely governs dynamic transport, and antiferromagnets are considered promising candidates for spintronic technology. In this work, we demonstrated antiferromagnet-based spintronic functionality on an itinerant Ising antiferromagnet of $Ca_{0.9}Sr_{0.1}Co_2As_2$ by integrating nanoscale spin-valve-type structure and investigating anisotropic magnetic properties driven by spin-flips. Multiple stacks of 1 nm thick spin-valve-like unit are intrinsically embedded in the antiferromagnetic spin structure. In the presence of a rotating magnetic field, a new type of the spin-valve-like operation was observed for anisotropic magnetoresistance and large anomalous Hall conductivity, whose effects are maximized above the spin-flip transition. In addition, a joint experimental and theoretical study provides an efficient tool to read out various spin states, which scheme can be useful for implementing extensive spintronic applications.
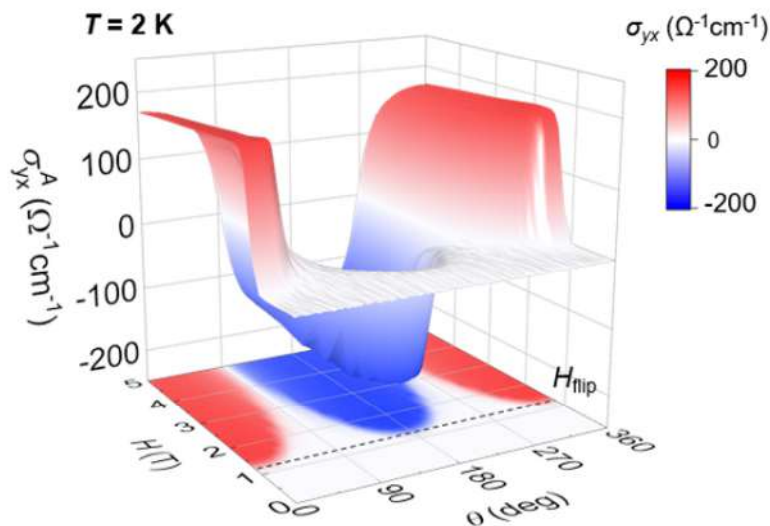
Fig. 1. Large anomalous Hall effect in CSCA

Magnetic property of directly exfoliated and dispersed magnetic 2-Demensional materials in pure water

Hyunjong Lim[1*], Hyobin Ahn[2], Changgu Lee[1*]

[1]School of Mechanical Engineering, Sungkyunkwan University, Suwon, Republic of Korea
[2]SKKU Advanced Institute of Nanotechnology (SAINT), Sungkyunkwan University, Suwon, Republic of Korea

Magnetic 2D materials have attracted lots of attention for atomically flat and stable surface which make them suitable for applications by maintaining their interface without intermixing between elements in many parts of industry. Even though their desirability of practical use, mass production of magnetic 2d material's thin film is still at the starting point because of extreme conditions for their deposition and elements which are more than three which make the choice of precursor and optimization of synthesis process complicated for conventional thin film synthesis method, for example, Chemical Vapor Deposition (CVD). Here we suggest simple and powerful method to make thin film of magnetic 2D materials via direct exfoliation and dispersion in pure water by sonication with controlling temperature of water. Compared to bulk crystal, we could get higher coercivity without disturbing their curie temperature and magnetic anisotropy, which means its magnetic property is well maintained even after direct exfoliation and dispersion process. We expect this simple method can make a breakthrough in mass production of magnetic 2D materials.
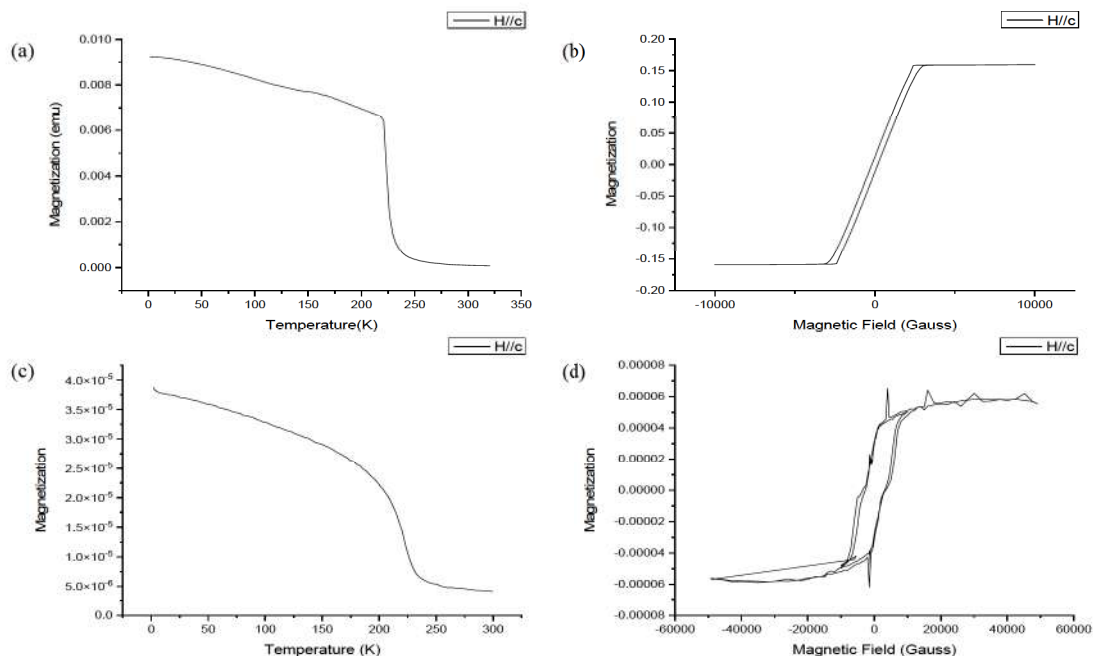
Figure 1. Magnetic properties of Fe_3GeTe_2 (FGT) bulk crystal and thin film. (a) M-T curve of bulk crystal. (b) M-H curve of bulk crystal at 2K. (c) M-T curve of thin film. (d) M-H curve of thin film at 2K.

Temperature and Current-dependent antisymmetric Magnetoresistance at Fe₅GeTe₂/Fe₃GeTe₂ heterostructure

Hyobin Ahn[1*], Srivastava Pawan Kumar[1], Budhi Singh[1], Changgu Lee[2†]

[1]SKKU Advanced Institute of Nanotechnology (SAINT), Sungkyunkwan University, Suwon, Republic of Korea, Korea

[2]School of Mechanical Engineering, Sungkyunkwan University, Suwon, Republic of Korea

Magnetic vdW materials have been researched for their exotic magnetic properties and quantum topological effect. Among them, Fe_XGeTe2 groups (X=3,4,5) which are ferromagnetic metalic materials have drawn lots of interst due to their relatively high curie temperature (T_C for Fe_3GeTe_2 = ~220K, T_C for Fe_5GeTe_2 = ~300K) and topological semimetalic characterstics. Furthermore, because of their atomically flat and stable surface, which is characteristic of vdW materials, they are oftenly refered to be the building blocks for next-generation spintronic device. Here, we fabricated hetero-structure of Fe_5GeTe_2/Fe_3GeTe_2 to study their interlayer coupling and interface between them. In contrast to our expectation, we observed temperature and current-dependent antisymmetric magnetoresistance at interface which is not commonly observed in ferromagnetic system. Antisymmetric MR was observed in two cases, in $Fe_3GeTe_2/Graphite/Fe_3GeTe_2$ and $Fe_3GeTe_2/MnPS_3$. However, in Fe_3GeTe_2/Fe_3GeTe_2 homo-junction, antisymmetric MR wasn't observed, which is different from our case. We expect the phenomenon that we observed originate from two factors, one is the spin current flowing at material itself which is not fully compensated at surface. The other one is the spin-momentum locking at the interface. Through our research, we may get deeper understandings in characteristic of spin current in materials and interface effect in magnetic vdW materials.
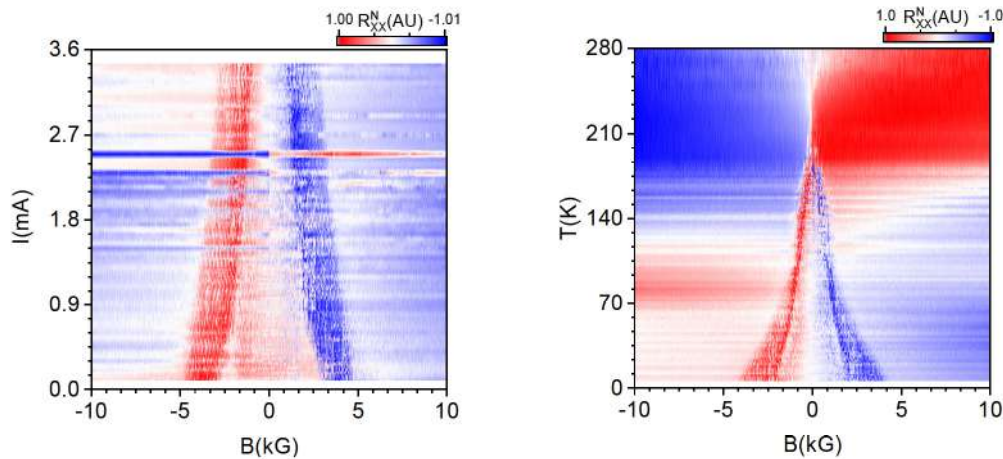
Fig. 1. Current and temperature dependence of R_{XX} at Fe_5GeTe_2/Fe_3GeTe_2 hetero-junction

Room-temperature anomalous Hall effect and anisotropic magnetoresistance reversal in a van der Waals antiferromagnet

Hyun Jun Shin[*], Mi Kyung Kim, Jong Hyuk Kim, Jin Seok Kim, Jae Min Hong, Ki Won Jeong, Jae Yeon Seo, Kyungsun Moon, Nara Lee[*] and Young Jai Choi[*]

Department of Physics, Yonsei University, Seoul 03722, Korea

Recent findings of van der Waals (vdW) antiferromagnetic crystals allow for exploring fundamentals of low dimensional spin-dependent phenomena and open opportunities for developing spin-processing functionalities. However, only a few has been known as itinerant vdW antiferromagnets that comprise an inherently low Néel temperature, limiting the feasible achievement of vdW-antiferromagnet-based spintronics. Here we achieve high-T_N itinerant antiferromagnetism with $T_N = 350$ K in Co-doped Fe_5GeTe_2, which reveals room-temperature large anomalous Hall conductivity and anisotropic magnetoresistance reversal driven by spin flops. Based on easy-axis anisotropic spin model, we associate the evolution of the spin structure by rotating a magnetic field with electrically measurable longitudinal and transverse resistive states. Our work offers an intrinsically magnetic platform to establish vdW-antiferromagnet-based spintroinics and more sophisticated vdW-heterostructures utilizing diverse 2D building blocks.
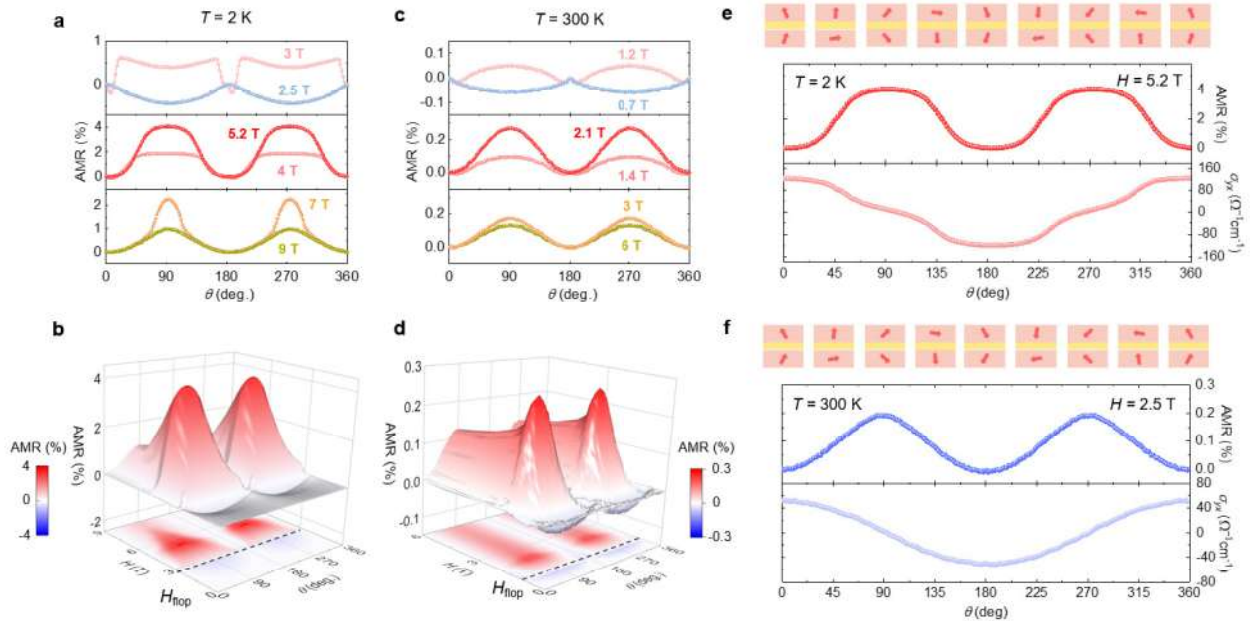
Fig. 1. Anisotropic magnetoresistance reversal and electrically-detectable spin states

Symmetry Breaking by Gradient Pt Thickness in Pt/Co Multilayer Structures

Han Seok Ko[1*], A. S. Samardak[2,3], Seok In Yoon[1], Taehyun Kim[1], Young Keun Kim[1]

[1]*Department of Materials Science and Engineering, Korea University, Seoul 02481, Republic of Korea*
[2]*School of Natural Sciences, Far Eastern Federal University, Vladivostok, Russia*
[3]*National Research South Ural State University, Chelyabinsk, Russia*

Broken inversion symmetry heterostructures comprising a nonmagnetic metal and a ferromagnetic layer are getting interest. Recent study showed that increasing number of stack N leads to enhancement of chiral interaction in $[Co/Pd/Pt]_N$ superlattices [1]. In this study, we investigated magnetic properties of $[Pt/Co]_4$ layer where Pt layer thickness is increasing or decreasing. Samples were prepared using DC magneton sputtering with base pressure of 5×10^{-9} Torr at room temperature. Three types of stacks were prepared;

type 1: Si/SiO$_2$(Substrate)/Ta2/[Pt2/Co(t)/Pt2/Co(t)/Pt2/Co(t)/Pt2/Co(t)]/Pt2/Ta2;

type 2: Si/SiO$_2$(Substrate)/Ta2/[Pt2/Co(t)/Pt1.6/Co(t)/Pt1.2/Co(t)/Pt0.8/Co(t)]/Pt0.4/Ta2

type 3: Si/SiO$_2$(Substrate)/Ta2/[Pt0.4/Co(t)/Pt0.8/Co(t)/Pt1.2/Co(t)/Pt1.6/Co(t)]/Pt2/Ta2, where Co thickness t were 0.4, 0.6, 0.8 nm. The samples were post-annealed at 300°C for 1 hour at 1×10^{-6} Torr. Magnetic properties were investigated by vibrating sample magnetometer (VSM). Saturation magnetization (M_S) of the samples was 2500 emu/cm^3, which is nearly 2.5 times larger than Ta/Pt3/Co1.2/Ta sample. Enhanced M_S can be explained by proximity effect [2]. M_S of the samples increased as the number of Pt/Co interfaces increases, where proximity effect occurs. Especially, for samples with Co thickness of 0.8 nm, magnetization switching occurred gradually rather than immediately. Also, the interfacial Dzyaloshinskii -Moriya interaction(DMI) energy was measured by polar magneto-optic Kerr effect(p-MOKE). The results show that symmetry breaking in [Pt/Co] multilayers cause enhancement of magnetic property by proximity effect which is related with Pt/Co interfaces.
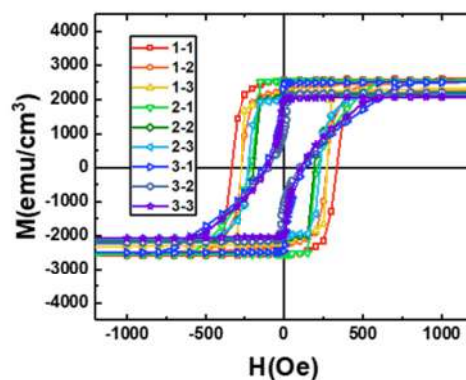
Fig. 1. Magnetic properties of Pt/Co multilayers

References

[1] W. S. Ham et al., Dzyaloshinskii–Moriya interaction in noncentrosymmetric superlattices, npj Comput. Mater. 7, 129 (2021)

[2] L. J. Zhu et al., Irrelevance of magnetic proximity effect to spin-orbit torques in heavy-metal ferromagnet bilayers, Phys. Rev. B 98, 134406 (2018)

Comparison of Thiele equation and experiment for skyrmion hall angle

Kitae Kim[1*], Seong-Hyub Lee[1], Yooleemi Shin[2], Ji-Wan Kim[2], Jung-Hyun Park[1], Jun-Young Chang[1] and Sug-Bong Choe[1†]

[1]Department of Physics and Astronomy, Seoul National University, Seoul, 08826, Republic of Korea
[2]Department of Physics, Kunsan National University, Kunsan, 54150, Republic of Korea

Magnetic skyrmion is topologically stable spin configuration, which is extensively studied nowadays as promising information carrier in future. Such skyrmion is composed of the Néel-type domain wall with energy stabilization by the Dzyaloshinskii-Moriya interaction. When an electric current is injected, the effect based on the Berry phase makes skyrmion deflected from the direction of the current. This effect is called skyrmion Hall effect (SkHE), which consequently causes information loss by inducing skyrmion annihilation near boundary of device. Therefore, the SkHE attracts great attention with caution in development of skymions to memory device.

In this study, we made series of samples, Ta (5) / Pt (2.5) / Co (X) / W (3) / Ta (2 nm), with varying the magnetic layer thickness X = 0.9, 1.0, 1.1, 1.2, 1.6, 1.7, and 1.9 nm using DC magnetron sputtering. We measure then the skyrmion Hall angle by means of a magneto-optical Kerr effect (MOKE) microscope. In Thiele equation, the skyrmion Hall angle is related to Gilbert damping α and anisotropy constant K_U. we experimentally measure independently Gilbert damping constant, and perpendicular magnetic anisotropy. Thus, comprehensive results are shown in Fig. 1. Skyrmion and half skyrmion have the same topological structure so that our result shows verification of Thiele equation experimentally.
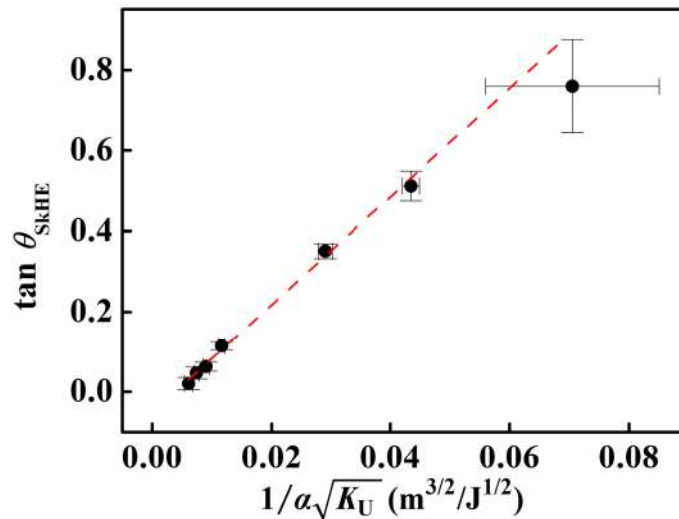
Fig.1 Skyrmion hall angle with respect to $1/\alpha\sqrt{K_U}$

Field-free Spin-Orbit Torque Switching in Ferrimagnet/Non-magnet/Ferromagnet Trilayer Structures

Donghyeon Han[*], Namhee Kim, Jeongmok Kim, Jaimin Kang, Jong-Guk Choi, Dohyoung Kim, Soogil Lee and Byong-Guk Park[†]

Department of Materials Science and Engineering, KAIST, Daejeon 34141, Korea

Field-free switching of ferromagnets, particularly by spin-orbit torque (SOT), has been extensively investigated to realize efficient and scalable spintronic devices. Notably, ferromagnet/non-magnet/ferromagnet trilayer structures were demonstrated to generate both in-plane and out-of-plane spin current at the interface between the bottom ferromagnet and non-magnet via spin filtering and spin precession, respectively. Therefore, spin precessional current replace the external magnetic field counterpart to achieve field-free SOT switching of the perpendicularly magnetized ferromagnet [1].

In this work, we report field-free switching in ferrimagnetic CoGd/Ti/Co trilayer structures. We show that field-free SOT switching polarity relies on the composition of the CoGd layer. In particular the sign of the switching polarity changes when crossing the magnetic compensation point. Furthermore, critical switching current density is found out to be $\sim 5 \times 10^6$ A/cm^2 at the composition of $Co_{74}Gd_{26}$, whose values are much lower than the previously reported conventional SOT switching current density of around 10^7 A/cm^2. Our result provides new possibility toward efficient SOT switching by embracing ferrimagnet/non-magnet interface as a new spin current source.
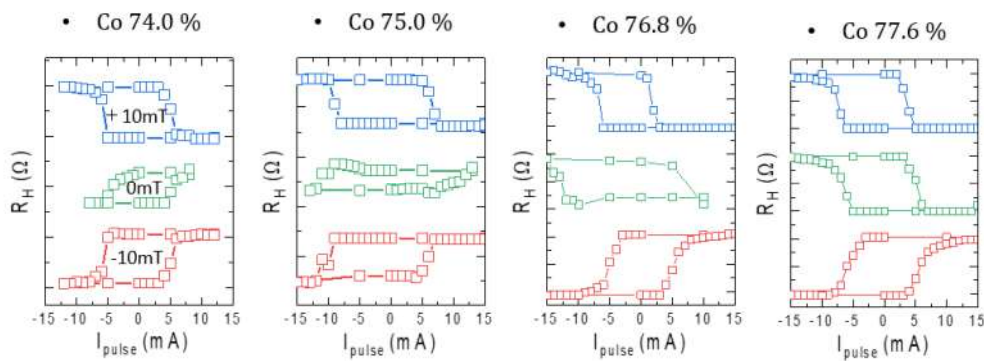
Fig. 1. CoGd composition dependent spin-orbit torque switching

Reference

[1] S. C. Baek, et al. spin currents and spin-orbit torques in ferromagnetic trilayer Nat. Mater. 17, 509 (2018)

Spin-orbit torque manipulation of exchange bias in IrMn/NiFe bilayer structures

Jaimin Kang[1*], Jeongchun Ryu[1], Jong-Guk Choi[1], Taekhyeon Lee[2], Jaehyeon Park[2], Soogil Lee[1], Kab-Jin Kim[2] and Byong-Guk Park[1†]

[1]Department of Materials Science and Engineering and KI for Nanocentury, KAIST, Daejeon 34141, Korea
[2]Department of Physics, KAIST, Daejeon 34141, Korea

Electrical manipulation of antiferromagnetic moment is a key technology of antiferromagnet-based spintronics with favorable device characteristics including ultrafast operation speed and high-density integration compared to the conventional ferromagnet-based one [1]. Electrical manipulation of antiferromagnetic moments through electric current has been demonstrated in epitaxial antiferromagnets with intrinsic broken inversion symmetry or antiferromagnet/heavy metal structures, in which spin-orbit torque (SOT) drives the antiferromagnetic domain wall [2].

Here, we report SOT manipulation of the exchange bias in IrMn/NiFe bilayers structures without a heavy metal [3]. We show that the direction of the exchange bias is gradually modulated in ranges from -22 degrees to 22 degrees by in-plane current, which is independent of the NiFe thickness. This suggests that spin currents originating from the IrMn layer exert SOTs on uncompensated interfacial moments of antiferromagnets and subsequently rotate the antiferromagnetic moments coherently. Furthermore, the multilevel switching characteristics are preserved in sub-micron devices, promoting nanoscale multi-level antiferromagnetic spintronic devices.

References

[1] Jungwirth, T., Marti, X., Wadley, P. & Wunderlich, J. Antiferromagnetic spintronics. *Nat. Nanotechnol.* **11**, 231–241 (2016).

[2] DuttaGupta, S. et al. Spin-orbit torque switching of an antiferromagnetic metallic heterostructure. *Nat. Commun.* **11**, 5715 (2020).

[3] Kang, J. et al. Current-induced manipulation of exchange bias in IrMn/NiFe bilayer structures. *Nat. Commun.* **12**, 6420 (2021).

Enhanced spin Seebeck effect induced by thermo-plasmonic using gold nanoparticles

Jong-Ryul Jeong[1,2*], Phuoc Cao Van[1], Ji-Hwan Seol[1]

[1]Department of Material Science and Engineering
[2]Graduate School of Energy Science and Technology, Chungnam National University,
Daejeon, 34134, Republic of Korea
Fax: +82-(42)-833-3206 E-mail: jrjeong@cnu.ac.kr (J.-R. Jeong)

In this report, we investigate the variation of longitudinal Spin Seebeck effect (LSSE) in $Pt/Y_3Fe_5O_{12}$ (YIG) bilayers embed gold nanoparticles (Au-NPs) grown on $Gd_3Ga_5O_{12}$ (GGG) substrate via rf-sputtering method under the co-existence of the generation of plasmonic spin current in company with plasmonic heating phenomena induced by laser illumination. The contribution of each type of spin source was observed by using particular samples under different laser power and wavelength. In the Pt/YIG/Au-NPs/GGG sample, the relative position of Au-NPs to YIG makes it generating the inverse thermal gradient (∇T) to the external ∇T caused by the laser source. There is a breakdown point of the SSE voltage dependence on laser power (P_{laser}) around 25 mW when the SPR condition is fulfilled. The experimental results show the dominance of plasmonic spin current contribution at the low laser power region. In contrast, the spin current originated from ∇T_{PH} significantly contributed to the overall SSE voltage signal when P_{laser} is increased. This implied the nonlinear increasing of the thermo-plasmonic effect which is induced by SPR in gold nanoparticles.

Substrate roughness dependence of the magnetic anisotropy and coercivity in ultrathin thulium iron garnet films

Duc Duong Viet[1*], Phuoc Cao Van[1*], Trinh Nguyen Thi[1], Jae Hyeon An[1], Viet Anh Cao[2], Junghyo Nah[2], Ji-Wan Kim[3†] and Jong-Ryul Jeong[1†]

[1]Department of Material Science and Engineering, Chungnam National University, Daejeon 34134, South Korea
[2]Department of Electrical Engineering, Chungnam National University, Daejeon 34134, South Korea
[3]Department of Physics, Kunsan National University, Kunsan, 54150, South Korea
[*]These authors contributed equally to this work
[†]Author to whom correspondence should be addressed: E-mail: hwoarang@kunsan.ac.kr, jrjeong@cnu.ac.kr

Nowadays, the control of magnetic anisotropy in magnetic insulators has great interest for non-volatile magnetic memory device applications. In this report, we have investigated the magnetic properties of thulium iron garnet ($Tm_3Fe_5O_{12}$, TmIG) thin films grown on gadolinium gallium garnet ($Gd_3Ga_5O_{12}$, GGG) {111} oriented substrates fabricated by the facing target sputtering method (FTS). The magnetic properties of the film systematically manipulated by the annealing temperature, thickness, and substrate roughness. Here, we revealed that the annealing temperature is a main key factor for obtaining the high quality of the surfaces and strong perpendicular magnetic anisotropy (PMA) in TmIG films. Besides, the easy axis of magnetization was also changed by increasing the thickness of the sample. In detail, the film, which has a thickness of less than 20 nm and is annealed at 1000 °C exhibited the perfect PMA property. In addition, the surface roughness of the substrate essentially contributes to the increase of the coercive field of the perpendicular magnetic anisotropic films. We supposed that this result is related to the behavior of the Néel domain wall motion.

Keywords: thulium iron garnet, facing target sputtering, surface morphology, perpendicular magnetic anisotropy, magnetic coercivity

Thickness dependent spin Seebck resistivity in $Y_3Fe_5O_{12}$ films grown by metal organic decomposition method

Trinh Nguyen Thi[1*], Phuoc Cao Van[1], Jong-Ryul Jeong[1,2*]

[1]Department of Material Science and Engineering
[2]Graduate School of Energy Science and Technology, Chungnam National University,
Daejeon, 34134, Republic of Korea
Fax: +82-(42)-833-3206 E-mail: jrjeong@cnu.ac.kr (J.-R. Jeong)

In this work, we studied the impact of spin Seebeck effect (SSE) voltages on the thickness of yttrium iron garnet (YIG) thin films produced on a silicon (Si) substrate using a metal-organic decomposition technique. Repeated spin coating and annealing cycles were used to control the thickness of the layers. Despite the increase in thickness, grazing incidence X-ray diffraction studies revealed that the YIG thin films had strong crystallinity with no secondary peaks. For samples with thicknesses ranging from 37 to 260 nm, scanning electron microscopy revealed homogenous, very dense films. Magnetic hysteresis loops showed similar coercivities of 36 Oe for all samples, demonstrating the high quality of the YIG films despite a mismatch between the YIG and substrate lattice constants. Spin Seebeck resistivity results showed a significant dependence on sample thickness and local maxima for 138-nm-thick YIG. This was attributable to the magnon energy relaxation length, which is less than that of a single-crystal YIG film produced on gadolinium gallium garnet. This work demonstrated how to easily fabricate hundreds of nanometer-thick YIG sheets on a Si substrate for thermoelectric energy harvesting applications.

Tunable Spin Valve Effect across Van der Waals Magnetic Tunnel Junction

Keun-Hong Min[1,2*], Duk Hyun Lee[1], Seongbin Yim[1], Sang-Jun Choi[3], Jonghwa Eom[2], Jun Sung Kim[4,5] and Suyong Jung[1]

[1]Interdisciplinary Materials Measurement Institute, Korea Research Institute of Standards and Science, Daejeon 34113, Korea

[2]Department of Physics and Astronomy, Graphene Research Institute, and GRI-TPC International Research Center, Sejong University, Seoul 05006, Korea

[3]Institute for Theoretical Physics and Astrophysics, University of Würzburg, Würzburg D-97074, Germany

[4]Department of Physics, Pohang University of Science and Technology, Pohang 37673, Korea

[5]Center for Artificial Low Dimensional Electronic Systems, Institute for Basic Science, Pohang 37673, Korea

Magnetic tunnel junctions (MTJs) with two-dimensional van der Waals (vdW) materials provide ideal spin-valve structures with atomically sharp and clean interfaces. vdW-assembled tunnel junctions minimize spin-dephasing disorders at the interfaces and allow tunnelling electrons to maintain their spin-polarized electronic states. Here, we demonstrate all-vdW-assembled MTJs using two-dimensional vdW ferromagnet Fe_3GeTe_2 (FGT) and insulator h-BN. FGT exhibits a strong perpendicular magnetic anisotropy and Curie temperature near 220K. With vdW MTJs, we are able to access high energy localized spin states of Fe_3GeTe_2 and observe interesting multiple tunneling magnetoresistance ratio polarity changes at low temperatures, which have been inaccessible in conventional thin-film MTJs.
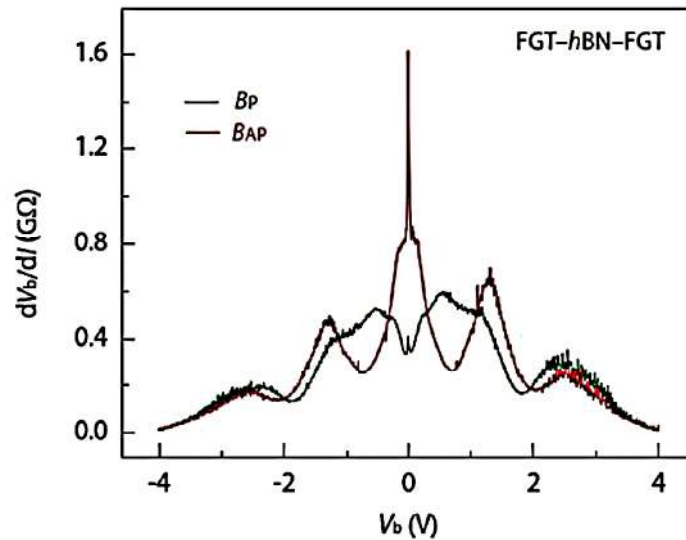
Fig. 1. Differential resistance dV_b/dI–V_b characteristics curve at 4.2K

RKKY 상호작용이 발생되는 p-MTJ 구조에서의 Joule heating 효과

이동현[1*], 임수빈[1], 정세엽[1], 이택현[2], 박정민[2], 김갑진[2], 김상훈[1]

[1]울산대학교 물리학과
[2]한국과학기술원 물리학과

Rudeman-Kittel-Kasuya-Yoshida (RKKY) 상호작용은 주로 비자성층에 인접한 두 자성층 사이에서 발생하는 층간 교환 결합에 기인한다. RKKY 상호작용은 자기 터널 접합의 열적 안정성을 높이기 활용될 수 있다. 최근에 발표된 열적 안정성을 높이기 위해 수직 자기 터널 접합 구조 (Perpendicular-magnetic tunnel junction, p-MTJ)에 수직 자기 이방성을 갖는 박막을 이용하여 RKKY 상호작용에 관한 연구가 발표되고 있다. [1]

스핀 토크를 이용하여 p-MTJ의 자화 반전 거동을 일으킬 때 전류에 의해 Joule heating이 일어나 소자의 자성 특성에 영향을 받을 수 있다. 이는 수직 자기 이방성 뿐만 아니라 교환 결합 바이어스 (exchange bias), RKKY 상호작용 등의 물성도 발열에 의해 변화할 것으로 예상되기 때문에, 해당 물리 변수들의 온도 의존성을 이해하는 것이 소자의 자성 특성을 판단하는데 매우 중요하다. RKKY 상호작용은 수평 자기 터널 접합 구조 (In plane magnetic tunnel junction, i-MTJ)에서 Joule heating이 증가함에 따라 감소한다고 알려져 있는 반면 [2], p-MTJ 구조에서의 RKKY에 온도에 대한 연구는 활발히 진행되지 않고 있다.

이번 발표에서는 수직 자기 이방성을 갖는 자성층/비자성층/자성층 구조를 magnetron sputtering 시스템을 이용하여 제작했으며 비자성층의 두께를 조절하여 인위적 준강자성체 (synthetic ferrimagnet)이 갖는 RKKY 상호작용의 온도 의존성 관측 결과를 다룬다. 자기장에 의한 비정상적인 홀 효과 (anomalous Hall effect)를 5 K에서 300 K까지 측정했으며 온도에 따른 보자력의 변화와 상온에서의 Joule heating에 의해 소자의 자성 특성 변화를 관측한다.

References

[1] Jyotirmoy Chatterjee, et al., Scientific Reports **8,** 11724 (2018)
[2] A. Chavent, et al., PHYS.REV.APPLIED **6**, 034003 (2016)

Large Perpendicular Magnetic Anisotropy in IrMn$_3$/Co Bilayer Grown on Graphene Buffer Layer

Trang Huyen Cao Pham[1*], Nga T. Do[1], Sehwan Song[2], Sungkyun Park[2], Chanyong Hwang[3], Tae Hee Kim[1†]

[1]Department of Physics, Ewha Womans University, 03760, Seoul, Korea
[2]Department of Physics, Pusan National University, 46241, Busan, Korea
[3]Korea Research Institute of Standards and Science, 34113, Daejeon, Korea

Nanomagnetic devices that could be energy efficient and non-volatile have led to the exploration of several switching strategies. In particular, electric field-induced switching has proved to be a promising route toward scalable ultra-low-power computing devices. We have investigated a new candidate for room temperature nanomagnetic devices based on symmetry breaking to achieve deterministic switching in perpendicular anisotropy devices. Here, we interface the magnetic layer Co with an anti-ferromagnetic material. An in-plane exchange bias is created and shown to enable magnetization reversal of perpendicularly magnetized Co/IrMn$_3$/graphene structure. 2.5 nm Co and 1.2 nm IrMn$_3$ films were prepared at room temperature using the UHV-Molecular Beam Epitaxy (MBE) film deposition technique beyond the wafer-scale CVD-grown graphene layer. Its magnetic and transport properties were characterized by the SQUID magnetometer and 4-probe method, respectively. Surface analysis was carried out by Raman spectroscopy and atomic force microscopy as well. Our experiment provides insight into the local spin structure at the magnetic layer/graphene interface.

Effect of sintering temperature on the formation of epsilon Fe₂O₃ nanoparticles encapsulated by SiO₂

Jihwan Seol[1*], Phuoc Cao Van[1], Trinh Nguyen Thi[1], Jong Ryul Jeong[1,2*]

[1]Department of Material Science and Engineering
[2]Graduate School of Energy Science and Technology, Chungnam National University,
Daejeon, 34134, Republic of Korea

The synthesis of ε-Fe₂O₃ has long been attractive within the scientific community due to its giant coercive field at room temperature, high-frequency millimeter-wave absorption, and the coupling of its magnetic and dielectric properties. This work investigated the effect of sintering temperature on the formation of ε-Fe₂O₃/SiO₂ composites which were fabricated by a combination of the reverse micelle and sol-gel methods. We performed sintering at various temperatures to determine the optimal temperature for obtaining the ε-Fe₂O₃ phase and the highest coercive field. The optimal conditions were sintering at 1150°C to achieve a giant coercive field up to 21.57 KOe(Fig 1.). Base on X-ray powder diffraction (XRD), the crystal structure ε-Fe₂O₃ was analyzed. TEM images show a wide size distribution of iron oxide nanoparticles (from 10 to 20nm). Our study illustrated that the ε-Fe₂O₃ are a promising candidate for a recording medium and unlock the door to possible applications in electronic devices intended for high-speed wireless communication.
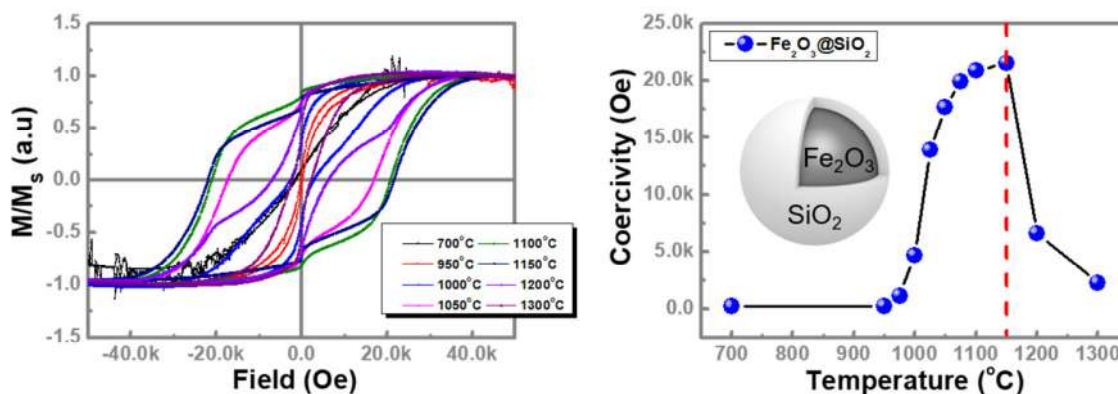
Figure 1. (a) Normalized magnetic hysteresis loop of Fe₂O₃@SiO₂ samples sintered at different temperatur. (b) The extracted of the coercivity dependence on the sintered temperature.

Keywords: ε-Fe₂O₃; sintering temperature; coercivity; reverse micelle and sol-gel

Spin Seebeck signal dependent on surface roughness in yttrium iron garnet thin films prepared by metal-organic decomposition method

Gun-Woo Park[1*], Phuoc Cao Van[1], Ji-Hwan Seol[1], Jong-Ryul Jeong[1,2*]

[1]Department of Material Science and Engineering
[2]Graduate School of Energy Science and Technology, Chungnam National University,
Daejeon, 34134, Republic of Korea
Fax: +82-(42)-833-3206 E-mail: jrjeong@cnu.ac.kr (J.-R. Jeong)

To investigate the dependence of surface morphology and spin Seebeck effect (SSE) voltages, yttrium iron garnet thin films were fabricated by metal-organic decomposition method on a silicon substrate with various poly[vinylpyrrolidone] (PVP) concentration. Base on atomic force microscopy and grazing incidence X-ray diffraction (XRD), the surface morphology and crystal structure were analyzed. The 1-g PVP sample's surface showed atomic steps with the root mean square roughness of 0.2 nm as well as high crystallinity which was confirmed by XRD reflection peaks. The SEM images showed a uniform film, high densification without pores. To obtain the spin Seebeck signal, a 10nm-thick platinum layer was added as a spin-detection layer. Repeatedly, the 1g-PVP presented the highest performance which indicates the importance of the crystallinity as well as morphology to the spin-to-charge conversion efficiency of YIG films.

Interlayer Exchange Coupling with Pt/Ru/Pt spacer layer

Seong Bok Kim, Woo Ri Ju, Da Hyeon Kim, Chan Kang Lee,
Joon Woo Kim, Jaehun Cho, June-Seo Kim[*]

Division of Nanotechnology, DGIST, Korea

Recently, the spin-transfer torque majority gate (STMG) is paid a great attention to develop the next-generation logic devices with an ultralow power consumption since STMG can reduce the circuit architectures such as number of transistors, circuit length, etc. Especially, NOT gate is essential. There are several methods to realize NOT gate in the spintronics based on logic devices [1,2]. In this study, the interlayer exchange coupling (IEC) is used to demonstrate NOT gate based on spintronics. Pt/Ru/Pt spacer layer would be one of the promising materials for the systematic investigation of the SOT on the antiferromagnetic structure.

Ta (3 nm)/Pt (5 nm)/Co (1.0 nm)/Ru (0 - 2 nm)/Pt (0.4 nm)/Co (0.8 nm)/Pt (3 nm) ware prepared by magnetron sputtering system to investigate IEC. To investigate the spacer layer thickness dependence of IEC, the Ru layers were grown in a wedge shape. The polar magneto-optic Kerr effect measurements were employed to measure the Ru thickness dependent magnetic hysteresis curve. Typical ferromagnetic coupling and antiferromagnetic coupling states are shown in Fig. 1. The exchange bias field is determined as 1681 Oe for 0.9-nm-thick Ru layer. From the hysteresis curve, the exchange bias field can be determined and found the oscillation between ferromagnetic and antiferromagnetic coupling as a function of the Ru layer thickness. We will also discuss the Pt insertion layer dependent IEC of Ta (3 nm)/Pt (5 nm)/Co (1.0 nm)/Pt (0, 0.2, 0.4 nm)/Ru (0 - 2 nm)/Pt (0.4 nm)/Co (0.8 nm)/Pt (3 nm) structured samples.
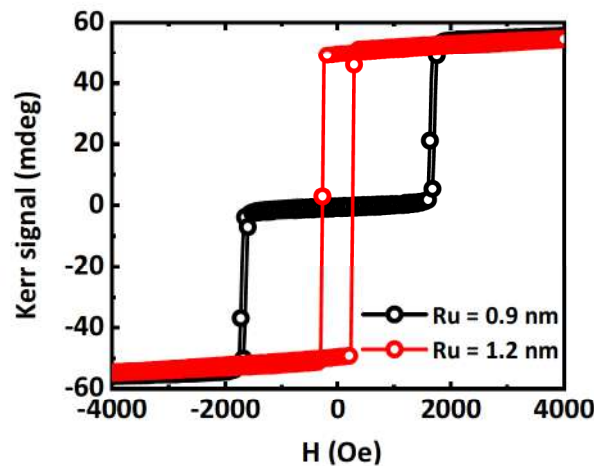
Fig. 1. Typical ferromagnetic and antiferromagnetic coupling states of our samples

References

[1] Z. Luo, *et al.* Current-driven magnetic domain-wall logic. *Nature* **579,** 214–218 (2020).

[2] S. Emori, U. Bauer, S. M. Ahn, E. Martinez, and G. S. Beach, Current-driven dynamics of chiral ferromagnetic domain walls. *Nat. Mater.* **12,** 611–616 (2013).

The Magnetic Properties of Pt/Co/Pt/Ru structure with inserted Pt overlayer

Woo Ri Ju, Seong Bok Kim, Da Hyeon Kim, Chan Kang Lee,
Joon Woo Kim, Jaehun Cho, June-Seo Kim[*]

Division of Nanotechnology, DGIST, Korea

At the interface between a heavy metal (HM) and a ferromagnet (FM), the interfacial phenomena such as a interfacial perpendicular magnetic anisotropy (iPMA), interfacial Dzyaloshinskii-Moriya interaction(iDMI) appear because of their strong spin-orbit coupling (SOC). Since dependence of iDMI and iPMA on the thickness of the Pt layer has been studied [1]. The element with large SOC strength as an interface at the HM/FM may provide a large modulation of the iPMA and iDMI values. It is reported that the presence of the interfacial Pt monolayer significantly enhances PMA to 11.06 mJ/m^2 at the Fe/MgO interface [2] calculated by the first principle calculation.

In this study, we investigate the inserted Pt overlayer dependence of the magnetic properties on the Ta (3nm)/Pt (5nm)/Co (0.5 – 2.5 nm)/Pt (0, 0.2, 0.4 nm)/Ru (3nm) structure fabricated by magnetron sputtering system. To investigate the FM layer thickness dependent magnetic properties, Co layer is fabricated as wedged type. The polar magneto-optic Kerr effect measurements were employed to measure the Co thickness dependent hysteresis curve. Typical perpendicularly magnetized states are shown in Fig. 1 for the 0.6-nm-thick Co thickness with Pt insertion layer. It is clearly shown that Pt insertion layer is led perpendicular magnetized for Pt (5nm)/Co (0.5 – 2.5 nm)/Pt (0.2, 0.4 nm)/Ru (3nm) sample. Based on the polar and longitudinal MOKE measurement, it will be discussed about the increment of iPMA while Pt insertion layer between Co and Ru layer. Furthermore, we will also discuss the magnetization dynamics study to determine magnetic parameters such as saturation magnetization, iPMA energy density, and iDMI energy density.
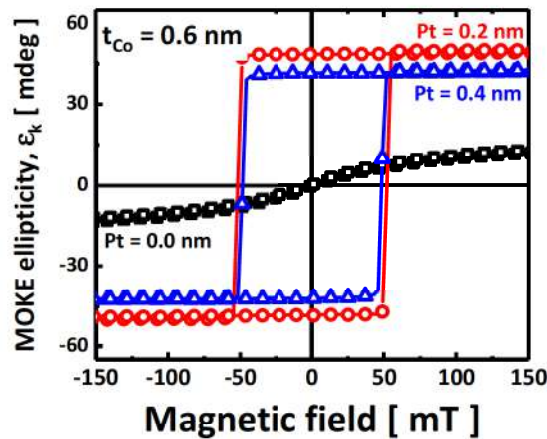
Fig. 1. Typical polar MOKE hysteresis for Pt (5 nm)/Co (0.6 nm)/Pt (0, 0.2, 0.4 nm)/Ru (3 nm) structured sample

References

[1] N.-H. Kim, et al., Appl. Phys. Expr. **10**, 103003 (2017).
[2] Y. Su, et al., J. Phys.: Condens Matter. **32**, 454001 (2020).

The dynamics of domain wall and skyrmion generation

Suyeong Jeong[1*], Dae-Han Jung[1], Hee-Sung Han[1,2], Ganghwi Kim[1] and Ki-Suk Lee[1*]

[1]School of Materials Science and Engineering, Ulsan National Institute of Science and Technology, Ulsan, Republic of Korea

[2]Advanced Light Source, Lawrence Berkeley National Laboratory, USA

The magnetic spin structure of magnetic skyrmions has high stability [1] from the topological charge invariance [2] and small size, which is a promising candidate as an information carrier for future spintronic devices [3]. To generate skyrmion, various types of creation concepts are suggested as switching domain using a local pinning site, changing from stripe domain to skyrmion with multiple pulses, point contact, and geometrical constructions [4,5,6]. In this work, we report micromagnetic simulation studies on the skyrmion generation from two-dimensional domain wall dynamics under external magnetic fields. We find that trivial bubbles are generated during domain wall propagation and they are stabilized to skyrmion or annihilated. Moreover, this process can be repeatable. Our results can provide an efficient way to generate magnetic skyrmions.

We believe that our results can contribute to skyrmion and domain wall-based devices.

References

[1] J. Sampaio, V. Cros, S. Rohart, A. Thiavile, and A. Fert, Nat. Nanotechnol. 8, 839-844 (2013).

[2] N. Nagaosa and Y. Tokura, Nat. Nanotechnol. 8, 899(2013).

[3] Fert, A., Reyren, N. & Cros, V. Nat. Rev. Mater. 2, 17031 (2017)

[4] Büttner, F. et al., Nat. Nanotechnol. 12, 1040–1044 (2017)

[5] Romming, N. et al. Science 341, 636–639 (2013)

[6] Jiang, W. et al. Science 349, 283–286 (2015).

The Skyrmion Dissipation via Radius and Domain Wall Width

Jaehun Cho[*], June-Seo Kim

Division of Nanotechnology, DGIST, Korea

Skyrmions are topologically protected spin textures which often originated from asymmetric exchange coupling as known Dzyaloshinskii-Moriya interaction(DMI)[1]. Recently, it has been attracted due to the possibility of the skyrmion based information devices and information storage units[2]. The motion of the skyrmion on two-dimensional film can be described by a modified version of Newton's equation. For sufficient slowly varying and not too strong forces, a symmetry analysis suggests the following equation [3]:

$$g \times \dot{R} + \alpha D \dot{R} = F \qquad (1)$$

Here, R is the center coordination of skyrmion, g is the gyrocoupling vector with the winding number of the skyrmion m, independent of microscopic details. α is the Gilbert damping constant, D the dissipation dyadic and F the external force e.g. by electric currents, magnetic field gradients, and thermal fluctuations. The component of dissipation dyadic, D_{xx} and D_{yy} can be express as follow [4]

$$D_{xx} = D_{yy} = \frac{2\pi M_s}{\gamma} f(x) = \frac{2\pi M_s}{\gamma}[f_1(x) + m^2 f_2(x)] \qquad (2)$$

$$f_1 = \int_0^\infty \frac{2t \sinh^2(x)\cosh^2(t)}{[\sinh^2(x) + \cosh^2(t)]}dt, \quad f_2 = \int_0^\infty \frac{2\sinh^2(x)\cosh^2(t)}{[\sinh^2(x) + \cosh^2(t)]}dt,$$

here, M_s is the saturation magnetization, γ the gyromagnetic ratio, x the ratio of skyrmion radius (r) to domain-wall width (w). Figure 1 (a) shows the $f(x)$ as a function of ratio of skyrmion radius and domain-wall width when $m = 1$ case. The micromagnetic simulations were performed using the Mumax^3 code [5] to investigate the relation with $f(x)$ and the shape of skyrmions. We selected a nanowire shape of 1000 nm × 100 nm × 1.2 nm in dimensions with a cell size 2 × 2 × 2 nm^3 at the zero temperature. We selected several independent skyrmions to investigate their dynamics. Fig 1 (b) shows m_z of selected two skyrmions which have different ratios of radius to width. The perpendicular magnetic anisotropy of two skyrmions (Skx I and Skx II) are 0.8 and 1.1 MJ/m^3, exchange stiffness constant 15 and 12 pJ/m, interfacial DMI energy densities 3.5 and 4.0 mJ/m^2, respectively. The M_s of both skyrmions is 580 kA/m, α is 0.3. Our setup of the simulation is following. We set the initial skyrmion in the center of the nanowire, and then 300 nsec later, we save the spin configuration to determine skyrmion displacement by external forces. We verify the theoretical argument given equation (2), in view of simulation results.
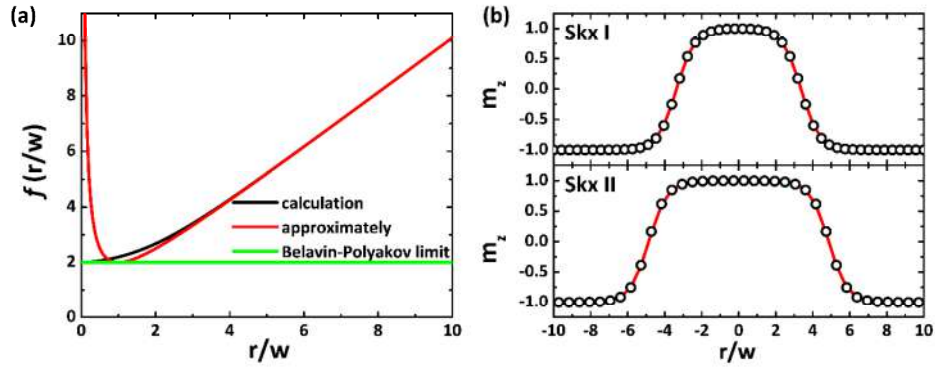
Figure 1(a) m_z of two skyrmions (b) The dissipation as a function of ratio of skyrmion radius to domain wall width.

References

[1] I. Dzyaloshinsky, J. Phys. Chem. Solids **4**, 241 (1958). T. Moriya, Phys. Rev. **120**, 91 (1960).

[2] J. Sampaio, *et al.*, Nat. Nanotech. **8**, 839 (2013).

[3] A. A. Thiele, Phys. Rev. Lett. **30**, 230 (1973).

[4] X. S. Wang, *et al.*, Commun. Phys. **1,** 31 (2018). A. Hrabec, *et al.*, Nat. Commun. **8**, 15765 (2017).

[5] A. Vansteenkiste, *et al.*, AIP Advances **4**, 107133 (2014).

In-Plane Anisotropy of Magnetic Damping Constant in Epitaxial Cr/Fe Bilayer

Thanh Huong Thi Nguyen[1*], Van Quang Nguyen[2], Jungmin Park[3], Nyun Jong Lee[4],
Sunglae Cho[4], Jung-Il Hong[1], Sanghoon Kim[4*]

[1]*Daegu Gyeongbuk Institute of Science & Technology (DGIST), Korea*
[2]*Korea Atomic Energy Research Institute (KAERI), Korea*
[3]*Korea Advanced Institute of Science & Technology (KAIST), Korea*
[4]*University of Ulsan (UOU), Korea*

The magnetic damping constant is an important parameter governing the magnetization dynamics of a ferromagnet. Especially in a bilayer system for spin torques (ST) devices, the effective damping constant determines the critical current density for current-induced magnetization switching. In this work, we report a study of dynamics properties of an epitaxially grown Cr/Fe bilayer by means of ferromagnetic resonance (FMR) techniques. The epitaxial film allows us to investigate the crystal orientation dependence of the damping parameter which is extracted from the slope of the linewidth dependence on the FMR frequency. We find that the magnetic damping constant in our film clearly shows an in-plane anisotropy which differs from its very weak magneto-crystalline anisotropy. Possible origins are also discussed in this presentation.

Study on the energy structure generating telegraph noise by domain wall motion

Seyyoung Jeon, Jiho Shin[*], Sug-Bong Choe

Department of Physics and Institute of Applied Physics, Seoul National University, Seoul, Korea

Telegraph noise, the certain type of signals which consists of sudden jumps between two or more levels, can be observed in several systems for example CMOS, memristor, and magnetic domain wall.

In this study, random telegraph noise generated when a magnetic domain wall in two metastable states is depinning was detected. And also, the statistical characteristics of telegraph noise according to depinning time was studied.

To detect telegraph noise, a notch structure was patterned on a Pt/Co/W sample with perpendicular magnetic anisotropy and the telegraph noise generated when the magnetic domain wall was depinning in the notch structure was obtained as a Polar MOKE signal.

As this method can provide large number of samples of depinning times compared to common methods, energy barriers of many different conditions can be obtained repeatedly to show clear linear dependencies to the field and current in certain ranges.

The extracted theoretical properties are well fitted in order range and dilute correlation related to the origin of the pinning potential can be seen in the analysis.

(a)

Depinning from	P_1	P_{-1}
V_0 [10^{-20} J] ([$k_B T_0$])	8.7 (15)	6.8 (12)
a [10^{-18} JT^{-1}]	8.9	-6.8
ε [10^{-14} Tm^{2}A^{-1}]	9.8	9.6

(b)
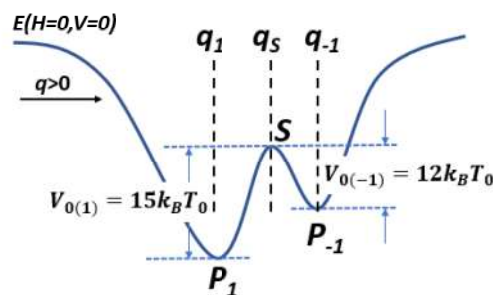
Fig. 1. (a) Extracted theoretical parameters involved in depinning energy barrier from each pinning sites. (b) Sketch of domain wall energy landscape with respect to the spatial coordinate q.

Origin of ultrafast lattice contraction in ferromagnets generated by femtosecond laser pulses

Yooleemi Shin and Ji-Wan Kim[*]

Department of Physics, Kunsan National University, Kunsan 54150, South Korea
[*]Email: hwoarang@kunsan.ac.kr

In Femtomagnetism community, it has been believed that the lattice dynamics induced by femtosecond laser pulses is much slower than the electron or the spin dynamics. Moreover, it was published that the ultrafast lattice contraction was shown up in a few ps and it was driven by magnetostrictive action after ultrafast demagnetization [1]. However, although the simultaneous measurement of the lattice and the spin is the most important criterion if the time sequences of events determine the causality, their conclusions have been drawn from experimental data measured separately with different setups.

To resolve this issue, we developed the modified ultrafast Sagnac interferometer capable of the simultaneous detection of the lattice displacement and the magneto-optical Kerr effect signals. Figure 1(a) shows the transient Kerr rotation (black) and the lattice displacement (red) for Al_2O_3(5nm)/Co(30nm)/sapphire measured with the probe wavelength of 625nm after femtosecond laser pump excitation (400nm). Here, we clearly find that the lattice contraction (negative sign) around 0 ps is preceded the demagnetization. This is the counter results to the earlier report where the demagnetization drives the lattice contraction through the magnetostriction. In order to find the origin of the lattice contraction rather than the expansion, we measured the dynamics with the different probe wavelength of 725nm as shown in Fig. 1(b). Here, the lattice contraction signal shows the dependence of the probe wavelength in terms of the peak value. Therefore, we suggest that the lattice contraction is originated from the nonthermal electrons, not from the magnetostrictive interaction mechanism driven by the demagnetization.
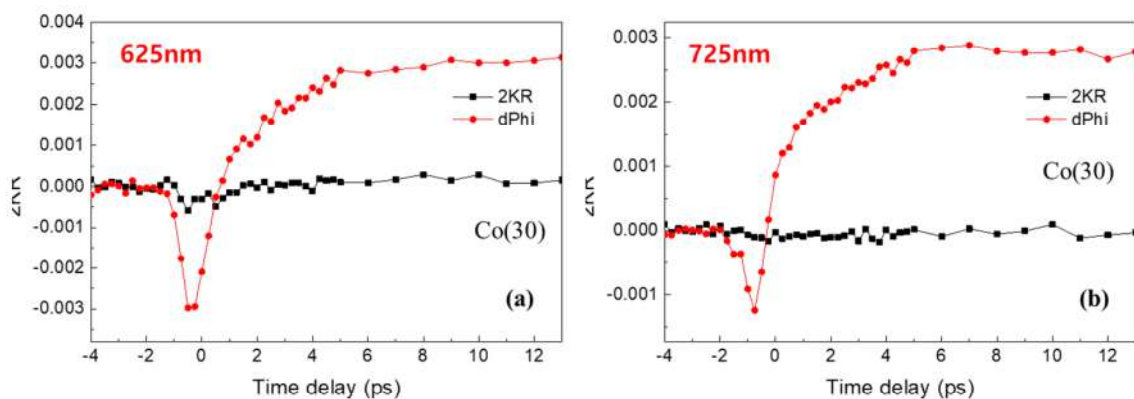
Figure 1. Time-resolved magneto-optical Kerr rotation (black) and lattice displacement (red) measured with the probe wavelength of 625nm (a) and 725nm (b) for Al_2O_3(5nm)/Co(30nm)/sapphire sample.

Reference

[1] A. H. Reid et al., Nat. Commun. 9, 388 (2018).

Dynamics of topological Bloch line

Jiseok Yang[1*], Kyoung-Woong Moon[2], Albert Min Gyu Park[1], Soogil Lee[1], Doo Hyung Kang[3], Mincheol Shin[3], Sanghoon Kim[4] and Kab-Jin Kim[1*]

[1]Department of Physics, Korea Advanced Institute of Science and Technology, Daejeon, 34141, Republic of Korea
[2]Quantum Spin Team, Korea Research Institute of Standards and Science, Daejeon, 34113, Republic of Korea
[3]School of Electrical Engineering, Korea Advanced Institute of Science and Technology, Daejeon, 34141, Republic of Korea
[4]Department of Physics, University of Ulsan, Ulsan, 44610, Republic of Korea

Magnetic racetrack memory has been proposed to a novel spintronic memory device [1], in which domain walls (DW) are used as data bits and moved through current-induced DW motion. During the last decade, DWs have been intensely researched owing to their promising application in DW-based racetrack memory. However, the limitation of the DW-based racetrack memory is that the DW motion exhibits stochastic features due to the pinning and depinning of the DW at the wire edge or defects. To solve this problem, other topological defects such as vortices, skyrmions, and Bloch lines have been proposed for magnetic memory devices [2-4]. The magnetic Bloch line (BL), a winding spin structure inside the DW, is also a topological defect with a nontrivial topological charge. The BL is a sub-structure of the DW, which is much smaller and stable than the DW. Although these outstanding features have led to attract much interest, the current-driven BL motion has not been considered as an operation mechanism for memory device.

In this presentation, we present that the current-driven BL motion can be utilized as a novel mechanism of BL memory [5]. Using micromagnetic simulations in Mumax3 code, we demonstrated that the writing and shifting process of the BLs are possible based on a spin-transfer-torque scheme. We also investigated that the BL has a much higher stability than the DW, and the BL motion is robust against the sample imperfections such as random defects or edge roughness. In addition to the simulations, we experimentally examined the current-driven BL motion in Permalloy (Py) films. The BL velocity was achieved about 100 m/s, which is higher than the DW velocity. Our results therefore open the possibility to utilize and realize the BL racetrack memory beyond the DW-based racetrack memory.

References

[1] S. S. P. Parkin et al., Science **320**, 190 (2008)
[2] A. Fert et al., Nat. Nanotechnol. **8**, 152 (2013)
[3] B. Pigeau et al., Appl. Phys. Lett. **96**, 132506 (2010)
[4] S. Konishi, IEEE Trans. Magn. **19**, 1838 (1983)
[5] J. Yang et al., Appl. Phys. Express. **14**, 103002 (2021)

Magnetic skyrmion hopping due to the structural topology

Moojune Song[1*], Mujin You[1], Seungmo Yang[2], Min Gyu Park[1], Kab-Jin Kim[1]

[1]Department of Physics, Korea Advanced Institute of Science and Technology (KAIST)
[2]Spin Convergence Research Team, Korea Research Institute of Standards and Science (KRISS)

Magnetic skyrmions are topological defects with topological quantum numbers. Skyrmions are not only topologically important but also attract a lot of attention as information carriers for future memory and logic devices. The scaling law of the creep, on the other hand, can explain the dynamics of various phenomena such as solid film growth, vortex dynamics, and liquid invasion into porous media [1, 2]. However, the scaling law of the magnetic skyrmion in a low-driving regime has not been well studied despite the importance of the efficiency of skyrmion devices in the low power range.

We use the W/CoFeB/Ta/MgO system to study the low-current-driven skyrmion and domain wall motion. By manipulating a magnetic field, a skyrmion bubble with a diameter of about 1 μm is nucleated [3] and an electric current is applied to induce SOT-driven skyrmion motion. Using the MOKE microscope and software-based image processing to track more than 700,000 current-driven skyrmions we analyze the relationship between the average velocity and applied current density. Our observations show that skyrmion does not follow the scaling law previously observed in domain wall creep in 2D systems. Instead, it follows the hopping behavior observed in the domain wall creep in the 1D system. On the other hand, domain wall motion in the same material is found to follow the previously reported scaling law of creep. We explain this theoretically using the domain wall segment theory [4], and we attribute the hopping behavior of the skyrmion to the bottleneck process of current-parallel segments on the skyrmion boundary. Furthermore, even if the topological charge of the skyrmions is removed by applying an in-plane magnetic field the skyrmionic bubbles follow the hopping law. We also analyze the properties of the 1D-confined skyrmion motion, which supports our theoretical interpretation. From this, we conclude that the shape of magnetic texture (for example, open-line for domain wall or closed-loop for skyrmion), in other words, *structural topology* can play an important role in a universality class of magnetic dynamics.

References

[1] K. -J. Kim *et al., Nature* **458**, 740 (2009)
[2] S. Lemerle *et al., Phys. Rev. Lett.* **80**, 849 (1998)
[3] K. -W. Moon *et al., NPG Asia Mater.* **13**, 20 (2021)
[4] J. Ryu *et al., Phys. Rev. B* **84**, 075469 (2011)

Magnetoelasticity-driven ultrafast spin precession in $Ni_x Fe_{100-x}$ alloy films

Yooleemi Shin[1], Seongsoo Yoon[2], Jung-Il Hong[2] and Ji-Wan Kim[1*]

[1]Department of Physics, Kunsan National University, Kunsan 54150, South Korea
[2]Department of Emerging Materials Science, DGIST, Daegu 42988, South Korea
[*]Email: hwoarang@kunsan.ac.kr

We find the clue that the spin precession induced by femtosecond laser pulses may be driven by magnetoelastic energy rather than the magnetocrystalline and the dipole energy terms. With $Ni_x Fe_{100-x}$ alloy films (x = 87.0 ~ 97.5) varying the magnetostriction values systematically, we measured the pump-induced magneto-optical Kerr rotation signals. As shown in Fig. 1(a), depending on the magnetostriction values materials, it is found that the phase inversion in spin precession is shown up around x = 92.3 and the phase varies from -90 deg to 0 deg with the increase of the pump intensity for x = 95.3 as presented in Fig. 1(b).

By solving Landau-Lifshitz-Gilbert equation considering both thermal and magnetoelastic effects, we found that for a low x, the thermal effect is dominant and for a high x, the magnetoelastic effect becomes dominant leading to the phase inversion. Interestingly, for x = 92.3 where there shows no precession, the thermal and magnetoelastic effects are in competition.
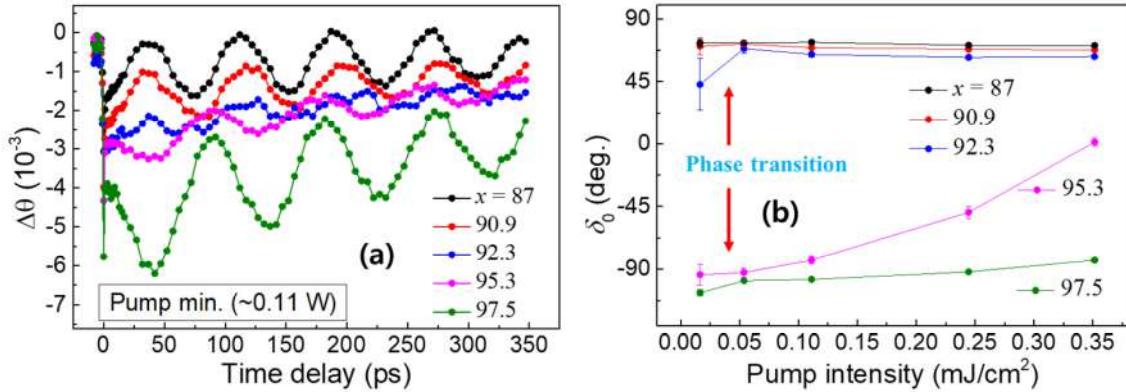
Fig. 1. (a) Differential Kerr rotation signals and (b) the phase of spin precession in $Ni_x Fe_{100-x}$ depending on their magnetostriction values

열간 변형 Nd-Fe-B 영구자석의 결정립 제어 연구

황진성[*], 안종빈

(주)디아이씨 신소재연구소

최근 열간 변형 소결법을 통한 Nd-Fe-B 소결자석의 제조 및 관련 연구가 많이 진행되고 있다. Nd-Fe-B 영구자석 제조 시 사용되는 분말, 온도, 압력, 시간 등 다양한 변수에 따라 자성 특성에 영향을 미치게 되는데, 이를 어떻게 제어하냐에 따라 보자력과 잔류자화 값이 달라지게 된다. 상용 MQU-G 분말을 650-750℃로 열간 가압 소결을 진행했다. 이후 변형률은 약 75%로 제어하고, 다른 변형 온도, 변형 속도의 변수로 열간 변형 공정을 진행했다. 보자력 값의 경우 변형 온도 차이에 비해 미미한 차이를 보였으며, 변형 속도가 빨라질수록 증가했다. 잔류자화 값의 경우 변형 온도가 높을수록 저하되며, 변형 속도를 빠르게 할수록 잔류자화 값은 감소했다. 보자력 값에 영향을 끼치는 결정립 크기는 변형 온도가 높고, 변형 속도가 느릴 때 성장이 일어나 입자 사이의 결합 강도를 약해지게 하며 결정립의 형태는 변형 온도가 높고, 변형 속도가 빠를수록 편평한 Platelet 형태에서 구형으로 변화됨을 확인했다. 또한, 잔류자화 값에 영향을 끼치는 결정립 정렬도의 경우 고온 변형에 의해 결정립의 정렬이 깨졌기 때문에 이러한 자성 특성 경향이 나타났다고 판단된다. 이 실험에서 사용했던 상용 MQU-G 분말은 잔류자화 값이 12.6~12.8kG 로 알려져 있지만, 열간 변형 공정 시 변형 온도와 변형 속도 제어를 통해 최고 13.15kG 의 기존 대비 높은 잔류자화 값을 얻을 수 있었다.

Synthesis and magnetic properties of Si^{4+}-$M^{1+,2+}$(M = Mg^{2+}, K^+, Li^+) co-substituted M-type Sr-hexaferrites

Jun-Pyo Lim[1], Young-Min Kang[1*], Min-Ho Kim[2], Kang-Hyuk Lee[3], Sang-Im Yoo[3]

[1]Department of Materials Science and Engineering, Korea National University of Transportation, Chungju, 27469, Korea

[2]R&D Team, Union Materials Corp., Pohang, 37865, Korea

[3]Department of Material Science and Engineering, Research Institute of Advanced Materials (RIAM), Seoul National University, Seoul, Korea

[*]Corresponding author email: ymkang@ut.ac.kr

In this study, M-type hexaferrites with the chemical formulae $SrFe_{12-2x}Si_xMg_xO_{19}$ (x = 0, 0.05, 0.1, 0.2), $Sr_{1-y}Fe_{12-y}Si_yK_yO_{19}$ (y = 0.05, 0.1, 0.2), and $SrFe_{12-z}(Si_{0.6}Li_{0.6})_zO_{19}$ (z = 0.05, 0.1, 0.2, 0.4, 0.6) were prepared using conventional solid-state reaction processes. A single M-hexaferrite phase could be formed in the charge-balanced Si^{4+}-Mg^{2+} and Si^{4+}-Li^+ co-substitution for Fe^{3+} up to x = 0.1 and z = 0.4, respectively. A fine microstructure could be obtained when the substitution level was in the range of $x \leq 0.1$ in the Si-Li-substituted SrM, whereas in the case of Si-Li substitution, it could be obtained at $z \geq 0.2$. When the magnetic properties according to x and z were evaluated through M-H measurements, the best hard magnetic properties were obtained at $x = z = 0.5$. When $Si_{0.03}$-$Li_{0.03}$ (z = 0.5) was substituted, the M_S value increased by 2.6%. This is because the intrinsic ferromagnetic properties of SrM changed owing to Si-Li substitution. When an anisotropic permanent magnet was prepared and evaluated after optimizing the sintering additive for the $SrFe_{11.5}Si_{0.03}Mg_{0.03}O_{19}$ composition, B_r also improved by 2.5% from 4207 to 4314 G compared to that of the unsubstituted SrM. The maximum energy product (BH_{max}) value also increased from 4.24 to 4.46 M·G·Oe. The improvement of the intrinsic magnetic characteristics of SrM by the substitution of Li-Si, a new composition besides La-Co, is an exciting development, expected to have wide-ranging applications.

Magentic properties in Nd reduced Nd-Ce-Fe-B Hot-deformed magnets

Ye Ryeong Jang[*], Wonjin Kim, Hyun-Sook Lee[*] and Wooyoung Lee[†]

Department of Materials Science and Engineering, Yonsei University, Seoul 03722, Republic of Korea

The price of Nd, which accounts for about 30% of the weight of Nd–Fe–B permanent magnets, has recently risen as the Nd–Fe–B magnet market expands. As the demand for Nd–Fe–B magnets increases, Ce-based magnets have received much attention in recent years due to their potential usefulness. A study on the substitution of Ce to improve magnetic performance while reducing the amount of expensive Nd by replacing Nd in Nd-Fe-B magnets has been reported. However, the substitution of Nd with Ce in the 2:14:1 main phase weakens the magnetic properties due to the low intrinsic magnetic properties of $Ce_2Fe_{14}B$ (saturation magnetization 11.7 kG and magnetocrystalline anisotropy field 30 kOe). The hot deformation process is an efficient method for manufacturing high-density anisotropic magnets, which can improve the low intrinsic magnetic properties of Ce-Fe-B magnets by ultra-fine grain size and aligned grains. However, the higher the Ce contents, the lower the coercivity values of the hot-deformed Nd-Ce-Fe-B magnet. Therefore, the fabrication of a high-performance magnet in which Nd is partially or completely replaced with Ce is still a challenging issue. In this work, we report the magnetic properties of hot-deformed Nd-Ce-Fe-B-based magnets by adding alloys of light rare-earth elements and transition metals. In particular, we investigated the effect of low melting alloy addition on the thermal stability of magnetic properties. The high thermal stability was discussed through microstructural analysis. Finally, we evaluated the availability of Nd-reduced Nd-Ce-Fe-B hot-deformed magnets as potential candidates for low-cost and intermediate-performance permanent magnets.

Grain boundary diffusion sources and temperature dependent coercivity in Nd-Fe-B sintered Magnets

Jaehyuk Kim[1,3*], Dong Hyun Lee[4], Seong Chan Kim[1,3], Dong Hwan Kim[1], Sangchul Lee[1], Donghwan Kim[2], Snag Hyub Lee[2], Dalhyun Do[3], Jong Wook Roh[4], Jeongmin Kim[1*]

[1]Division of Nanotechnology, DGIST, 333 Techno Jungang-daero, Hyeonpung-eup, Dalseong-gun, Daegu 42988, Republic of Korea

[2]R&D Center, Star Group, Daegu 42714, Republic of Korea

[3]Department of Advanced Materials Engineering, Keimyung University, 1095, Dalgubeol-dareo, Dalseo-gu, Daegu, Republic of Korea

[4]Department of hydrogen & renewable energy Graduate School, Kyungpook National University Daegu, Republic of korea

Commercially used Nd-Fe-B sintered permanent magnets have been widely used in various applications such as hard disc drives, wind power generators, efficient air-conditioner compressors and motors for electric vehicles. Since these applications are often used in high-temperature environments, the required coercivity and remanence have been simultaneously obtained by using the heavy rare earth (HRE) grain boundary diffusion process (GBDP). In this study, we report the effect of a low-melting diffusion material mixed with Al and Co in HRE diffusion material to reduce the HRE content of GBDP-based high-performance magnets on the magnetic properties of sintered magnets and the heat treatment temperature dependence. TbH, TbH-Al and TbH-Co coated commercial Nd-Fe-B sintered magnets were annealed under various temperatures and the coercivity and remanence were systematically measured. Further description of the microstructure will be discussed in detail.

Synthesis and characterization of SmFe$_{12}$-based compounds prepared by reaction-diffusion reaction

Kang-Hyuk Lee[1][*], Jun-sun Hwang[1], Min Kyung Seng[2] and Sang-Im Yoo[1][†]

[1]*Department of Material Science and Engineering, Research Institute of Advanced Materials (RIAM), Seoul National University, Seoul, Korea*
[2]*Department of Physics, Sookmyung Women's University, Seoul 04310, Republic of Korea*

The ThMn$_{12}$-type structure has attracted attention as permanent magnetic material due to the high anisotropy field, saturation magnetization (M_s), and Curie temperature (T_C). The Sm(Fe$_{0.8}$Co$_{0.2}$)$_{11}$Ti (SFCT) materials have been intensively studied to synthesize high permanent magnets by controlling the doping element. In this study, we tried to investigate SFCT materials prepared by reaction-diffusion reaction. we prepared the SFCT precursor was prepared by a common co-precipitation method. The samarium nitrate hexahydrate, cobalt nitrate hexahydrate, titanium tetrachloride, and iron nitrate hexahydrate were dissolved in deionized water at 70 C to form a homogeneous solution. The 3M KOH solution was slowly dropwise in the solution. Then the pH of the solution was adjusted slowly to pH 12 by adding dropwise ammonium hydroxide solution. The precipitates were collected by filtration. The precursors were heat-treated at 600°C for 4h in H2 gas. And other SFCT precursor was prepared by solid state reaction. The samarium oxide and iron oxide was weighed, milled with anhydrous ethanol. The raw materials were ball-milled for 24 h with anhydrous ethanol and calcined at 1000 °C for 6 h in air. The precursors were heat-treated at 600°C for 4h in H$_2$ gas. The hydrogen-reduced powders were mixed with calcium granules and pelletized. The pelletized samples were heated at 850 - 1050 °C for 1~6 h in Ar gas. Samples were characterized by using an x-ray diffractometer (XRD) with Cu-Kα radiation source, a vibrating sample magnetometer (VSM), and scanning electron microscopy (SEM). The samples were obtained ThMn$_{12}$-type phase at 1050 °C for 1 h in Ar gas. The M_s and H_c values of Sm(Fe$_{0.8}$Co$_{0.2}$)$_{11}$Ti samples were 95 emu/g and 1935 Oe. Detailed microstructures and magnetic properties will be presented for discussion.

SmFe12-based compounds, ThMn12-type, hard magnetic material

Finite-element micromagnetic simulation study of multi-main phase core-shell Janus spherical particle clusters

Hyeon-Kyu Park[*], Jae-Hyeok Lee, Sang-Koog Kim[†]

National Creative Research Initiative Center for Spin Dynamics and Spin-Wave Devices, Nanospinics Laboratory, Department of Materials Science and Engineering, Seoul National University, Seoul 151-744, South Korea
[*]Correspondence and requests for materials should be addressed to S.-K. K. (sangkoog@snu.ac.kr).

$Nd_2Fe_{14}B$ magnetic materials are facing supply risks due to limited deposits and high prices of precious Neodymium metals. Cerium and Lanthanum are relatively abundant and cheap rare-earth elements, and they are considered as substitute materials for Nd. Nonetheless, alloys containing Ce and La have been considered difficult for practical applications owing to their magnetic performances typically inferior to pure $Nd_2Fe_{14}B$ materials [1-5]. Recently, J. Jin *et al.* [6] developed a special material called as multi-main phase (MMP) magnets, which have a performance comparable to pure ones in spite of Ce and La contents in the material. They turned out to have a microstructure composed of core-shell Janus grains according to microscopy techniques [7]. Here, we further investigate concrete and detailed reversal processes of magnetic materials composed of two types of core-shell Janus spherical particles with different atomic ratio of Ce to Nd by finite-element micromagnetic simulations. We will discuss the dependence of the overall magnetic performances of this model on the Ce composition as well.

References

[1] X. Fan *et al.*, *J. Magn. Magn. Mater.* 419, 394-399 (2016).

[2] Z. Li *et al.*, *J. Magn. Magn. Mater.* 426, 70-73 (2017).

[3] Y. Zhang *et al.*, *Acta Mater.* 128, 22-30 (2018).

[4] K. P. Skokov *et al.*, *Scr. Mater.* 154, 289-294 (2018).

[5] G.-Y. Kim *et al.*, *Scr. Mater.* 214, 114676 (2022).

[6] J. Jin *et al.*, *Sci. Rep.* 6, 32200 (2016).

[7] T. Ma *et al.*, *Acta Mater.* 142, 18-28 (2018).

Structure and Magnetic Properties of La-Ca-Co substituted SrM-type hexaferrites synthesized by solid-state reaction method

Min-Kyung Seong[1*], Kang-Hyuk Lee[2], Seo-Hyuk Jin[2], Sang-Im Yoo[2†], Hae-In Yim[1†]

[1]Department of Physics, Sookmyung Women's University, Seoul 04310, Korea
[2]Department of Material Science and Engineering, Seoul National University, Seoul 08826, Korea

M-type hexaferrites ($SrFe_{12}O_{19}$ and $BaFe_{12}O_{19}$) are the most useful materials for permanent magnets due to relatively low price, high coercivity, large magnetocrystalline anisotropy, and outstanding chemical stability. Numerous studies were reported to enhance magnetic properties such as saturation magnetization (M_S) and coercivity (H_C). Among these studies, La-Ca-Co substituted Sr-M hexaferrites are suggested with high magnetic properties.

Our previous research was focused on the ratio of Fe/Sr=12, but the composition was hard to obtain the single phase. Therefore, in this work, we reduced the ratio to 11 to get the single M-type phase.

$Ca_{0.15}La_{0.3}Sr_{0.55}Fe_{10.7}Co_{0.3}O_{19}$ were prepared by a solid-state reaction using four different procedures. First, Ca and La were mixed either before calcination or after calcination. Second, the heating process was with or without additives, respectively. Through these different procedures, we tried to find the optimum synthesis process by checking the additive's effect.

The precursor powders were weighed according to the target cation composition of $Ca_{0.15}La_{0.3}Sr_{0.55}Fe_{10.7}Co_{0.3}O_{19}$ and mixed. To the additives were added sample, SiO_2 was added at a dose of 0.3 wt% of the total precursor powder. The powder mixture was ball-milled in ethanol for 24 hours. The calcination temperature was 1280 °C for 2 hours. The calcined powders were crushed and ball-milled in ethanol for 24 hours. While ball-milling, 0.4 wt% of SiO_2 and 0.7 wt% of $CaCO_3$ were added again to the mixture which contains the additive. After ball-milling, the powders were dried and pressed in a mold with a diameter of 15mm at a pressure of 11.7 MPa to produce a disk-shaped green compact pellet. The pelleted samples were sintered in air at 1100 – 1230 °C for 2 hours. The heating range during calcination and sintering was 5 °C/min, and the samples were then furnace-cooled to room temperature.

The density of the sintered sample was calculated by the Archimedes method. The phase and micrographs of sintered magnets were characterized using X-ray diffraction (XRD) and emission scanning electron microscope (SEM). Magnetic properties were analyzed by the vibrating sample magnetometer (VSM).

Magnetic Performance and Microstructures of Hot-deformed Nd-Ce-Fe-B Magnets

Wonjin Kim[*], Ye Ryeong Jang, Hyun-Sook Lee and Wooyoung Lee

Department of Materials Science and Engineering, Yonsei University, Seoul 03722, Republic of Korea

Replacing Nd with more abundant and low cost Ce has been widely studied in recent years. However, the intrinsic magnetic properties, such as saturation magnetization and anisotropy field, of Ce2Fe14B are lower than those of Nd2Fe14B. In order to improve magnetic properties and reduce the manufacturing cost, it is necessary to develop an appropriate prepare method and to modify the phase constitution. Hot-deformation process has been proved as an efficient method for manufacturing high-density anisotropic magnets and can prevent microstructure deterioration at a lower temperature and shorter time compared to the conventional sintering process. In this study, we investigated the magnetic properties of hot deformed Nd-Fe-B magnets by replacing Ce. The composition of Nd-Ce-Fe-B was adjusted during the fabrication process of the melt-spun ribbons. The magnetic properties of the as-prepared magnets were analyzed by comparing the microstructures of grains and compositional distributions of low-melting alloys. Finally, in order to obtain the best magnetic performance of Nd-Ce-Fe-B hot deformed magnets. the optimal compositions of Nd and Ce and the optimal conditions of high-press and hot-deformation were determined.

SrM Nanoparticles에 다양한 알칼리 염의 치환에 따른 상형성 및 자기적 특성변화

최재영[1,2*], 이정민[1], 백연경[1], 이정구[1], 김양도[2], 김영국[1]

[1]한국재료연구원, 자성재료연구실
[2]부산대학교, 재료공학과

본 연구에서는 다양한 pH 조절체인 알칼리 염을 사용하여 이들이 $SrFe_{12}O_{19}$ 나노입자 (SrM NPs)에 어떠한 영향을 미치는지에 대한 연구를 진행하였다. SrM NPs 는 공침법을 통해 합성 되었으며 pH 조절체로는 다양한 알칼리 염을 함유한 용액과 혼합하였다. 하소 전 증류수를 통해 세척을 하나 잔류한 알칼리 염들이 SrM NPs에 영향을 미치는 것을 확인하였다. NaOH를 사용하여 합성한 SrM NPs는 매우 우수한 단일상과 자기적 특성을 가진다. 하지만 KOH, LiOH를 사용한 SrM NPs는 이차상이 생성되었으며 자기적 특성이 감소하였다. XRD 분석결과 NaOH, KOH를 포함한 SrM NPs는 소결하였을 때 단일상이 형성되었고 Na보다 큰 K가 첨가된 SrM NPs의 경우 오히려 격자상수가 감소하였다. Li를 포함한 SrM NPs의 경우 하소 후 비정질로 존재하였고, 소결 후에는 Li-rich 상이 1차상이었으며 M-type SrM상이 2차상으로 존재하였다. KOH를 첨가하면 입자크기가 작고 결정성이 좋지않아 자화 및 보자력이 감소한다.
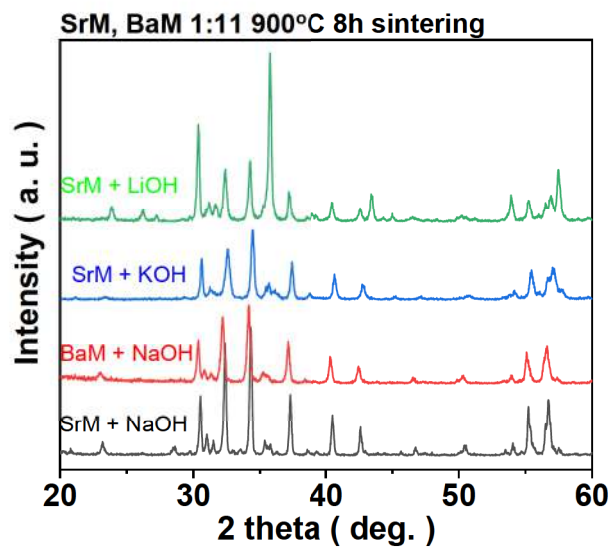
Fig. 1. XRD data, SrM + NaOH, KOH, LiOH

Magnetic Properties of Ce-Fe-B magnets produced by reduction-diffusion process

Jun-Sun Hwang[*], Kang-Hyuk Lee, Sang-Im Yoo[†]

Department of Material Science and Engineering, Research Institute of Advanced Materials (RIAM),
Seoul National University, Seoul, Korea

Nd-Fe-B permanent magnets have been widely used due to the high saturation magnetization (M_s), remanence magenetization (M_r), and coercivity (H_c). However, the high cost of Nd ions prevents their application. Considering the cost reduction of rare earth metals, there is a growing requirement for usage of low-cost rare earth metals, such as Ce, La in Nd-Fe-B magnets. Despite its low magnetic properties of Ce-Fe-B magnet($4\pi M_s$ = 11.7kG) compared to Nd-Fe-B magnet($4\pi M_s$ = 16kG), but it is usable. RSP process is commonly used to synthesize $Ce_2Fe_{14}B$, but the process costs much more than reduction-diffusion process, so we synthesized $Ce_2Fe_{14}B$ using reduction-diffusion process. First, $CeFeO_3$ was synthesized using CeO_2, Fe_2O_3, and Fe at 1050°C for 6h in Ar. The mole ratio was 3 : 1 : 19, which satisfies with the mole number of Ce and Fe in $Ce_2Fe_{14}B$. After that, we mixed $CeFeO_3$, Fe, and H_3BO_3. The H_3BO_3 was added satisfying $Ce_2Fe_{14}B_x$ (x=4,5,6). Then we conducted reduction-diffusion process by adding Ca at 1050°C for 6h in Ar. $Ce_2Fe_{14}B$ single phase was synthesized at B=5. $Ce_2Fe_{14}B$ was also synthesized, but much Fe still remained, at B=4 and B=6. The M_s, M_r, and H_c of $Ce_2Fe_{14}B$ at B=5 was 143.63 emu/g, 4.4421 emu/g, 74.905Oe, respectively. The phase and the magnetic properties were characterized using X-ray diffraction (XRD) and the vibrating sample magnetometer (VSM) at room temperature, respectively.

High-performance Ce-substituted (Nd,Ce)-Fe-B hot-deformed magnets fabricated from amorphous melt-spun powders

Ga-Yeong Kim[1,2*], Tae-Hoon Kim[1], Hee-Ryoung Cha[1], Yang-Do Kim[2*] and Jung-Goo Lee[1†]

[1]Department of Magnetic Materials, Korea Institute of Materials Science, Changwon, Korea
[2]Department of Materials Science and Engineering, Pusan National University, Busan, Korea

Ce is the most abundant rare earth elements and its price is about 1/40 of the price of Nd. Hence, it is a technologically interesting challenge to develop high-performance Nd-saving Nd-Fe-B magnets by substitution of Ce for Nd. However, the magnetic properties of Nd-Fe-B magnets could be drastically deteriorated after replacing Nd with Ce due to inferior intrinsic magnetic properties of $Ce_2Fe_{14}B$ ($4\pi M$ = 11.7 kG, Ha = 26 kOe) compared to $Nd_2Fe_{14}B$ ($4\pi M$ = 16 kG, Ha = 73 kOe). Furthermore, according to previous investigations on (Nd,Ce)-Fe-B magnets, a Ce-dissolved $REFe_2$ secondary phase is formed at the triple junction region, this leads to further deterioration in both remanence and coercivity of the high-Ce-content magnets with a Ce-substitution level of 25 % or more because the $REFe_2$ phase is paramagnetic and hinders the formation of RE-rich grain boundary phase that is essential for the coercivity generation of the Nd-Fe-B based magnets. The hot deformation is well known porcess to fabricate high-performance Nd-Fe-B magnets comprising ultra-fine grains. According to our previous study, the $REFe_2$ phase hinders not only the RE-rich grain boundary phase formation but also the grain boundary sliding and grain rotation during the hot-deformation. If we obtain a method to inhibit the formation of $REFe_2$ phase in the high-Ce-content (Nd,Ce)-Fe-B hot-deformed magnets, we can expect development of cost-effective (Nd,Ce)-Fe-B magnets with sufficient permanent magnetic properties to replace commercial Nd-Fe-B magnets. In this study, we investigate a method to produce high-performance and cost-effective Ce-substituted Nd-Fe-B hot-deformed magnets with 30% Nd reduction. To suppress the formation of Ce-dissolved $REFe_2$ phase, which is a main obstacle for [001] texture development and RE-rich grain boundary phase formation, the amorphous melt-spun precursors were used in fabricating 30% Ce-substituted hot-deformed magnets. To prepare amorphous precursors, the $(Nd_{0.7}Ce_{0.3})_{30.0}Fe_{62.0}B_{1.0}Ga_{1.0}Co_{6.0}$ (wt.%) alloy ingots were melt-spun with a wheel speed of 35 m/s and then pulverized into powders. For comparison, the crystalline melt-spun powders were also prepared by pulverizing the $(Nd_{0.7}Ce_{0.3})_{30.0}Fe_{62.0}B_{1.0}Ga_{1.0}Co_{6.0}$ ribbons fabricated at a wheel speed of 28 m/s. The melt-spun powders were then hot-pressed and subsequently die-upsetted. By suppressing the formation of $REFe_2$ phase from the precursors, the c-axis alignment of 2:14:1 platelets in the magnets by grain boundary sliding and grain rotation was improved, and the Nd/Ce-concentration of grain boundary phases in the magnets was increased. As a result, both the coercivity and remanence of the magnets noticeably increased to 15 kOe and 13 kG, respectively, compared to those of the magnets fabricated from crystalline precursors containing REFe2 phase (H_{cj} = 13.4 kOe, $4\pi M_r$ = 12.1 kG). The magnetic performance of the 30%-Ce-substituted magnets developed in this work is sufficient to replace the N42M-graded commercial Ce-free magnets.

Versatile MBE Growth of Tetrataenite L1$_0$-FeNi Film

Van Quang Nguyen[*] and June Hyuk Lee[†]

Neutron Science Division, Korea Atomic Energy Research Institute (KAERI), Daejeon 34057, Republic of Korea

Ordered hard magnetic L1$_0$-FeNi, tetrataenite, has attracted attentions as a good candidate for rare earth free permanent magnet with comparable maximum magnetic energy product. Fabricating tetrataenite is challenge using conventional method due to its low order-disorder transition temperature, 320 °C. In this work, high quality FeNi films were fabricated using molecular beam epitaxy (MBE) on Al$_2$O$_3$ (0001) substrate with different deposition route i.e., co-deposition (CD), alternative monatomic layer deposition (AMLD), and 2 steps co-deposition (2SCD). XRD patterns indicated that the L1$_0$-FeNi phase was successfully obtained using these three deposition routes from low to moderate substrate temperatures. Surprisingly, the CD films show decrease in crystallinity with increasing substrate temperature, where the best substrate temperature is 50 °C. By using 2SCD, it is possible to fabricate sample at higher substrate temperature in order to obtain larger uniaxial magnetic anisotropy energy, K$_u$. Whereas lower quality films were achieved using AMLD, attributed to the smaller diffusion of Fe and Ni in this growth route. Other characterizations using vibrating sample magnetometer and neutron reflectivity will be discussed. Our work provides a comprehensive picture on MBE growth of the L1$_0$-FeNi film for the development of next-generation rare earth free hard magnetic materials.
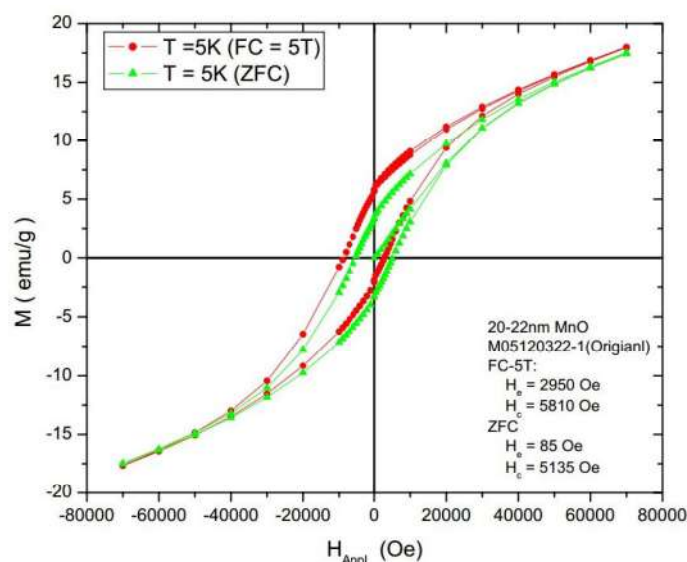
Fig. 1. A sample line graph
(1line spacing / image size: 300 dpi)

A Halbach Magnet Prototype for Low Field MR Systems

Yeong-Jae Jeon[1,2*], Shin-Eui Park[1], Ji-Yeon Suh[1], Hyeon-Man Baek[1,2]

[1]Lee Gil Ya Cancer & Diabetes Institute, Gachon University, Incheon, the Republic of Korea
[2]Department of Health Sciences and Technology, GAIHST, Gachon University, Incheon, The Republic of Korea

Conventional MRI systems use superconducting electromagnets to create high magnetic fields. However, researches on low-field MRI using low-cost permanent magnets are also being actively conducted [1]–[3]. In this work, we introduce a Halbach magnet for the construction of low-cost and low-field MRI scanner. As an alternative to the H-shape or C-shape design, if a permanent magnet is placed in a specific position to make a Halbach array, a magnetic field for NMR or MRI can be created. Halbach magnet is flexible in design and relatively easy to make compared to other types of design in terms of manufacturing. A simulation study is conducted to make a prototype, and the Larmor frequency and bandwidth for magnetic resonance could be determined by measuring the magnetic field strength after fabrication (**Fig. 1**).
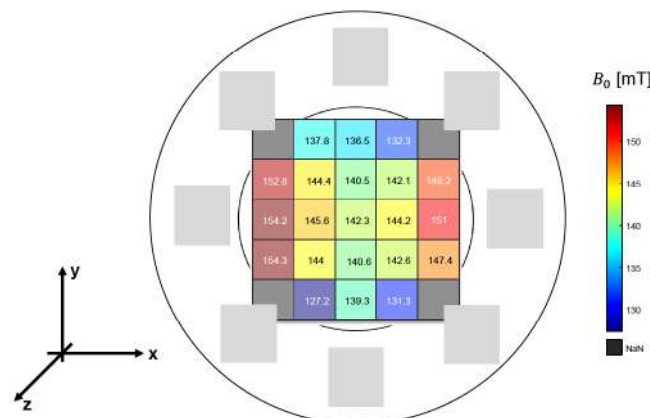
Fig. 1. Magnetic field (B_0) measurements at the center of the bore.

References

[1] C. Z. Cooley *et al.*, "Design and implementation of a low-cost, tabletop MRI scanner for education and research prototyping," *J. Magn. Reson.*, vol. 310, p. 106625, (2020).

[2] C. Z. Cooley *et al.*, "A portable scanner for magnetic resonance imaging of the brain," *Nat. Biomed. Eng.*, vol. 5, no. 3, pp. 229–239, (2021).

[3] Y. Liu *et al.*, "A low-cost and shielding-free ultra-low-field brain MRI scanner," *Nat. Commun.*, vol. 12, no. 1, pp. 1–14, (2021).

Magnetic properties and high frequency characteristic of M-type hexaferrite synthesized by the molten salt method

Minyeol Kim[*], Kyoo-sung Park, Jongryoul Kim

Department of Materials and Chemical Engineering, Hanyang University, Ansan 15588, South Korea

차세대 통신 기술과 자율주행기술이 발달함에 따라 이에 활용되는 자성소재들의 작동 주파수가 상승하고 있다. 따라서, 페라이트 자성소재는 높은 전기저항과 이방성 자기장을 가지도록 연구개발이 진행되고 있다. 이에 따라, 밀리미터 파 대역에서 강자성 공명(Ferromagnetic resonance, FMR)을 가지는 것으로 알려져 있는 M-type 헥사페라이트는 통신장비 및 자율주행기술에 활용 가능한 우수한 소재 중 하나이다. M-type 헥사페라이트의 자기적 특성은 조성변화에 따라 포화자속밀도와 보자력을 제어 할 수 있으며, 용융염 합성공정을 활용하여 분말의 형상을 제어하는데 매우 용이하다. 따라서, 이러한 M-type 헥사페라이트 분말의 자기적 및 고주파 특성에 대한 지속적인 연구가 필요하다.

본 연구에서는 다양한 조성의 M-type 헥사페라이트 분말이 용융염 공정을 활용하여 합성하였다. 모분말은 $SrCO_3$, $BaCO_3$, Fe_2O_3, NaCl을 볼 밀링을 통해 균질하게 교반하였으며, 박스로에서 다양한 열처리 조건 하에 하소를 진행하였다. 우선 자가적 특성 변화에 따른 M-type 헥사페라이트의 고주파 특성 변화를 관찰하기 위해 동일한 열처리 조건에서 서로 다른 입도를 가지는 스트론튬 페라이트 분말을 합성하였다. 합성된 스트론튬 페라이트 분말의 입도를 제어하기 위해 모분말 제조 시 각각 0.3 μm와 1.0 μm 크기의 Fe_2O_3 분말을 사용하였다. 또한 조성변화에 의한 고주파 특성 분석을 위해 바륨 페라이트와 스트론튬 페라이트 분말을 합성하였다. 합성된 모든 M-type 헥사페라이트 분말들은 VSM(Vibrating sample magnetometer)를 활용하여 자기적 특성을 분석하였으며, network analyzer를 이용하여 투자율 측정을 진행하였다. 시료의 미세구조와 분석은 XRD(X-ray diffractometer)을 사용하였다.

합성된 M-type 헥사페라이트 분말들은 VSM 분석 결과 포화자속밀도가 이론값에 가까우며, 결정구조가 M-type 헥사페라이트 상을 가지는 것을 XRD 분석을 통해 확인하였다. 합성된 분말을 활용하여 시트 형태의 복합자석을 제작하여 network analyzer로 투자율을 측정하였다.

그림 1은 스트론튬 페라이트 분말의 입도 크기에 따른 자기적 특성 및 투자율 측정 결과를 비교 한 것이다. 그림 1 a) 분말은 0.3 μm Fe_2O_3 분말을 사용하여 합성한 스트론튬 페라이트 분말이며 b)는 0.3 μm Fe_2O_3 사용하여 합성한 시료이다. 두 시료 모두 동일한 열처리 조건 아래에서 하소를 진행하였으며, 용융염 공정에 활용한 NaCl 제거를 위해 증류수를 활용하여 NaCl을 모두 제거 한 이후 자기적 특성분석과 투자율 측정을 진행하였다. 자기적 특성 분석 결과 a)와 b) 시료 모두 포화자속밀도는 비슷한 수치를 나타내었으며, 이는 이론값에 매우 근접한 것을 확인하였다. 반면 보자력은 시료 합성에 활용된 초기 Fe_2O_3 입자의 크기에 따라 달라진 것을 확인 할 수 있었다. 투자율 측정 결과 서로 다른 보자력 특성에도 불구하고 두 시트 모두 FMR이 50 GHz 근처에서 발생 하였다.

그림 2는 M-type 헥사페라이트 분말의 조성변화에 따른 자기적 특성 및 투자율 측정 결과를 비교 한 것이다. 그림 2 a)는 스트론튬 페라이트 분말이며 b)는 바륨 페라이트 분말이다. 합성된 시료는 XRD 분석 결과 불순물 없이 M-type 헥사페라이트 구조를 가지는 것을 확인하였다. 해당 시료의 투자율 측정 결과 스트론튬 페라이트와 바륨 페라이트의 FMR 발생 위치가 차이를 보이는 것을 확인하였다. 이러한 차이는 바륨 페라이트와 스트론튬 페라이트 분말이 가지는 이방성 자기장 차이에 의한 것으로 보인다.

결과적으로, M-type 헥사페라이트에서의 투자율 거동은 포화자속밀도와 보자력과 같은 자기적 특성차이에 의한 변화보다, 이방성 자기장이 더 큰 영향을 미치는 것으로 보인다. 따라서, M-type 헥사페라이트의 FMR 제어를 위해서는 열처리 공정제어를 통한 자기적 특성과 분말 입도를 제어하는 방법이 아니라, 조성변화를 통해 헥사페라이트 분말의 이방성 자기장을 제어하는 것이 더 효과적인 접근방법인 것으로 보인다.
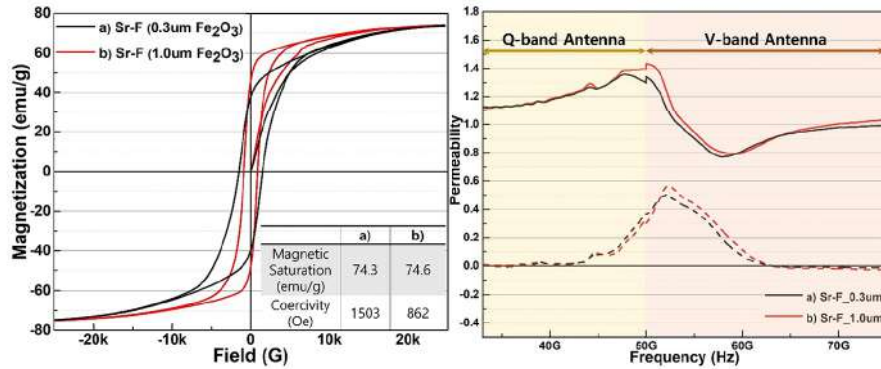
그림. 1 Magnetic properties and permeability of synthesized M-type strontium hexaferrite powders, a) using 0.3 μm Fe_2O_3, b) using 1.0 μm Fe_2O_3
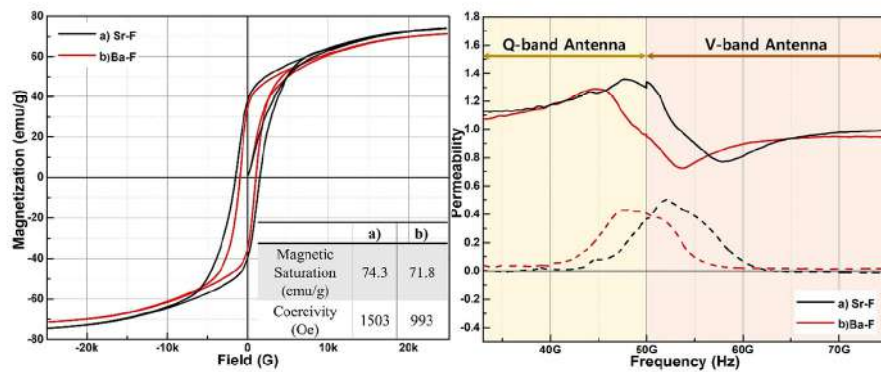
그림. 2 Magnetic properties and permeability of synthesized M-type strontium hexaferrite powders, a) $SrFe_{12}O_{19}$, b) $BaFe_{12}O_{19}$
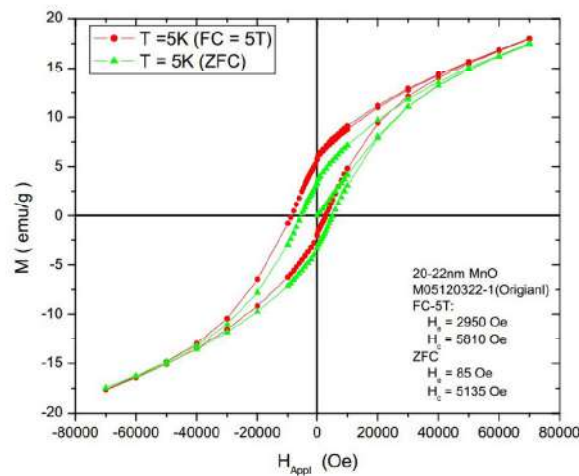
Fig. 1. A sample line graph
(1line spacing / image size: 300 dpi)

나노 결정립을 갖는 ThMn$_{12}$-type Sm$_x$Fe$_{11}$Ti (x=0.9, 1.0, 1.1) 합금의 자기적 특성과 미세조직에 관한 연구

이한솔[*], 강민규, 김종렬[†]

한양대학교 재료화학공학과

ThMn$_{12}$ 결정구조를 갖는 SmFe$_{12}$ 기반 합금은 뛰어난 자기적 특성을 보유하여 차세대 영구자석으로서 최근 활발한 연구가 진행중이다. 이 합금의 자기이방성장은 7 ~ 12 T으로 가장 강력한 영구 자석인 Nd$_2$Fe$_{14}$B의 자기이방성장(약 7 T)을 상회한다. 그러나 실질적으로 중요한 자기 특성 지표인 보자력(H$_c$)은 자기이방성장의 10%도 채 구현되지 않고 있는 실정이다. 본 연구에서는 급속응고법으로 제조된 합금 내 Sm 조성과 열처리 조건을 변화시키면서 합금의 자기적 특성과 미세조직의 관계를 파악하고 저보자력의 원인에 대하여 고찰하였다.

합금 조성 별로 최대 보자력을 나타내는 열처리 온도(T$_A$)는 Sm 함량에 비례하여 증가하며 이는 Sm 함량이 높아질수록 ThMn$_{12}$ 결정 구조의 형성이 지연되기 때문인 것으로 확인되었다. 가장 높은 보자력을 보인 합금은 SmFe$_{11}$Ti로서 850℃에서 15분간 열처리 후 6.3 kOe의 보자력을 나타내었으며 이 때의 결정립 크기는 약 40 nm 으로 확인되었다. 합금의 결정립 크기는 열처리 온도가 더욱 증가함에 따라 지속적으로 증가하는 반면 보자력은 감소하는 경향을 나타내었다. 따라서 본 합금의 보자력은 Sm 함량과 열처리 조건에 매우 민감하게 변화하는 것을 알 수 있다.
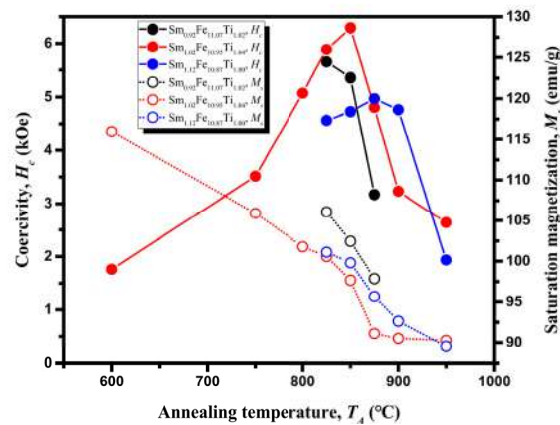
Fig. 1. Magnetic properties of Sm$_x$Fe$_{11}$Ti (x=0.9, 1.0, 1.1) with various annealing temperature measured at maximum applied field of 2.5 T
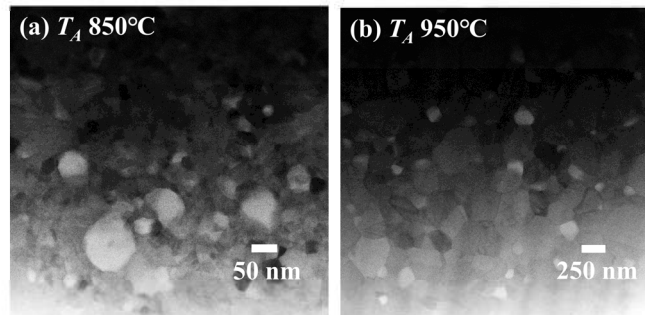
Fig. 2. Bright field images of Sm$_{1.0}$Fe$_{11}$Ti annealed at (a)850℃ and (b)950℃ for 15 minutes using Transmission Electron Microscopy. The intermetallic compound, Fe$_2$Ti, was showed on bright contrast in images.

Fabrication of hot-deformed magnets prepared by Ce-substituted (Nd,Ce)-Fe-B HDDR powders

Jae-Gyeong Yoo[1,2*], Tae-Hoon Kim[1], Hee-Ryoung Cha[1], Yang-Do Kim[2†], Jung-Goo Lee[1†]

[1]Department of Magnetic Materials, Korea Institute of Materials Science, Changwon, Korea
[2]Department of Materials Science and Engineering, Pusan National University, Busan, Korea

In recent times, increasing demand for Nd-Fe-B permanent magnets for high-efficiency motors in hybrid/ electric vehicles and wind turbines has attracted growing attention in the development of Nd-lean RE-Fe-B magnet using abundant and low-cost alternatives, such as La or Ce, instead of Nd. However, the magnetic properties of (Nd,Ce)-Fe-B magnets could be outstandingly deteriorated after replacing Nd with Ce since the $Ce_2Fe_{14}B$ phase ($4\pi M_s$ = 11.7 kG, H_a = 26 kOe) has lower intrinsic magnetic properties than those of the $Nd_2Fe_{14}B$ phase ($4\pi M_s$ = 16 kG, Ha = 73 kOe). Furthermore, the Ce-dissolved $REFe_2$ secondary phase is inevitably formed in the $(Nd_{1-x}Ce_x)$-Fe-B magnets at x≥0.3 because Ce reveals quasi-complete substitutional solubility in $(Nd_{1-x}Ce_x)_2Fe_{14}B$ phase. The $REFe_2$ phase would lead to further deterioration of both remanence and coercivity because the $REFe_2$ phase is paramagnetic at room temperature (Tc = 235K) and interrupts the formation of RE-rich grain boundary phase, which is essential for conferring coercivity to Nd-Fe-B-based magnets. Conventionally, the $REFe_2$ phase plays positive role on densification and the formation of continuous and uniform RE-rich grain boundary phases caused by good wettability during sintering above the melting point of $REFe_2$ phase (925ºC) in the (Nd,Ce)-Fe-B sintered magnets whereas that is harmful to the (Nd,Ce)-Fe-B hot-deformed magnets. This is because the $REFe_2$ phase does not melt during hot-deformation process at a temperature(600-800ºC) below the melting point of $REFe_2$ phase, which hinders not only the deformation of the main phase grains but also development of [001] texture. Therefore, the formation of the $REFe_2$ phase is expected to be more serious influence on the deterioration of the magnetic properties in the hot-deformed magnets than that in the sintered magnets. Hence, various attempts for suppression of the $REFe_2$ phase formation have been carried out by addition of element, such as La, Ta, and Si in the initial alloy of (Nd,Ce)-Fe-B hot-deformed magnets. Interestingly, the $REFe_2$ phase was easily inhibited by reforming of RE-rich grain boundary phase from decomposition of $REFe_2H_x$ into REH_x and α-Fe during HDDR (hydrogenation-disproportionation-desorption-recombination) process, which could be a powerful method to inhibit the formation of $REFe_2$ phase in the high-Ce-content (Nd,Ce)-Fe-B hot-deformed magnets. However, most of the studies have been concerned with (Nd,Ce)-Fe-B hot-deformed magnets produced by melt-spun powder and studies on HDDR powders are limited.

Thus, in this work, we fabricated the anisotropic hot-deformed magnet using the Ce-substituted $(Nd_{1-x}Ce_x)$-Fe-B HDDR powder, and observed the influences of the magnetic and microstructural properties of initial HDDR powders containing different Ce content on the magnetic alignment and hot-deformation behaviours. Especially, in spite of formation of REFe2 phase in the alloys over X=0.3, obtained HDDR powders are not formed $REFe_2$ phase until x=0.5 after HDDR treatment. This implies that the $REFe_2$ phase in high Ce-containing HDDR powders is spread to amorphous $CeFe_2H_x$ and further decomposed into CeH_x and α-Fe under hydrogenation-disproportionation stage, and formed RE-rich grain boundary phase instead $REFe_2$ under desorption-recombination

stage during HDDR process [1]. By suppressing the formation of $REFe_2$ phase through HDDR process, the remenance of hot-deformed magnet until Ce-substitution level of 50 % show the gradual deterioration. A detailed method to control the magnetic and microstructural properties of the initial HDDR powders will be explained, and the magnetic and microstructural differences between the hot-deformed magnets produced from HDDR powders containing different Ce content will be discussed.

Reference

[1] I. Poenaru *et al*, J. Alloys Compd., 152-215, 814 (2020).

분말 기반 Fe-6.5%Si 전기 강판의 자기적 성질 연구

김도희[1*], 권기혁[1†], 김우열[1], 나태욱[2], 최용석[3], 백운경[3], 권민호[3]
[1]포항산업과학연구원
[2]한국생산기술연구원
[3]제닉스 주식회사

Fe-6.5%Si 전기 강판은 높은 포화자속밀도 및 고주파 대역에서 철손이 낮은 특징을 가지고 있다. 그러므로 고효율 구동모터를 구현하기에 가장 적합한 소재이다. Si의 함량을 높임으로써 우수한 전·자기적 성질을 확보할 수 있지만, 그로 인해 냉간 압연성이 저해되어 생산성이 낮은 단점이 있다. 이로 인해 일반 판재 제조공정으로는 고품위의 판재를 대량생산하기에 부적합하여 상업적으로 사용되지 못하고 있다. 이러한 문제점을 해결하기 위한 다양한 공정이 연구개발 되고 있다. 그중 분말압연 공정은 Fe-6.5%Si 전기 강판을 저비용으로 생산할 수 있다. 또한, 원료소재를 변화시켜 다양한 합금계를 구현할 수 있는 장점이 있다.

이에 본 연구에서는 Fe-6.5%Si 분말 압연을 통한 고밀도의 판재 제조가 가능한지 확인하고, 분말 기반 Fe-6.5%Si 전기 강판 제조 가능성을 제시하고자 한다. 본 연구에서는 고순도Fe 분말 및 고순도 Si 분말을 활용하였다. 전기 강판의 자기적 성질 확보를 위해 Fe 분말 형상 제어, Si 함량 다변화, 액상 소결, 바인더 접합 분말을 적용하여 다양한 연구를 진행하였다. 본 결과를 통해 분말 기반 Fe-6.5%Si 전기 강판의 최적의 제조 조건을 확립하고자 한다.

DPI 시스템 연료분사기 부품용 페라이트계 연자성재의 국산화를 위한 선행 연구

정해혁[*], 박헌준, 이진한

현대자동차그룹-현대케피코

본 연구는 자동차 파워트레인 연료분사 시스템에 적용되는 듀얼인젝터 내 페라이트계 연자성재 SUS430FR의 국산화를 위한 선행 연구에 관한 것이다.

친환경차의 글로벌 시장 점유율이 점차 높아지고 있으나 하이브리드를 포함한 내연기관이 적용되는 차량의 비율은 여전히 전체 자동차 시장에서 80% 이상을 차지하고 있다.

이에 따라 자동차 업계에서는 친환경차 관련 개발은 물론 지속적으로 기존 파워트레인 부품의 원가경쟁력을 위한 연구가 진행되고 있다.

인젝터는 차량의 운전 조건에 따라 ECU로부터 산정된 연료 분사 시간 동안, 정확한 양의 연료를 최적의 분무상태로 흡기포트에 분사하는 솔레노이드 형태의 정밀 제어 밸브로서 제품의 주요 성능은 자성 부품의 자기특성에 의해 결정된다. 그 중 리드파이프는 주요 자기회로를 구성하고 응답성능에 영향을 주는 매우 중요한 자성 부품 중 하나이다.

듀얼인젝터는 Dual multi Point Injection(DPI)로 기존 Port Fuel Injection (PFI)과는 다르게 하나의 실린더(흡기포트)에 두 개의 인젝터를 장착하여 연료 분사의 정밀도를 높여 기존 대비 연비와 배기성능을 개선한 인젝터이다.

본 연구는 듀얼인젝터 리드파이프용 페라이트계 연자성재 SUS430FR의 국산화를 통한 원가경쟁력 강화를 그 목표로 하였으며, 1) 기존 원소재 대비 소재 특성 동등 이상 (Hc ≤ 2.0 A/cm, Permeability ≥ 2500, Electrical Resistance ≥ 0.76 $\Omega \cdot$ ㎟/m), 2) 부품화를 통한 가공성 확인, 3) 부품 및 완제품 단위 특성 확인 (BH 트레이서, ICP-OES, GD-OES, XRF, 만능시험기, 비커스경도기, 완제품 성능시험기)과 같은 순으로 연구를 진행하였다.

특히 자기적 특성 만족을 위해 열처리 온도, 시간 등 열처리 조건을 다양하게 설정하여 최적의 열처리 조건을 도출하였고, 이를 통해 기존 원소재와 동등한 수준의 특성을 확보할 수 있었다.

Electromagnetic wave absorbing properties of Mn-substituted Ni-Zn ferrites

Ji-Hye Lee[1], Min-Gu Kang[1], Young-Min Kang[1*], Sang-Min Lee[2]

[1]Department of Materials Science and Engineering, Korea National University of Transportation, Chungju, 27469, Korea

[2]Division of Creative Convergence, Korea National University of Transportation, Chungju 27469, Korea

*Corresponding author email: ymkang@ut.ac.kr

In this study, Mn-substituted Ni-Zn spinel ferrite ($Ni_{0.5}Zn_{0.5}Fe_2O_4$) were prepared by both sol-gel and solid-state reaction methods. The respective powders were mixed with epoxy binder (10 wt %) and pressed into toroidal shapes, which were finally cured at 180 °C 1h in air. Spinel phase was confirmed by X-ray diffraction (XRD) analysis. Scanning electron microscope (SEM) was used for the microstructure observation. The complex permittivities (ε', ε'') and permeabilities (μ', μ'') spectra ($0.1 \leq f \leq 18$ GHz) were measured by using a vector network analyzer on the toroidal samples. The reflection loss (RL), which shows the electromagnetic (EM) wave absorbing performance were calculated and the RL map as functions of absorber thickness (d) and frequency (f) also plotted for each sample. The dependence of the EM wave absorption characteristics on the Mn substitution site (Fe, Ni, Zn) and the Mn substitution amount will be revealed and discussed.

Effect of Heat Treatment on Magnetic Properties of Fe-based Amorphous Alloys

Jihye Park[*], Hyunsol Son, Haein Choi-Yim[†]

Department of Applied Physics, Sookmyung Women's University, Seoul, 04310, Korea

Fe-based amorphous/nanocrystalline alloys have been widely applied in commercial products such as magnetic cores due to their excellent soft magnetic properties. In particular, nanocrystalline materials are well known for their high saturation flux density and high permeability comparable to Fe-based amorphous alloys, which drastically improves soft magnetic characteristics. This study aimed to research the magnetic properties of Fe-Co-B-P-Cu amorphous ribbons by giving variations on heat treatment conditions. Nanocrystalline ribbons were fabricated by rapid quenching melt spinning method followed by heat treatment. We obtained differential scanning calorimetry (DSC) curves of as-spun specimens to investigate the annealing condition. Structural properties were examined via X-ray diffraction (XRD) and magnetic properties via vibrating sample magnetometer (VSM). Among the alloys investigated, an annealing time of 10 min over a temperature of 440°C exhibits highest magnetic flux density of 1.88T in combination with desirable coercivity, which entitles Fe-Co-B-P-Cu alloy as an advantageous candidate in industrial applications.

FeSiCr 연자성 복합체의 입자 크기에 따른 마이크로파 흡수 특성

최연준[*], 이민영, 김상우, 이보화[†]

Department of Physics and Oxide Research Center, Hankuk University of Foreign Studies, Yongin, South Korea

GHz 대역에서의 통신기술 사용이 확대됨에 따라 스마트폰을 비롯한 전자기기에서 발생하는 전자파 간섭 (EMI)으로 인한 기기 오작동 및 인체 유해성에 대한 문제가 발생하고 있다. 이에 따라 EMI 방지를 위한 GHz 대역에서의 전자파 차폐 물질 개발이 진행되고 있다. 본 연구에서는 페라이트 물질에 비해 비교적 제조하기 쉽고 저렴한 가격을 가지는 Fe 기반 합금의 입자 크기에 따른 마이크로파 흡수 특성을 분석하였다. Gas-atomization에 의해 제조된 FeSiCr 합금을 25 μm이하, 25-38 μm, 38-53 μm, 53-63 μm, 63 μm 이상의 입자 크기로 나누었다. 각 사이즈 별 파우더의 입자 크기 분포는 particle size analyzer, morphology는 scanning electron microscopy, 결정 구조는 X-ray diffractometer, 자기적 특성은 vibrating sample magnetometer을 사용해 분석하였다. 각 파우더는 3.0 wt%의 epoxy resin과 섞어 2.0 mm 두께의 toroidal core로 만들었고, network analyzer을 사용하여 0.1-18 GHz대역에서의 투자율과 유전율을 측정하여 reflection loss(RL)를 계산하였다. 전체적인 마이크로파 흡수 특성은 입자 크기가 작아짐에 따라 점차 증가하는 경향성을 보였으며, 25 μm 이하의 파우더의 RL은 약 4 GHz에서 -9.4 dB로, 이는 약 90 %의 마이크로파 흡수 성능에 해당한다.

CIP와 Fe nano 분말 첨가에 따른
FeSiCrB 연자성 복합체의 자기적 특성

김대유[*], 박봉태, 우혁준, 이보화[†]

한국외국어대학교 물리학과, 산화물 연구센터

칩 인덕터는 핸드폰이나 전기차와 같은 전자 장비에 전원을 공급해주는 주된 수동소자이다. 최근 고성능 전자 장비의 소형화에 따라 칩 인덕터 또한 소형화, 고성능화가 요구되고 있어 소재의 높은 투자율과 포화자속 밀도, 낮은 코어 손실 등의 성능 향상이 필요하다. 본 연구에서는 gas-atomization에 의해 제조된 평균 크기가 25.3um인 FeSiCrB 비정질 합금에 미분과 초미분으로 각각 3.8~5.4um인 CIP와 95~105nm인 Fe nano 분말을 첨가하여, 이에 따른 자기적 특성을 분석하였다. 각 파우더의 입자 크기 분포는 particle size analyzer, 결정 구조 는 X-ray diffractometer, 자기적 특성은 vibrating sample magnetometer을 사용해 분석하였다. 혼합 비에 따라 준비된 각 파우더는 3.5wt%의 epoxy resin과 섞어 20.00 x 12.88 mm 규격의 toroidal core로 성형하였고, 분말 첨가에 따른 입자 분포의 morphology를 scanning electron microscopy 로 파악하였다. B-H analyzer 로 100kHz ~ 1MHz 대역에서의 core loss를 측정한 결과, CIP와 Fe nano 분말의 첨가에 따라 코어 손실이 감소하였다.

Microwave absorption properties of partially Zn-substituted strontium W-type hexaferrites in Ka band (26.5-40 GHz)

Seung-Min Choi[1,2*], Hyuk-Jin Seo[1] and Sang-In Yoo[1]

[1]Department of Materials Science and Engineering, Research Institute of Advanced Materials (RIAM),
Seoul National University, Seoul 151-744, Korea
[2]Chang Sung Co Ltd, 1840-29, Seohae-ro, Cheongbuk-eup, Pyeongtaek-si, Gyeonggi-do, 17794, Korea

Recently, many researchers have reported the microwave absorption properties of hexaferrites, including M-, W-and Y-type hexaferrites. It has been, however, a challenging task to achieve an enhancement microwave absorber in the Ka band (26.5 – 40 GHz) which can exhibit the reflection loss (RL) less than -20 dB (i.e., absorption higher than 90%) for the absorber thickness less than 1mm. In this study, we report that such thin and excellent microwave absorber in Ka band are obtainable from flexible sheet with partially Zn-substituted Strontium W-type (SrW) hexaferrites ($SrFe_{1.75}Zn_{0.25}Fe_{16}O_{27}$). We fabricated flexible absorber sheet with various filler contents through the tape casting method by mixing SrW powders and acryl resin. The measurements of complex permittivity ($\varepsilon_r = \varepsilon' - j\varepsilon''$) and permeability ($\mu_r = \mu' - j\mu''$) were carried out using the Vector Network Analyzer(E8364A), their complex permittivity and permeability values were calculated from S-parameters in the Ka band frequency region. Consequently, the microwave absorbing properties will be presented including reflection loss, various thickness and filler contents.

The Effect of Si/B Ratio on the Soft magnetic properties and microstructure of $Fe_{80+x}(B_aSi_b)_{15-x}C_1Cu_1Nb_3$ Nanocrystalline Soft Magnetic Ribbons

Subong An[1,2*], Hyun Ah Im[1,2], Yeong Gyun Nam[1,2], Sangsun Yang[1],
Jung Woo Lee[2] and Jae Won Jeong[1†]

[1]Metal Powder department, Korea Institute of Materials Sciene(KIMS),
797 Changwondae-ro Seongsan-gu, Changwon 51508, Korea
[2]Department of Materials Science and Engineering, Pusan National University, Pusan 46241, Republic of Korea
*E-mail of Corresponding Author: jeongjw1204@kims.re.kr

The $Fe_{80+x}(B_aSi_b)_{15-x}C_1Cu_1Nb_3$ (a : b, a=1~6, b=1) nanocrystalline soft magnetic ribbons were fabricated to obtain a high saturation flux density (B_s) and a high glass forming ability (GFA) by consisting of over 80 at% Iron (Fe) content and controlled with different ratio of the Boron (B) and the Silicon (Si). The ribbons were manufactured by a Rapid Solidification Processing (RSP) with a melt spinner and the aspects of nanocrystalline matrix were examined by progressing the heat treatment with different temperatures (380 °C ~ 620 °C) on muffle furnace in Argon atmosphere. To find optimal temperature for the heat treatment was analyzed using a Differential Scanning Calorimetry (DSC). The magnetic properties, coercivity, permeability, core loss and saturation flux density, were measured with a DC Loop Tracer, BH Analyzer and Vibrating-Sample Magnetometer (VSM). The microstructures of ribbons from surface part to inner part were observed to compare a formation of nanocrystals in matrix by a Transmission Electron Microscope (TEM). The results of that, the magnetic properties and microstructures of the ribbons became a more improvement characteristic with high ratio of B/Si. Optimized components of alloy, the $Fe_{80}B_{12.5}Si_{2.5}C_1Cu_1Nb_3$ ribbon (B : Si = 5 : 1) annealed 580 °C for 10 min, exhibited the saturation flux density of 1.62 T and the coercivity of 14.7 A/m relatively with other ribbons.
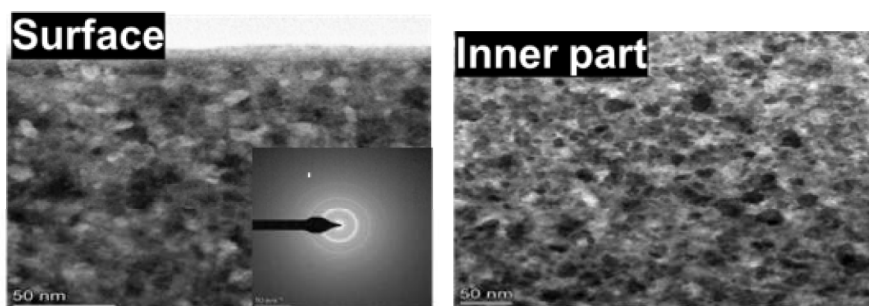
Figure 1. The TEM images of surface and inner part of nanocrystalline ribbons

Keywords: Soft magnetic materials, Rapid solid process, Glass forming ability, Nanocrystals, Magnetic properties

Effect of magnetic field on morphological and magnetic properties of FeNi₃

Su Jeong Park[1*], Akshay Kumar[2], Kavita Kumari[3], Mohit, K Sharma[2],
Seok Hwan Huh[4] and Bon Heun Koo[5†]

[1]Department of Materials Convergence and System Engineering, Changwon National University,
Changwon, Gyeongnam, 51140, Republic of Korea
[2]Mechatronics Research Institute, Changwon National University, Changwon, Gyeongnam, 51140, Republic of Korea
[3]Industrial Technology Research Institute, Changwon National University,
Changwon, Gyeongnam, 51140, Republic of Korea
[4]Department of Mechatronics Conversion Engineering, Changwon National University,
Changwon, Gyeongnam, 51140, Republic of Korea
[5]School of Materials Science and Engineering, Changwon National University,
Changwon, Gyeongnam, 51140, Republic of Korea
[*]Corresponding Author - bhkoo@changwon.ac.kr

With the advancement of portable wireless devices, it is essential to develop a soft magnetic material with a high investment rate for the efficient use of power consumption. Many studies have been conducted mainly on powder to improve the magnetic properties of ferromagnetic materials. However, there is a limit to increasing the investment rate only with the packing density, so this study seeks to develop a soft magnetic material with shape magnetic anisotropy, and Fe-Ni with high saturation magnetism and high magnetic flux density was selected. This study reports the various shapes of nanoparticles formed under magnetic induction. Fe-Ni nanoparticles were prepared by chemical reduction using $FeCl_2 \cdot 4H_2O$, $NiCl_2 \cdot 6H_2O$, $N_2H_4 \cdot H_2O$, NaOH, etc. in this research. Magnets of various strengths are used in the process of generating nanoparticles. The produced sample was washed several times using DI water and ethanol. Then dry using a vacuum oven. The collected samples are analyzed the crystal structure and lattice constant through XRD. Then, we are analyzed the shape, diameter, length, and distribution through SEM, and the hysteresis curve, the saturation magnetization and the coercive force are identified through the Physical Property Measurement System equipment.

Keywords: Fe-Ni nanoparticles, magnetic properties, magnetic field, Fe-Ni nanowires

1-Dimensional morphological evolution of FeCo using static magnetic field

Kavita Kumari[1*], Seok-Hwan Huh[2], Akshay Kumar[3], Mohit.K Sharma[3],
Naveen Yadav[4], Su-Jeong Park[4] and Bon-Heun Koo[5†]

[1]Industrial Technology Research Institute, Changwon National University,
Changwon, Gyeongnam 51140, Republic of Korea
[2]Department of Mechatronics Conversion Engineering, Changwon National University,
Changwon, Gyeongnam 51140, Republic of Korea
[3]Mechatronics Research Institute, Changwon National University, Changwon, Gyeongnam, 51140, Republic of Korea
[4]Department of Materials Convergence and System Engineering, Changwon National University,
Changwon, Gyeongnam 51140, Republic of Korea
[5]School of Materials Science and Engineering, Changwon National University,
Changwon, Gyeongnam, 51140, Republic of Korea
[*]Corresponding Author - bhkoo@changwon.ac.kr

The additional degree of freedom in the nanowires included due to their shape enables to tune the magnetic properties of the material. The shape anisotropy thus generated enhances the effective anisotropy of the material useful for high density data storage applications. Therefore, in the present work, the FeCo nanowires have been prepared using an external magnetic field during synthesis allowed the 1-dimensional growth of the nanowires. The nanowires were characterized through x-ray diffraction (XRD), high resolution field emission scanning electron microscopy (HR-FESEM) and dc-magnetization. The structural analysis revealed the base centred cubic symmetry of the nanowires with the space group: Ia3. The lattice parameter is found to be 2.8 Å with a strain of 2.5×10^{-3}. The morphological evaluation demonstrated the formation of continuous wires with an average length of ~ 7 μm and an average diameter less than 300 nm. The saturation magnetization calculated form the magnetization (M) vs magnetic field (H) hysteresis curve is found to be greater than 200 emu/g corresponding to the coercivity > 500 Oe. The Law of approach estimated the magnetic anisotropy $\sim 2.5 \times 10^5$ erg/cm^3.

Key words: Magnetic nanowires, Magnetic anisotropy, Saturation magnetization, high resolution field emission scanning electron microscopy

Fe-based hybrid soft magnetic composites utilizing the shape anisotropy of Fe-Si chip for high-performance electric motors

Bonuk Koo[1,2*], Jong-Min Park[1], Min Sun Jang [1], Young-Tae Kwon[1], Sangsun Yang[1], Yong Ho Park[2] and Jae Won Jeong[1]

[1]Powder/Ceramic Research Division, Korea Institute of Materials Science(KIMS), 797 Changwondae-ro, Seongsan-gu, Changwon, 51508, Korea
[2]School of Materials Science and Engineering, Pusan National University, Busandaehak-ro 63beon-gil, Geumjeong-gu, Busan, 46241, Korea

Soft magnetic composites (SMCs) have been pursued in many research for the efficiency and low-cost electronic devices such as inductor, transformer, and electric motor. In particular, SMCs for the electric motors have advantages of design freeform and better power efficiency when compared with conventional electrical steels. SMCs are fabricated through a metallurgical process after insulating coating on the surface of the Fe powder, so that it is possible to efficiently control core loss and to manufacture complex-shaped cores.

On the other hand, Fe-6.5wt%Si alloys have excellent magnetic properties such as high permeability, low core loss, and magnetostriction close to zero. Recently, studies have been reported about the fabrication of near-net shaping of Fe-Si alloys through the melt spinning and compression molding. Fe-6.5wt%Si chips has very thin thickness and the high aspect, so it shows shape anisotropy, and results in very high permeability in a specific direction.

Although many studies are being conducted on SMCs and near-net shaping of Fe-Si chips, researches on mixing of them to improve magnetic properties has net been conducted. In this work, to develop a material with excellent magnetic properties for applying to electric motors, we intend to make a novel hybrid SMC which comprises both Fe powder and chip-type Fe-Si fillers. The hybrid SMC has a low core loss and overcomes low permeability of previous powder-based SMCs. The surface insulation coating (TEOS coating) was proceeded on both of the water-atomized irregular Fe powder (average particle size of 225 μm) and Fe-Si chip fabricated by melt spinning. Then, they were mixed in different ratio and formed into a toroidal core. The green body was heat treated at 600 °C for 2 hours, and then the magnetic properties were evaluated.

The novel hybrid SMC composing anisotropic Fe-Si plate fillers shows a tendency that the permeability is increased and the iron loss is decreased according to the mixing ratio of the chips and powders. In addition, the saturation magnetization of the core was maintained high even though Fe-Si having poor moldability was incorporated.

Effect of Nb/ Zr co-addition on the soft magnetic properties and microstructures of $Fe_{77.5}Si_{11.5}B_7Nb_xZr_{3-x}Cu_1$ nanocrystalline Alloys

Hyun Ah Im[1,2*], Subong An[1,2], Yeong Gyun Nam[1,2], Sangsun Yang[1], Jung Woo Lee[2] and Jae Won Jeong[1†]

[1]Metal Powder department, Korea Institute of Materials Sciene(KIMS), 797 Changwondae-ro Seongsan-gu, Changwon 51508, Korea

[2]Department of Materials Science and Engineering, Pusan National University, Pusan 46241, Republic of Korea

*E-mail of Corresponding Author: jeongjw1204@kims.re.kr

Soft magnetic materials require magnetic properties such as high permeability(μ), high saturation magnetic flux density(B_s), and low core loss. Silicon electronical is widely used due to high saturation flux density and low material cost, however it is difficult to satisfy low coercivity (H_c) and low core loss. Soft magnetic Fe-Si-B-Nb-Cu (Finemet) nanocrystalline alloys have been used as magnetic components in high frequency transformers, inductors due to their low coercivity, high permeability. Comparing to Silicon electronical Finemet has low saturation magnetic flux density(1.23T). Therefore, it is inevitable to develop Fe-based nanocrystalline soft magnetic materials with high saturation magnetic flux density and excellent soft magnetic properties. Nanocrystalline materials have the best soft magnetic properties when the crystal size is 10-15 nm. The purpose of this study is to minimize grain size and to enhance the soft magnetic properties. Zr distributed in amorphous residual matrix suppress grain growth, increasing the permeability and lowering the core loss and coercivity. Nb atoms also suppress grain growth and impending Fe_2B formations. However, Nb is problematic in terms of cost. To improve cost problem, we design our nanocrystlline alloys substitute Nb with Zr. Also according to previously studies **W. Lu et al.**, it has been reported that simultaneous co-addition of transition elements resulted in a significant reduction in particle size to 10-20 nm. In this study, nanocrystalline ribbons with a composition of $Fe_{77.5}Si_{11.5}B_{7.5}Nb_xZr_{3-x}Cu_1$(x=0-3) have been fabricated by rapid-quenching melt spinning and thermal annealing. The ratio of (Zr/Nb) effects on microstructure and magnetic properties. Among the alloys investigated in this work, $Fe_{77.5}Si_{11.5}B_{7.5}Nb_1Zr_2Cu_1$ nanocrystalline ribbon annealed at 580 °C exhibits excellent soft-magnetic properties including low coercivity, low core loss, and high saturation magnetization. The uniform nanocrystallization in $Fe_{77.5}Si_{11.5}B_{7.5}Nb_1Zr_2Cu_1$ alloy has been also confirmed through high-resolution TEM analysis.

Keywords: soft magnetic materials. nanocrystalline, amorphous, magnetic properties, microstructures

Magnetic Properties of Fe-B-Si-P-Cu-Nb Alloy System by Heat Treatment

Hyunkyung Lee[*], Hyunsol Son, Haein Choi-Yim[†]

Department of Applied Physics, Sookmyung Women's University, Seoul 04310, Korea

Fe-based amorphous alloy systems are based on soft magnetic with high saturation magnetization and low coercivity. According to the (Fe-B-Si-P-Cu) alloy system with Nb added, soft magnetic and thermal properties are created without compromising amorphous properties, but adding Nb results in relatively low saturation magnetization.

In this study, the decreased saturation magnetization was identified when investigating the effect of Nb on the properties of FeBSiPCu alloys. And we proceeded to anneal to overcome this. Based on the first crystallization temperature (T_{x1}) of the differential scanning calorimeter (DSC) result of the as-spun ribbon, the annealing condition was determined, which is every ten minutes from (T_{x1}-20K) to (T_{x1}+120K) at intervals of 20K.

With the annealed ribbon sample, we identified the α-Fe phase by X-ray diffraction (XRD) for the structural characteristics of the ribbon sample. When examining for magnetic properties using a vibrating sample magnetometer (VSM), the highest saturation magnetization was 192.12 emu/g, and the coercivity was approximately 1.97 Oe.

As a result, the reduction in saturation magnetization of the alloy system (Fe-B-Si-P-Cu) to which Nb was added was overcome through annealing. New soft magnetic materials with high saturation magnetization and low coercivity loss will contribute to a variety of industries.

Magnetic properties of double-layer-insulated soft magnetic composites after high-temperature heat treatment

Jong-Min Park[1,2*], Min-Sun Jang[1], Bonuk Koo[1,2], Hea-Ran Kim[1,3], Young-Tae Kwon[1], Sangsun Yang[1], Jung Woo Lee[2] and Jae Won Jeong[1†]

[1]Metal Powder Department, Korea Institute of Materials Science (KIMS),
797 Changwondae-ro, Seongsan-gu, Changwon 51508, Korea
[2]School of Materials Science and Engineering, Pusan National University, 2, Busandaehak-ro 63beon-gil, Geumjeong-gu, Busan, 46241, Republic of Korea
[3]Department of Materials Science and Engineering, Sungkyunkwan University (SKKU),
2066, Seobu-ro, Jangan-gu, Suwon-si, Gyeonggi-do 16419, Korea

In recent years the remarkable kind of soft magnetic materials named soft magnetic composites (SMCs) has drawn significant attention of scientists and rapidly increased its application range. in addition, SMC has superior output density compared to electric steel sheets and SMC is expected to account for a large application of next generation motor parts. In the case of SMCs, comprising $Fe@PO_4$ powders, which is currently widely used, heat treatment above 650 °C damage of insulation properties. In order to solve this problem, this study focused on manufacturing SMC with low core loss characteristics, excellent magnetic properties, and maintaining insulation at heat treatment above 650 °C. this study Fe powder was coated magnesium chloride and tetraethyl orthosilicate by sol-gel method, and core was manufactured by pressing and heat treatment for 1 hour at 600 °C, 700 °C, 800 °C, and 900 °C in the argon atmosphere. Herein, the multi-layer contains both the coating retention of MgO and the excellent electrical resistivity of SiO_2. For all of these reasons the core has superior coating retention and core loss property at high temperature. The phase identification was carried out by X-ray diffractometer (XRD) and the insulation coating layer was measured by scanning electron microscope and energy dispersive X-ray spectroscopy. Also, magnetic characteristics were figured out through vibrating sample magnetometer (VSM) as well as the core loss value were compared for each frequency band; 0.05 kHz, 0.4 kHz, and 1 kHz using AC BH analyzer (AC) and DC BH loop tracer (DC). XRD patterns were observed the α-Fe peak, VSM results suggested that the saturation magnetization value was reduced, which confirmed the existence of coating layers. The results of AC and DC measurements on the cores heat-treated at 600 °C, 700 °C, 800 °C, and 900 °C have presented that the core loss property of core is better than the $Fe@PO_4$ due to added MgO and SiO_2. And this result shows the possibility that multi-layers can be applied at high temperature.

Keywords: soft magnetic composite, sol-gel, magnetic properties, heat treatment, multi-layer

Reference

[1] Zuzana Bircakova et al., J. Magn. Magn. Mater., **485**, 1-7, (2019).

Effect of carbon addition on the amorphours formation ability of $Fe_{76}Si_9B_{10}P_5$ soft magnetic amorphours alloy

Yeong Gyun Nam[1*], Hearan Kim[1], Hyun Ah Im[1], Su Bong An[1],
Jung Woo Lee[2], Sangsun Yang[1] and Jae Won Jeong[1*]

[1]*Metal Powder Research Division, Korea Institute of Materials Science,
797 Changwondae-ro, Seongsan-gu, Changwon, 51508, Korea*
[2]*Department of Materials Science and Engineering, Pusan National University, Pusan 46241, Republic of Korea*
Corresponding Author :jeongjw1204@kims.re.kr

As the operating frequency of the power conversion element increases for the purpose of miniaturization and weight reduction, the development of a soft magnetic material with high saturation magnetization is required to cope with the increase in current while exhibiting low iron loss even at high frequencies above 100. In the case of crystalline powder materials such as Fe-Ni, Fe-Si-Al, and Fe-Si, which were previously used, the iron loss due to eddy current increases rapidly as the frequency increases above 100 kHz. Current limiting use at high frequencies. Amorphous soft magnetic powder material is emerging as an alternative because it has no crystalline magnetic anisotropy and high specific resistance compared to conventional crystalline powder material and shows low iron loss even at high frequencies. For the production of amorphous powder, a high-pressure water injection method using an inert gas is used. Although the water injection method is helpful for the production of amorphous soft magnets, it has disadvantages such as a decrease in saturation magnetization and an increase in Core loss due to oxidation. As another manufacturing method, there is a gas injection method, but it is important to select and manufacture a composition that achieves high GFA (glass forming ability) because the cooling rate is limited and it is difficult to make amorphous powder. In this study, in order to obtain a powder composition with high saturation magnetization and GFA, it was designed using the well-known Fe76Si9B10P5 composition. In the case of this composition, there is not enough GFA to make an amorphous powder when actually produced by a gas jet method. It was designed to reduce Si and add 1 to 3% of C. Since it is reported that carbon is effective in improving GFA without significantly reducing saturation magnetization, the composition of $Fe_{76}Si_{9-x}P_5B_{10}C_X$ was designed by adding carbon. After alloy production through arc melting, a ribbon was manufactured using a stainless wheel with a lower cooling rate than the Cu wheel under the conditions of 1200rpm, 1000rpm,800rpm through melt spinning. Through the coercive force (H_c) and Xrd measurement through the DC loop tracer, it was confirmed whether the composition is capable of forming an amorphous pattern through evaluation of the amorphous pattern, and the saturation magnetization value (M_s) was evaluated through the Vibrating Sample Magnetometer (VSM). Among the evaluated compositions, the composition C1% judged to be high in GFA was selected, the basic composition $Fe_{76}Si_9B_{10}P_5$ and C1% powder were prepared by gas injection method, magnetic properties through VSM and amorphous pattern through XRD were checked, basic composition and carbon addition method In comparative analysis of the differences, it was confirmed that the composition with 1% carbon added had a higher GFA than the basic composition and reduced saturation magnetization less.

Electromagnetically induced transparency-like effect based on a high-Q ferrite metamaterial in microwave regime

김태한, 김상우[*], 이보화[†]

Department of Physics and Oxide Research Center, Hankuk University of Foreign Studies, Yongin, South Korea

In this paper, we have designed a high-Q ferrite metamaterial (MM) in microwave regime, which exhibits a significant slow-light effect in gigahertz (GHz) frequencies, based on an electromagnetically induced transparency phenomenon. Electromagnetically induced transparency (EIT)-like behavior originates from the bright-bright mode coupling or the bright-dark mode coupling through the near-field interaction in metamaterial unlike EIT in atomic system. It is employed a linearly coupled Lorentz model to theoretically study the coupling mechanism on the transmission characteristics of the system. Simply by appropriately adjusting the coupling distance of the proposed MM structure, EIT-like effect with a high-quality factor can be dynamically tuned and simulation results show the spectral properties. Furthermore, the electromagnetic field distributions and group delay of the ferrite MM are investigated as well as transmission spectral responses. It should be note that the increased Q-factor leads to large group index (of the order of 262) and the proposed MM structure provides a useful method for various potential applications, such as, tunable switching, bio-sensors and slow-light devices in microwave regime.
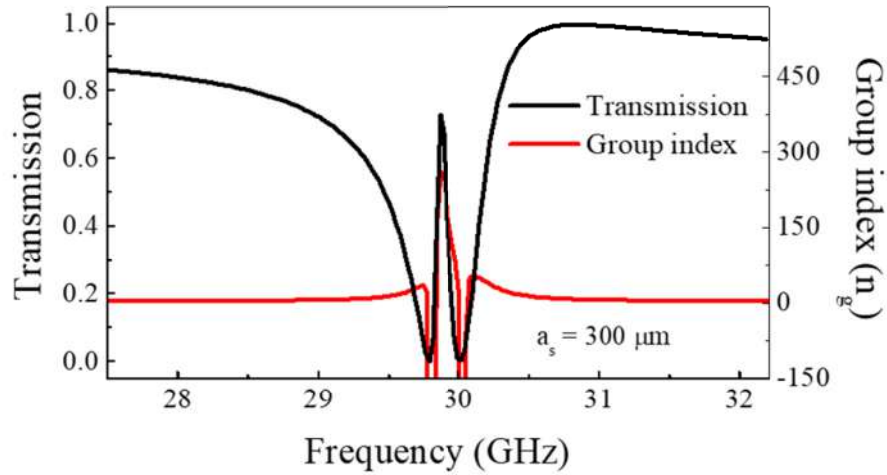
Fig. 1. Relationship between the transmission spectrum and group index (n_g) of the proposed ferrite MM as a function of frequency at the coupling distance (a_s =100 μm).

3-Dimensional Magnetostatic Interactions in Controllable Magnetic Fe/Au Barcode Nanowire Arrays

Eunjin Jeong[1*], Aleksei Yu. Samardak[2], Yoo Sang Jeon[3], Vadim Yu. Samardak[2],
Aleksei G. Kozlov[2], Kirill A. Rogachev[2], Alexey V. Ognev[2], Gyu Won Kim[1], Min Jun Ko[1],
Alexander S. Samardak[2*] and Young Keun Kim[1*]

[1]Department of Materials Science and Engineering, Korea University, Seoul 02841, Republic of Korea
[2]Institute of High Technologies and Advanced Materials, Far Eastern Federal University, Vladivostok 690922, Russia
[3]Center for Hydrogen · Fuel Cell Research, Korea Institute of Science and Technology,
Seoul 02792, Republic of Korea

A multilayered barcode nanowire (BNW) can change its properties by adjusting the length of each segment made of different components. Since various functions can be realized even within a single structure, it can provide diverse applications in magnetic, electrical, mechanical, and biomedical fields.[1]-[4] Especially in the field of computational technologies, the study of 3-dimensional magnetostatic interactions is in high demand since the field generated by complex interactions between densely arranged magnetic nanoelements inside a memory device can even damage the written information. Nevertheless, studies on the basic 3-dimensional magnetic properties according to the changes in shape and structure of materials are still insufficient. Therefore, we tried to analyze the various magnetic interactions within the Fe/Au BNW array, which is electrochemically synthesized by the one bath electrodeposition method.

The composition and length of each segment of BMWs were conveniently and finely modulated by controlling applied current density and elapsed time of electrodeposition. Experiments and measurements were carried out with a series of samples, varying the length of Au segments from 30 to 200 nm, when the Fe segments' length was fixed to 100 and 200 nm, respectively, to investigate the magnetic properties in the Fe/Au BNW array. The microstructure and composition of each segment were analyzed using diffraction patterns and energy dispersive X-ray spectroscopy (EDS), and both segments had different Fe-Au concentration ratios.

Analysis of the hysteresis curve revealed that the Fe/Au BNW is a soft magnetic material composed of strong ferromagnetic Fe segments and weak ferromagnetic Au segments. Magnetic force microscopy (MFM) has shown the different positions of the magnetic poles when an applied external field direction is parallel and perpendicular to the main axis of the BNW. In addition, micromagnetic simulations presented that the spin configuration of all samples was a vortex.

Combining the above analysis results with the FORC diagram, we came up with three different types of complex magnetostatic interactions with the alternating magnetization of segments. Each of these three types is interactions between: 1. opposite magnetic poles of adjacent Fe segments within the same nanowire, 2. poles within one Fe segment, 3. closest poles in the Fe segments of neighboring BNWs in an array. For Fe(100) samples, the type of interaction changed from the coexistence of type 1 and 2 to only type 2 prevalence, as the length of the Au segment increased. Whereas in the Fe(200) samples, only type 1 interaction was possible when

Au segments were 30 nm, but all three types of interactions coexisted when Au segments were 200 nm since the distances between poles of adjacent Fe segments in the same nanowire, in one Fe segment, and of neighboring nanowires in the array are become comparable.

References

[1] S. Min *et al., Adv. Mater. 32, 2004300* (2020)

[2] S. Min *et al., Nano Lett. 20, 7272* (2020)

[3] S. Bochmann *et al., RSC Adv. 7, 37627* (2017)

[4] J. A Moreno *et al., J. Magn. Magn. Mater. 484, 110* (2019)

Hall effect property of
Multilayer Thin Films according to Pt thickness

Y.K. Kim[*], T.W. Kim[†]

Department of Nanotechnology & Advanced Materials Engineering, Sejong University, Seoul, Korea

Magnetic recording media and magnetic sensors using magnetic recording films, magnetic recording films have been extensively studied in magnetic recording media and magnetic sensors. The materials used in this study give a wide range of Hall effects suitable for Hall sensors. This study was conducted as an experiment on the Hall effect.

The deposition was carried out on the structure currently being studied using a sputtering system, a thin film manufacturing equipment, and deposition conditions were CoSiB-0.04 nm/s, Pt-0.08 nm/s, and Ta-0.05 nm/s.

The structures were deposited for [Pt3/(CoSiB0.3/Pt(x))*5/Pt5nm]. Proceeded for Pt(x)=1, 1.2, 1.3, 1.4, 1.5, 1.6 nm.

It was confirmed that the perpendicular magnetic anisotropy (PMA) was well-formed through the data after deposition, and if you look at the measurement results for the V-H curve, you can check the correlation between V_H, Hall resistivity, and Hall angle with respect to Pt thickness. As the thickness of Pt increases, it can be seen that V_H, Hall resistivity, and Hall angle decrease in a similar pattern. In Hall Voltage, Hall resistivity, and Hall angle, it was confirmed that V_H was generally similar between 0.25mV, which is the largest value at Pt=1nm, and Pt=1.3~1.6nm. Additional experiments should be conducted, but it was confirmed that there was no increase or decrease in Hall Voltage above Pt=1.3nm.

A study hall effect property on multilayer Thin Films

Y.K. Kim[*], T.W. Kim[†]

Department of Nanotechnology & Advanced Materials Engineering, Sejong University, Seoul, Korea

It is STT-MRAM that opened up the possibility of commercializing high-density magnetic random access memory (MRAM). STT-MRAM is a magnetic tunnel junction based on perpendicular magnetic anisotropy in order to use Spin Transfer Torque (STT) as a recording medium or sensor, with an emphasis on securing large signal voltage and thermal stability.

In this study, the thin film fabrication was performed at Ta(8)/Pt(3)/CoSiB(x)/Pt(0.8)/CoSiB(x)/Pt(3)nm to confirm the perpendicular magnetic anisotropy (PMA). The experiment was carried out while changing the conditions for x=1.5, 1.8, 2.3, and 2.8. For deposition, a [CoSiB/Pt] multilayer was prepared using sputter. During deposition, the initial pressure was set to 7×10^{-7}, and the working pressure was maintained at 3×10^{-3}. For bulk production, a 1cm×1cm dicing wafer was used. As a result of checking the hall voltage as a result of the data, the hysteresis shape of the switch type was maintained at CoSiB=1.5 and 1.8, and the linear shape was slightly exhibited at CoSiB=2.3, but disappeared completely without showing the PMA effect at CoSiB=2.8 confirmed that there is.

Magneto-transport effect in CoSiB/Pt/CoSiB thin films

T.W. Kim[*†]

Department of Nanotechnology & Advanced Materials Engineering, Sejong University, Seoul, Korea

Magnetic multilayer films with perpendicular magnetic anisotropy (PMA) have been widely investigated and expected to be used for magnetic recording media, magnetic sensor, and magnetic memories. We have studied PMA magnetic multilayer films with amorphous materials due to their smooth surface and soft magnetic properties. The CoSiB 1000 Å single layer film shows soft magnetic properties with 1.6 Oe coercivity and 407 emu/cm^3 saturation (M_s). The as-deposited CoSiB 1000 Å film has amorphous structure even with post-annealing treatment up to 350 °C. The Hall effect in [CoSiB/Pt] multilayer films were measured by using Van der Pauw method and showed spontaneous Hall angle (ρ_H/ρ). Even though the observed Hall resistivity in [CoSiB/Pt] multilayer is smaller than that in amorphous rare earth-transition metal (RE-TM) alloy films, the Hall angle of 8% is much larger than amorphous RE-TM alloy films. The trilayer films of the structure [CoSiB 15 Å/Pt (t) Å/CoSiB 15 Å] (t_{Pt} from 11Å to 39Å) have out-of-plane easy axes and show strong antiferromagnetic exchange coupling especially for the films of t_{Pt} = 22Å and 27Å. Hall voltage curve show two hysteresis loops. This is a clear evidence of antiferromagnetic coupling. This is a clear evidence of antiferromagnetic coupling. It is believed that the CoSiB/Pt/CoSiB is a candidate system for use in hall sensor.

A study hall effect property on multilayer Thin Films

Y.K. Kim, T.W. Kim[*†]

Department of Nanotechnology & Advanced Materials Engineering, Sejong University, Seoul, Korea

It is STT-MRAM that opened up the possibility of commercializing high-density magnetic random access memory (MRAM). STT-MRAM is a magnetic tunnel junction based on perpendicular magnetic anisotropy in order to use Spin Transfer Torque (STT) as a recording medium or sensor, with an emphasis on securing large signal voltage and thermal stability.

In this study, the thin film fabrication was performed at Ta(8)/Pt(3)/CoSiB(x)/Pt(0.8)/CoSiB(x)/Pt(3)nm to confirm the perpendicular magnetic anisotropy (PMA). The experiment was carried out while changing the conditions for x=1.5, 1.8, 2.3, and 2.8. For deposition, a [CoSiB/Pt] multilayer was prepared using sputter. During deposition, the initial pressure was set to 7×10-7, and the working pressure was maintained at 3×10-3. For bulk production, a 1cm×1cm dicing wafer was used. As a result of checking the hall voltage as a result of the data, the hysteresis shape of the switch type was maintained at CoSiB=1.5 and 1.8, and the linear shape was slightly exhibited at CoSiB=2.3, but disappeared completely without showing the PMA effect at CoSiB=2.8 confirmed that there is.

Manufacturing and characterization of Fe-Si based soft magnetic composite materials for energy conversion

Kwiyoung Lee*, Gyutae Lee and Jongryoul Kim

Department of Materials and Chemical Engineering, Hanyang University, Ansan 15588, South Korea

전자기 장비의 고효율화를 달성하기 위해서는 특히 전력변환용 소재의 고주파화, 고특성화를 필연적으로 요구하고 있다. 따라서 연자성 소재는 포화자화 증가와 동시에 히스테리 손실과 와전류 손실 저감이 요구되고 있다. 현재 사용되고 있는 단일 조성 소재의 경우 포화자화 증가와 손실 저감 두 특성을 동시에 만족하는데 한계를 나타내고 있어서, 이를 극복하기 위해서 복합재료에 대한 연구가 활발히 진행되고 있다. 연자성 복합재는 높은 포화자화와 동시에 모터 및 인덕터의 고주파화에 대응하기 위한 특성 향상이 요구된다[1, 2]. 그러므로, 연자성 복합재(soft magnetic composites, SMCs)는 고주파 특성 개선을 위해 와전류 손실 저감에 필요한 전기 절연층으로 둘러싸인 Fe계 자성 분말, 리본 강판에 대해 많은 연구가 진행되고 있다. 분말이 갖고 있는 특성 때문에 복합재료는 높은 투자율 및 자속 밀도를 달성하기 위해 고밀도 적층 및 성형성이 요구된다. Fe에 첨가된 Si는 이방성 상수(K_1)와 자기변형율(λ_s)을 감소시킴과 동시에 전기비저항을 증가시킴으로써 Fe 연자성 소재의 특성을 향상시키게 된다. 그러나, Si의 농도가 증가하면 재료의 연성이 감소하여 강판으로 가공하거나, 분말 성형체의 제작이 어려워지고 포화자화도 감소한다.

이러한 문제의 해결을 위해, 본 연구에서는 Fe-Si 합금의 낮은 성형성을 극복하고자 Si 함량을 감소시킨 Fe-1.5wt%Si 합금 분말을 제조하였고, 표면에 인산염을 코팅하여 Fe-1.5wt%Si@Fe$_3$(PO$_4$)$_2$ 복합재를 제조하였다. 제조된 복합재는 1950MPa의 압력으로 성형하여 97%의 상대밀도를 가졌으며, 높은 저기저항으로 인한 와전류 감소로 고주파 영역에서의 낮은 손실이 측정되었다. 또한, 이슬점(dew point) 열처리를 이용하여 SiO$_2$ 산화막이 형성된 Fe-3wt%Si@SiO$_2$ 합금 분말과 Fe 나노 분말을 이용하여 복합재를 제조하였고, Fe 나노 분말의 함량에 따른 복합재의 성형성 및 자기적 특성을 조사하였다. 그 결과, 20wt%의 Fe 나노 분말을 함유한 복합재는 높은 성형밀도로 인해 우수한 고주파 특성을 나타내었다. 이러한 결과는 다양한 방법으로 제조된 Fe-Si 연자성 복합재가 고주파 영역에서 전기강판의 대체제로써의 가능성을 보여준다.

References

[1] Choi, Moosung, et al. "The effects of Fe nano-powders on compaction behaviors and magnetic properties of SMCs." Journal of Magnetism and Magnetic Materials 480 (2019): 33-39.

[2] Lee, Kwiyoung, et al. "Magnetic properties of Fe-1.5 wt% Si high-frequency powder cores." AIP Advances 9.12 (2019): 125340.
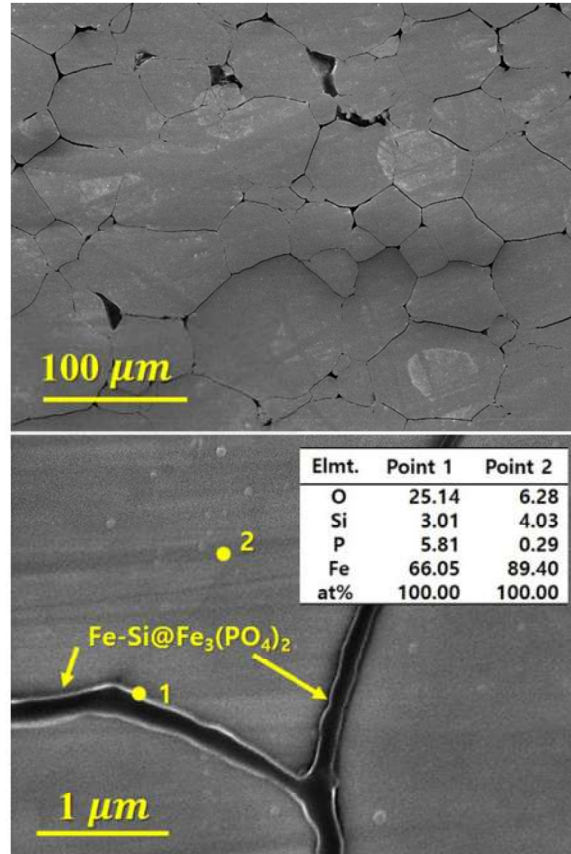
Figure 1. 인산염 코팅된 Fe-1.5wt%Si 성형체 단면 SEM 이미지

Elmt.	Point 1	Point 2
O	25.14	6.28
Si	3.01	4.03
P	5.81	0.29
Fe	66.05	89.40
at%	100.00	100.00

wt% NPs	0	5	10	15	20	25	30	35	100
Density [g/cm³]	6.03	6.31	6.44	6.53	6.62	6.59	6.55	6.46	5.71
σ [S/m]	0.044	1.52	5.86	83.6	190.7	793.5	1007	1953	179530
TS [MPa]	0.44	1.71	6.31	8.28	9.73	17.17	23.74	31.34	277.1
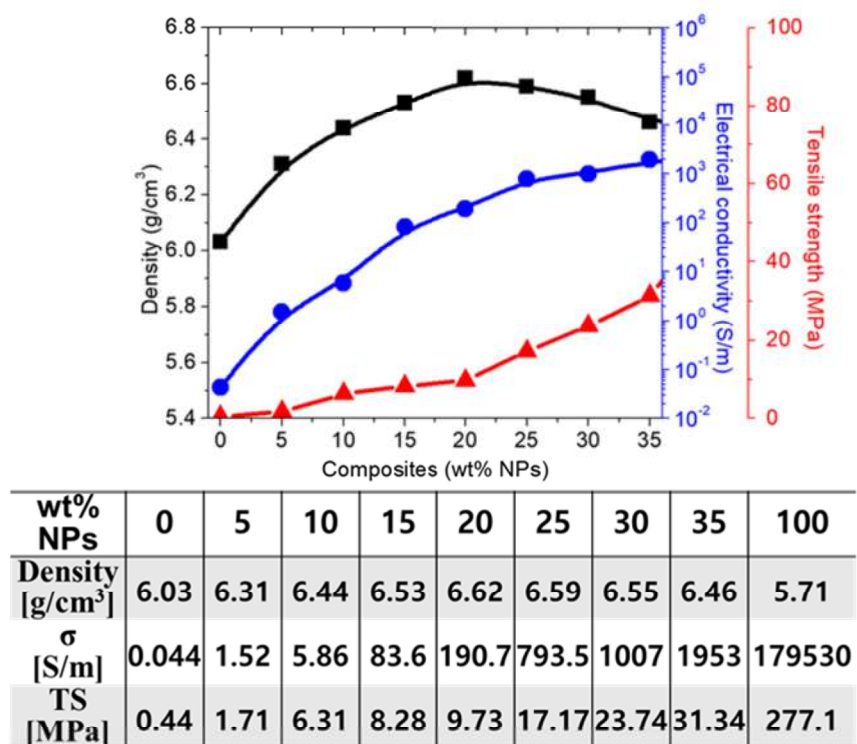
Figure 2. Fe-3wt%Si 합금 분말과 Fe 나노 분말 혼합율에 따른 특성

Effect of powder sized distribution and sintering temperature on soft magnetic properties of Fe-Si-Al-P soft magnetic composite with Fe-P powder

Dae Won Jung[1,2*], Min Woo Lee[1], Sung Min Kim[1], Kee Ahn Lee[2], Hwi Jun Kim[1†]

[1]Advanced Process and Materials R&D Group, Korea Institute of Industrial Technology, Incheon 21999, Korea
[2]Department of Materials Science and Engineering, Inha University, Incheon 22201, Korea

Fe-Si based soft magnetic core is excellent materials for magnetic devices such as inductor cores and motor cores. Due to its advantages such as high effective permeability, low coercivity, and core loss, it is attracting attention as a representative magnetic material for maximizing electrical energy efficiency, miniaturization and high performance. In this study, the Fe-Si-Al-P powder to be used as the main powder was manufactured by high pressure gas atomization. Powder distribution and magnetic properties measured by particle size analyzer and vibrating sample magnetometer. Fe-Si-Al-P powder and Fe-P powder were mixed in various ratio to evaluate soft magnetic properties determined by saturation magnetization and coercivity according to each particle size. The Fe-Si-Al-P powder was classified into ~63, 63~90, 90~150, 150~300 μm. The optimal values of Fe-P for insulation and the desirable microstructure through soft magnetic properties according to frequency was confirmed. Also, changes in core density of soft magnetic composite fabricated by various pressure was investigated with the amount of Fe-P added. Fe-P powder is smaller than Fe-Si-Al-P powder, the Fe-P powder was ground at 300 RPM added tungsten carbide balls with powder mixing and it 1 to 10 wt.% was added to Fe-Si powder. After preparing a soft magnetic composite, it was sintered and heat treated. As for the manufacturing process conditions of the Fe-Si-Al-P and Fe-P soft magnetic composite, the temperature, time, and atmosphere of the heat treatment processes were variously performed.

In this study, the correlation between soft magnetic properties such as saturation magnetic flux density, microstructure with various condition of manufactured core was examined.
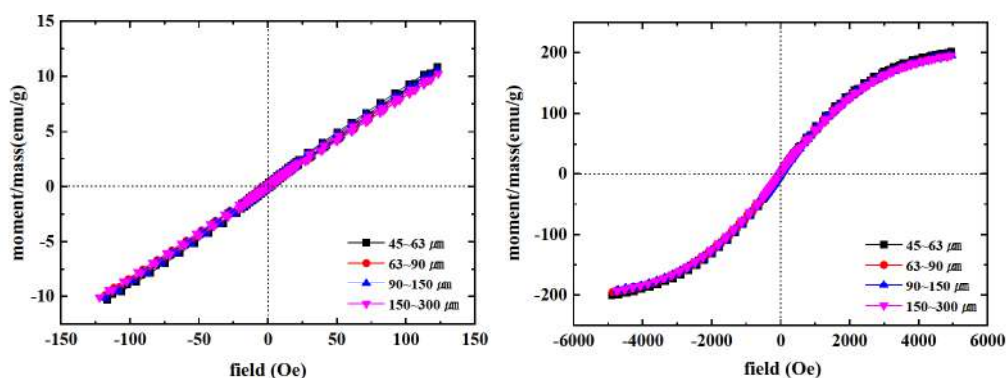
Fig. 1. The hysteresis loop of size distribution of Fe-Si-Al-P powder.

Keywords: Fe-Si-Al-P alloys, Core, Saturation magnetic flux density, Sintering, Ball milling

Electroless plated FeCoNi on cellulose sheet for electromagnetic shielding

Minji Gu[1*], Jinu Kim[2] and Ki Hyeon Kim[1†]

[1]*Department of Physics, Yeungnam University, Gyeongsan, 38541, Republic of Korea*
[2]*Institute of Photonics and nanotechnology, Yeungnam University, Gyeongsan, 38541, Republic of Korea A, Korea*

현재 전자기기들에 적용하는 차폐재는 주로 단순 반사 위주의 고전도성 물질을 이용하고 있으며, 이로 인한 내부 반사는 신호 간섭의 요인이 될 수 있음으로 이를 방지하기 위한 흡수 특성을 가진 차폐재가 요구되고 있다. 이러한 흡수 특성을 만족할 수 있는 소재로는 주로 고주파수 특성의 고투자율 연자성 소재가 이용되고 있다. 대표적으로 고포화자화를 갖는 FeCo에 Cu, Ni, B 등을 추가하여 보자력을 감소시켜 활용하고 있다. 그러므로 본 연구에서는 다중 반사에 의한 높은 차폐 효과를 가지는 3차원 다공성 구조의 자성 필름을 제조하기 위해 FeCoNi을 약 150mm 두께의 셀룰로오스 종이 위에 무전해도금한 뒤 열처리하여 셀룰로오스 제거 후 그림 1과 같이 $Fe_{55}Co_{36}Ni_9$ 다공성 자성 필름을 제조하였다. 제조된 FeCoNi 중공형 다공성 필름은 1mm 두께의 중공형으로 총 필름 두께는 180mm이다. 코팅된 FeCoNi은 (110), (200), (211) 결정방향을 갖는 BCC구조를 확인하였으며[그림 2(a)], 198 emu/g과 37 Oe 포화 자화와 보자력의 우수한 연자성 특성을 보였다[그림2(b)]. 이들 필름에 대한 원역장에서 차폐효과는 동축관과 벡터 네크워크 아날라이저(VNA)를 이용하여 18 GHz까지 측정하였으며 그림 2(c)에 나타낸 바와 같이 총 차폐능(SE_T)은 60-85dB, 흡수능(SE_A)은 42-75dB, 반사능은 21-12dB의 값을 보임으로써 반사능에 비해 흡수능의 기여가 매우 큰 것을 확인하였다. 결론적으로 다중반사 손실 특성을 증가시킨 FeCoNi 중공형 다공성 필름이 전자 부품 등에 EMI 차폐재로서 여러 분야에 응용될 수 있을 것으로 판단된다.
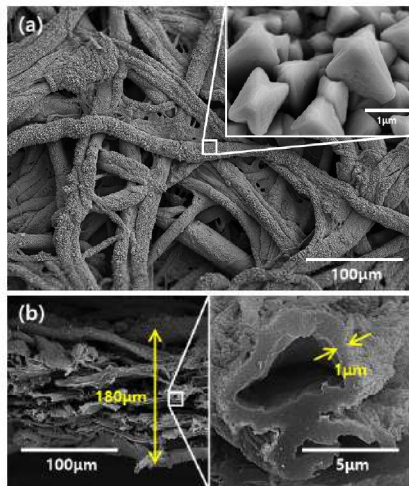
그림 1. SEM Image of FeCoNi film
(a) surface, (b) cross-section view
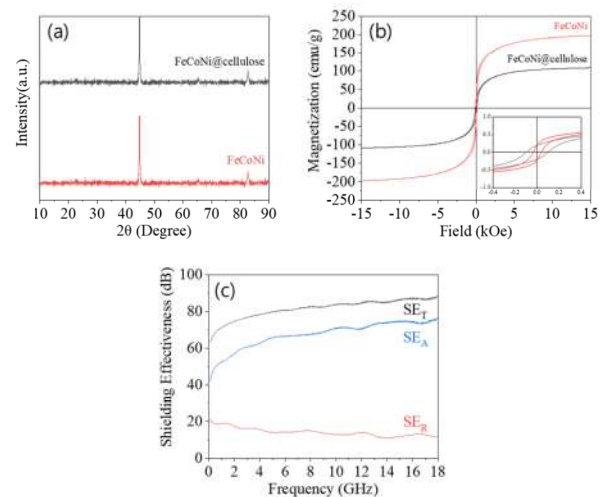
그림 2. (a) XRD, (b) VSM,
(c) Shielding Effectiveness of FeCoNi film

References

[1] Yuping, D., Yahong, Z., et al., Materials Science and Engineering: B, 185, 86-93, 2014

[2] Kim, T., Lee, J., et al., Chemical Engineering Journal, 361, 1182-1189, 2019

[3] B.Y.Yoo, S.C. Hernandez, et al., Electrochimica Acta, 51, 6346-6352, 2006

Effect of Annealing on Magnetic Properties in Fe-Si-B-P-Cu-C Alloy System

Jiyoon Lim[*], Hyunsol Son, Haein Choi-Yim[†]

Department of Applied Physics, Sookmyung Women's University, Seoul 04310, Korea

Fe-based amorphous soft magnetic alloy systems have been prominent for magnetic properties with high saturation magnetization(M_S), low coercivity(H_C), and good permeability. Above all, Fe-Si-B-P-Cu-C alloy system has attractive magnetic properties. Nonetheless, it needed to improve the saturation magnetization.

In this study, to enhance the magnetic properties of Fe-Si-B-P-Cu-C alloy system, we focused on the variation of M_S by various annealing temperatures and proceeded to anneal the as-spun sample.

After preparing the as-spun ribbon samples by induction melting, arc melting, and melt-spinning process under the argon atmosphere, we investigated heat treatment to improve saturation magnetization(M_S). We used experimental equipment to analyze the thermal and structural properties of the specimens, such as differential scanning calorimeter(DSC) and X-ray diffractometer(XRD). Furthermore, measuring the magnetic properties of the ribbons used vibrating sample magnetometer(VSM).

Fe nano 첨가에 따른 Fe-Ni 기반 연자성 복합체 특성 변화

김예래[*], 박봉태, 이보화

한국외국어대학교 물리학과, 산화물 연구센터

bwlee@hufs.ac.kr

주변에서 흔히 볼 수 있는 전자기기의 중요부품인 인덕터는 전류 변화에 저항하는 수동소자로, 전자기 유도 현상을 기본 원리로 작동한다. 하나의 전자기기에 다수의 인덕터가 들어가기 때문에, 각 소자의 손실 값을 낮추는 것이 중요하다. 본 연구에서는 코어의 에어 갭을 줄여 코어 손실을 줄이고자, 입자 크기가 다른 분말을 혼합하였다. 기본 분말로 결정질의 Fe-Ni를 선정하였고, Fe nano를 미분 분말로 첨가하였다. X-ray diffractometer를 통해 각 분말의 결정구조를, scanning electron microscope을 통해 morphology를 확인하였다. 두가지 종류의 분말과 함께, 코어 성형 및 절연특성을 높이기 위한 epoxy를 3.0wt% 첨가하여 섞어 준 후, 외경 20mm 내경 13mm의 몰드로 코어를 성형하였다. Fe nano의 첨가로 코어밀도가 증가하였고, 분말 밀도와 코어 밀도로 계산한 충진율 또한 향상되었다. 인덕터 코어 주요 특성인 코어 손실 값은 감소한 것으로 확인되었다. 이는 충진율이 향상됨에 따라 입자간 상호작용이 줄어들어 inter-particle손실 값에 영향을 준 것으로 보인다.

A study on soft magnetic properties of Fe-B-Cu-Nb(Mo) nano-crystalline alloys with various heat treatment process

Young-Sin Choi[1,2*], Min-Woo Lee[1], Eun-Ji Cha[1], Yeon-Joo Lee[1],
Jong-Ryoul Kim[2] and Hwi-Jun Kim[1†]

[1]Advanced Process and Materials R&D Group, Korea Institute of Industrial Technology, Incheon 21999, Korea
[2]Department of Materials Science and Chemical Engineering, Hanyang University, Ansan 15588, Korea
[*]khj@kitech.re.kr

Fe-based amorphous soft magnetic materials has low coercivity and high saturation magnetization compared with soft ferrite material and alloy designs were facilitating for design various chemical compositions by rapid solidification processing. Fe-Ni alloys are high flux materials with low coercivity and high permeability, so it is desirable for used in industry. But the price of Ni is expensive compared with Fe, we develop for new composition alloys reduce Ni elements in Fe-based alloys with maintaining low coercivity. In this study, soft magnetic properties were evaluated in Fe-based nano-crystalline alloys fabricated by single melt spun process of adding B of metalloid elements, Cu for nucleation site, and Nb and Mo to suppress grain growth. Fe-B-Cu-Nb (Mo) alloys were controlled with optimized annealing process of saturation magnetization up to 180 emu/g over and low coercivity. $Fe_{85-x}B_{13+x}Cu_{0.5}Nb(Mo)_1$ (x=0 to 4) at.% were investigated with substitute Nb to Mo. We evaluate the saturation magnetization increasing through annealing process and influence of Nb and Mo effects in Fe-based alloys. The soft magnetic properties were measured by vibrating sample magnetometer (VSM) and thermal properties of the specimens by differential scanning calorimetry (DSC) and phase analysis was performed by X-ray diffraction (XRD) analysis, respectively.
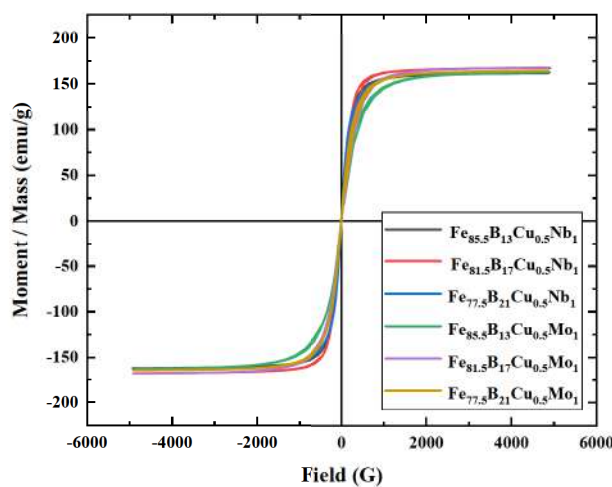
Fig. 1. The hysteresis loop of Fe-B-C-Nb(Mo) ribbons in as-quenched states.

Keywords: Fe-based nano-crystalline, Metalloids, Transition metal, Saturation magnetization, Annealing

Effect of insulating layers on microstructure and soft magnetic properties of Fe-Si-Al soft magnetic cores

Young-kyun Kim[1*], Min-woo Lee[2], Sang-min Lee[1]

[1]Institute for Advanced Engineering, Repubic of Korea
[2]Korea institute of inductrial technology,Repubic of Korea

Soft magnetic composite (SMC) is an attractive electromagnetic material which is obtained by coating thin insulating layers on the surface of a ferromagnetic particles. The soft magnetic materials with high magnetic flux density and permeability can significantly reduce the mass and volume of the magnetic core leading to compact energy converting parts. The proper insulating layers improve eddy current loss and core loss due to higher electrical resistance, while excess thickness of insulating layers resulting in degrading the permeability and saturation magnetization. Fe-Si alloys have been used as transformer magnets and magnetic cores because of their excellent soft magnetic properties. The addition of Si in Fe matrix results in the decrease of magnetic anisotropy and core loss caused by increase of electrical resistivity. To further reduce the loss of cores at high frequency of over 1000 Hz, the researchers have been developing various kinds of insulation coatings to decrease eddy current of soft magnet core thanks to reducing inter-particle contact and increasing electrical resistance. In this study, we tried to form various insulation layers on the Fe-3.5 wt.% Si-Al powder to minimize core loss by increasing the electrical resistance and investigate the effect of various oxide layer like Si-Al-O and Si-P-O on microstructure and soft magnetic properties of Fe-Si-Al-P magnetic cores. Fe-3.5Si-Al wt.% powders were fabricated by a high pressure gas atomization process. The chamber was evacuated to 5×10^{-5} Torr and then maintained in an Ar atmosphere. The powders were sieved to ensure a size of 90~150 μm and 150~300 μm for high-frequency applications. Fe-3.5Si-Al wt.% powder were heat-treated in mixed gas of 80 vol.% Ar and 20 vol.% O_2 at various temperature. The oxidized powders were compacted at 1600 MPa into toroidal shape, and toroidal samples were annealed at 850 °C for stress relaxation. Annealed SMC samples were investigated by SEM for microstructure. The electrical resistivity of the SMCs was measured by the four-point probe method. The initial permeability and soft magnetic properties measured by VSM, AC B-H curve tracer. Furthermore, we evaluated the relationship between kinds of oxide layers and soft magnetic properties (Bs, Ph, Pe and Pw) of Fe-3.5Si-Al wt.% SMC cores.
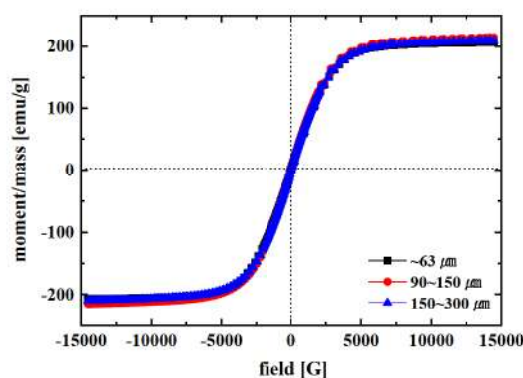
Figure 1 Magnetic properties of Fe-Si-Al soft magnetic powder

First-principles study of antiferromagnetic coupling in $3d^9$-$5d^3$ double perovskite BaLaCuOsO$_6$

Dong Hyun David Lee[*], Myung-Chul Jung and Myung Joon Han[†]

Department of Physics, KAIST, Daejeon 34141, Republic of Korea
[†]Corresponding author e-mail: mj.han@kaist.ac.kr

We carried out density functional theory calculation for a newly synthesized antiferromagnetic (AFM) $3d^9$-$5d^3$ double perovskite, BaLaCuOsO$_6$,[1] to understand its electronic and magnetic behaviors. As observed in the experiment, our numerical results show that the system exhibit energetically stable AFM ordering and reduced magnetic moment. Spin-orbit coupling as well as p-d hybridization are found to be responsible for this reduction of moment. We also estimated exchange couplings, all of which have AFM type. These AFM couplings could be understood based on the superexchange mechanism, owing to the half-filled nature of the orbitals. In addition, finite next-nearest-neighbor coupling is found to be essential for the C-type ordering to be stabilized in spite of the much suppressed out-of-plane nearest-neighbor coupling. Our results provide an extensive understanding and insights of this $3d^9$-$5d^3$ double perovskite by explaining the experimentally observed electronic and magnetic behaviors.

Reference

[1] G. S. Thakur, H. L. Feng, W. Schnelle, C. Felser, and M. Jansen, Structure and Magnetism of New A- and B-Site Ordered Double Perovskites ALaCuOsO$_6$ (A = Ba and Sr), J. Solid State Chem. 293, 121784 (2021).

Magneto-crystalline Anisotropy of Co/Pt Thin Film: Role of Ti

GyeongHye Kim[*], Thi H. Ho, Soon Cheol Hong and S. H. Rhim

Department of Physics and Energy Harvest-Storage Research Center, University of Ulsan, Republic of Korea

Magneto-crystalline anisotropy (MCA) is a tendency of magnetization to align along a preferred direction, which is one important property for spintronics applications [1-3]. In this study, we investigate the role of Ti in magneto-crystalline anisotropy of Co/Pt thin film. Two types of stacking sequence are considered. First, Ti-insertion, which indicate Co/Pt film with insertion of Ti between Co and Pt, Co/Ti/Pt. Second, Ti-capping, Ti on the top layer, Co/Pt/Ti film. EMCA of Ti-capping is twice as large as that with Ti-insertion, 1.11 and 0.54 meV/film, respectively. With different stacking sequence, different interfacial effect occurs. Pt next to Co in Ti-capping has relatively high positive MCA energy. However, Pt next to Ti in Ti-insertion has small negative MCA energy. MCA is investigated in the flamework of the perturbation theory [4], where occupation change of bands is responsible.

References

[1] S. Wolf et al., Science **294**, 1488 (2001).

[2] I. et al., Rev. Mod. Phys. **76**, 323 (2004).

[3] A. Brataas et al., Nat. Mater. **11**, 372 (2012).

[4] Ding-Sheng Wang et al., Phys. Rev. B **47**, 14932 (1993).

Strain engineering and the role of magnetism for charge density waves in monolayer VTe$_2$

Do Hoon Kiem[*], Min Yong Jeong, Hongkee Yoon and Myung Joon Han[†]

Department of Physics, Korea Advanced Institute of Science and Technology, Daejeon 34141, Korea

Two-dimensional transition-metal dichalcogenides have attracted lots of attention. Motivated by a recent study of crystalline bulk VTe$_2$, we theoretically investigated the spin-charge-lattice interplay in monolayer VTe$_2$. To understand the controversial experimental reports on several different charge density wave (CDW) ground state, we paid a special attention to the 'hidden' role of antiferromagnetism as its direct experimental detection may be challenging. Our first-principles calculations show that the 4×1 charge density wave and the corresponding lattice deformation are accompanied by the 'double-stripe' AFM spin order in its ground state. This phase has not only the lowest total energy but also the dynamical phonon stability, which supports a group of previous experiments. Interestingly enough, this ground state is stabilized only by assuming the underlying spin order. Other previously reported phases were found to have either significantly larger total energy or unstable phonon profile. By noticing this intriguing and previously unknown interplay between magnetism and other degrees of freedom, we further suggest a possible strain engineering. By applying tensile strain, monolayer VTe$_2$ exhibits phase transition first to a different charge density wave phase and then eventually to a ferromagnetically ordered one.

Reference

[1] Won, Kiem et al. Adv. Mater. 32 (11), 1906578 (2020).

The role of isotropic strain on anomalous Hall and Nernst conductivity in compensated ferrimagnet Mn₃Al

Guihyun Han[1*], Minkyu Park[2], Soon Cheol Hong[1,3] and S.H. Rhim[1,3]

[1]Department of Physics, University of Ulsan, Republic of Korea
[2]Research Institute of Basic Sciences, University of Ulsan, Ulsan, Republic of Korea
[3]Energy Harvest-Storage Research Center, University of Ulsan, Republic of Korea
(schong@ulsan.ac.kr, sonny@ulsan.ac.kr)

The evolution of lattice constant under strain varies electronic structures and Berry curvatures. Consequently, anomalous Hall (AHE) and Nernst effects (ANE), formulated by Berry curvature for its intrinsic contributions, can be controlled by tuning lattice constant. In this work, we apply isotropic strains to compensated ferrimagnet Mn₃Al and investigate its influence on AHE and ANE. Interestingly, with hole doping, linear and quadratic behaviors under isotropic strains are observed in AHE and ANE respectively as shown by dashed line in the figures. We further present the analysis on Berry curvatures and band structures for each isotropic strain.
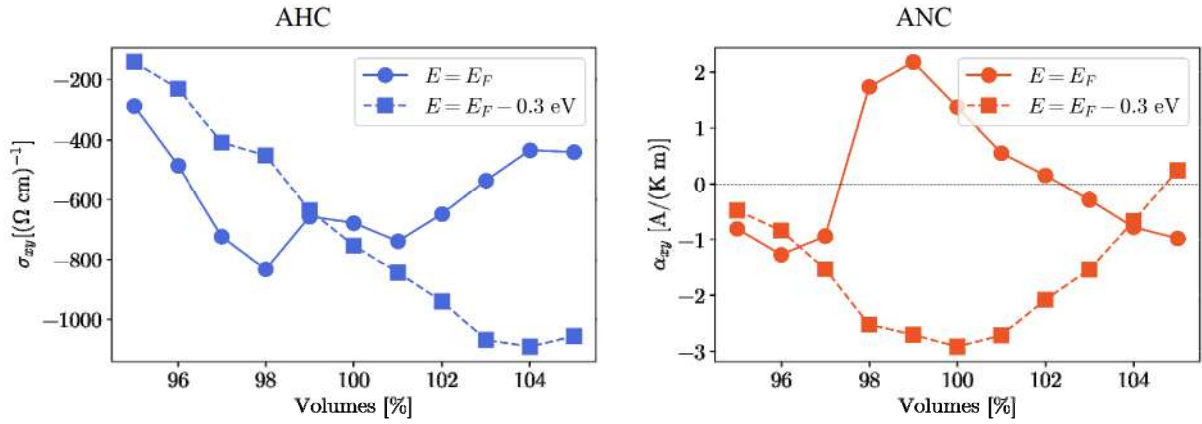
A bandgap opening at the Fermi level in Ba$_2$NaOsO$_6$ driven by an orbital ordering

Taesu Park[1], Je Young An[1], Ji Hoon Shim[1], Changhoon Lee[2*]

[1]Department of Chemistry, Pohang University of Science and Technology, Pohang 37673, Korea
[2]Max Planck POSTECH Center for Complex Phase of Materials, Pohang University of Science and Technology, Pohang, 37673, Korea

The origin of metal-insulator transition of correlated solid are not clearly explained. The origin of insulating behavior for the Ba$_2$NaOsO$_6$ double-Perovskite Ba$_2$NaOsO$_6$ also is still in the controversy. Liu et al., suggest that Ba$_2$NaOsO$_6$ was the Mott insulator developed from strong SOC effect, and magnetic ordering of Ba$_2$NaOsO$_6$ was responsible for insulting behavior proposed by Lu et al. From Xiang *et al*, the insulating behavior of Ba$_2$NaOsO$_6$ was shown to originate from a cooperative effect of electron correlation and spin-orbit coupling. The magnetic susceptibility of Ba$_2$NaOsO$_6$ between 75 and 200 K follows a Curie-Weiss law with a negative Weiss temperature (i.e. $\theta \approx -10$ K), which shows that the dominant spin exchange interaction between Os^{7+} ions is antiferromagnetic, even though the Os^{7+} ion of Ba$_2$NaOsO$_6$ has one electron on 5d state predicting structural distortion caused by Jahn-Teller (JT) instability, the material has an undistorted double-perovskite structure, space group Fm-3m indicating that JT instability is very weak on OsO$_6$ octahedra in which OsO$_6$ octahedra persists an ideal octahedral. However, Ba$_2$NaOsO$_6$ undergoes a ferromagnetic (FM) ordering below T$_C$ = 6.8 K with a very low magnetic moment, i.e., ~0.2 μB and a (110) easy axis. According to Lu et al., a long range FM ordering of Ba$_2$NaOsO$_6$ is connected an orbital ordering. When a phase transition occur caused by as an orbital ordering and a charge density wave (CDW) formation leading to an electronic density modulation, a band gap opens at the Fermi level, and DOS peaks are generated at the edges of the resulting CBM and VBM. Therefore, we explored a relationship between orbital ordering and insulating behavior in Ba$_2$NaOsO$_6$ based on DFT approach. We suggest that the orbital ordering transition of Ba$_2$NaOsO$_6$ should be responsible for as a metal-to-insulator transition driven by a bandgap opening at the Fermi level.

Symmetry-preserving strain engineering of Hundness and Mottness in a two-dimensional correlated system

Eun Kyo Ko[1,2,†], Sungsoo Hahn[1,2,†], Changhee Sohn[3], Sangmin Lee[4], Byungmin Sohn[1,2], Jeong Rae Kim[1,2], Jaeseok Son[1,2], Youngdo Kim[1,2], Donghan Kim[1,2], Miyoung Kim[4], Choong H. Kim[1,2*], Changyoung Kim[1,2*], Tae Won Noh[1,2*]

[1]Center for Correlated Electron Systems, Institute for Basic Science (IBS), Seoul 08826, Republic of Korea
[2]Department of Physics and Astronomy, Seoul National University, Seoul 08826, Republic of Korea
[3]Department of Physics, Ulsan National Institute of Science and Technology, Ulsan, Republic of Korea
[4]Department of Materials Science and Engineering and Research Institute of Advanced Materials, Seoul National University, Seoul 08826, Republic of Korea

The electronic states of materials with partially filled d- or f-orbitals are governed by strong correlations. The electron correlation due to strong on-site Coulomb repulsion has been a central paradigm in physics since the 1940s. Recently, the correlation due to Hund's rule coupling (J) has attracted much theoretical attention to describe the novel quantum phases of matter. Here, we developed a strain engineering method to systematically investigate the role of J in the energetics of the Mott gap. By growing $SrRuO_3$ monolayers on various substrates with a symmetry-preserving interlayer, we gradually tuned the crystal field. This lifted the degeneracy of the Ru t_{2g} orbitals and effectively varied the numbers of involved orbitals and electrons. Using in situ angle-resolved photoemission spectroscopy, we observed progressive changes from a metal to a Mott insulator. This study shows that this experimental approach can be useful for exploring the physics of Hundness and Mottness, particularly in two dimensions.
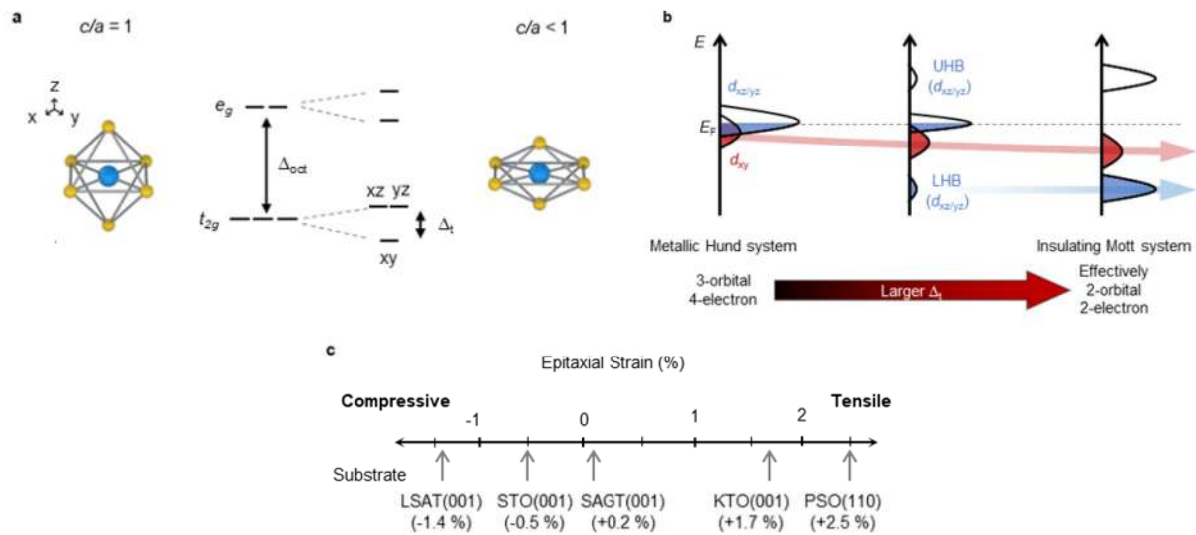
Fig. 1. Engineering crystal field splitting in the $SrRuO_3$ (SRO) monolayer via epitaxial strain. a, Crystal field splitting between t_{2g} orbitals (Δ_t) attributable to structural distortion. b, Schematic of the band configuration of Ru t_{2g} with Δ_t and a Coulomb interaction (U). c, Epitaxial strain imparted to SRO monolayers on various substrates.

Realization of perpendicular anisotropic ferromagnetic semiconductor in strain-induced Sr_2FeReO_6

Gahee Noh[†], Hansol Lee[1][†], Yongjin Kim, Yeongrok Jin, Jaekwang Lee, Chan-Ho Yang, Changhee Sohn[1*], Ho Nyung Lee[*] and Si-Young Choi[*]

[1]Ulsan National Institute of Science and Technology (UNIST), Department of Energy Engineering, Ulsan 44919, Republic of Korea

[†]These authors contributed equally to this work.

Ferromagnetic semiconductors, rarely found in nature, have the potential for spintronics applications due to their enhanced tunneling magneto-Seebeck effect and high spin filter efficiency. However, since ferromagnetic exchange interaction is usually accompanies metallicity along with the Ruderman–Kittel–Kasuya–Yosida (RKKY) interaction where the conduction electrons mediate the alignment of ferromagnetic spin. Thus the ferromagnetic properties dissipate in the semiconductor state. Here, ferromagnetic Sr_2FeReO_6 (SFRO) thin films were grown on different substrates applying strain to modify their crystal and electronic structures. We confirmed that SFRO under tensile stress has successfully synthesized semiconductors with robust ferromagnetic ground states at high Curie temperatures ($T_c \sim 400K$) through dc transport and optical conductivity data. We found that the magnetic anisotropy of the tensiled SFRO originates from the $a^-a^-c^+$ structure since the oxygen octahedral structure prefers to rotate along the in-plane direction under tensile stress. We have demonstrated that the in-plane (out-of-plane) orbitals of Re are preferentially occupied under compressive (tensile) stress, both theoretically and experimentally. This result is consistent with the previous first-principle calculation that C-type octahedral distortion induces an orbital-ordered insulating state. Our work is expected to increase interest in future research on developing spin filters, spin current generation, and anomalous Hall effects.
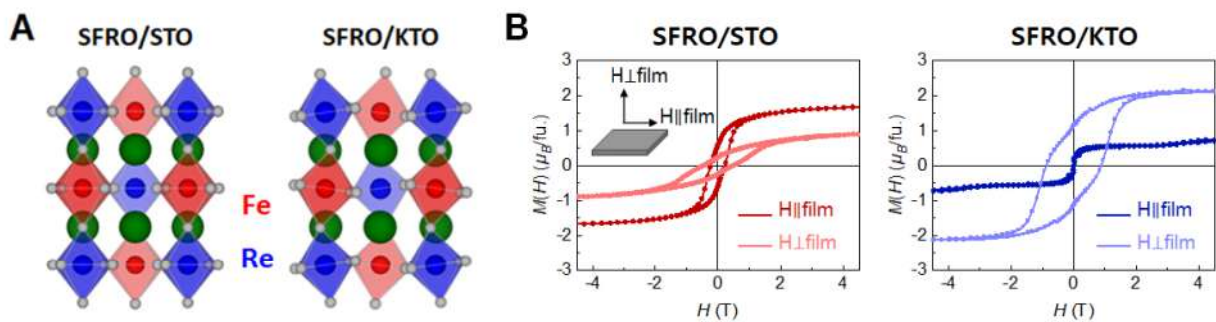
Fig. 1. Schematics of the distorted crystal structures and $M(H)$ curves of SFRO grown on (A) KTO and (B) STO substrates

Construction of Entangled Many-body States via the Higgs Mechanism

Pureum Noh[*] and Eun-Gook Moon

Department of Physics, Korea Advanced Institute of Science and Technology (KAIST), Daejeon 34141, Korea

We provide a guiding principle to generate entanglement of quantum many-body states by applying the Higgs mechanism to systems without gauge structures. A unitary operator associated with the Higgs mechanism is constructed, named as mean-operator, and employed to prepare an entangled many-body state out of a trivial state. We uncover a symmetry-protected-topological state with two Ising symmetries on a square lattice and find entangled states with different symmetries and lattice. Plausible applications to quantum simulators such as Rydberg atoms and trapped ions, are also discussed, interpreting the mean-operators as the Ising coupling gates.
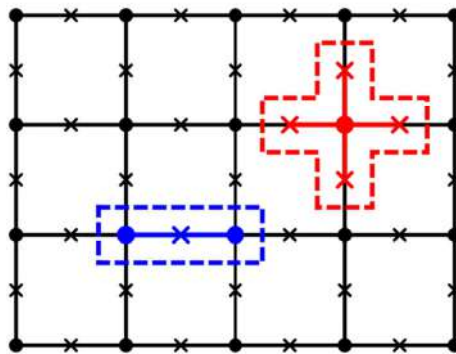
Fig. 1. The interaction terms of our model on a square lattice.

Signatures of Orthogonal Metals at Non-zero Temperatures

Inho Song[*], Minsoo Park[*], Hanit Oh and Eun-Gook Moon[†]

Department of Physics, Korea Advanced Institute of Science and Technology (KAIST), Daejeon 34141, Korea
[*]These authors contributed equally to this work.

Orthogonal metals are massively entangled states, characterized by the emergence of fractionalized carriers instead of electronic quasi-particles. The absence of electronic quasi-particles in orthogonal metals makes tunneling conductance and angle-resolved photoemission spectroscopy (ARPES) significantly distinct from conventional metals.

Here, we employ the Kitaev's toric code model minimally coupled to fermions and provide characteristic signatures of tunneling conductance and ARPES at non-zero temperatures. We discuss implications of our results in connection with recent intriguing experiments in metallic quantum magnets such as Sr2VO3FeAS.

Dipolar Braiding Statistics in Two Dimensions

Yun-Tak Oh[1*], Jintae Kim[2], Jung Hoon Han[2]

[1]Department of Physics, Korea Advanced Institute of Science and Technology, Daejeon 34141, Republic of Korea
[2]Department of Physics, Sungkyunkwan University, Suwon 16419, Republic of Korea

In our earlier work, we recently studied a variant of the TC called the rank-2 toric code (R2TC), which can be derived by lowering the U(1) symmetry of the rank-2 lattice gauge theory. Interestingly, the quasiparticles emerging in R2TC show braiding statistics seems to break the conventional wisdom of Abelian anyon braiding and the flux attachment picture. We argue that this novel statistical phase captures the total dipole moment of quasiparticles encompassed in the braiding, whereas conventional anyonic braiding sees the total charge. An Aharonov-Bohm interpretation of such dipolar braiding statistics can be made in terms of emergent, rank-1 vector potentials built from the underlying rank-2 gauge fields. Pertinent field theories of the quasiparticle dynamics in the R2TC are developed, accompanied by the dipole conservation and the charge conservation law. A dipolar BF theory of the rank-2 gauge fields is constructed and shown to correctly capture the dipolar braiding statistics, in contrast to the conventional BF theory capturing the monopolar braiding statistics of anyons in the rank-1 toric code.

Atomically flat Li$_2$TiO$_3$ single crystal substrate as a new platform for quantum phenomena

Jin-Hyun Choi[1*], Minjae Kim[2], Jong Mok Ok[2], Changhee Sohn[1†]

[1]Department of Physics, Ulsan National Institute of Science and Technology, Korea
[2]Department of Physics, Pusan National University, Korea

Since the Kitaev model is suggested, numerous research about exotic quantum phenomena with using honeycomb or triangular lattice have been reported. However, to our best knowledge, heterostructure studies on honeycomb lattices have been barely conducted. The lack of suitable substrates is one of the major obstacles to synthesize high-quality thin film with triangular or hexagonal lattice materials. Herein we introduce an atomically flat Li$_2$TiO$_3$ single crystal substrate with triangular lattice. The single crystal of Li$_2$TiO$_3$ is synthesized by solid-state reaction of Li$_2$CO$_3$ and TiO$_2$ with heated in air at 1273 K for 12 h. To establish atomically flat surface, mechanical polishing is carried out. Polished Li$_2$TiO$_3$ crystals are annealed at 1400 K for 1 h followed by wet cleaning with HF for 10 – 60 s. As a result, step-terraces of about 0.5 nm height are observed in AFM measurements, which is a strong evidence for atomically flat surface. With processed Li$_2$TiO$_3$ substrates, we demonstrate epitaxial growth of Na$_3$Co$_2$SbO$_6$ (NCSO).
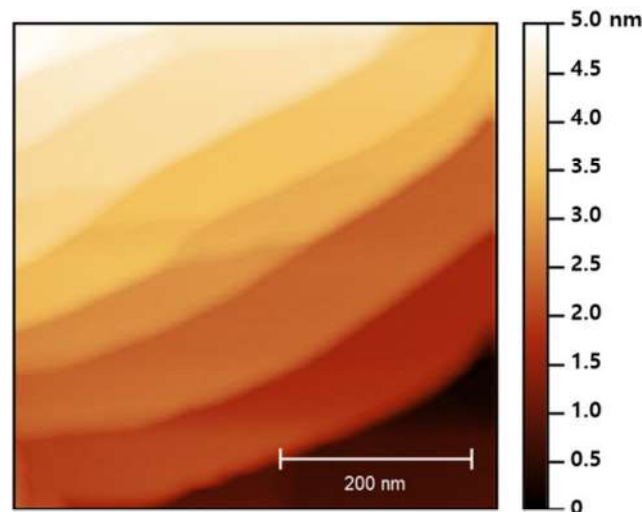
Figure 1. Atomically flat surface of single crystal Li$_2$TiO$_3$ substrate

Magnetic octupole induced oscillation of Hall effect in an antiferromagnetic semimetal

Jeongkeun Song[1,2*], Taekoo Oh[1,2], Eunkyo Ko[1,2], Ji Hye Lee[1,2], Woo Jin Kim[3],
Yangyu Zhu[4], Bohm-Jung Yang[1,2], Yangyang Li[4*] and Tae Won Noh[1,2†]

[1]Department of Physics and Astronomy, Seoul National University, Seoul, 08826, Korea
[2]Center for Correlated Electron Systems, IBS, Seoul, 08826, Korea
[3]Department of Physics, Stanford University, CA, 94305, USA
[4]School of Physics, Shandong University, Jinan, 250100, China

Recent observations of anomalous Hall effect in the antiferromagnets (AFMs) have attracted attention for exploring novel topological phenomena and realizing AFM spintronics. Since these materials are AFM, magnetic dynamics are expected to be different from that of conventional ferromagnets. Here, we report the observation of anomalous oscillation of the Hall effect of AFM $Nd_2Ir_2O_7$ film. The observed anomalous oscillation is decoupled with the behaviors of dipole order-driven magnetization, indicating the presence of hidden order other than a magnetic dipole in AFM. We have found that the appearance of the anomalous response coincides with the orthogonal magnetization (OM) induced by cluster magnetic order. Moreover, the OM causes magnetic field-dependent behaviors of the Hall effect when magnetic field (H) and current (I) are parallel, in which the Hall effect conventionally should vanish. Our study provides a platform to investigate novel topological functionalities by highlighting magnetic dynamics of multipole arising from the interplay between multipole and topology in AFM.

Heterostructure approach on Kitaev quantum spin liquid

Baekjune Kang[1*], Miju Park[1*], Seunghyun Noh[2], Daeseong Choe[2], Minsik Kong[3], Minjae Kim[3], Choongwon Seo[1], Eun Kyo Ko[4,5], Gangsan Yi[1], Jung-woo Yoo[2], Eun-Gook Moon[6], Jongmok Ok[3*] and Changhee Sohn[1†]

[1]Department of Physics, Ulsan National Institute of Science and Technology, Ulsan, 44919, Republic of Korea
[2]Department of Materials Science and Engineering, Ulsan National Institute of Science and Technology, Ulsan, 44919, Republic of Korea
[3]Department of Physics, Pusan National University, Pusan, 46241, Republic of Korea
[4]Center for Correlated Electron Systems, Institute for Basic Science (IBS), Seoul, 08826, Republic of Korea
[5]Department of Physics and Astronomy, Seoul National University, Seoul, 08826, Republic of Korea
[6]Department of Physics, Korea Advanced Institute of Science and Technology, Daejeon, 34141, Republic of Korea

Quantum magnets are an attractive quantum phase in both new paradigms beyond the classical Landau-Ginzberg-Wilson paradigm and future quantum technologies. The Kitaev quantum spin liquid is one of the recent quantum spin systems with exactly solvable anisotropic spin Hamiltonian. However, the materialization of genuine Kitaev quantum spin liquid remains challenging due to the additional isotropic exchange interaction derived from structural deformation. Here, we utilize heterostructure approaches to eliminate structural deformation. We synthesize single phase, high quality, epitaxial, and fully relaxed $Na_3Co_2SbO_6$ thin film, a promising candidate for Kitaev quantum spin liquid. We obtained quantitative parameters of spin Hamiltonian from optical spectroscopy, consistent with the recent theoretical prediction. Field-dependent magnetic susceptibility shows the clear signature of quantum phase transition from zigzag long-range ordered to quantum disordered phases. In particular, the critical magnetic field in $Na_3Co_2SbO_6$ is about 1 T, noticeably smaller than the case of well-known α-$RuCl_3$. We believe that the heterostructure approach is a new platform for implementing the Kitaev quantum spin liquid and future applications of quantum technologies.

Optical-pump Terahertz-probe spectroscopy on epitaxial La$_{0.7}$Sr$_{0.3}$MnO$_3$ films

Jaewoo Han[*], Jeonghoon Kim, Hyeong-Ryeol Park and Changhee Sohn

Ulsan National Institute of Science and Technology (UNIST), Department of Physics Ulsan 44919, Republic of Korea

대표적인 거대자기저항 물질인 La$_{0.7}$Sr$_{0.3}$MnO$_3$는 상온 근처에서 도체-부도체 전이를 일으킨다. 이러한 자성 바닥상태에 따른 큰 저항 변화는 La$_{2/3}$Sr$_{1/3}$MnO$_3$ 가 근적외선 볼로미터로 응용이 가능함을 시사한다. 우리는 LSMO를 근적외선 볼로미터로 새롭게 응용하는 물질로 만들기 위하여 실험을 진행하였다. LSMO 박막은 펄스 레이저 증착 방식을 통하여 (LaAlO3)0.3-(Sr2AlTaO6)0.7 기판 위에 제작하였고 X선 회절 측정을 통하여 LSMO 박막이 증착 되었음을 확인하였다. LSMO의 특성을 확인하기 위하여 물성특성측정시스템을 통하여 온도에 따른 저항의 변화를 측정하여 TCR 값을 계산하였다. 가시광-펌프 테라헤르츠-프로브 실험을 통하여 LSMO 박막 에서 자유 캐리어가 1ps 시간동안 들떴다가 수십 ps 안에 다시 에너지가 내려가게 되며 광-펌프로 인한 열로 온도가 증가하여 Thz 투과의 증가를 확인하였다. 이러한 결과는 기존에 사용하던 VO$_2$보다 최대 10만배 빠르다 는 점을 확인할 수 있다. 이런 점을 토대로 보아 LSMO 필름위에 나노갭을 만들어 에너지를 집속시키는 방식 을 통하여 상온 초고속 근적외선 볼로미터에 응용할 수 있음을 시사한다.

Advancing Hybrid Quantum-Classical Algorithm via Mean-Operators

Donggyu Kim[1*], Pureum Noh[1], Hyun-Yong Lee[2,3,4*] and Eun-Gook Moon[1†]

[1]*Department of Physics, Korea Advanced Institute of Science and Technology (KAIST), Daejeon 34141, Korea*
[2]*Department of Applied Physics, Graduate School, Korea University, Sejong 30019, Korea*
[3]*Division of Display and Semiconductor Physics, Korea University, Sejong 30019, Korea*
[4]*Interdisciplinary Program in E · ICT-Culture-Sports Convergence, Korea University, Sejong 30019, Korea*

The hybrid quantum-classical algorithms have been suggested to control quantum entanglement of many- body systems in noisy intermediate-scale quantum (NISQ) technology, and yet their applicability is limited by the numbers of qubits and quantum operations. Here we propose a mean-operator-theory (MOT) which overcomes the limitations by combining advantages of the hybrid algorithms and the standard mean-field-theory. We demonstrate that an introduction of a mean-operator prepares an entangled target many-body state with the significantly reduced number of quantum operations. We also show that a class of mean-operators is expressed as time-evolution operators, which indicates that our theory is directly applicable to quantum simulations with Rydberg atoms and trapped ions.

La$_{1-x}$Sr$_x$MnO$_3$/NdNiO$_3$ 이중층에서 발생하는 전하이동에 의한 금속 -절연체 전이

조하은[1,3*], 이종민[2], 이년종[1], 양미현[3], 심은지[4], 박정민[5], 이상한[2†], 임규욱[3†], 김상훈[1†]

[1]울산대학교 물리학과
[2]광주과학기술원 신소재공학부
[3]포항가속기연구소 나노계면연구팀
[4]성균관대학교 지능형 팹테크 융합전공
[5]한국과학기술원 물리학과

강자성/비자성층 접합으로 이루어진 이중층에서 계면의 라쉬바-에델스타인 효과 혹은 벌크의 스핀 홀 효과로 인해 전하전류가 스핀전류로 전환될 수 있다[1]. 비자성층 물질이 금속-절연체 전이를 가지는 경우, 상전이에 따라 전하에서 스핀으로 전환되는 효율을 제어 가능[2]하며 이러한 소재는 스핀 전류에 의한 자화제어 연구분야에서 중요성이 높아지고 있다. 본 연구에서는 La$_{1-x}$Sr$_x$MnO$_3$(LSMO)/NdNiO$_3$(NNO)를 강자성층/비자성층 구조를 가진 강상관계 전자 시스템으로 구성하여 NNO 두께에 따른 전자기적 상전이 특성에 대해 연구하였다. 강자성층 LSMO는 반금속 성질[3]을 가진 강자성 산화물이며, 비자성층 물질은 기존에 알려진 금속-절연체 재료인 VO$_2$와 유사한 상전이를 가지지만 그 원리가 다른 희토류 니켈산염 NNO로 채택하였다. NNO는 전자 사이의 강한 결합 및 상호작용으로 인해 상자성-반강자성 자기상전이 및 금속-절연체 전이[4]를 함께 가지는 강상관계 산화물의 일종이다.

상전이 과정에 대한 연-X선 흡수 분광법 관찰을 통하여, 시료가 저온의 절연상에서 상온의 금속상으로 전이할 때 527.6 eV 근처에서 Ni^{2+} 피크[5]가 새로이 생성되는 것이 관찰되었다. 이는 LSMO의 망간에서 NNO의 니켈로 국부적인 전하이동[6]이 발생했다는 증거이며, 해당 피크의 출현 여부는 상전이 과정에 대한 I–V 실험 결과와 일치한다. 이는 LSMO/NNO 이중층 계면에서 전하이동에 의해 라쉬바-에델스타인 효과가 온도에 따라 제어될 수 있음을 의미한다.

References

[1] LUQIAO LIU, SCIENCE, Vol **336**, No.6081, pp. 555-558 (2012)

[2] Taqiyyah S. Safi, Nature Communications, Vol. **11**, No. 11, pp. 476 (2020)

[3] B Nadgorny, Journal of Physics: Condensed Matter, Vol. **19**, No. 31, pp. 315209 (2007)

[4] María Luisa Medarde, Journal of Physics: Condensed Matter, Vol. **9**, No. 8, pp.1679–1707 (1997)

[5] Natalia Palina, Nanoscale, Vol. **9**, pp.6094-6102 (2017)

[6] Zedong Xu, ACS Appl. Mater. Interfaces, Vol. **10**, No. 36, pp. 30803–30810 (2018)

Instrumentation for Thermal Conductivity Measurement

Jin Ho Kim[1*], Heejun Yang[2], Je Geun Park[2], Yoon Seok Oh[1*]

[1]Department of Physics, Ulsan National Institute of Science and Technology, Ulsan 44919, Korea
[2]Department of Physics and Astronomy, Seoul National University, Seoul 08826, Korea

Recently, thermal transport measurement has attracted much attention to probe quasiparticles associated with exotic magnetic excitation and to understand their dynamic properties. We have reported that quasi-one-dimensional $S=1$ chain system $NiTe_2O_5$ exhibits unconventional critical phenomena and anomalous critical exponents below the Néel temperature T_N[2]. Above T_N, $NiTe_2O_5$ shows unexpected strong spin fluctuation even in the paramagnetic state[3]. The thermal transport could be a good experiment probe to understand those intriguing phenomena. We prepare our thermal conductivity measurement apparatus with electronic devices based on the Quantum Design Thermal Transport assemblies. Here, we present the instrumentation for thermal conductivity measurement and discuss further improvements.

References

[1] Mingda Li and Gang Chen, Thermal transport for probing quantum materials, *MRS Bulletin* **45**, 348-356 (2020).

[2] Jun Han Lee, Marie Kratochvílová, Huibo Cao, Zahra Yamani, JS Kim, Je-Geun Park, GR Stewart, Yoon Seok Oh, Unconventional critical behavior in the quasi-one-dimensional $S=1$ chain $NiTe_2O_5$, *Physical Review B* **100**, 144441 (2019).

[3] Seung-Ho Baek, Jun Han Lee, Yoon Seok Oh, Kwang-Yong Choi, Bernd Büchner, Persistence of Ising-like easy-axis spin correlations in the paramagnetic state of the spin-1 chain compound $NiTe_2O_5$, *Physical Review B* **104**, 214431 (2021).

Spin-flip-driven reversal of the angle-dependent magnetic torque in layered antiferromagnetic Ca$_{0.9}$Sr$_{0.1}$Co$_2$As$_2$

Jae Yeon Seo[*], Jong Hyuk Kim, Mi Kyung Kim, Ki Won Jeong, Hyun Jun Shin,
Jae Min Hong, Jin Seok Kim, Kyungsun Moon, Nara Lee and Young Jai Choi

Department of Physics, Yonsei University, Seoul 03722, Korea

A spin–flip transition can occur in antiferromagnets under strong magnetocrystalline anisotropy, inducing a significant modification of the anisotropic magnetic properties through phase conversion. In contrast to ferromagnets, antiferromagnets have not been thoroughly examined in terms of their anisotropic characteristics. In this study, we investigate the magnetic field and temperature evolutions of the anisotropic aspects of Ising-type antiferromagnet Ca$_{0.9}$Sr$_{0.1}$Co$_2$As$_2$ using torque magnetometry measurements. We found that an A-type antiferromagnetic order emerges below $T_N = 97$ K, aligned along the magnetically easy c axis. The reversal of the angle-dependent torque across the spin–flip transition was observed, revealing the influence of the magnetocrystalline anisotropy on the anisotropic magnetic properties. Specific spin configurations associated with the magnetic torque variation in the presence of a rotating magnetic field were theoretically identified, and the experimental torque data could be fully reproduced, based on an easy-axis anisotropic spin model. Our results provide insight into fundamental and applied research on diverse antiferromagnetic compounds by opening new possibilities for distinct magnetic aspects.
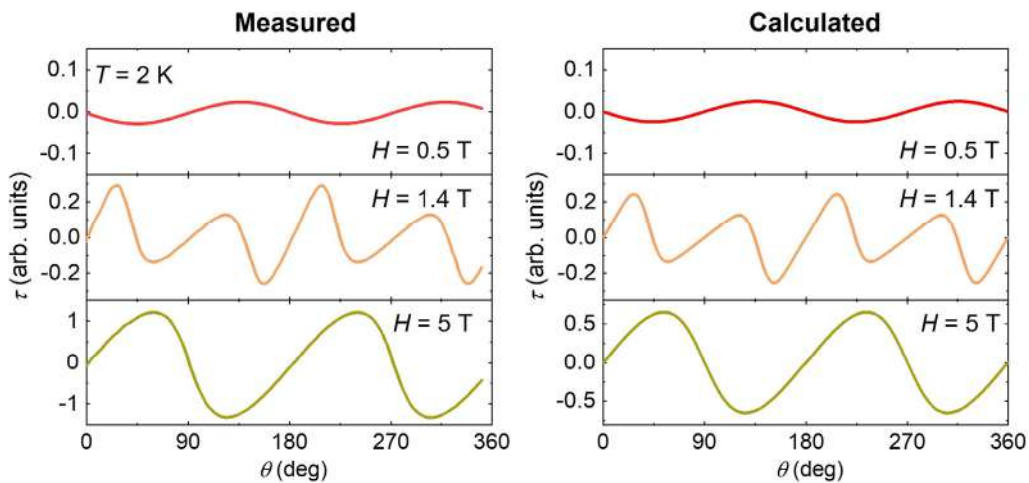
Fig. 1. Temperature evolution of angle-dependent magnetic torques.

Competing orders in monolayer AV_3Sb_5 (A=Na, Rb, Cs)

Sun-Woo Kim[1,2*], Hanbit Oh[2*], Eun-Gook Moon[2†] and Youngkuk Kim[1†]

[1]Department of Physics, Sungkyunkwan University, Suwon 16419, Republic of Korea
[2]Department of Physics, KAIST, Daejeon, 34126, Republic of Korea (Dated: February 24, 2022)

Recently, layered kagome metals AV_3Sb_5 (A=K, Rb, and Cs) have emerged as a fertile platform for exploring frustrated geometry, correlations, and topology. Here we demonstrate that AV_3Sb_5 can crystallize in a mono-layered form, revealing a range of properties that render the system unique by using first-principles and mean-field calculations. Most importantly, the two-dimensional monolayer preserves intrinsically different symmetries from the three-dimensional layered bulk, enforced by stoichiometry. Enrichment of the van Hove singularities, a logarithmic divergence of electronic density of states, consequently appears, leading to a variety of competing instabilities such as doublets of charge density waves and s and d-wave superconductivity. We show that the competition between orders can be fine-tuned in the monolayer via electron-filling of the van Hove singularities. Thus, our results suggest the monolayer kagome metal AV_3Sb_5 as a promising platform for designer metallic quantum phases.
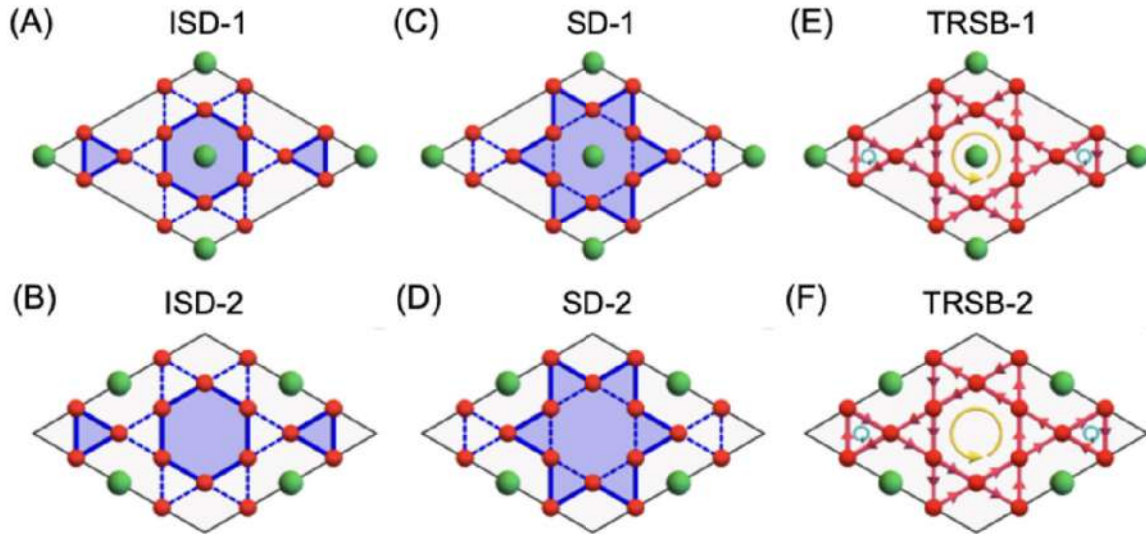
Fig. 1. Schematic illustration of six distinct CDW configurations. (A-B) Inverse star of David (ISD)-1,2, (C-D) star of David (SD)-1,2, (E-F) time-reversal symmetry breaking (TRSB)-1,2. In (A-D), solid and dashed blue lines indicate distinct bonding strengths. In (E,F), red arrows on the bonds indicate the direction of current bond orders. The yellow and green oriented circles represent magnetic fluxes threading the hexagons and triangles in opposite directions, respectively.

Evolution of anisotropic magnetic properties through helix-to-fan transition in a helical antiferromagnet EuCo₂As₂

Jae Min Hong[*], Jong Hyuk Kim, Mi Kyung Kim, Hyun Jun Shin, Ki Won Jeong,
Jin Seok Kim, Kyungsun Moon, Nara Lee and Young Jai Choi

Department of Physics, Yonsei University, Seoul 03722, Korea

A helimagnet comprises a noncollinear spin structure formed by competing exchange interactions. Recent advances in antiferromagnet-based functionalities have broadened the scope of target materials to noncollinear antiferromagnets. Here we have explored anisotropic magnetic aspects in a layered helimagnet of EuCo₂As₂ by measuring magnetic-field and angle dependences of magnetic toques. The helimagnetic order arises below T_N = 46 K, in which the magnetic-moment direction is rotated spatially in the ab plane, propagating along the c axis. The conversion of helix to fan phase occurs at H_m = 4.7 T at 2 K. Two distinctive magnetic phases are characterized by the reversal of magnetic torque variation in the presence of rotating magnetic field. The development of spin configuration and corresponding magnetic torques across the helix-to-fan transition was established by hosting an easy-plane anisotropic spin model. This work renders an in-depth understanding of anisotropic properties in noncollinear-type antiferromagnet and a useful guidance of potential application for spin-processing functionalites.
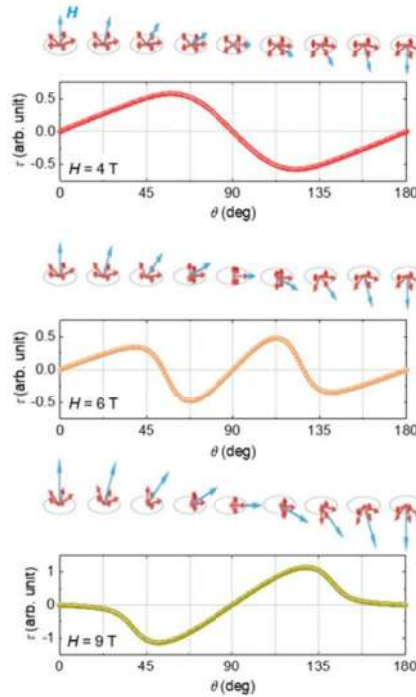
Fig. 1 Detailed magnetic-moment configurations of angular-dependent magnetic torques.

A Brief Survey on 2D vdW Ferromagnetic Metal Family Fe_nGeTe_2 $(3\leq n \leq 7)$

Pradeep Raj Sharma[*], Jang Bogeun and Jongill Hong[†]

Department of Materials Science and Engineering, Yonsei University, Seoul 03722, Korea

[*]E-mail: hong.jongill@yonsei.ac.kr

Two-dimensional van der Waals (vdW) magnetic materials are promising for long-range spin transport and spin manipulation in the development of advanced spin-based technologies. Room temperature ferromagnetism is essential to realize the device applications. Among the vdW magnetic materials Fe_nGeTe_2 $(3\leq n \leq 7)$ possesses ideal characteristics to explore various spin-related phenomena. They are high magnetic anisotropic energy (MAE), metallic conductivity, strong PMA, higher Curie temperature, and layer-dependent ferromagnetism and make Fe_nGeTe_2 highly desirable materials for spintronic devices though the origin of its ferromagnetism is still under debate and needs further understanding to overcome the ambiguities. Herein, this survey is motivated to provide a brief description to understand the 2D Fe_nGeTe_2 family, which could provide a perfect platform for the study of room-temperature 2D spincaloritronics and their potential device applications.

Anomalous Ferromagnetism of Ni Nanowires Embedded in Anodic Alumina Oxide

Hae Jun Ahn[*] and Seung Hun Huh[†]

Korea Institute of Ceramic Engineering and Technology (KICET), Korea

The most of 3-d ferromagnetic(FM) nanomaterials(NMs) have shown the excellent magnetic properties compared to the corresponding bulks due to larger magnetic spin moments per atom. Coercivity (H_c) and remanence to saturation magnetization(M_r/M_s) of FM NMs have become also enhanced with decreasing temperature because of suppression of thermal perturbation. Figure 1 shows the magnetic hysteresis loops for the parallel (//) and perpendicular direction ($\perp$) to the long axis of the Ni nanowires, clearly indicating that the coercivity of $H_{c//}$ becomes smaller at 2 K than at 300 K, while that of $H_{c\perp}$ becomes larger. This is due to the magnetoelastic effects. The behaviors for $M_{r//}$ and $M_{r\perp}$, and $M_{r//}/M_{s//}$ and $M_{r\perp}/M_{s\perp}$ exhibit similar tendency. The phase transition-like behavior (FM→FM) was also observed at zero-field-cooling(ZFC)/field-cooling(FC) measurement for the first time. Temperature-dependent cyclic properties are further discussed.
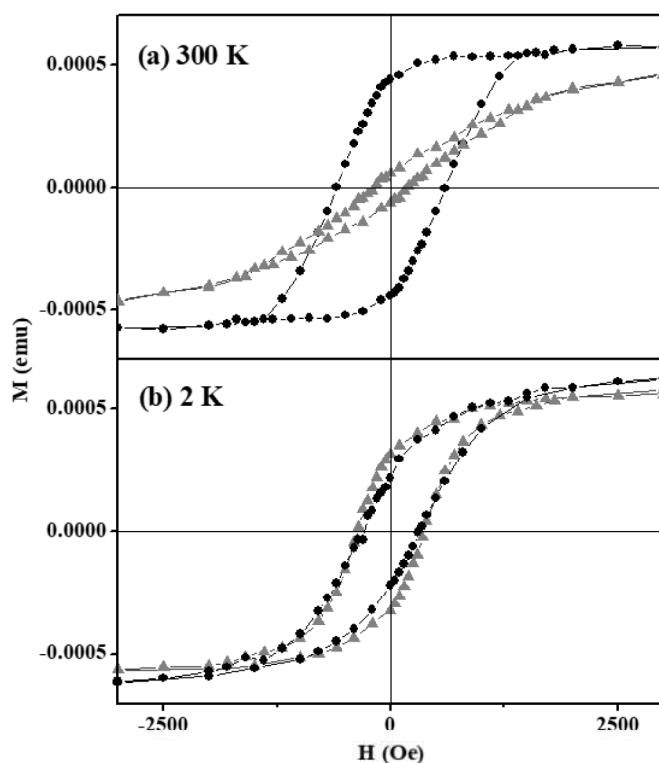

Fig. 1. Magnetic hysteresis curves of Ni nanowirea at 300K and 2K

Enhancement Rashba Effect in Conducting STO Surface by Capping Layer

Seunghyun Noh[*], Daeseong Choe, Jung-Woo Yoo[†]

Department of Materials Science and Engineering, Ulsan National Institute of Science and Technology, Ulsan, 44919, Korea

Systems having inherent structural asymmetry retain the Rashba-type spin-orbit interaction, which ties spin and momentum of electrons in the band structure leading to coupled spin and charge transport. One of the electrical manifestations of the Rashba spin-orbit interaction is nonreciprocal charge transport, which could be utilized for rectifying devices by unidirectional feature. Further tuning of Rashba spin-orbit interaction allows additional functionalities in spin-orbitronic applications. In this work, we present our study of nonreciprocal charge transport in conducting $SrTiO_3$ (001) surface and its significant enhancement by capping layer. The conductive STO (001) surface was created through oxygen vacancies by Ar^+ irradiation and nonreciprocal signal was probed by angle and magnetic field dependent second harmonic voltage measurement with AC current. We observed clear nonreciprocal signal in Ar^+ irradiated sample at low temperature. The magnitude of nonreciprocal signal is highly dependent on the irradiation time as it affects the depth of conducting layer and the strength of Rashba effect on itinerant electrons. Moreover, the nonreciprocal resistance was significantly enhanced by simply adding MoO_3 capping layer on conductive STO surface. This result shows MoO_3 capping layer enhances Rashba effect on STO surface states and controllable feature of Rashba effect by capping layer.
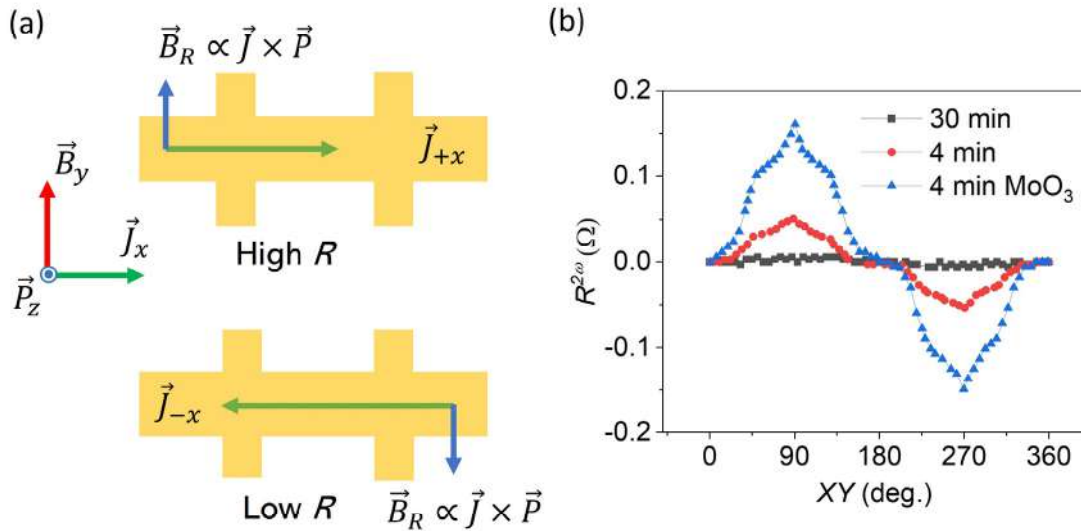
Fig. 1. Rashba effect and nonreciprocal charge transport. (a) Schematic illustration of directional charge transport induced by Rashba effect. The combination of applied current and Rashba effect induces effective magnetic field B_R (Rashba field). (b) The xy angle dependent AC second harmonic resistance ($R^{2\omega}$) with applied magnetic field of $B = 8$ T and $I = 80$ μA at 2 K. The 30 min and 4 min are represented Ar^+ etching times on $SrTiO_3$ surface. The 4 min MoO_3 is represented MoO_3 capping layer deposited at 4 min Ar^+ etched sample.

Electrical and magnetic properties of graphene/graphene oxide heterostructure

Eun Hee Kee[1*], Mohd Musaib Haidari[1], Sohwi Kim[1], Duc Minh Tran[1],
Ji Hye Lee[2,3], Jin Sik Choi[1] and Bae Ho Park[1†]

[1]Division of Quantum Phases & Devices, Department of Physics, Konkuk University, Seoul 143-701, Korea
[2]Department of Physics, Seoul National University, Seoul 08826, Korea
[3]Center for Correlated Electron Systems (CCES),Institute of Basic Science (IBS), Seoul 08826, Korea
E-mail address: *baehpark@konkuk.ac.kr

In the past decade, the study of graphene has been tremendously exploited due to its phenomenal physical and electromagnetic properties such as high flexibility, high thermal conductivity, high electron mobility and long spin diffusion length. Especially, research using long spin life-time and spin diffusion length of graphene have been extensively investigated for the application to spintronics. However, low spin-injection efficiency (~1%) of graphene is an obstacle to realize for spintronic devices. Recently, there have been reports to overcome this problem by using insulating oxide films or a material which has a similar hexagonal lattice constant of graphene such as Ni (111) between the ferromagnetic electrode and graphene. Also, it has been known that a magnetic exchange field (MEF) induced by a magnetic insulator adjacent to graphene can effectively control local spin generation and spin modulation in a 2D device without modulating the structural properties of the material.

In this study, we fabricated graphene (G) / graphene oxide (GO) junction devices in which GO was formed by oxidation technique by applying ultraviolet(UV) light, directly. One of the shortcut to fabricate large area GO, which can make the process of fabrication device easy, minimizing contamination on graphene surface is using ozone induced by UV light. We examined the proximity effect of GO adjacent graphene in the transport of this G/GO heterostructure device with external magnetic field. We showed that week localization and Shubinikov-de Haas oscillations were larger than that of pristine graphene. And we measured magnetoresistance(MR) that revealed negative MR at low temperature in this G/GO heterostructure device. We expect the ferromagnetic properties of GO improve the spin-orbit coupling of the graphene.
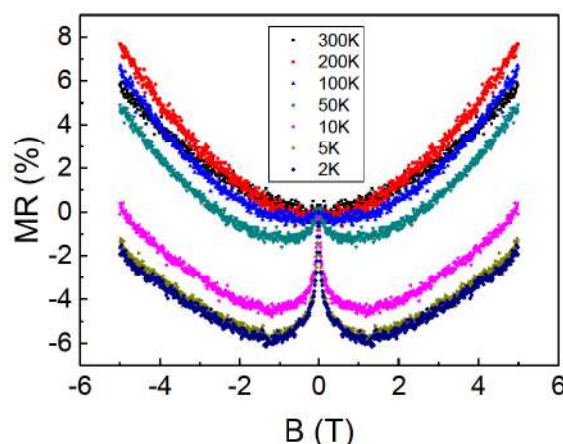

Fig. 1. Magnetoresistance (MR) VS Magnetic field
MR (%) = {Rxx(B)-Rxx(B=0)/Rxx(B=0)}*100, graph shows enhanced weak localization effect at low temperature.

Investigation of magnetism difference of oxidized MoS$_2$ caused by structural change

DaYea Oh[1*], Duk Hyun Lee[2], Won Dong Kim[2], Gwang Taek Oh[1], Chansoo Yoon[1], Bae Ho Park[1*]

[1]Department of Physics, Konkuk University, Seoul 05029, South Korea
[2]Quantum Technology Institute, Korea Research Institute of Standards and Science, Daejeon 34113, Korea

As the demand for nano scaled devices is increasing, Two dimensional (2D) materials have been theoretically and experimentally investigated in the last few decades. Among 2D materials, TMD(Transition Metal Dichalcogenide) materials which have layered structure shows extensively magnetic, electrical, and mechanical properties. Especially, hydrogenation of MoS$_2$ by high temperature and MoS$_2$ irradiated by proton shows unexpected ferromagnetic behavior which would lead to new spintronics devices .

In this works, we fabricate locally hydrogenated or oxidized MoS$_2$ using AFM lithography and confirm specific magnetic properties. Through Raman measurement, we identify that the pure MoS$_2$ surface modify hydrogenated or oxidized one under different lithographic condition. Also, Magnetic Force Microscopy (MFM) measurement support that hydrogenated or oxidized MoS$_2$ using AFM lithography shows novel magnetic properties comparing with pristine MoS$_2$. This result may attribute to the H or O atoms deposited on MoS$_2$ defect by AFM lithography.
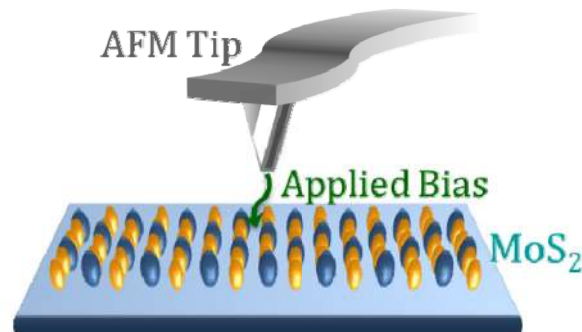

Fig. 1 Schematic image of AFM lithography method

Unexpected electromagnetic behavior of van der Waals transition metal chalcogenide TaCo$_x$Te$_2$

손원혁[1*], 고경태[2], 김규[1], 김재욱[1], 지성대[1], 이성수[1]

[1]한국원자력연구원, 대한민국

[2]한국기초과학지원연구원, 대한민국

반데르발스 자성체는 2차원 기능성 스핀트로닉 소자의 후보로 기초물성부터 소자화 연구에 이르기까지 다양한 연구들이 진행되고 있다. 전이금속계 칼코겐족 반데르발스 물질인 TaCo$_x$Te$_2$는, 두 물질 모두 상온에서 반강자성의 자기적인 정렬을 나타낼 것이라는 이론적인 예측이 있으며, 특히 TaCoTe$_2$의 경우 방향에 따라 위상학적 물리 현상이 나타날 것으로 예상된다. 우리는 기상증착법을 이용하여 TaCo$_x$Te$_2$(x=1,2) 단결정을 성장했다. 성장된 단결정은 X 선 회절, 스캐닝전자현미경을 통해 구조와 조성을 확인하였으며, 전자기 수송 분석을 통해 두 물질 모두 전기적으로 금속임을 확인했다. 자화율 측정 결과 이론적 예측과는 다르게 상온에서 2 K 저온까지 자기적 정렬이 관찰되지 않았다. 또한 포항방사광가속기 6A 빔라인을 이용한 실험에서 Co 가 2+ 상태로 존재하며 전기적으로 금속이지만 국소화된(localized) 상태를 가지는 것을 확인하였으며, 추가적으로 밀도범함수(DFT) 계산을 진행하여 TaCo$_x$Te$_2$이 가지는 전자구조적인 특성을 기존에 알려진 이론적 분석과 비교했다. 우리는 이번 발표를 통해 TaCo$_x$Te$_2$에서 나타나는 자기적 현상에 대해 논의하고자 한다.

Theory of Moiré Magnets and Topological Magnons: Applications to Twisted Bilayer CrI₃

Kyoung-Min Kim[1*], Do Hun Kim[2], Grigory Bednik[1],
Myung Joon Han[2] and Moon Jip Park[1]

[1]Center of Theoretical Physics of Complex Systems, Institute for Basic Science, Daejeon 34126, Republic of Korea
[2]Department of Physics, Korea Advanced Institute of Science and Technology, Daejeon 34141, Republic of Korea

We develop a concrete theory of twisted bilayer magnetism. Starting from the first-principles calculations of two-dimensional honeycomb magnet CrI₃, we construct the generic spin models that represents a broad class of twisted bilayer magnetic systems. Using the Monte-Carlo method, we discover a variety of non-collinear magnetic order that has been overlooked in the previous theoretical and experimental studies. As a function of the twist angle, the collinear magnetic order undergoes the phase transitions to the non-collinear order and the magnetic domain wall phase. Within the domain wall phase, the magnetic skyrmion phase is additionally identified even in the absence of the Dzyaloshinskii–Moriya interaction, which is the consequence of the non-trivial spatially varying interlayer exchange coupling. To describe the critical phenomena, we construct the field theoretical model of moiré magnet, which correctly captures the phase transitions observed from the simulations. Finally, we classify the topological magnons, characterized by massive Dirac magnons with different physical origin of the mass terms, for each of magnetic phases we uncovered. In the collinear magnetic order, higher-order topological magnonic insulator (HOTMI) phase occurs. This is a unique example of the HOTMI, as it does not require any non-collinear order or asymmetric interactions. In the noncollinear phases, the magnons of the noncollinear domain wall harbors one-dimensional topological edge mode, which is confined at the domain walls. As the domain walls form a network, the confined edge mode extends to form a network model of the topological magnons.

Analysis of Planar Hall Magnetoresistive sensors with sub-nT Detectivity

Taehyeong Jeon[1*], Proloy Taran Das[2], Mijin Kim[1], Changyeop Jeon[1],
Byeonghwa Lim[2], CheolGi Kim[1†]

[1]Department of Physics and Chemistry, DGIST, Daegu 42988, Korea
[2]Magnetics Initiative Life Care Research Center, DGIST, Daegu 42988, Korea

We investigated the detectivity of planar Hall magnetoresistive (PHMR) sensors in the 0.5 Hz to 200 Hz frequency range. Analysis of PHMR sensors is performed by varying parameters such as power operating mode, geometry, sensor stack, and temperature. Sensor sensitivity and voltage noise characteristics are measured in an unshielded environment. In the PHMR sensor configuration, Barkhausen noise was revealed in 1/f noise component and found less significant. In the measurement at optimized conditions, we achieved the best magnetic field detectivity reaching to 521 pT/√Hz at 100 Hz and close to 1.1 nT/√Hz at 10 Hz, using a tri-layer multiring PHMR sensor.[1]

Keywords: Planar Hall Magnetoresistance, Magnetic Sensors, Low frequency noise, Detectivity.

Reference

[1] T. Jeon *et al.* "Operational parameters for sub Nano-Tesla field resolution of PHMR sensors in Harsh environments," *Sensors,* vol.21, no.20, pp.6891, (2021).

Self-Balanced PHMR Sensor integrated with Bridge Resistance Compensation for offset and Noise Reduction

Changyeop Jeon[1*], Jae Hoon Lee[1], Taehyeong Jeon[1], Proloy Taran Das[1],
Yong-Ho Lee[3], Byeonghwa Lim[2] and Cheol Gi Kim[1†]

[1]Department of Emerging Materials Science, DGIST, Daegu 42988, Korea
[2]Magnetics Initiative Life Care Research Center, DGIST, Daegu 42988, Korea
[3]Quantum Magnetic Measurement Team, KRISS, Daejeon 34113

The application of advanced microelectromechanical systems (MEMS) magnetoresistance sensors requires very high resolution in the low magnetic field range. To improve the resolution of magnetoresistance sensor, a self-balancing bridged sensor incorporating a resistance compensator is designed to reduce low frequency noise in the range of 0.5 Hz to 200 Hz. The self-balancing bridge sensor is made of PHMR (Planar Hall Magnetoresistance Effect) with a NiFe (10 nm)/IrMn (10 nm) Bilayer structure. A resistance compensator integrated with its magnetic bridge sensor architecture is an alternative to marketable MEMS MR sensors, allowing for adjustable offset voltage compensation at the wafer level and significantly improving the noise level of the sensor. Additionally, sensor noise components of electronic and magnetic origin are identified by measuring the sensor noise spectral density as a function of temperature and operating power. The lowest noise achievable with the device architecture is estimated to be 3.34 nV/√Hz at 100 Hz.
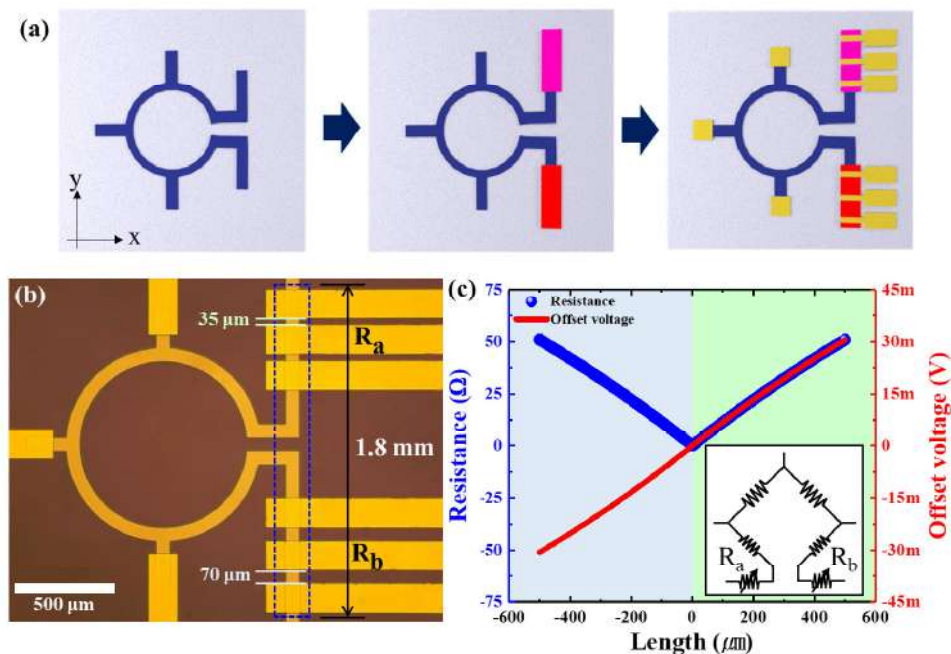
Fig. 1. Structure diagram of self-balancing bridge type PHMR sensor with resistance compensator applied

내장형 제어봉구동장치의 모터하우징 설계 영향분석 연구

이재선*

한국원자력연구원, SMART계통기술개발부, 대전광역시 유성구 대덕대로989번길 111, 34057

제어봉구동장치는 원자로 노심 내에서 제어봉집합체를 상하로 구동하여 원자로 노심 반응도를 제어하는 전기기계로, 원자로의 주요 기기 중 하나이다. 자석잭 형식의 제어봉구동장치가 상용 및 SMART 원자로덮개 상부에 설치되는 외장형으로 개발되었는데, 제어봉구동장치 내부에는 원자로의 일차냉각재가 채워져 원자로 압력경계의 일부로 설계된다. 외장형 제어봉구동장치의 인양력은 전자기장 해석을 통해 예측하고, 이를 설계에 적용한 바 있다 [1]. 혁신 SMART 는 전기출력 200MW 의 일체형원자로로 개발 중이며, 원자로 압력경계 내부에 제어봉구동장치를 배치하는 자석잭 형식의 원자로내장형 제어봉구동장치가 적용된다 [2]. 내장형 제어봉구동장치는 기존 상용 및 SMART 와 다르게 제어봉구동장치 하우징(모터하우징)이 원자로압력경계를 구성하지 않아 모터집합체의 구동을 가이드하고 코일집합체로부터의 전자기장이 효율적으로 모터집합체로 전달되도록 하는 전자기장 경로로서의 기능을 수행하게 된다. 모터하우징은 자성체와 비자성체가 번갈아 배치될 경우에 최적의 인양력을 얻을 수 있음을 선행 연구를 통하여 확인하였으며[3], 본 연구에서는 모터하우징의 유무와 두께에 따른 인양력의 변화를 예측하여 내장형 제어봉구동장치의 최적 설계인자를 확인하고자 한다.
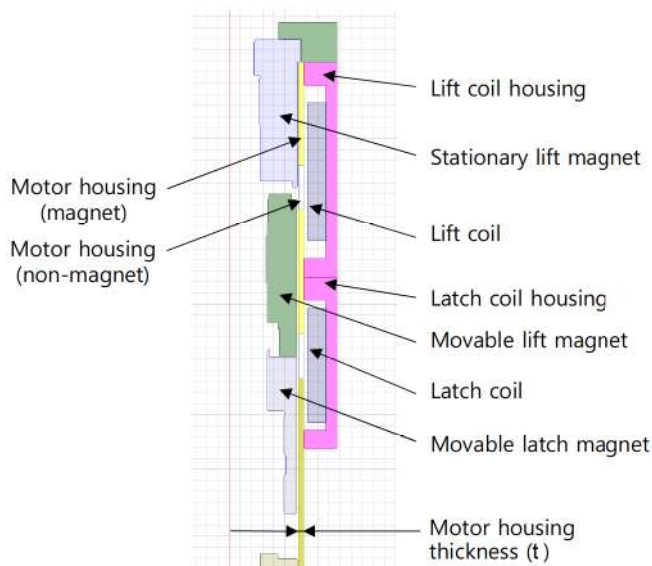
Fig. 1. 2D Axisymmetric analysis model
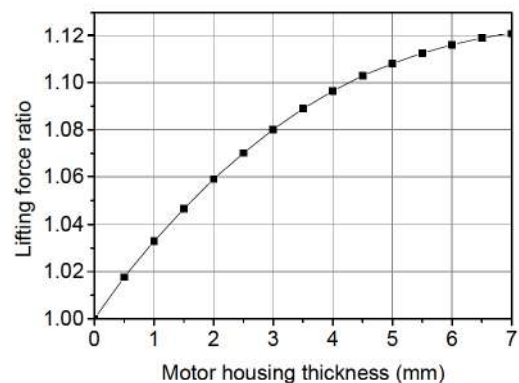
Fig. 2. Relative lifting force with respect to motor housing thickness

전자기장 해석을 위해 Ansys Electromagnetics Suite 2022를 이용하여 Fig. 1과 같이 2차원 축대칭 모델을 구성하였으며, 모터하우징의 자성체와 비자성체의 길이는 동일한 것으로 모델링하였다. 코일집합체의 지름은 200mm 이하로 제한되며, 코일의 크기를 고려하여 모터하우징의 두께(t)를 0 ~ 7mm 까지 증가시키면서 이동인양마그넷과 이동래치마그넷 (Movable lift magnet and movable latch magnet)에 발생하는 인양력을 계산하였다. 모터하우징이 없을 경우 인양력은 약 2600N 으로 예상되었는데, 이는 경향성 분석을 위해 자성재료는 410 스테인리스강으로 가정한 결과로 추후 각 자성체의 선정 결과에 따라 인양력은 변경될 예정이다. Fig. 2의 해석

결과에서와 같이 모터하우징 두께가 증가할수록 인양력이 증가하는 것으로 예측되어 모터하우징이 두꺼울수록 효율적인 설계가 진행됨을 확인하였다. 모터하우징 두께가 증가할수록 인양력의 증가 기울기는 감소하며, 제어봉구동장치의 최대 지름이 원자로 설계에 따라 제한받기 때문에 설계 가능한 범위 내에서 증가량은 제한된다.

해석 결과로부터 모터하우징은 모터집합체의 구동 가이드 역할 뿐 아니라, 모터집합체로 전달되는 전자기장의 경로를 개선하여 인양력 향상에 기여함을 확인하였다. 향후 참고문헌 3과 같이 모터하우징의 자성체와 비자성체 배열의 최적 설계를 통해 내장형 제어봉구동장치의 설계최적화가 가능하다.

References

[1] JaeSeon Lee et al., IEEE T MAGN. **50**, 11 (2014)

[2] JaeSeon Lee et al., US patent 9,853,817 (2017)

[3] JaeHan Lee et al., *KNS Autumn Meeting* 21-22 (2021)

A Study on the eddy current simulation technique by rolling of a ship

Sang Hyeon Im[*]

Dong Eui University, Korea

Recently, magnetic materials capable of generating a large magnetic flux have been developed due to the development of high-performance magnetic materials. In general, when a large magnetic flux is generated, it becomes possible to design high-performance electric devices, thereby increasing efficiency. However, in the defense field, especially in the case of the navy, the risk of attack by magnetic-sensitive mines increases because the magnetic materials constituting the ship generate magnetic field signals to the outside.

In order to prevent this, studies such as demagnetization and demagnetization have been actively conducted. However, although the permanent and induced magnetic fields are sufficiently reduced due to demagnetization and demagnetization, the proportion of the eddy current magnetic field is relatively large, so research on techniques for reducing the eddy current is also required.

n this paper, modeling for predicting eddy currents and eddy current magnetic fields generated in ships is proposed. The ship inevitably oscillates during the voyage. If the ship fluctuates while a constant earth magnetic field is occurring, the amount of magnetic flux linkage to the ship changes, resulting in eddy currents. In order to reduce this eddy current, the magnitude and phase of the eddy current generated in the ship must be predicted first. The analysis to predict the eddy current was carried out through the modeling shown in Figure 1, and the verification was completed through the experiment. In the future, based on the results of this study, we plan to develop a plan to reduce the eddy current magnetic field.
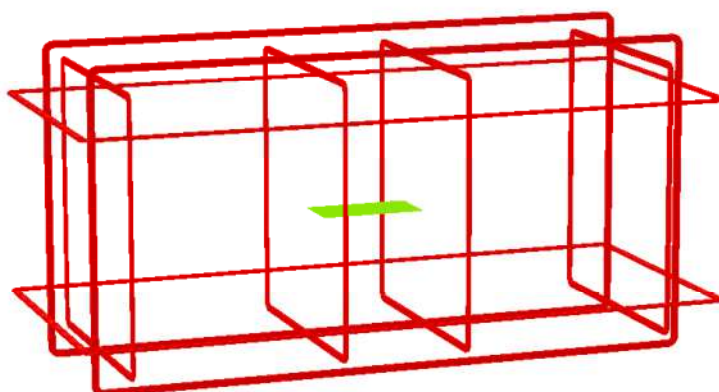

Fig. 1. Model of analysis on eddy current of a ship by

Stability of Topologically Ordered Quantum Magnets at non-zero Temperatures

Minsoo Park[*], Inho Song[*], Hanit Oh and Eun-Gook Moon[†]

Department of Physics, Korea Advanced Institute of Science and Technology (KAIST), Daejeon 34141, Korea
[*]These authors contributed equally to this work.

We study effects of thermal fluctuations on topologically ordered quantum magnets. It is well known that Kitaev's toric code model in three spatial dimensions has a non-zero thermal phase transition between a topologically ordered magnetic state and a paramagnetic state. Here, we argue that the presence of such thermal phase transitions is generic. By utilizing the transfer matrix method in statistical mechanics extensively, we investigate behaviors of the two largest eigenvalues of Kitaev's toric code model with generic perturbations on one cube and prove the stability of the thermal phase transitions. We also discuss implications of our calculations in the context of highly entangled metallic states such as orthogonal metals.

초전도 자기장발생장치의 자기차폐장치 설계 제작

손대락[*], **류권상**[2], **김병국**[3]

[1]㈜센서피아, 대전, 대한민국
[2]한국표준과학연구원, 대전, 대한민국
[3]중앙분석센터, 한국과학기술원, 대전, 대한민국

분석기기용으로 초전도 자석을 사용하여 수십 Tesla의 자기장을 발생시킨다. 이 경우 장비를 사용하는 사람이 큰 자기장에 노출되지 않아야 된다. 가장 이상적인 방법은 초전도 자석으로부터 먼 곳에 작업자가 있으면 된다. 그러나 현실적으로 실험실의 공간이 협소하기 때문에 초전도 자석으로부터 발생되는 자기장을 차폐를 하여야 되는 경우가 발생한다.

본 연구에서는 14 T 자기장을 발생시키는 초전도 자석으로부터 자석의 중심으로부터 1.6 m 반경에서 500 μT (5 Gauss)이하의 자기장이 되게 자기차폐장치를 설계·제작하였다.

기존의 초전도 자석에서 자기장을 차폐하기 위한 구조로 설계를 진행하였으며, Maxwell 사용 FEM simulation을 수행하여 중심으로부터 자기장이 500 μT 이하인 조건을 찾은 후에 제작을 수행하였다. 차폐재료는 가공이 쉽고 투자율이 비교적 큰 저탄소강인 SPHC강을 사용하였다. Fig. 1-a)는 제작된 차폐장치를 조립하는 과정에서 하부에 차폐강판을 설치하는 사진이고, Fig. 1-b)는 원통형 내부 차폐 구조를 설치한 후의 사진이며, Fig. 1-c)는 원통형 외부 차폐 구조를 설치하고 그 위에 무방향성 규소강판을 덮은 마지막 조립이 된 상태의 사진이다. 제작된 차폐장치는 14 T로 초전도자석을 구동할 경우 차폐장치가 없을 경우 중심으로부터 반경 1.6 m의 거리에서 자기장 평균이 2,000 μT였으나, 차폐장치를 한 후 자기장 평균이 480 μT였으며, 컴퓨터 시뮬레이션 결과와 잘 일치하였다.
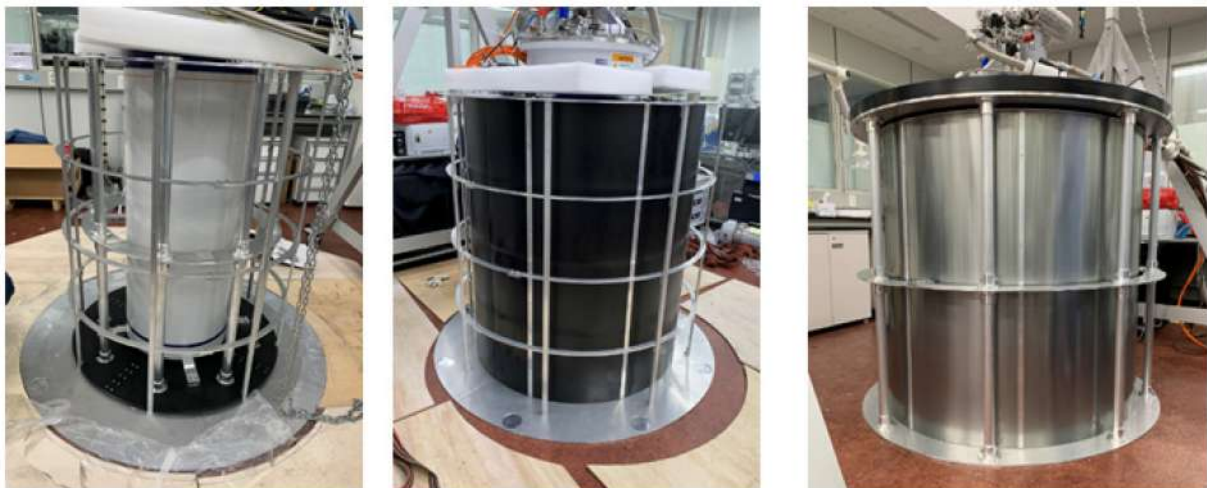
Fig. 1. Photography of constructed magnetic shield chamber; a) after butom layer, b) after inner cylinder layer, and c) after final outer cylinder layer.

Synthesizing polycrystalline-$Y_3Fe_5O_{12}$ matrix with different sequences and observation of ε-phase Fe_2O_3

H.-J. Ok[1*], M.-S. Jang[2] and K.-S. Lee[1]

[1]Department of Materials Science and Engineering, Ulsan National Institute of Science and Technology (UNIST), Ulsan, Republic of Korea

[2]Metal Powder Department, Korea Institute of Materials Science (KIMS), Changwon, Korea

Yttrium iron garnet ($Y_3Fe_5O_{12}$, YIG) is ferrimagnetic insulator that has significant properties as magnetic and optical. Since the spin Seebeck effect that used pure spin current was discovered in the insulator [1], YIG was one of the attractive materials for many researchers. There are many synthesizing methods, however, the polycrystalline bulk-YIG is proper to applicate the YIG in cooling system was absented real life than single-crystalline thin film-YIG. In this research [2], the sol-gel method was used for synthesizing YIG matrix that was the mixture phase as not included perfectly crystallized but was able to phase transition. We focused on the relation of heat treatment (HT) and mechanical pressing (P) at YIG matrix for observing the increment of saturation magnetization (M_s). As a result, the increment of M_s was measured when the HT before P was processed. This relation between H.T. and P was able to understand due to the effect of agglomeration and densification on particles of YIG matrix. Though the grinding process existed before the HT, slight difference of adjacent particles was affected to phase transition that could determine the magnetic properties. Also, especially, completely different wasp-waisted hysteresis loop as a giant coercive field (H_c) and low M_s value was measured in YIG matrix when undergoing HT at the specific temperature, 850°C. The wasp-waisted hysteresis loop is able to appear when two hysteresis loops are mixed [3]. From the analysis of XPS and crystal structure, yttrium iron perovskite ($YFeO_3$) and iron oxide (Fe_2O_3) were able to exist. The phase of iron oxide was determined by the comparison the hysteresis loop of each phase, the existence of ε-Fe_2O_3 was confirmed. The $YFeO_3$ has very low M_s and H_c [4] whereas ε-Fe_2O_3 has around 20 kOe of H_c [5]. Consequently, from the 1.5 times improvement of M_s value, the probability of affection on the perfectly crystallized YIG through more densify and aggregate of YIG matrix. And the existence of thermodynamically unstable ε-Fe_2O_3 in the synthesizing process by sol-gel method guarantees an easy mechanism to synthesize.
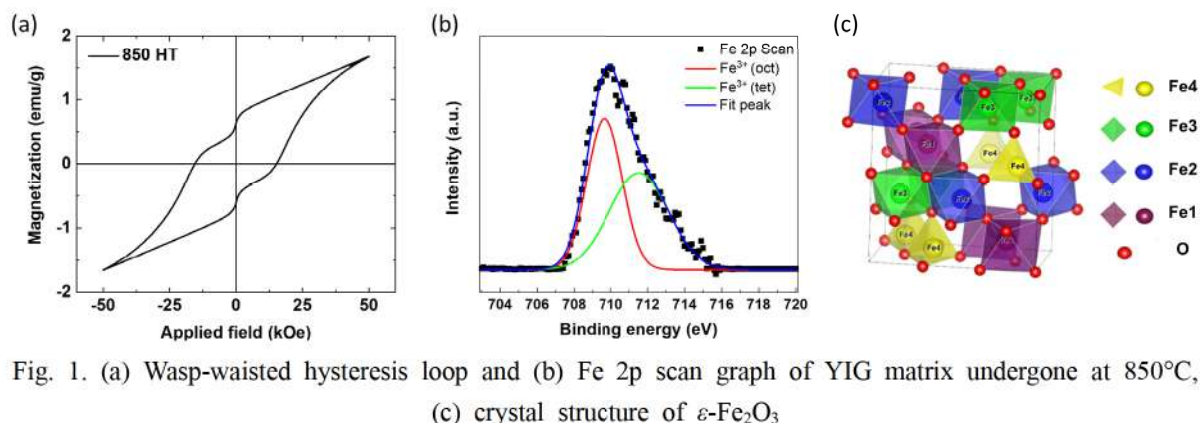

Fig. 1. (a) Wasp-waisted hysteresis loop and (b) Fe 2p scan graph of YIG matrix undergone at 850°C, (c) crystal structure of ε-Fe_2O_3

References

[1] Phys. Rev. Lett. **99** (2007) 066603 1-4.

[2] J. of Mag. and Mag. Mater. **552**, (2022) 169218.

[3] J. Am. Ceram. Soc. **97**, (2014) 1-27.

[4] J. Amighian, A. Yousif, M. Mozaffari, Life Sci. **10**, (2013) 155-161.

[5] J. Nogués Phys. Rev. B, **79**, (2009) 094404.

Design and optimization of a high-performance alumina-based wire wound chip inductor for GHz frequency

Rachida Lamouri[1*], Minji Gu[1], Jinu Kim[2] and Ki Hyeon Kim[1]

[1]Department of Physics, Yeungnam University, Gyeongsan, 38541, Republic of Korea
[2]Institute of Photonics and nanotechnology, Yeungnam University, Gyeongsan, 38541, Republic of Korea A, Korea

Miniaturized chip inductors with high performance are essential components in radio-frequency integrated circuits technology. The inductor characteristics, mainly Q-factor, the inductance, and the self-resonance frequency, are strongly influenced by the design and model parameters. Contrary to the multi-layer chip inductors, the wire-wound inductors present excellent advantages such as low wire resistance and low parasitic capacitance between the coils leading to high Q-factor and Self-resonance frequency. In this work, we simulated an inside-wire wounding alumina (300mm ´ 600mm ´ 100mm; $w'l't$) -based inductor with an optimized distance from the edge of the substrate to the via-hole using ANSYS HFSS software. The improvement of the Q-factor was achieved by controlling the designed structure parameters in terms of the coil diameter, Number of turns, and space between coils. Unlike the influence of the space between coils, the Increase in the number of turns leads to an increase in the inductance while the SRF and the Q-factor values decrease.
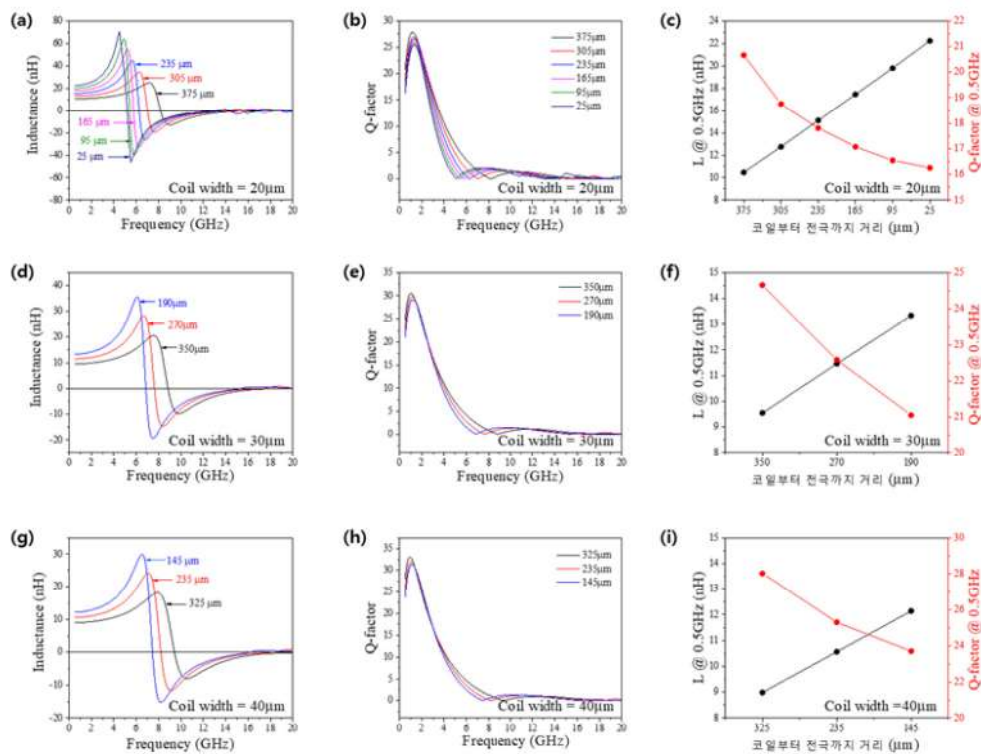
Fig. 1. (a-d-g) inductance (b-e-h) Q-factor (c-f-i) inductance and Q-factor at 0.5 GHz as a function of the space between coils, for coil width of 20 μm, 30 μm, and 40 μm, respectively.

Symposium 2

'Magnetization Dynamics'
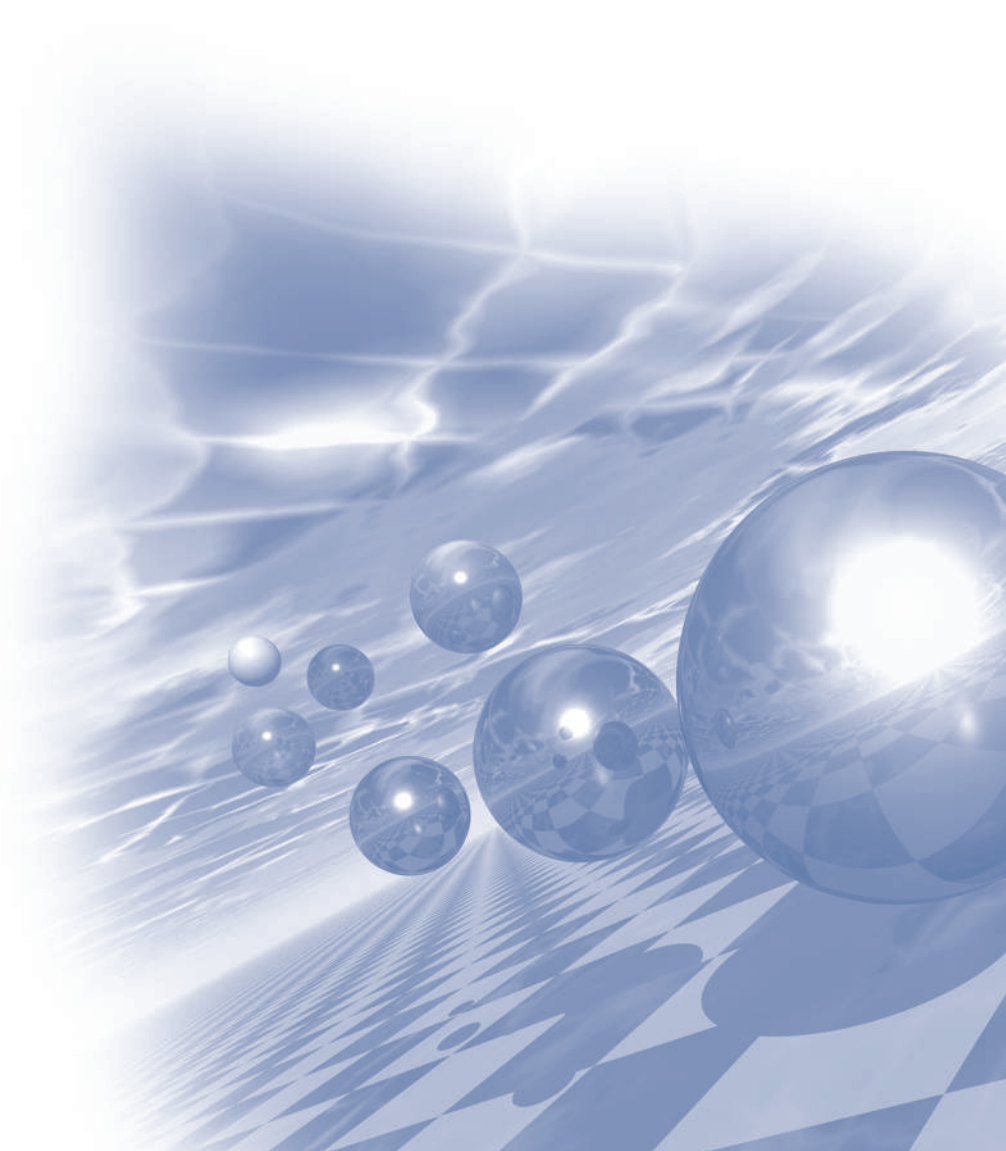
Generation of Transverse Spin Current and its Transport in Ferromagnets

Kyoung-Whan Kim[*]

Cente for Spintronics, Korea Institute of Science and Technology

Spin current generated by an external electric field enables electrical manipulation of magnetization dynamics. While spin current generation in normal metals has been studied for several decades, that in ferromagnets has not been studied intensively. This is attributed to the common belief that the exchange interaction of typical $3d$ transition metals is much stronger than spin-orbit coupling, and thus the transverse component of spin quickly dephases in ferromagnetic bulk. However, a recent theoretical report implies the spin Hall conductivities of Fe, Co, and Ni are large and can be comparable to that of Pt. Therefore, it becomes important to explore transport of transverse spin current in ferromagnets and its impact on the magnetization dynamics. In this talk, I would like to introduce a theoretical formalism to describe transport of transverse spin current. The formalism implies the existence of a self-generated spin-orbit torque without any external spin current source. In addition, due to the orbital degree of freedom, the spin current generated in ferromagnets has different physical features from that generated in normal metals, as demonstrated by the spin swapping conductivities shown in Fig. 1.
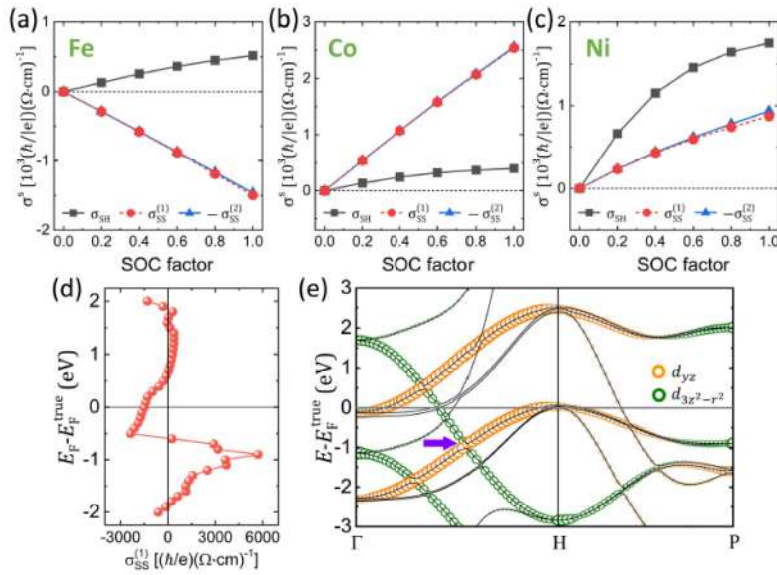
Fig. 1. Spin swapping current induced by Fe, Co, Ni

Spin generation driven by ultrafast phase-transition of FeRh

Kyuhwe Kang[1], Tomoyasu Taniyama[2], Kyung-Jin Lee[3] and Gyung-Min Choi[1,4*]

[1]Department of Energy Science, Sungkyunkwan University, Suwon 16419, Korea
[2]Department of Physics, Nagoya University, Nagoya 464-8601, Japan
[3]Department of Physics, KAIST, Daejeon 34141, Korea
[4]Center for Integrated Nanostructure Physics, Institute for Basic Science, Suwon 16419, Korea

Magnetization dynamics can generate spin current. A representative example is the spin pumping: a steady-state precession of magnetization of a ferromagnet metal (FM) generates DC spin current to an adjacent non-ferromagnetic metal (NM). More recently, an ultrafast version of spin pumping has been achieved: an ultrafast demagnetization (UDM) of FM generates a transient spin current to a NM. Despite that the UDM-driven spin current has been confirmed by various experimental observations, such as spin accumulation on NM and spin-transfer-torque on another FM, a theoretical interpretation of it remains controversial. One of the possible mechanisms is the angular momentum transfer between magnons and electrons during the magnetization dynamics. In this work, we examine the role of angular momentum transfer in an entirely different magnetization dynamic, ultrafast phase transition (UPT) of FeRh. We demonstrate that UPT generates a transient spin current, whose sign, time delay, and magnitude are well explained by angular momentum transfer between electrons and magnons.

자성동역학의 단계적인 이해 및 자성나선도메인의 형성

Kyoung-Woong Moon[*]

양자스핀팀, 한국표준과학연구원, 대전 34113

이번 발표에서는 수직자성 박막에서 스핀토크에 의해 일어나는 다양한 자성동역학에 대해서 계산 및 시뮬레이션으로 연구한 결과를 소개한다. 자화벡터가 오직 1개만 존재하는 0차원 상황에서 시작하여 자화벡터들이 한 줄로 배열되어 있는 1차원 모델에 대한 결과를 설명하고 자화벡터들이 평면상에 균일하게 위치하고 있는 2차원 상황에 대하여 다룬다. Mumax3 시뮬레이션 툴을 이용하여 각 차원의 상황을 효율적으로 계산하는 방법을 소개한다. 마지막으로 방사형 전류에 의해 형성될 수 있는 나선모양의 특이한 자화상태에 대해 설명한다. 자성나선도메인이라고 부를 수 있는 특이한 자화상태는 시간에 따라 회전하는 특성을 가지며 스커미온의 생성자로 역할을 할 수 있다.

하드웨어 기반 보안기술을 위한 스핀트로닉 물리적 복제 불가능성 (physical unclonable function)

이수길[1*], 강재민[1], 김정목[1], 김남희[1], 이택현[2], 이성준[1], 한동현[1],
이상화[1], 이지성[3], 노수정[3], 이한샘[3], 권준현[3], 김갑진[2], 박병국[1]

[1]한국과학기술원 신소재공학과, 대전 34141, 대한민국
[2]한국과학기술원 물리학과, 대전 34141, 대한민국
[3]현대자동차 연구개발부, 화성 18280, 대한민국

최근 정보 통신 기술의 눈부신 발전과 함께 수많은 IoT (Internet-of-Thing)기기를 통해 방대한 양의 정보가 생성되고 공유되고 있다. 이러한 환경에서 정보 보안의 중요성이 더욱 부각되고 있는데, 기존의 소프트웨어 기반 보안 기술은 해킹에 의한 공격에 상대적으로 취약하기 때문에 새로운 정보 보안에 대한 연구가 진행되고 있다. 특히, 기존 소프트웨어 기반 보안에 대한 대안으로 하드웨어의 물리적 복제 불가능성(physical unclonable function)을 이용한 보안 기술이 고려되고 있다. 물질의 합성 혹은 소자공정과중에 얻어질 수 있는 제어불가능(uncontrollable)하고 예측불가능(unpredictable)한 무작위성에서 비롯된 물리적 복제 불가능 기능(PUF)은 동일한 방법으로 제작된 물질 혹은 소자에서 같은 외부입력 값을 인가했을 때 각각의 구분되는 고유한 출력 값을 생성하여 각 전자 장치에 독자적으로 식별 가능한 암호 키를 생성할 수 있다. 기존의 complementary-metal-oxide-semiconductor (CMOS) 소자뿐만 아니라 resistive random-access memory (ReRAM)등의 비휘발성 메모리 소자를 이용해서 보안 소자를 개발하려는 연구가 활발히 진행되고 있고, magnetic random-access memory (MRAM)를 기반으로 한 스핀트로닉 소자의 물리적 복제 불가능성을 이용한 보안 기술 연구도 태동기에 있다. 본 연구에서는 하부 강자성체/비자성체/상부 강자성체 삼중층 구조에서 무장 스핀-궤도 토크(spin-orbit torque) 스위칭을 활용하는 스핀트로닉 PUF 를 소개하고자 한다. 우리 연구에서 물리적 복제 불가능성은 탈자화(demagnetization) 과정을 통해 얻어진 하부강자성체 층의 무작위적인 자구 분포를 기반으로 얻어진다. 이렇게 생성된 하부강자성층의 무작위적인 자구 분포는 전류 유도 무자기장 SOT 스위칭 극성에 의해 전기적으로 읽을 수 있다. 이를 바탕으로 우리가 제작한 스핀트로닉 보안소자는 SOT 스위칭 극성으로 구분되는 고유한 패턴을 식별 키로 사용될 수 있음을 증명했다. 추가적으로 스핀트로닉 PUF 의 동작 안정성(reliability)과 재구성(reconfigurable) 가능성에 대해서도 논의하고자 하며 특히, 지금까지의 스핀트로닉 장치를 기반으로 하는 하드웨어 기반 보안연구에서 거론되지 않던 외부 자기장에 대한 공격 내성을 가지고 있음을 보이고자 한다.

X-선 강자성공명을 이용한 강자성/금속/강자성 삼층 구조에서의 약한 비접촉 상호작용 측정

김창수[*1], 김원동[2], 최원창[3], 문경웅[1], 김현중[1], 안경모[1], 홍정일[2], 김호영[4],
김영학[4], 박병규[4], 김재영[4], Z. Q. Qiu[5], 황찬용[1]

[1]양자기술연구소, 한국표준과학연구원
[2]소재융합측정연구소, 한국표준과학연구원
[3]신물질과학전공, 대구경북과학기술원
[4]산업기술융합센터, 포항가속기연구소
[5]Department of Physics, University of California at Berkeley, Berkeley, California 94720, USA

거대자기저항 효과가 발견된 이후, 두 박막 자성층 사이에 금속을 삽입한 삼층구조의 상호작용에 대한 연구가 진행되었다. 금속 삽입층 두께에 따라 강자성, 반강자성 비접촉 상호작용이 번갈아 나타나는 RKKY (Ruderman-Kittel-Kasuya-Yosida) 같은 상호작용이 잘 알려져 있다. 또 한 강자성체에서 강자성공명이 일어날 때 스핀펌핑에 의해 다른 강자성체로 각운동량이 전달되어 세차운동에 변조가 일어나는 현상도 연구되고 있다. 우리는 이 구조에서 비교적 두꺼운 두께의 금속을 삽입하여 두 자성체 사이의 상호작용을 X-선 강자성공명을 통해 연구했다. X-선 자기원형이색성은 자성물질의 미시적인 스핀 구조를 이해하는데 널리 사용되고 있는데, X-선 강자성공명은 이 원리를 이용하여 스핀의 세차 동역학을 원소별로 측정할 수 있다. 우리는 Py(50)/Ti(0, 2, 5, 10, 20)/CoFeB(3) 삼층구조에서 X-선 강자성공명을 이용하여 Py와 CoFeB 층의 세차운동을 측정했다. 그리고 두 강자성층사이의 상호작용을 알아내기 위해 두 개의 란다우-립쉬츠 방정식을 이용해서 강자성과 반강자성 상호작용, 스핀 펌핑이 있을 때 두 자성층의 세차운동을 모사했다. 강자성 상호작용 모델이 우리의 실험결과와 일치했으며, 10 nm의 삽입층 두께에서까지 비접촉 상호작용이 나타났다. Ti 10 nm의 삽입층이 있을 때, 비접촉 강자성 상호작용 상수는 1.2 μJ/m^{2}였으며 자기장으로 환산하면 0.36 mT이다.

Synthetic Rashba Spin-Orbit Coupling in n-Si Metal-Oxide Semiconductor

Soobeom Lee[1][*][†], Hayato Koike[2], Minori Goto[3], Shinji Miwa[3], Yoshishige Suzuki[3], Naoto Yamashita[1], Ei Shigematsu[1], Ryo Ohshima[1], Yuichiro Ando[1] and Masashi Shiraishi[1]

[1]Department of Electronic Science and Engineering, Kyoto University, Kyoto, 615-8510, Japan
[2]Advanced Products Development Center, TDK Corporation, Chiba, 272-8558, Japan
[3]Graduate School of Engineering Science, Osaka University, Osaka, 560-8531, Japan
[†]Present address: Department of Emerging Materials Science, Daegu Gyeongbuk Institute of Science Technology, Daegu, 42988, Republic of Korea

Spin–orbit coupling plays a significant role in magnetization dynamics including current-induced magnetization manipulation. Well-known material with large spin–orbit coupling is a bulk of single heavy elements such as Pt, Ta, and Bi. Breaking structural inversion symmetry is also one of the pivotal approaches to generate the spin–orbit coupling, called Rashba-type. For this reason, materials with inversion symmetry and light elements have been outside the scope of spin–orbit coupling study. Indeed, Si has been believed to be unsuitable for study of spin–orbit coupling, because of its small atomic number and inversion symmetric crystal structure. Here, we focus on Si metal-oxide semiconductor (MOS). Application of gate voltage in Si MOS modulates carrier density adjacent to the Si/oxide interface, and an interplay of a gate electric field and carrier accumulation at the interface could synthetically induce Rashba-type spin–orbit coupling. In this talk, we present an observation of spin lifetime anisotropy of propagating spins in n-Si induced by the formation of an emergent effective magnetic field due to the Rashba-type spin–orbit coupling, when a gate voltage is applied to the n-Si MOS.

Spin-polarization in n-Si is electrically generated, transported, and detected in a non-local spin transport device, which consists of ferromagnetic electrodes and non-magnetic reference electrodes on an n-type silicon-on-insulator substrate. Gate voltage (V_g) is applied to backside oxide [Fig. 1(a)]. To investigate an anisotropy of spin lifetime in the n-Si channel, spin precession measurement is exploited at 300 K, applying an oblique magnetic field. In this measurement, the non-local spin signal (V_{NL4T}) under an applied magnetic field
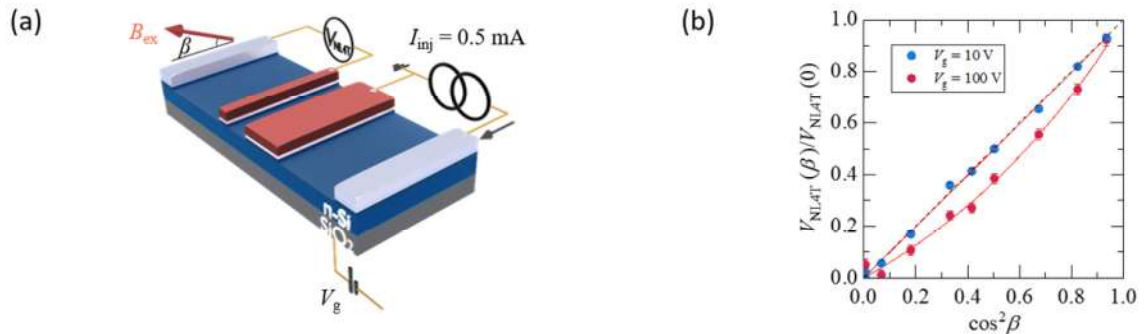
Figure 1. (a) Schematic illustration of n-Si based non-local spin transport device and experimental setup. (b) $\cos^2\beta$ dependences of a normalized spin signal under V_g = 10 V (blue dots) and 100 V (red dots). Red lines indicate theoretical fits.

is measured as a function of the tilt angle (β) of the magnetic field. In a system with an isotropic spin lifetime, a linear relationship between the magnitude of $V_{\text{NL4T}}(\beta)/V_{\text{NL4T}}(0)$ and $\cos^2\beta$ is predicted in the theoretical equation [1]. By fitting experimental angular dependence in Fig. 1(b), the anisotropy ratio, which is quantified by a ratio of an out-of-plane spin lifetime to an in-plane spin lifetime, is extracted. Anisotropy ratios are 0.99 ± 0.02 and 0.75 ± 0.02 in gate voltages of 10 V and 100 V, respectively. Our results indicate that synthetic Rashba-type spin–orbit coupling is indeed induced in n-Si MOS by a field-effect when a strong gate voltage is applied [2]. A more detailed discussion will be given in the presentation.

References

[1] B. Raes *et al.*, Nature Communications **7**, 11444 (2016).

[2] S. Lee, M. Shiraishi *et al.*, Nature Materials **20**, 1228 (2021).

Symposium 3

'Permanent Magnetics' &
'Electro-Magnetic Energy Conversion'
공동세션
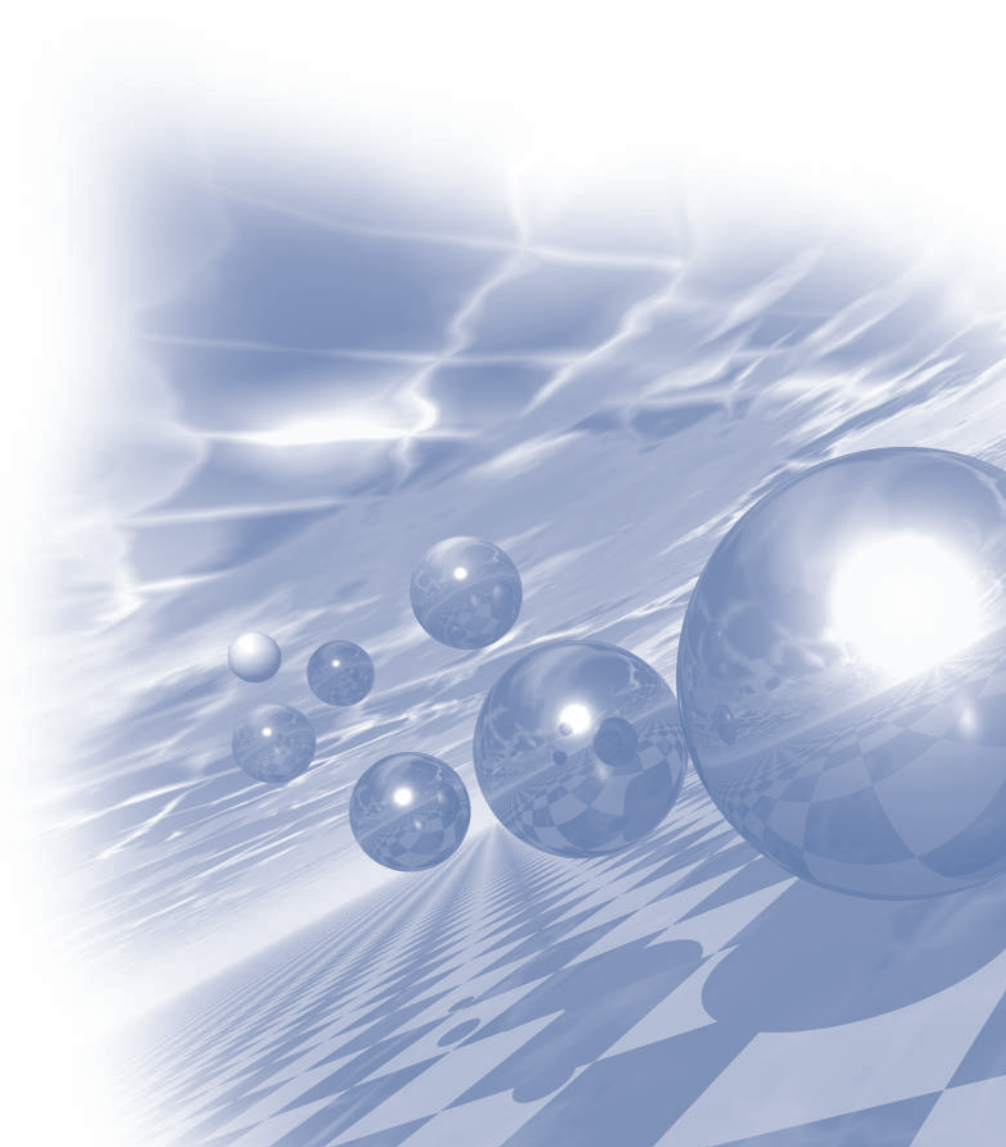
Toward the Development of Permanent Magnets for Compressor Motor

Jin Bae Kim[*]

H&A Research Center, LG Electronics, Seoul, Korea

High performance permanent magnets have become the subject of considerable attention because of the potential applications in electrical appliances and devices, such as motors and speakers. Nd-Fe-B permanent magnets have considerable interest due to a large maximum energy product. The recent concern of the scare supply of Nd has stimulated worldwide research on the development of Nd-reduced high coercivity magnets. At the same time, many scientists have even started exploring rare-earth-free permanent magnetic materials. In this talk, we will discuss the possibility of finding a new magnetic compound for high performance permanent magnets with a reduced amount of rare-earth elements.

열간-변형 Nd 영구자석 제조방법과 적용분야

안종빈*, 황진성, 방희련

(주)디아이씨 신소재연구소

Nd 영구자석은 스마트폰, 전기차, 가전제품, 각종 전동공구뿐만 아니라 전기자동차, 수소차, 플라잉 카, 로봇, 퍼스널 모빌리티 등 최근 탄소배출권과 관련하여 탄소중립 달성에 필수적으로 사용되는 소재이다.

NdFeB 영구자석을 제조할 때 사용되는 원료 분말은 일반적으로 Strip casting 으로 만들어진 분말을 이용하는데 이러한 분말로 제조된 영구자석을 'NdFeB 소결영구자석(NdFeB sintered permanent magnet)'이며, Melt spinning 법으로 제조된 분말을 원료로 소성변형 공정을 통해 고이방성 NdFeB 영구자석을 제조하면 '열간-변형 NdFeB 영구자석(Hot deformed NdFeB permanent magnet)'이라고 한다.

'열간-변형 NdFeB 영구자석(Hot deformed NdFeB permanent magnet)'은 등방성 상태의 성형 자석을 소성변형 공정을 통해 나노 결정립 상태의 이방성 자석으로 제조하기 때문에 소성변형이 열간-변형 영구자석을 제조하는데 핵심 기술이다. (주)디아이씨에서는 기존의 한계로 알려진 열간-변형 영구자석의 고보자력 & 고잔류자화 값을 구현하는 열간-변형 영구자석 제조기술을 확보하였으며, 이를 응용하여 radial ring 자석, bar type 열간-변형 영구자석 등을 개발하고자 한다.

최근 Nd 영구자석을 제조하는데 필수가 되는 희토류 원소 가격은 지속적 증가하고 있지만, 탄소중립 및 고효율 전동화 장비의 needs 도 늘어나고 있기 때문에 Nd 영구자석은 더 많은 수요가 예상되며, 중희토류와 희토류를 대체하는 영구자석 개발 핵심기술인 열간-변형 영구자석 기술에 대한 수요는 지속적으로 증가 될 것으로 예상된다. 뿐만 아니라, 자석 제조시 Loss 를 최소화 하면서 소형모터 및 고효율모터에 적용할 수 있는 '열간-변형 NdFeB 영구자석(Hot deformed NdFeB permanent magnet)'은 기존 'NdFeB 소결영구자석(NdFeB sintered permanent magnet)'으로 구현하기 힘든 Nd 영구자석을 제조하는데 좋은 대안이 될 것이다.

희토류 자원 무기화에 대응하기 위한
저희토함유 Nd계 소결자석 개발동향 및 제어방법

배경훈[*], **이상협**, **김동환**, **공군승**

성림첨단산업㈜ 연구소, 대구광역시 달서구 달서대로85길 49

Nd-Fe-B 계 희토 소결 영구자석은 최대에너지적이 가장 높은 자석으로써 모터, 발전기 등 다양한 동력을 변화시키는 기기의 에너지 절감 및 소형화를 위한 필수 소재이다 [1, 2]. 특히, 첨단산업 및 친환경산업의 발전에 따라 모터 사용의 급증함으로써 Nd-Fe-B 소결자석의 글로벌 수요는 매년 연평균 3.7% 증가하고 있다. 중국은 희토류 생산 프로세스 전반에 걸쳐 세계 최대 공급국으로써 최근 세계 각국의 생산량 증가로 중국의 점유율은 축소 수세이지만, 여전히 희토류 세계 생산국의 시장 지배력을 이용한 자원무기화 가능성은 상존하고 있다. 또한, 국내 영구자석 수급의 중국의존도는 93%로 여전히 매우 높은 상황이다. 따라서, 희토류 자원이 무기화되고 Nd-Fe-B 소결자석의 사용량이 급증하고 있는 시점에서 자석의 희토 함량 저감 기술 개발은 절실히 요구되고 있다.

미세 결정립 제어, 입계확산공정 그리고 Ce-La 첨가는 Nd-Fe-B 소결자석의 희토 함량 저감을 위한 효과적인 방법이다 [1,2]. 자석의 미세 결정립 제어 방법은 중희토 함량 첨가 없이 자석의 보자력 특성을 가장 효과적으로 개선할 수 있는 방법이다. 하지만, 결정립 크기가 미세화 됨에 각 공정 마다 고도 기술이 요구되고 있고 산화를 제어하기 어렵다. 특히, 합금 단계부터 시작해서 자성분말의 조분쇄, 미분쇄 공정의 최적화가 요구되고 있으며 결정립이 미세 해질수록 계면의 미세구조 결함이 효과적으로 제어되지 않기 때문에 자기적 특성 향상이 쉽지 않다. 입계확산공정은 자석의 표면에서 내부로 중, 경희토를 확산시켜 결정립 계면에서의 core-shell 미세구조 형성 및 입계상 제어를 통해 희토 첨가량을 최소화하며 자기적 특성을 개선하는 방법이다. 잔류자화 감소를 최소화하면서 보자력을 향상시킬 수 있는 대표적인 공정이지만, 표면에서 내부로 확산되는 물질의 확산 깊이가 제한적이기 때문에 적용할 수 있는 자석 두께 또한 제한된다. 입계확산공정 적용으로 중희토 (Dy, Tb) 사용량이 최소화 되었지만 반대로 경희토 (Nd, Pr) 사용량이 높아지면서 가격 또한 증가되고 있다. 이를 대체하기 위해 상대적으로 매장량이 높은 Ce-La 을 첨가하여 Nd 함량을 저감하는 연구가 활발히 진행되고 있다. 그러나, Ce-La 첨가 자석은 고유자기특성이 낮기 때문에 자기적 특성은 자연스럽게 감소되고 Ce-La 첨가에 따른 새로운 상 형성은 추가 공정 개발 및 최적화가 필요하게 되었다. 그러므로, Nd-Fe-B 계 소결 자석의 희토 함량을 저감 하면서도 높은 자기적 특성을 얻기 위해서는 고도의 기술 개발이 필요하고 첨가 물질 및 해당 공정의 문제점을 잘 이해할 필요가 있다.

본 발표에서는 Nd-Fe-B 소결자석의 희토 함량 저감을 위한 개발 방법 및 연구 동향을 제시하고 각 공정의 장, 단점 규명을 통해 희토 함량이 효과적으로 저감된 고특성 Nd-Fe-B 소결자석 개발 방법과 발전 방안에 대해 고찰하고자 한다.

References

[1] J. Li, H. Sepehri-Amin, T. Sasaki, T. Ohkubo, and K. Hono, Sci. Technol. Adv. Mater, 22, 1, (2021)

[2] S. Liu, J. He, R. V. Ramanujan, Mater. Design, 209, 110004, (2021)

MnBi마그넷과 페라이트 마그넷의 에어컨 Fan모터 적용 성능 비교

나현민[1*], 임현석[1], 이정기[1], 최광기[1], 배석[1], 박예지[2], 이주[2]

[1]LG이노텍
[2]한양대학교

마그넷은 산업용, 가전제품, 자동차 분야 등에 적용 중이며, 최근 전기차 시장 성장과 함께 Nd마그넷 중심으로 사용량이 증가하고 있다. 한편, Nd 마그넷은 희토류 시세에 따른 가격 변동 Risk 및 원재료 공급 국가의 자원 무기화로 인해 희토류 Free 마그넷 사용에 대한 요구는 점차 커지고 있다. 본 연구에서는 에어컨 Fan 모터의 효율 성능을 개선하기 위해 기존 적용된 페라이트 마그넷(FB9H)과 MnBi 마그넷의 성능을 비교하였으며, MnBi 마그넷 적용 시 동일 모터 크기에서 전류 저감에 따른 동손 저감으로 3.74% 효율 증가를 확인하였다. MnBi 마그넷 사용 시 페라이트 마그넷 대비 영구자석의 사용량 또는 전동기 사이즈 저감도 가능할 것으로 판단된다.

Table 1. 페라이트 마그넷(FB9H)과 MnBi 마그넷 성능 비교

항목		FB9H	MnBi	단위
마그넷 성능	(BH)max	4.4	12.0	MGOe
	Br	4.3	7.1	kG
	Hc	5.0	7.1	kOe
모터 크기	외경	44.0	44.0	mm
	높이	50.0	50.0	mm
모터 중량	마그넷 중량	150.5	261.1	g
	코어 중량	819.6	819.6	g
	구리 중량	950.8	903.0	g
입력전류		23.0	14.9	Arms
정격출력		303	303	W
정격토크		1.5	1.5	Nm
동손		31.74	13.32	W
철손		11.54	15.53	W
효율		87.50	91.24	%
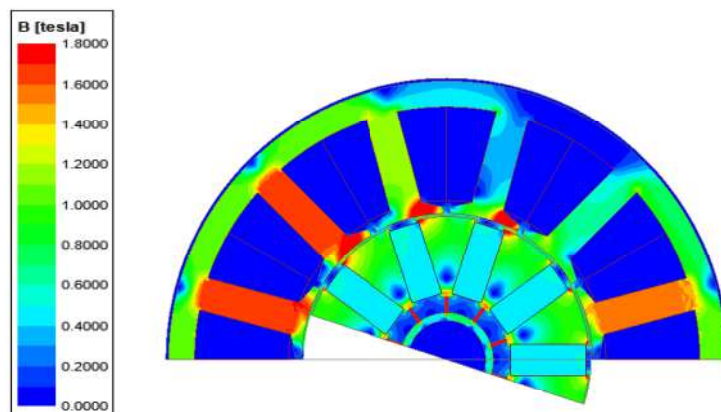
Fig. 1. MnBi 마그넷의 부하 시 자속 포화도

마그네틱 커플링 Outer Part 구조의
영구자석 누설에 따른 출력 저하 분석

윤명환*, 김지용, 이기덕, 유세현, 이정종

한국전자기술연구원 지능메카트로닉스 연구센터

마그네틱 커플링은 비접촉식 동력 전달 장치로써 화학공정용 펌프에 많이 적용된다. Inner Part와 Outer Part로 구조가 나뉘게 되는데 Inner Part는 임펠러와 연결되고 Outer Part는 외부 동력원인 유도기에 연결된다. 아래 그림 1과 같이 Outer Part는 영구자석과 코어로 이루어지는데, 바깥쪽 코어는 아래 그림 구조에서 좌측으로 연장되어 유도기의 축과 이어진다. 여기서 공극 즉 영구자석간 거리가 커질수록 영구자석에서 발생한 자속이 공극으로 흐르지 못하고 옆 코어로 누설되게 된다. 따라서 출력 저하, 토크 감소를 방지하기 위해서는 영구자석과 코어 그리고 공극 길이에 따른 자기저항 관계를 분석하여 누설을 최소화하는 안이 필요하다. 본 논문에서는 마그네틱 커플링의 구조에 따른 누설 분석 및 개선안에 대해 분석한다.
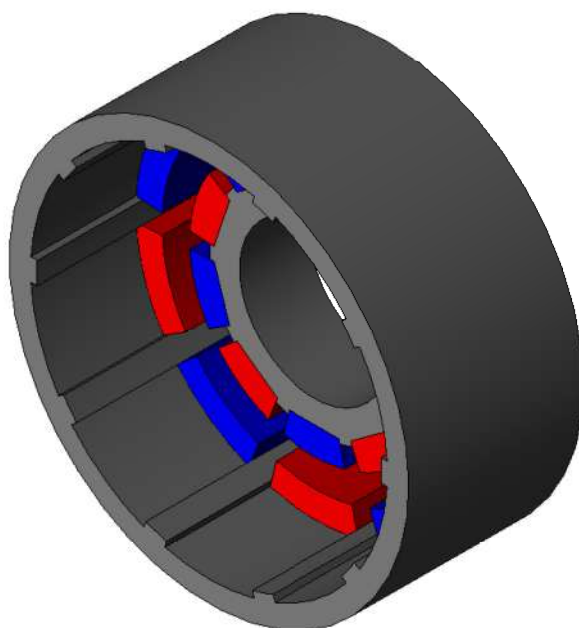
그림 1. 마그네틱 커플링 구조

Analysis of electromagnetic field characteristics considering thermal characteristics to establish an optimized design model for 15kW-class motors

Insoo Song[1*], Eunsil Han[1], Myeonggyun Choi[2], Yunyong Choi[2]

[1]MOASOFTWARE Korea, Seoul 05770
[2]DRIVETECH Korea, Bucheon 14558

This paper discusses the change in thermal analysis characteristics according to the size reduction of a 15kW class motor with a water-cooled structure. When designing an electric motor, equation (1) is related to output power and torque.

$$T = \frac{1}{4} D^2 L_{stk} [m^2 / T] \qquad (1)$$

The heating area of the motor varied according to the change of the electromagnetic field analysis model. In other words, the saturation level can vary according to the rotor shape. To analyze the effect of the thermal conditions, the analysis is performed by applying the thermal equivalent circuit technique as shown in Figure 1. The housing is spiral structure and it is analyzed by a two-way method. Thermal solution is performed by inputting a loss value based on the electromagnetic field analysis result. Also, the compensating loop for temperature and loss is performed. The effect of electromagnetic characteristic changes on thermal analysis is analyzed as shown in Fig 2. The operating point is defined as illustrated in Fig. 3 to compare the temperature conditions and characteristics according to the electromagnetic field analysis.
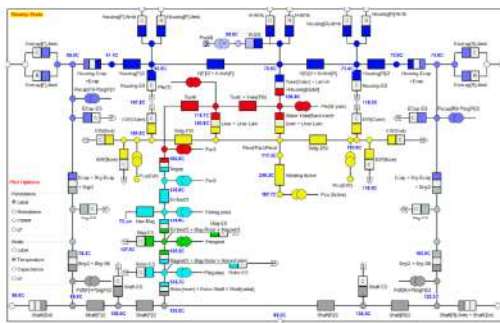
Figure 1. 15kW Motor Thermal Equivalent Circuit
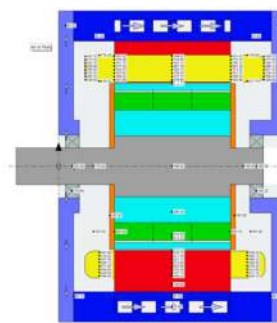
Figure 2. Thermal Analysis Results
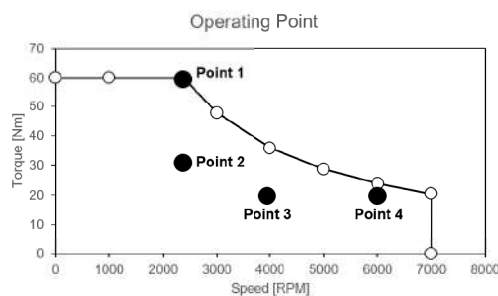
Figure 3. Operating Point (Point 1 ~ Point 4)

115kW급 HEV용 매입형 영구자석 동기기의
PWM 전류 고조파를 고려한 철손 및 AC동손 분석

김현수[1]*, 박진철[2], 배예나[1], 유준열[2], 임명섭[1]†

[1]Department of Automotive Engineering (Automotive-Computer Convergence), Hanyang University, Korea
[2]Department of Automotive Engineering, Hanyang University, Korea

최근 국제 정세로 인한 화석연료의 공급불안정과 세계 각국의 환경 규제로 인해 Hybrid Electric Vehicle (HEV), Electric Vehicle(EV) 등 친환경차량의 수요가 증가하고 있다. 친환경차량의 구동모터는 제한된 배터리 용량내에서 구동하고, 넓은 운전영역으로 인해 고조파를 반영한 모터의 효율을 정확하게 예측하는 것이 중요하다. 따라서 모터 효율의 정확성을 향상시키기 위해서는 인버터의 스위칭으로 인한 Pulse Width Modulation (PWM) 전류 고조파를 고려한 모터의 손실을 분석해야 한다. 모터의 손실 중 철손은 히스테리시스 현상과 와전류로 인해 주파수의 함수이고, Alternating Current(AC) 동손은 표피효과와 근접효과로 인해서 고조파에 영향을 받는다. 따라서 본 논문에서는 정현파 전류와 PWM 고조파를 고려한 전류의 철손 및 AC 동손을 분석한다. 대상모델은 16극24슬롯 HEV용 Interior Permanent Magnet Synchronous Motor(IPMSM)이다.

PWM고조파를 고려한 철손 및 AC동손 해석 프로세스는 Fig.1에 제시하였다. 우선 정현파 전류 기준으로 대상모터의 전류와 전류 위상각에 따른 인덕턴스를 계산하였다. 그리고 정현파와 고조파에 의한 포화도는 동일하다고 가정하여 포화에 따른 인덕턴스의 변화를 고려하기 위해 앞서 계산된 인덕턴스를 인버터 시뮬레이션에 반영하여 부하 포인트의 전류를 계산하였다. 그 이후, 대상 모터의 Finite Element Analysis(FEA) 모델에 계산된 전류를 인가하여 철손 및 AC동손을 계산했다. 철손해석 시에는 특정 고주파 차수를 고려하여 공극 mesh
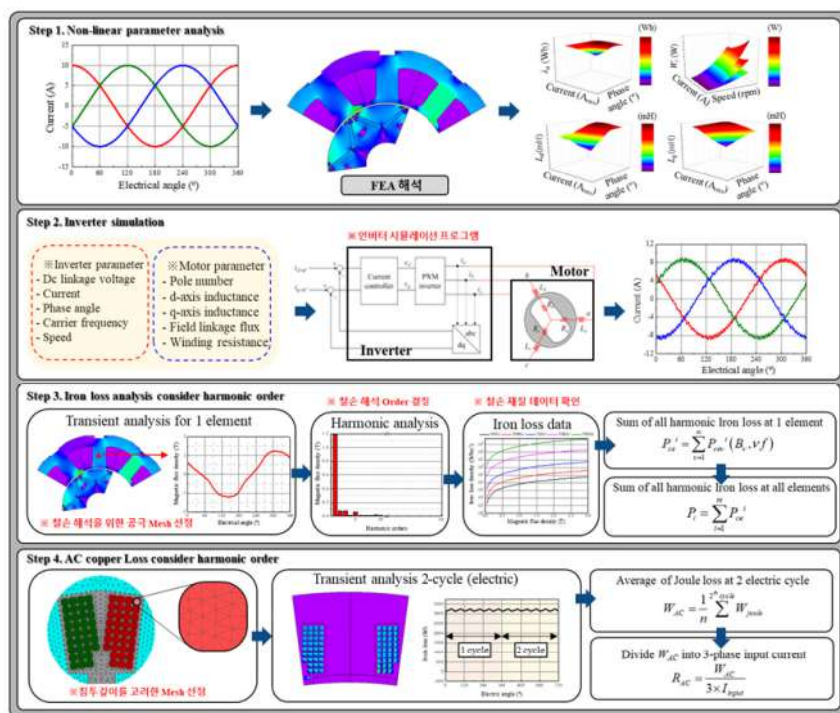
Fig. 1. PWM 전류 고조파를 반영한 철손 및 AC 동손 해석 프로세스
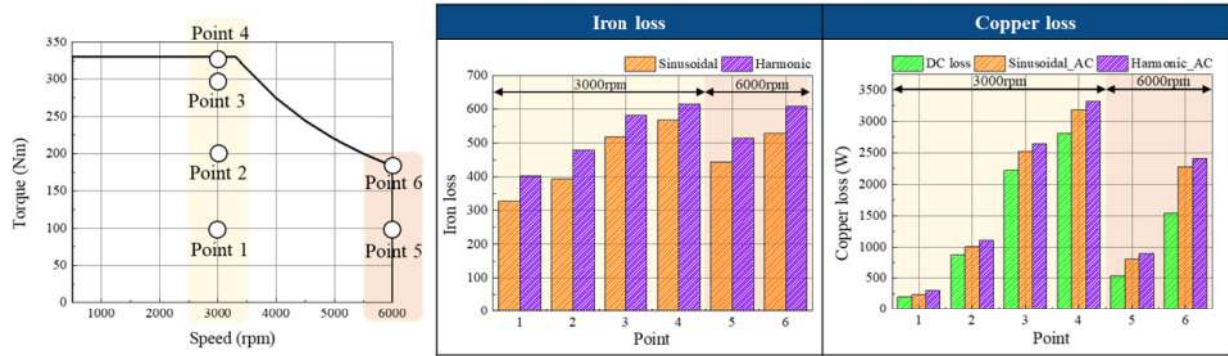
Fig. 2. 정현파 전류 및 PWM고조파를 반영한 전류의 철손 및 AC동손 비교

를 선정하였고, AC동손 해석시에는 표피효과의 침투 깊이를 고려하여 mesh를 선정하였다. 그리고 정현파 전류를 인가한 철손과 AC동손도 동일한 mesh를 이용하여 계산하였다. Fig.2에 정현파 전류와 PWM 고조파를 반영한 전류의 철손과 AC동손 해석결과를 제시하였다. PWM 전류 고조파로 인해 철손 및 AC동손 모두 증가함을 확인했다. 따라서 모터의 효율을 정확하게 계산하기 위해서는 PWM 전류 고조파를 반영해야 한다.

1kW급 로봇용 SPMSM의 효율 개선을 위한 수식 기반 모터 설계

배예나[1*], 박진철[2], 김현수[1], 유준열[2], 임명섭[1†]

[1]Department of Automotive Engineering (Automotive-Computer Convergence), Hanyang University, Korea
[2]Department of Automotive Engineering, Hanyang University, Korea

최근 협동 로봇이 낮은 인건비와 높은 생산성으로 제조산업 전 분야에 걸쳐 빠르게 보급되는 추세이다. 이에 협동 로봇에 적용되는 Surface Permanent Magnet Synchronous Motor(SPMSM)의 고효율화 및 소형화를 통한 공정 소비전력 절감에 관심이 대두되고 있다. SPMSM의 고효율 및 고출력 설계를 위해서는 설계 단계에서 적절히 모터 사이즈 결정하고 정확한 효율 예측하는 것이 중요하다. 설계된 모터의 효율은 Finite Element Analysis(FEA)를 이용해 파악할 수 있지만, 적절한 사이즈 선정을 위해 FEA를 이용할 경우 형상 변화에 따라 모델링 해야 하므로 오랜 시간이 소요된다. 이에 본 논문에서는 모터 형상 변화 비율을 이용해 사이즈 변화 시의 모터 파라미터를 수식적으로 계산하고 효율을 빠르게 예측하는 방법을 제시한다.

Fig. 1은 본 논문에 적용된 1kW급 로봇용 SPMSM의 초기 모델 형상을 나타낸다. 그림과 같이 모터 사이즈는 고정자 외경(Ds), 회전자 외경(Dr), 적층 길이(Lstk)를 변수로 결정된다. Fig. 2는 사이즈 변화 비율을 이용해
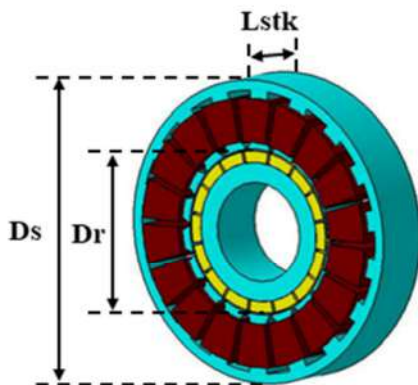
Fig. 1. 초기 모델 형상

Fig. 2. 고정자 권선 수 계산 예시
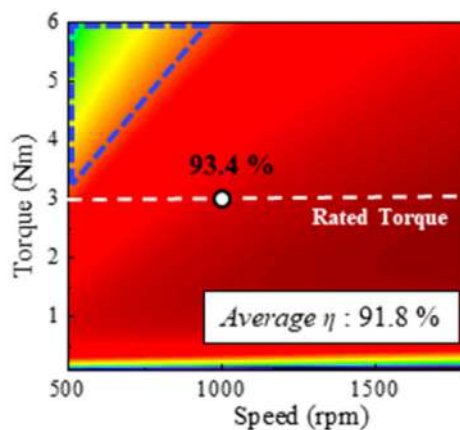
Fig. 3. 초기 모델 효율 맵
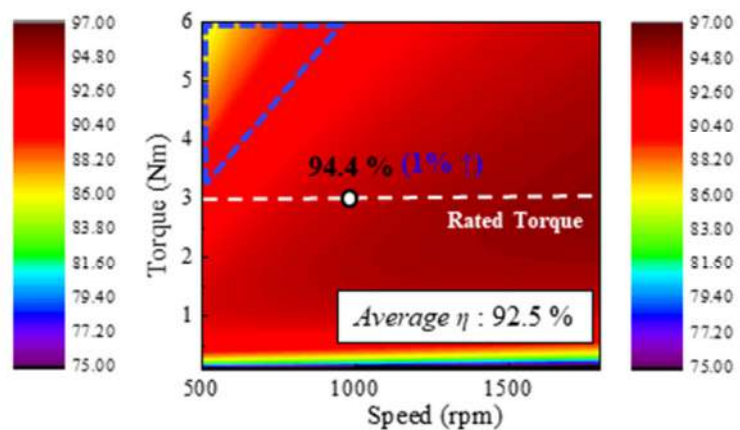
Fig. 4. 개선 모델 효율 맵

수정된 모터의 고정자 권선 수(Ns)를 계산하는 과정을 나타낸다. 이처럼 모터 파라미터는 Ds, Dr, Lstk에 대한 함수로 표현할 수 있다. 따라서 수정된 모델의 인덕턴스, 권선 저항, 철손 저항과 같은 전기 파라미터는 초기 모델의 전기 파라미터를 사이즈 변화 비율에 따라 비례식으로 계산하여 예측할 수 있다. 이때 사이즈 변화 전후의 역기전력, 무부하 공극 자속밀도, 치·요크 폭 자속밀도, 점적률, 샤프트 외경은 동일하다고 가정하였다.

본 논문에서는 모터 사이즈 변화 시 고정자 외경(Ds)은 일정한 조건에서 회전자 외경(Dr) 및 적층 길이 (Lstk)가 변화하는 경우에 대해 검토하였다. 이를 위해 초기 모델의 전기 파라미터를 FEA을 통해 계산하였고, 회전자 외경 및 적층 길이 변화에 따른 파라미터 변화를 수식적으로 도출하였다. 최종적으로 모터의 전압 방정식을 이용해 변화된 파라미터에 따른 효율을 예측하였다. 모터 효율은 입력된 전력과 발생한 손실을 이용해 계산하였으며, 동손, 철손, 베어링 마찰 및 풍손에 의한 기계손을 고려하였다. 이때 모터 입력 전력은 사이즈 변화 전후에 동일 정격 토크를 만족시키기 위한 최소 크기의 전기자 전류를 계산해 적용하였다.

Fig. 3과 Fig. 4는 각각 FEA를 이용해 파악한 초기 모델과 개선 모델의 효율맵을 나타내며, 초기 모델 대비 개선 모델의 전 영역 평균 효율 및 정격 운전점에서의 효율이 향상됨을 확인하였다.

Symposium 4

'Magnetic Sensors and Micro–Devices'
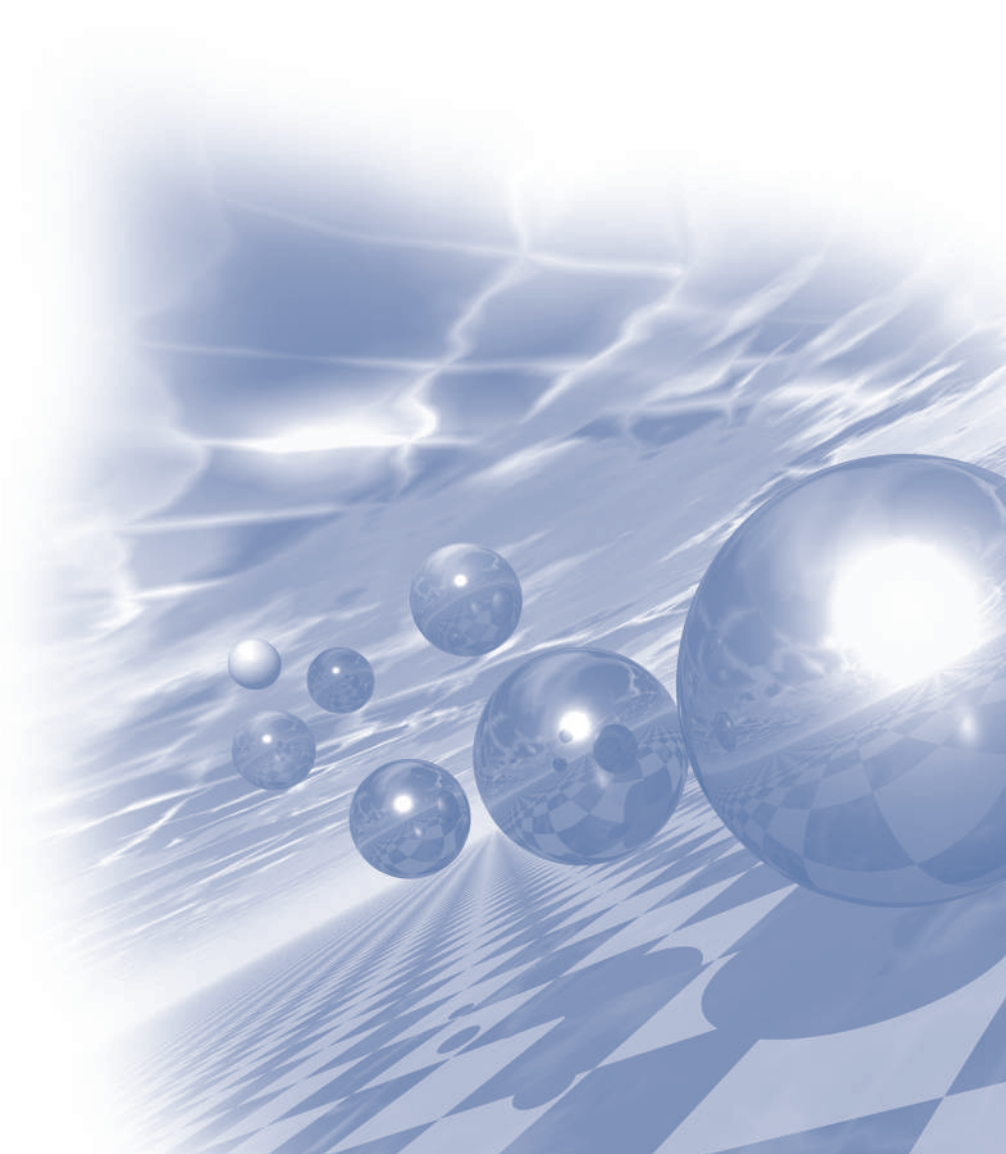
높은 열 안정성과 자기장 감지 성능을 갖춘 평면 홀 자기저항센서의 발전과 핵심기술

임병화*, 전태형, 전창엽, 김미진, 김철기

DGIST, Korea

나노/마이크로 기술의 발전으로 인해 저장 매체와 그 외의 응용 분야에서 자기저항 센서가 빠르게 채택되었습니다. 자기저항센서는 사물 인터넷(IoT), 모바일 장치, 우주, 항공 분야 만이 아니라 스마트 홈, 환경, 건강 분야 등 스마트 감지 성능이 필요한 첨단 응용 분야의 요구 사항을 충족하는 높은 성능을 가지고 있습니다. 그 중에서도 평면 홀 효과 기반 자기저항 센서는 초 저자기장 감지에 적합한 높은 감도와 낮은 잡음 특성을 넓은 온도 범위에 적용 가능합니다. 그리고 간단한 구조로 인해 비용 효율적이면서 용도에 맞춰 제작하거나 소형화를 하기 용이하여 통합이 쉽기 때문에 다양한 새로운 응용 분야에서 활용할 수 있는 유망한 센서입니다. 최근, 평면 홀 자기저항 센서와 마이크로 유체 채널을 결합하여 국소화 된 자기장에 대한 높은 감지성능을 보여준 연구가 보고되었습니다. 이러한 특성은 평면 홀 자기센서가 상온에서 몇 pT수준의 분해능을 요구하는 POS(Point-of-Care) 기술에도 응용될 수 있음을 보여줍니다. 이번 논의를 통해 우리는 평면 홀 자기센서 개발의 역사와 최근 몇몇 응용 분야에서 극적인 발전에 대해 이야기하고, 센서 재료의 특성 요구 사항과 설계 아키텍처, 잡음 감소기술 및 감지기능에 대해 이야기할 것입니다.

마이크로 직교플럭스게이트 센서의 개발

김경원[1,2*], 이형만[1], 홍성민[1], 이대성[1], 신광호[3], 임상호[2*]

[1]한국전자기술연구원 스마트 센서 연구센터
[2]고려대학교 신소재공학과
[3]경성대학교 정보통신공학과

센서 중 한 종류인 자기 센서는 스마트폰, 자동차, 가전, 국방 등 여러 분야에서 사용되고 있고, 다양한 응용이 계속 제안됨에 따라 시장의 규모가 계속 증가할 것으로 예측되는 고성장 산업이다. 본 논문에서는 마이크로 직교플럭스게이트 센서의 개발 및 관련 연구내용들을 보고한다. 현재 개발 중인 직교플럭스게이트 타입의 센서는 자성체의 코어와 픽업코일로써 이루어져 있으며, 자성체의 코어에 직접 여자전류를 인가하여 유도되는 자계로써 자성체 코어에 자계를 인가한다. 자성체의 코어에 여자 전류에 의한 자계와 직교하는 외부자계가 인가 시 자성체 코어의 자화는 두 축을 두고 진동하게 되며 이를 픽업 코일로 검출한다. 따라서 센서의 감도 및 분해능은 자성체 코어의 자기특성에 크게 의존 하며 자성체 코어의 보자력을 줄일수록 센서의 분해능은 향상된다. 본 연구에서는 센서의 코어로써 Co계 아몰퍼스 박막을 마그네트론 스퍼터링으로 증착하였으며 이때 박막의 보자력은 0.15 Oe 이하로 확인되었다. 그리고 소모전력을 절감하기 위해 자성체 코어는 FM/NM/FM 과 같은 다층막 구조가 사용되었으며 이때 NM은 전도율이 좋은 Cu를 사용하였고, 자성체 코어에 유도되는 자계 방향으로 자기열처리를 하여 유도이방성을 부여하였다. 그리고 형상 별 반자화 및 형상이방성을 조사하여 이를 최적화하였다. 본 논문에서 제안되는 직교플럭스게이트 센서의 구조는 자기임피던스 센서의 구조와 동일하며 박막의 두께를 최적화함에 따라 자기임피던스 효과도 추가적으로 얻을 수 있을 것으로 기대된다.

면적형 홀센서 배열을 사용한 누설 자속 측정

박덕근[1,2*], 신정우[2], 이진이[3]

[1]한국원자력연구원
[2]주식회사 아이피트
[3]조선대학교

산업현장에서 사용하는 배관에 자성 비파괴 검사를 적용할 때에는 검사 대상에 자기장을 인가하는데, 검사 대상에 결함이 있는 경우 결함부에서 자속 누설이 발생한다. 넓은 범위의 자속 누설를 가진 시험편을 측정하기 위해선, 동시에 대면적을 측정할 수 있도록 면적형으로 센서가 배열된 탐촉자가 필요하다. 본 연구에서는 다채널 홀센서로 구성된 배관 내삽용 면적형 탐촉자를 제작했다. 연구에 사용된 홀센서는 입력과 출력을 위해 센서 하나 당 4개의 단자가 필요한데 이를 배열로 구성할 경우 필요한 도선의 수량이 많아지고 이로 인해 도선 다발의 두께가 두꺼워지게 된다. 또한 각 센서의 신호를 수집할 DAQ가 많이 필요하며 이는 장비 제작 비용 증가로 이어진다. 이런 문제를 해결하고자 홀센서 배열에서 각 열의 신호 단자를 병렬로 연결하였고, 각 행의 전원 단자를 병렬로 연결한 뒤 멀티플렉서와 FET로 각 행마다 전원을 순차적으로 입력시키는 방식을 사용해 필요한 도선과 DAQ의 수량을 줄였다. 이렇게 제작된 면적형 탐촉자는 배관 또는 금속 평판의 용접부 검사나 항공기 리벳 검사 등 다양한 분야의 안전 검사에 적용 가능할 것으로 예상된다.
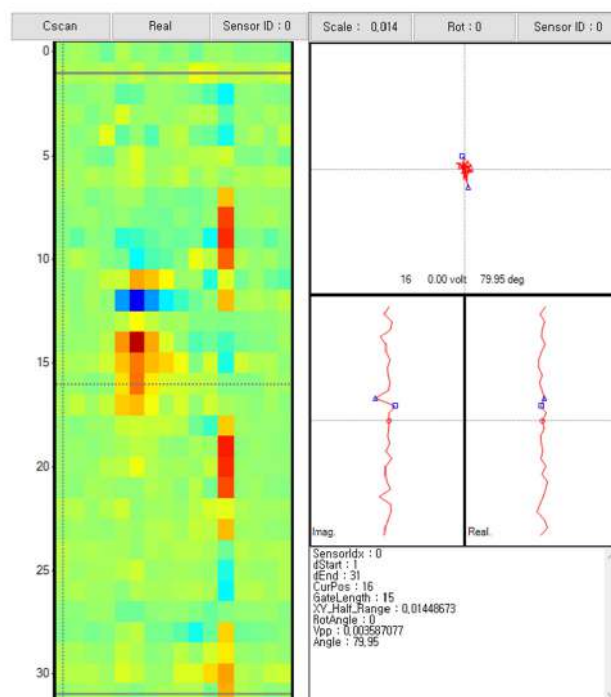
Fig. 1. 면적형 홀센서 배열을 사용한 누설 자속 측정 결과

Application of Magnetoplethysmogram Sensor as the Measuring Device of Cuffless Blood Pressure and Peripheral Blood Flow Velocity

Sang-Suk Lee[*], Jong-Gu Choi and Mahbub Hasan

Department of Digital Healthcare Engineering, Sangji University, Wonju 220-702, Korea

A wrist-wearable MPG(Magnetoplethysmogram) sensor equipped with a magnetic field-sensing semiconductor Hall device and a permanent magnet attached to silicon housing at the centre of the radial artery was developed for BP(blood pressure) monitoring. This MPG sensor can acquire precise BP and pulse rate values by using a cuffless device containing a hardware and software system for measuring radial artery pulse waves transformed into voltage signals. The systolic and diastolic areas and the systolic and notch amplitudes of the radial artery pulse wave were used simultaneously for obtaining systolic and diastolic BP. The clinical tests for three human subjects (normal BP, hypotension, and hypertension) yielded precise BP similar to the BP values measured using conventional devices. Two estimated BP equations obtained using the cuffless arterial pulsimeter during 5 s show the analysis of the pulse wave measured during the testing of the arterial pulsimeter. Based on the theoretical background, we developed a MPG sensor for BP measurements, which enables measuring the brachial pressure and the CAP(central arterial pressure. Classifying BP in terms of hypertension, normal blood pressure, and
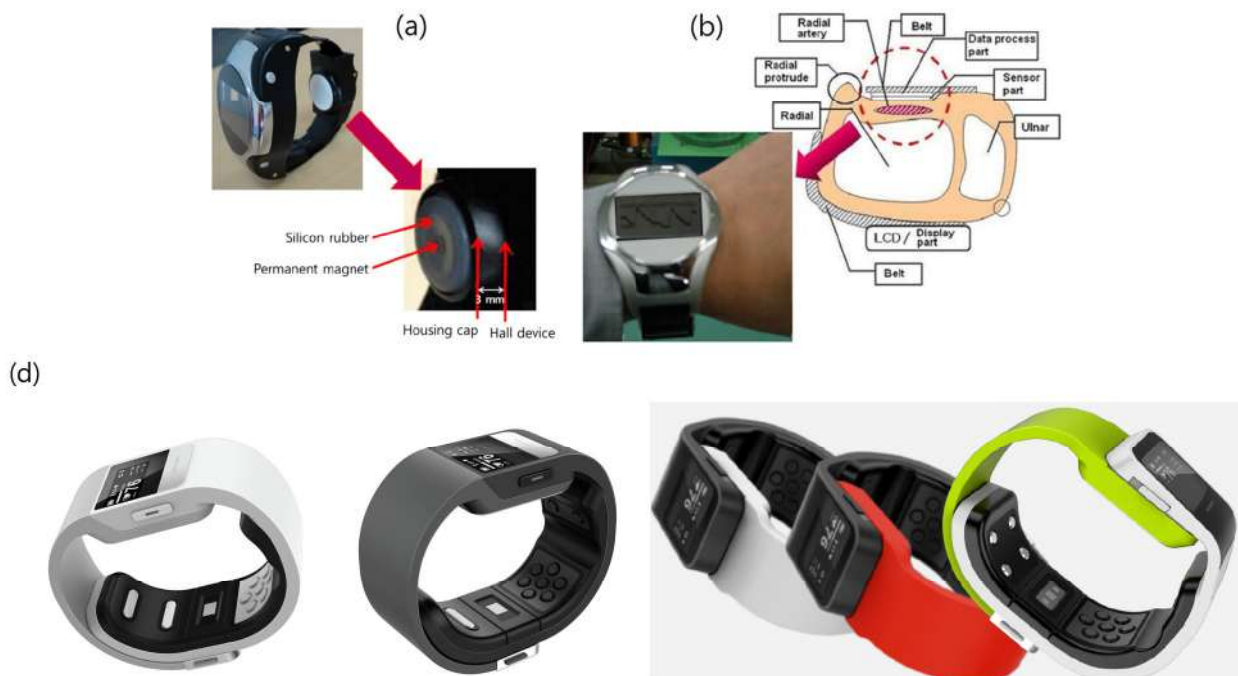
Fig. 1. Photographs of (a) a mockup radial artery used for clinical testing and (b) a fully functioning wrist-wearable MPG pulsimeter. Schematic shows the cross-section with a detailed description of the device's components. (c) Several designs and proto-type of a wrist-wearable smart watch-type band for accurate BP measurement.

hypotension is not efficient for preventing a cerebral vascular disease or a cardiovascular disease. Therefore, accurate self-adjustment is recognized as an essential and fundamental factor of any successful BP therapy. One important advantage of the proposed MPG sensor is its portability, which allows using it as a wrist-wearable smart watch-type band for accurate BP measurement, as shown in Fig. 1. This medical device can also yield data that are usually obtained by performing complicated procedures, such as for measuring the brachial pressure and the CAP, allowing to efficiently obtain precise BP.

To measure the PBFV(peripheral blood flow velocity), the radial artery MPG sensor was simultaneously connected to the PPG. Analysis and comparison of two pulse waves' data have been obtained from a clinical test of forty subjects of 20 ages. The blood velocity simultaneously measured from an RAP(radial artery pulse) wave and PPG(photoplethysmography) was had an average value of 0.27-0.50 m/s, as shown in Fig. 2. The PPWV(peripheral pulse wave velocity) had a wider scope, with an average value of 1.25-1.52 m/s. The new method provided more precise values of PWV(pulse wave velocity) than the conventional biomedical signal monitoring system, implying that the data measured by this oriental medical diagnosis apparatus may be clinically useful in the future. Both PPWV and PBFV are important measurements that may help normal people understand their health status and motivate them to take better care of themselves. Predicting a blood vessel's elasticity from the analysis of PPWV may be useful for developing an oriental-western diagnostic medical signal device for the ubiquitous health care system in the future. The developed MPG sensor may be useful for developing a biomedical signal storage device for mobile U-health applications.
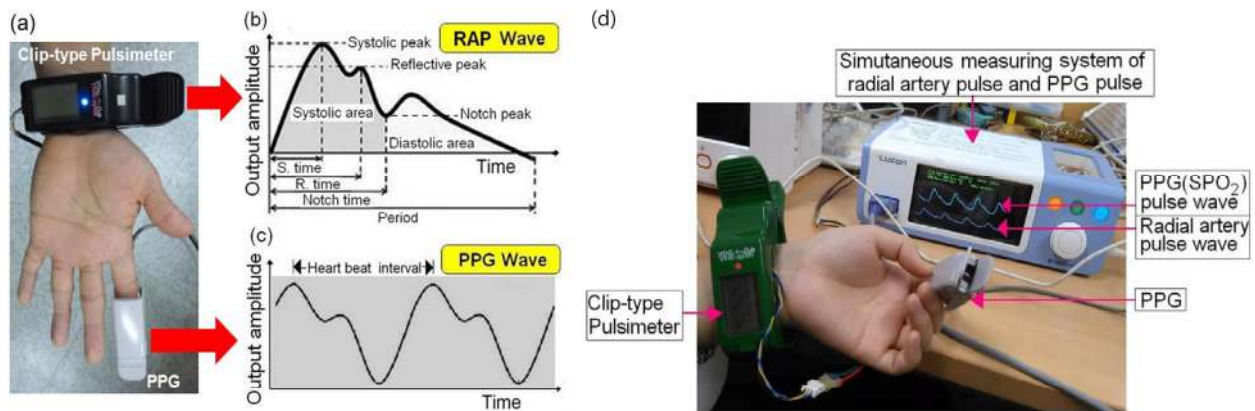
Fig. 2. (a) A real feature of two simultaneous measuring devices consisted of one MPG sensor in the wrist and one PPG in the index finger. (b) The major parameters, such as the period of pulse wave, the systolic time, the reflective time, and the notch time. (c) The typical waveforms of PPG. (d) RAP graph and PPG signals obtained from the simultaneous measurements by the MPG sensor and PPG mounted on the wrist and fingertip of the left hand. Here, $\Delta\tau_i$ is the time interval measured from ith phase difference of the two pulse waveforms.

References

[1] W. H. Lee, Y. H. Rho, S. S. Hyeon, J. B. Song, and S. S. Lee, Insights in Blood Pressure 2(2), 1-8 (2016).

[2] K. H. Kim and S. S. Lee, Journal of Magnetics 20(1), 47-51 (2015).

[3] D. H. Nam, W. B. Lee, Y. S. Hong, and S. S. Lee, Sensors 13(4), 4714-4723(2013).

자기 통신을 위한 자기센서-기반 수신기의 설계 및 분석

김장열*, 이현준, 이재호, 오정훈, 조인귀

한국전자통신연구원, 전파원천기술연구실

자기 센서는 무선통신 분야에서 수신기의 수신 소자로서 활발히 연구되고 있다 [1-4]. 특히 자기 센서를 수신소자로 활용하여 대기, 지중, 및 수중 환경의 자기장 통신에 응용되는 연구들이 진행되고 있다 [5], [6]. 이러한 자기 센서는 투자율이 높은 자성 물질을 재료로 사용하기 때문에 pT/Hz$^{1/2}$ 수준의 초고감도(ultra-high sensitivity) 특성을 갖는 자기 센서를 구현할 수 있다. 따라서 높은 감도 특성을 갖는 자기 센서는 미약한 자기장 신호를 감지할 수 있어 통신 거리를 비약적으로 증가시킬 수 있다. 본 연구에서는 초고감도 특성을 갖는 거대자기임피던스(giant magnetoimpedance) 센서와 자기 인덕션(magnetic induction) 센서를 수신 소자로 선정 하여 이를 분석하였고, 자기장 통신에 응용 하기위해 자기센서-기반 수신기 2종을 설계 및 제작하여 실험적 검증을 수행하고 분석하였다. 100 kHz 이하의 주파수 대역에서 수중 및 지중환경에서 구현된 자기센서-기반 수신기를 이용한 통신 실험을 통해 변조 및 복조 결과를 확인하였다. 결과적으로, 제안된 자기센서-기반 수신 기의 자기장 통신 응용 가능성을 확인하였다.

References

[1] J.Y. Kim et al, "A novel experimental approach to the applicability of high-sensitivity giant magneto-impedance sensors in magnetic field communication", IEEE Access, vol. 8, pp. 193091-193101, 2020.

[2] K. Kim et al, "Giant magnetoimpedance receiver with a double-superheterodyne topology for magnetic communication," IEEE Access, vol. 9, pp. 82903-82908, 2021.

[3] Z. Sun et al, "Underground wireless communication using magnetic induction", in Proc. IEEE Int. Conf. Commun., pp. 1-5, Jun. 2009.

[4] H. Guo et al, "Practical design and implementation of metamaterial-enhanced magnetic induction communication," IEEE Access., vol. 5, pp. 17213–17229, 2017.

[5] T. E. Abrudan et al, "Impact of rocks and minerals on underground magneto-inductive communication and localization," IEEE Access, vol. 4, pp. 3999-4010, 2016.

[6] M. C. Domingo, "Magnetic induction for underwater wireless communication networks," IEEE. Trans. Antennas Propag., vol. 60, no. 6, pp. 2929-2939, Jun. 2012.

자기센서 맞춤형 증폭 회로 설계 및 성능 분석

윤석수[1*], 김동영[1], 전태형[2]
[1]안동대학교 물리학과
[2]대구경북과학기술원, 화학물리학과

자기센서 소자는 다이나믹 레인지를 맞추거나 AD 변환기와 연결하기 위해 증폭 회로를 필요로 한다. 그런데 증폭 회로는 추가적인 노이즈를 발생하여 자기 센서의 분해능을 나쁘게 할 수 있으므로 자기센서 소자의 자기장 분해능을 최대한 발휘하기 위해서 증폭 회로를 맞춤형으로 설계하는 것이 요구된다. 본 발표에서는 Planar Hall Magneto-Resistance (PHMR) 자기센서 맞춤형으로 증폭 회로를 설계할 시 앰프의 노이즈를 최소화하기 위해 고려해야할 요소와 센서의 1/f 노이즈를 제거할 수 있는 일반적인 방법에 대해 소개한다. 그리고 실제 설계 및 제작한 Instrumentational Amplifier IC 기반 증폭 회로와 Dual matched bipolar transistor 기반 증폭 회로의 동작 과정과 노이즈 스펙트럼 측정결과를 제시한다. PHMR 자기 센서 소자에 제작한 증폭 회로를 연결하여 지구자기장을 검출하는 성능도 제시한다. 마지막으로 자기장 분해능을 더 향상하기 위해 PHMR 자기 센서 소자 측면과 증폭 회로 측면에서 향후 개선되어야 할 사항에 대해서도 논의한다.

Circuit design optimization for PHR sensor module targeting for highly integrated PCB analysis

Nam Young Lee[1*], Joong Hong Ji[2] and Dae Sung Lee[3]

[1]DNJTECH, 503, 65, Dongpyeon-ro 13beon-gil, Dongan-gu, Anyang-si, Gyeonggi-do, Korea
[2]MINDSEYE, 502, 65, Dongpyeon-ro 13beon-gil, Dongan-gu, Anyang-si, Gyeonggi-do, Korea
[3]Korea Electronics Technology Institute, 68, Yatap-dong, Bundang-gu, Seongnam-si, Gyeonggi-do, Korea

Recent years, we developed a high-sensitivity Planar Hall Resistance (PHR) sensor targeting for the application on highly integrated PCBs. The PHR sensor was composed of Wheatstone bridge with 4 symmetric magnetic resistance (MR) sensors, which processed to have a tri-layer structure of NiFe/Cu/IrMn. When magnetic field is applied, some mismatch occurs in the symmetric Wheatstone bridge and the sensor output signal is generated in the range of mV.

We designed an instrumental amplifier with electrical chopping function to amplify the signal and remove 1/f noise. The developed magnetic sensor showed good enough features of an ultra-small size of below 100um, 10nT magnetic field resolution, 1mA current resolution, and 1MHz operating frequency, to be applied for the PCBs.

During its characterization, however, we experienced a monotonously changing output noise in the long-time range of a few ten minutes. (Fig.1) Although the amplitude and the period of the noise differ from sample to sample, they all show the same pattern on which the output signal gradually drift in time and become saturated in a few ten minutes. This noise was analyzed that the temperature mismatch occurred inside the Wheatstone bridge and the signal drift occurred in the long-time range.

In this report, we will introduce the basic circuit operation of the PHR sensor module, and the physical modeling of the thermal drift noise. It will be presented that the drift noise can be significantly removed by adding the pulse width modulation technique to the circuit. And we will propose several other solutions of reducing the noise by tuning PHR sensor layout, manufacturing processes and electric operation conditions
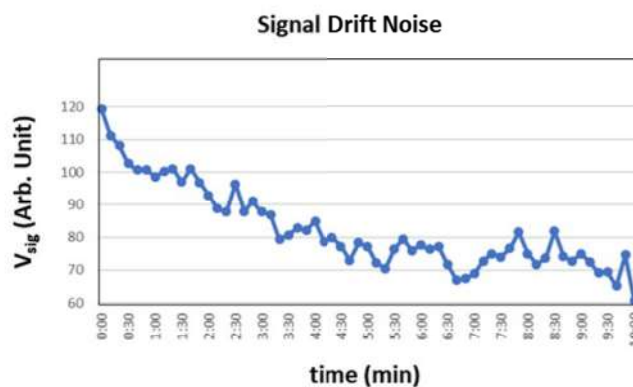
Fig. 1. Typical signal drift noise. Output signal of PHR sensor drifts in a few 10 minutes.

자기센서 성능 향상을 위한 전자회로 설계

손대락*

㈜센서피아, 유성구, 대전, 대한민국

자기센서를 개발·제작하기 위해서는 자기센서를 전기적으로 구동을 하여야 되고, 센서로부터 나오는 신호는 적절한 아날로그 신호처리를 한 후에 ADC(Analog to Digital Converter)를 사용 digital 신호로 변환시킨 후 MCU(Micro-Controller Unit)에서 센서의 offset과 gain을 연산하고 필요한 경우 digital signal processing을 한 후 통신포트로 데이터를 출력시키는 방법을 많이 사용되고 있다.

센서를 구동시키기 위해서는 센서의 종류에 따라서 다르지만 일반적으로 직류나 교류로
1. 일정한 전압으로 구동하는 방법
2. 일정한 전류로 구동하는 방법이 있다.

전력소비를 감소시키기 위해서는 반도체 S/W를 사용 전력을 짧은 시간만 공급하는 방식을 사용하기도 한다. 특히 전력을 공급받지 못하는 센서의 경우 전력공급시간의 duty cycle에 따라서 구동시간이 결정된다.

센서의 전자회로 설계 시 고려하여야 될 전자부품의 종류가 매우 다양하고 각각의 전자부품마다 자기고 있는 변수가 매우 다양하기 때문에 전자회로를 설계하는데 많은 경험이 필요한 경우가 발생한다.

많이 사용되는 전자부품의 주요 특성을 보면
-연산증폭기 : noise, frequency band width, offset and offset drift, supply voltage and current,
-MOSFET S/W : on resistance, maximum current.
-MCU : bit, memory size, clock speed, Internal ADC and DAC
-ADC : bit resolution, conversion speed 등이 있다.

Fig. 1은 한 예로 Pulse Eddy Current NDT를 설계한 장치의 개략도를 보여주고 있다. 자기장 발생코일에 펄스전류를 공급하기 위하여 Embedded controller의 I/O port(TP)를 사용 MOSFET S/W를 구동시키고, 공급되는 전력공급장치의 전력소비도 줄이기 위하여 I/O port(PSON)을 사용 측정이 필요한 시간에만 구동할 수 있게 하였다. 또한 탐지 probe의 search coil에서 유도되는 기전력으로부터 자속밀도를 구하기 위하여 전자적분기를 적용하였는데 적분기를 reset하기 위한 switch pulse(TR)도 발생시켰다.

탐지 probe의 솔레노이드에 공급되는 전류를 측정하기 위한 current shunt양단의, Hall센서신호, MEMS flux-gate신호 및 적분기 신호는 24 bit ADC를 Embedded controller로 SPI통신으로 digital data로 받아서 센서의 교정 값을 연산한 후에 RS-232C 통신으로 PC에 출력할 수 있게 하였다.
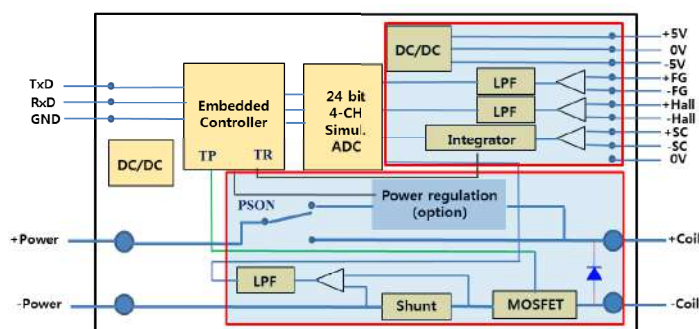
Fig. 1. Diagram of electronics block for pulse current eddy current NDT

Symposium 1

'Quantum Magnetism'
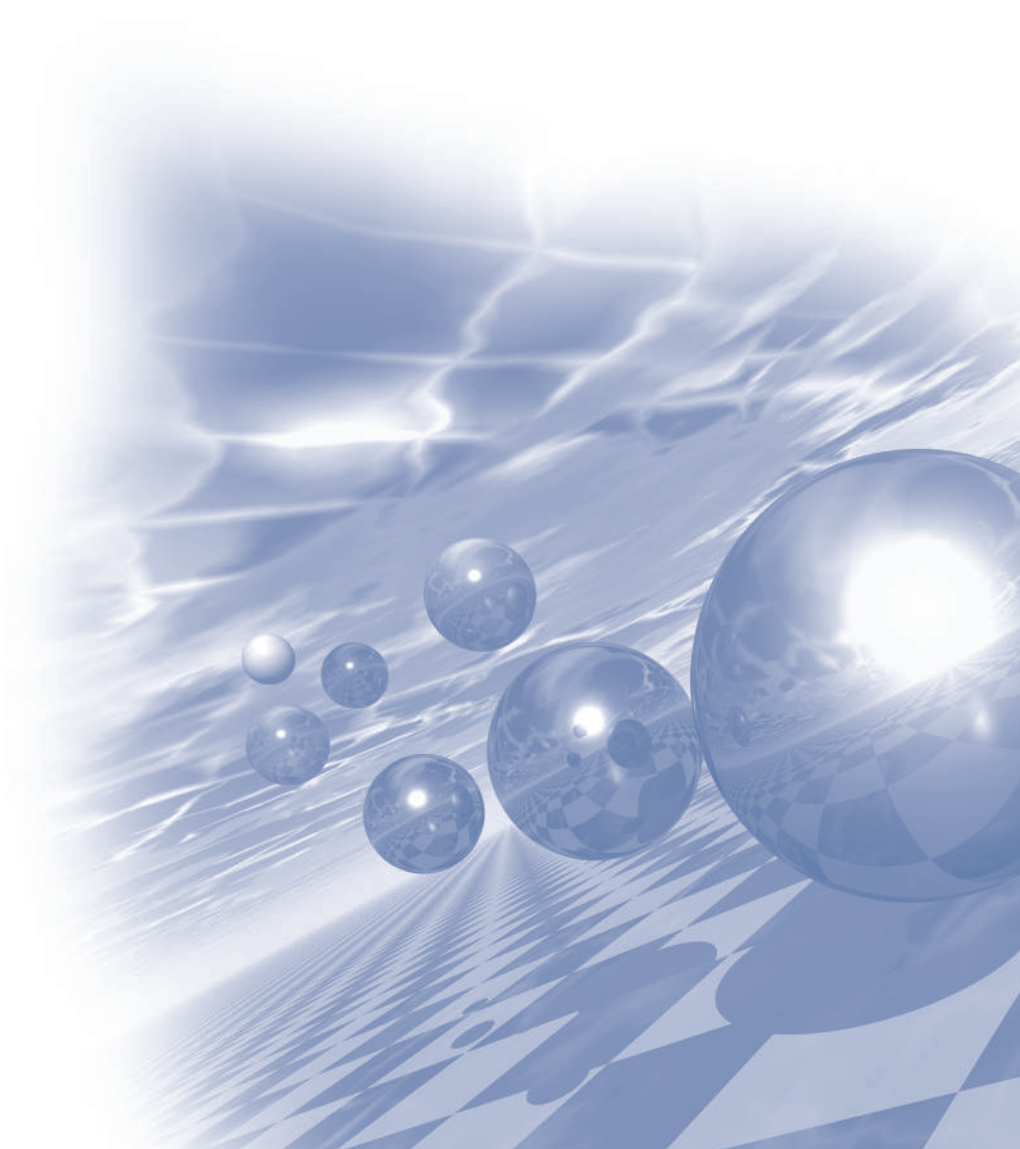
Single crystal growth, magnetotransport, and temperature-dependent Raman scattering of Kagome metals

Kee Hoon Kim[1*]

[1]Center for Novel States of Complex Materials Research, Department of Physics and Astronomy, Seoul National University, Seoul 08826, Republic of Korea

[2]Institute of Applied Physics, Department of Physics and Astronomy, Seoul National University, Seoul 08826, South Korea

Kagome metals refer to a new class of metallic quantum magnetss hosting Kagome lattice and topological band structure. Various forms of Kagome metals have been recently documented; they include 3-1 (e.g. paramagnet Ni3In, antiferromagnet Mn3Sn), 1-1 (e.g paramagnet CoSn), 1-6-6 (e.g ferrimagnet TbMn6Sn6), 3-2-2 (e.g. hard ferromagnet Co3Sn2S2), and 3-2 materials (e.g, soft ferromagnet Fe3Sn2), thus demonstrating a variety of crystal and magnetic structures. They generally feature a 3d transition metal based magnetic Kagome lattice with an in-plane lattice constant of about 5.5Å. Their 3d electrons dominate the low-energy electronic structure, thus exhibiting electronic correlation. Most importantly, the Kagome lattice electrons generally feature Dirac band crossings and flat band, which are the source for nontrivial band topology. Moreover, they all contain heavy elements like Sn, which can provide strong spin-orbit coupling to the system. Therefore, the system can be an ideal platform to explore the rich interplay between geometry, correlation, and topology.

In this presentation, we summarize our group's efforts to grow all of the above-mentioned structures that have formed Kagome metallic magnets. In this presentation, we focus on temperature dependent transport/magnetism in Ni shandites ($Ni_3(Tl,In)_2S_2$) materials, in which large magnetoresistance is coined to the presence of two types of carriers, i.e. holes and electrons with strong temperature dependent variation of carrier density. These the Hall effect signals of these materials shed light into the possible Dirac/Weyl fermions, Berry curvature, and spin-orbit coupling. Moreover, we provide the temperature dependent Raman scattering spectra in of Ni_3In, in which we trace out the phonon spectra and quasi-elastic electronic signals to discuss the implications of the electron correlation in this compound. Our research efforts are likely to provide promising hints for the development of technologies in quantum computing, spin superconductors, and low power electronics based on the Kagome metals.

In close collaboration with Kwangtak Kim, Donghyun Kim, Yeahan Sur, Sangjin Kim, and Dirk Wulferding

Spin-Split Band Hybridization in Graphene Proximitized with α-RuCl3 Nanosheets

Youngwook Kim[*]

Department of Physics and Chemistry, Korea

Proximity effects induced in the two-dimensional Dirac material graphene potentially open access to novel and intriguing physical phenomena. Thus far, the coupling between graphene and ferromagnetic insulators has been experimentally established. However, only very little is known about graphene's interaction with antiferromagnetic insulators. Here, we report a low-temperature study of the electronic properties of high quality van der Waals heterostructures composed of a single graphene layer proximitized with α-RuCl3. The latter is known to become antiferromagnetically ordered below 10 K. Shubnikov-de Haas oscillations in the longitudinal resistance together with Hall resistance measurements provide clear evidence for a band realignment that is accompanied by a transfer of electrons originally occupying the graphene's spin degenerate Dirac cones into α-RuCl3 band states with in-plane spin polarization. Left behind are holes in two separate Fermi pockets, only the dispersion of one of which is distorted near the Fermi energy due to spin selective hybridization with these spin polarized α-RuCl3 band states. This interpretation is supported by our density functional theory calculations. An unexpected damping of the quantum oscillations as well as a zero-field resistance upturn close to the Néel temperature of α-RuCl3 suggest the onset of additional spin scattering due to spin fluctuations in the α-RuCl3.

A newcomer of one-dimensional S = 1 chain, NiTe$_2$O$_5$

Yoon Seok Oh[*]

Department of Physics, Ulsan National Institute of Science and Technology (UNIST), Ulsan, Korea

Investigation of the exotic quantum phenomena near the phase transition has attracted a lot of attentions in condensed matter physics. The one-dimensional transverse-field Ising model (1DTFIM) is a prototype for quantum phase transitions and quantum criticality, and the transverse magnetic field could suppress the magnetic order, which induces an order-disorder quantum phase transition, and a gap could be closed at a quantum critical point (QCP). Recently, we have found a new one-dimensional S = 1 chain compound NiTe$_2$O$_5$, in which spin-1 of Ni^{2+} ions form a one-dimensional chain structure through NiO$_6$ octahedra's edge-sharing, Fig.1(a). The long-range antiferromagnetic order of NiTe$_2$O$_5$ has the ferromagnetically ordered longitudinal magnetic moments but alternating ferromagnetic-antiferromagnetically ordered transverse magnetic moments along the chain, Fig. 1(b). Using the single crystal Neutron scattering and a ^{125}Te nuclear magnetic resonance (NMR) experiments, we have found unconventional critical behavior near Néel temperature and persistent spin fluctuation at high temperature in the paramagnetic state of NiTe$_2$O$_5$. In this talk, I present comprehensive experimental results for the magnetic properties of NiTe$_2$O$_5$ and discuss about physical origin of the intriguing magnetic phenomena.
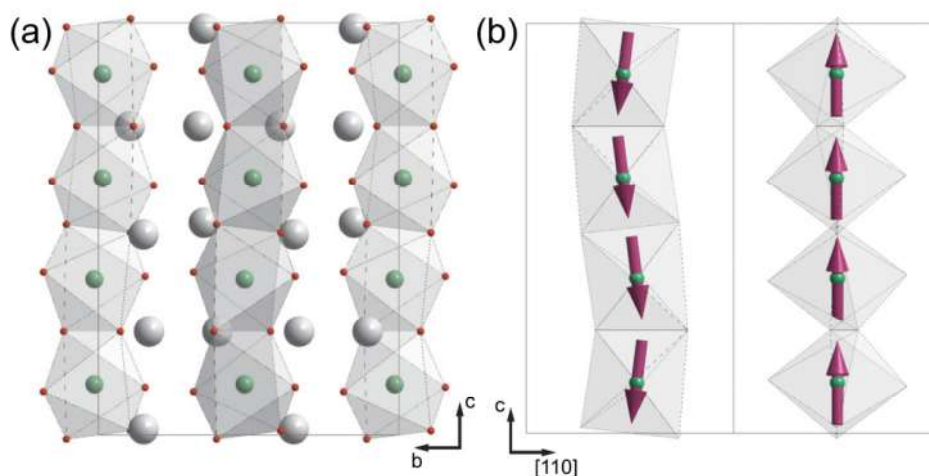
Fig. 1. (a) Crystallographic and (b) magnetic structure of NiTe$_2$O$_5$

Towards Quantum Skyrmionics

Seungmo Yang[1], Taesung Joo[1,2], Jongwan Son[1], Kyoung Woong Moon[1],
Sungkyun Park[2], Chanyong Hwang[1*]

[1]Quantum Spin Team, KRISS, Korea
[2]Physics Department, Pusan National Univ., Korea

Magnetic skyrmion has drawn a lot of attention in spintronic device. From memory to logic devices, its manipulation(creation, deletion, movement) with pure electric external variables is needed. On the contrary to its expectation working at a very low critical current, even the generation of this magnetic skyrmion at the place aimed has not been possible. Now we will show our recent work on the manipulation of this magnetic skyrmion. The next step for its use is leading the quantum effects with skyrmions. Several reports have been shown so far, all theoretical. We will discuss several examples of quantum skyrmions, such as skyrmion qubit, control of Majorana bound state with the chiral magnetism of skrmions and edge state formation in skrymions in confined geometry.

Proving the origin of magnetically inhomogeneity of FeRh film using polarized neutron reflectometry

Sehwan Song[1], Jiwoong Kim[1], Chang-woo Cho[1], Jisung Lee[1,2], Dooyong Lee[1], Doukyun Kim[1], Hyegyoung Kim[1,3], Haeyong Kang[1], Chul-Hong Park[4], Jun Kue Park[5], Jae Hyuck Jang[2], Noboru Miyata[6], Neeraj Kumar[7], Yeong-Ah Soh[7], Chanyoung Hwang[8], Brian J. Kirby[9], Sungkyun Park[1*]

[1]Department of Physics, Pusan National University, Busan 46241, Korea
[2]Korea Basic Science Institute, Daejeon 34133, Korea
[3]Core Research Facilities, Pusan National University Busan 46241, Korea
[4]Department of Physics Education, Pusan National University, Busan 46241, Korea
[5]Multi-Purpose Accelerator Complex, Korea Atomic Energy Research Institute, Gyeongju 38180, Korea
[6]Neutron Science and Technology Center, Compressive Research Organization for Science and Society, 162-1 Shirakata, Tokai, Naka, Ibaraki 319-1106, Japan
[7]Paul Scherrer Institute, 5232 Villigen, Switzerland
[8]Quantum Spin Team, Korea Research Institute of Standards & Science, Daejeon 34113, Korea
[9]NIST Center for Neutron Research, National Institute Standard & Technology, Gaithersburg, MD 20878, USA

FeRh films, knowns as antiferromagnetic (AFM) materials, exhibits magnetic phase transition from AFM to ferromagnetic (FM) system accompanied by structural and electrical variations. Furthermore, utilizing the phase transition characteristics in modern AFM-based spintronic applications is an important research subject. Moreover, the interface characteristics of FeRh film is essential for heterostructure formation in potential device application. Previously, it has been known that the pristine FeRh films exhibit residual ferromagnetism in the AFM state (i.e., below transition temperature). Therefore, it is disadvantageous to obtain magnetically clean interfaces owing to the formation of residual ferromagnetism at the interfaces.

In this presentation, we examined the temperature- and depth-dependent magnetic properties of DC sputtered FeRh films to enhance our understanding on the residual ferromagnetism in the AFM state. As a result, we found that the presence of non-uniform magnetic properties at the interfaces. Furthermore, we showed the different origins of residual ferromagnetism at the top and bottom interfaces.
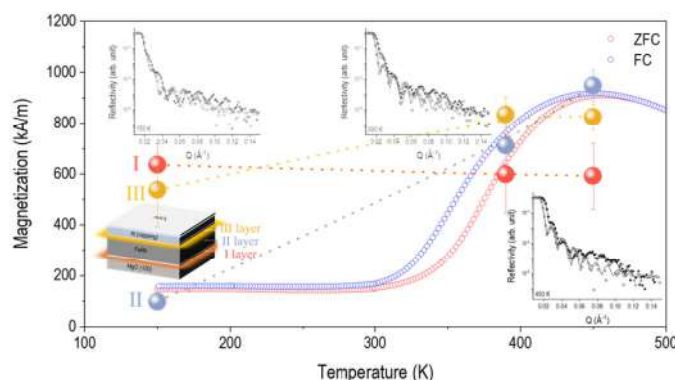
Fig. 1. Temperature- and depth-dependent magnetic characteristics of FeRh film

Unusual spin pseudogap behavior in the spin web lattice Cu_3TeO_6 probed by ^{125}Te nuclear magnetic resonance[*]

Seung-Ho Baek[1*], Kwang-Yong Choi[2] and Bernd Büchner[3]

[1]Department of Physics, Changwon National University, Changwon, Korea
[2]Department of Physic, Sungkyunkwan University, Suwon, Korea
[3]IFW Dresden, Germany

We present a ^{125}Te nuclear magnetic resonance (NMR) study in the three-dimensional spin web lattice Cu_3TeO_6 which harbors topological magnons. The ^{125}Te NMR spectra and the Knight-shift K as a function of temperature show a drastic change at $T_S \sim 40$ K much lower than the Néel ordering temperature $T_N \sim 61$ K, providing evidence for the first-order structural phase transition within the magnetically ordered state. Most remarkably, the temperature dependence of the spin-lattice relaxation rate T_1^{-1} unravels spin-gap-like magnetic excitations, which sharply sets in at $T^* \sim 75$ K, the temperature well above T_N. The spin-gap behavior may be understood by weakly dispersive optical magnon branches of high-energy spin excitations originating from the unique corner-sharing Cu hexagon spin-1/2 network with low coordination number.

Session 1

구두발표 I
'Spintronics I'
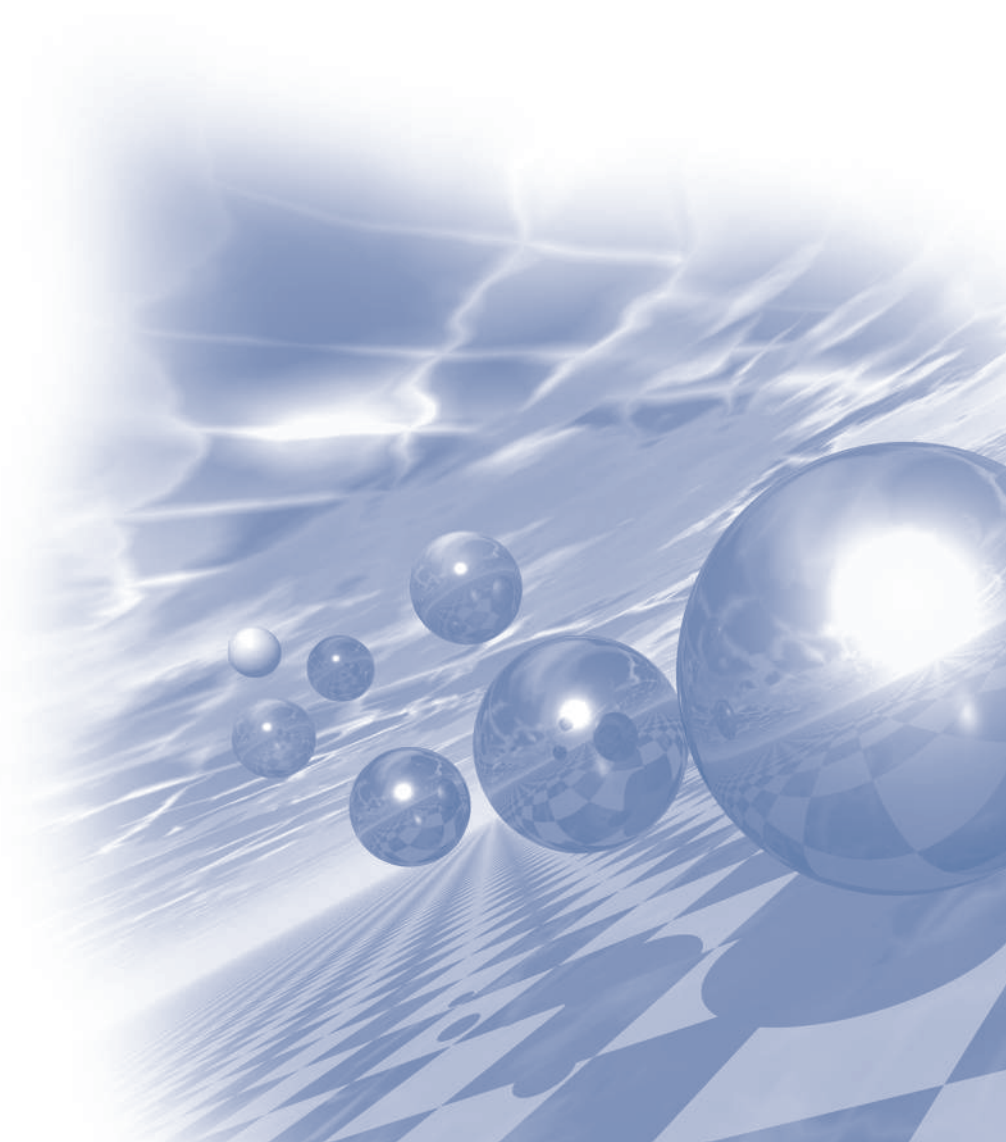
Spin Hall Conductivities in W-Si Alloys

Quynh Anh T. Nguyen[*], S. C. Hong and Sonny H. Rhim

Department of Physics and Energy Harvest Storage Research Center, University of Ulsan,
Ulsan 44610, Republic of Korea

Recently in spintronics, W compounds have attracted attentions owing to large spin Hall angle [1,2]. Motivated by recent experiment [3], we investigate spin Hall conductivities (SHC) of $W_{100-x}Si_x$ alloys using first-principles calculations, where β-W is considered as mother material. Among various concentration of Si, x = 0, 3.125, 6.25, 12.5, and 25 are taken into account with possible configurations. For each concentration x, thermodynamic average of SHC is taken, where Boltzmann factor at 300K corresponding to formation energy is used. When x = 3.125, SHC exhibit highest magnitude of -1306 $\hbar$/e S/cm, which is enhanced by 59.9 % over β-W. When x > 3.125, after reaching highest value, SHC decreases. When x = 6.25, SHC (-835 $\hbar$/e S/cm) is comparable to β-W, but x > 6.25, SHC is smaller than β-W. Underlying analyses are discussed in term of k-resolved Berry curvature and orbital resolved band structure.

References

[1] K.-U. Demasius, T. Phung, W. Zhang, B. P. Hughes, S.-H. Yang, A. Kellock, W. Han, A. Pushp, and S. S. P. Parkin, Nat. Commun. **7**, 10644 (2016).

[2] X. Sui, C. Wang, J. Kim, J. Wang, S. H. Rhim, and W. Duan, Phys. Rev. B **96**, 241105(R) (2017).

[3] Y. J. Kim, M. H. Lee, G. W. Kim, T. Kim, I. H. Cha, Q. A. T. Nguyen, S. H. Rhim, and Y. K. Kim, Acta Mater. **200**, 551 (2020).

Effects of Interlayer on Magnetotransports In Graphene-based Spintronic Devices

Nga T. Do[1,2*], Youngrok Jang[3], Sijin Park[4], Chanyong Hwang[4] and Tae Hee Kim[1*]

[1]Deparment of Physics, Ewha Womans University, 03760, Seoul, Korea
[2]IBS Center for Quantum Nanoscience, Ewha Womans University, 03760, Seoul, Korea
[3]Department of Physics, Incheon National University, 22012, Incheon, Korea
[4]Korea Research Institute of Standards and Science, 34113, Daejeon, Korea

In this work, we focused on the interplay between graphene and Pt layer by introducing an ultrathin Co interlayer. As Co thickness increases from 0.5 to 25 Å in Pt/Gr/SiO$_2$/Si perpendicular stacks, different magnetoresistance behaviors have been observed in the intermediate temperature range (77-300K). The Co films were prepared on the wafer-scale CVD-grown graphene layers, and covered with a 3-nm-thick of Pt using the UHV-Molecular Beam Epitaxy (MBE) films deposition technique. For the transport measurement, Pt-Hall bar devices were also prepared using the *in-situ* shadow mask system in the same UHV-MBE chamber. Our results showed that the quantum interference effect could observed even at 77 K for the samples with the Co thickness less than 2 Å. Particularly, for the sample of 0.5-Å-thick Co, the WL-WAL crossover was clearly shown in the perpendicular MR measured at 77 K. To explore in more detail the Co-interlayer effects on the transport properties at the Pt/Gr interface, a theoretical analysis was performed using modified the Hikami-Larkin-Nagaoka (HLN) equation. A comparative study of the effect of different interlayer thickness on magnetotransport phenomena was performed to elucidate the role of interlayer in the dependent scattering mechanisms. For microstructural characterizations of the heterostructures, the careful analysis of interface properties was also carried out using the atomic force microscope (AFM), high resolution-TEM.

Our results provide further insights into the transport phenomena and highlight the defect engineering of 2D-material with other ferromagnetic materials to manipulate and develop highly effective spintronic devices with new functionalities.

Sign-tunable anisotropic magnetoresistance and electrically detectable dual magnetic phases in a helical antiferromagnet

Jong Hyuk Kim[*][†], Hyun Jun Shin[†], Mi Kyung Kim[†], Jae Min Hong, Ki Won Jeong, Jin Seok Kim, Kyungsun Moon, Nara Lee[*] and Young Jai Choi[*]

Department of Physics, Yonsei University, Seoul 03722, Korea
[†]These authors contributed equally to this work.
Correspondence: Nara Lee (eland@yonsei.ac.kr) or Young Jai Choi (phylove@yonsei.ac.kr)

The helimagnetic order describes a non-collinear spin texture of antiferromagnets, arising from competing exchange interactions. Although collinear antiferromagnets are elemental building blocks of antiferromagnetic (AFM) spintronics, the potential of implementing spintronic functionality in non-collinear antiferromagnets has not been clarified thus far. Here, we propose an AFM helimagnet of $EuCo_2As_2$ as a novel single-phase spintronic material that exhibits a remarkable sign reversal of anisotropic magnetoresistance (AMR). The contrast in the AMR arises from two electrically distinctive magnetic phases with spin reorientation driven by magnetic field lying on the easy-plane, which switches the sign of the AMR from positive to negative. Further, various AFM memory states associated with the evolution of the spin structure under magnetic fields were identified theoretically, based on an easy-plane anisotropic spin model. These results reveal that non-collinear antiferromagnets hold potential for developing spintronic devices.
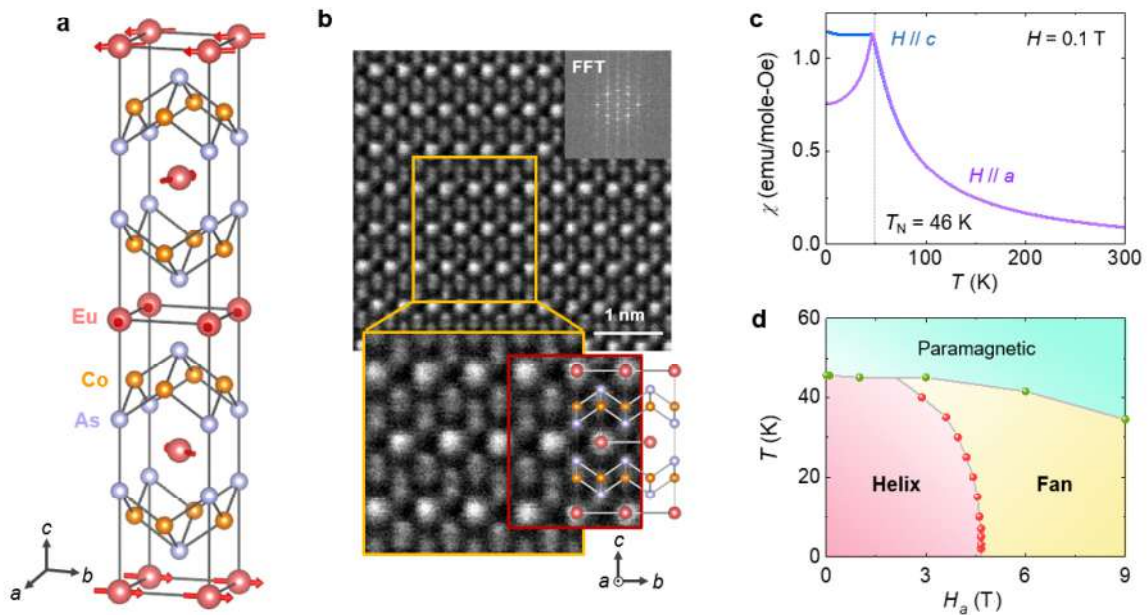
Fig. 1. Structure and magnetic susceptibility of $EuCo_2As_2$

Spin Seebeck voltage in yttrium-iron-garnet embed Au-NPs structure

Phuoc Cao Van, Jong-Ryul Jeong[†]

Department of Material Science and Engineering, Chungnam National University, Daejeon 34134, South Korea
[†]Author to whom correspondence should be addressed: E-mail: jrjeong@cnu.ac.kr

In this report, we present the fabrication of high-quality yttrium-iron-garnet (YIG, $Y_3Fe_5O_{12}$) thin film grown on a single-crystal garnet $Gd_3Ga_5O_{12}$ (GGG) substrate using RF sputter followed by a crystallization process. The narrowest ferromagnetic resonance (FMR) linewidth of 1.9 Oe at 9.43 GHz for a 60-nm-thick YIG film was obtained. This value is comparable to the recently published value even for the film grown by the pulsed laser deposition method. The thickness and temperature dependence of FMR linewidth and surface morphology were systematically investigated. The result shows the optimal condition for growing YIG with our self-made target was 60 nm of thickness and 875°C of annealing temperature. Furthermore, we studied the spin Seebeck effect voltage (V_{SSE}) in the YIG embed gold NPs (Au-NPs) using a laser-based SSE measurement system. For the matching condition of surface plasmon resonance (SPR) dip caused by Au-NPs and laser's wavelength (λ_{laser} = 660 nm), there is a break-down of V_{SSE} which is attributed to the contribution of the plasmonic heating effect. For λ_{laser} = 830 nm, meaning off-resonance case, there is still enhancement of V_{SSE} signal which is assigned to the contribution of the interfacial magnons.

Keywords: $Y_3Fe_5O_{12}$; interfacial magnons; spin Seebeck effect; surface plasmon resonance

Comparison between Perpendicular and Longitudinal Exchange Bias Effects in (Mn, Co)$_3$Ga/Mn$_3$Ga Bilayers

Hyeon-Su Kim[*], Woosuk Yoo and Myung-Hwa Jung[*]

Department of Physics, Sogang University, Seoul 04107, South Korea

The exchange bias (EB) effect originates from the magnetic interaction at the interface between ferromagnetism (FM) and antiferromagnet (AFM), FM/AFM bilayer, which is practically used to pin the spin direction of giant magnetoresistance head in hard disk drives. Nevertheless, its mechanism is still unveiled. From the material viewpoint, most studies on the EB effect have been performed in FM/AFM bilayers with in-plane magnetic anisotropic (IMA) geometry, and there are few reports on FM/AFM bilayers with perpendicular magnetic anisotropic (PMA) geometry. In this study, we report the EB characteristics for IMA and PMA, where the spin structure is controlled by the amount of Co of Mn$_{3-x}$Co$_x$Ga. We fabricated two distinct bilayers systems composed of two magnetic components; Mn$_{3-x}$Co$_x$Ga ferrimagnetic layer and Mn3Ga antiferromagnetic layer. We could change the magnetic anisotropy of Mn$_{3-x}$Co$_x$Ga ferrimagnet layer simply by adjusting the Co composition. For $x \leq 0.3$, it is hard ferrimagnet with PMA, and for $x \geq 0.57$ it is soft ferrimagnet with IMA. Furthermore, since the antiferromagnetic Mn$_3$Ga is cubic with no magnetic anisotropy, we could tune the magnetic anisotropy of Mn$_3$Ga through the field cooling process. We explain the complex EB effect of ferrimagnetic Mn$_{3-x}$Co$_x$Ga/ antiferromagnetic Mn$_3$Ga bilayer systems by using the spin-glass model.

Symposium 5

'뫼스바우어 자성'
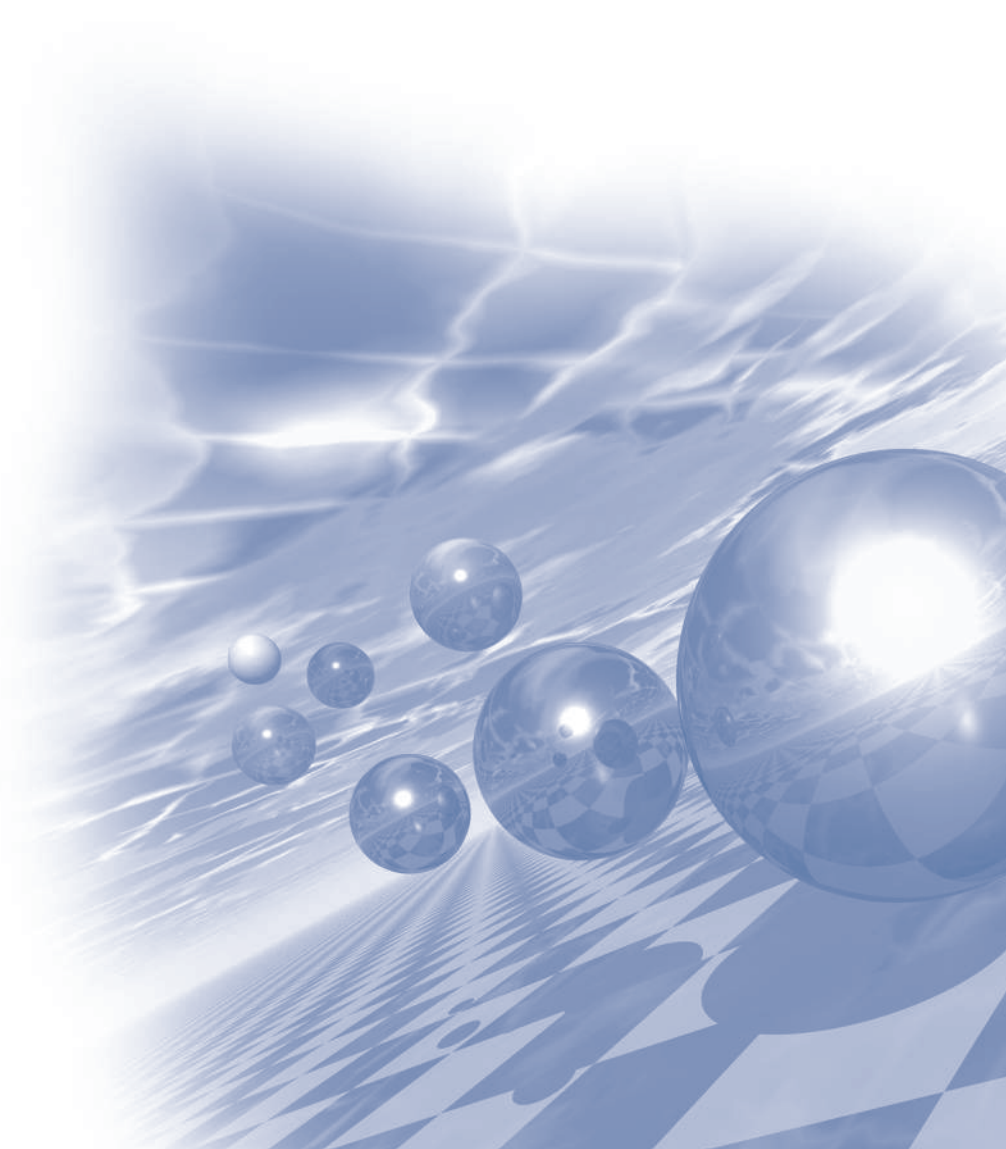
Mössbauer studies of inter/deintercalation process features in cathode

Hyunkyung Choi[*] and Chul Sung Kim[†]

Department of Physics, Kookmin University, Seoul 02707, Korea

As the energy industry develops, the demand for large-sized secondary batteries has increased, and the development of next-generation batteries has been concentrated. The fastest-growing lithium-ion battery in the Energy Storage System is lightweight, has no memory effect, and easily maintains it charge capacity. It is widely used in portable electronic devices and electric vehicles because it can save energy without loss for a long time because of a low natural discharge. Lithium ions, which exist in an ionic state, generate electricity by moving from the cathode to the anode during charging and from the anode to the cathode during discharging. These cathode materials are a reactant participating in an actual electrochemical reaction, and they are required to have an energy density, an output characteristic, increased lifetime characteristics, and improved stability. Therefore, the lithium-on activation capability of the cathode material determines the performance of the battery. The electrode material undergoes repeated use and degradation beyond its normal operating potential due to irreversible structural changes caused by inter/deintercalation process of lithium(or sodium) ions. In order to minimize irreversible structural deformation, the development of cathode materials is becoming more important in terms of inherent properties, including the interrelationship between the crystal structure and electromagnetic properties of cathode materials.

In this presentation, the magnetic properties of iron-based cathode materials were analyzed X-ray diffraction and Mössbauer spectroscopy. The Mössbauer spectroscopy allowed us to determine the valence states of iron in the crystal structures of cathode and also to unveil the presence of different iron-containing phases. In addition, we present the relation of structural transition and magnetic property by deintercalation of lithium(or sodium) intercalation cathode.

철계 촉매를 활용한 연료전지용 전극 구조 제어 연구

지윤성*, 우성현, 김성민, 정지수, 우승희, 강윤식, 이은직, 박구곤, 박석희, 임성대

연료전지연구실, 한국에너지기술연구원

고분자 전해질막 연료전지는 산소와 수소가스를 이용하여 전기를 생산하는 친환경 고효율 에너지 변환기술로 주로 자동차, 가정, 건물의 발전시스템으로 사용된다. 고분자 전해질막 연료전지의 전극은 반응물의 화학 에너지를 전기에너지로 변환하는 전기화학 반응을 수행한다. 전극은 주로 백금, 탄소, 이오노머를 혼합한 분산액을 사용해 제조합니다. 각 물질의 특성이 다르기 때문에 분산 방법, 분산매 특성 등에 따라 용액 내 입자들의 거동이 달라지며, 제조된 전극의 최종 형태에도 영향을 미친다. 전극층의 특성은 반응물의 전달현상에 영향을 주어 연료전지의 전력 출력특성을 결정짓기 때문에, 전극재료들의 성질, 배열 및 전극 구조의 제어를 통해 연료전지의 출력특성을 개선하기 위한 연구들이 진행되고 있다.

본 연구는 자성을 띄는 촉매를 활용하여 전극 특성을 조절하고 그 효과를 확인하기 위해 수행되었다. 물과 노말프로필알콜의 혼합용매와 불소계 이오노머를 사용하여 연료전지용 촉매 분산액을 제조하고, 혼합용액의 조성비에 따른 용액 내 촉매의 거동을 다양한 방법으로 분석하였다. 자성제어에 유리한 조건에서 자기력선을 따라 입자를 배열하여 전극을 제조한 후 전극의 특성을 살펴보았다.

Iron-Based Catalysts for Production of Synthetic Waxes from Syngas: Selectivity Innovation by Mössbauer Spectroscopy

Dong Hyun Chun[1,2*], Geun Bae Rhim[1], Min Hye Youn[1]

[1]Carbon Conversion Research Laboratory, Korea Institute of Energy Research,
152 Gajeong-Ro, Yuseong-Gu, Daejeon 34129, Republic of Korea
[2]Advanced Energy and System Engineering, University of Science and Technology,
217 Gajeong-Ro, Yuseong-Gu, Daejeon 34113, Republic of Korea

Fischer-Tropsch synthesis (FTS) is a promising way to convert syngas ($CO + H_2$) into high value-added products.

One of the most valuable products in FTS is a synthetic wax, also called an FTS wax, mostly composed of C_{19+} n-paraffins. The FTS wax can be used as a substitute for a polyethylene wax in various fields such as adhesive industry, ink, coating, and polymer processing. Furthermore, the FTS wax is reported to possess excellent physical properties in terms of melting point, viscosity, and molecular weight. Iron-based catalysts are highly promising for the FTS, due to their low cost and high activity. In general, iron carbides are known to be active phases for the FTS. However, it is very difficult to specify iron carbide phases more selective to wax production because several iron oxide and carbide phases evolve in the iron-based catalysts in the FTS condition. In this study, we report our recent understanding on the relationship between the type of iron carbide phase and the wax selectivity in the FTS. We used Mössbauer spectroscopy, which is known as a proven technique for detailed and quantitative analyses of multiple iron phases. We found that the higher the ε`-carbide ($Fe_{2.2}C$) to χ-carbide (Fe_5C_2) ratio, the higher the selectivity of FTS waxes.

Development of potable Mössbauer Spectroscopy Instrumentation

Jaegi Lee[*], Gwang-Min Sun and Young Rang Uhm

Department of Quantum and Convergence Science, Korea Atomic Energy Research Institute, Daejeon, South Korea

Potable Mössbauer spectrometer is also focused in our research to apply in-situ detection in the fields of material science, culture heritages, and geo-science of earth and space. Mössbauer Spectroscopy is well-known technique in material research, especially in a filed of iron-based materials research. Typical problem the researchers need to solve is to have proper and precise instrument, keeping simple and user friendly usage. Recently, our department was developed potable instrument of conversion & advanced Mössbauer spectrometers (CAMS 1.0). We are also advancing Mössbauer spectrometers for Lunar project in KOREA(South). In this study, the main technical principles of Mössbauer spectroscopy instruments are presented. The last advances and experiences in instrumentation is mentioned, including different detection systems, and velocity drives.

Symposium 6

'스핀트로닉스'
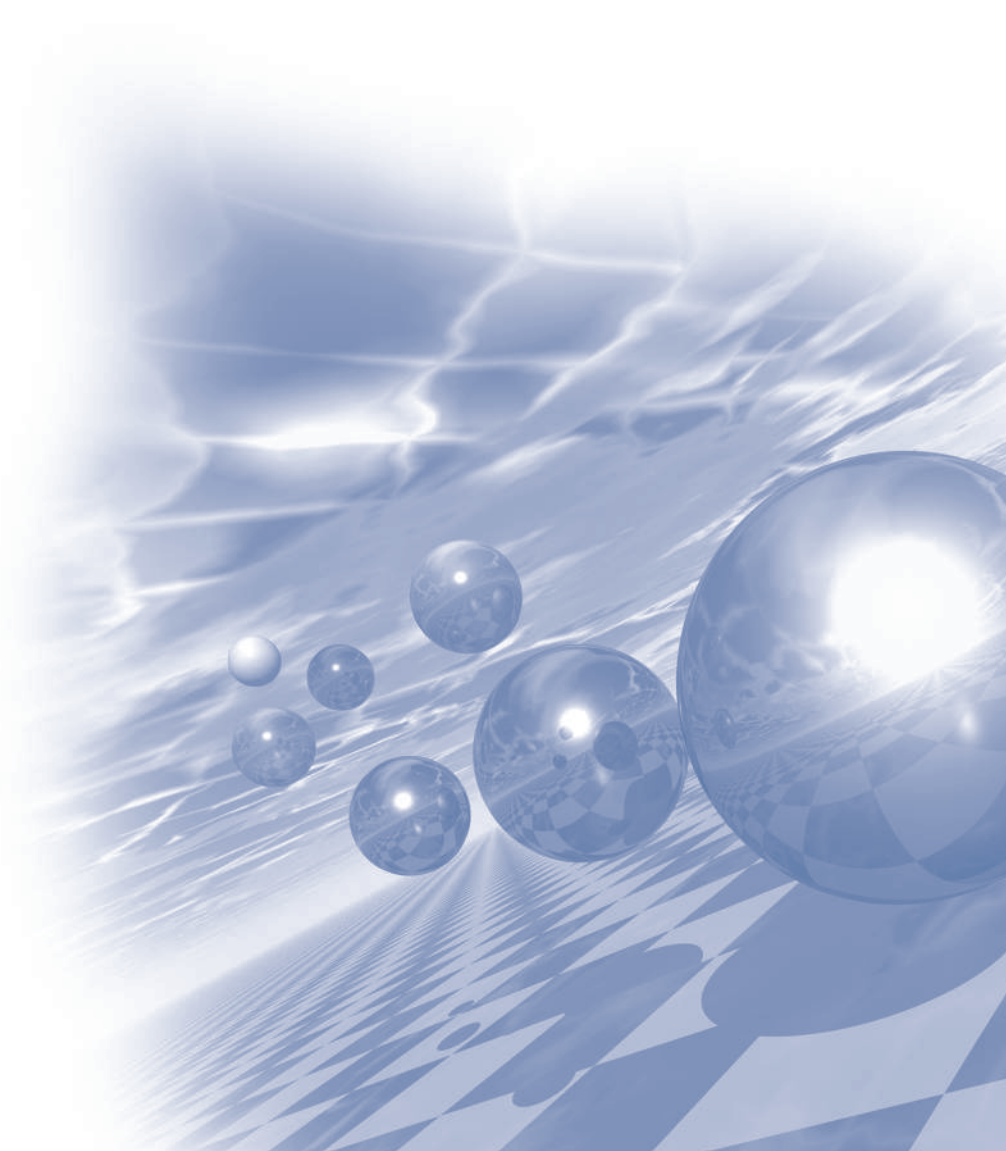
Dynamics of Skyrmions in Curved Geometry

Sang-Koog Kim[1][†], Jaehak Yang[1*], Hyeon-Kyu Park[1], Gyuyoung Park[1],
Claas Abert[2,3] and Dieter Suess[2,3]

[1]National Creative Research Initiative Center for Spin Dynamics and Spin-Wave Devices, Nanospinics Laboratory,
Research Institute of Advanced Materials, Department of Materials Science and Engineering,
Seoul National University, Seoul 151-744, South Korea
[2]Faculty of Physics, University of Vienna, Vienna, Austria
[3]University of Vienna Research Platform MMM Mathematics - Magnetism – Materials,
University of Vienna, Vienna, Austria
[†]Correspondence and requests for materials should be addressed to S.-K. K. (sangkoog@snu.ac.kr)

We found a rich variation of the topological magnetic textures of vortices, skyrmions, and skyrmioniums in a curved geometry, e.g., magnetic hemispherical shells as functions of surface-normal uniaxial magnetic anisotropy constant (K_u), Dzyaloshinskii-Moriya interaction (DMI) constant (D_{int}), and the shell diameter 2R. The combination of K_u and D_{int} plays a crucial role in the stabilization of those different spin textures [1]. An interesting feature is that skyrmions can be stabilized even in the absence of intrinsic DMI for 2R < 25 nm. In this talk, we also report on the characteristic dynamic properties of skyrmions excited by in-plane and out-of plane oscillating magnetic fields. Moreover, we present a novel switching behavior of skyrmion polarity through a transient skyrmionium state using very-low-strength AC magnetic fields [2-4]. This work provides further physical insight into the static and dynamic properties of skyrmions in curved-geometry nanodots and suggests potential applications to low-power consumption and ultra-high-density information-storage devices.

References

[1] J. Yang, C. Abert, D. Suess, and S. -K. Kim, *Sci. Rep.* **11**, 3886 (2021)

[2] J. Yang, H. -K. Park, G. Park, C. Abert, D. Suess, and S. -K. Kim, *Phys. Rev. B* **104**, 134427 (2021)

[3] S. -K. Kim, J. Yang, Y. Song, K. Lee, and J. Kim, *U.S. Patent* No. 506,859,107 (2021)

[4] S. -K. Kim, J. Yang, Y. Song, K. Lee, and J. Kim, *K.R. Patent* No. 10-2021-0069421 (2021)

Disparate field-response of magnetic submoment in ferrimagnetic TbCo

Ji-Ho Park[1], Won Tae Kim[1], Woonjae Won[1], Jun-Ho Kang[1], Soogil Lee[2],
Byong-Guk Park[2], Byoung S. Ham[3], Fabian Rotermund[1] and Kab-Jin Kim[1*]

[1]Department of Physics, Korea Advanced Institute of Science and Technology (KAIST), Daejeon, Republic of Korea
[2]Department of Materials Science and Engineering and KI for Nanocentury,
KAIST, Daejeon 34141, Republic of Korea
[3]School of Electrical Engineering and Computer Science, GIST, Gwangju 61005, Republic of Korea

Rare earth (RE)–transition metal (TM) ferrimagnetic alloys are receiving renewed interest, because the unique coupling of RE and TM sub-moments enables the antiferromagnetic spin dynamics. As the RE sub-moment originates primarily from the 4f-electrons which locates far below the Fermi level while the TM sub-moment arises from the 3d-electrons near the Fermi level, microscopic mechanism of antiferromagnetic spin dynamics requires to understand the individual magnetic moment configuration at different energy levels, which has so far been ignored. Here we present the experimental evidences for the energy-level-dependent disparate magnetic moment configuration in ferrimagnetic TbCo alloys. Multiple techniques that can access the different energy levels have been employed, and reveal that magnetic moment at deeper energy level is rather easily altered by the magnetic field than that at Fermi level, suggesting that the magnetic moment responds differently to the magnetic field depending on the energy level. Further investigation on the temperature dependence shows that the Tb sub-moment exhibits the spin glass-like freezing possibly induced by the random anisotropy of Tb. Our results demonstrate the important aspects of RE-TM ferrimagnets and therefore pave the way towards a complete understanding of antiferromagnetic spin dynamics in RE-TM ferrimagnets.

Magnetic tunnel junctions with two-dimensional van der Waals magnets: Bias controlled and spin-transfer-torque induced spin-valve operations

Suyong Jung[1*], Keun-Hong Min[1,2], Dun Hyun Lee[1], Sang-Jun Choi[3],
Jonghwa Eom[2] and Jun Sung Kim[4]

[1]Interdisciplinary Materials Measurement Institute,
Korea Research Institute of Standards and Science, Daejeon, Korea
[2]Department of Physics and Astronomy, Sejong University, Seoul, Korea
[3]Institute for theoretical physics and astrophysics, University of Wurzburg, Wurzburg, Germany
[4]Department of Physics, Pohang University of Science and Technology, Pohang, Korea

Van der Waals (vdW) heterostructures with two-dimensional magnets offer an idealized magnetic junction with an atomically sharp and clean interface. This unique physical attribute ensures that the magnetic layers maintain their intrinsic spin-polarized electronic states and spin-flipping scattering processes at a minimum level, a trait that can expand spintronic device functionalities. Here, using a vdW assembly of ferromagnetic Fe_3GeTe_2 with nonmagnetic hBN and WSe_2 layers, we demonstrate electrically tunable, highly transparent spin injection and detection across the vdW interfaces. By varying an electrical bias, the net spin polarization of the injected carriers can be modulated and remarkably reversed in polarity, which leads to compelling sign changes of the tunneling magnetoresistance. The unique spin polarization reversals are attributed to sizable contributions from high-energy localized spin states in the metallic ferromagnet, so far inaccessible in conventional magnetic tunnel junctions (MTJs). Moreover, the current required for spin-transfer-torque induced spin-valve operations ($< 10^4$ A/cm^2) is found to be two-to-three orders of magnitude lower than those of conventional MgO-based MTJs. Such exceptionalities of the spin-valve operations open a promising route for the electronic control of upcoming low-dimensional spintronic device applications.
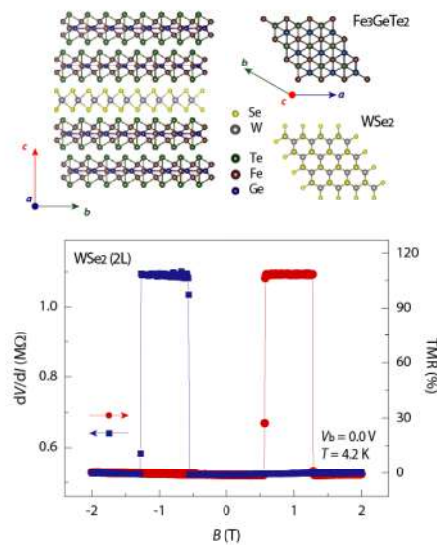
Fig. 1. Schematic of all van der Waals assembled magnetic tunnel junctions and spin-valve operation

Two-fluid magnon transport : experimental evidences

Kyongmo An[*], Changsoo Kim, Chanyong Hwang

Quantum Spin Team, Korea Research Institute of Standards and Science, Daejeon, Republic of Korea
[*]E-mail: Kyongmo.an@kriss.re.kr

Converting heat into spin current has recently drawn a lot of attention due to its potential usage on heat recovery via the spin Seebeck effect (SSE) [1] -the generation of spin current upon thermal gradient- as well as fundamental interests including generation of spin super currents [2] and Bose-Einstein condensation of magnons [3]. The underlying mechanism of SSE is understood as thermally induced nonequilibrium between magnons and phonons [4]. Initial attempts to measure such nonequilibrium have failed under small temperature gradients, but suggested the spectral range of magnons involved in SSE [5].

In this talk I will present the first optical experiment that reveals the existence of such nonequilibrium between magnons and phonons under strong temperature gradient [6]. The spectral range of spin current generated in this condition turned out to be on the order of hundreds μeV, much lower than room temperature (300 K = 25 meV) [7]. In these optical measurements, the spin diffusion length is estimated to be on the order of microns. While similar length scales of micron ranges have been reported in the nonlocal spin transport measurements [8], there are other studies suggesting the existence of much shorter length scales of submicron range [9-11]. To reconcile the discrepancy, we performed a nonlocal spin transport experiment with a controlled heat profile, which is often a complicating factor in determining the length scale of spin diffusion. By putting an Al heat sink, the magnon profile deviates significantly from an exponential decay and shows double sign reversals in a short range within 1 μm from the heat source suggesting a competition between multiple sources. Using a phenomenological spin transport model, we calculate the spatial profile of nonequilibrium spin density. The observed sign reversal can only be accounted for if the relevant decay length is on the order of submicrons. Our results demonstrate the existence of the shorter decay length in the nonlocal magnon transport experiments. All these results point to the fact that magnons behave as two fluids, short decaying magnons at thermal energy and long distance propagating low energy magnons.

References

[1] S. R. Boona et al., Spin caloritronics. Energy & Environmental Science 7(3), 885-910 (2014)

[2] D. A. Bozhko et al., Nature Physics 12(11), 1057-1062 (2016)

[3] Y. Tserkovnyak et al., Physical Review B 93(10), 100402 (2016)

[4] H. Adachi et al., Reports on Progress in Physics 76(3), 036501 (2013)

[5] M. Agrawal et al., Physical review letters 111 (10), 107204 (2013)

[6] K. An et al., Physical Review Letters 117 (10), 107202 (2016)

[7] K. Olsson et al., Physical Review X 10 (2), 021029 (2020)

[8] L. J. Cornelissen et al., Nature Physics 11(12), 1022-1026 (2015)

[9] A. Kehlberger et al., Physical review letters 115(9), 096602 (2015)

[10] A. Prakash et al., Physical Review B 97(2), 020408 (2018)

[11] J. S.Jamison et al., Physical Review B 100(13), 134402 (2019)

Chiral induced spin selectivity in halide perovskites enables spin light-emitting diodes

Young-Hoon Kim[*]

Department of Energy Engineering, Hanyang University, Seoul, 04763, Republic of Korea

In traditional opto-electronic approaches, control over spin, charge, and light requires the use of both electrical and magnetic fields. In a spin-polarized light-emitting diode (spin-LED) charges are injected and circularly polarized light is emitted from spin-polarized carrier pairs. Typically, injection of carriers occurs with the application of an electric field, while spin-polarization can be achieved using an applied magnetic field or the use of polarized ferromagnetic contacts.

Here we employ chiral induced spin selectivity (CISS) to produce spin-polarized carriers and demonstrate a spin-LED that operates at room temperature and without magnetic fields or ferromagnetic contacts. The CISS layer consist of oriented self-assembled small chiral molecules within a layered organic/inorganic metal-halide hybrid semiconductor framework. The CISS layer is used to transport spin-polarized holes into an achiral colloidal perovskite nanocrystal with a spin-injection selectivity of up to 80%. In perovskite nanocrystal emitting layers, injected spin-polarized holes recombine with electrons which have proper spin direction and emit light with a matching polarization. Additionally, mixed-halide is utilized to facilitate the radiative recombination of spin-polarized excitons while suppressing spin-dephasing. The spin-LED achieves ± 2.6% circularly-polarized electroluminescence at room temperature. Thus, here we control of spin, charge, and light with only an applied electric field.

Keywords: chiral induced spin selectivity, halide perovskites, light-emitting diodes, spin injection, polarization

Damping-Induced Superluminal-like Motion of Antiferromagnetic Magnons at nm Scale

Kyusup Lee[1*], Dong-Kyu Lee[2], Dongsheng Yang[1], Rahul Mishra[1,3], Dong-Jun Kim[1], Sheng Liu[4], Qihua Xiong[5,6,7], Se Kwon Kim[8], Kyung-Jin Lee[8] and Hyunsoo Yang[1]

[1]Department of Electrical and Computer Engineering, National University of Singapore, Singapore
[2]Department of Materials Science and Engineering, Korea University, Seoul, Korea
[3]Centre for Applied Research in Electronics, Indian Institute of Technology Delhi, New Delhi, India
[4]Division of Physics and Applied Physics, Nanyang Technological University, Singapore
[5]State Key Laboratory of Low-Dimensional Quantum Physics and Department of Physics, Tsinghua University, Beijing, P. R. China [6]Beijing Academy of Quantum Information Sciences, Beijing, P. R. China
[7]Beijing Innovation Center for Future Chips, Tsinghua University, Beijing, P. R. China
[8]Department of Physics, Korea Advanced Institute of Science and Technology (KAIST), Daejeon, Korea

Solid-state devices based on spin degree of freedom are of interest for information technology with energy-efficient, fast and non-volatile features over contemporary complementary metal-oxide-semiconductor (CMOS) devices. Magnetoresistive random access memories (MRAMs) have been recently commercialized owing to the discovery of spin-transfer torque, whereas a complete overhaul of the charge-based counterpart with the spin devices yet requires constant discoveries and innovations. Electrical switching of magnetization ("writing") lies at the heart of the modern spin-torque MRAM devices. The "reading" current, on the other hand, inevitably undergoes the current shunting through the write channel, which disturbs the system and induces energy dissipation via thermal loss (*i.e.* Joule heat). In this respect, a number of recent works have been devoted to magnetic insulators, which are electrically insulating but magnetically conducting by means of magnons. Magnons, quanta of spin waves, carry the angular momentum without moving charges and thus enable the Joule-heat-free spin transport.

Antiferromagnetic (AFM) insulators are of considerably important for energy-efficient devices due to exceptionally low magnetic dissipation that enables, for instance, a long-range spin transport. In addition, AFM resonance frequencies are typically in the range of the sub-terahertz (sub-THz) to THz, while the ferromagnetic (FM) resonance frequencies are limited on the order of GHz. These intriguing AFM features further promise the energy-efficient information devices. Nonetheless, for the energy-efficiency, not only low dissipation of magnons but also a high magnon velocity is required because the power consumption is proportional to the device operation time. The magnon velocity at the nanoscale is therefore of particular importance for the operation speed of nanodevices, whereas the experimental observation remains elusive.

We discuss the recent major progress on the AFM spin transport. Particularly, we introduce the current limitations on probing the fast AFM magnon propagation on the sub-ps time scale and at the nm scale, and propose a simple idea to estimate the AFM magnon velocity over nm distances. Here, we utilize the optically-driven spintronic THz emission scheme based on a non-magnetic/ferromagnetic (NM/FM) bilayer, which has demonstrated to probe the ultrafast spin current generation in the FM layer. Moreover, we use a NM/AFM insulator/FM trilayer to probe the spin transport [1]. The optically-excited spin current in the FM layer can be transferred to the NM layer through the AFM insulator layer via the magnon current. The magnon current is

subsequently converted into the transverse charge current in the NM layer via spin-charge conversion such as the inverse spin Hall effect (Fig. 1). Because the emitted THz waveform is recorded in the time domain, this enables the direct estimation of the magnon propagation time and subsequently the magnon velocity over nm distances [2]. In the experiment, Bi_2Te_3 (6 nm)/NiO (0–50 nm)/Co (3 nm) trilayers are used. Interestingly, the magnon velocity is not constant but varying with the NiO thickness over the nm scale. More importantly, the maximum velocity is found to be ~650 ±50 km/s for the NiO thickness of 15 nm. With considering the fundamental magnon group velocity of ~40 km/s that was estimated by indirect methods such as inelastic neutron scattering, our direct estimation reveals the superluminal-like propagation of AFM magnons over the nm scale. Our theory suggests that for the magnon propagation at the nanoscale a finite damping makes the dispersion anomalous at a low wavenumber regime and subsequently yields the superluminal-like magnon velocity. Magnon linewidth estimation using low-wavenumber Raman scattering agrees with the theory and further supports the damping-induced superluminal-like magnon propagation. This superluminal-like magnon velocity owing to the damping is of considerable interest from the viewpoint of fundamental science as it has been believed that the damping always results in a detrimental effect on various spin-related phenomena. It is also of importance from the application point of view because it allows one to operate nanoscale magnonic devices at a far higher speed than what has been thought to be the fundamental limit of magnonic devices.
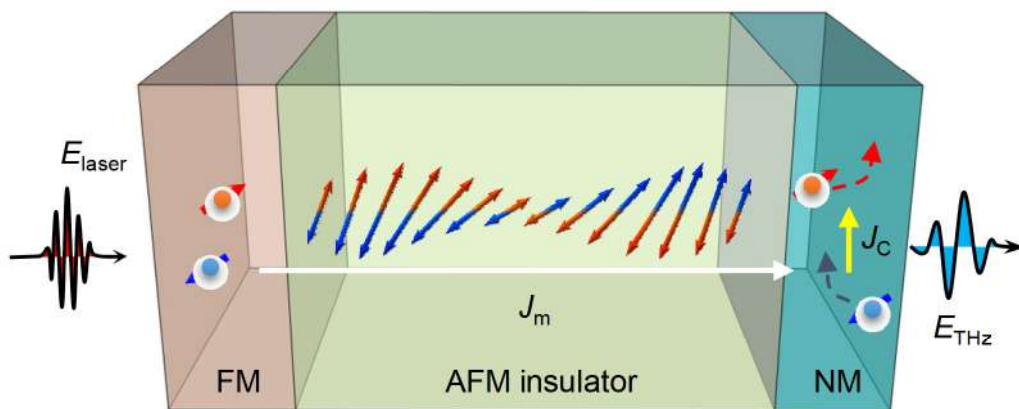
Fig. 1. Schematics of optically-driven terahertz emission via spin-charge conversion mediated by antiferromagnetic magnon transport

References

[1] Yi Wang, Dapeng Zhu, Yumeng Yang, Kyusup Lee, Rahul Mishra, Gyungchoon Go, Se-Hyeok Oh, Dong-Hyun Kim, Kaiming Cai, Enlong Liu, Shawn D. Pollard, Shuyuan Shi, Jongmin Lee, Kie Leong Teo, Yihong Wu, Kyung-Jin Lee and Hyunsoo Yang, Magnetization switching by magnon-mediated spin torque through an antiferromagnetic insulator, *Science* **366**, 1125-1128 (2019).

[2] Kyusup Lee, Dong-Kyu Lee, Dongsheng Yang, Rahul Mishra, Dong-Jun Kim, Sheng Liu, Qihua Xiong, Se Kwon Kim, Kyung-Jin Lee and Hyunsoo Yang, Superluminal-like magnon propagation in antiferromagnetic NiO at nanoscale distances, *Nat. Nanotechnol.* **16**, 1337-1341 (2021).

Introduction of Magnetic Tunnel Junction Materials (Sputtering Target)

Young Jin Park[*]

Materion Advanced Material Group

There is an increased demand for a variety of superior quality magnetic tunnel junction (MTJ) materials to support the expanding market for mass data storage, mobile platforms and other automotive/industrial applications.

These materials lay the cornerstone for the transition to STT-RAM (Spin-Transfer Torque Random-Access memory) technology. As the Number One global supplier of MTJ materials, Materion manufactures critical components for the advanced memory and data storage industry.

CoFeB: Recent Target Improvements
- Enhancement: Low Oxygen, High Density for low-through-high boron content – goal to reduce particles
- Method Improved: Powder formation, pressing tech
- This optimization is part of a larger effort within Materion to develop advanced powder metallurgical methods for future CoFeB compositions.

Materion utilizes two distinct fabrication methods for CoFeB-based sputtering targets, depending on composition and application:

Melting, Casting, Rolling

Induction coil
Refractory crucible
Mold
Vacuum Melting
Rolling and Heat Treat
Waterjet, Lathe, Grind, Bond

Powder Metallurgy

Powder Formed in Varied Morphologies
Uniaxial Hot Press
Lathe, Grind, Bond
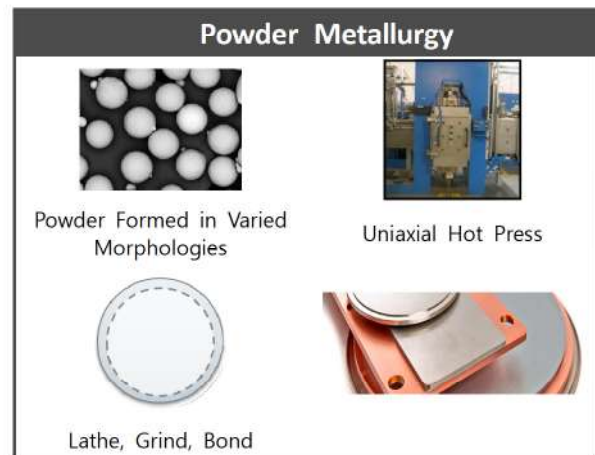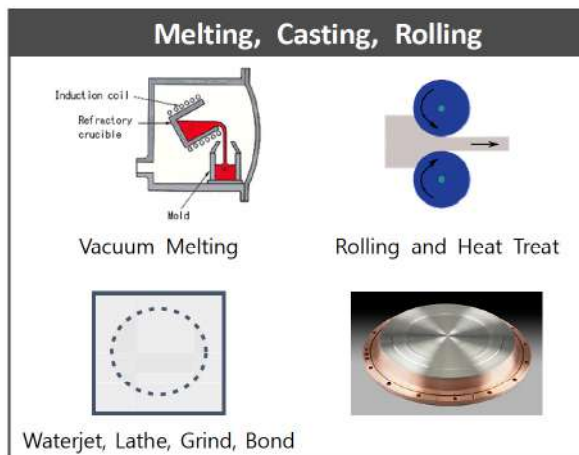
Session 2

구두발표 II
'Spintronics II' / 'Magnetization Dynamics'
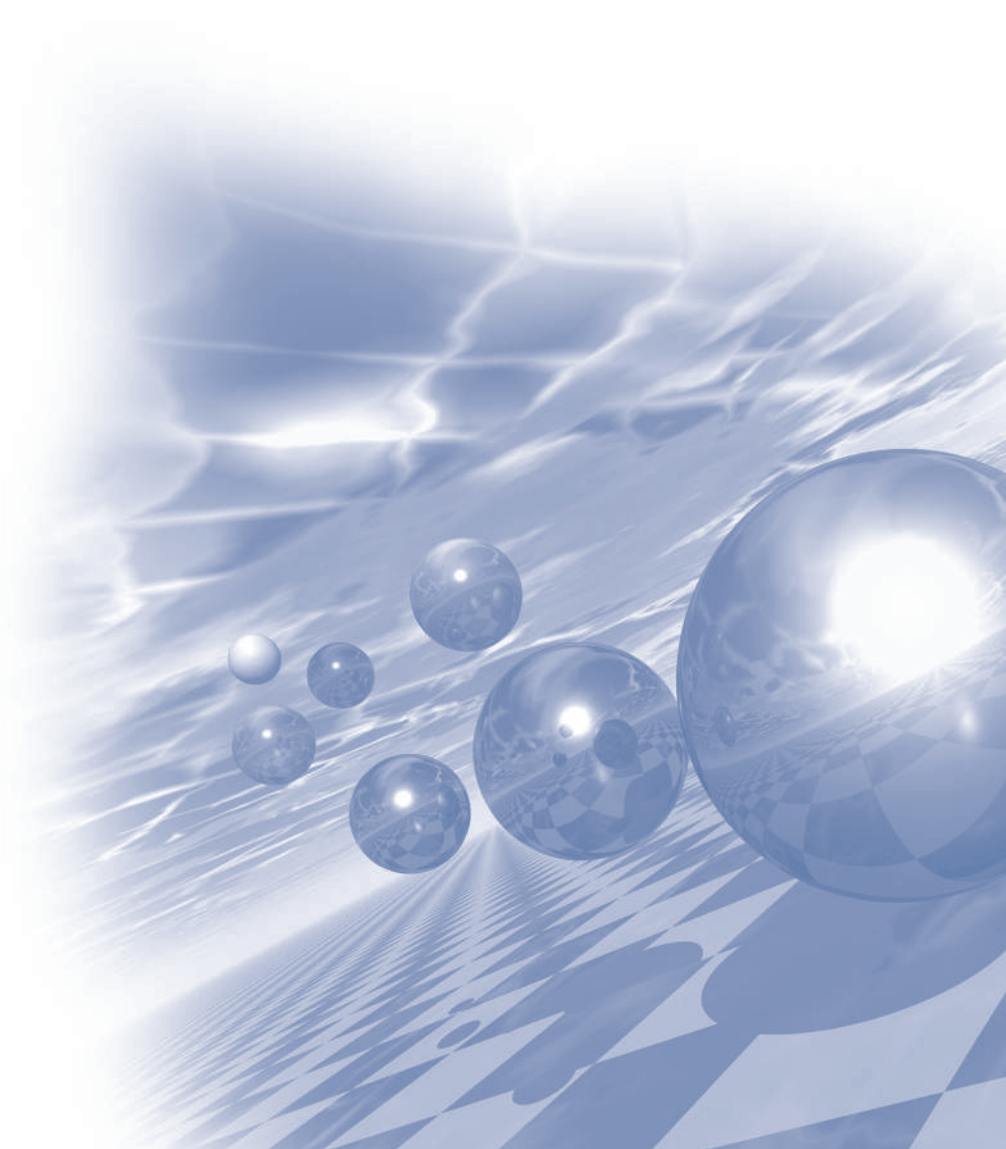
Optical methodologies for detections of spin, magnon, and orbital

Young-Gwan Choi[1*] and Gyung-Min Choi[1,2†]

[1]Department of Energy Science, Sungkyunkwan University, Suwon 16419, Korea
[2]Center for Integrated Nanostructure Physics, Institute for Basic Science, Suwon 16419, Korea

Observation of an angular momentum of a system is a key element of studying magnetic properties in condensed matters. For example, electrical measurements have been widely used to characterize angular momentum transports related to the spin/orbital effects, such as magneto resistance, anomalous Hall effect, spin-torque ferromagnetic resonance measurements, and so on. However, electronics-based methodologies have limitations in terms of a time-resolved measurement in a picosecond time scale and a selective detection of a surface region. Here, we introduce optical methodologies for observations of net angular momentum of thin metallic films driven by spin, magnon, and orbital generations with the advantages of ultrafast and surface sensitive detections. At first, we observe ultrafast dynamics of a magnetization driven by the spin Hall effect in a ferromagnet thin film (FM)/normal metal (NM) heterostructure. To excite the ferromagnetic resonance mode in the FM, an electric pulse is used with a photo-switch and a pulsed laser. The magnetization vectors are measured by magneto-optical Kerr effect (MOKE). Second, we show the spin wave modes in a soft magnet thin film, Co_xB1-x, in picosecond timescales *via* the optical spin-orbit torque. Moreover, we directly measure the spin/orbital accumulations without the ferromagnet layer with an application of the electric bias as evidence of spin/orbital Hall effects in transition metals. We argue that static and time-resolved optical technique can provide efficient ways of exploring magnetic properties of spin, magnon, and orbital in condensed matters.

Controlling Chaos in Skyrmion Dynamics

Gyuyoung Park[*] and Sang-Koog Kim

National Creative Research Initiative Center for Spin Dynamics and Spin-Wave Devices, Nanospinics Laboratory, Research Institute of Advanced Materials, Department of Materials Science and Engineering, Seoul National University, Seoul 151-744, South Korea

Nonlinear dynamics is a root of unpredictability in nature. Prominent examples include a motion of planet. Orbital trajectories of planets lose their order when chaos arises. The absence of order leads to the emergence of a complex pattern. Magnetic skyrmion, a robust topological defect, also shows non-trivial core trajectories when its nonlinearity increases. Based on skyrmion's nonlinear dynamics [1,2], here we step further into chaotic dynamics. This chaos can be anticipated with nonlinear Thiele's equation of motion [3-5]. The skyrmion dynamics within the chaotic regime show highly sensitive dependence on their initial condition. In addition, different types of chaotic behaviors exist in a single skyrmion when they are driven by different methods. Complex patterns inside the chaotic skyrmion motion can be the potential for device implementations. Understanding the chaotic behavior helps to control its complex dynamics such as phase-locking and condition mapping. The chaotic controlling may offer new-paradigm logic devices.

References

[1] Y. -f. Chen et al., *J. Magn. Magn. Mater.* **458,** 123 (2018).

[2] C. Reichhardt et al., *Phys. Rev. B* **104**, 064441 (2021).

[3] K. Y. Guslienko et al., *Phys. Rev. B* **82**, 014402 (2010).

[4] J. -H. Shim et al., *Appl. Phys. Lett.* **99**, 142505 (2011).

[5] A. Dussaux et al., *Phys. Rev. B* **86**, 014402 (2012).

Tunable magnetic transition temperature and enhanced magnetoresistance of FeRh thin film by Co doping

Sang-Il Seo[*], Mintae Park and Myung-Hwa Jung

Department of Physics, Sogang University, Seoul 04107, Republic of Korea

FeRh is an interesting material with a temperature-induced first-order magnetic transition from antiferromagnetic (AFM) to ferromagnetic (FM) phase This magnetic transition occurs near 370 K above room temperature, and it is accompanied with giant magnetoresistance, which make FeRh expected to be applied to spintronics. For FeRh to be applied as a spintronic element, it is necessary to adjust the transition temperature to a desired one. Since the magnetic transition is closely associated with a small volume change (less than 1%), doping with different transition metals is one of the methods to effectively tune the transition temperature. In this study, we fabricated pristine FeRh(001) and Co-doped FeRh(001) thin films on MgO(001) substrates by using the magnetron co-sputtering method with FeRh alloy and Co targets. We controlled the Co target gun current and obtained 1~2% Co-doped FeRh thin films. From the energy dispersive spectroscopy measurements, the Co atom seems to be substituted for the Rh site, which can influence a change of magnetic interaction. Both magnetic and transport data revealed that the magnetic transition temperature dramatically decreases by more than 100 K for the Co doping of 1%, while the lattice parameters of Co-doped FeRh is same to the pristine FeRh. As the amount of Co doping increases, the transition temperature difference between heating and cooling process, ΔT becomes large, and the magnetization difference between AFM and FM phase, ΔM becomes small. Nevertheless, the magnetoresistance change of Co-doped FeRh films between the two phases becomes large about 60%, which is larger than that (40%) for the pristine FeRh film. These results offer potential applications in the fields of magnetic random access memory and antiferromagnetic spintronics.

Spin-orbit torque of W-V alloy based magnetic heterostructures

Jeong Kyu Lee[1*], Gyu Won Kim[1], Taehyun Kim[1], Min Hyeok Lee[1],
In Ho Cha[1], Jiung Cho[2], Young Keun Kim[1]

[1]Department of Materials Science and Engineering, Korea University, Seoul 02481, Republic of Korea
[2]Western Seoul Center, Korea Basic Science Institute, Seoul 03759, Republic of Korea

Materials used for spin-orbit torque (SOT) switching-based magnetic memory device fabrication affect its properties. Even though β-W is well known for its incredible charge-to-spin conversion property, alloys based on it have been rarely studied because they lack phase stability [1]. Here, we study spin-orbit torque properties of W-V alloy based magnetic heterostructures.

We sputtered $W_{100-x}V_x$ (5)/CoFeB (2.5)/MgO (1)/Ta (2) magnetic heterostructures onto thermally oxidized Si wafers under a base pressure below 5×10^{-9} Torr. The compositions of W-V alloys were controlled by changing sputtering power densities during co-sputtering. X-ray diffraction confirmed that β-W maintained up to a V content of 20 at%. Co-V alloys were formed when V content exceeded 60 at%. Spin-orbit torque properties were measured by utilizing harmonic Hall measurement [2]. The maximum damping-like torque efficiency was obtained when W and V contents were 80 at% and 20 at%, respectively. Phase transition from β-W to α-W occurred as V content exceeded 20 at%, leading to a dramatic decrease in damping-like torque efficiency [3]. We also fabricated W (5)/CoFeB (0.9)/MgO (1)/Ta (2) and $W_{80}V_{20}$ (5)/ CoFeB (0.9)/MgO (1)/Ta (2) heterostructures that exhibit perpendicular magnetic anisotropies. These samples were used to obtain optical microscope images and determine switching current densities. We used Magneto-Optical Kerr Effect microscope to observe and obtain current-induced spin-orbit torque switching images. The switching current is greatly reduced when $W_{80}V_{20}$ is used instead of pristine W and we expect $W_{80}V_{20}$ alloys to function as outstanding spin current source layers in magnetic memory devices in the future.
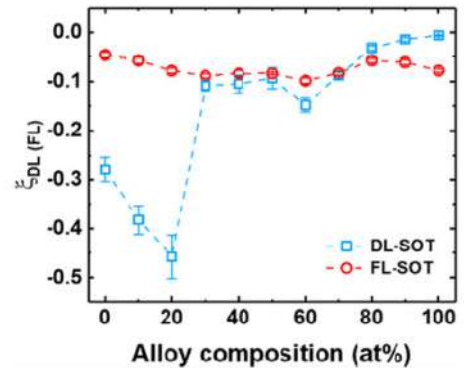
Fig. 1. SOT efficiencies of $W_{100-x}V_x$/CoFeB/MgO/Ta structures

References

[1] K.U. Demasius *et al.*, Nat. Commun. 7, 10644 (2016)
[2] C. O. Avci *et al.*, Phys. Rev. B 90, 224427 (2014)
[3] C.F. Pai *et al.*, Appl. Phys. Lett. 101, 122404 (2012)

Symposium 3

'Permanent Magnetics' &
'Electro-Magnetic Energy Conversion'
공동세션
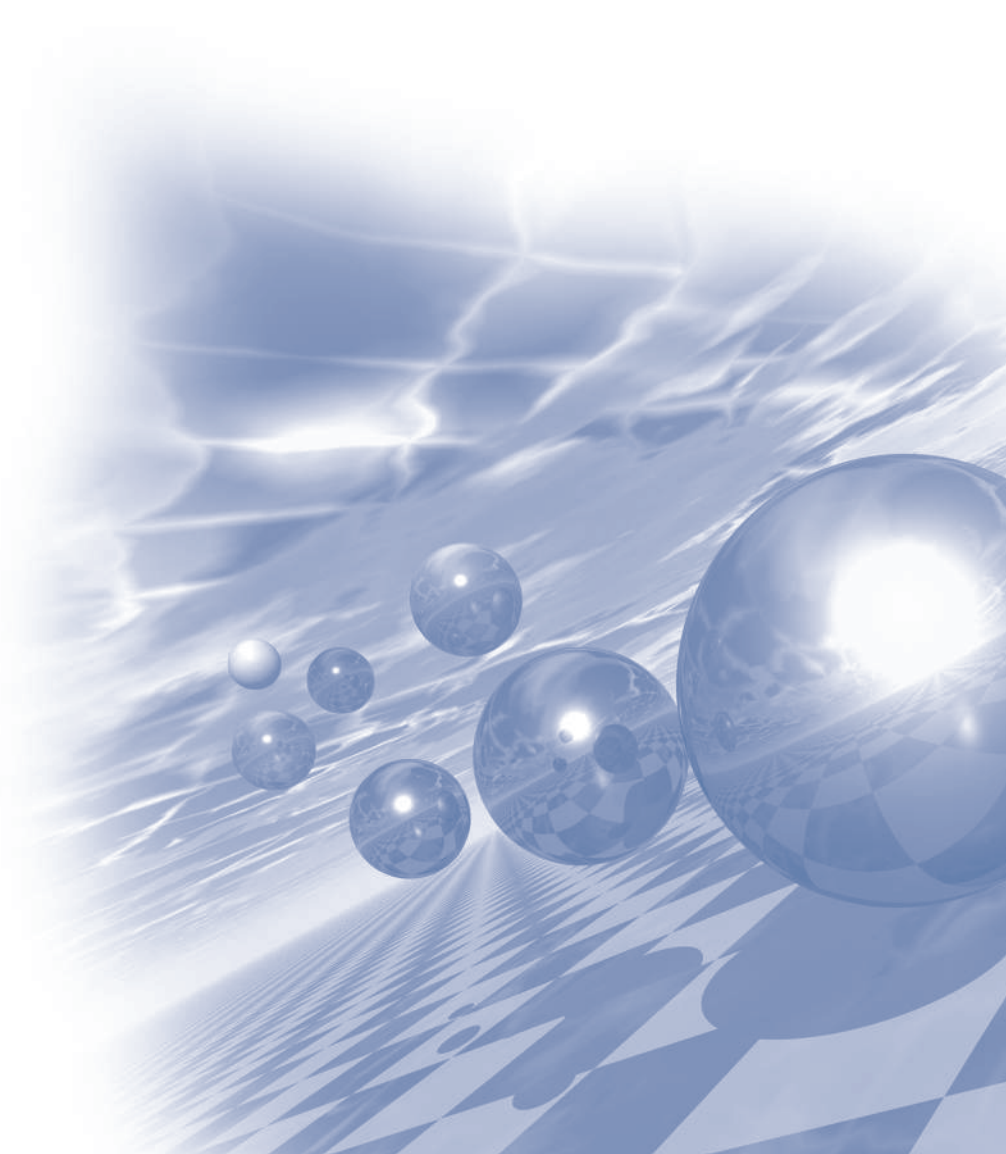
Current Status and Research & Development Trend of magnetic materials used for Home appliance Motors

Song E Park[*]

Motor Element Technology R&D, Component Solution Business, LG Electronics, Changwon, Korea

Magnetic materials, which are electrical steels used in motor cores material and that permanent magnets, are one of the important components in motors. In particular, Nd sintered magnets have the best magnetic properties among permanent magnets and are being applied to various motor developments, and the motor industry is considering attention to not only the research and development trend of Nd sintered magnets but also the Rare earth trend after the cost soared in 2011.

According to the correlation between permanent magnets and motors, the technology of permanent magnets has great influence on the technology development of motors. Therefore, for the continuous improvement of the motor and magnet industries, motor developers should understand the trend of permanent magnet and magnet developers should develop technologies that reflect the properties required in applied products.

This article describes the type of magnet used in motors for home appliances, development direction of motors, and the technology of magnet necessary for motors in the future.

Development of high-performance and cost-effective Nd-saving Nd-Fe-B hot-deformed magnets

Tae-Hoon Kim[1*], Ga-Yeoung Kim[1,2], Hee-Ryoung Cha[1], Jung-Goo Lee[1†]

[1]Department of Magnetic Materials, Korea Institute of Materials Science, Changwon, Korea
[2]Department of Materials Science and Engineering, Pusan National University, Busan, Korea

In this presentation, we report a state-of-the-art development of high-performance and cost-effective 30% Ce- and/or La-substituted Nd-Fe-B hot-deformed magnets [1-3]. We found that the [001] texture and microstructure of the RE-rich grain boundary phases, which are the factors that determine the remanence and coercivity of hot-deformed magnets, were deteriorated by the Ce- and Ce-La-substitution. This is because the volume fraction of the RE-rich liquid formed in the grain boundaries during the hot-press and hot-deformation decreased due to the Ce- and Ce-La-substitution, thereby increasing the friction between the 2:14:1 grains while the c-axes of grains were aligned by grain rotation and decreasing the RE concentration of grain boundary phases. This indicates that there is room for further improvement in both the remanence and coercivity of the Ce- and Ce-La-substituted magnets by introducing additional liquid into the grain boundaries prior to hot-press and hot-deformation. By applying the Nd-Cu infiltration process to the melt-spun ribbons (intermediate infiltration, I-infiltration), both the remanence and coercivity of the Nd-saving $(Nd_{0.7}Ce_{0.3})$-Fe-B and $(Nd_{0.7}Ce_{0.225}La_{0.075})$-Fe-B hot-deformed magnets were successfully improved, as shown in Fig. 1-i. In addition, in order to increase the magnetic performance of 30% Ce-substituted hot-deformed magnets further by suppressing the formation of the Ce-dissolved $REFe_2$ phase, which primarily limits [001] texture development and RE-rich grain boundary phase formation, amorphous melt-spun precursors were used to fabricate 30%-Ce-substituted hot-deformed magnets. By suppressing the
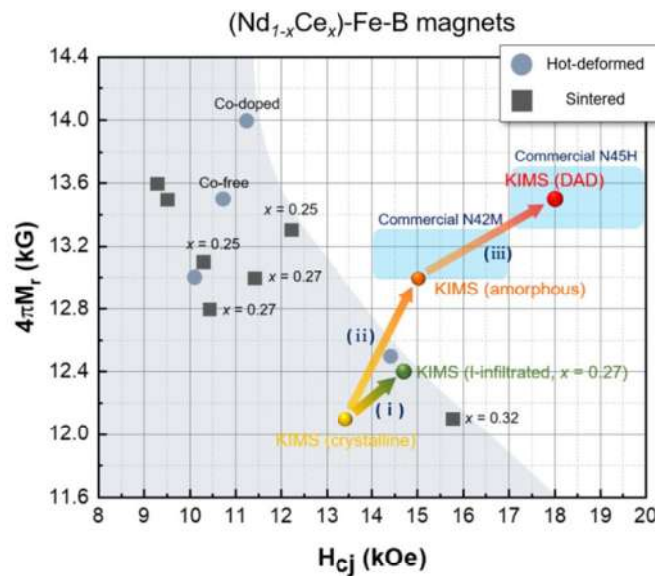
Figure 1. H_{cj} versus $4\pi M_r$ of $(Nd_{1-x}Ce_x)$-Fe-B anisotropic magnets with $0.25 \leq x \leq 0.32$. The data points without information about x correspond to magnets with x = 0.3.

formation of REFe$_2$ phase from the precursors, the c-axis alignment of 2:14:1 platelets in the magnets due to grain boundary sliding and rotation improved, and the Nd/Ce-concentration of grain boundary phases in the magnets increased. As a result, both coercivity (H$_{cj}$) and remanence (4πM$_r$) of the magnets noticeably increased to 15 kOe and 13 kG, respectively, in relation to those of the magnets fabricated from crystalline precursors containing an REFe$_2$ phase (H$_{cj}$ = 13.4 kOe, 4πM$_r$ = 12.1 kG), as shown in Fig. 1-ii. The magnetic performance of the 30%-Ce-substituted magnets developed in this work is sufficient to replace the N42M-graded commercial Ce-free magnets, as shown in Fig. 1. Furthermore, by developing a new method (DAD, Dual-Amorphous precursor-Deformation), we finally succeeded in fabricating the 30%-Ce-substituted Nd-Fe-B hot-deformed magnets with a very high hard magnetic performance comparable to N45H-graded commercial Nd-Fe-B magnets, as shown in Fig. 1-iii.

References

[1] G. Y. Kim, T. H. Kim, H. R. Cha, S. H. Lee, D. H. Kim, Y. D. Kim, J. G. Lee, J. Mater. Sci. Technol. In-press (2022).

[2] G. Y. Kim, T. H. Kim, H. R. Cha, S. H. Lee, D. H. Kim, Y. D. Kim, J. G. Lee, Scripta Mater. **214**, 114676 (2022).

[3] G. Y. Kim, T. H. Kim, H. R. Cha, T. H. Kim, S. H. Lee, D. H. Kim, J. G. Lee, To be submitted (2022).

Phase Transformation and Deformation Behavior of Fe-rich Permanent Magnetic Materials

Jihoon Park[*], Jung Tae Lim, Hui-Dong Qian, Chul-Jin Choi[†]

Powder Materials Division, Korea Institute of Materials Science, Changwon,
Gyeongsangnam-do 51508, Republic of Korea

The magnetic properties of $ThMn_{12}$-type Fe-rich compound, including magnetic anisotropy field (H_A), saturation magnetization (M_s), and Curie temperature (T_C), are known to be superior to those of Nd-Fe-B magnets. However, the low intrinsic coercivity (H_{ci}) and difficulties in grain alignment due to nano-scaled single domain size hinder the $ThMn_{12}$-type Fe-rich compound to be used as a permanent magnet. Although many studies have been conducted to overcome these problems, the achieved remanent magnetization (M_r) and H_{ci} were far lower than the theoretical values [1-4]. The obstacles that must be overcome to achieve high M_r and H_{ci} are difficulties in precisely controlling the phase transformation and grain growth during heat treatment and aligning the nano-scaled grains. However, attaining nano-sized grains of $ThMn_{12}$-type phase through high-temperature heat treatment is a very difficult process due to rapid grain growth. Moreover, pulverization into nano-sized powder and their magnetic alignment have oxidation and decomposition problems and difficulties in achieving high squareness, respectively.

Therefore, in this study, the phase transformation mechanism, formation of grain boundary phases, and deformation behavior of the Fe-rich compound were investigated to obtain high performance rare-earth lean permanent magnetic materials. Ingots of Fe-rich compounds were prepared using arc-melting process, followed by obtaining nanocrystalline ribbons by melt spinning method. The as-prepared ribbons were pressed into bulk samples and heat treated for the phase transformation and sintering. The fabricated bulk samples were subjected to hot deformation process to align the grains and achieve high squareness in the hysteresis loops. The compositional dependence of the phase transformation from the amorphous phase to the $ThMn_{12}$-type phase and the formation of grain boundary phases will be introduced. In addition, the physical and magnetic properties of the hot deformed bulk samples will be discussed.

References

[1] P. Tozman, H. Sepehri-Amin, Y. Takahashi, S. Hirosawa, K. Hono, *Acta Mater.* 153 (2018) 354–363.

[2] I. Dirba, H. Sepehri-Amin, T. Ohkubo, K. Hono, *Acta Mater.* 165 (2019) 373–380.

[3] I. Dirba, Y. Harashima, H. Sepehri-Amin, T. Ohkubo, T. Miyake, S. Hirosawa, K. Hono, *J. Alloys Compd.* 813 (2020) 152224.

[4] I. Dirba, J. Li, H. Sepehri-Amin, T. Ohkubo, T. Schrefl, K. Hono, *J. Alloys Compd.* 804 (2019) 155–162.

In-situ Observation of Magnetic Skyrmion Crystal Formation from the Conical phase : Kinetics

Tae-Hoon Kim[*]

Department of Materials Science and Engineering, Chonnam National University, Gwangju 61186, South Korea

Magnetic skyrmion is a nanoscale vortex-like spin structure that have attracted considerable interests as information carriers for future spintronic devices. In spite of extensive previous research on skyrmion imaging and formation mechanisms, the microscopic mechanisms that control their formation and evolution are still unclear, and the kinetic of the SkX development is much less understood because of the ultrafast spin rotation and high sensitivity to external perturbations. Here, using in-situ Lorentz transmission electron microscopy, we demonstrate that skyrmion crystals (SkXs) can nucleate, grow, and evolve from the conical phase in the same ways that real nanocrystals form from vapors or solutions. And the dynamics of SkX formation was successfully measured with precise control of both the temperature and the magnetic field. The Avrami equation and constant describe the transition process suggesting one-dimensional heterogeneous nucleation of individual skyrmions. A modified Arrhenius rate law is established, with an energy barrier that has a square-root dependence on temperature and a quadratic dependence on the magnetic field. This study paves the way toward precise and predictable manipulation of topological spin structures.

Ce-based RE-Fe Permanent Magnet Designing; First principles calculation approach

Ji Hoon Shim[*]

Department of Chemistry, Pohang University of Science and Technology, Korea

We have investigated the enhanced magnetic properties for Nd-free RE-Fe permanent magnet based on computational materials design using density function theory calculations. Based on Ce-based permanent magnet, we have searched the permanent magnet candidates through the database of the available crystal structures. By calculating the saturated magnetic moment, magnetic anisotropy, and transition temperatures, we selected the possible Ce-based permanent magnet. We also discuss the strategy for designing the permanent magnet by the tuning of crystalline electric field and geometry of the atoms surrounding Ce atoms.

Enhanced magnetic anisotropy in $Fe_{16-x}Al_xN_2$ alloy

Jinho Byun and Jaekwang Lee[*]

Department of Physics, Pusan National University, Busan 46241, Korea

Electronic properties and magneto crystalline anisotropy energy (MAE) of $Fe_{16-x}Al_xN_2$ alloy were investigated in the framework of Density Functional Theory (DFT) combined with Cluster Expansion (CE) method. Based on the second-order perturbation theory, the MAE was evaluated by the spin-orbital coupling (SOC) between the occupied and unoccupied states. We found that the MAE enhancement of $Fe_{16-x}Al_xN_2$ alloy is predominated by the SOC term associated with the dxy-orbital. Moreover, from the orbital decomposed density of states analysis, the MAE is inversely proportional with dxy-orbital -orbital occupation in this alloy. Interestingly, we showed that the MAE of $Fe_{16-x}Al_xN_2$ alloy, with an optimized ratio of Al/Fe of 0.14, significantly enhances about 250% compared to that of the pristine $Fe_{16}N_2$ We thus expect that these $Fe_{16-x}Al_xN_2$ alloy will be promising candidates for strong rare-earth free permanent magnets.
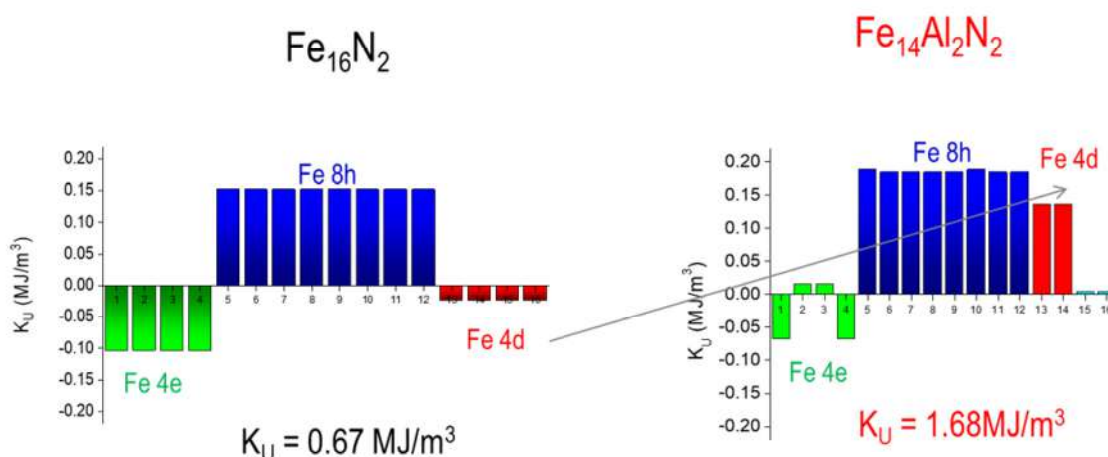
Fig. 1. Enhanced magnetic anisotropy in $Fe_{14}Al_2N_2$ alloy

해석적 방법을 이용한 마그네틱 기어의 자속밀도 및 토크 해석

이훈기[*], 최장영[†]

충남대학교

기어는 가전제품이나 자동차 시스템 그리고 풍력 발전기, 컨베이어 벨트, 고속 및 저속으로 회전하는 기기 등 많은 산업 분야에서 사용되고 있는 기계적 장치로, 1차측 톱니와 2차측 톱니가 서로 맞물리며 동력이나 회전을 전달하는 원리를 가진다. 기계식 기어는 주로 금속 재질을 이용하여 제작되며 톱니의 맞물림을 통한 물리적인 접촉으로 인해 기계적인 마찰을 가진다. 이로 인해 기어의 동작 시 진동 및 소음이 발생하고 심한 경우 비틀림 힘에 의한 파손 및 마모가 발생하여 시스템의 수명을 단축시킨다. 이러한 기계식 맞물림을 통해 동력을 전달하는 기계식 기어의 대안으로 자기적 힘의 상호작용으로 동력을 전달하는 마그네틱 기어가 제안되었다. 1900년대 후반 스퍼기어, 웜기어, 베벨기어 같은 기계식 기어의 동력 전달 구조를 단순히 모방한 비접촉식 마그네틱 기어가 제안되었다. 마그네틱 기어는 소음 및 진동 저감, 마찰 손실 제거, 과부하 시 자체 보호 기능 등의 장점을 가지고 있으나, 전체 영구자석 중 일부만이 동력 전달에 사용되는 비효율적인 구조를 가진다는 큰 단점이 존재했다. 또한 기계식 기어에 비해 현저히 낮은 전달 토크 밀도로 인해 산업분야의 관심을 얻지는
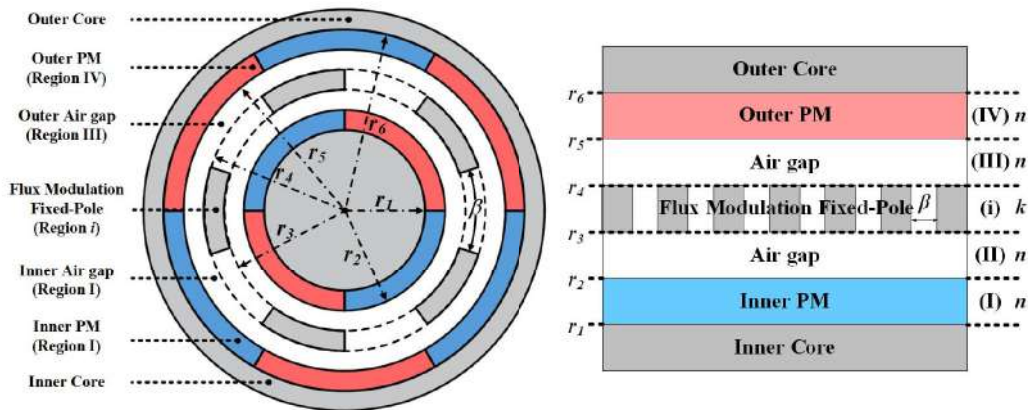
Fig. 1. 해석적 방법을 적용하기 위한 단순화 모델
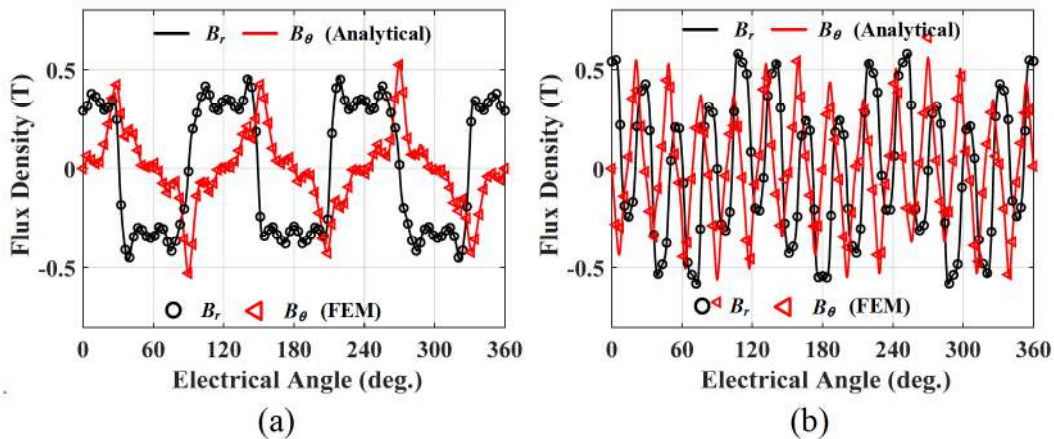
Fig. 2. 자속밀도 해석 결과: (a) 내측 공극 자속 밀도, (b) 외극 자속 밀도

못하였다. 그러나 2001년 영국의 Sheffied 대학의 K. Atallah 교수에 의해 동축 상에 놓인 내, 외측 회전자에서 나오는 자계를 다수개의 변조 철심을 통해 변조시켜 두 회전자 간의의 기어비를 만들어 내는 동축 마그네틱 기어가 제안되었다. 동축 구조를 통해 모든 영구자석이 동력전달에 사용되어 전달 토크 밀도 또한 크게 향상시킬 수 있었다.

　　동축 마그네틱 기어를 해석 및 설계하는 방법에는 일반적으로 알려진 전자계 해석 방법인 수치해석법과 해석적 방법이 존재한다. 수치해석법 중의 하나인 유한요소법은 재질의 비선형 특성을 고려할 수 있을 뿐만 아니라 복잡한 형상을 보다 정확하게 해석 가능하다. 그러나 해석시간이 오래 걸리며 요소 분할 조건 및 설계자의 숙련도에 따라 해석 결과에 영향을 줄 수 있다. 이에 반해, 해석적 방법은 수치해석법에 비해 해석 시간이 짧고 설계 변수 변화에 대한 특성 변화를 이해하는데 유리하다. 마그네틱 기어에 대해 해석적 방법을 적용하는데 어려운 점은 변조 철심 구조를 고려하는 것이고, 1차측에서 2차측으로 전달되는 힘을 예측하기 위해서는 변조 철심 영역을 고려하는 것이 필수적인 과정이라 할 수 있다. 따라서 본 논문에서는 해석적 방법을 적용하기 위해서 해석 모델을 단순화하고, 몇 가지 가정 및 적절한 경계조건을 통해서 각 해석 영역에서의 자계 및 토크 특성 해석을 수행하였다. 해석 결과는 유한요소해석 결과와 비교함으로서, 제시된 해석 방법의 타당성을 검증하였다.

해석적 기법과 랜덤 워크 알고리즘을 사용한
영구자석 동기 전동기의 사이즈 최적 설계

김수민*, 우종현, 이훈기, 이영근, 최장영

충남대학교 전기공학과, 대전시 유성구 99, 34134

영구자석 동기 전동기(Permanent Magnet Synchronous Motor, PMSM)는 고출력, 고효율, 소형화가 가능한 이점을 가지고 있는 전기기기이다. 이러한 이점으로 PMSM는 차량, 선박, 발전기와 같은 다양한 분야에 적용되고 있다. 일반적으로 PMSM의 설계 목표는 저비용, 저소음 및 출력 밀도 향상으로 볼 수 있다. PMSM의 출력 밀도는 단위 부피 또는 무게 당 출력으로 표현된다. 따라서 동일한 토크 및 속도에서 부피 또는 무게를 저감한다면 출력 밀도를 높일 수 있는 결과를 얻을 수 있다. 또한, 부피와 무게가 감소되는 만큼 제작 비용을 절감할 수 있을 것이다. 하지만 설계과정에서 PMSM의 적절한 부피와 무게를 선정하기 위해 전자기 해석을 하는 과정에서 많은 시간이 소모된다. 기존에 사용된 단위 회전자 체적당 토크(Torque per Rotor Volume, TRV)와 전기장하, 자기장하를 사용한 설계 방법은 경험적인 데이터에 의존적인 설계 방법이다. 이를 통한 설계 방법은 설계 사양을 충족시키기 위해 많은 설계 변수를 변경하며 전자기 해석을 수행하게 되면서 상당히 많은 시간을 소모하게 된다. 이를 보완하기 위한 방법으로 해석적 기법과 확률론적 알고리즘을 사용한 최적 설계에 관한 연구가 꾸준히 진행되고 있다.

본 논문에서는 공간고조파법 및 랜덤 워크 알고리즘(Random Walk Algorithm, RWA)을 사용한 PMSM의 최적 설계를 수행하였다. 공간고조파법을 기반으로 PMSM의 전자기 해석 시간을 단축하였으며 확률론적 알고리즘의 전역 최적화 능력은 유지한 채로 PMSM의 설계 과정을 단축시켰다. 해석적 기법에는 크게 유한요소법(Finite element method, FEM)과 해석적 기법으로 나누어 볼 수 있다. FEM은 신뢰할 수 있는 해석 결과를 제공하지만 PMSM의 초기 설계에서 FEM을 이용한 해석은 설계 변수와 성능 간의 분석 결과를 얻기에는 시간이 많이 소요되는 단점이 있다. 또 다른 해석적 기법은 일반적으로 자기등가회로(Magnetic equivalent circuit, MEC)와 공간고조파법을 사용한다. MEC는 간소화된 등가회로를 통해 다양한 형상에 대한 빠른 해석이 가능하지만 재질의 비선형적 요소를 고려한 해석은 어려움이 있어 FEM 해석결과보다 정밀성이 떨어지는 단점을 가지고 있다. 공간고조파법은 FEM보다 빠른 해석이 가능하며 맥스웰 방정식의 복잡한 수식을 통해 전자장을 해석하기 때문에 MEC보다 정확한 결과를 보여준다.

또한, 확률론적 알고리즘은 PMSM의 부피 또는 무게 저감에 초점을 맞추어 목적 함수의 최소 값을 탐색하는 RWA기법을 사용하였다. RWA기법의 가장 기본적인 원리는 현재 위치에서 함수 값이 감소 또는 증가하는 방향으로 조금씩 변수 값을 이동해 나가는 것이다. 즉, 임의의 방향으로 한걸음을 내딛은 후 그 위치에서 어느 방향이 가장 최소 값인지를 탐색 후 그 방향으로 한 걸음을 내딛고, 또 다시 그 위치에서 가장 최소 값 방향을 찾는 과정을 더 이상 감소할 수 없는 최소 값에 다다를 때까지 반복한다. RWA 기법은 이러한 과정을 반복하여 목적 함수의 전역 최소 값이 되는 지점을 탐색한다. 이를 통해 최적화된 PMSM의 사이즈를 탐색하여 최적설계점을 찾는데 이점을 가질 수 있다. 제한 조건으로는 효율 저하를 방지하기 위해 동손과 철손을 선택하였다. PMSM의 동손은 계산식을 통해 산출하였고 철손은 자기장하를 통한 비례식을 사용하여 FEM 해석결과와 비교하였다. 이를 통해 도출된 최적화 모델에 대해 FEM의 해석결과와 비교하여 설계 기법의 타당성을 검증하였다. 따라서 공간고조파법 및 RWA 기법을 사용한 PMSM의 최적 설계는 PMSM의 초기설계과정에서 유용한 설계 방법으로 사료된다.

A Study on the Development Trend of Major Technology for Electric Motor for the Automobile Application

Dong-woo Kang[*]

Depart of Electronic and Electrical Engineering, Keimyung University, Daegu 42601, South Korea

Historically, motor technology was implemented in the early 1800s. As a representative example, various types of motors have been researched and developed, such as a DC motor having a brush and commutator structure to use the stored DC, and an AC motor to which the principle of a rotating magnetic field is applied to use an AC power source. Today, typical commercialized motor technologies can be classified into a total of six types. These are DC motors, brushless motors, induction motors, switched reluctance motors, stepping motors, and universal motors. Each motor technology has been developed to suit different industries. In addition, the performance of the motor is becoming more advanced through the development of materials and production technology. Before the eco-friendly car market opened in earnest, the actuator technology based on DC motor was the mainstream for motor technology for automobiles. In the 2000s, brushless motors with various structures using permanent magnets began to be widely applied to automobile systems.

Motors for eco-friendly vehicles can be divided into traction motors and automotive motors. Automotive motors can be further divided into performance motors, convenience function motors, and safety function motors. Traction motors have different types and roles depending on the power transmission platform technology of P0~P5.

Suitable motor technologies include induction motors, brushless motors, and wound field synchronous motors, which have been recently applied as mass production technologies. The performance motor serves to increase power performance and fuel economy, the convenience function motor drives parts that are not essential but provides convenience functions, and the safety function motor functions to increase the driving stability of the vehicle.

For such automotive motors, DC motors and brushless motors are applied as mass production technologies depending on the purpose, and appropriate technologies are applied and developed according to the required specifications. According to the Japanese industry announcement, the number of major automotive motors is expected to increase from 45.5 per vehicle in 2020 to 63.9 by 2030. Traction motor technology requires high capacity, high cooling, high speed, and light weight, and automotive motors are expected to be developed requiring BLDC, high precision control, and miniaturization.

In 2035, the traction motor technology will become common with an 800V voltage system with a continuous rated output of 70kW, and the output/weight ratio is expected to reach a maximum of 10. In addition, the motor technology for eco-friendly vehicles will focus its capabilities on machine architecture and integration technology, thermal management technology, material (winding, hard magnetic material, soft magnetic material) technology, manufacturing innovation technology, and life cycle industrial management technology.

상미분방정식을 이용한 고전압 충전 커패시터와 공심요크를 이용한 고자속밀도 발생과정에 관한 연구

이성구[1*], 이규원[1], 배재남[2]

[1]동아대학교 전기공학과, Korea
[2]동양미래대학교 전기공학, Korea

이방성 영구자석의 제조를 위해서는 이방화 방향으로 충분히 높은 자속밀도의 외부 자기장을 인가하는 공정이 필요하다. 높은 자속밀도의 외부 자기장 내에서 영구자석의 자구들은 외부 자기장 방향으로 정렬되며, 이후 공정을 통해 정렬된 자구들을 고정시키면 결과적으로 자구들이 한방향으로 정렬된 고성능 이방성 영구자석을 얻게 된다. 최근 영구자석의 추가적인 성능 개선을 위해 높은 압력을 자석재료에 가하여, 재료의 밀도를 높이는 연구가 수행되고 있다. 이를 통해 영구자석의 잔류자속밀도의 개선이 가능하지만, 반대로 이의 이방화를 위해서는 기존보다 더 높은 자속밀도의 외부 자기장이 필요하다는 문제점을 가진다. 본 연구에서는 이와 같은 문제점을 해결하기 위하여, 충전된 커패시터로 여자되는 공심형 솔레노이드 코일에서 발생하는 자기장의 정량적인 크기를 예측할 수 있는 해석모델을 제안하였다. 해당 해석모델은 솔레노이드 코일의 턴수, 솔레이노이드 코일 내부의 직경, 코일의 선경과 같은 주요 설계변수의 닫힌 함수 형태로 표현된다. 이와 같은 해석모델을 이용하면, 주어진 제약조건에서 가장 높은 자속밀도를 생성할 수 있는 솔레노이드 코일의 사양을 단시간에 정확하게 찾을 수 있다는 장점을 가진다. 해당 해석모델은 RLC 직렬회로와 RL 직렬회로로부터 유도된 상미분방정식의 수학적인 해석해로부터 도출되었다. 제안된 해석모델의 타당성은 축대칭성을 이용한 2차원 유한요소해석과의 비교를 통해 검증하였다.

Symposium 7

'Soft Magnetics'
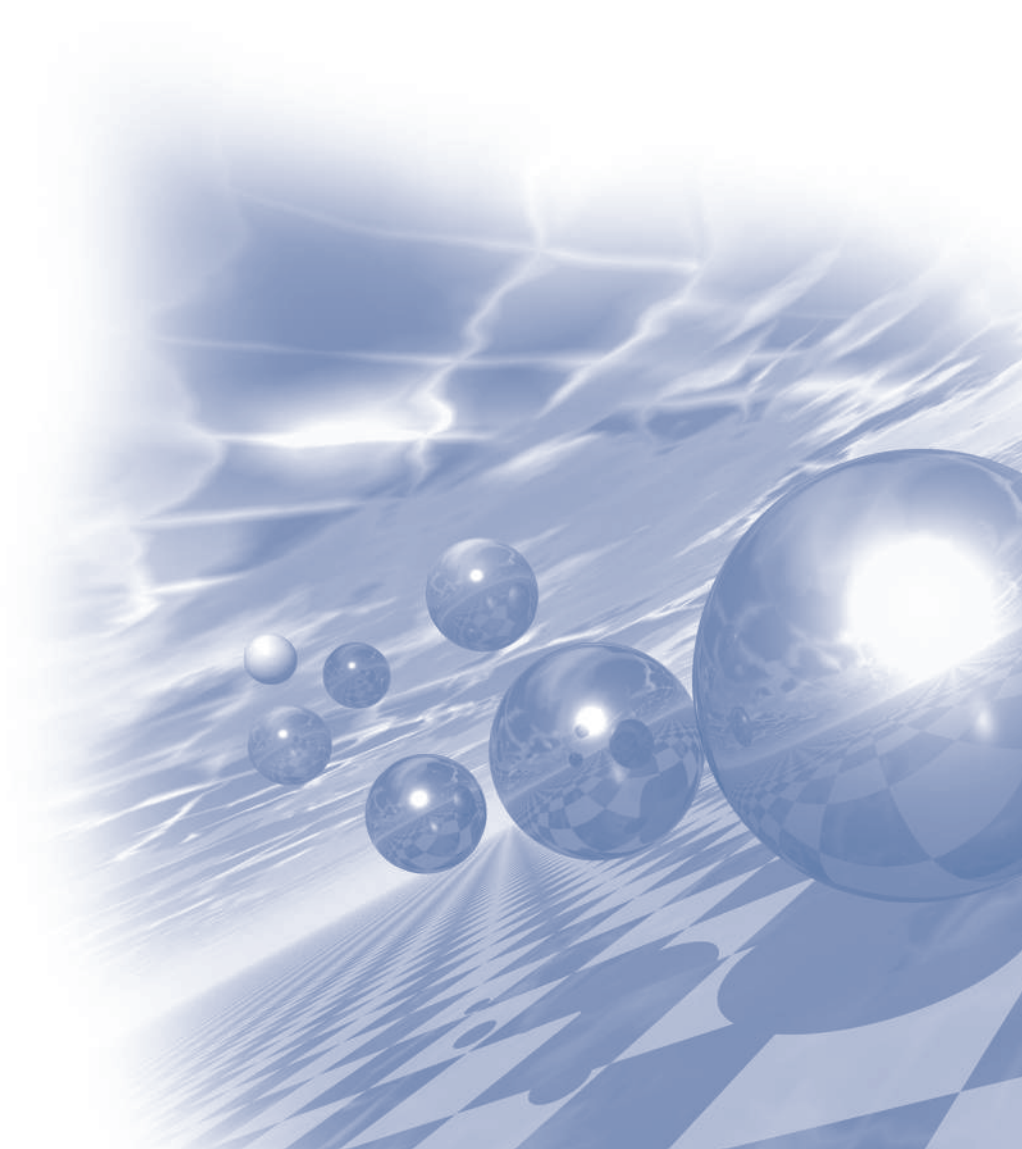
Modulation of electromagnetic wave absorbing properties in hexaferrites composites

Su-Mi Lee, Young-Min Kang[*]

Department of Materials Science and Engineering, Korea National University of Transportation,
Chungju, 27469, Korea
[*]Corresponding author email: ymkang@ut.ac.kr

The recent growth of the multi-functionalization of smart devices, wearable, Internet of Things, and automotive electronics markets has highlighted the importance of electromagnetic (EM) wave shielding or absorbing materials. Ferrimagnetic hexaferrite is one of the promising candidates for EM wave absorbers working at several tens gigahertz (GHz) range owing to its high magneto-crystalline anisotropy. Hexaferrite are divided into six types of M, W, U, X, Y, and Z phases, depending on the stacking structure and composition and exhibit various electromagnetic properties. EM wave absorption of insulating hexaferrites is mostly dependent on the magnetic loss mechanism, which is closely related to the imaginary part of the permeability (μ''). The μ'' of hexaferrites increases when ferromagnetic resonance (FMR) occurs and the FMR frequency varies with the phase type and cation substitution. In this study, it is revealed that various types of hexaferrite including M, Z, X, and W phases can be formed depending on the synthesis temperature and substitution composition, and accordingly, their magnetic and electromagnetic wave absorption properties are changed. It is also derived that series of substitution composition with a trend in permeability spectra which varies step by step according to the gradual change of the substitution composition. In conclusion, a method for designing the material composition to actively control the absorption band of electromagnetic wave in 1-18 GHz range.

New route to manufacture microwave absorbing materials with high magnetic permeability

Young-Tae Kwon[1*], Mi Se Chang[1], Jae Won Jeong[1], Min-Sun Jang[1],
Byeongjin Park[2] and Sang-Sun Yang[1]

[1]Metal Powder Department, Korea Institute of Material Science (KIMS), Changwon, Republic of Korea
[2]Composites Research Division, Korea Institute of Material Science (KIMS), Changwon, Republic of Korea
*E-mail: ykwon87@kims.re.kr

To meet the consumer demands in high-speed wireless communications, fifth generation (5G) telecommunications are rapidly developing for reliable data transmission and better connection in users. However, the high frequency bands around 10-30 GHz have an effect on serious problems in human health and malfunctioning in devices. Notable examples are the recent breakthroughs in electromagnetic wave absorbing materials (EWAMs), composed of dielectric and magnetic materials for eliminating or attenuating electromagnetic waves. From this point of view, FeCo-based soft magnetic alloys is particularly attractive EWAMs due to their performances, including high saturation magnetization (M_s) of 2.45 T, small coercivity (H_c), and complex permeability. In addition, a structural modulation of the soft magnetic materials provides the magnetic anisotropy, resulting in enhancing the limit of ferromagnetic resonance (f_{mr}) to achieve high initial permeability.

Here, we prepare the FeCo nanowires using a highly-productive thermal plasma synthesis to be utilized as an electromagnetic absorber with exceptionally low reflection loss in the high frequency bands. The composition of FeCo nanowires ranging from 7:3 to 3:7 shows high saturation magnetization of 151 - 227 emu g^{-1}. Subsequently, the planetary ball milling is also implemented for a shape modulation in order to enhance the complex permeability and the reflection loss performance. The shape-modulated FeCo nanochains offer the enhancement in the imaginary part of the complex permeability. The shape modulation is one of the technological advancements in improving the complex permeability of FeCo alloys.

냉각속도 맞춤형 비정질 연자성 합금 개발 및 분말 제조 공정 적용 사례

Jae Won Jeong[1*], Yeong Gyun Nam[1,2], Hea-Ran Kim[1,3], Hyun Aha Im[1,2], Su-Bong An[1,2], Yong-Jin Kim and Sangsun Yang[1]

[1]*Metal Powder Department, Korea Institute of Materials Science (KIMS), 797 Changwondae-ro, Seongsan-gu, Changwon 51508, Korea*
[2]*School of Materials Science and Engineering, Pusan National University, Busandaehak-ro 63beon-gil, Geumjeong-gu, Busan 46241, Korea*
[3]*Department of Materials Science and Engineering, Sungkyunkwan University (SKKU), Suwon 16419, Korea*

Soft magnetic materials are widely used in diverse fields of applications including electronics, motor/generators, electromagnetic wave shielding/absorbing. As the working frequency of electronic devices is continuously increasing and high-efficiency operation is required, the development of reliable and low-loss soft magnetic materials has become an import work.

Fe-based soft magnetic amorphous/nanocrystalline materials are considered ideal materials for magnetic powder cores due to their excellent magnetic properties such as low coercivity, high resistance, and good DC bias characteristics. Due to the disordered configuration of atoms in amorphous alloys, these materials have zero magnetocrystalline anisotropy, which ensures high permeability and low coercivity. In addition, due to their high resistivity, Fe-based amorphous alloys exhibit extremely-low eddy current loss at high frequencies, making them suitable as high frequency soft magnetic composite (SMC) materials.

The most significant limitation of SMCs comprising low-M_s amorphous/nanocrystalline materials is poor DC bias. Enhancing the M_s of amorphous/nanocrystalline materials by carefully managing alloy composition is the best way to enhance permeability retention even with high bias field; however, increasing Fe content in the alloy significantly deteriorates the glass-forming ability of the alloy, and processing through gas or water atomization becomes extremely difficult due to the limited cooling rate ($10^2 \sim 10^6$ K/s) of the process

In this presentation, the fabrication and processing of novel amorphous/nanocrystalline soft magnetic materials for high-frequency and high-efficiency electromagnetic applications will be discussed. Ultra-fine soft magnetic micro powders having amorphous phase were prepared by high-pressure gas/liquid co-injection atomization and their soft magnetic properties were examined. In particular, cooling rates for each process were evaluated and amorphous soft magnetics alloys were developed and applied for each process. Finally, we demonstrate successful fabrication of amorphous soft magnetic powders through gas atomization.

딥러닝을 이용한 Fe-based Metallic Glass 소재의 자기특성 예측

남충희*

한남대학교 전기전자공학과, 대전광역시 대덕구 한남로 70

소재의 설계는 실험을 통한 try-and-error 방법과, 양자역학을 기반으로 하는 계산과학을 이용한 방법 (예, 범밀도함수이론)등이 있다. 이러한 방법을 통한 새로운 소재의 발굴과 응용은 지구상에 존재하는 제한적인 소재의 한계성으로 인해서 배터리소재, 모터소재, 에너지 소재 등 여러 분야에서 중요해지고 있다. 본 연구에서는 연자성소재로 사용되는 대표적인 소재중 하나인 철을 기반으로 하는 비정질 합금(Fe based metallic glass)의 자기적 특성을 예측하였다. 소재의 조성(composition)을 바탕으로 특성인자(feature)를 파이썬 모듈인 pymatgen 과 matminer를 통해서 얻었다. 지도학습의 모델을 적용하기 위해서 144개의 특성인자와 목표값(target value)인 포화자속밀도(saturation flux density: Bs)를 185개 소재에 대해서 데이터 전처리를 통해서 생성시킨 후 딥러닝을 적용하였다. 컴퓨터 비전에서 주로 사용되는 합성곱 신경망(convolutional neural network: CNN)을 이용하기 위해서 네트워크를 구성하였으며, 성능지표는 R^2 값을 사용하였다. 최적의 CNN 네트워크는 Conv2D-Maxpooling2D-Flatten-Dense-Dropout-Dense로 이루어졌으며, convolution 과정에서는 'relu' 활성화 함수를, 마지막 단계는 회귀값 도출을 위해서 'linear'를 사용하였다. 비용함수(loss function)는 'mean_squared_error'를 사용하였으며 최적화(optimizer)는 'Adam'을 사용하였다. 전체데이터의 15%는 test data로 사용하였으며, 이에 대한 예측결과(parity plot)는 그림 1과 같으며, R^2는 0.962이다. 마지막으로, 최근 논문에 XGBoost 등 다른 기계학습 모델을 이용하여 소개된 4개 소재에 대한 포화자속밀도 예측값을 상호 비교하였다[1].
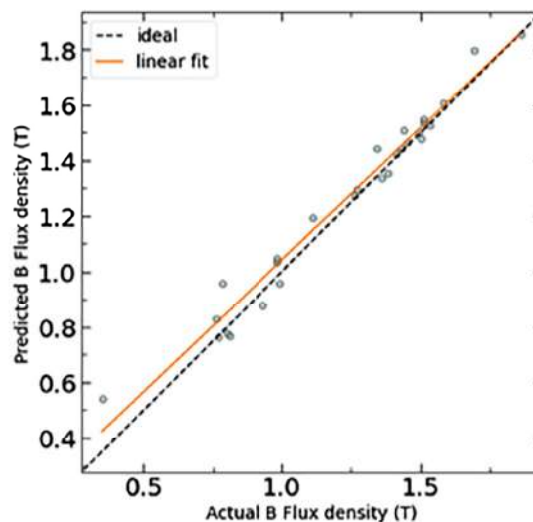
Fig. 1. Parity plot of predicted and actual magnetic flux density of test data

Reference

[1] Zhichao Lu et al., npj Computational Materials 6, 187 (2020)

Magnetic properties of Fe-rich amorphous powders produced by high speed water screen atomization process (HWSP) for power inductor

Tae Kyung Lee[1*], Young Woo Kim[2], Dae Yong Jeong[3]

[1,2]Changsung R&D Center, Korea
[3]Inha University, Korea

Fe-rich $Fe_{93}Si_aB_bC_cP_d$ (wt.%) amorphous powders with high magnetic flux density were prepared in an extremely high cooling rate of over 10^5 K/sec by high speed water screen atomization process(HWSP). The rich $Fe_{93}Si_aB_bC_cP_d$ (wt.%) (wt.%) powders showed the amorphous phase and the Bs value was over 166 emu/g, which is 20% higher than that of conventional product Fe Si B C P alloy powder. Furthermore, consolidated cores of amorphous powders were also fabricated by compact-pressing techniques. The initial permeability of the core in the frequency range up to 10 MHz was about 25, and the core loss at 1 MHz for Bm=0.2T was 250 mw/cm³.
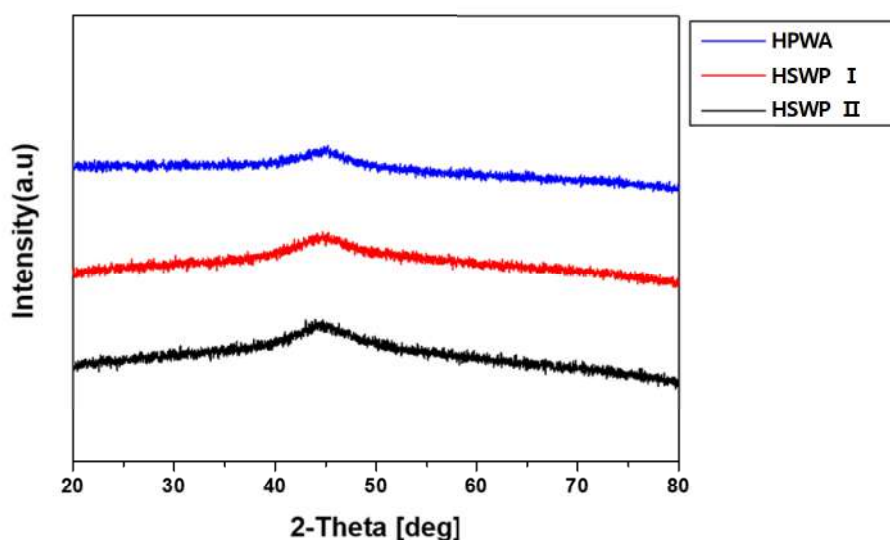
Fig. 1. X-ray diffraction patterns of Fe-rich amorphous powders.
(HPWA: High Pressure Water Atomization, HSWPI: Previous High Speed Water Screen atomization Process, HWSPII : Advanced High Speed water Screen atomization Process)

전력변환부품용 페라이트 코어 개발동향

황득규[*], 이희혁, 이기양

현대모비스 금속재료셀

최근 전기차 등 친환경차 전력변환부품의 고효율화 및 컴팩트화 트렌드에 따른 변압기 및 인덕터 등 자성부품 성능향상을 위한 연구개발이 가속화 되고 있다. 페라이트는 이러한 자성부품에 필수적으로 사용되는 산화물계 연자성 코어 소재로 높은 비저항 값으로 인한 고주파 손실 저감을 구현할 수 있는 장점이 있다. 한편 차량 내 극한 환경을 고려할 때 기존 소재 대비 고온 손실특성이 크게 향상된 페라이트 코어가 요구되므로 현재 해외 선진업체 및 국내 업체간 원소재 관련 기초 연구 및 코어 양산화 개발이 활발히 진행되고 있다.

본 연구에서는 전동화 차량에 적용되는 페라이트 코어 특성 및 기술동향에 대해 고찰하였다. 기존 전력변환 부품에 적용된 페라이트 소재 물성 및 업체별 기술동향을 분석하고 이를 통해 향후 페라이트 소재개발 방향에 대해 제시하고자 한다. 또한 저손실 페라이트 코어 국산화 개발 및 300kHz 이상 고주파 시스템에 적합한 소재 개발사례를 소개하고 향후 고주파 페라이트 개발방향에 대해서도 같이 논의하고자 한다.

High-temperature-resistant soft magnetic composite comprising layered anisotropic Fe-Si chips with tunable double insulation layer *via* high temperature annealing: Synergy of MgO and SiO$_2$

Min-Sun Jang[1*], Bonuk Koo[1,2], Jong-Min Park[1,2], Hea-Ran Kim[1,3], Young-Tae Kwon[1], Sangsun Yang[1] and Jae Won Jeong[1]

[1]Metal Powder Department, Korea Institute of Materials Science (KIMS), 797 Changwondae-ro, Seongsan-gu, Changwon 51508, Korea

[2]School of Materials Science and Engineering, Pusan National University, Busandaehak-ro 63beon-gil, Geumjeong-gu, Busan 46241, Korea

[3]Department of Materials Science and Engineering, Sungkyunkwan University (SKKU), Suwon 16419, Korea

Soft magnetic composite (SMC) which can produce an innovative 3-dimensional core has attracted much attraction as the potential applications in various electrical machinery fields. However, the practical applications of 3D-formed SMC especially for the electric motor have been hindered due to their lower permeability, higher core loss compared to widely-used electrical steels. Furthermore, lack of mechanical strength of SMC can cause safety issues when adopted traction motors for electric vehicles. So, the need for developing high-strength SMC parts is being raised against the material is damaged by fatigue due to exposure to continuous vibration or external shock.

In general, SMC is composed of pure iron powders, and the surface of the iron powders is covered with an inorganic or organic insulation layer, which improve the surface resistance and thus remarkably reduce the eddy-current losses [1]. There is a method to develop high-strength SMC by the densification of the surface insulating materials through annealing at high temperature (>700 °C). However, in general, there is a disadvantage in that insulation is weakened after annealed at high temperature, so an evaluation is necessary to secure both strength characteristics and insulation coating layer retention.

Herein, SMC with different inorganic coating materials which is well-known to withstand at high temperature; SiO$_2$, MgO, and PO$_4$ and stacking layer; mono or double parameters have been considered for magnetic characterization. All of the coated iron particles were prepared by a chemical sol-gel method, and the thickness of the formed coating layer was confirmed to be 500-600 nm on average through a scanning electron microscope and an energy dispersive X-ray spectrometer. In addition, novel SMCs comprising anisotropic chip-type soft magnetic materials are also presented, and demonstrate their enhanced magnetic properties including high permeability and low core loss. It is believed that newly developed high-temperature-resistant SMCs comprising layered anisotropic Fe-Si chips will offer both enhanced magnetic and mechanical properties, and will be the appropriate materials candidates for electric machines with high powder density and high efficiency.

Reference

[1] S.H. Lee, et al., IEEE Trans. Power Syst. 53, 1-4 (2017).

Effects of compressibility on the Magnetic Properties of Soft Magnetic Powder using Water Atomized Iron Powder for Eco-Friendly Automotive Application

Joonchul Yun[*], Hyungon Lyu, Jinwoo Kim and Wonseog Koo

Powder Development & Quality Management Team, Hyundai Steel, Korea

최근 연자성 분말소재는 고주파수 영역에서의 낮은 철손과 3차원 성형에 따른 복잡한 형상 구현 용이성으로 전기강판으로의 접근이 어려운 AFM(Axial Flux Motor) 타입의 모터 적용에 있어 긍정적인 평가를 듣고 있다. AFM 모터용 코어로 요구되는 연자성 분말의 자기적 특성은 높은 자속밀도와 투자율, 그리고 낮은 철손이다. 특히 높은 자속밀도와 투자율을 구현하기 위해서는 재료의 순도와 고밀도의 성형성이 필요함에도 불구하고, 낮은 철손 구현을 위해 Fe 소재에 Si 등을 첨가하는 합금화 공정, 인산이나 산화물 재질의 절연 코팅 공정 등은 성형 시 고밀도화를 방해하고 이로 인해 자속밀도를 감소시키는 원인이 된다. 또한 전자제품 산업 대비 부품의 크기가 대형화 되어 있는 자동차 산업에 연자성 분말소재 적용을 위해서는 고밀도 성형 공정이 필수적이다.

본 연구에서는 연자성 분말소재 중 성형성이 가장 우수하다고 알려진 수분사 공정 및 절연코팅된 Fe 연자성 분말소재를 이용하여, 분말야금 공정 기반으로 윤활제, 분말혼합방법, 성형공정별 성형성과 이 때 성형성이 자기적 특성에 미치는 영향력에 대해 분석하였다. 인산염 코팅이 된 Fe 연자성 분말소재는 다양한 실험 조건에서 성형체 밀도는 7.2g/cc에서 최대 7.5g/cc까지 증가시킬 수 있었으며, 자속밀도는 1.2~1.65T의 범위를 갖는 것으로 확인되었다. 이는 성형밀도와 비례하였고, 투자율은 400~600의 범위로 조사되었는데 성형밀도 외에도 코어 표면의 외관품질과 유의미한 상관관계를 나타내었다. 이는 코어 표면 외관품질이 우수할수록 결정립 내 결함이 적어 자화가 용이하였기 때문이라 판단된다.

Fe$_{48}$Co$_{48}$V$_2$ 합금의 열처리 조건변화에 따른 자기적 특성

Eonbyeong Park[*], Yongchan Kim

Research Institute of Industrial Science and Technology, Materials & Processing Research Laboratory, Korea

Fe$_{48}$Co$_{48}$V$_2$ 합금은 2.4 T 수준의 높은 포화자속밀도와 낮은 철손 그리고 작은 보자력을 가지고 있는 자성재료로서 고성장의 전기자동차와 향후 도래할 UAV시장에서 고효율 모터의 소재로 활용될 가능성이 매우 높다. 그러나, 본 합금 판재를 제조하기 위해서는 단조, 균질화열처리, 열간압연, 급냉열처리, 냉간압연, 풀림열처리 등 다양한 공정의 최적화가 필요하여, 특히 조직을 정밀하게 제어하지 못하면 냉간압연 공정에서 크랙이 발생하거나 낮은 연신율로 인해 압연공정 주 파단이 발생하여 0.15mm수준의 박판 냉간압연이 곤란한 합금으로 알려져 있어, 일부 선진사 업체에서만 생산 및 공급이 가능한 합금이었다.

본 연구에서는 Fe$_{48}$Co$_{48}$V$_2$ 합금을 진공상태에서 용해하여 잉곳을 제조한 후 열간압연을 실시하여 6mm 두께의 판상으로 제조하였으며, 이후 냉간압연 공정을 원활히 진행하기 위해 brittle한 ordering 조직이 발생하지 않도록 730℃ 이상의 온도조건에서 각각 열처리 후 급냉을 실시하여 α+γ phase가 형성될 수 있도록 조직을 제어한 후 냉간압연을 통해 0.2mm두께의 박판을 제조할 수 있었다. 또한 동일한 판재에서 풀림 열처리 유무에 따라 인장강도, 연신율이 크게 변화하였으며, 특히 조직제어를 위한 급냉 열처리 및 풀림 열처리 온도 및 시간에 따라 내부조직 및 잔류응력이 달라져 포화자속밀도, 철손 등의 자성특성값에 큰 영향을 줄 수 있음을 확인하였다.

Manufacturing strategy for a powder-based Fe-6.5%Si steel by powder rolling

Ki Hyuk Kwon[1*], Yong Seok Choi[2], Do Hee Kim[1], Un-Gyeong Baek[2],
Min-Ho Kwon[2], Eon Sik Lee[3]

[1]Materials Research Division, RIST, Pohang, Korea
[2]Material Division R&D part, ZENIX Co., Ltd., Gumi, Korea
[3]Department of Material Science and Engineering, POSTECH, Pohang, Korea

In order to manufacture the high performance of high speed and high horsepower electric vehicles, it is essential to use the traction motors that operate efficiently in higher frequency. However, since the core loss of soft magnetic materials increase in the high frequency band, it is required to develop the soft magnetic material capable of exhibiting low core loss with high magnetic flux density even in high frequency. Among the several soft magnetic materials, Fe-6.5%Si steel is a promising candidate because it can simultaneously show high magnetic flux density, low core loss and low magnetostriction in high frequency compared to the existing Fe-3.5%Si steel and amorphous materials. However, in order to realize the mass production of this material, it is needed to develop the new manufacturing process with lower cost compared to the commercial CVD process even using $SiCl_4$ toxic gas.

Among the various candidate of manufacturing processes, the powder rolling process is promising with the advantage of low cost and being able to manufacture alloys containing high Si and Al, which are traditionally difficult to cast. In order to commercialize this process, manufacturing the steel sheets with high density and design of manufacturing process are important. In this study, the technical ideas for the densification of steel sheet were verified such as a modification of powder size distribution and addition of metal, and the optimization of powder rolling process was carried out.

Introduction of trends in motors with soft magnetic materials

Won-Ho Kim[*]

Department of Electrical Engineering, Gachon University, Seongnam 13120, Korea

최근 출력밀도 향상 및 다품종 소량 생산의 시장 트랜드에 맞추어 연자성 소재를 활용한 전동기에 대한 연구가 많이 이루어지고 있다. 기존 전기강판을 사용하여 제작된 모터는 적층 구조의 제작 특성상 원통형에 방사 방향으로 자속이 통과하는 형태가 대부분이다. 그러나 최근 로봇 관절, 차량용 모터 등 박형 구조에 모터 수요가 늘며 기존 방사 방향 자속보다 효율적으로 토크를 발생시키는 축방향 전동기에 많은 관심이 집중되고 있으며 이를 효율적으로 제작하기 위한 연자성 소재를 활용하는 연구가 다양하게 진행중이다. 연자성 소재를 활용한 연구는 설계 자유도의 극대화를 위하여 3D 프린터의 활용까지 이어지며 최근 다양한 연구가 진행되고 있다.

본 발표에서는 연자성 소재를 활용한 모터의 토크 발생 원리 및 구조, 적용 사례, 3D 프린터 활용 연구 사례 및 향후 전동기에 적용될 연자성소재의 특성에 대한 제안을 포함하고 있다.
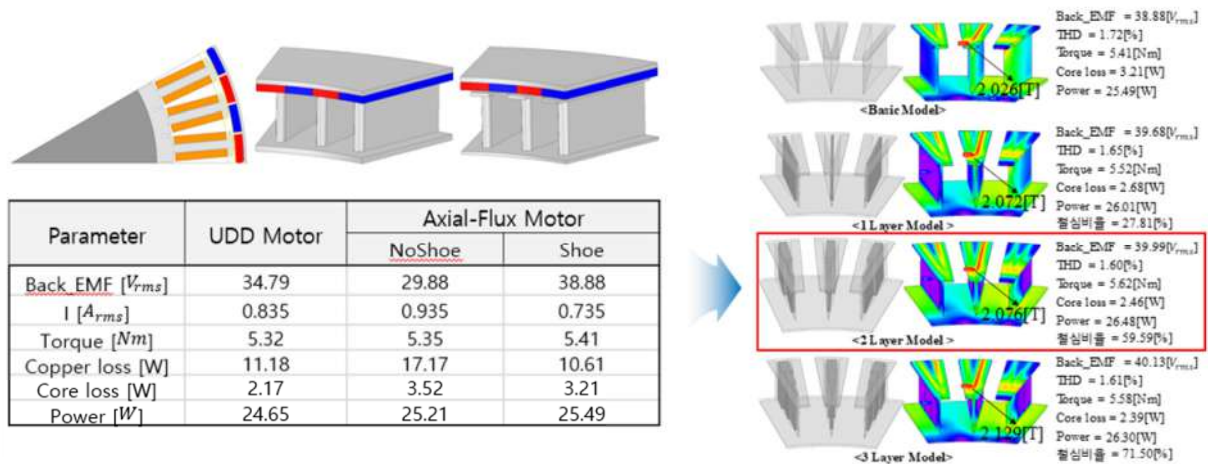
Fig. 1. Comparison of Axial Flux Motor Performance Using 3D Printing

Symposium 1
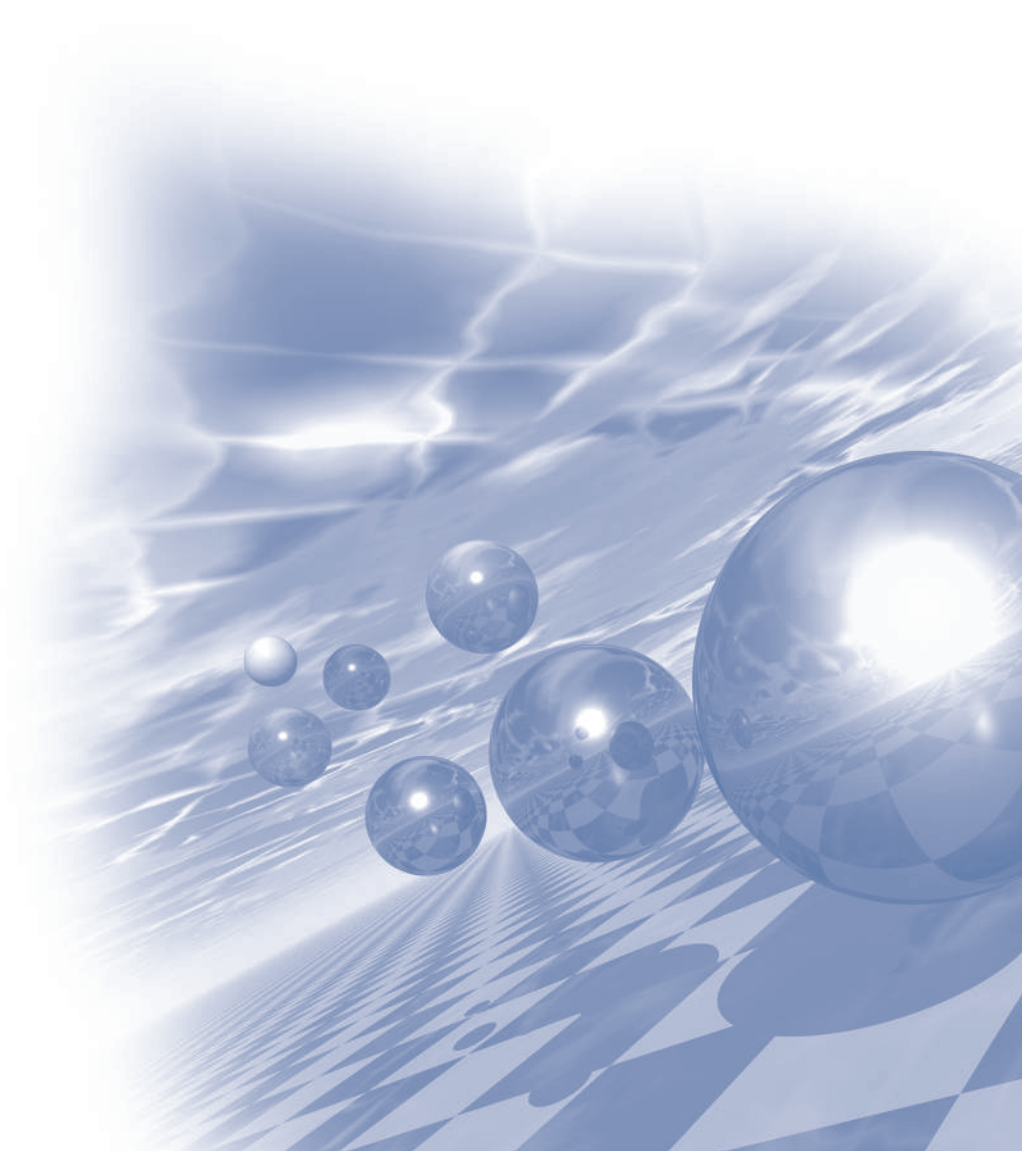
'Quantum Magnetism'

Detecting spin liquids in quantum simulation of frustrated magnetism

Gil Young Cho[1,2*]

[1]Department of Physics, Pohang University of Science and Technology (POSTECH),
Pohang 37673, Republic of Korea
[2]Center for Artificial Low Dimensional Electronic Systems, Institute for Basic Science (IBS),
Pohang 37673, Republic of Korea

Recently, a rapid technological development in quantum simulators allow the simulations of frustrated spin systems including quantum spin liquids. For example, Rydberg atoms and Google sycamore have been used to simulate the Z2 spin liquids. However, there are a number of different classes for completely-symmetric spin liquids. For example, there are four distinct, completely symmetric and fully gapped Z2 spin liquids on the Kagome lattice. This makes them very difficult to distinguish them in quantum simulations (and in solid-state experiments). In this talk, we will discuss how the different spin liquids and symmetry-breaking phases can be diagnosed from the measurement data of the quantum simulators. For this, we will combine the quantum-information theoretic approach with the machine learnings. We will demonstrate the feasibility of our approach on the classically-simulated data.

Interaction of spin superfluid and magnonic topological phases

Seunghun Lee, Gyungchoon Go and Se Kwon Kim[*]

Department of Physics, KAIST, Daejeon 34141, Republic of Korea

In certain magnetic systems, magnon bands can exhibit topologically nontrivial phases, which are often referred to as magnonic topological insulators due to their similarities to electronic topological insulators. The conventional methods to manipulate the magnon-band topology have hitherto required the bulk manipulation of the systems via, e.g., the application of an external magnetic field. In this work, we lift the previous limitation of the magnon topology control on the bulk manipulation by showing that the magnon-band topology can be controlled from the boundary by injecting a spin chirality from the boundary into the bulk, which can be realized, e.g., by utilizing the proximate heavy metal and the resultant interfacial spin Hall effects. More specifically, we propose a scheme to manipulate magnonic topological phases of ferromagnets and antiferromagnets on a honeycomb lattice via chirality injection from the boundaries of the sample [1]. We find that the magnon Hamiltonian subjected to the spin chirality injection possesses a sublattice-symmetry-breaking mass term resulting from the coupling between the spin chirality and the Dzyaloshinskii-Moriya interaction on top of the previously studied bosonic counterpart of the Haldane model [2, 3]. This chirality-induced mass term competes with the known Haldane mass term, which allows us to nonlocally tune the bulk topology from nontrivial to trivial and vice versa by the boundary manipulation. For experimental probes of the chirality-induced topological phase transition, we propose the magnon thermal Hall effect arising from the band topology. The "shoulders" in the thermal Hall conductivity can herald the presence of the proposed phase boundary. Our work leads us to envision that the interfacial chirality injection may offer a nonintrusive means to manipulate the static and the dynamics bulk properties of general magnetic systems.
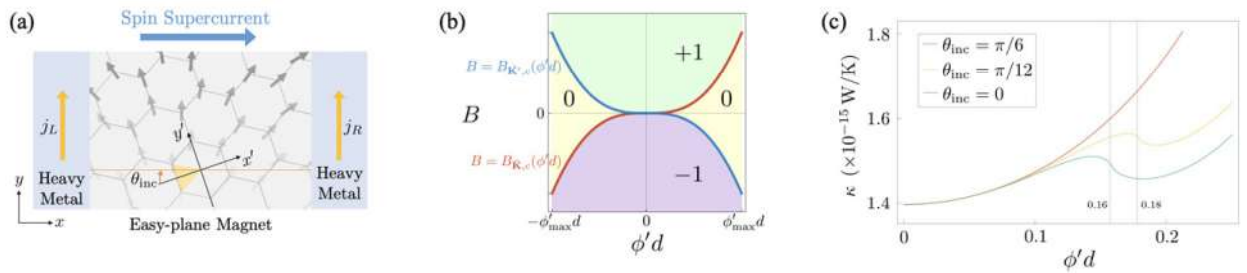
Figure 1: (a) The chirality of spin texture is induced by injecting spin supercurrent into the sample with the incident angle of θ_{inc} via spin Hall effect from the proximate heavy metals. (b) The topological phase diagram for a honeycomb ferromagnet as a function of the injected chirality and the external . The red and blue curves show the phase boundaries between the trivial and nontrivial phase. (c) Thermal Hall conductivity as a function of spin chirality. The "shoulders" appear at the phase boundary when $\theta_{inc} = \pm\pi/6$.

References

[1] G. Go, S. Lee, and S. K. Kim, "Generation of nonreciprocity in gapless spin waves by chirality injection," Phys. Rev. B 105, 134401 (2022)

[2] S. K. Kim, H. Ochoa, R. Zarzuela, and Y. Tserkovnyak, "Realization of the Haldane-Kane-Mele Model in a System of Localized Spins," Phys. Rev. Lett. 117, 227201 (2016)

[3] S. A. Owerre, "A first theoretical realization of honeycomb topological magnon insulator," J. Phys. Condens. Matter 28, 386001 (2016)

Orbital physics and engineering in LaMnO$_3$ films

Chan-Ho Yang[1,2*]

[1]Department of Physics, KAIST, Daejeon 34141, Republic of Korea
[2]Center for Lattice Defectronics, KAIST, Daejeon 34141, Republic of Korea

The Jahn-Teller (JT) effect, through geometric deformation of molecules or local ionic lattices, lowers the overall energy of the system by removing electron degeneracy from partially occupied orbitals. Crystal symmetry lowered by JT distortion inevitably creates multiple variants of elastic and orbital-anisotropic states. Visualization and control of the domain/wall textures create a cornerstone to understand various correlated phenomena and explore wall properties. Here, we report the real-space observation of JT phonon and orbiton-related domains in a LaMnO$_3$ thin film using confocal Raman spectromicroscopy [1]. The characteristic symmetries of the JT-originated Raman modes allow us to detect and visualize the local population and orientation of the JT planes. Combined with a crystal structural analysis, we find that the formation of ferroelastic domains with W or W' walls provides the basic framework for understanding JT domain textures. We also demonstrate the JT domains can be manipulated by applying local external stress. Furthermore, we introduce our recent results on the melting of orbital order at reduced dimension [2] and summarize this talk with future perspective for electronic and magnetic functionalities.

References

[1] Y.-J. Kim *et al.*, Raman imaging of ferroelastically configurable Jahn–Teller domains in LaMnO$_3$, *npj Quantum Mater.* **6**, 62 (2021).

[2] Y.-J. Kim *et al.*, Orbital order melting at reduced dimensions, *Nano Lett.* **22**, 1059 (2022).

[3] G. A. Safarina *et al.*, Raman spectroscopy of the Jahn-Teller phonons in a magnetic LaMnO$_3$ thin film grown on KTaO$_3$, *J. Appl. Phys.* **131**, 025302 (2022).

토크 마그네토미터리를 이용한 반강자성 산화물 연구

옥종목[*]

부산대학교 물리학과

복잡한 상호작용을 가지는 물질에 자기장을 가하면, 기존의 균형이 깨지면서 독특한 자성 상태가 발현될 가능성이 있다. 하지만 대부분의 경우, 높은 자기장이 필요하여 독특한 자성 상태를 관측하는 데는 어려움이 있다. 토크 마그네토미터리(Torque magnetometry)는 piezoresistive micro-cantilever를 이용하여 시료의 자성을 측정하는 방법이다. 다른 측정방법과 비교하여 측정감도가 뛰어나 작은 시료를 극한 환경(저온, 고자기장)에서 측정할 수 있다는 장점이 있다. 본 연구에서는 토크 마그네토미터리를 이용하여 반강자성 산화물의 특이 자성 상태를 발견하고자 한다. 본 발표에서는 삼각격자 기반의 이종층상구조를 가지는 $PdCrO_2$와 양자스핀액체가 발현될 가능성이 있는 $Na_3Co_2SbO_6$를 소개하고, 토크 마그네토미터리를 이용하여 관측한 독특한 자성 상태에 대해서 논의한다.

Quasi-two-dimensional square lattice S = 2 antiferromagnet Ba₂FeSi₂O₇: Magnetic properties and quantum transition

Jae-Hoon Park[1,2*]

[1]Department of Physics, POSTECH, Korea
[2]Center for Complex Phase Materials, MPK, Korea

Quasi 2D Heisenberg antiferromagnets have often been exhibited exotic low-dimensional magnetism involving lattice topology and spin-orbit coupling. Here we introduce a new quasi 2D square lattice antiferromagnet $Ba_2FeSi_2O_7$ with an integer spin S = 2 (Fe^{2+}), which exhibits a non-trivial magnetic transition with temperatures and external magnetic fields. In this talk, we will present experimental results such as the magnetization (χ, M), specific heat (C_P), neutron diffraction and inelastic scattering on this new quasi 2D antiferromagnet as well as the theoretical Monte Carlo simulations. We also discuss nature of the ground state and the non-trivial quantum transition.
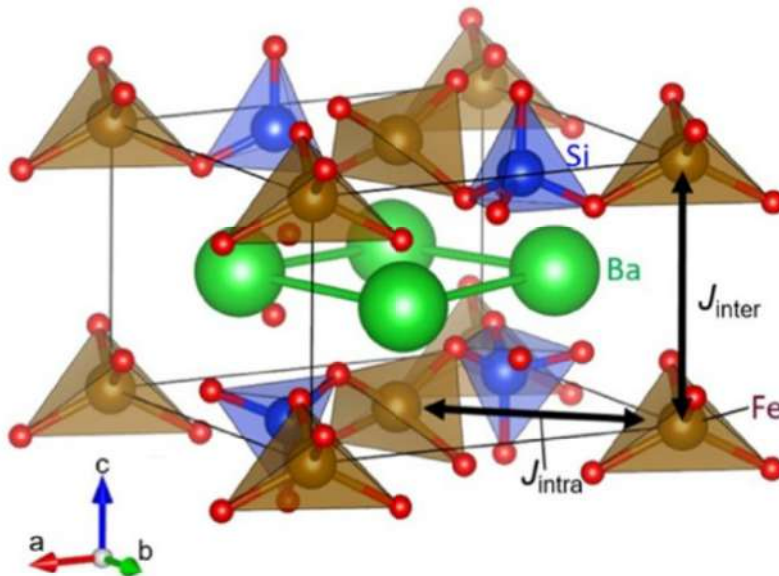
Fig. 1. Crystal structure with exchange couplings

Symposium 8

'Low Dimensional Magnetics'
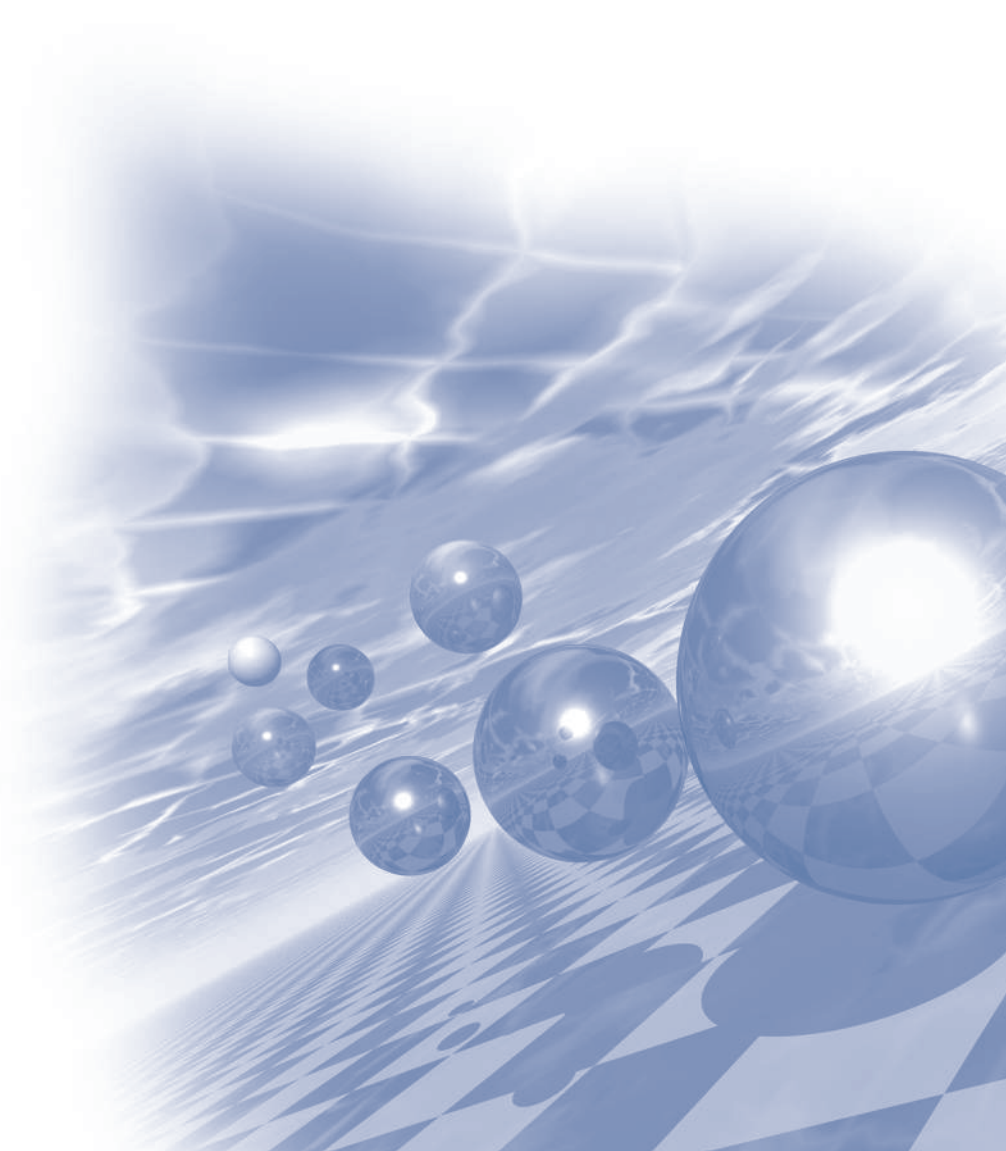
Ferroelectricity-driven phonon Berry curvature and nonlinear phonon transports

Hosub Jin[*]

Department of Physics, Ulsan National Institute of Science and Technology (UNIST), Ulsan 44919, Korea

In symmetry-broken crystalline solids, pole structures of Berry curvature can emerge, which have been utilized for various electronics and spintronics applications. In this talk, we show that polar lattice distortion gives rise to phonon Berry curvature in a way that induces a nonlinear phonon Hall effect. In group-IV monochalcogenide monolayers, ferroelectric distortion induces the phonon Rashba effect that opens a mass-gap in tilted Weyl phonon modes, resulting in a large phonon Berry curvature dipole. Our ab-initio molecular dynamics simulations reveal that the nonlinear phonon Hall transports occur in a controllable manner via ferroelectric switching.

Fe$_5$GeTe$_2$의 나선형 자성특성과 자기저항의 전류밀도 의존성 연구

김상훈[*]

울산대학교 물리학과

Fe$_5$GeTe$_2$(이하 F5GT)은 2차원 자성체 중에 가장 높은 큐리온도(~320 K)를 가지고 있는 물질 중 하나로, 최근 연구가 많이 되고 있다. 본 발표에서는 크게 두가지 주제에 대해서 다룰 예정이다. 첫번째는 F5GT의 온도에 따른 자성특성, 두번째는 저온에서 발현되는 수송현상 관련 연구결과이다. 첫번째 주제의 경우, 이 연구를 통해 약 270 K에서 F5GT가 나선형 자성 특성을 갖게 되며, 이는 결정 비대칭구조에 의한 쟐로우신스키-모리야 상호작용에 의한 것임을 주사 터널 현미경 측정을 통해 증명할 예정이다. 또한, 나선형 자성특성이 자기 공명 현상에 어떤 영향을 미치는지 논의될 것이다. 두번째 주제에서는 F5GT가 전류밀도에 따라 자기 저항의 크기가 바뀌고, 이것이 자기상변화와 관련되어 있음을 논의할 예정이다.

Effective magnetic field in a Ca-doped Bi$_2$Se$_3$ Topological Insulator

Hyun Cheol Koo[1*], Youn Ho Park[1], Sung Jong Kim[1], Tae-Eon Park[1], Kyoung-Whan Kim[1], Chaun Jang[1], Byoung-Chul Min[1], Hyung-jun Kim[1], Andrzej Hruban[2], Andrzej Materna[3], Stanislawa G. Strzelecka[3]

[1]Center for Spintronics, Korea Institute of Science and Technology, Seoul 02792, Korea
[2]Institute of Physics Polish Academy of Sciences, 02-668 Warsaw, Poland
[3]Institute of Electronic Materials Technology, 01-919 Warsaw, Poland

A topological insulator gives a great interest in the field of spintronics because it supplies a conducting state and a high spin polarization. In spite of the strong potential for spin transport devices, the quantitative analysis of spin polarization in topological insulators has not yet been clearly demonstrated. In this research, Ca is doped inside the well-established topological material Bi$_2$Se$_3$ to enhance the spin–orbit interaction and gate controllability. From the anisotropic magnetoresistance of the Ca-doped Bi$_2$Se$_3$ channel, we extract an effective magnetic field of ~10 T. Also, we modulate the carrier types both p- and n-channels, as well as the effective magnetic field by applying a gate voltage. To investigate the interfacial coupling between ferromagnet and topological insulator, the anisotropic magnetoresistance (AMR) in a Ni$_{81}$Fe$_{19}$/SiO$_2$/Ca-doped Bi$_2$Se$_3$ structure is observed. The AMR is determined by the alignment between the magnetization orientation of a ferromagnet and the bias current direction. The bias current induces a strong spin-momentum locking and an effective magnetic field along the transverse direction which changes the magnetic anisotropy and switching process of the ferromagnetic layer. These results not only suggest a measurement platform to estimate the quantitative value of a topological insulator but also provide an efficient technique for manipulating magnetization reversal of the ferromagnetic material in spin-based devices.
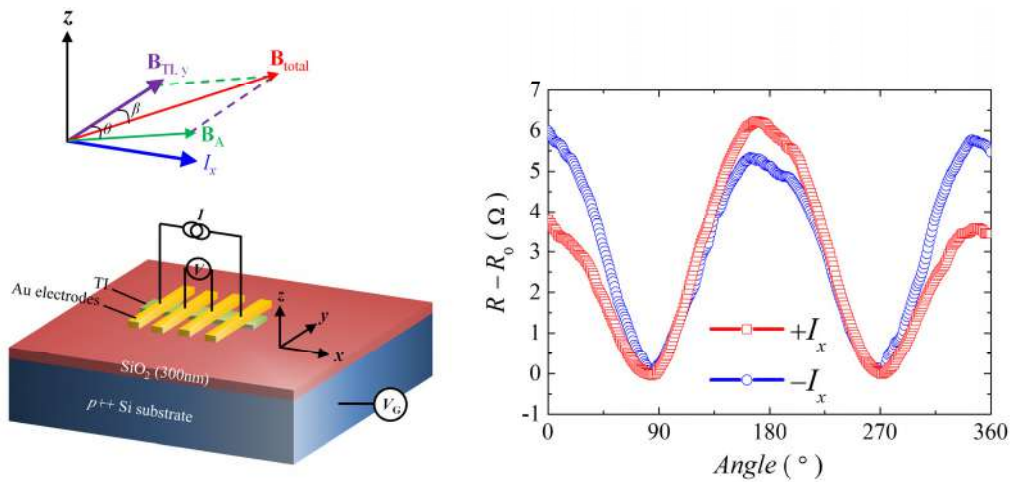
Fig. 1. Measurement geometry and results of angle dependent of anisotropic magnetoresistance.

Pure spin current driven by strong spin orbit coupling at defect dominant 2-dimensional conducting SrTiO₃ surface

Mi-Jin Jin[1,2*], Doo-Seung Um[3], Kohei Ohnishi[1,4], Sachio Komori[2], Nadia Stelmashenko[2], Daeseong Choe[5], Jung-Woo Yoo[5], Jason W.A. Robinson[2*]

[1]Center for Multidimensional Carbon Materials (CMCM), Institute for Basic Science (IBS), Ulsan 44919, Republic of Korea

[2]Department of Materials Science & Metallurgy, University of Cambridge, 27 Charles Babbage Road, Cambridge CB3 0FS, United Kingdom

[3]Department of Electrical Engineering, Sejong University, Seoul 05006, Republic of Korea

[4]Department of Physics, Kyushu University, 744 Motooka, Fukuoka 819-0395, Japan

[5]School of Materials Science and Engineering, Ulsan National Institute of Science and Technology (UNIST), Ulsan, 44919, Republic of Korea

The field of spintronics now expands and diversifies into new opportunities such as spin-caloritronics of spin and magnon, spin-orbitronics using spin orbital coupling, and spinterface using spin at the material interface. Here we bypass the problem by generating a spin current not through the spin injection from outside but instead through the inherent spin Hall effect, and demonstrate the non-local spin transport. The analysis on the non-local spin voltage, confirmed by the signature of a Larmor spin precession and its length dependence. And this 2D polar conductor may exhibit directional propagation of itinerant electrons, i.e. the rightward and leftward currents differ from each other, when the time-reversal symmetry is further broken by applying a magnetic field. Further, we report nonlocal spin-transport on two-dimensional surface-conducting SrTiO₃ (STO) without a ferromagnetic spin injector via the spin Hall effect (and inverse spin-Hall effect). By applying magnetic fields to the Hall bars at different angles to the nonlocal spin-diffusion, we demonstrate an anisotropic spin-signal that is consistent with a Hanle precession of a pure spin current.
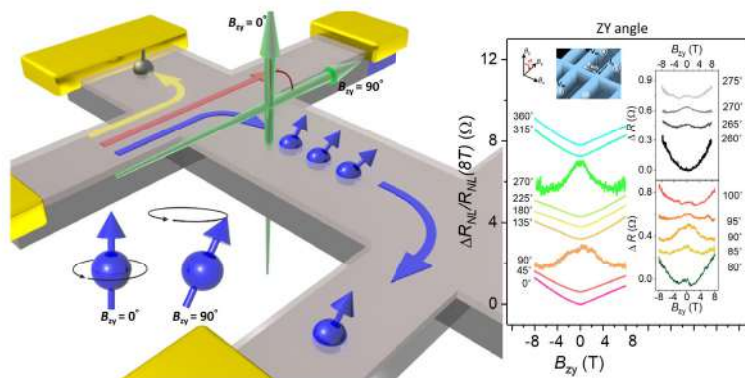
Fig. 1. Illustration(left) of electron spin transport depens on spin orbit coupling and angle dependent spin precession courve.

Coherent quantum control and sensing of individual atoms and molecules

Taeyoung Choi[*]

Department of Physics, Ewha Womans University, Seoul, Republic of Korea

In recent years, controlling quantum systems and utilizing them for certain computation and sensing have been one of highly active research areas across fields of physics, chemistry, and material science. In particular, individual atoms and molecules have been one of leading quantum platforms since the system intrinsically bears quantumness. Such quantum control on individual atoms and molecules can be applied to condensed matter systems via combining electron spin resonance with scanning tunneling microscopy. In this talk, I will introduce how to coherently control spin states of atoms and molecules on surfaces and build various nanostructures to possibly utilize them for quantum sensing. On the other hand, individual atoms and molecules can be trapped under ultrahigh vacuum, where the atoms are well-isolated from their environment, demonstrating full quantum control and entanglement. Here, I will share our recent effort for the trapped ion system to develop the trapped ion based scanning probe.

Quantitative analysis of individual magnetic nanowires based on wide-field diamond magnetometry

Jungbae Yoon[1], Junhwan Moon[2], Jugyeong Jeong[1] , Yujin Kim[2],
Youngkeun Kim[2] and Donghun Lee[1*]

[1]Department of Physics, Korea University, Seoul, Korea
[2]Department of Materials Science and Engineering, Korea University, Seoul, Korea

Wide-field magnetometry based on diamond nitrogen-vacancy (NV) centers has been used to image solid-state magnetic materials, current-flowing devices, magnetic particles or nuclear spins in biomedical samples etc. Here, we use a custom-built ambient wide-field diamond magnetometer to study magnetic properties of various nanowires including Fe, Co, Fe-Au, Fe-Co alloy, etc. From the magnitude and spatial distribution of static magnetic field around nanowires, we are able to extract magnetization of individual ferromagnet nanowires which varies depending on relative size, material composition and so on. The imaging technique can provide quantitative analysis method of studying magnetism in various nanostructures at ambient conditions.

Session 3

구두발표 Ⅲ
'Low Dimensional Magnetics' /
'Magnetic Sensors and Micro-Devices'
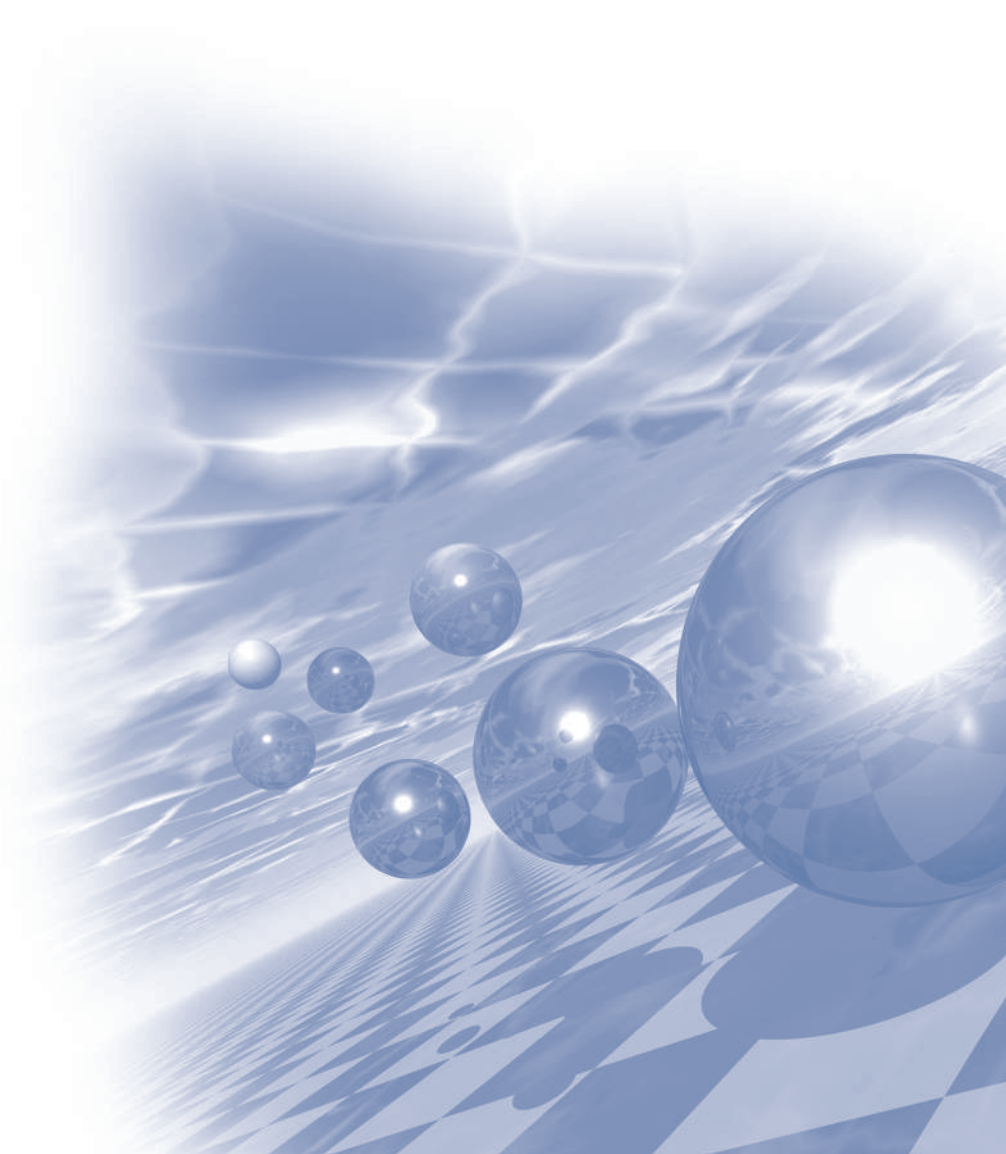
Understanding Enhanced Low-Field Magnetic Hyperthermia via Synthetic Parameters of Monodisperse MnZn Ferrite Nanocubes

Bo Kyeong Choi[*], Tae Won Lim and Kwan Lee

Department of Advanced Materials Engineering, Kyungsung University, Busan, 48434, Republic of Korea

Magnetic nanoparticles have significantly attracted interest because of their intrinsic properties depending on their size, shape, and composition. In particular, Mn–Zn ferrite nanoparticles has attracted as hyperthermia agents because of their high specific absorption rate (SAR) and good biocompatibility. Although various synthetic approaches have been developed for highly efficient induction heating characteristics via control of metal ion doping, however, lack of reproducibility of monodisperse magnetic nanoparticles synthesis is a persistent problem for enhanced magnetic hyperthermia. Here, we demonstrate the effect of synthetic parameters effect of Mn-Zn ferrite nanocubes on the magnetic hyperthermia with high intrinsic low power in a range of 5 nHm^2/kg at $H_{app}F_{app}$ = $1X10^9$ A/ms, in which the optimized synthetic condition enables 50 times higher heating induction than that of commercial magnetic hyperthermia agents. We elucidated the critical roles of precursor nature, heating rate, and reductive-oxidative environment while organic phase synthetic process, which are significantly relevant to enhanced heat induction characteristics. Our demonstrations provide the underlying mechanism of size and shape control of Mn-Zn ferrite nanocubes and the voyage of synthetic procedures for the realization of phase-controlled ferrite nanocubes are critical to an outcoming magnetism and their enhanced heating induction.

Low frequency noise and sub-nT field resolution in planar-Hall magnetoresistive (PHMR) sensors

Proloy T. Das[1*], T. Jeon[2], C. Jeon[2], J. Kim[2], M. Kim[2], B. Lim[1] and C. G. Kim[1,2]

[1]Magnetics Initiative Life Care Research Center, DGIST, Daegu 42988, Korea
[2]Department of Physics and Chemistry, DGIST, Daegu 42988, Korea

Using special designed planar Hall magnetoresistive (PHMR) sensors[1], we measure magnetic signals at frequencies below 100 Hz at room temperature. We show that for measuring time of up to 30 seconds it is possible to detect fields below 1 nT at 100 Hz. In order to enhance the detection limit of the magnetic sensor, a resistance compensator integrated self-balanced bridge type PHMR sensor is also devised for low-frequency noise reduction in the frequency range[2]. Moreover, the sensor noise components of electronic and magnetic origin have been identified by measuring the sensor noise spectral density as a function of temperature and operating power. In addition, the sensors exhibit a wide linearity field range of 3 mT with a very high thermal stability. These specific features of the PHMR sensors combined with the low power consumption, low cost, and miniature size pave the way for a wide range of applications[3-5].

Keywords: Planar Hall Effect, Magnetic Sensors, Low frequency noise, Detection limit, Self-balancing feature

References

[1] T. Jeon *et al.* "Operational parameters for sub Nano-Tesla field resolution of PHMR sensors in Harsh environments," *Sensors,* vol.21, no.20, pp.6891, (2021).

[2] J. H. Lee *et al.* "Bridge Resistance Compensation for Noise Reduction in Self-Balanced PHMR sensor," *Sensors,* vol.21, no.11, pp.3585, (2021).

[3] V. Mor, et al., "Planar hall effect (PHE) magnetometers," in High Sensitivity Magnetometers. New York, NY, USA: Springer, 2017, pp. 201–224

[4] M. Hott, *et al.*, "Magnetic Communication Using High-Sensitivity Magnetic Field Detectors," *Sensors,* vol. 19, pp.3415, Aug. 2019.

[5] B. Lim *et al.* "Advances and key technologies in magnetoresistive sensors with high thermal stabilities and low field detectivities" *APL Materials, 2022 (Accepted).*

MEMS flux-gate 센서를 사용한 탄의 자세 측정

김은애[1*], 홍기민[1], 손대락[2]

[1]충남대학교, 물리학과
[2]㈜센서피아

본 연구에서는 회전하며 날아가는 탄의 탄의 회전속도와 궤적을 자기적인 방법으로 추적할 수 있는 방안을 고안하였다. 탄이 지구자기장 하에서 회전하며 진행하는 동안의 자기장 변화를 측정하기 위해 MEMS flux-gate 센서를 채택하였는데, 탄의 회전을 고려하여 2-축 센서로 설계하였다. 두 축의 센서는 서로 수직방향으로 배치하여 탄의 회전축에 수직인 성분과 탄의 회전축의 성분을 측정할 수 있도록 하였다. MCU를 적용하여 2-축 자기센서 조립체의 offset과 gain을 교정하였고, 자기장 값은 telemetry 보드를 이용하여 지상관측소에서 데이터를 취득하였다.

탄이 회전하면서 날아갈 때 측정된 자기장 데이터는 강자성체로 된 탄의 영구 자기장 성분(B_p)과 지구자기장에 의하여 탄이 자화되는 유도 자기장 성분(B_i)을 가지게 된다.

탄에서 측정한 회전축에 수직인 방향의 자기장을 B_{rm}, 탄의 회전축 방향의 자기장을 B_{xm}이라고 한다면 탄의 회전축 방향의 자기장 B_{xm}에서 영구 자기장 성분과 유도 자기장 성분을 제거한 값을 B_x, 탄의 회전축과 수직방향의 자기장 B_{rm}에서 영구 자기장 성분과 유도 자기장 성분을 제거한 값을 B_r이라고 한다. 이 때의 total field 값은 $B_t = \sqrt{B_x^2 + B_{rmax}^2} = 50 \mu T$가 된다.

Fig.1-(a)는 본 연구에서 제작된 155 mm 탄의 신관에 장착된 2-축 자기센서 조립체이고, Fig.1-(b)는 telemetry 보드로부터 취득한 데이터이다. Fig.2-(a)는 탄의 영구 자기장 성분 및 유도 자기장 성분을 포함한 데이터와 total field를 나타낸 그래프이다. Fig.2-(b)는 측정된 데이터를 이용하여 total field B_t가 50 μT가 되도록 B_{xm}과 B_{rm}에서 영구자기장 성분과 유도자기장 성분을 적절히 제거한 데이터와 total field를 나타낸 그래프이다. 영구자기장 성분과 유도자기장 성분이 제거된 데이터를 이용하여 시험 조건 (탄의 1회전 시 이동거리, 발사 각도 등)을 적용하여 계산하면 Fig.3과 같이 탄의 회전속도(a)와 궤적(b)을 추적할 수 있다.

결과적으로 자기적인 방법으로 측정된 데이터를 실제 탄의 회전속도와 날아간 궤적과 비교했을 때 잘 일치하고 있어 자기적 방법으로도 탄의 궤적과 운동을 측정할 수 있음을 확인하였다.

(a)　　　　　　　　　　(b)
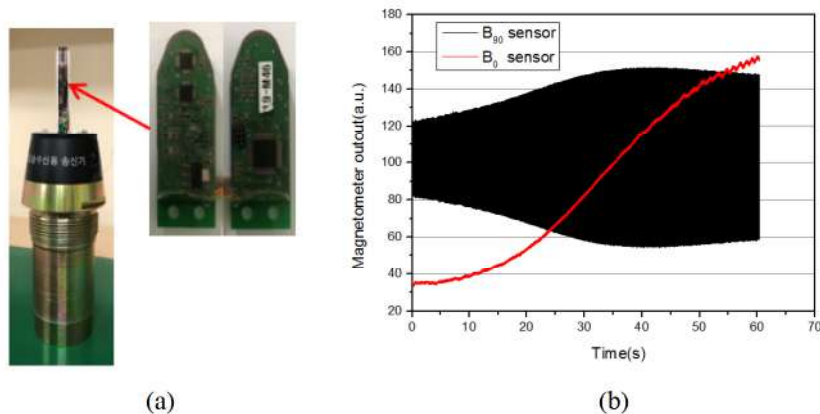
Fig. 1. 제작된 2-축 자기센서조립체(a), 지구자기장 측정데이터(b)

(a)   (b)
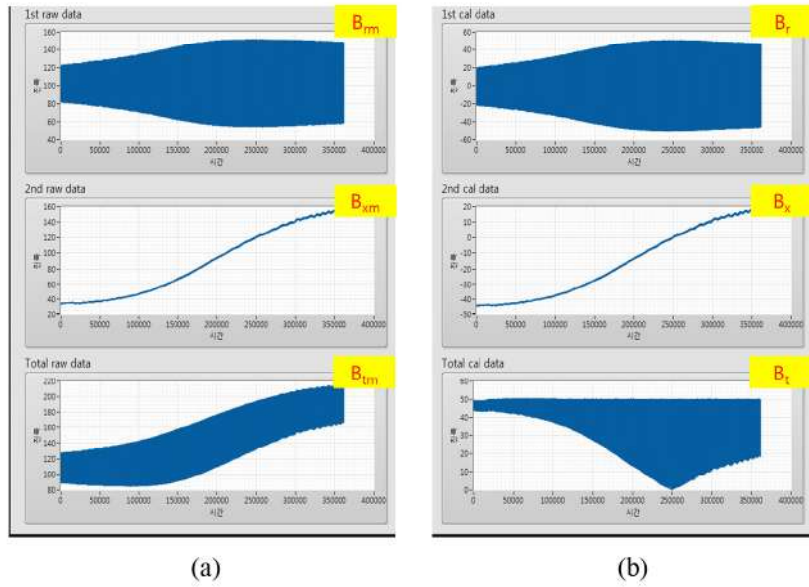
Fig. 2. 탄의 영구 자기장 성분 및 유도 자기장 성분 포함된 데이터(a),
탄의 영구 자기장 성분 및 유도 자기장 성분이 제거된 데이터(b)
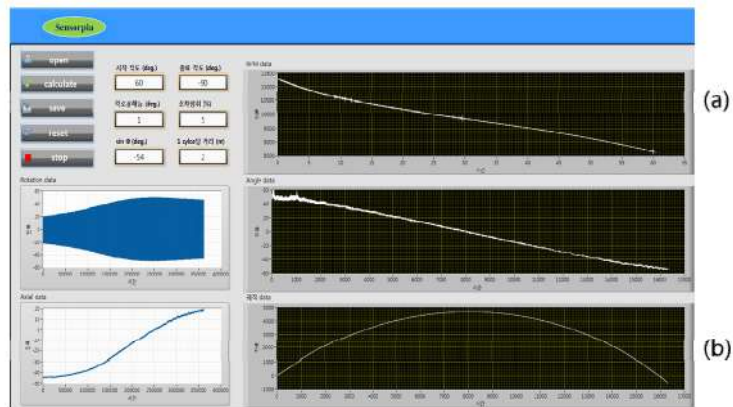
Fig. 3. 탄의 회전속도(a), 탄의 궤적(b)

Analysis of magnetic noises in continuous reliquefaction of helium for high-sensitivity SQUID systems

Yong-Ho Lee[*], Kwon-Kyu Yu, Jin-Mok Kim, Bokyoung Kim

Korea Research Institute of Standards and Science

High-sensitivity magnetometer systems made of superconducting quantum interference devices (SQUIDs) provide low-magnetic-noise performance for precision measurements. Among the superconducting materials, SQUIDs made from low-temperature Nb/AlO$_x$/Nb Josephson junctions are reliable physically and chemically against repeated thermal cycling between room temperature and liquid helium temperature, and they have low noise characteristic. The Nb-based SQUIDs need regular refill of liquid helium to cool them down to 4.2 K. However, the recent crisis of liquid helium deficiency requires refill-less operation of the SQUID system, by using either cryocooler based conduction cooling or reliquefaction of the evaporated helium gas. In the direct cooling configuration using a cryocooler, big vibration and magnetic interferences from the cryocooler's cold head make now-noise operation of the SQUID system difficult. Thus, conduction cooling concept is not suitable for especially multichannel SQUID systems of high thermal load. For refill-free operation of the Nb SQUID systems while using the liquid helium, we developed a cooling configuration with continuous reliquefaction of the evaporating helium gas from the dewar. To realize low-noise operation of the reliquefier-based SQUID system, we installed the SQUID array in the vacuum space of the dewar without the mechanical insert structure from the dewar neck, thus eliminating the vibration transmission from the conventional SQUID insert. Furthermore, the vibration from the cryocooler was minimized by using a flexible transfer tube between the reliquefier chamber and the SQUID dewar. We fabricated whole-head magnetoencephalography (MEG) systems and magnetocardiography (MCG) systems cooled by this concept, and showed that the overall noise performance is quite similar to those multichannel SQUID systems cooled by the direct liquid helium of regular refill type.

Session 4

'신진과학자 콜로키움'
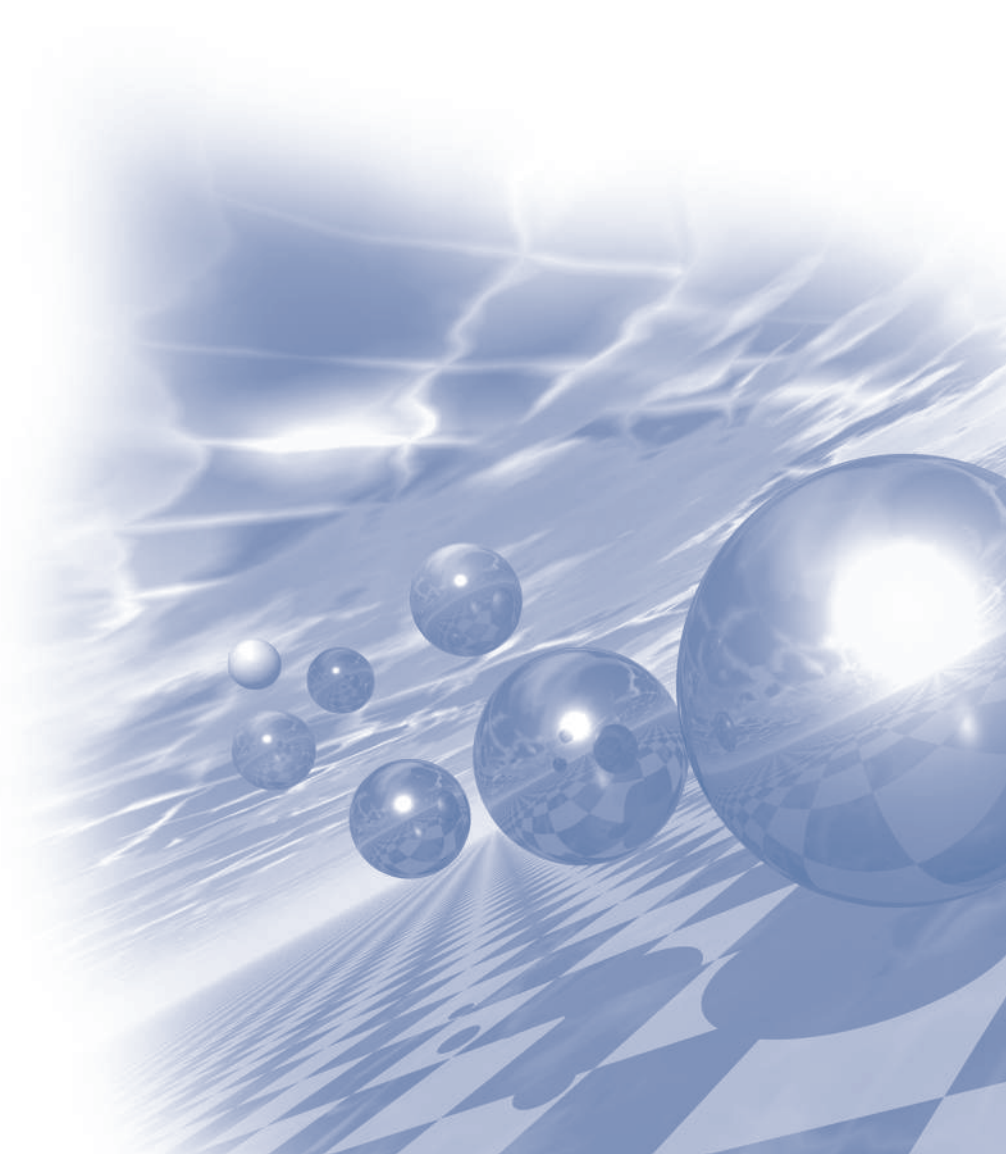
Bias current dependence of spin accumulation voltage in n-Si spin MOSFET

Soobeom Lee[1*†], Hayato Koike[2], Minori Goto[3], Shinji Miwa[3], Yoshishige Suzuki[3],
Fabien Rortais[1], Ei Shigematsu[1], Ryo Ohshima[1], Yuichiro Ando[1] and Masashi Shiraishi[1]

[1]Department of Electronic Science and Engineering, Kyoto University, Kyoto, 615-8510, Japan
[2]Advanced Products Development Center, TDK Corporation, Chiba, 272-8558, Japan
[3]Graduate School of Engineering Science, Osaka University, Osaka, 560-8531, Japan
[†]Present address: Department of Emerging Materials Science, Daegu Gyeongbuk Institute of Science Technology,
Daegu, 42988, Republic of Korea

Si spintronics has attracted a lot of interest, and much effort has been paid to the room temperature operation of Si-based spin metal-oxide-semiconductor field-effect transistor (spin MOSFET) using non-degenerate n-Si [1]. Furthermore, recent research reported the output spin accumulation voltage of more than 1 mV at room temperature due to the spin drift effect [2]. In the previous research, the spin accumulation voltage exhibited saturation under a large electric current injection regime, suggesting a possibility of modification of spin transport properties, such as spin diffusion length and spin injection efficiency, in the non-degenerate n-Si. In this study, we clarify the origin of the bias current dependence of spin accumulation voltage in the non-degenerate n-Si spin MOSFET.

A structure of a non-degenerate n-Si spin MOSFET and a measurement setup are schematically shown in Fig. 1(a). Spin MOSFET consists of two ferromagnetic source and drain on non-degenerate n-Si. Spin accumulation voltage at one ferromagnetic electrode (ΔV_{L3T}) is experimentally measured in local three terminal configuration as a function of source-drain bias current. All measurements are carried out at 300 K. Spin accumulation voltage is theoretically calculated using previously established one-dimensional model based on spin drift diffusion
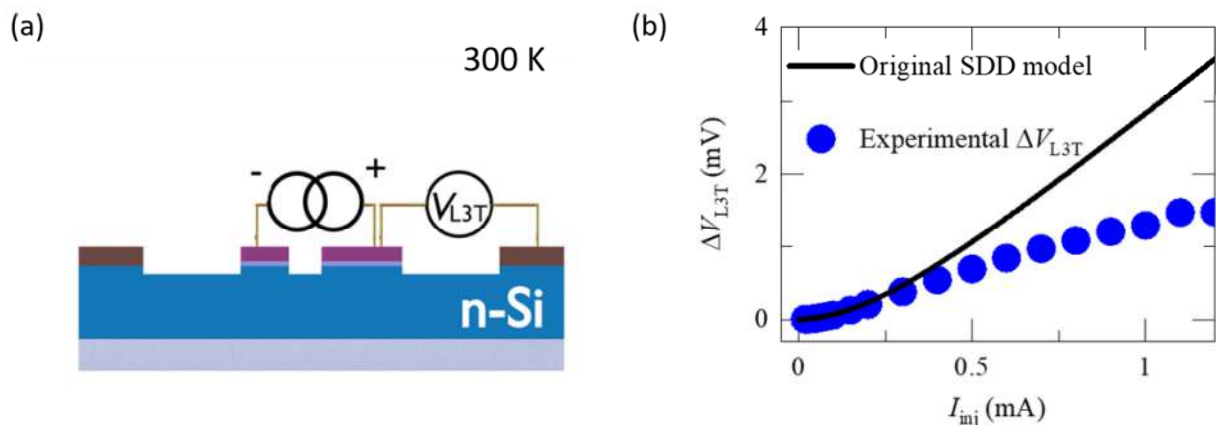
Figure 1. (a) Schematic illustration of non-degenerate n-Si based spin MOSFET device and local three-terminal experimental setup. (b) Bias current (I_{inj}) dependences of ΔV_{L3T} experimentally measured (blue circle) and theoretically calculated by means of spin drift diffusion (SDD) model (black line).

equation [2]. Figure 1(b) presents a bias current dependence of spin accumulation voltage experimentally measured (blue circles) and theoretically calculated (black line). As previously reported [2], the spin accumulation voltage is saturated under a large applied bias current exhibiting the disagreement between the experiment and calculation. The non-local four-terminal measurement and the Hall measurement reveals that spin lifetime of the non-degenerate n-Si channel is independent of the bias current in this study, while interface resistances of ferromagnetic source and drain are reduced to the same order of spin resistance of the Si channel. We implement a model calculation considering these results and the detail will be discussed in the presentation [3].

References

[1] T. Tahara, Y. Ando, M. Shiraishi *et al*., Appl. Phys. Express **8**, 113004 (2015).

[2] T. Tahara, Y. Ando, M. Shiraishi *et al*., Phys. Rev. B **93**, 214406 (2016).

[3] S. Lee, Y. Ando, M. Shiraishi *et al*., Phys. Rev. B **99**, 064408 (2019).

Orbital torque in magnetic bilayers

Dongjoon Lee[1*], Dongwook Go[3,4], Hyeon-Jong Park[2], Wonmin Jeong[1,5], Hye-Won Ko[6],
Deokhyun Yun[1,7], Daegeun Jo[3], Soogil Lee[8], Gyungchoon Go[6], Jung Hyun Oh[5],
Kab-Jin Kim[6], Byong-Guk Park[8], Byoung-Chul Min[1], Hyun Cheol Koo[1,2], Hyun-Woo Lee[3,9],
OukJae Lee[1] and Kyung-Jin Lee[6]

[1]Center for Spintronics, Korea Institute of Science and Technology, Seoul 02792, Korea
[2]KU-KIST Graduate School of Converging Science and Technology, Korea University, Seoul 02841, Korea
[3]Department of Physics, Pohang University of Science and Technology, Pohang 37673, Korea
[4]Basic Science Research Institute, Pohang University of Science and Technology, Pohang 37673, Korea
[5]Department of Materials Science and Engineering, Korea University, Seoul 02841, Korea
[6]Department of Physics, Korea Advanced Institute of Science and Technology, Daejeon 34141, Korea
[7]Department of Electrical Engineering, Korea University, Seoul 02841, Korea
[8]Department of Materials Science and Engineering, Korea Advanced Institute of Science and Technology,
Daejeon 34141, Korea
[9]Asia Pacific Center for Theoretical Physics, Pohang 37673, Korea

The spin Hall effect is a phenomenon which longitudinal electric field with spin-orbit coupling generates transverse flow of the spin angular momentum. The flow of the spin angular momentum generates torque on ferromagnetic layer, which is spin-orbit torque. Theories [1,2] of spin hall effect suggested that spin Hall effect is not fundamental effect but is a concomitant effect of the orbital Hall effect. An electric field generate the flow of orbital angular momentum, orbital Hall effect, and the orbital angular momentum subsequently convert to spin angular momentum via spin-orbit coupling. However, it is hard to distinguish orbital current from spin current. Because the symmetry transformations of both current are identical. More recent study [3] predict that the orbital Hall effect can generate a torque, called orbital torque, in normal metal/ferromagnet bilayer system when an orbital current is injected into ferromagnetic layer. Still spin-orbit torque and orbital torque have identical properties with symmetry transformations, but both torques have different dependency of spin-orbit correlations in normal metal and ferromagnet(Fig. 1.). From this theoretical prediction, we investigate current-induced torque in various heavy metal/ferromagnet bilayer. we find that the direction of net torque in Ni/Ta bilayers is opposite to the conventional spin Hall theory prediction but instead consistent with the orbital Hall theory, which confirms the orbital torque generated by the orbital Hall effect.
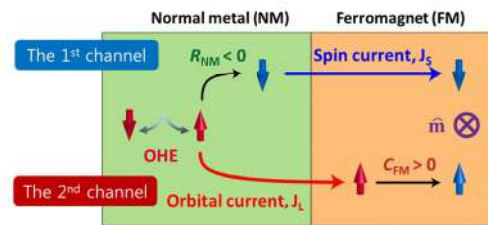
Fig. 1. Schematic illustration of the orbital Hall effect and orbital torque

References

[1] T. Tanaka et al., Phys. Rev. B **77**, 165117 (2008).

[2] H. Kontani et al., Phys. Rev. Lett. **102**, 016601 (2009).

[3] D. Go. et al., Phys. Rev. Res. **2**, 0131777 (2020).

Magnetotransport at Pt/YCrO$_3$ interfaces

Jin Hong Lee[1,2*], Sara Varotto[2], Julien Bréhin[2], Javier Herrero-Martín[3],
Alexandre Gloter[4] and Manuel Bibes[2]

[1]Center for Spintronics, Korea Institute of Science and Technology (KIST), 02792 Seoul, Korea
[2]Unité Mixte de Physique, CNRS, Thales, Université Paris Sud, Université Paris-Saclay, 91767 Palaiseau, France
[3]ALBA Synchrotron Light Source, Cerdanyola del Valles, 08290 Barcelona, Catalonia, Spain
[4]Laboratoire de Physique des Solides, CNRS, Université Paris-Saclay, 91405 Orsay, France

Interfaces between two very different materials have been attractive as they show not only the intrinsic two dimensionality but also emergent phenomena totally distinct from their bulk properties. Here, we study the interfacial magnetotransport in heterostructures composed of nonmagnetic spin-orbit metal Pt and noncollinear antiferromagnetic insulator YCrO$_3$. Unexpected anomalous Hall effect is observed at room temperature while the X-ray magnetic circular dichroism measurement proves that the Pt layer is still nonmagnetic. The first- and second-harmonic components of in-plane magnetoresistance are investigated at low temperature and their temperature behavior is different from the onset of canted magnetic moment in YCrO$_3$. Our investigation provides an opportunity to achieve emergent phenomena at interfaces between heavy metals and noncollinear antiferromagnetic oxides.

Enhancing Spin-Orbit Coupling of Graphene

Jungmin Park[*]

Department of Physics, Korea Advanced Institute of Science and Technology, Daejeon 34131, Korea

Graphene having weak spin-orbit coupling (SOC) is crucial for spin transporting channel because it has a long spin relaxation length and time. Spin–orbit coupling (SOC) offers an alternative technique for generating pure spin currents in non-magnetic materials and controlling spin precessions for spin-field effect transistors. In addition, introducing SOC into graphene causes pristine graphene to evolve into a new condensed matter phase, such as the topological insulator state (quantum spin Hall state). Thus, the control of SOC in graphene is essential for its functional spin-orbitronic applications. In this session, I present the way to enhance SOC of graphene. First, I introduce Au clusters on graphene to enhance spin-orbit coupling and employ a nonlocal geometry to study the spin Hall induced nonlocal resistance. The results show that nonlocal resistance of Au-clustered graphene depends on the applied gate voltage due to various current channels. However, the spin Hall induced nonlocal resistance becomes dominant at a particular carrier concentration, which is further confirmed through Hanle curves. The obtained spin Hall angle is as high as ~ 0.09 at 2 K. Finally, I show the nonvolatile tuning of SOC in graphene through the proximity effect from a ferroelectric substrate, $Pb(Zr_{52},Ti_{48})O_3$ (PZT). Ferroelectric poling by applying a gate voltage induces a change in the SOC strength in addition to shifting the charge neutral point in graphene. The variations in SOC were extracted from weak localization within the quantum interference theory of graphene. Our analyses show that the dipole moments from the PZT polarization significantly enhance the $z \rightarrow -z$ asymmetric and symmetric SOCs of graphene. Unlike the impurity doping and/or gating, this methodology leads to the nonvolatile electrical control of SOC, thereby paving the way for versatile spin-orbitronic applications of graphene.

Investigation of Magnetic Frustration Effects in Quasicrystal Approximants

Takayuki Shiino[*]

Department of Materials Science and Engineering, KAIST, Daejeon 34141, Korea

Quasicrystals (QCs) are unique crystals that do not have translational symmetry but have long-range order with diffraction symmetries prohibited in conventional crystals. Approximant crystals (ACs) are periodic and compositionally similar crystals related to their corresponding QCs. Among ACs, Tsai-type 1/1 AC is the most abundant and commonly studied with a special interest in its periodicity and unique polyhedral structures. Interestingly, Tsai-type 1/1 ACs contain all the Platonic-solid structures (tetrahedral, cubic, octahedral, dodecahedral, and icosahedral structures) in their crystal structures, among which octahedral and icosahedral structures consist of rare-earth (RE) atoms (thus the system can become magnetic). From the magnetic point of view, the RE-based octahedral/icosahedral magnetic network may yield geometrical magnetic frustration. However, the possible geometrical frustration in such a unique octahedral/icosahedral magnetic network remains to be clarified. In this presentation, I will mainly talk about the experimental results of the $(Gd_{1-x}Y_x)Cd_6$ 1/1 AC [1], which has a good localization of 4f electrons. Interestingly, the system exhibits an abrupt change in its physical property by diluting magnetic Gd only by a few percent (with nonmagnetic Y) from the pure $GdCd_6$ (x = 0). This dilution behavior might be associated with the unique geometrical network of the present system.

Reference

[1] T. Shiino, F. Denoel, G. H. Gebresenbut, D. C. Joshi, Y.-C. Huang, C. P. Gómez, U. Häussermann, A. Rydh, and R. Mathieu, Singular magnetic dilution behavior in a quasicrystal approximant, Phys. Rev. B **104**, 224411 (2021).

Colossal Angular Magnetoresistance in a Ferrimagnetic Nodal-line Semiconductor Mn₃Si₂Te₆

Junho Seo[1,2*], Chandan De[1,3], Hyunsoo Ha[4], Ji Eun Lee[5], Sungyu Park[1], Joonbum Park[6], Yurii Skourski [6], Eun Sang Choi[7], Bongjae Kim[8], Gil Young Cho[1,2,9], Han Woong Yeom[1,2], Sang-Wook Cheong[3,10], Jae Hoon Kim[5*], Bohm-Jung Yang[4,11,12*], Kyoo Kim[13*], Jun Sung Kim[1,2*]

[1]Center for Artificial Low Dimensional Electronic Systems, Institute for Basic Science
[2]Dept. of Physics, POSTECH
[3]Laboratory of Pohang Emergent Materials, Pohang Accelerator Laboratory
[4]Dept. of Physics and Astronomy, Seoul National University
[5]Dept. of Physics, Yonsei University
[6]Hochfeld-Magnetlabor Dresden, Helmholtz-Zentrum Dresden-Rossendorf
[7]National High Magnetic Field Laboratory, Florida State University
[8]Dept. of Physics, Kunsan National University
[9]Asia-Pacific Center for Theoretical Physics(APCTP)
[10]Rutgers Center for emergent Materials and Department of Physics & Astronomy, Rutgers University
[11]Center for Correlated Electron System, Institute for Basic Science
[12]Center for Theoretical Physics, Seoul National University
[13]KAERI

Topological magnets, where both magnetism and nontrivial band topology coexist, have emerged as promising candidates to realize novel electronic and spintronic functionalities, because their topological band degeneracy can be readily tuned by spin configurations, thus dramatically modulating electronic conduction. Here we propose a new class of topological magnets, namely, magnetic nodal-line semiconductors, in which spin-polarized conduction or valence bands possess topological nodal-line degeneracy. Taking a layered ferrimagnet Mn₃Si₂Te₆ as a model system, we show that the topological band degeneracy, driven by chiral molecular orbital states, is lifted depending on the spin orientation, which leads to a metal-insulator transition in the same ferrimagnetic phase. As a result, we have observed extremely large angular magnetoresistance exceeding a trillion percent per radian, which we call colossal angular magnetoresistance. Our findings highlight that magnetic nodal-line semiconductors are a promising platform for realizing extremely sensitive spin- or orbital-dependent functionalities.

Unconventional Interlayer Exchange Coupling via Chiral Phonons in Atomically Controlled Oxide Superlattices

Seung Gyo Jeong[1*], Jiwoong Kim[2], Ambrose Seo[3], Sungkyun Park[2], Hu Young Jeong[4], Young-Min Kim[5], Valeria Lauter[6], Takeshi Egami[7,8], Jung Hoon Han[1], Woo Seok Choi[1]

[1]Department of Physics, Sungkyunkwan University, Suwon 16419, Korea
[2]Department of Physics, Pusan National University, Busan 46241, Korea
[3]Department of Physics and Astronomy, University of Kentucky, Lexington, KY 40506, USA
[4]Graduate School of Semiconductor Materials and Devices Engineering,
Ulsan National Institute of Science and Technology, Ulsan 44919, Korea
[5]Department of Energy Science, Sungkyunkwan University, Suwon 16419, Korea
[6]Neutron Scattering Division, Oak Ridge National Laboratory, Oak Ridge, TN 37831, USA
[7]Materials Science and Technology Division, Oak Ridge National Laboratory, Oak Ridge, TN 37831, USA
[8]Department of Materials Science and Engineering, University of Tennessee, Knoxville, TN 37996, USA

Chiral symmetry broken phonons, i.e., chiral phonons, are intriguing concepts to understand various spin-related quantum phenomena, such as phonon Hall effect, optically driven effective magnetic field, AC Stark effect, topologically-induced viscosity split, and pseudogap phases. However, a direct experimental manifestation of chiral phonons determining a ground state with long-range spin ordering has not been realized.

In this study, we use atomic-scale precision-controlled oxide heterostructures where two ferromagnetic ($SrRuO_3$) layers are separated by a nonmagnetic-insulating spacer ($SrTiO_3$)[1-9]. We observe an unexpected oscillation of in-plane magnetization as a function of the nonmagnetic-insulating spacer layer thickness. Since itinerant electrons are absent in the spacer layer, Ruderman-Kittel-Kasuya-Yosida interaction cannot explain the observed behavior. Instead, we propose that chiral phonons created in the $SrRuO_3$ layer penetrate through the $SrTiO_3$ layer mediating the unprecedented interlayer exchange interaction, as shown in the Figure below. The structural similarity between the perovskite layers provides a facile pathway for the chiral phonons, and depending on the insulating spacer thickness, the interaction is shown to effectively change the relative spin orientation. The presence of chiral phonons is conclusively supported by the observation of phonon Zeeman effect in the heterostructure.
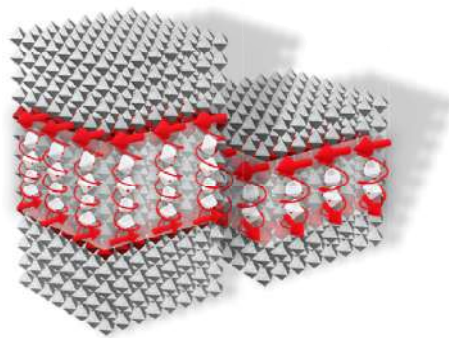
Fig. 1. Schematic representations of interlayer exchange coupling across nonmagnetic-insulating spacers via chiral phonon-mediated exchange interaction with different spacer thicknesses.

References

[1] Jeong *et al., Appl. Phys. Lett.* **115**, 092905 (2019).

[2] Jeong *et al., Phys. Rev. Lett.* **124**, 026401 (2020).

[3] Jeong *et al., Nanoscale* **12**, 13926 (2020).

[4] Jeong *et al., Adv. Sci.* **7**, 2001643 (2020).

[5] Seo *et al., Phys. Rev. B* **103**, 045104 (2021).

[6] Jeong *et al., ACS Appl. Nano Mater.* **4**, 2160 (2021).

[7] Cho *et al., Acta Mater.* **216**, 117153 (2021).

[8] Jeong *et al., Adv. Sci.* **8**, eabm4005 (2022).

[9] Jeong *et al., Sci. Adv.* **9**, 2103403 (2022).

Session 5

구두발표 IV
'Soft Magnetics'
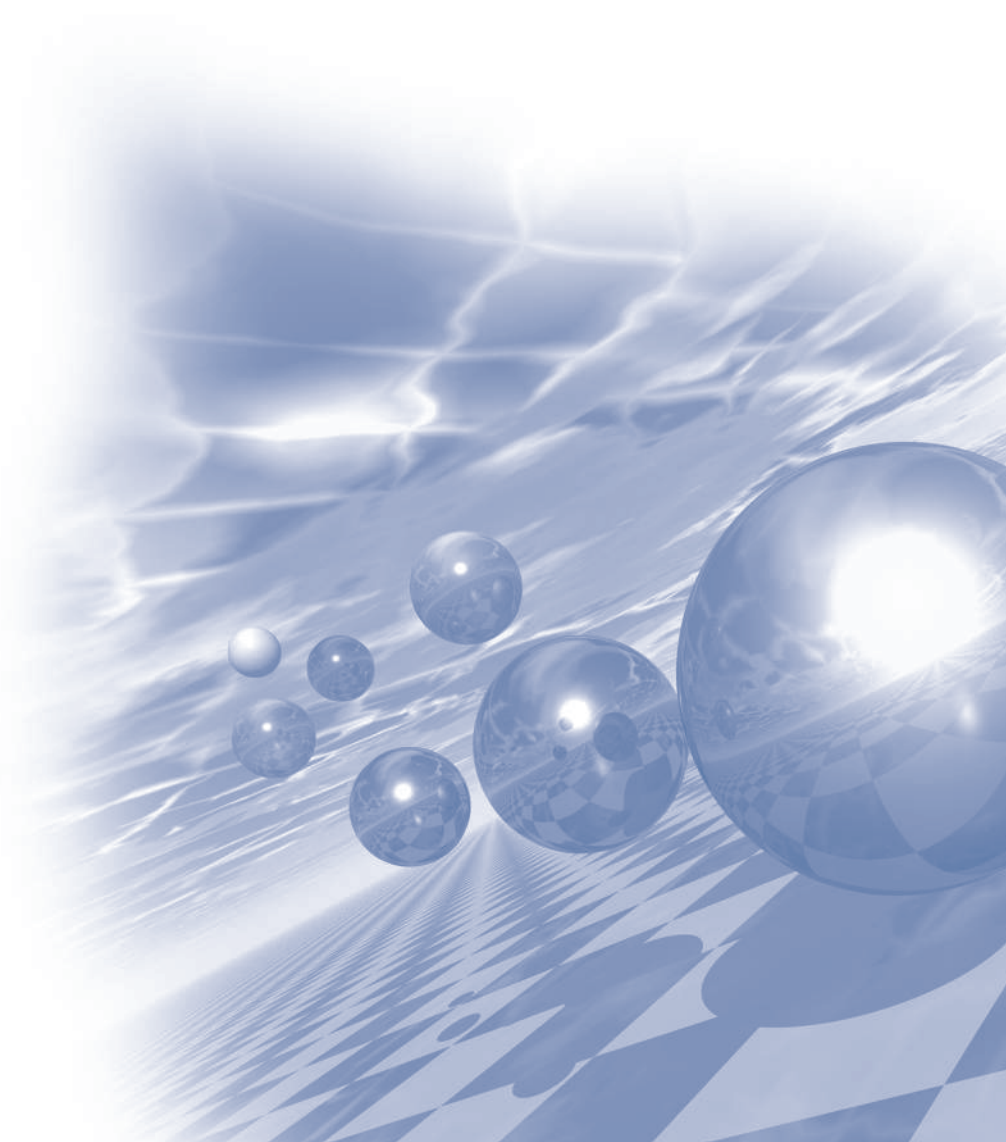
산화물-레진 2층 절연막 순철 SMC 코어

최광덕[1,2], 이소연[1,3], 황종승[4], 허주열[3], 이경우[2], 변지영[1*]

[1]A, Korea a Korea Institute of Science and Technology, Seoul, Korea
[2]Seoul National University, Seoul, Korea
[3]Korea University, Seoul, Korea
[4]Tech University of Korea, Gyeonggi-do, Korea

본 연구에서는 산화물 막과 레진을 2층으로 코팅한 순철분말을 이용하여 제조된 SMC (Soft Magnetic Composites) core의 특성에 대해 보고한다. 순철 분말 표면에 산화물 절연막을 형성하기 위해 closed system을 도입하였다. 산화제로는 산소 가스를 사용하였고, 산화 반응 온도는 500℃로 하였다. 순철분말과 산소와의 균일한 반응을 위해 회전식 원통형 반응기를 채용하였다. 산소농도 분석기를 설치하여 반응기 내부에서 산화반응의 진행 정도를 모니터링 할 수 있도록 하였다. 순철 분말 1 그램당 1~4 ㎤의 산소를 주입하였고 주입된 산소가 완전히 반응에 소모될 때까지 반응시켰다. 주입되는 산소의 양을 조절하면 산화물의 두께를 조절할 수 있음을 확인하였다. 산화물은 대부분이 Fe_3O_4로 구성되어 있었다. 산화물 절연막의 두께가 증가하면 철손의 뚜렷한 감소가 관측되었는데 이는 절연특성의 증가로 인한 와전류 손실의 감소에 기인한 것이었다. 상세한 결과는 현장에서 발표하고자 한다. 또한 산화물 절연막 두께 변화에 따른 순철 SMC 코어의 자기적 특성 변화를 관찰하여 그 결과를 보고한다. Fe_3O_4의 비저항이 크지 않아 보다 절연특성을 향상시키고자 산화물 막 위에 실리콘 레진을 코팅하였다. 산화물-레진 2층 절연막 순철 SMC 코어를 제조하여 그 특성을 측정해 본 결과, 1 T, 400 Hz에서의 철손이 190 W/kg(레진 층이 없음)에서 56 W/kg로 급격히 감소하는 것을 확인하였다. 이는 레진 층의 존재에 의한 절연특성의 증가에 기인한 것으로 판단된다.

Characteristics of crystalline and amorphous soft magnetic cores from Fe-based soft magnetic powders

Minwoo Lee, Dohun Kwon, Youngsin Choi, Dae Won Jung, Hwijun Kim[*]

Korea Institute of Industrial Technology, Korea

Soft magnetic materials are used in powder generation, transfer, and convertor, and are extensively used in electric machines, power electronics, sensors, and electromagnetic interference shielding. Soft magnetic composites (SMCs) components are normally manufactured by modified powder metallurgy processes which are combined with new techniques, such as compaction, warm compaction, multi-step annealing followed by a heat treatment at relatively low temperature.

The recent increase in demand for high-efficiency electric motors, especially for electric vehicles (EVs) is finally starting to make a meaningful push into the global market, so the demand is growing in the global automotive industry. The properties of soft magnets depend on diverse manufacturing technologies and materials. The requirement for new soft magnetic materials in the field of the electric motors, high frequency power conversion parts and telecommunications has significantly caused the improvement of soft magnetic materials in Korea for the past decades. To meet the growing need for energy efficiency in power electronics and electric machines, we have been studying on a number of new soft magnetic composite cores with various structures like crystalline, amorphous and nanocrystalline. Compared to the currently most widely used crystalline SMCs, the amorphous SMCs exhibit more favorable properties, including high electrical resistivity, good saturation magnetization and low coercivity.

This presentation will introduce the results on frequency dependence of the soft magnetic cores manufactured from crystalline and amorphous powders by means of conventional powder metallurgy processes. While crystalline SMC cores show useful soft magnetic characteristics in low frequency range ($\sim$1000 Hz), amorphous SMCs cores exhibit valuable properties in high frequency ranges ($\sim$100 kHz). Furthermore, characteristics of SMC cores such as permeability, coercivity and core loss will be estimated in the various frequency ranges.
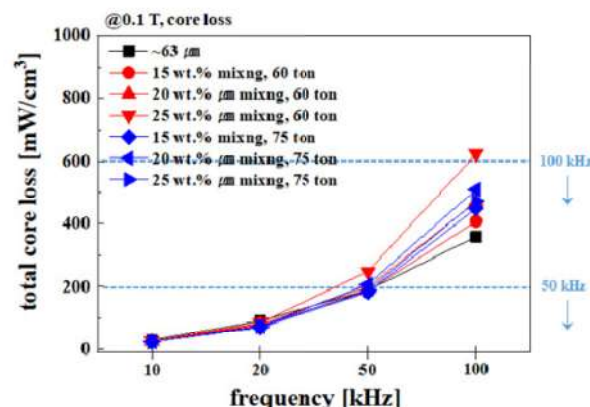
Figure. 1. manetic properties of Fe-based amorphous soft magnetic core

Keywords: Soft magnetic composites, Amorphous alloys, Nanocrystalline alloys, Soft magnetic properties, Powder metallurgy process, Soft magnetic core

Symposium 9

'Magnetics in Medical Science'
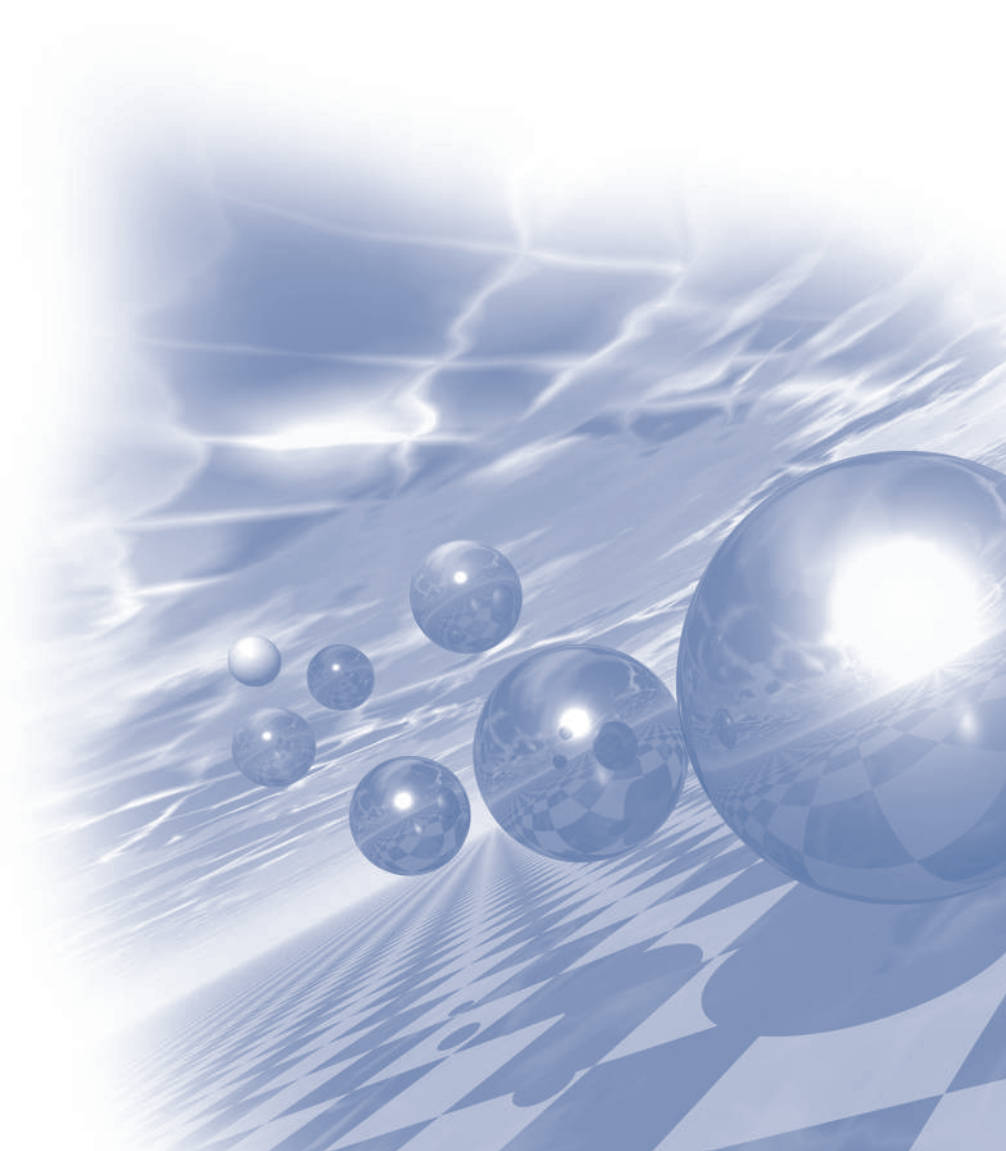
Performance Analysis of Multi-functional Compact Gamma Camera System for Radiation Monitoring

Dong-Hee Han[1], Seung-Jae Lee[2], Jang-Oh Kim[3], Da-Eun Kwon[1], Cheol-Ha Baek[1,4*]

[1]Department of Medical Health Science, Kangwon National University, Samcheok, Republic of Korea
[2]Departemt of Radiological Science, Dongseo University, Busan, Republic of Korea
[3]Health and Medical Education Research Institute, Kangwon National University, Samcheok, Republic of Korea
[4]Departemt of Radiological Science, Kangwon National University, Samcheok, Republic of Korea

Conventional gamma cameras have heavy and large volume disadvantages due to photomultiplier tube, and high voltages must be applied. The compact gamma camera evaluated in this study was developed by ARALE Co., Ltd. and it has 934 g of $86 \times 65 \times 78.5$ mm^3 and can be equipped with a diverging collimator of metal 3D printing manufactured as a field of view of 45 degrees, enabling high-resolution images to be obtained. The use of system-on-chip and field-programmable-gate-array in the detector parts was able to make it compact and lightweight, providing hardware and software good connection. In addition, by tiling the photodetector in 2×2, the detection area was expanded and the sensitivity was improved. Therefore, it can be mounted on a system of drones or robots that require miniaturization, so it can be used in various fields. As a result of the experiment using a software called MAETEL Manager version 1.42 and radioisotopes such as ^{57}Co, ^{54}Mn, ^{22}Na etc., an energy spectrum and a segmentation gamma images were obtained. Currently, performance evaluations such as full width at half maximum calculation, intrinsic and extrinsic uniformity measurement are in progress.

Fig. 1. Appearance of the compact gamma camera and proposed SoC-FPGA and SiPM

Fundamental Study on Radiation Therapy Application of Alanine/ESR System

Ki-Taek Han[1], Chul Hee Min[2], Hyojun Park[2], Woo Sang Ahn[3], Da Yeong Gwon[1], Sung Jin Noh[1*]

[1]Radiation Technology and Research Center, Korean Association for Radiation Application, Korea
[2]Department of Radiation Convergence Engineering, Yonsei University, Korea
[3]Department of Radiation Oncology, Gangneung Asan Hospital, University of Ulsan College of Medicine, Korea

This study is the fundamental research on the development of optimization and measurement protocols of the alanine/ESR system for radiation therapy application. Alanine/ESR dosimetry system is a method which is used as secondary standard by several national metrology institutions [1]. Especially, alanine dosimeter is a tissue-equivalent material and is suitable for medical radiation application. Recently, with the development of various radiation treatments such as boron neutron capture therapy(BNCT) and FLASH, a technology capable of quantitatively evaluating these new technologies is required. In the case of alanine/ESR dosimetry, dose evaluation was performed using the dose response curve for absorbed dose to water using Co-60 gamma ray source, but further development of neutron measurement technology is required for quantitative evaluation of new radiation therapy using neutrons like BNCT. For radiation therapy, an accurate measurement and a small uncertainty of the applied dose is required. Therefore, we carried out the experiment to develop an optimized measurement protocols for the alanine/ESR dosimetry for neutrons and photons in this study. In this study, a dose evaluation process using the alanine/ESR system was developed, including fabrication of reference material(RM), optimization of alanine/ESR system, preparation of dose response curves for neutron and photon beams, and uncertainty evaluation.

First of all, dose response curves for photon and neutrons were measured using Co-60 gamma-ray sources and Cf-252 neutron sources as reference radiation sources, respectively. It was confirmed that the R-square values of the dose response curves were 99.99%, and the linearity was very good. Next, a study was conducted to minimize uncertainty of the dose evaluation method using the Alanine/ESR system. It was confirmed that the uncertainty for each dose response curve was 4% or less, satisfying the conditions required for medical radiation quality assurance.

In conclusion, it was confirmed that it is appropriate to apply the dose evaluation method using the alanine/ESR system to therapeutic radiation quality management. In the future, research will be conducted on the development of mathematical models and dose assessment processes that can further reduce uncertainty.

Reference

[1] R. Ahmad, P. Kuppusamy, Chem Rev. 110(5), 3212 (2010).

Deep Learning-Based Auto-Segmentation of Small-Volume of Brain Metastasis

Hojin Kim[*]

Department of Radiation Oncology, Yonsei Cancer Center, Yonsei University College of Medicine

Magnetic resonance imaging (MRI) is a very powerful imaging modality in the sense that it maximizes soft-tissue contrast by manipulating pulse sequence, facilitating accurate diagnosis. Beyond diagnostic purpose, it has been stretched out to therapeutic applications, especially focusing on the image guidance before actual treatment. Throughout efforts made over several decades, the MR-guided radiation therapy has been installed in over several hundred clinics around the world. MRIs in 0.35T and 1.5T are currently used with linear accelerator for X-ray radiotherapy. The inevitable trend demands so-called MR-only radiotherapy, which also required for addressing a couple of technical barriers. It is believed that a recent breakthrough, deep learning, is able to help advance the technology. At the same time, the deep learning network could be applied to tumor localization on MR imaging automatically. In radiotherapy, auto-segmentation is the most active field in radiation oncology that the deep learning is the most widely used. It should be more challenging with respect to tumor segmentation. Of various types of tumor segmentation, brain metastasis is one of the most difficult parts as the volumes are very small (< 0.5 cc in median). Thus, more elaborated approaches need to be proposed to enhance the segmentation approach. This presentation shows how to escalate the performance throughout deep neural networks and additional pre- and post-processing.

국가RI신약센터 및 생체영상이용 신약개발 지원소개

박장우[*]

Korea Radioisotope Center for Pharmaceuticals, Korea Institute of Radiological & Medical Sciences, Seoul, Korea

국가RI신약센터는 약 6년간 938억 원의 예산이 투입된 '방사성동위원소 이용 신개념 치료기술 개발 플랫폼 구축사업'을 통해 2019년 8월에 개소하였습니다. 또, 국가RI신약센터는 서울특별시 노원구에 위치하고 있으며, 1만7112㎡의 연면적에 지상 7층, 지하 2층 규모로 초감도가속질량분석기, 생체영상장비 등 연구장비와 방사성동위원소 기반의 비임상평가시설, 임상시험시설, 방사성의약품 생산시설 등을 갖추고 있습니다.

그리고 국가RI신약센터는 국내 제약사들이 해외에 나가지 않아도 국내에서 방사성동위원소를 이용하는 비임상/임상 시험을 할 수 있도록 지원하고, 치료용 방사성의약품 개발에서 후보물질 발굴, 유효성 평가, 비임상 독성평가(GLP) 및 임상용 방사성의약품 제조(GMP)에 이르는 전주기 과정을 진행할 수 있도록 지원하고 있습니다. 국내 제약사 및 연구자들이 신속하고 용이하게 이용 가능한 방사성동위원소이용 비임상 시험과 신약개발지원 위탁업무를 수행하며, 연구자가 직접 시설과 장비를 이용할 수도 있는 개방형 연구실도 운영하고 있습니다.

또, 실험동물을 이용한 비임상 유효성평가를 수행하며, 수요자 맞춤형 질환모델의 구축 및 세포주를 이용한 평가 그리고 비침습적 생체영상평가를 통하여 생체내 약물의 이동 및 치료 효능평가를 지원하고 있습니다. 특히, 구축된 최신 생체영상장비(MRI, PET/CT, SEPCT/CT 등)중 국내 최초로 CryoProbe coil을 도입하여 소동물용 고자장 9.4T MRI에서 높은 SNR의 영상획득이 가능하며, PET insert를 이용하여 PET과 MR의 동시영상획득이 가능합니다. 이처럼, 국가RI신약센터는 최신 장비 및 시설을 연구개발에 지원하고 있으며, 글로벌 수준의 연구지원체계를 갖추어가고 있습니다.
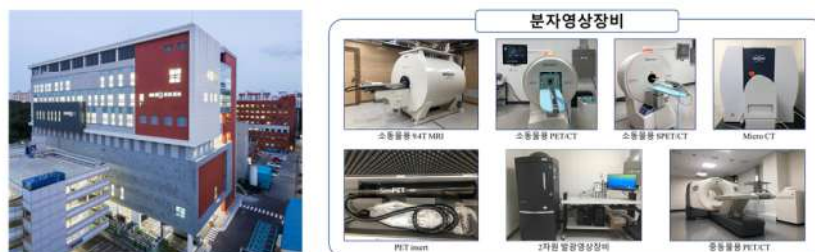
Fig. 1. 국가RI신약센터 전경(좌) 및 운영중인 소동물용 생체영상장비(우)
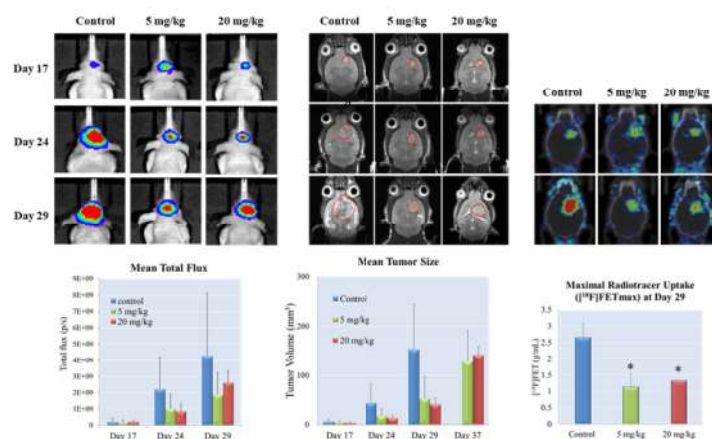
Fig. 2. 생체영상이용 약물의 유효성평가

Compact Superconducting Synchrocyclotron with Active Magnetic Shielding and Variable Beam Energy for Proton Therapy: MEVION S250 Series[TM]

Sung Hoon Oh[*]

HanBeam Technology, Seongnam, Korea
e-mail: shoh@hanbeamtek.com

Proton therapy is one of cnacer treatments to treat patients using separated protons obtained by accelerating hydrogen nuclei. Proton beams are also known to best provide the purpose of radiation therapy by minimizing the risk of damage to surrounding normal tissues, while to deposit most energy to only to cancer cells using a physical property called "Bragg peak". Mevion transformed radiation oncology by inventing compact proton therapy - shrinking the equipment footprint and the operational and financial costs significantly while still delivering a powerful cancer-fighting tool. The MEVION S250 Series[TM] is elegantly designed to deliver high-quality, efficient proton therapy treatments—optimizing both the outcomes and the economics of proton therapy.

Brain imaging : A comparison of 2D High resolution PROPELLER with 3D Fast spin echo imaging on multi-planar reconstruction

Ho Beom Lee[1*], Ji sung Jang[1], Yong Soo Han[2]

[1]Department of Radiology and Research Institute of Radiology, Asan Medical Center, Korea
[2]Department of Radiological Science, Hallym polytechnic University, Korea

The motion insensitive PROPELLER (Periodically Rotated Overlapping Parallel Lines with Enhanced Reconstruction) have been improved enabling high resolution images even with excellent contrast along the slice selection direction and other directions which can obtain similar quality to 3D sequences. Therefore, the aim of this study was to compare high resolution (HR) 2D PROPELLER and 3D CUBE T2-weighted sequence for image quality of general brain imaging. 13 healthy volunteers underwent cine MRI at 3 T (Signa Architect, GE Healthcare, USA) using 48-channel head coil. The axial data sets were reconstructed on a free-standing workstation to generate 1mm reformatted images in the sagittal and coronal, and sagittal planes. Contrast-to-noise ratios (CNR)s were calculated and measured in five regions of interest (ROIs). ROI were selected on frontal white matter, occipital gray matter and red nucleus, hippocampus, cerebellar tonsils. Overall image quality was graded on a scale of 1–5 (1, excellent, 2, good, probably no artifact; 3, fair, no sure on artifact; for each sequence, 4,

(C) Coronal(top), Sagittal(bottom) multi-planar reconstruction
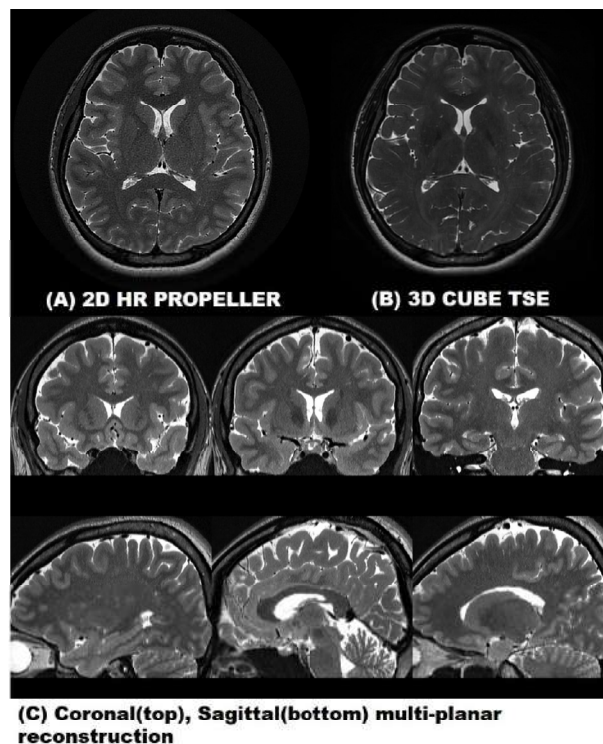
Fig.1. (A) 2D HR PROPELLER(Left), (B) 3D CUBE TSE(Right), (C) coronal(top), sagittal(bottom) multi-planar reconstruction

poor, probable artifact; definitely no artifact 5, unacceptable, definite artifact; Statistical significance was verified using paired t-test on quantitative analysis and Wilcoxon-signed rank test was performed on qualitative analysis. Parameters of the two sequences were maintained similar: TRs= [HR PROPELLER 4000msec, 3D CUBE; 2000msec], FOV=220*220 mm2, effective TE= [94msec, 96msec], voxel size=[0.6* 0.6 * 1, 1*1*1], acquisition time=[5min 17sec, 5min 43sec], acceleration factor=[3, 2*1.5]. As a result, in the slice selection direction (AX), 2D HR had high CNRs in all 5 ROIs (p<0.01). In particular, the difference in contrast between WM and GM was even stronger. In the reconstructed images, COR and SAG, although the difference was smaller than that of the section selection surface, the 2D HR PROPELLER was higher. Qualitative evaluation of the reconstructed images showed no significant differences between the two groups. In addition, artifacts were rather reduced in the 2D HR PROPELLER images. In conclusion, HR PROPELLER has excellent contrast and motion compensation, and also maintains the same image quality as the slice selection surface in MPR reconstruction.

Comparison of a zero-filling interpolation with a real matrix size at 1.5 Tesla based on spin-echo weighted imaging with various spatial resolutions: an ACR phantom study

Ji Sung Jang[1*], Ho Beom Lee[1], Min Cheol Jeon[2], Seong Ho Kim[2]

[1]Department of Radiology and Research Institute of Radiology, Asan Medical Center, Korea
[2]Department of Radiological Technology, Daejeon Health Institute of Technology, Korea

This study aimed to assess the effect of zero-filling interpolation (ZIP) and various spatial resolutions on quality assurance (QA). Two important variables for the assessments of magnetic resonance image quality were included with recommended acceptance criteria: high-contrast spatial resolution and low-contrast object detectability with reference limits. All acquired data were divided into two groups according to whether the ZIP technique was applied: group A (without ZIP) and group B (with ZIP). The spatial resolutions of both slice-1 images of T1-weighted and T2-weighted imaging in both directions fulfilled the American College of Radiology (ACR) criterion of 1.0 mm in group B. The observed high-contrast spatial resolution values were significantly different between the two groups up to a matrix size of 320 × 320 ($p < 0.05$). On the other hand, with a matrix size $\geq$ 384 × 384, no significant differences between the two groups were observed in terms of high-contrast spatial resolution ($p > 0.05$, Fig.1). For low-contrast object detectability, the total number of measured spokes in all groups fulfilled the ACR criterion. However, the low-contrast object detectability values without ZIP tended to decrease as the matrix size decreased. The use of ZIP can improve high-contrast spatial resolution and low-contrast object detectability while reducing image blurriness.
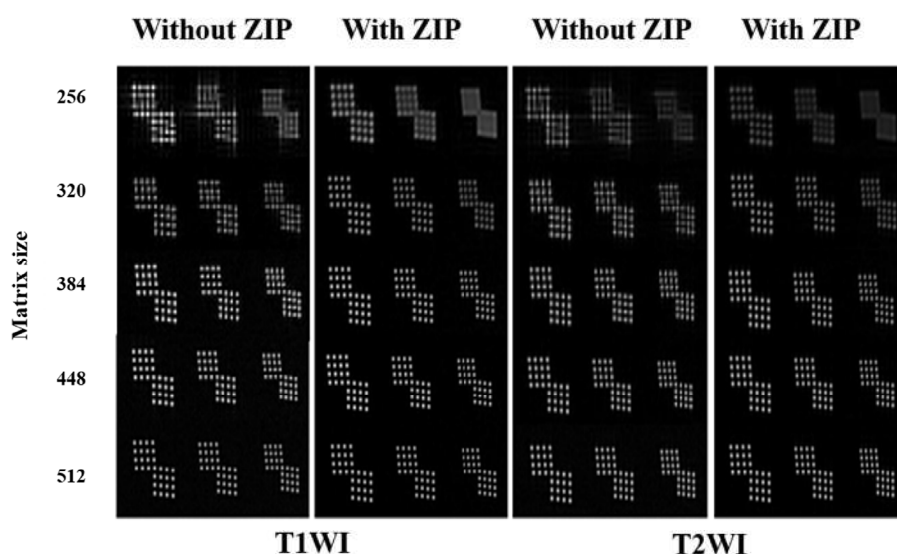
Fig.1. Images of the high-contrast spatial resolution obtained with and without ZIP according to different matrix sizes.

Effects of Stimulation Method and Frequency of rTMS on Motor Cortex Activation in Stroke Patients

Sung-Ryong Ma[1*], Byung-Il Yang[2], Bo-Kyoung Song[3]

[1]Department of Occupational Therapy, Chosun University, Gwnagju, Republic of Korea
[2]Department of Physical Therapy, Sangji University, Wonju, Republic of Korea
[3]Department of Occupational Therapy, Kangwon National University, Samcheok, Republic of Korea

Stroke is characterized by neurological deficits in sensory, cognitive, language, and motor functions due to cerebral vascular hemorrhage or cerebral ischemia, resulting in weakness of the body. In particular, damage to the lateral corticospinal tract leads to disruption of the opposite upper limb and hand movement. Recently, various rehabilitation approaches have been introduced to improve upper limb motor function of stroke patients. Especially repetitive transcranial magnetic stimulation (rTMS) was introduced as a therapeutic modality for post-stroke upper limb hemiparesis. TMS is a brain stimulation method that non-invasively stimulates the cerebral cortex safely and effectively, with little or no pain, due to the fact that it is not weakened by strong resistance such as the skull or scalp and does not form a strong current density. The effect of TMS is different depending on the type of stimulation. Therefore, rTMS may increase or decrease excitability to the cortical spinal cord depending on the strength of the stimulus, the direction and frequency of the coil. rTMS is divided into high frequency and low frequency depending on frequency. A high frequency of 5 to 20 Hz increases the response of the cerebral cortex, which can be seen to decrease the MEP threshold. Low frequency stimuli also stimulate below 1 Hz or at the same frequency, resulting in suppression of cortical responses.

Fig. 1. rTMS application
(https://www.med.unc.edu/psych/patient-care/interventional-psychiatry/tms/)

Robust resonant spin dynamics of magnetic nanoparticles for magnetic hyperthermia application

Jae-Hyeok Lee, Min-Kwan Kim, Yongsub Kim, Bosung Kim and Sang-Koog Kim[*]

National Creative Research Initiative Center for Spin Dynamics and Spin-Wave Devices, Nanospinics Laboratory, Department of Materials Science and Engineering, Seoul National University, Seoul 151-744, South Korea

Magnetic nanoparticles of different sizes exhibit very unique magnetization dynamics such as uniform magnetization precession, vortex-core gyration, and spin waves [1,2]. Since such magnetization dynamics are followed by energy dissipation owing to the intrinsic damping of individual spins' precession, low-power-driven heat generation can be established through resonant spin excitations driven by microwave magnetic fields [3,4]. In this talk, we introduce the relevant characteristic spin dynamics of nanoparticles and present how such novel dynamic behaviors can be used for heat generation; additionally, we present an amazing result of heat generation rates, the values of which have yet to be found for conventional magnetic hyperthermia [5]. In detail, we experimentally demonstrated that highly efficient heat-dissipation power in MFe_2O_4 (M = Fe, Mn, Ni) ferrite nanoparticles gives rise to a targeted temperature increment [6]. The power is two orders of magnitude greater than those of conventional Néel-Brownian mechanism. From micromagnetic simulation and analytical derivation, we also found close correlations between the temperature increment and the intrinsic material parameters of the damping constant as well as saturation magnetizations of nanoparticles' constituent materials. Our experimental results and theoretical formulations provide for a better understanding of the effect of resonant spin dynamics on the efficiency of heat generation as well as a straightforward guidance for the design of advanced materials for controls of highly localized incrementation of targeted temperatures using magnetic particles. This work may offer a precisely controllable and highly efficient means of heat generation for bio-applications, e.g., magnetic hyperthermia.

References

[1] S.-K. Kim et al., Sci. Rep. **5**, 11370 (2015)

[2] S.-K. Kim et al., Sci. Rep. **6**, 31513 (2016)

[3] M.-K. Kim and S.-K. Kim et al., Phys. Rev. Applied **9**, 054037 (2018)

[4] M.-K. Kim and S.-K. Kim et al., J. Appl. Phys. **125**, 063901 (2019)

[5] J.-H. Lee and S.-K. Kim et al., Sci. Rep. 11, 4969 (2021)

[6] J.-H. Lee and S.-K. Kim et al., Sci. Rep. 12, 5232 (2022)

Symposium 10

'Bio-Convergence Magnetics'
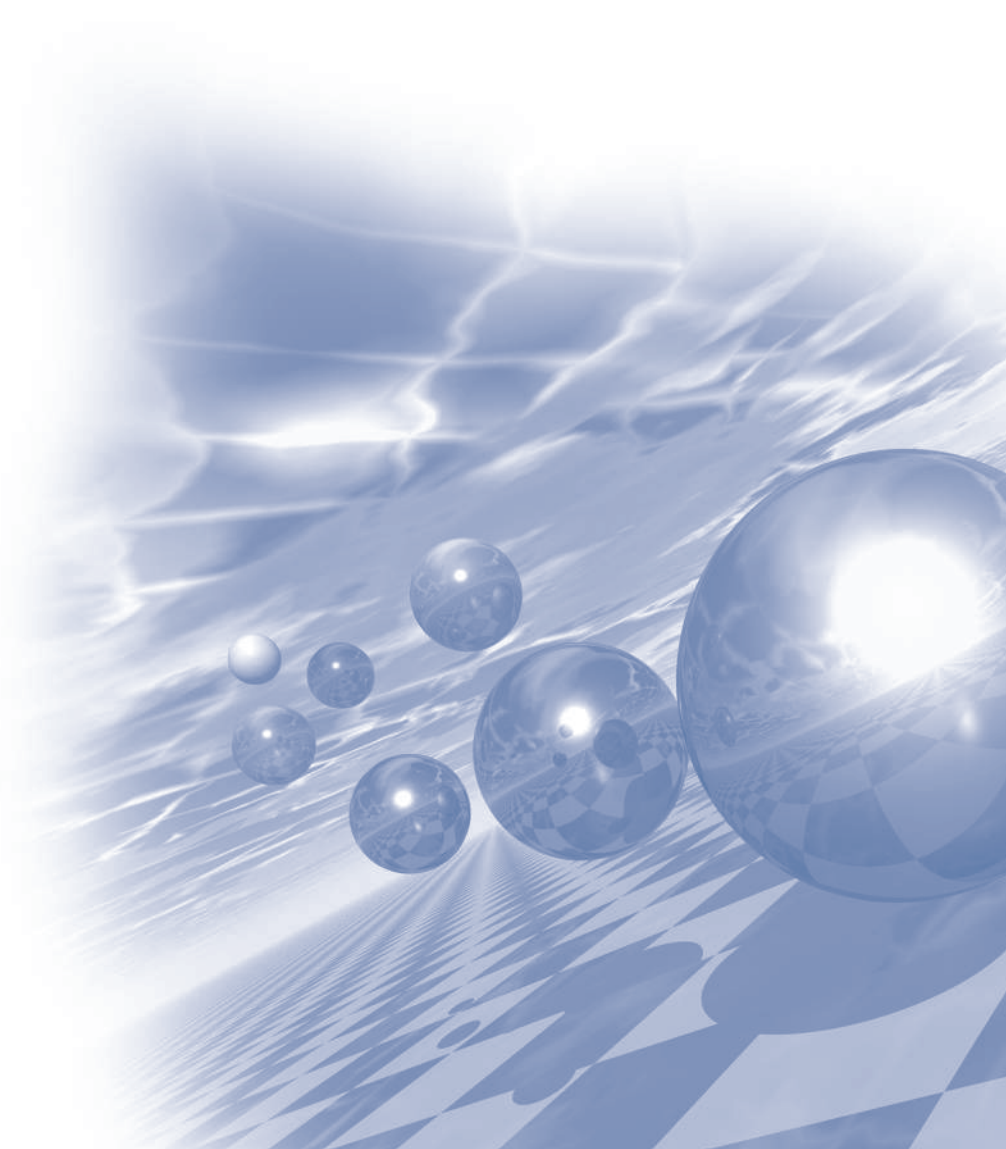
Single-crystalline-level properties of ultrathin, clean, wide, and flexible SrRuO₃ membranes for surface-related applications

Dongha Kim[1], Wook Ki Jung[2], Shinbuhm Lee[1*]

[1]Department of Physics and Chemistry, DGIST, Korea
[2]Agency for Defense Development, Korea

Transferring single-crystalline (SC) membranes to flexible substrates has attracted much attention, enabling new functionality and enhanced performance of various devices. A commonly used support-assisted transfer process inevitably leaves dirty residue on the material surfaces, limiting further development of surface-related applications. Here, we scaled down the thickness of SC SrRuO₃ (SRO) flexible membranes to 15 nm with a clean surface area of 2.5×2.5 mm², by reducing the surface tension on polyethylene terephthalate (PET) substrates via oxygen-plasma-treated conversion to a hydrophilic PET surface. The concomitant satisfaction of thinness, clean and wide surface, and flexibility in SC SRO membranes guarantees a high transmittance of up to 60%, a low resistivity of 10^{-4}-10^{-3} Ω cm at room temperature, and band ferromagnetism below 150 K with a high magnetic moment of ~0.5 μ_B/Ru at 10 K. These values are comparable to those of SC SRO solid films. The excellent optical, electrical, and magnetic properties of our ultrathin, clean, wide, and flexible SC SRO membranes imply their potential use in state-of-the-art platforms for next-generation electronics and energy devices.

Magnetic-based Pressure Sensor and Its Applications for Bio-medical Instruments

Sungwon Lee[*]

Department of Emerging Materials Science, Daegu Gyeongbuk Institute of Science & Technology (DGIST),
333, Techno Jungang-daero, Hyeonpung-myeon, Dalseong-gun, Daegu 711-873, Korea

Pressure sensors have been integral in the development of biomedical industry and health monitoring devices. Their versatility in applications as well as their simple, straightforward mechanisms have led to massive production of sensors which are typically based on the electrical properties of the active materials. This, however, introduces some risks in sensor reliability due to difficulties in maintaining the materials' uniformity. To address this issue, a unique magnetic-based pressure sensor is fabricated utilizing a planar Hall resistive sensor. The stability of the magnetic sensor and its small hysteresis value ensures high reproducibility. The successful integration of the magnetic-based pressure sensor into health monitoring processes such as pulse monitoring, respiration and phonetic recognition also promises its wide expanse of possibilities as a wearable diagnostic device. We demonstrate here grasping force measurement system for infant that require precise pressure signal detection from unambiguous force application.

자성기반 펜슬형 맥박패턴 측정 시스템

오선종[1*], 김성기[1], 이보연[1], 정영도[1], 김미진[2], 김철기[2]

[1]한국기계연구원, 자연모사응용연구실
[2]대구경북과학기술원, 나노소자연구실

사람의 혈관은 노화, 당뇨, 심혈관 질환 등에 의한 질병, 흡연, 비만 등의 이유로 혈관의 탄력조직(elastin)의 감소 또는 파괴됨에 따라 경직도(stiffness)가 상승하게 된다. 혈관 경직도가 상승하면 심장의 수축기 때 혈압이 크게 상승하게 되어 심혈관, 뇌혈관, 관상동맥, 말초혈관에 문제를 발생시킬 수 있다. 혈관의 경직도는 맥박패턴 분석 (PWA; pulse wave analysis) 또는 맥파전달 속도 (PWV; pulse wave velocity) 측정을 통해 분석하고 있으며 고감도/고신뢰도의 측정 소자 및 시스템이 요구되고 있다.

본 연구에서는 미세한 맥박패턴 측정이 가능한 자성기반 유연센서를 펜슬형으로 제작하여 민감도와 신뢰성을 동시에 높인 맥박패턴 측정 시스템을 개발하였다. 개발한 자성기반 펜슬형 맥박 패턴 측정시스템은 손목과 같은 맥박패턴 측정부에 접촉하는 맴브레인과 물리적 힘을 전기적 신호로 변환해주는 자성기반 센서부, 맥박패턴 측정 부위와 맴브레인의 거리를 제어하는 모터 제어부 그리고 신호분석 소프트웨어로 구성되어 있다.

맥박패턴 측정부로부터 맴브레인의 위치를 조절하여 맴브레인이 피부에 접촉하는 힘을 정밀하게 제어할 수 있기 때문에 보다 정확한 맥박 패턴을 얻을 수 있었다. 또한, 피부에 가해지는 힘에 따른 맥박패턴 측정 및 분석을 통하여 혈관 경직도와의 상관관계를 파악하였고, 신호분석 소프트웨어 개발을 통해 혈관 건강상태에 따른 정확한 물리적 혈관특성을 모니터링 할 수 있는 측정시스템을 개발 하였다.

그림 1. 자성기반 펜슬형 맥박 패턴 실시간 측정 시스템

Analysis of Reflected Wave Characteristics using Cardiovascular Simulator : Wave Separation Analysis

Min-Woo Lee[1*], Jae-Yeon Choi[2]

[1]Daegu Gyeongbuk Institute of Science & Technology, Korea
[2]Department of Physics and Chmistry, Daegu Gyeongbuk Institute of Science & Technology, Korea

A aim of this study is to analysis the reflected wave characteristics through a waveform separation algorithm using a cardiovascular simulator. The simulator can be divided into three parts, consisting of a pulse generator part, which act as the heart of the human body, a vascular part, and a distal part to set the terminal conditions. Heart rate, stroke volume, and SD ratio were controlled by the pulse generator, and a uniform-one tube model was used for the vascular part to most easily interpret the results. To investigate the effect of vascular terminal conditions on reflected waves, the terminal was set with a compliance chamber and a resistance valve at the end of the one tube to control resistance and compliance. In this study, the effect of the resistance and compliance characteristics at the end of the vascular on the reflected wave was objectively analyzed in the frequency domain, not in the time domain. Wave separation was performed using the verified wave separation algorithm that has been used for a long time using the actual measured pressure and flow waveform. The reflected wave obtained in the above process was analyzed in the frequency domain by FFT.
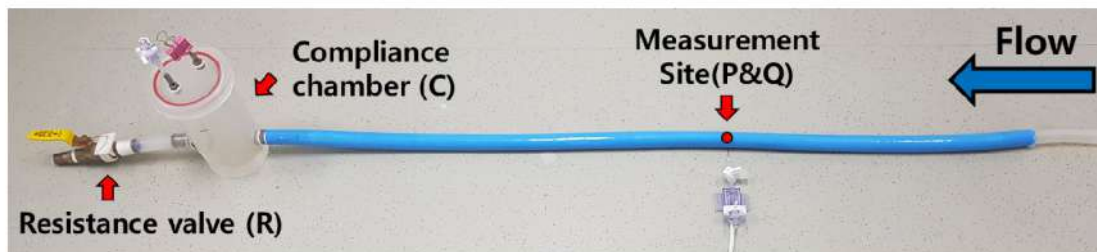
Fig. 1. Experiment System with one tube model
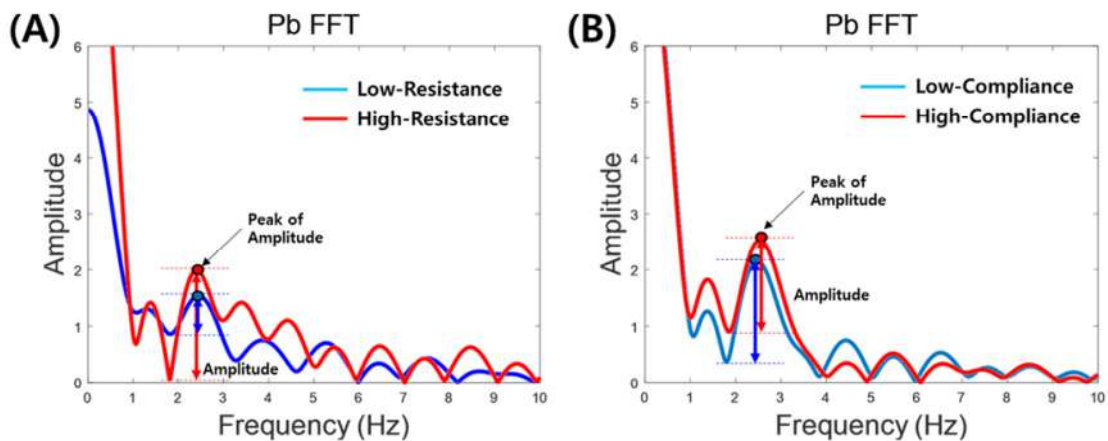
Fig. 2. FFT of reflected wave of one tube model (A) effect of resistance (B) effect of compliance

As a result of adjusting the resistance and compliance at the end of the One-Tube, the trends in the frequency domain were different. As the resistance increases, both Amplitude and Peak of Amplitude increase in the corresponding frequency section, and there is no change in the corresponding frequency section. On the other hand, as compliance increased, there is little change in the amplitude, but the peak of amplitude increased the same as the resistance characteristics. In addition, the corresponding frequency section to the peak of amplitude increased. Through this study, the possibility of developing new evaluation index was confirmed through frequency analysis of the reflected wave.

Large-scale Atomic/Molecular Massively Parallel Simulator (LAMMPS) for Bio-Convergence Magnetics

Chun-Yeol You[*]

Department of Emerging Materials Science, DGIST, Daegu, Korea

LAMMPS (Large-scale Atomic/Molecular Massively Parallel Simulator) is one of the widely used open source simulator for the molecular dynamics in the chemistry, biology, and materials science societies. It is scalable for practical problems which involve huge number of particles, molecules, proteins. Many kinds of potential are implemented including electrostatics potential and metallic bonding. In this presentation, we would like to discuss about possibilities of the LAMMPS applications for the bio-convergence magnetics. In order to study the external magnetic field in the molecular dynamics, we implanted Lorentz force by introducing fix bfield command. Some examples of the LAMMPS results will be discussed.

Symposium 1

'Quantum Magnetism'
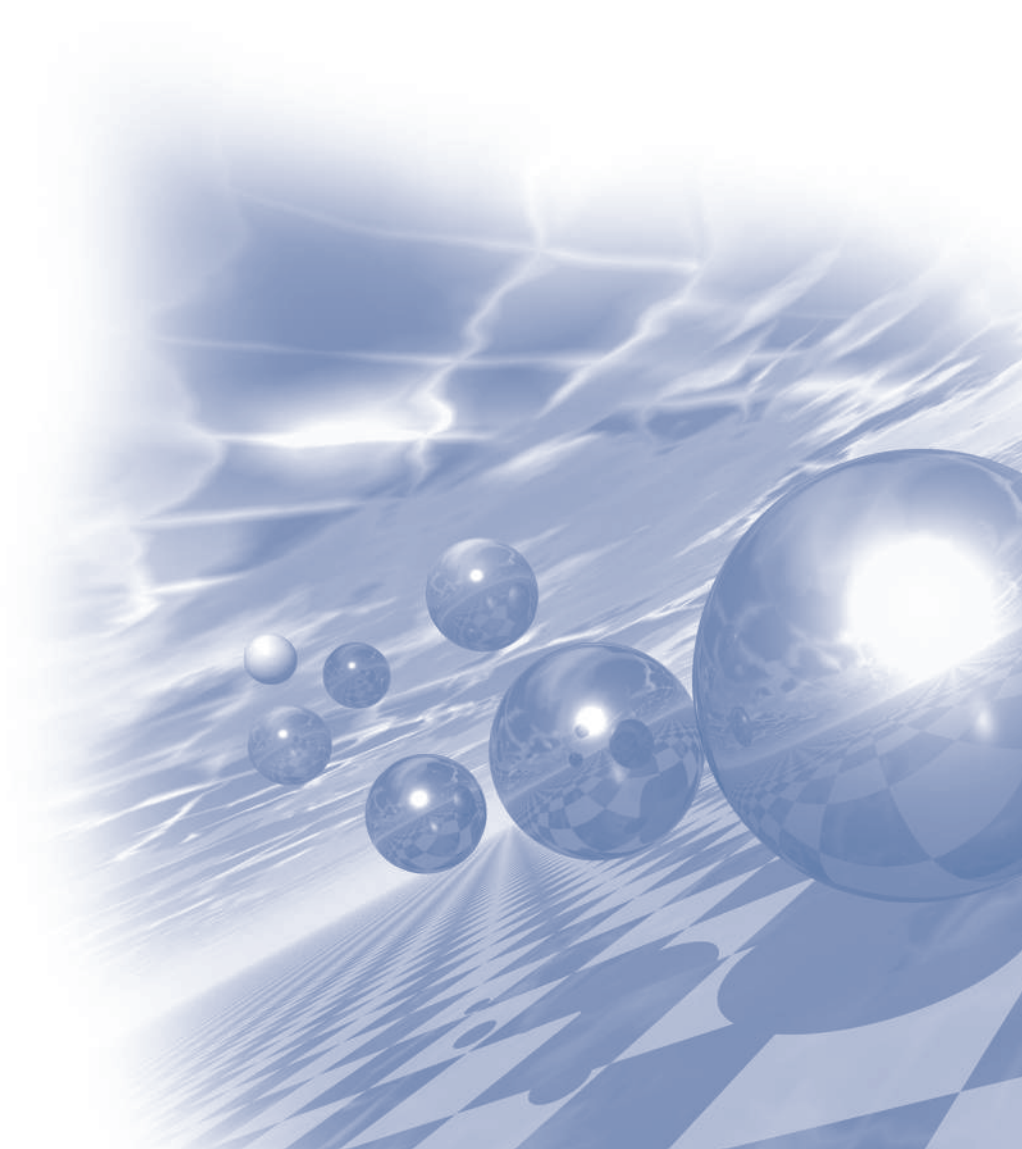
Quantum entanglement in Co compounds

Je-Geun Park[*]

Center for Quantum Materials, Department of Physics & Astronomy, Seoul National University, Korea

The relativistic spin-orbit coupling can, in principle, entangle the two quantum states leading to the entangled Hilbert space of J-manifold. However, this term is usually the smallest among the relevant energy scales, and often we witness it is intervened by other stronger terms, most notably the Jahn-Teller term. For this reason, it has so far been extensively studied for Ir and Ru, where the situations are more favorable for the J-physics. Nevertheless, it is still worthy of exploring the possibility of finding examples among 3d transition metal compounds. If found, it would provide a new platform to study the spin-orbit entanglement under strong electron correlations. In this talk, I will pick up the specific case of Co^{2+} and examine several compounds in the search for hints of spin-orbit entanglement.

1/9 Magnetization Plateau and Fractionalized Excitations in the S=1/2 Kagome Antiferromagnet YCu$_3$[OD]$_{6+x}$Br$_{3-x}$

Kwang-Yong Choi[1*], Seongmin Jeon[1], Seungyeol Lee[2], Youngsu Choi[3], Dirk Wulferding[4], Mingseong Lee[5], Suheon Lee[6], Sungkyun Choi[6], Tae-Hwan Jang[7], Ki Wan Nam[8], Kee Hoon Kim[8]

[1]Department of Physics, Sungkyunkwan University, Korea
[2]Department of Physics, Chung-Ang University, Korea
[3]Department of Energy Science, Sungkyunkwan University, Korea
[4]Center for Correlated Electron Systems, IBS, Korea
[5]The National High Magnetic Field Laboratory, NANL, USA
[6]Center for Integrated Nanostructure Physics, IBS, Korea
[7]MPPHC-CPM, Planck POSTECH/Korea Research Initiative, Korea
[8]Department of physics and astronomy, SNU, Korea

One of the most sought-after many-body phenomena in quantum magnets is a quantum spin liquid (QSL)-a long-range entangled spin state that defies the standard symmetry-breaking paradigm. A S=1/2 kagome Heisenberg antiferromagnet (KHAF)- a two-dimensional lattice formed by corner-sharing triangles is proposed for a paradigmatic setting for achieving QSLs. Singularly, recent numerical calculations are converging on the notion that the KHAF stabilizes a QSL ground state at zero field as well as the fractional magnetization plateaus m=1/9, 3/9, 5/9, and 7/9 under an external field. The kinetic frustration leads to the crystallization of magnons localized on the hexagon of the kagomé lattice at m=3/9, 5/9, and 7/9, while the 1/9 magnetization plateau is controversially discussed in terms of a topological Z_3 spin liquid vs valence bond crystal.

To date, a number of S=1/2 kagome compounds are reported to be QSL candidates. Nonetheless, the 1/9 plateau predicted in theory is not observed in the kagome candidate materials, thereby constituting one of the fundamental quests in KHAFs. In this talk, we address this issue in the recently discovered YCu$_3$(OH/D)$_{6+x}$Br$_{3-x}$. Our high-field magnetization curve $M(H)$ unveils the characteristic 1/9 and 1/3 plateaus at $\mu_0 H_{1/9} \approx 22$ T and $\mu_0 H_{1/3} \approx$ 60 T expected for the perfect KHAF model. Raman spectroscopy probes fractionalized spinon excitations. Further, the specific heat and thermal conductivity data evince that a zero-field ground state bears signatures of a gapless U(1) liquid, yet some deviations are evitable due to bond randomness.

Structural glassy behavior on the Coulomb frustrated magnet

Hyeok-Jun Yang, Eun-Gook Moon, SungBin Lee[*]

Department of Physics, Korea Advanced Institute of Science and Technology, Daejeon, 34141, Korea

The interplay of competing interactions and global constraint on the magnet is a wealth of unusual phenomena such as spin liquids, glass-forming liquids and non-equilibrium physics. Here, we study the standard Monte-Carlo simulation supported by a mean-field theory of the Coulomb frustrated magnet. The competition of short-ranged ferromagnetic and long-ranged antiferromagnetic interactions forbids the formation of static magnetic order, instead develops a heterogeneous structure due to global neutrality. When the Coulomb interaction dominates the system, it stabilizes the regular pattern of striped phases whose period depends on the frustration parameter and temperature. However, for small but nonzero Coulomb interaction, it stabilizes the sluggish phase whose auto-correlation function features the slow dynamics without quenched disorder. We also estimate the structure factor to investigate the liquid-like correlation. Our analysis is relevant to spin ice and Coulomb Ising model, whose kinematic constraint generically imposes the slow relaxation and non-equilibrium dynamics.

Terahertz Evidence of Room-Temperature Quantum Spin Liquid Behavior in TbInO₃

Taek Sun Jung[1], Xianghan Xu[2,3], Jaewook Kim[4], Beom Hyun Kim[5], Eun-Gook Moon[6], Sang-Wook Cheong[2,3], Jae Hoon Kim[1*]

[1]Department of Physics, Yonsei University; Seoul 03722, Republic of Korea
[2]Department of Physics and Astronomy, Rutgers University; Piscataway, New Jersey 08854, USA
[3]Rutgers Center for Emergent Materials, Rutgers University; Piscataway, New Jersey 08854, USA
[4]Korea Atomic Energy Research Institute; Daejeon 34057, Republic of Korea
[5]School of Computational Sciences, Korea Institute for Advanced Study; Seoul 02455, Republic of Korea
[6]Department of Physics, Korea Advanced Institute of Science and Technology; Daejeon 34141, Republic of Korea

Quantum spin liquids (QSLs) are extremely entangled Mott insulating states, manifested by exotic emergent excitations. Signatures of such excitations, if any, are commonly believed to be observable only at low temperatures, as in α-RuCl₃ and herbertsmithite (ZnCu₃(OH)₆Cl₂). Here, we challenge this common belief and show, by using terahertz time-domain spectroscopy (THz-TDS), that exotic emergent excitations indicating QSL behavior in TbInO₃ survive even at room temperature. Over the entire temperature range of 1.5–300 K, we observe a parabolic frequency dependence in the real part of the in-plane optical conductivity and the Fano asymmetry of an optical phonon strongly interacting with the excitation continuum. These features are robust even under external magnetic fields up to 7 T. Our data confirm the presence of emergent charge carriers within the Mott charge gap of TbInO₃, opening up a possibility to probe and manipulate highly entangled QSL states at room temperature.

Magnetic phase diagram of the 2-dimensional triangular lattice antiferromagnet Na$_2$BaMn(PO$_4$)$_2$

Jaewook Kim[1*], Kyoo Kim[2], Eunsang Choi[1], Young Joon Ko[3], Dong Woo Lee[1], Sang Ho Lim[1], Jong Hoon Jung[3] and Seongsu Lee[1]

[1]Korea Atomic Energy Research Institute, Daejeon 34057, Republic of Korea
[2]National High Magnetic Field Laboratory, Florida State University, Tallahassee, FL 32310-3706, U.S.A.
[3]Department of Physics, Inha University, Incheon 22212, Republic of Korea

We report the magnetic phase transitions of the 2-dimensional triangular lattice antiferromagnet Na$_2$BaMn(PO4)$_2$ with spin-5/2. From specific heat measurement, we observe two magnetic transitions at temperatures 1.15 and 1.30 K in zero magnetic field. Detailed AC magnetic susceptibility measurements, with magnetic field applied along the c direction, show multiple phases including the ↑↑↓ phase between 1.9 T and 2.9 T at 0.047 K. These observations imply that Na$_2$BaMn(PO$_4$)$_2$ is a classical $2d$-TL Heisenberg AFM with easy-axis anisotropy. However, it deviates from an ideal model as evidenced by additional magnetic field-induced phases and a hysteresis region between the ↑↑↓ and V-phases. Our work provides another experimental example to study frustrated magnetism in $2d$-TL AFM which also serves as a reference to understand the possible quantum spin liquid behavior observed in isostructural systems with quantum spins.

Noncollinear magnetic order and spin dynamics in a polar honeycomb antiferromagnet Ni$_2$Mo$_3$O$_8$

Sungkyun Choi[1,2*]

[1]Center for Integrated Nanostructure Physics (CINAP), Institute for Basic Science (IBS), Suwon 16419, Republic of Korea

[2]Sungkyunkwan University (SKKU), Suwon 16419, Republic of Korea

Multiferroic in condensed matter physics is an intriguing topic owing to the potential future application, including spintronics, and a promising subject to discover new electronic phases and their transitions. Motivated by finding novel magnetism and understanding its role in electric polarisation in multiferroics, we studied a polar honeycomb antiferromagnet Ni$_2$Mo$_3$O$_8$ using a primary tool of neutron scattering. This material is attractive owing to highly frustrated magnetic exchange interactions in the honeycomb lattice of S=1 (Ni^{2+}) magnetic ions in the context of finite electric polarisation. Its uniqueness lies in an unusual structural motif of alternating octahedral and tetrahedral oxygen environments in the bipartite honeycomb layer, a model to be able to learn about a new aspect of the coupling between magnetisation and polarisation. In this study, we determined a noncollinear magnetic order using powder and single-crystal neutron diffraction supported by direction-dependent magnetic susceptibility. Our magnetic structure can be understood by the local magnetic anisotropy calculated by the crystal electric field theory. We also performed inelastic neutron scattering measurements on the powder sample to explore the magnetic excitation emerging from the noncollinear magnetic structure. We will discuss how we could understand its electric polarisation related to magnetism.

Symposium 11

'자기이론분과 심포지움'
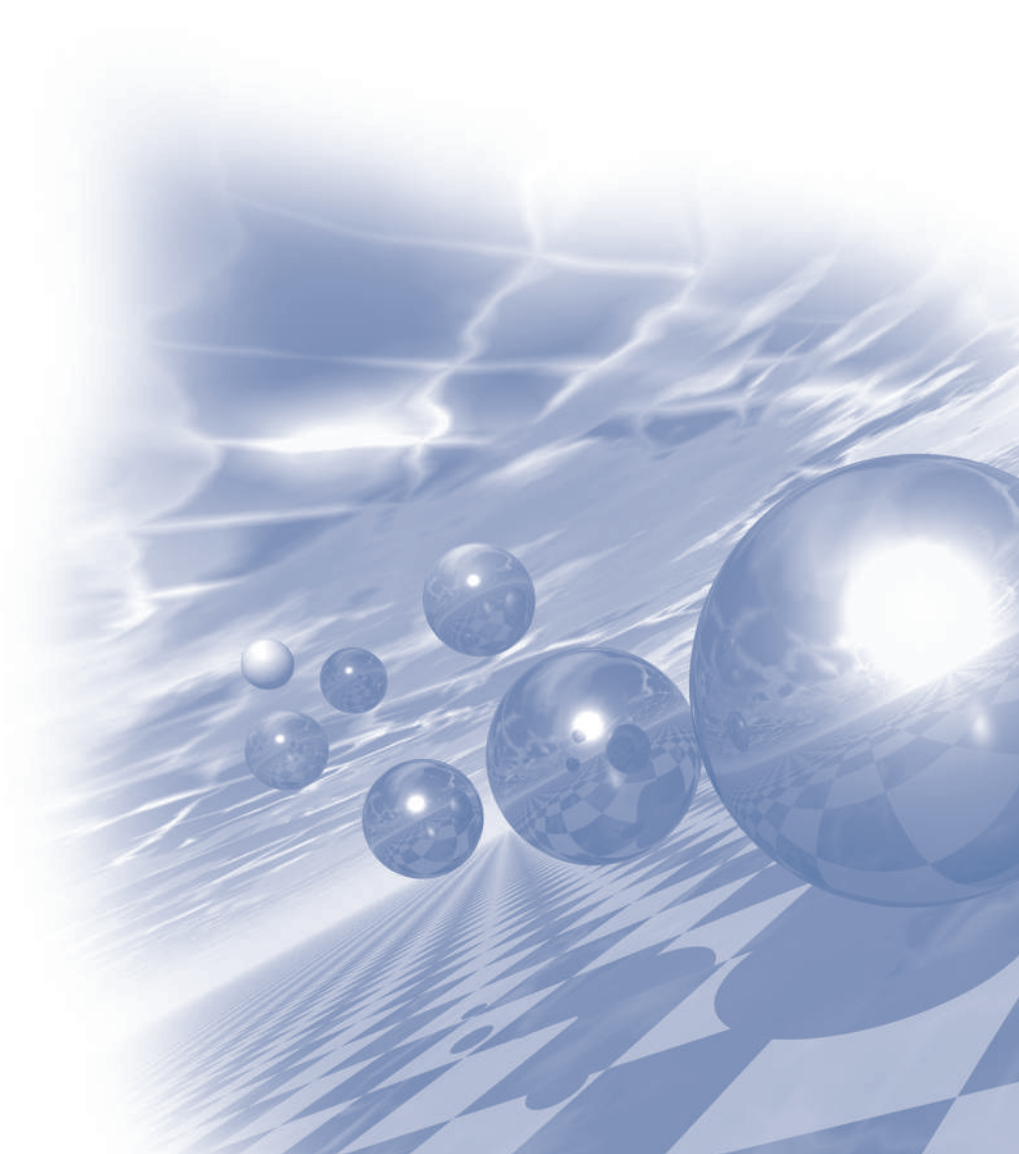
Anomalous Hall signatures of nonsymmorphic nodal lines in the doped chromium chalcospinel CuCr$_2$Se$_4$

Subhasis Samanta[1], Gang Chen[2] and Heung-Sik Kim[1]

[1]Department of Physics and Institute of Quantum Convergence and Technology, Kangwon National University
[2]Department of Physics and Center of Theoretical and Computational Physics, University of Hong Kong

An emerging phase of matter among the class of topological materials is nodal line semimetals, possessing symmetry-protected one-dimensional gapless lines at (or close to) the Fermi level in k space. When the k dispersion of the nodal line is weak, van Hove singularities generated by the almost flat nodal lines may be prone to instabilities introduced by additional perturbations such as spin-orbit coupling or magnetism. Here, we study the Cr-based ferromagnetic chalcospinel compound CuCr$_2$Se$_4$ (CCS) via first-principles electronic structure methods and reveal the true origin of its dissipationless anomalous Hall conductivity, which was not well understood previously. We find that CCS hosts nodal lines protected by nonsymmorphic symmetries, located in the vicinity of Fermi level, and that such nodal lines are the origin of the previously observed distinct behavior of the anomalous Hall signature in the presence of electron doping. The splitting of the nodal line via spin-orbit coupling produces a large Berry curvature, which leads to a significant response in anomalous Hall conductivity. Upon electron doping via chemical substitution or gating, or rotation of magnetization via external magnetic field, noticeable change of anomalous Hall behavior occurs, which makes CCS a promising compound for low-energy spintronics applications.

Anti-Hund's Singlet State in
an Insulating layered Nickelate

Kwan-Woo Lee[*]

Division of Display and Semiconductor Physics, Korea University, Sejong
Department of Applied Physics, Graduate School, Korea University, Sejong

Spin singlet physics in two-dimensional systems has played an important role in high T_c superconducting cuprates. Recently, similarities of layered nickelates to cuprates have stimulated extending this concept to superconducting nickelates. The major concept in cuprates has been the Zhang-Rice singlet that categorizes undoped cuprates as charge-transfer insulators (CHIs) rather than Mott-Hubbard insulators (MHIs). Even for undoped $NdNiO_2$ that has been considered to be in the middle of CHI and MHI, this concept may account for the observed low temperature behavior.

In this presentation, we will focus on a novel singlet phase in an infinite layered d^8 nickelate $Ba_2NiO_2(AgSe)_2$. The unprecedented singlet in the e_g orbital has compensating $d(x^2-y^2)$ up-spins with $d(z^2)$ down-spins inside of each Ni ion that violates the Hund's first rule, resulting in zero net spin moment. We propose that our anti-Hund's singlet accounts for the experimental observations of the signature of magnetic reconstruction in susceptibility at 130 K without any Curie-Weiss background (no moment). We will provide more analysis of the d^8 anti-Hund's singlet state in the presentation.

Fig. 1. Anti-Hund's Singlet (Red: spin-up, Green: spin-down)

References

[1] K.-W. Lee and W. E. Pickett, Phys. Rev. B 70, 165109 (2004).

[2] H.-S. Jin, W. E. Pickett, and K.-W. Lee, Phys. Rev. Research 2, 033197 (2020).

[3] A. S. Botana, K.-W. Lee, M. R. Normal, V. Pardo, and W. E. Pickett, Frontiers in Phys. 9, 813532 (2021).

[4] H.-S. Jin, W. E. Pickett, and K.-W. Lee, J. Phys. Materials 5, 024008 (2022).

[5] W.-L. Tu, E.-G. Moon, K.-W. Lee, W. E. Pickett, and H.-Y. Lee, Commnu. Phys. (in press).

Competing magnetisms in Sr_2RuO_4

Bongjae Kim

Department of Physics, Kunsan National University, Korea

In this study, we report the magnetic energy landscape of Sr_2RuO_4 employing generalized Bloch approach within density functional theory. We identify the two dominant magnetic instabilities, ferromagnetic and spin-density-wave, together with *other* instabilities. We show that epitaxial strain can change the overall magnetic tendency of the system, and tune the various magnetic instabilities of the system. Especially, the balance between spin-density-wave and ferromagnetic instabilities can be controlled by the strain, and, eventually can lead to the new static magnetic phases as well as possibly altering the superconducting channels. Our findings are compared with previous theoretical models and experimental reports on the various magnetic features of the system, and offers first-principles explanation to them.

Dynamical mean-field theory study of a ferromagnetic CrI3 monolayer

Chang-Jong Kang[1,2,*], Jeongwoo Kim[3]

[1]Department of Physics, Chungnam National University, Daejeon 34134, Korea
[2]Institue of Quantum Systems, Chungnam National University, Daejeon 34134, Korea
[3]Department of Physics, Incheon National University, Incheon 22012, Korea

We have employed one of the well-known many-body techniques, density functional theory plus dynamical mean-field theory (DFT + DMFT), to investigate the electronic structure of ferromagnetic monolayer CrI3 as a function of temperature and hole-doping concentration. The computed magnetic susceptibility follows the Curie's law, indicating that the ferromagnetism of monolayer CrI3 originates from localized magnetic moments of Cr atoms rather than Stoner-type itinerant ones. The DFT + DMFT calculations show a different coherent temperature for each spin component, demonstrating apparent strong spin-dependent electronic correlation effects in monolayer CrI3. Furthermore, we have explored the doping-dependent electronic structure of monolayer CrI3 and found that its electronic and magnetic properties is easily tunable by the hole-doping.

Session 6

구두발표 ∨
'Theory and Computational Magnetics'
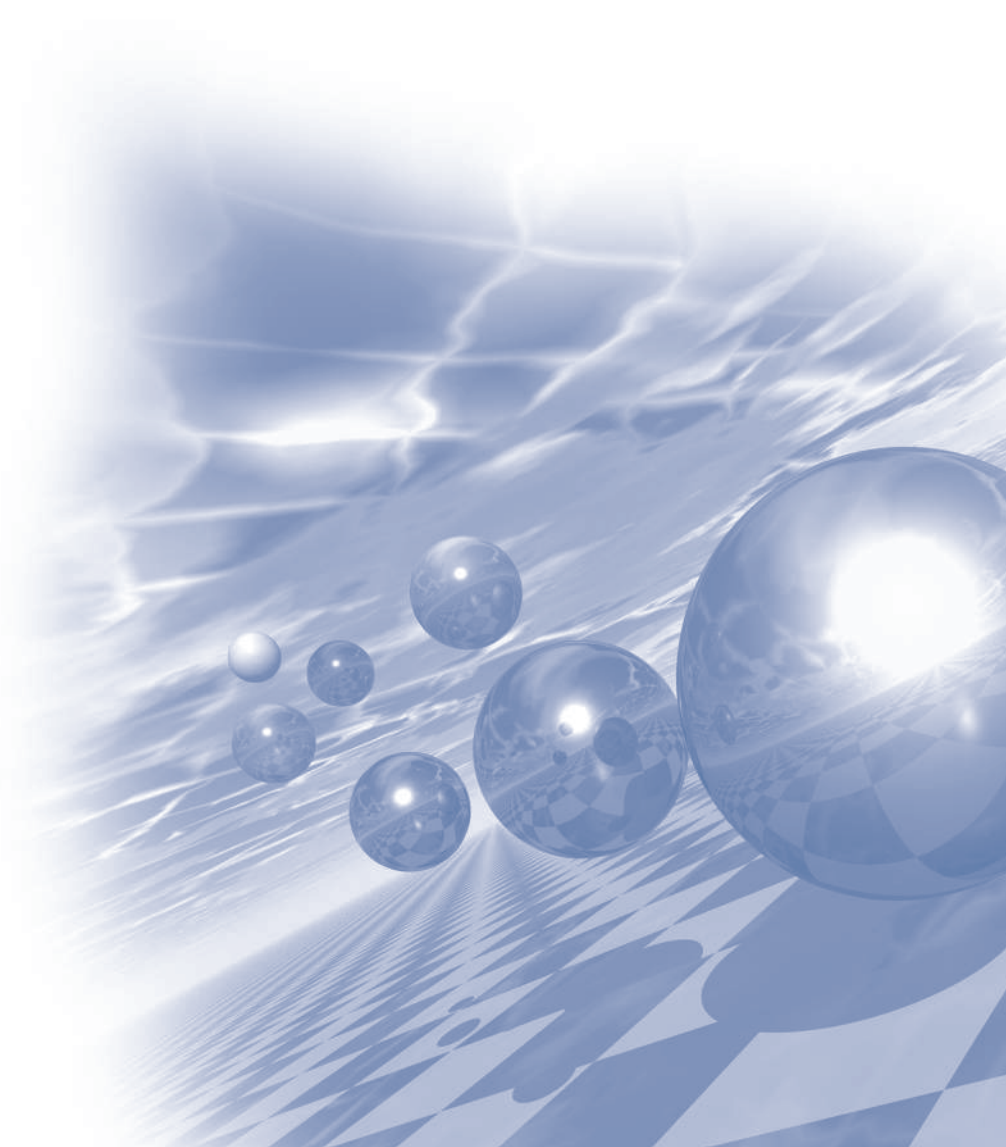
Electric field induced giant anomalous Nernst effect and switching in 2D MoTe₂/VSe₂ heterostructure

Brahim Marfoua and Jisang Hong[*]

Department of Physics, Pukyong National University, Busan 48513, Korea

Generation of the transverse electric current by a longitudinal charge or heat current is receiving extensive research efforts because of its potential applications in information-processing devices. Therefore, we investigated the electric field dependent Curie temperature, anomalous Hall conductivity (AHC), and anomalous Nernst conductivity (ANC) of the 2H-MoTe₂/1T-VSe₂ heterostructure. The MoTe₂/VSe₂ heterostructure had a Curie temperature of 270 K, and the Curie temperature was substantially increased to 355 K under the electric field. We obtained the electric field induced switching of the AHC in the electron doped system, whereas no switching was found in the hole doped system. Also, the electric field dependent ANC of the MoTe₂/VSe₂ heterostructure was investigated. The electric field dependence of the ANC was more prominent in the electron doping system. We obtained a giant ANC of 6.2 A/K.m when the electric field was applied from VSe₂ to MoTe₂ layer, and this was switched to -1.5 A/K.m with an opposite electric field. This finding may indicate the 2D MoTe₂/VSe₂ heterostructure can be used for potential applications in energy conversion and spin caloritronics devices.

Topological singularities and avoided crossings in compensated ferrimagnet Mn₃Al

Minkyu Park[*] and S. H. Rhim

Department of Physics, University of Ulsan, Ulsan 44610, Republic of Korea

Recently, topological singularities such as Weyl points and nodal lines have been a main interest of condensed matter physics. Such topological singularities and avoided crossings are sometimes formed at the same energy. In this work, we analyze such degeneracies and avoided crossings in compensated ferrimagnet Mn₃Al using first-principles calculations. In particular, we quantify their contributions to the anomalous Hall effects. The analysis shows avoided crossings are more crucial than Weyl points and nodal lines in general.

Magnetic interaction in Sr$_2$RuO$_4$ and superconducting gap symmetry

Jae-Ho Han[1*], Bongjae Kim[2]

[1]Center for Theoretical Physics of Complex Systems, Institute for Basic Science (IBS),
Daejeon 34126, Republic of Korea
[2]Department of Physics, Kunsan National University, Gunsan, 54150 Republic of Korea

The superconductivity of Sr$_2$RuO$_4$ has been studied for almost three decades, but the nature of the order parameter is still under intensely disputed. The superconducting gap was expected to have chiral p-wave symmetry, which is an electron analog of the A-phase of superfluid ^{3}He. Experimentally, however, there have been many results that contradict each other: nuclear magnetic resonance, polarized neutron scattering, and muon spin relaxation results support p-wave symmetry while the strain dependences of transition temperature, Pauli limit of the in-plane critical field, and absence of edge states support even symmetry. Recently, the revisit of nuclear magnetic resonance experiment has further increased the interests on the system, but no consensus on the order parameter has been made yet. One of the main difficulties in the theoretical prediction of gap symmetry is the small difference in critical temperatures between different gap symmetries, which makes it harder to identify the correct symmetry, and, thus, almost degeneracy of different states is also discussed. Considering the pairing glue of the Cooper pair is spin-fluctuations, the explicit consideration of magnetic interactions can be important in determining the symmetry of the superconducting gap. Here, we investigate gap symmetry within the mean-field level, including magnetic interactions explicitly. We obtain a phase diagram of gap symmetry upon spin-orbit coupling and magnetic interaction strength and discuss the role of the magnetism on the order parameter. Further, we study the implications of our approaches to the recent uniaxial strain experiments.

Author Index

Name	Abstract ID	Page	Name	Abstract ID	Page
Lee, Ji-Hye	SM03	130	Lee, Nyunjong	SS02	61
Lee, Jin Hong	조O-4-3	324	Lee, OukJae	SS05	64
Lee, Jinseo	SS21	82	Lee, OukJae	SS08	67
Lee, Jisung	조S-1-9	235	Lee, Oukjae	SS09	68
Lee, Jiyoung	SS21	82	Lee, OukJae	SS10	69
Lee, Joon Woo	SS14	73	Lee, OukJae	조O-4-2	323
Lee, June Hyuk	PM12	121	Lee, Sang-Beom	MS07	43
Lee, Jung Woo	SM08	135	Lee, Sangchul	PM04	113
Lee, Jung Woo	SM12	139	Lee, Sangho	SS01	60
Lee, Jung Woo	SM14	141	Lee, Sang-Kon	EM13	28
Lee, Jung Woo	SM15	142	Lee, Sangmin	QM01	163
Lee, Jung-Goo	PM11	120	Lee, Sang-Min	SM03	130
Lee, Jung-Goo	PM16	126	Lee, Sang-min	SM28	157
Lee, Jung-Goo	조S-3-10	270	Lee, Sang-Suk	MS15	54
Lee, Jun-Seok	MS09	46	Lee, Sang-Suk	조S-4-4	222
Lee, K.-S.	OS05	192	Lee, Seong-Hyub	SS27	88
Lee, Kang-Hyuk	PM02	111	Lee, Seongsu	조S-1-20	361
Lee, Kang-Hyuk	PM05	114	Lee, Seung-Heon	EM04	17
Lee, Kang-Hyuk	PM07	116	Lee, Seung-Heon	EM11	26
Lee, Kang-Hyuk	PM10	119	Lee, Seunghun	조S-1-12	298
Lee, Kee Ahn	SM23	152	Lee, Seung-Jae	MS16	56
Lee, Ki-Suk	MD03	101	Lee, Seung-Jae	조S-9-1	337
Lee, Ki-Suk	SS12	71	Lee, Seungyeol	조S-1-17	358
Lee, Ki-Suk	SS15	74	Lee, Seung-Youl	MS09	46
Lee, Ki-Suk	SS20	81	Lee, Shinbuhm	조S-10-1	349
Lee, Kwan	O-3-1	313	Lee, Snag Hyub	PM04	113
Lee, Kwan-Woo	조S-11-2	366	Lee, Soobeom	조O-4-1	321
Lee, Kwiyoung	SM22	150	Lee, Soobeom	조S-2-6	202
Lee, Kyung-Jin	조O-4-2	323	Lee, Soogil	MD08	107
Lee, Kyung-Jin	조S-2-2	198	Lee, Soogil	SS28	89
Lee, Kyung-Jin	조S-6-6	258	Lee, Soogil	SS29	90
Lee, Kyusup	조S-6-6	258	Lee, Soogil	조O-4-2	323
Lee, Min Hyeok	O-2-4	266	Lee, Soogil	조S-6-2	254
Lee, Min Woo	SM23	152	Lee, Sooseok	SS15	74
Lee, Mingseong	조S-1-17	358	Lee, Sooseok	SS20	81
Lee, Minwoo	O-5-2	334	Lee, Suheon	조S-1-17	358
Lee, Min-Woo	SM27	156	Lee, Su-Mi	조S-7-1	283
Lcc, Min-woo	SM28	157	Lcc, Sung Bin	조S-1-18	359
Lee, Min-Woo	조S-10-4	352	Lee, Sungwon	BM02	31
Lee, Mo Kwon	MS10	49	Lee, Sungwon	조S-10-2	350
Lee, Nam Young	조S-4-7	226	Lee, Tae Kyung	조S-7-5	287
Lee, Nara	O-1-3	241	Lee, Taekhyeon	SS29	90
Lee, Nara	QM13	175	Lee, Won Jeong	MS10	49
Lee, Nara	QM15	177	Lee, Won Jeong	MS12	51
Lee, Nara	SS22	83	Lee, Wooyoung	PM03	112
Lee, Nara	SS25	86	Lee, Wooyoung	PM08	117
Lee, Nyun Jong	MD05	104	Lee, Yeon-Joo	SM27	156
Lee, Nyun Jong	SS14	73	Lee, Ye-Seo	EM10	24

Name	Abstract ID	Page
Oh, Yun-Tak	QM05	167
Ohnishi, Kohei	조S-8-4	308
Ohshima, Ryo	조O-4-1	321
Ohshima, Ryo	조S-2-6	202
Ok, H.-J.	OS05	192
Ok, Hye-Jin	SS15	74
Ok, Hye-Jin	SS20	81
Ok, Jong Mok	QM06	168
Ok, Jongmok	QM08	170
Park, Albert Min Gyu	MD08	107
Park, Bae Ho	LM04	181
Park, Bae Ho	LM05	182
Park, Bae Ho	SS11	70
Park, Bum Chul	BM05	34
Park, Byeongjin	조S-7-2	284
Park, Byong-Guk	SS28	89
Park, Byong-Guk	SS29	90
Park, Byong-Guk	조O-4-2	323
Park, Byong-Guk	조S-6-2	254
Park, Chang-Won	MS09	46
Park, Chul-Hong	조S-1-9	235
Park, Eonbyeong	조S-7-9	291
Park, Gun-Woo	SS37	98
Park, Gyuyoung	O-2-2	264
Park, Gyuyoung	조S-6-1	253
Park, Hee Gyum	SS03	62
Park, Hyeong-Ryeol	QM09	171
Park, Hyeon-Jong	조O-4-2	323
Park, Hyeon-Kyu	PM06	115
Park, Hyeon-Kyu	조S-6-1	253
Park, Hyojun	조S-9-2	338
Park, Jae-Hoon	조S-1-15	302
Park, Jaehyeon	SS29	90
Park, Je Geun	QM12	174
Park, Je-Geun	조S-1-16	357
Park, Ji-Ho	조S-6-2	254
Park, Jihoon	조S-3-11	272
Park, Jihyc	SM04	131
Park, Jong-Min	SM11	138
Park, Jong-Min	SM14	141
Park, Jong-Min	조S-7-7	289
Park, Joonbum	조O-4-6	327
Park, Jun Kue	조S-1-9	235
Park, Jung-Hyun	SS27	88
Park, Jungmin	MD05	104
Park, Jungmin	SS02	61
Park, Jungmin	조O-4-4	325
Park, Kyoo-sung	PM14	123

Name	Abstract ID	Page
Park, Miju	QM08	170
Park, Min Gyu	MD09	108
Park, Minkyu	O-6-2	372
Park, Minkyu	TC04	161
Park, Minsoo	OS03	190
Park, Minsoo	QM04	166
Park, Mintae	O-2-3	265
Park, Moon Jip	LM07	184
Park, Moon Jip	조S-1-2	4
Park, Shin-Eui	PM13	122
Park, Sijin	O-1-2	240
Park, Song E	조S-3-9	269
Park, Su Jeong	SM09	136
Park, Su-Jeong	SM10	137
Park, Sujeong	SS13	72
Park, Sungkyun	SS35	96
Park, Sungkyun	조O-4-7	328
Park, Sungkyun	조S-1-8	234
Park, Sungkyun	조S-1-9	235
Park, Sungyu	조O-4-6	327
Park, Tae-Eon	조S-8-3	307
Park, Taesu	TC05	162
Park, Yong Ho	SM11	138
Park, Youn Ho	조S-8-3	307
Park, Young Jin	조S-6-7	260
Park, Younggun	SS15	74
Park, Yunchang	SS19	79
Pham, Trang Huyen Cao	SS35	96
Pyo, Hyun-Jo	EM09	23
Pyo, Hyun-Jo	EM11	26
Qian, Hui-Dong	조S-3-11	272
Qiu, Z. Q.	조S-2-5	201
Rhim, Geun Bae	조S-5-3	249
Rhim, S. H.	O-6-2	372
Rhim, S. H.	TC02	159
Rhim, S.H.	TC04	161
Rhim, Sonny H.	O-1-1	239
Robinson, Jason W.A.	조S-8-4	308
Rogachev, Kirill A.	SM17	144
Roh, Jong Wook	PM04	113
Rortais, Fabien	조O-4-1	321
Rotermund, Fabian	조S-6-2	254
Ryu, Jeongchun	SS29	90
Ryu, Woohyeon	SS11	70
Samanta, Subhasis	조S-11-1	365
Samardak, A. S.	SS26	87
Samardak, Aleksei Yu.	SM17	144
Samardak, Alexander S.	SM17	144

Digests of the KMS 2022 Summer Conference
The Korean Magnetics Society
사단법인 한국자기학회

KimTech sells various high pressure cells and tools

Piston Clamp Cells (0 - 4 GPa) w/ hydostatic oil medium
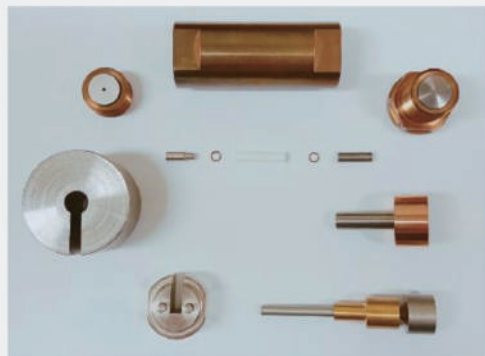
|	
Product	PC Oil Transport Cell (for PPMS™ or other Cryostats)
Material	Hyrid walls: CuBe & NiCrAl
Parts	Teflon tube, metal rings, obturators
Target *P*	3 GPa (KTO3) / 4 GPa (KTO4)

Product	PC Oil Magnetization Cell (for MPMS™ or SQUID-VSM™)
Material	CuBe
Target *P*	1.5 GPa

- A PCC for neutron scattering at Hanaro research reactor is being developed too

Diamond Anvil Cells (0-100 GPa) w/ gasket and *P* medium

Product	Diamond Anvil Transport Cell (for PPMS™ or other Cryostats)
Material	NiCrAl
Target *P*	60 GPa (300 μm culet diamond)
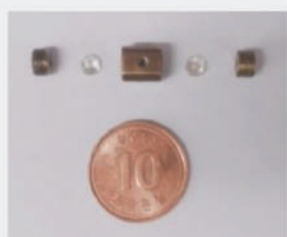
Product	Diamond Anvil Magnetization Cell (for MPMS™)
Material	CuBe
Target *P*	10 GPa (800 μm culet diamond) 15 GPa (600 μm culet diamond)

Product	Diamond Anvil Optics Cell (for XRD / Raman)
Material	WC / SUS/ CuBe
Target *P*	60 GPa (300 μm culet diamond)

- Other types of oil cells with different diameters can be also fabricated per order.
- For details, please contact : kimtech2019@gmail.com or visit http://kimtech.kr

KimTech co. ltd: Rm 56-427, Dept. of Physics and Astronomy, Seoul National University